

THIRD EDITION

Reaction
Mechanisms
of Inorganic
and
Organometallic
Systems

Robert B. Jordan

Reaction Mechanisms of Inorganic and Organometallic Systems

TOPICS IN INORGANIC CHEMISTRY

A Series of Advanced Textbooks in Inorganic Chemistry

Series Editor

Peter C. Ford, University of California, Santa Barbara

Chemical Bonding in Solids, J. Burdett

Reaction Mechanisms of Inorganic and Organometallic Systems,
3rd Edition, R. Jordan

Reaction Mechanisms of Inorganic and Organometallic Systems

Third Edition

Robert B. Jordan

OXFORD
UNIVERSITY PRESS
2007

OXFORD
UNIVERSITY PRESS

Oxford University Press, Inc., publishes works that further
Oxford University's objective of excellence
in research, scholarship, and education.

Oxford New York

Auckland Cape Town Dar es Salaam Hong Kong Karachi
Kuala Lumpur Madrid Melbourne Mexico City Nairobi
New Delhi Shanghai Taipei Toronto

With offices in

Argentina Austria Brazil Chile Czech Republic France Greece
Guatemala Hungary Italy Japan Poland Portugal Singapore
South Korea Switzerland Thailand Turkey Ukraine Vietnam

Copyright © 2007 by Oxford University Press, Inc.

Published by Oxford University Press, Inc.
198 Madison Avenue, New York, New York 10016

www.oup.com

Oxford is a registered trademark of Oxford University Press

All rights reserved. No part of this publication may be reproduced,
stored in a retrieval system, or transmitted, in any form or by any means,
electronic, mechanical, photocopying, recording, or otherwise,
without the prior permission of Oxford University Press.

Library of Congress Cataloging-in-Publication Data

Jordan, Robert B.

Reaction mechanisms of inorganic and organometallic systems / Robert

B. Jordan.—3rd ed

p. cm.

Includes bibliographical references and index.

ISBN 978-0-19-530100-7

1. Reaction mechanisms (Chemistry) 2. Organometallic compounds. 3. Inorganic
compounds. I. Title.

QD502.J67 2006

41'.39—dc25 2006052498

9 8 7 6 5 4 3 2 1

Printed in the United States of America
on acid-free paper

Preface

This book evolved from the lecture notes of the author for a one-semester course given to senior undergraduates and graduate students over the past 20 years. This third edition presents an updating of the material to cover the literature through to the end of 2005, with occasional excursions to early 2006. As a result, the total number of references has increased from about 660 in the second edition to over 1570 in the present one, and 140 pages of text have been added; this seems to be a clear testament to the vitality of the subject area. A new Chapter 9 on kinetics in heterogeneous systems has been added. This area has long been the domain of chemical engineers, but it is of increasing relevance to inorganic kineticists who are studying catalytic processes, such as hydrogenation and carbonylation reactions, where gas/liquid mass transfer is involved. This chapter also covers the kinetic aspects of adsorption and reaction of species on solids, and the question of whether the reaction is really homogeneous or heterogeneous.

The overall organization of the first edition has been retained. The first two chapters cover basic kinetic and mechanistic terminology and methodology. This material includes new sections on the analysis of data under second-order conditions, Curtin–Hammett conditions and an expanded discussion of pressure effects. New material has been added at various points throughout Chapters 3 and 4. The coverage of organometallic systems in Chapter 5 has been increased substantially, primarily with material on metal hydrides, catalytic hydrogenation and asymmetric hydrogenation. The inverted region and activation parameters for electron-transfer reactions predicted by Marcus theory have been added to Chapter 6, along with an expanded discussion of intervalence electron transfer. The recently revised assignment of the electronic spectra of metal carbonyls has resulted in substantial revisions to photochemical interpretations in Chapter 7. The coverage of selected bioinorganic systems in Chapter 8 has been extended to include methylcobalamin as a methyl transferase and the chemistry of nitric oxide synthase. Chapter 10 on experimental methods and their applications is largely unchanged. Some new problems for each chapter have been added.

There is more material than can be covered in depth in one semester, but the organization allows the lecturer to omit or give less coverage to certain areas without jeopardizing an understanding of other areas. It is assumed that the students are familiar with elementary crystal field

theory and its applications to electronic spectroscopy and energetics, and concepts of organometallic chemistry, such as the 18-electron rule, π bonding and coordinative unsaturation. For the material in the first two chapters, some background from a physical chemistry course would be useful, and familiarity with simple differential and integral calculus is assumed.

It is expected that students will consult the original literature to obtain further information and to gain a feeling for the excitement in the field. This experience also should enhance their ability to critically evaluate such work. Many of the problems at the end of the book are taken from the literature, and original references are given; outlines of answers to the problems will be supplied to instructors who request them from the author.

The issue of units continues to be a vexing one in this area. A major goal of this course has been to provide students with sufficient background so that they can read and analyze current research papers. To do this and be able to compare results, the reader must be vigilant about the units used by different authors. Energy units are a special problem, since both joules and calories are in common usage. Both units have been retained in the text, with the choice made on the basis of the units in the original work as much as possible. However, within individual sections the text uses one energy unit. Bond lengths are given in angstroms, which are still commonly quoted for crystal structures. The formulas for various calculations are given in the original or most common format, and units for the various quantities are always specified.

The author is greatly indebted to all of those whose research efforts have provided the core of the material for this book. The author is pleased to acknowledge those who have provided the inspiration for this book: first, my parents, who contributed the early atmosphere and encouragement; second, Henry Taube, whose intellectual stimulation and experimental guidance ensured my continuing enthusiasm for mechanistic studies. I am only sorry that I did not finish this edition soon enough for Henry to see that I did make the changes he suggested. Finally and foremost, Anna has been a vital force in the creation of this book through her understanding of the time commitment, her comments, criticisms and invaluable editorial assistance in producing the camera-ready manuscript. However, the inevitable remaining errors and oversights are entirely the responsibility of the author.

R. B. J.

Edmonton, Alberta
June 2006

Contents

1 Tools of the Trade, 1

- 1.1 Basic Terminology, 1
- 1.2 Analysis of Rate Data, 3
- 1.3 Concentration Variables and Rate Constants, 12
- 1.4 Complex Rate Laws, 15
- 1.5 Complex Kinetic Systems, 15
- 1.6 Temperature Dependence of Rate Constants, 17
- 1.7 Pressure Dependence of Rate Constants, 21
- 1.8 Ionic Strength Dependence of Rate Constants, 24
- 1.9 Diffusion-Controlled Rate Constants, 25
- 1.10 Molecular Modeling and Theory, 28

2 Rate Law and Mechanism, 31

- 2.1 Qualitative Guidelines, 31
- 2.2 Steady-State Approximation, 32
- 2.3 Rapid-Equilibrium Assumption, 34
- 2.4 Curtin–Hammett Conditions, 36
- 2.5 Rapid-Equilibrium or Steady-State?, 37
- 2.6 Numerical Integration Methods, 38
- 2.7 Principle of Detailed Balancing, 39
- 2.8 Principle of Microscopic Reversibility, 40

3 Ligand Substitution Reactions, 43

- 3.1 Operational Approach to Classification of Substitution Mechanisms, 43
- 3.2 Operational Tests for the Stoichiometric Mechanism, 44
- 3.3 Examples of Tests for a Dissociative Mechanism, 49
- 3.4 Operational Test for an Associative Mechanism, 54
- 3.5 Operational Tests for the Intimate Mechanism, 57
- 3.6 Some Special Effects, 73
- 3.7 Variation of Substitution Rates with Metal Ion, 83
- 3.8 Ligand Substitution on Labile Transition-Metal Ions, 94
- 3.9 Kinetics of Chelate Formation, 100

4 Stereochemical Change, 114

- 4.1 Types of Ligand Rearrangements, 114
- 4.2 Geometrical and Optical Isomerism in Octahedral Systems, 119
- 4.3 Stereochemical Change in Five-Coordinate Systems, 128
- 4.4 Isomerism in Square-Planar Systems, 130
- 4.5 Fluxional Organometallic Compounds, 130

5 Reaction Mechanisms of Organometallic Systems, 150

- 5.1 Ligand Substitution Reactions, 150
- 5.2 Insertion Reactions, 168
- 5.3 Oxidative Addition Reactions, 177

- 5.4 Reductive Elimination Reactions, 188
- 5.5 Reactions of Alkenes, 188
- 5.6 Catalytic Hydrogenation of Alkenes, 195
- 5.7 Homogeneous Catalysis by Organometallic Compounds, 225

6 Oxidation–Reduction Reactions, 253

- 6.1 Classification of Reactions, 253
- 6.2 Outer-Sphere Electron-Transfer Theory, 256
- 6.3 Differentiation of Inner-Sphere and Outer-Sphere Mechanisms, 273
- 6.4 Bridging Ligand Effects in Inner-Sphere Reactions, 274
- 6.5 Intervalence Electron Transfer, 281
- 6.6 Electron Transfer in Metalloproteins, 285

7 Inorganic Photochemistry, 292

- 7.1 Basic Terminology, 292
- 7.2 Kinetic Factors Affecting Quantum Yields, 294
- 7.3 Photochemistry of Cobalt(III) Complexes, 295
- 7.4 Photochemistry of Rhodium(III) Complexes, 301
- 7.5 Photochemistry of Chromium(III) Complexes, 304
- 7.6 Photochemistry of Ruthenium(II) Complexes, 310
- 7.7 Organometallic Photochemistry, 313
- 7.8 Photochemical Generation of Reaction Intermediates, 327

8 Bioinorganic Systems, 337

- 8.1. Basic Terminology, 337
- 8.2 Terms and Methods of Enzyme Kinetics, 338
- 8.3 Vitamin B₁₂, 341
- 8.4 A Zinc(II) Enzyme: Carbonic Anhydrase, 356
- 8.5 Enzymic Reactions of Dioxygen, 361
- 8.6 Enzymic Reactions of Nitric Oxide, 373

9 Kinetics in Heterogeneous Systems, 391

- 9.1 Gas/Liquid Heterogeneous Systems, 391
- 9.2 Gas/Liquid/Solid Heterogeneous Systems, 400
- 9.3 Where is the Catalyst?, 409

10 Experimental Methods, 422

- 10.1 Flow Methods, 423
- 10.2 Relaxation Methods, 428
- 10.3 Electrochemical Methods, 431
- 10.4 Nuclear Magnetic Resonance Methods, 435
- 10.5 Electron Paramagnetic Resonance Methods, 446
- 10.6 Pulse Radiolysis Methods, 448
- 10.7 Flash Photolysis Methods, 451

Problems, 457

Chemical Abbreviations, 488

Index, 491

Reaction Mechanisms of Inorganic and Organometallic Systems

This page intentionally left blank

1

Tools of the Trade

This chapter covers the basic terminology and theory related to the types of studies that are commonly used to provide information about a reaction mechanism. The emphasis is on the practicalities of determining rate constants and rate laws. More background material is available from general physical chemistry texts^{1,2} and books devoted to kinetics.³⁻⁵ The reader also is referred to the initial volumes of the series edited by Bamford and Tipper.⁶ Experimental techniques that are commonly used in inorganic kinetic studies are discussed in Chapter 9.

1.1 BASIC TERMINOLOGY

As with most fields, the study of reaction kinetics has some terminology with which one must be familiar in order to understand advanced books and research papers in the area. The following is a summary of some of these basic terms and definitions. Many of these may be known from previous studies in introductory and physical chemistry, and further background can be obtained from textbooks devoted to the physical chemistry aspects of reaction kinetics.

Rate

For the general reaction



the reaction rate and the rate of disappearance of reactants and rate of formation of products are related by

$$\text{Rate} = -\frac{1}{a} \frac{d[A]}{dt} = -\frac{1}{b} \frac{d[B]}{dt} = \frac{1}{m} \frac{d[M]}{dt} = \frac{1}{n} \frac{d[N]}{dt} \quad (1.2)$$

In practice, it is not uncommon to define the rate only in terms of the species whose concentration is being monitored. The consequences that can result from different definitions of the rate in relation to the stoichiometry are described below under the definition of the rate constant.

Rate Law

The rate law is the experimentally determined dependence of the reaction rate on reagent concentrations. It has the following general form:

$$\text{Rate} = k[\text{A}]^m[\text{B}]^n \dots \quad (1.3)$$

where k is a proportionality constant called the rate constant. The exponents m and n are determined experimentally from the kinetic study and have no necessary relationship to the stoichiometric coefficients in the balanced chemical reaction. The rate law may contain species that do not appear in the balanced reaction and may be the sum of several terms for different reaction pathways.

The rate law is an essential piece of mechanistic information because it contains the concentrations of species necessary to get from the reactant to the product by the lowest energy pathway. A fundamental requirement of an acceptable mechanism is that it must predict a rate law consistent with the experimental rate law.

Order of the Rate Law

The order of the rate law is the sum of the exponents in the rate law. For example, if $m = 1$ and $n = -2$ in Eq. (1.3), the rate law has an overall order of -1 . However, except in the simplest cases, it is best to describe the order with respect to individual reagents; in this example, first-order in $[\text{A}]$ and inverse second-order in $[\text{B}]$.

Rate Constant

The rate constant, k , is the proportionality constant that relates the rate to the reagent concentrations (or activities or pressures, for example), as shown in Eq. (1.3). The units of k depend on the rate law and must give the right-hand side of Eq. (1.3) the same units as the left-hand side.

A simple example of the need to define the rate in order to give the meaning of the rate constant is shown for the reaction



From Eq. (1.2), and assuming the rate is second-order in $[\text{A}]$, then

$$\text{Rate} = -\frac{1}{2} \frac{d[\text{A}]}{dt} = \frac{d[\text{B}]}{dt} = k[\text{A}]^2 \quad (1.5)$$

If the experiment followed the rate of disappearance of A, then the experimental rate constant would be $2k$ and it must be divided by 2 to get the numerical value of k as defined by Eq. (1.5). However, if the formation of B was followed, then k would be determined directly from the experiment.

Half-time

The half-time, $t_{1/2}$, is the time required for a reactant concentration to change by half of its total change. This term is used to convey a qualitative idea of the time scale for the reaction and has a quantitative relationship to the rate constant in simple cases. In complex systems, the half-time may be different for different reagents and one should specify the reagent to which the $t_{1/2}$ refers.

Lifetime

The lifetime, τ , for a particular species is the concentration of that species divided by its rate of disappearance. This term is commonly used in so-called lifetime methods, such as NMR, and in relaxation methods, such as temperature jump.

1.2 ANALYSIS OF RATE DATA

In general, a kinetic study begins with the collection of data of concentration versus time of a reactant or product. As will be seen later, this can also be accomplished by determining the time dependence of some variable that is proportional to concentration, such as absorbance or NMR peak intensity. The next step is to fit the concentration–time data to some model that will allow one to determine the rate constant if the data fits the model.

The following section develops some integrated rate laws for the models most commonly encountered in inorganic kinetics. This is essentially a mathematical problem; given a particular rate law as a differential equation, the equation must be reduced to one concentration variable and then integrated. The integration can be done by standard methods or by reference to integration tables. Many more complex examples are given in advanced textbooks on kinetics.

1.2.1 Zero-Order Reaction

A zero-order reaction is rare for inorganic reactions in solution but is included for completeness. For the general reaction



the zero-order rate law is given by

$$\frac{d[B]}{dt} = k \quad (1.7)$$

and integration over the limits $[B] = [B]_0$ to $[B]$ and $t = 0$ to t yields

$$[B] - [B]_0 = kt \quad (1.8)$$

This predicts that a plot of $[B]$ or $[B] - [B]_0$ versus t should be linear with a slope of k .

1.2.2 First-Order Irreversible System

Strictly speaking, there is no such thing as an irreversible reaction. It is just a system in which the rate constant in the forward direction is much larger than that in the reverse direction. The kinetic analysis of the irreversible system is just a special case of the reversible system that is described in the next section.

For the representative irreversible reaction



the rate of disappearance of A and appearance of B are given by

$$-\frac{d[A]}{dt} = \frac{d[B]}{dt} = k_1[A] \quad (1.10)$$

The problem, in general, is to convert this differential equation to a form with only one concentration variable, either $[A]$ or $[B]$, and then to integrate the equation to obtain the *integrated rate law*. The choice of the variable to retain will depend on what has been measured experimentally. One of the concentrations can be eliminated by considering the reaction stoichiometry and the initial conditions. The most general conditions are that both A and B are present initially at concentrations $[A]_0$ and $[B]_0$, respectively, and that the concentrations at any time are defined as $[A]$ and $[B]$.

For this simple case, the rate law in terms of A can be obtained by simple rearrangement to give

$$-\frac{d[A]}{[A]} = k_1 dt \quad (1.11)$$

Then, integration over the limits $[A] = [A]_0$ to $[A]$ and $t = 0$ to t , gives

$$\ln [A] - \ln [A]_0 = -k_1 t \quad (1.12)$$

and predicts that a plot of $\ln [A]$ versus t should be linear with a slope of $-k_1$. The linearity of such plots often is taken as evidence of a first-order rate law. Since the assessment of linearity is somewhat subjective, it is better to show that the slope of such plots is the same for different initial concentrations of A and that the intercept corresponds to the expected value of $\ln [A]_0$.

The equivalent exponential form of Eq. (1.12) is

$$[A] = [A]_0 e^{-k_1 t} \quad (1.13)$$

and it is now common to fit data to this equation by nonlinear least squares to obtain k_1 .

In order to obtain the integrated form in terms of B, it is necessary to use the mass balance conditions. For a 1:1 stoichiometry, the changes in concentration are related by

$$[A]_0 - [A] = [B] - [B]_0 \quad (1.14)$$

At the end of the reaction, $[A] = 0$ and $[B] = [B]_{\infty}$, and substitution of these values into Eq. (1.14) gives

$$[A]_0 = [B]_{\infty} - [B]_0 \quad (1.15)$$

After rearrangement of Eq. (1.14) and substitution from Eq. (1.15), one obtains

$$[A] = [B]_{\infty} - [B] \quad (1.16)$$

Then, substitution for $[A]$ from Eq. (1.16) into Eq. (1.10) gives an equation that can be integrated over the limits $[B] = [B]_0$ to $[B]$ and $t = 0$ to t , to obtain

$$\ln ([B]_{\infty} - [B]) - \ln ([B]_{\infty} - [B]_0) = -k_1 t \quad (1.17)$$

This equation also can be obtained by substitution for $[A]_0$ and $[A]$ from Eq. (1.15) and (1.16) into Eq. (1.12) and predicts that a plot of $\ln ([B]_{\infty} - [B])$ versus t should be linear with a slope of $-k_1$.

The half-time, $t_{1/2}$, can be obtained from Eq. (1.12) for the condition $[A] = [A]_0/2$, or from Eq. (1.17) for $[B] = 1/2([B]_{\infty} - [B]_0) + [B]_0$. In either case, the result is

$$t_{1/2} = \frac{\ln 2}{k_1} = \frac{0.693}{k_1} \quad (1.18)$$

Therefore, *the half-time is independent of the initial concentrations.*

An important practical advantage of the first-order system is that *the analysis can be done without any need to know the initial concentrations.* Therefore, the collection of concentration–time data can be started at any time arbitrarily defined as $t = 0$. This is a significant difference from the second-order case that is described later in this chapter.

1.2.3 First-Order Reversible System

For a system coming to equilibrium, both the forward and reverse reactions must be included in the kinetic analysis and one must take into account that significant concentrations of both reactants and products will be present at the end of the reaction. A first-order system coming to equilibrium may be represented by



The rate of disappearance of A equals the rate of appearance of B, and these are given by

$$-\frac{d[A]}{dt} = \frac{d[B]}{dt} = k_1[A] - k_{-1}[B] \quad (1.20)$$

Just as with the irreversible system, the problem is to convert this equation to a form with only one concentration variable, either [A] or [B], and then integrate the equation to obtain the *integrated rate law*. The initial concentrations are defined as $[A]_0$ and $[B]_0$, those at any time as [A] and [B], and the final concentrations at equilibrium as $[A]_e$ and $[B]_e$. Then, mass balance gives

$$[A]_0 + [B]_0 = [A] + [B] = [A]_e + [B]_e \quad (1.21)$$

To obtain the rate law in terms of B, Eq. (1.21) can be rearranged to obtain the following expressions for [A] and $[A]_0$:

$$[A] = [A]_0 + [B]_0 - [B] \quad \text{and} \quad [A]_0 = [A]_e + [B]_e - [B]_0 \quad (1.22)$$

so that

$$[A] = [A]_e + [B]_e - [B]_0 + [B]_0 - [B] = [A]_e + [B]_e - [B] \quad (1.23)$$

Substitution for [A] from Eq. (1.23) into Eq. (1.20) gives

$$\frac{d[B]}{dt} = k_1([A]_e + [B]_e) - (k_1 + k_{-1})[B] \quad (1.24)$$

Note that the initial concentrations have been eliminated.

Since Eq. (1.24) contains only one concentration variable, [B], it can be integrated directly. However, it is convenient in the end to eliminate $[A]_e$ by noting that, at equilibrium the rate in the forward direction must be equal to the rate in the reverse direction:

$$k_1[A]_e = k_{-1}[B]_e \quad (1.25)$$

and substitution for $k_1[A]_e$ into Eq. (1.24) gives

$$\begin{aligned} \frac{d[B]}{dt} &= k_{-1}[B]_e + k_1[B]_e - (k_1 + k_{-1})[B] \\ &= (k_1 + k_{-1})([B]_e - [B]) \end{aligned} \quad (1.26)$$

This equation can be rearranged and integrated over the limits $[B] = [B]_0$ to $[B]$ and $t = 0$ to t to obtain

$$\ln([B]_e - [B]) - \ln([B]_e - [B]_0) = -(k_1 + k_{-1})t \quad (1.27)$$

Therefore, a plot of $\ln([B]_e - [B])$ versus t should be linear with a slope of $-(k_1 + k_{-1})$. Note that the kinetic study yields the sum of the forward and reverse rate constants. If the equilibrium constant, K , is known, then k_1 and k_{-1} can be calculated since $K = k_1/k_{-1}$.

Just as in the irreversible first-order system, *the analysis can be done without any need to know the initial concentrations*, and the collection of concentration–time data can be started at any time defined as $t = 0$.

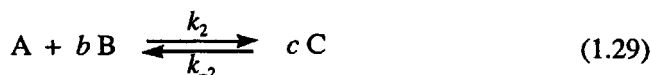
At the half-time, $t = t_{1/2}$, $[B] = 1/2([B]_e - [B]_0) + [B]_0$, and substitution into Eq. (1.27) gives

$$t_{1/2} = \frac{\ln 2}{k_1 + k_{-1}} = \frac{0.693}{k_1 + k_{-1}} \quad (1.28)$$

The irreversible first-order system is a special case of the reversible system. For the irreversible system, $k_1 \gg k_{-1}$ so that $(k_1 + k_{-1}) = k_1$.

1.2.4 Second-Order Reversible System

The second-order reversible system will be described next and the simpler irreversible system will be developed later as a special case of the reversible one. This reversible system can be described by



where b and c are stoichiometric coefficients defined relative to a coefficient of 1 for the deficient reagent A. The rate of disappearance of A is given by

$$-\frac{d[A]}{dt} = k_2[A][B] - k_{-2}[C] \quad (1.30)$$

It will be assumed that there is no C present initially so that mass balance gives the concentrations of B and C in terms of A as

$$[B] = [B]_0 - b([A]_0 - [A]) \quad \text{and} \quad [C] = c([A]_0 - [A]) \quad (1.31)$$

and at equilibrium

$$[B]_e = [B]_0 - b([A]_0 - [A]_e) \quad \text{and} \quad [C]_e = c([A]_0 - [A]_e) \quad (1.32)$$

It is convenient to eliminate k_{-2} before integrating by noting that the forward and reverse rates are equal at equilibrium:

$$k_2[A]_e\{[B]_0 - b([A]_0 - [A]_e)\} = k_{-2}c([A]_0 - [A]_e) \quad (1.33)$$

which, after rearrangement, gives

$$k_{-2} = \frac{k_2[A]_e\{[B]_0 - b([A]_0 - [A]_e)\}}{c([A]_0 - [A]_e)} \quad (1.34)$$

Substitution for [B] and [C] from Eq. (1.31) and for k_{-2} from Eq. (1.34) into Eq. (1.30) gives the following equation which can be integrated because [A] is the only concentration variable:

$$-\frac{d[A]}{dt} = \frac{k_2\{[A] - [A]_e\}\{[A]_0[B]_0 - b([A]_0 - [A]_e)([A]_0 - [A])\}}{[A]_0 - [A]_e} \quad (1.35)$$

Integration over the limits $[A] = [A]_0$ to $[A]$ and $t = 0$ to t gives the following solution:

$$\ln \left(\frac{[A]_0[B]_0 - b([A]_0 - [A]_e)([A]_0 - [A])}{[A] - [A]_e} \right) - \ln \left(\frac{[A]_0[B]_0}{[A]_0 - [A]_e} \right) = \frac{\{[A]_0[B]_0 - b([A]_0 - [A]_e)^2\}k_2t}{[A]_0 - [A]_e} \quad (1.36)$$

A plot of the first term on the left-hand side of Eq. (1.36) versus t should be linear with a slope related to k_2 , as indicated by the right-hand side of Eq. (1.36). It is apparent that *one must know the stoichiometry coefficient, b , in addition to the initial concentrations, $[A]_0$ and $[B]_0$, and the final concentration, $[A]_e$, in order to do the analysis and to determine the value of k_2 from the slope.* In practice, all of these requirements can be difficult to satisfy so that this is an unpopular and uncommon situation for experimental studies. The methods used to circumvent these requirements are described in Sections 1.2.6 and 1.2.8.

1.2.5 Second-Order Irreversible System

This system can be obtained as a special case of the reversible system by simple consideration of the stoichiometry conditions. If B is the excess reagent and reaction (1.29) goes essentially to completion, then $[A]_e = 0$, and substitution of this condition into Eq. (1.36) gives

$$\ln \left(\frac{[B]_0 - b([A]_0 - [A])}{[A]} \right) - \ln \left(\frac{[B]_0}{[A]_0} \right) = ([B]_0 - b[A]_0)k_2t \quad (1.37)$$

In this case, the initial concentrations of both reactants are required in order to plot the first term on the left versus t and to determine k_2 from the slope. These conditions are not as restrictive as those for the reversible second-order system, but they are still worse than those for the first-order system.

At the half-time for this second-order reaction, $[A] = [A]_0/2$, and substitution into Eq. (1.37) shows that

$$t_{1/2} = \frac{1}{([B]_0 - b[A]_0)k_2} \ln \left(\frac{2[B]_0 - b[A]_0}{[B]_0} \right) \quad (1.38)$$

1.2.6 Pseudo-First-Order Reaction Conditions

The pseudo-first-order reaction condition is very widely used, but it is seldom mentioned in textbooks. Although many reactions have second-order or more complex rate laws, the experimental kineticist wishes to optimize experiments by taking advantage of the first-order rate law because it imposes the fewest restrictions on the conditions required to determine a reliable rate constant. The trick is to use the pseudo-first-order condition.

The *pseudo-first-order condition* requires that the concentration of the reactant whose concentration is monitored is at least 10 times smaller than that of all the other reactants, so that the concentrations of all the latter remain essentially constant during the reaction. Under this condition, the rate law usually simplifies to a first-order form and one gains the advantage of not needing to know the initial concentration of the deficient reagent.

In the preceding irreversible second-order example, if it is assumed that the conditions have been set so that $[B]_0 \gg [A]_0$, then $[B]_0 \gg [C]$ and $[C] = [A]_0 - [A]$. In addition, the concentration of B will remain constant at $[B]_0$, and the final concentration of C is $[C]_\infty = [A]_0$ if the reaction is irreversible and has a 1:1 stoichiometry. Substitution of these conditions into Eq. (1.37) gives

$$\ln \left(\frac{[C]_\infty}{[C]_\infty - [C]} \right) = [B]_0 k_2 t \quad (1.39)$$

This equation predicts that a plot of $\ln ([C]_\infty - [C])$ versus t should be linear

with a slope of $-k_2[B]_0$. This is identical in form to the first-order rate law except that k_1 is replaced by $k_2[B]_0$. The latter constant is often called the observed, k_{obsd} , or experimental, k_{exp} , rate constant. Since $[B]_0$ is known, it is possible to calculate k_2 .

In a more general case, if the rate of disappearance of reactant A is a function of the concentrations of other species X, Y and Z, then the rate of disappearance of A may be given by

$$-\frac{d[A]}{dt} = k[X]^x [Y]^y [Z]^z [A] \quad (1.40)$$

If the conditions are such that $[X]_0, [Y]_0, [Z]_0 \gg [A]$, so that $[X], [Y]$ and $[Z]$ remain essentially constant, then

$$-\frac{d[A]}{dt} = k[X]_0^x [Y]_0^y [Z]_0^z [A] = k_{\text{exp}}[A] \quad (1.41)$$

and the rate law has the first-order form.

1.2.7 Comparison of First-Order and Second-Order Conditions

The differences between second-order and first-order kinetic behavior, and the transition from second-order to pseudo-first-order conditions are illustrated by the curves in Figure 1.1. These curves are based on the system



and show the time dependence of the formation of C. The deficient reagent is A, with $[A]_0 = 0.10$ M, different initial concentrations of B of 0.50, 0.70, 0.85 and 1.0 M are used, and $k_2 = 3 \times 10^{-3} \text{ M}^{-1} \text{ s}^{-1}$. The lower curve, with $[B]_0 = 0.50$ M, represents a typical time dependence for second-order conditions. Note that this time dependence has a more gradual approach to the final value than the others in Figure 1.1. Thus, a qualitative examination can provide an indication of the second-order nature of the reaction. The fact that the rate is slower under second-order conditions can be used to advantage if the limits of the experimental method are being strained.

As $[B]_0$ is increased, C is formed more rapidly and the curves approach a first-order shape. When $[B]_0 = 1.0$ M, $[B]_0 \geq 10[A]_0$ and the pseudo-first-order condition has been reached. Then, the curve calculated from Eq. (1.37) for second-order conditions is almost indistinguishable from the line calculated from Eq. (1.39) for pseudo-first-order conditions. The correspondence of these curves is the rationale for the general rule that *pseudo-first-order conditions require at least a 10-fold excess of the reagents whose concentrations are to remain constant.*

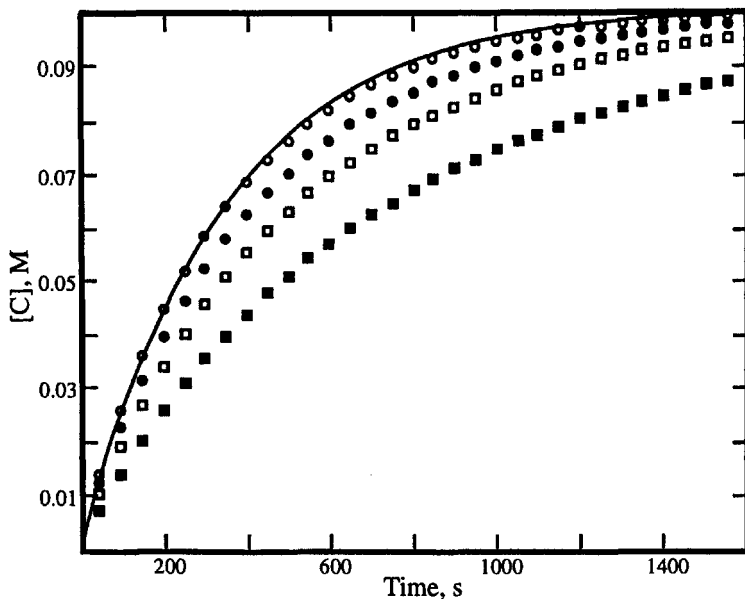


Figure 1.1. The time dependence for formation of product C with the initial deficient reagent $[A]_0 = 0.10$ M. Results are calculated for pseudo-first-order (—) conditions and concentrations (M) of the excess reagent B of 0.50 (■), 0.70 (□), 0.85 (●), 1.0 (○).

1.2.8 Initial Rate Method

This is a method for determining the concentration dependence of a rate law that avoids the need for an integrated rate law or pseudo-first-order conditions. It is based on the assumption that the reactant concentrations are essentially constant during the initial ~10% of reaction. The use of this method requires that observation can begin very soon after mixing the reactants and that the detection method is sensitive enough to provide precise data over the small extent of reaction. The latter condition usually means that the reaction half-time is about ten seconds or longer, so that this method is convenient and efficient for slow reactions. Observation over a short initial period may avoid, but also may hide, kinetic and chemical complications that only are clearly apparent later in the reaction.

The kinetic runs simulated in Figure 1.2 are for a second-order rate law with varying initial concentrations of the reactants A and B, with A as the deficient reagent. The absorbance, I_A , which is proportional to the concentration of A, has been measured at 2 s intervals. For illustrative purposes, the concentrations have been chosen so that the initial rate, $k_2[A]_0[B]_0$, is the same for all the runs. More commonly, the reagent concentrations are varied one at a time in a series of kinetic runs in order to determine the rate law.

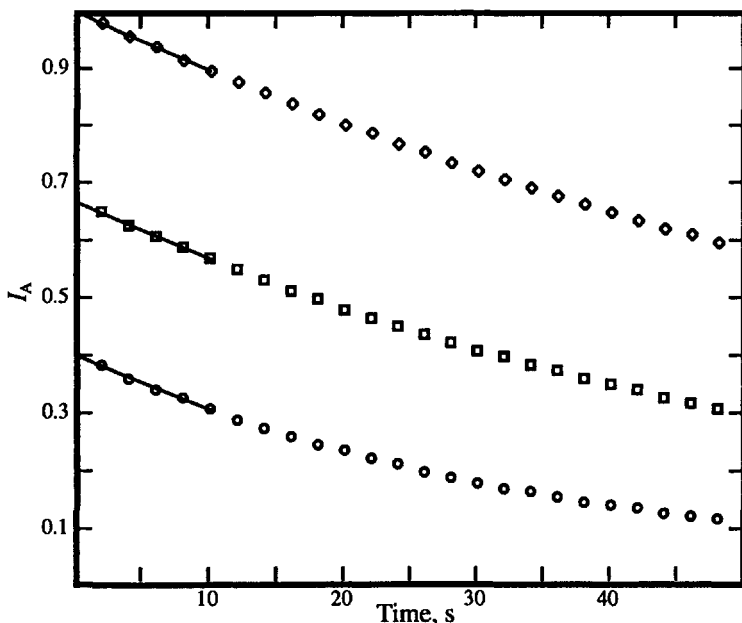


Figure 1.2. The time dependence of the absorbance, I_A , of reactant A during the initial stages of its reaction with B with a rate law $-d[A]/dt = k_2[A][B]$ and $k_2 = 3.0 \times 10^{-2} \text{ M}^{-1} \text{ s}^{-1}$. Initial concentrations (M) are: $[A]_0 = 0.050$, $[B]_0 = 0.400$ (\diamond); $[A]_0 = 0.033$, $[B]_0 = 0.600$ (\square); $[A]_0 = 0.020$, $[B]_0 = 1.0$ (\circ).

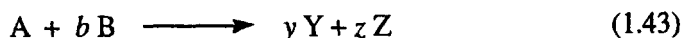
The simplest way of determining the initial rate is to take the slopes of the lines through the initial points, as shown in Figure 1.2. Strictly speaking, the slopes should be taken for lines which cover the same extent of reaction but this is not always obvious when one just observes a small portion of the reaction. In the Figure, the more common practice of taking the slope over a fixed time is illustrated, even though the extent of reaction is greatest for the fastest (lower) data set. As a result, the slopes actually range from 0.103 to 0.112 s^{-1} , although they should be equal. In this case, the error probably is not too significant for the purpose of determining the rate law. This difficulty can be minimized by fitting the data over a greater extent of the reaction to a power series in t , such as $I_t = I_0 + \alpha t + \beta t^2$, in which case α will be the initial slope. In order to determine the actual rate constant, one must know the relationship between the property being observed and the concentration.

1.3 CONCENTRATION VARIABLES AND RATE CONSTANTS

The rate laws have been developed in terms of concentrations, but in many cases it is not practical or possible to determine actual molar concentrations as a function of time. However, it is easy to measure some property that is

known to be directly proportional to molar concentration, such as absorbance in the electronic or infrared spectrum, NMR integrated peak intensity, conductance or refractive index.

The following development shows the general relationship between the concentration of the limiting reagent and the property being measured for the irreversible reaction



The equation is balanced so that A has a coefficient of 1 in order to simplify the ratios b/a , y/a and z/a which otherwise would appear in the equations. The property being measured is designated as I and its proportionality constant with concentration is ϵ . At any time, the value of I is given by

$$I_t = \epsilon_A[A] + \epsilon_B[B] + \epsilon_Y[Y] + \epsilon_Z[Z] \quad (1.44)$$

and the initial value is given by

$$I_0 = \epsilon_A[A]_0 + \epsilon_B[B]_0 \quad (1.45)$$

If A is the limiting reagent, then the final value of I is given by

$$I_\infty = \epsilon_B([B]_0 - b[A]_0) + (y\epsilon_Y + z\epsilon_Z)[A]_0 \quad (1.46)$$

The following stoichiometric relationships can be used to express the concentrations of B, Y and Z in terms of A:

$$\begin{aligned} [B] &= [B]_0 - b([A]_0 - [A]) & [Y] &= y([A]_0 - [A]) \\ [Z] &= z([A]_0 - [A]) \end{aligned} \quad (1.47)$$

Substitution of these values into Eq (1.44) gives

$$I_t = \epsilon_A[A] + \epsilon_B\{[B]_0 - b([A]_0 - [A])\} + (y\epsilon_Y + z\epsilon_Z)([A]_0 - [A]) \quad (1.48)$$

Then, taking the difference $I_t - I_\infty$ and solving for $[A]$ gives

$$[A] = \frac{I_t - I_\infty}{(\epsilon_A + b\epsilon_B) - (y\epsilon_Y + z\epsilon_Z)} \quad (1.49)$$

Similarly, $I_0 - I_\infty$ gives $[A]_0$ as

$$[A]_0 = \frac{I_0 - I_\infty}{(\epsilon_A + b\epsilon_B) - (y\epsilon_Y + z\epsilon_Z)} \quad (1.50)$$

Combination of the last two equations gives

$$[A] = \left(\frac{I_t - I_\infty}{I_0 - I_\infty} \right) [A]_0 \quad (1.51)$$

Substitution for $[A]$ into the integrated rate law gives equations that can be used to determine a k from measurements of I .

1.3.1 First-Order Irreversible System

A simple rearrangement of the previous solution for this system (Eq. (1.12)) and substitution for $[A]$ and $[A]_0$ from Eq. (1.49) and (1.50) gives

$$\ln \left(\frac{[A]}{[A]_0} \right) = \ln \left(\frac{I_t - I_\infty}{I_0 - I_\infty} \right) = -k_1 t \quad (1.52)$$

This shows that a plot of $\ln(I_t - I_\infty)$ versus t should be linear with a slope of $-k_1$. It is not necessary to know the concentration of A or any values of ϵ in order to determine the rate constant, but one does need I_∞ . Sometimes, it is impossible to measure I_∞ because of secondary reactions, or it is inconvenient because the reaction is slow. Such systems can be analyzed by nonlinear least-squares fitting of the data over as much of the reaction as possible, or in a more classical way by the Guggenheim method, described in more detail by Moore and Pearson³ (p 71), Mangelsdorf⁷ and Espenson⁸ (p 25).

1.3.2 Second-Order Irreversible System

The integrated rate law for this system is given by Eq. (1.37) which may be rewritten as

$$\ln \left(\frac{[B]_0 - b[A]_0}{[A]} + b \right) - \ln \left(\frac{[B]_0}{[A]_0} \right) = ([B]_0 - b[A]_0)k_2 t \quad (1.53)$$

Then, substitution for $[A]$ from Eq. (1.51) gives

$$\ln \left(\frac{[B]_0 - b[A]_0}{[A]_0} \left(\frac{I_0 - I_\infty}{I_t - I_\infty} \right) + b \right) - \ln \left(\frac{[B]_0}{[A]_0} \right) = ([B]_0 - b[A]_0)k_2 t \quad (1.54)$$

Therefore, a plot of the first term on the left-hand side versus t should be linear with a slope of $([B]_0 - b[A]_0)k_2$. Clearly in this case, it is necessary to know the stoichiometry coefficient, b , as well as the initial concentrations, $[B]_0$ and $[A]_0$, in order to determine k_2 . However, only b and the ratio of $[B]_0$ to $[A]_0$ are needed in order to make the plot.

1.4 COMPLEX RATE LAWS

It is not unusual for a rate law to be more complex than the simple zero-, first- or second-order cases we have considered. In general, the rate law has the following form:

$$-\frac{d[A]}{dt} = f([X], [Y], [Z])[A] = k_{\text{exp}}[A] \quad (1.55)$$

where $f([X], [Y], [Z])$ is some function of the concentrations of X, Y and Z.

In inorganic systems, the concentration dependence of k_{exp} can be quite complex, but some common forms of k_{exp} are

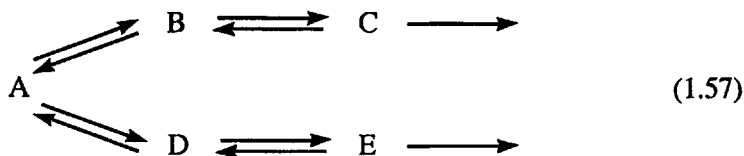
$$\begin{aligned} k_{\text{exp}} &= k'[X] & k_{\text{exp}} &= k' + k''[X] \\ k_{\text{exp}} &= \frac{k'[X]}{k'' + [Y]} & k_{\text{exp}} &= \frac{k'[Y] + k''}{k''' + [Z]} \end{aligned} \quad (1.56)$$

Most commonly, the dependence of k_{exp} on [X], [Y] and [Z] is determined from a series of kinetic experiments under pseudo-first-order conditions, keeping [Y] and [Z] constant and changing [X] to determine the dependence of k_{exp} on [X], and then repeating the process for [Y] and [Z]. In the case of H^+ , buffers can be used to keep its concentration constant during an experiment.

In many elementary considerations of kinetic data, it is suggested that the order of a reaction with respect to a particular reagent can be determined from a plot of the logarithm of the rate constant versus the logarithm of the reagent concentration. This procedure is only appropriate for simple forms, such as the first example in Eq. (1.56). Although log-log plots may appear linear for the more complex forms, the plots will yield meaningless fractional orders and should be avoided. Unfortunately, there is no truly general method of analysis to yield the reaction order, but this is seldom a serious problem when the reagent concentrations have been varied over a reasonable concentration range, using pseudo-first-order conditions (Section 1.2.6) or the initial rate method (Section 1.2.8).

1.5 COMPLEX KINETIC SYSTEMS

Sometimes, even under pseudo-first-order conditions, the kinetic observations do not obey the first-order integrated rate law. This may indicate a number of chemical problems, such as impurities, a nonlinear analytical method or precipitate formation. However, it is also possible that the system is more complex, with parallel and/or successive reactions, as shown in the following system:

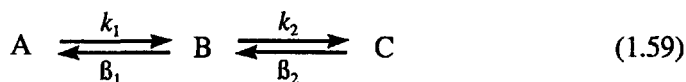


If pseudo-first-order conditions are maintained, it is always possible to solve the differential equations to determine the integrated rate law.^{9,10} The solution has the general form

$$[\text{Product}] = Me^{-\gamma_1 t} + Ne^{-\gamma_2 t} + \dots \quad (1.58)$$

where M, N, \dots and $\gamma_1, \gamma_2, \dots$ are constants that depend on the rate constants for the individual steps. The number of exponential terms equals the number of steps in the reaction network. For such systems, the time dependence of the concentration variable is usually fitted by nonlinear least squares to determine the constants. In practice, exceptionally good data are required to extract more than two γ values.

The following system of successive reactions is often encountered:



If one measures some property, I , that is directly proportional to concentration, then the integrated rate law predicts that the time dependence of I is given by

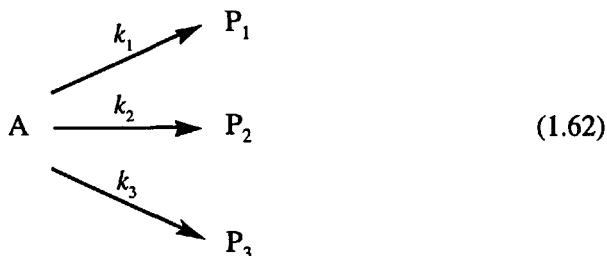
$$\begin{aligned}
 I = I_\infty + \left(\frac{1}{\gamma_2 - \gamma_1} \right) \times \\
 \{ [k_1(I_B - I_A) - \gamma_2(I_\infty - I_A)]e^{-\gamma_1 t} - [k_1(I_B - I_A) - \gamma_1(I_\infty - I_A)]e^{-\gamma_2 t} \}
 \end{aligned} \quad (1.60)$$

where I_A and I_B are the values of the property I for species A and B, respectively, I_∞ is the final value of I at "infinite time" and γ_1 and γ_2 are the apparent rate constants. The latter are related to the specific rate constants in reaction (1.59) by

$$\begin{aligned}
 \gamma_{1,2} = \frac{k_1 + \beta_1 + k_2 + \beta_2 \pm \\
 \sqrt{(k_1 + \beta_1 + k_2 + \beta_2)^2 - 4(k_1 k_2 + k_1 \beta_2 + \beta_1 \beta_2)}}{2}
 \end{aligned} \quad (1.61)$$

The form of Eq. (1.60) is useful for computer fitting procedures because one usually has some idea of reasonable values of I_A and I_B and an experimental value for I_∞ . The equation for simpler schemes in which either or both of the reverse rate constants are zero can be obtained by setting the appropriate terms in Eq. (1.61) equal to zero.

A somewhat simpler example of a system that proceeds by parallel paths to give different products is shown by the following:



The rate and integrated rate law are given by

$$-\frac{d[A]}{dt} = (k_1 + k_2 + k_3)[A] \quad (1.63)$$

and

$$[A] = [A]_0 e^{-(k_1 + k_2 + k_3)t} \quad (1.64)$$

In this case, the kinetics will determine $k_{\text{exp}} = (k_1 + k_2 + k_3)$. In order to evaluate the individual k_i values, it is necessary to determine the final product amounts, $[P_i]_{\infty}$, and use the relationship

$$[P_i]_{\infty} = \frac{k_i[A]_0}{k_1 + k_2 + k_3} \quad (1.65)$$

Such systems are discussed in more detail by Espenson⁸ (pp 55–56).

1.6 TEMPERATURE DEPENDENCE OF RATE CONSTANTS

To obtain information about the energetics of a reaction, the temperature dependence of the rate constant is determined. For complex rate laws, this also will involve a study of the concentration dependence of the rate at different temperatures, in order to determine the temperature dependence of the various terms contributing to the rate law. Once the experimental information is available for the specific rate constants, it is usually analyzed in terms of one of the following formalisms.

1.6.1 Arrhenius Equation

Arrhenius seems to have been the first to find empirically that rate constants have a temperature dependence analogous to that of equilibrium constants, given by

$$k = Ae^{-E_a/RT} \quad (1.66)$$

where A is the Arrhenius pre-exponential factor, E_a the Arrhenius activation energy, R the gas constant ($1.987 \text{ cal mol}^{-1} \text{ K}^{-1}$ or $8.314 \text{ J mol}^{-1} \text{ K}^{-1}$) and T the absolute temperature. The units of A will be those of k and

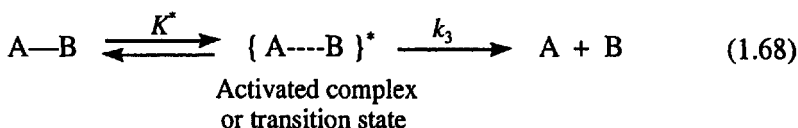
E_a will have the energy units of R . The k is determined by experiments at several temperatures, and the logarithmic form of Eq. (1.66) is

$$\ln k = \ln A - \frac{E_a}{RT} \quad (1.67)$$

which shows that a plot of $\ln k$ versus T^{-1} has a slope of $-E_a/R$. The rate constant is predicted to increase with increasing temperature. Typical values are 10 to 30 kcal mol⁻¹ for E_a and, if k is a first-order rate constant, 10¹⁰ to 10¹⁴ s⁻¹ for A . The Arrhenius equation is still widely used in certain areas of kinetics and for complex systems where the measured rate constant is thought to be a complex composite of specific rate constants.

1.6.2 Transition-State Theory

This theory was developed originally for a simple dissociation process in the gas phase and it assumes that the reaction can be described by the following sequence:



The theory proposes that the activated complex or transition state will proceed to products when the A—B bond has a thermal energy $k_B T$, so that the rate constant, k_3 , will be proportional to the bond's vibrational frequency, $\nu = k_B T/h$ s⁻¹, with a proportionality constant, κ , known as the transmission coefficient ($k_B \equiv$ Boltzmann's constant, 1.381×10⁻¹⁶ erg K⁻¹; $h \equiv$ Planck's constant, 6.626×10⁻²⁷ erg s). It also is assumed that the activated complex is always in equilibrium with the reactant with a normal equilibrium constant, $K^* = [A\cdots B]^*/[A-B]$, so that

$$\frac{d[B]}{dt} = k_3[A\cdots B]^* = k_3 K^*[A-B] = \kappa \frac{k_B T}{h} K^*[A-B] \quad (1.69)$$

and

$$\ln K^* = -\frac{\Delta G^\circ}{RT} = -\frac{\Delta H^\circ}{RT} + \frac{\Delta S^\circ}{R} \quad (1.70)$$

where ΔG° , ΔH° and ΔS° are the standard molar free energy, enthalpy and entropy differences, respectively, between the activated complex and the reactants.

If the first-order rate expression, $d[B]/dt = k_{\text{exp}}[A-B]$, is compared to Eq. (1.69), then substitution for K^* from Eq. (1.70) shows that

$$k_{\text{exp}} = \kappa \frac{k_B T}{h} K^* = \kappa \frac{k_B T}{h} e^{-\Delta G^\circ/RT} \quad (1.71)$$

Rearrangement and substitution from Eq. (1.70), along with the common assumption that $\kappa = 1$, gives the logarithmic form as

$$\ln\left(\frac{k_{\text{exp}}}{T}\right) = \ln\left(\frac{k_B}{h}\right) - \frac{\Delta H^{\circ*}}{RT} + \frac{\Delta S^{\circ*}}{R} \quad (1.72)$$

Therefore, a plot of $\ln(k_{\text{exp}}/T)$ versus T^{-1} should be linear with a slope of $-\Delta H^{\circ*}/R$. The value of $\Delta S^{\circ*}$, in $\text{cal mol}^{-1} \text{K}^{-1}$, can be calculated from a known value of k_{exp} at a particular T from

$$\Delta S^{\circ*} = 4.576\left\{\log\left(\frac{k_{\text{exp}}}{T}\right) - 10.319\right\} + \frac{\Delta H^{\circ*}}{T} \quad (1.73)$$

Commonly, the standard state designations are dropped and ΔH^* and ΔS^* are called the activation enthalpy and entropy, respectively. The Arrhenius parameters are related to ΔH^* and ΔS^* by the following relationships:

$$\Delta H^* = E_a - RT \quad \text{and} \quad \Delta S^* = 4.58(\log A - 13.2) \quad (1.74)$$

Results of Sargeson and co-workers¹¹ for the temperature dependence of the linkage isomerization of $(\text{H}_3\text{N})_5\text{Co}-\text{ONO}^{2+}$ to $(\text{H}_3\text{N})_5\text{Co}-\text{NO}_2^{2+}$ are shown in Figure 1.3.

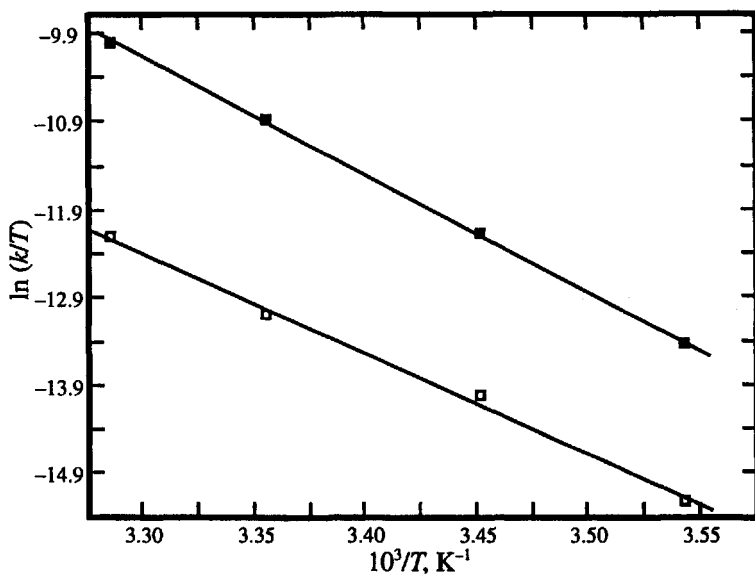


Figure 1.3. The temperature dependence of k for the linkage isomerization of $(\text{H}_3\text{N})_5\text{Co}-\text{ONO}^{2+}$ in alkaline solution: for k_{OH} (\blacksquare , $\Delta H^* = 110 \text{ kJ mol}^{-1}$) and for $10 \times k_s$ (\blacksquare , $\Delta H^* = 95 \text{ kJ mol}^{-1}$).

The rate law for the reaction in alkaline solution under pseudo-first-order conditions shows a spontaneous path, k_s , and an OH^- -catalyzed path, k_{OH} . The ΔH^\ddagger is somewhat higher for the k_{OH} path, as indicated by the steeper slope in Figure 1.3.

The transition-state theory parameters are used commonly to describe the temperature dependence of k_{exp} even for processes in solution that are far more complex than assumed in the original formulation of the theory. If $\kappa \neq 1$, its true magnitude is included in ΔS^\ddagger . It seems best to consider ΔH^\ddagger and ΔS^\ddagger as experimental parameters that are useful for calculating k_{exp} at other temperatures and for comparisons of closely related systems. Lente et al.¹² have discussed common misconceptions about the reliability and numerical precision of experimental ΔS^\ddagger values.

Within transition-state theory, reactions are often depicted in terms of "reaction coordinate diagrams". These are plots of the energy of the system versus the "reaction coordinate", which is an ambiguous measure of the extent to which reactant has been converted to product. Examples of such diagrams are shown in Figure 1.4. In the Figure, ΔH is the energy function, but ΔG or $T\Delta S$ also could be used, in which case the energy difference between the transition state and the reactant state would be ΔG^\ddagger or $T\Delta S^\ddagger$, respectively.

The *transition state* (or activated complex) is the species at the highest energy point on the reaction coordinate diagram. The full rate law will involve all species necessary to form the transition state. An *intermediate* is the species present at any valley on a reaction coordinate diagram. When a valley is shallow, it can be ambiguous whether or not an intermediate really is formed. In chemistry, an intermediate is expected to have a lifetime longer than a few vibrational lifetimes ($>10^{-13}$ s) and the valley should be deeper than the thermal energy ($RT = 2.5 \text{ kJ mol}^{-1}$ at 25°C).

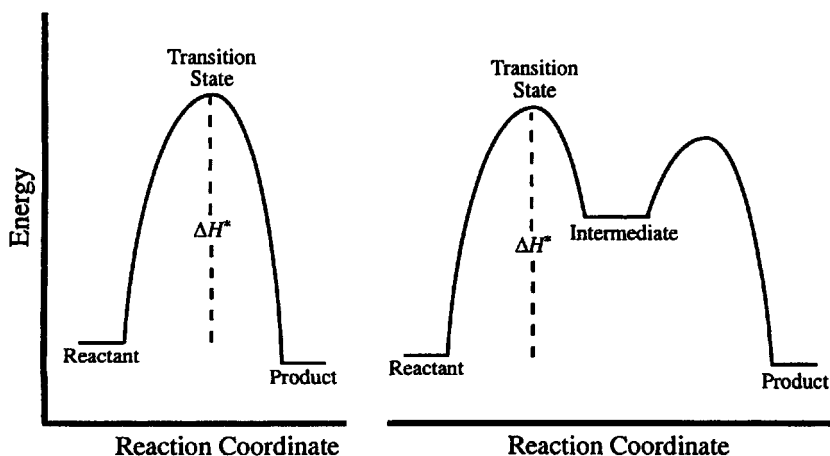


Figure 1.4. Reaction coordinate diagrams.

1.7 PRESSURE DEPENDENCE OF RATE CONSTANTS

It is possible to measure the rate of a reaction at various applied pressures and determine the variation of k with P . In recent years, such measurements have become increasingly widespread for a variety of inorganic reactions, and the interpretation of the pressure dependence adds a further tool to the arsenal of parameters available for mechanistic interpretations. The recommended units of pressure are megapascals, MPa, (1 atm = 0.1013 MPa = 1.013 bar).

The variation of K with P is given by the van't Hoff equation:

$$\left(\frac{\delta \ln K}{\delta P}\right)_T = -\frac{\Delta V^\circ}{RT} \quad (1.75)$$

where ΔV° is the difference in the partial molar volume between the products and reactants. Since $K = k_1/k_{-1}$, it is logical to express the variation of k_1 with P by

$$\left(\frac{\delta \ln k_1}{\delta P}\right)_T = -\frac{\Delta V_1^*}{RT} \quad (1.76)$$

where ΔV_1^* is defined as the volume of activation for the forward step and is equal to the partial molar volume of the transition state minus the partial molar volume of the reactant(s). If ΔV_1^* is independent of pressure, then integration of Eq. (1.76) at constant temperature over the limits $P = 0$ to P and $k_1 = (k_1)_0$ to k_1 gives

$$\ln k_1 = \ln (k_1)_0 - \frac{\Delta V_1^* P}{RT} \quad (1.77)$$

and a plot of $\ln k_1$ versus P should be linear with a slope of $-\Delta V_1^*/RT$. Since these studies usually cover pressures up to several thousand atmospheres, $\ln (k_1)_0$ is taken as the value at ambient pressure. If the plot is not linear, it is assumed that the reactant and/or transition state may be compressible and their volumes as a function of pressure can be described by

$$\Delta V_1^* = (\Delta V_1^*)_0 - \Delta \beta^* P \quad (1.78)$$

where $\Delta \beta^*$ represents the compressibility of the system. Substitution of Eq. (1.78) into Eq. (1.76) and integration over the same limits yields

$$\ln k_1 = \ln (k_1)_0 - \frac{(\Delta V_1^*)_0 P}{RT} + \frac{\Delta \beta^* P^2}{2RT} \quad (1.79)$$

More complex explanations of nonlinearity also are possible.¹³

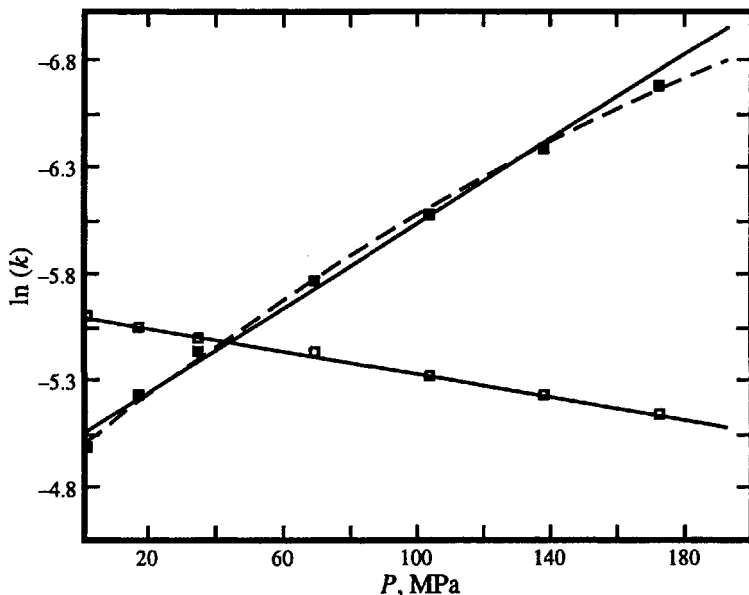


Figure 1.5. The pressure dependence of k for the linkage isomerization of $(\text{H}_3\text{N})_5\text{Co—ONO}^{2+}$ in alkaline solution: for $10^2 \times k_s$ (\square , $\Delta V^\ddagger = -6.6 \text{ cm}^3 \text{ mol}^{-1}$) and for k_{OH} (\circ , $\Delta V^\ddagger = 29.5 \text{ cm}^3 \text{ mol}^{-1}$, $\Delta\beta^\ddagger = 0.05 \text{ cm}^3 \text{ MPa}^{-1} \text{ mol}^{-1}$).

Results for the pressure dependence of the linkage isomerization of $(\text{H}_3\text{N})_5\text{Co—ONO}^{2+}$ are shown in Figure 1.5. For the pathway catalysed by OH^- , k_{OH} , the authors¹¹ have ascribed the slight curvature of the plot to the effect of compressibility with $\Delta\beta^\ddagger = 0.05 \text{ cm}^3 \text{ MPa}^{-1} \text{ mol}^{-1}$. The difference between the upper straight line and the dashed curve shows the extent of the deviation from linearity.

The density and viscosity of liquids normally increase with increasing pressure and decrease with increasing temperature. For water, these properties change much less than for most other solvents.

The density change affects molar concentrations and should be taken into account, except for first-order kinetics. In practice, this is rarely done because the density change over normal pressure and temperature ranges often is small relative to other errors.

As the viscosity of a solvent increases, the diffusion coefficients of species dissolved in the solvent decrease. Therefore, the rates of processes that are at or near the diffusion-controlled limit will decrease and this will appear as a positive contribution to ΔV^\ddagger or a positive contribution to ΔH^\ddagger . The solvent's viscosity can influence the rates of rearrangements within intermediates and thereby affect the products of the reaction. This effect has been exploited in recent years by Trofimov and co-workers¹⁴ to elucidate reaction pathways in several organic reactions, and is the basis of

the “cage effect” which sometimes is used in photochemistry to control the lifetime of the immediate products of photochemically induced dissociation. However, changes in the solvent can affect reactivity for reasons other than just the change in viscosity.

Jonas and co-workers¹⁵⁻¹⁷ reported somewhat unusual pressure effects in several systems in which the rate constant first increased and then decreased with increasing pressure. Representative results¹⁷ for the rotation of ethylene in $(\eta^5\text{-C}_3\text{H}_5)(\text{C}_2\text{F}_4)\text{Rh}(\text{C}_2\text{H}_4)$ are shown in Figure 1.6. These effects were related to the solvent viscosity through its effect on the efficiency of energy transfer from the solvent to the reacting solute.¹⁸ The efficiency increases with increasing pressure until the solvent-solvent interactions become dominant, at which point the diffusion of solvent towards the solute becomes a controlling factor. The energy transfer affects the rate constant by changing the transmission coefficient, κ , in Eq. (1.71) from transition-state theory.

In recent years, there has been an extended controversy about the effect of solvent viscosity on reaction rates that are much below the diffusion-controlled limit. In 1999, Swiss and Firestone¹⁹ used a series of hydrocarbon solvents to study the dimerization of cyclopentadiene and the 1,3-dipolar cycloaddition of diphenyl-diazomethane to ethyl phenylpropiolate. In both cases, the rate constant seemed to increase as the solvent's viscosity increased to ~ 1.5 cp, and then decreased at

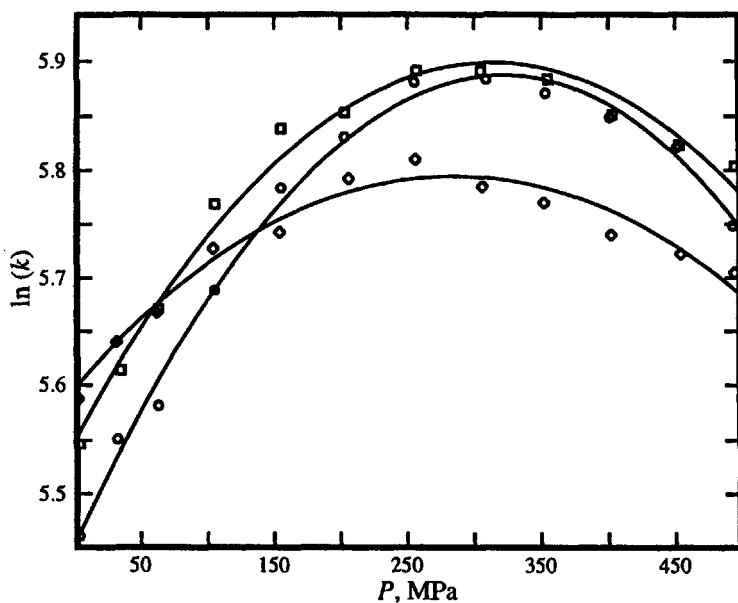


Figure 1.6. The pressure dependence of k at 0°C for the rotation of ethylene in $(\eta^5\text{-C}_3\text{H}_5)(\text{C}_2\text{F}_4)\text{Rh}(\text{C}_2\text{H}_4)$ in: (●) methylcyclohexane, (○) n-pentane, (□) CS_2 .

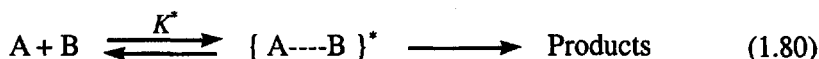
higher viscosities. The authors noted the implications for pressure induced viscosity changes on the interpretation of ΔV^\ddagger values. The experimental results of both these systems have been criticized by Weber and van Eldik,²⁰ and by Hamann and le Noble,²¹ respectively. Firestone and Swiss have questioned²² the chemical integrity in the new experiments by Weber and van Eldik on cyclopentadiene, but acknowledge²³ that Hamann and le Noble's reanalysis is correct and that there is no viscosity effect for the diphenyl-diazomethane reaction. In the meantime, Kumar and Deshpande²⁴ examined the viscosity dependence of the rates and products of thirteen earlier studies on similar reactions and repeated some experiments. Although these thirteen studies cover a range of solvents with many different properties, Kumar and Deshpande focused on the viscosity dependence and generally found a maximum in the product ratios and rate constants between 0.8 and 1 cp. Other workers²⁵ have tended to rationalize such results in terms of solvent polarity effects.

At this point, it is unclear what types of reactions are affected by viscosity, aside from diffusion-controlled reactions. To either detect or minimize viscosity effects in pressure studies, it is helpful to know how the viscosity varies with pressure. There is very little effect of pressure on the viscosity of water,²⁶ and the variation is modest in methanol²⁷ but more substantial in 2-propanol.²⁶ For hydrocarbon solvents, such as cyclohexane,²⁸ *n*-decane and *n*-tetradecane,²⁹ the variation is nearly the same, but larger than for the others mentioned.

1.8 IONIC STRENGTH DEPENDENCE OF RATE CONSTANTS

For reactions of ions in solution, the variation of the activity coefficients with reagent concentrations is sometimes ignored or, more commonly, assumed to be held constant by carrying out the reaction in the presence of some "inert electrolyte" which is at a much higher concentration than that of the reactants.

The kinetic effect of ionic strength can be illustrated for a bimolecular reaction of the following type:



for which transition-state theory predicts that the rate is given by

$$\text{Rate} = \left(\frac{k_B T}{h}\right) K^\ddagger \left(\frac{\gamma_A \gamma_B}{\gamma^\ddagger}\right) [A][B] = k[A][B] \quad (1.81)$$

where γ_A , γ_B and γ^\ddagger are the activity coefficients of the reactants and transition state, respectively. At infinite dilution (zero ionic strength), the activity coefficients are equal to 1 and the rate constant is defined as k_0 .

Therefore

$$k = \left(\frac{\gamma_A \gamma_B}{\gamma^*} \right) k_0 \quad (1.82)$$

The simplest relationship between the activity coefficients, γ_i , and the ionic strength, μ , is given by the Debye–Hückel limiting law, which applies for $\mu \leq 0.01$ M:

$$\log \gamma_i = -A z_i^2 \sqrt{\mu} \quad (1.83)$$

where A is a constant for a given solvent ($A = 0.509 \text{ M}^{-1/2}$ for water at 25°C) and z_i is the charge of the ion. Using this limiting law, and realizing that $z^* = z_A + z_B$, it follows from Eq. (1.82) and (1.83) that

$$\log k = \log k_0 + 2A z_A z_B \sqrt{\mu} \quad (1.84)$$

and a plot of $\log k$ versus $\sqrt{\mu}$ should be linear with a slope of $2A z_A z_B$.

Many kinetic studies are done at ionic strengths beyond the range of applicability of the Debye–Hückel limiting law. The law was extended by Debye and Hückel to take into account the finite size of the ions to give the following relationship, that is applicable for $\mu < 0.1$ M:

$$\log k = \log k_0 + \frac{2A z_A z_B \sqrt{\mu}}{1 + \alpha B \sqrt{\mu}} \quad (1.85)$$

where α is the average effective diameter of the ions and B is a constant depending on the solvent properties ($B = 0.328 \text{ \AA}^{-1} \text{ M}^{-1/2}$ for water at 25°C). Values of α for various ions in water have been tabulated by Klotz.³⁰ Empirical equations have been developed for higher ionic strengths; an example is the Davies equation,³¹ for $\mu \leq 0.5$ M.

The ionic strength dependence of k is essentially a property of the rate law. Therefore, the ionic strength dependence seldom affords new mechanistic information unless the complete rate law cannot be determined. These equations more often are used to "correct" rate constants from one ionic strength to another for the purpose of rate constant comparison. Ionic strength effects have been used to estimate the charge at the active site in large biomolecules, but the theory is substantially changed³² because the size of the biomolecule violates basic assumptions of Debye–Hückel theory.

1.9 DIFFUSION-CONTROLLED RATE CONSTANTS

The upper limit on a rate constant for a reaction is imposed by the rate at which the reactants can diffuse together. This limit can be of significance when a particular mechanism would require a rate constant beyond the

diffusion-controlled limit; then, the mechanism can be eliminated as a reasonable possibility. In addition, certain classes of reactions are known to proceed at or near diffusion-controlled rates, and this information can be useful in constructing and analyzing mechanistic models.

If two reactants A and B with radii r_A and r_B , respectively, diffuse together and react at an interaction distance ($r_A + r_B$), then theories developed from Brownian motion predict that the diffusion-controlled second-order rate constant is given by

$$k_{\text{diff}} = \frac{4\pi N(D_A + D_B)(r_A + r_B)}{1000} \left(\frac{U}{e^U - 1} \right) \quad (1.86)$$

where

$$U = \frac{z_A z_B e^2}{4\pi \epsilon_0 \epsilon (r_A + r_B) k_B T}$$

N is Avogadro's number, D_A and D_B are the diffusion coefficients for A and B, respectively, z_A and z_B are their respective charges, e is the electron charge (1.602×10^{-19} C), ϵ is the dielectric constant of the solvent, ϵ_0 is the vacuum permittivity ($4\pi \epsilon_0 = 1.113 \times 10^{-12}$) and k_B is Boltzmann's constant (1.381×10^{-23} J K⁻¹). If one or both of the species are neutral, then $U = 0$ and the right-hand term in brackets in Eq. (1.86) equals 1.

Diffusion coefficients can be approximated from the Stokes–Einstein equation, $D = k_B T / 6\pi\eta r$, where $k_B = 1.381 \times 10^{-16}$ erg K⁻¹, η is the solvent viscosity and r is the radius of the species, so that

$$k_{\text{diff}} = \frac{2RT(r_A + r_B)^2}{3000\eta r_A r_B} \left(\frac{U}{e^U - 1} \right) \quad (1.87)$$

with $R = 8.314 \times 10^7$ erg mol⁻¹ K⁻¹, r in cm and η in poise. This equation shows that k_{diff} will be relatively independent of the size of the reactants, as long as $r_A \approx r_B$, and its magnitude will depend inversely on the solvent viscosity. The temperature dependence of k_{diff} will be governed largely by that of the solvent viscosity, so that apparent activation energies for diffusion-controlled processes are found to be in the 1 to 3 kcal mol⁻¹ range for common solvents. It should be noted that the Stokes–Einstein equation greatly underestimates the diffusion coefficients of the proton and hydroxide ions in water.

One can estimate k_{diff} from Eq. (1.87) without knowing the diffusion coefficients. Some values for various reactant sizes and charge products in water ($\eta = 0.00894$ poise, $\epsilon = 78.3$), are given in Table 1.1. It is apparent from these data that diffusion-controlled rate constants in water can be expected to be in the range of 10^9 to 10^{10} M⁻¹ s⁻¹. For a solvent with $\epsilon = 20$, k_{diff} is ~5 times larger for $z_A z_B < 0$ and smaller for $z_A z_B > 0$.

Table 1.1. Estimated Diffusion-Controlled Rate Constants (25°C) in Water

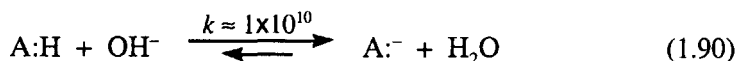
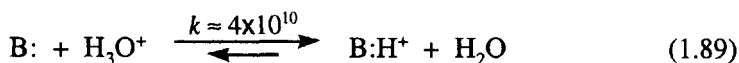
$r_A = 5.0$ (Å) $z_A z_B$	$r_B = 2.0$ (Å)	$r_B = 5.0$ (Å) $k_{\text{diff}} (\text{M}^{-1} \text{s}^{-1})$	$r_B = 8.0$ (Å)
-2	8.54×10^9	14.0×10^9	20.7×10^9
-1	5.81×10^9	10.4×10^9	16.3×10^9
0	3.64×10^9	7.42×10^9	12.5×10^9
+1	2.09×10^9	5.03×10^9	9.40×10^9
+2	1.11×10^9	3.34×10^9	6.68×10^9

For a unimolecular dissociation, such as A—B forming A + B, the rate is controlled by the diffusion of the products out of the solvent cage. Theory predicts that the limiting dissociation rate constant is given by

$$k_{\text{diff}} = \frac{3(D_A + D_B)}{(r_A + r_B)^2} \left(\frac{U}{1 - e^{-U}} \right) \quad (1.88)$$

that can be further simplified using the Stokes–Einstein equation. The predicted unimolecular dissociation rate constants (s^{-1}) are of the same magnitude as the bimolecular constants in Table 1.1.

The most important general class of reactions that have diffusion-controlled rates in water are protonation of a base by H_3O^+ and deprotonation of an acid by OH^- , as shown in the following reactions, with rate constants at 25°C in $\text{M}^{-1} \text{s}^{-1}$:



These results stem from the pioneering work of Eigen and co-workers.³³ The reverse rate constants for these reactions can be calculated from the equilibrium constants that are known for a wide range of such acids and bases. It is important to note that the reverse rate constants may not be extremely large. For example, trimethylamine is a strong base with a protonation rate constant of $6 \times 10^{10} \text{ M}^{-1} \text{ s}^{-1}$, but the acid dissociation constant of the trimethylammonium ion is $1.6 \times 10^{-10} \text{ M}$. Therefore, the rate constant for deprotonation by water is $(6 \times 10^{10})(1.6 \times 10^{-10}) \approx 10 \text{ s}^{-1}$.

The main exceptions to the preceding generalizations are so-called carbon acids, such as nitromethane or acetylacetone, for which the rate constants are usually much smaller and dependent on the nature of the acid.³⁴ Such reactions are thought to be slower because of the bonding

rearrangements required at the carbon center as the conjugate base is formed. The same constraint may apply to the deprotonation of organometallic hydrides.

1.10 MOLECULAR MODELING AND THEORY

For years chemists have built models as an aid to visualizing molecules and to help in understanding reactivity patterns. The advent of the desktop computer provided the opportunity to easily create three-dimensional pictures of molecules that could be rotated freely in space, and these have gradually replaced the old ball and stick models. This type of modeling is capable of providing an indication of the effects of steric interactions on reactivity, but gives no measure of the actual energetics of the reaction.

More recently, modeling of reactions has become the serious business of theoreticians and computational chemists. The theory takes the further step of providing the reaction energetics for various proposed reaction pathways. This allows for the selection between mechanisms on the basis of the predicted lowest energy pathway. This area has grown enormously in the past few years, largely due to the introduction of Density Functional Theory (DFT). It is now common to find an experimental kinetic study supported by a theoretical analysis, as well as many purely theoretical papers. As with experiments, the theoretical treatment is driven by practical considerations and inevitably contains assumptions that affect the reliability of the results. Some assumptions, such as simplification of the chemical system (e.g. $\text{P}(\text{CH}_3)_3$ replaced by PH_3) are easy to assess because of their steric consequences. However, more esoteric assumptions about basis sets and electron correlation effects remain difficult for the non-specialist to evaluate, in part because of the sea of alphabet soup that seems to dominate the theoretical discussions. Some insight into these acronyms and the strengths and weaknesses of various treatments in inorganic systems are provided in reviews by Niu and Hall,³⁵ Ziegler³⁶ and Poli and Harvey.³⁷ The WEB site Computational Chemistry Archives³⁸ provides translations of many acronyms and general information on the strengths and weaknesses of various methods.

Quantum mechanics (QM) calculations commonly produce potential energy surfaces for reactions at 0°K. In recent years, there has been an increasing effort to include entropy effects in the models, through a combination of QM and molecular mechanics (MM) methods, and thereby to calculate free energy surfaces at a particular temperature. Examples of the calculated entropic effects in inorganic systems can be found in the work of Ziegler and co-workers.³⁹

Finally, it should be noted that theoretical predictions are not necessarily unequivocal. They have some dependence on the methodology and interpretation, just like any experimental result. The only conditions that the experimental kineticist can impose are that the theory must predict the

correct rate law and a reasonable approximation to the energetics, as determined from the temperature dependence of the rate.

References

1. Levine, I. N. *Physical Chemistry*, 3rd ed.; McGraw-Hill: New York, 1988.
2. Atkins, P. W.; de Paula, J. *Physical Chemistry*, 7th ed.; Freeman: New York, 2002.
3. Moore, J. W.; Pearson, R. G. *Kinetics and Mechanism*, 3rd ed.; Wiley-Interscience: New York, 1980.
4. Laidler, K. J. *Chemical Kinetics*, 3rd ed.; Harper & Row: New York, 1987.
5. Pilling, M. J.; Seakins, P. W. *Reaction Kinetics*; Oxford University Press: Oxford, 1995.
6. *Comprehensive Chemical Kinetics*; Bamford, C. H.; Tipper, C. F. H., Eds.; Elsevier: Amsterdam, 1969; Vol. 1, 2.
7. Mangelsdorf, P. C. *J. Appl. Phys.* **1959**, *30*, 443.
8. Espenson, J. E. *Chemical Kinetics and Reaction Mechanisms*; McGraw-Hill: New York, 1981.
9. Rodiguin, N. M.; Rodiguina, E. N. *Consecutive Chemical Reactions*, English Ed., translated by R. F. Schneider; Van Nostrand: Princeton, N.J., 1969.
10. Capellos, C.; Bielski, B. H. *Kinetic Systems*; McGraw-Hill: New York, 1972.
11. Jackson, W. G.; Lawrance, G. A.; Lay, P. A.; Sargeson, A. M. *Inorg. Chem.* **1980**, *19*, 904.
12. Lente, G.; Fábíán, I.; Poč, A. J. *New. J. Chem.* **2005**, *29*, 759.
13. Asano, T.; le Noble, W. J. *Chem. Rev.* **1978**, *78*, 407.
14. Adam, W.; Trofimov, A. V. *Acct. Chem. Res.* **2003**, *36*, 571.
15. Hasha, D. L.; Eguchi, T.; Jonas, J. *J. Am. Chem. Soc.* **1982**, *72*, 5019.
16. Xie, C.-L.; Campbell, D.; Jonas, J. *J. Chem. Phys.* **1988**, *88*, 3396.
17. Peng, X.; Jonas, J. *J. Chem. Phys.* **1990**, *93*, 2192.
18. Kramers, H. A. *Physica (Amsterdam)* **1940**, *7*, 284; Grote, R. F.; Hynes, J. T. *J. Chem. Phys.* **1980**, *73*, 2715; Nadler, W.; Marcus, R. A. *J. Chem. Phys.* **1987**, *86*, 3906; Basilevsky, M. V.; Ryaboy, V. M.; Weinberg, N. N. *J. Phys. Chem.* **1991**, *95*, 5533.
19. Swiss, R. A.; Firestone, R. F. *J. Phys. Chem. A* **1999**, *103*, 5369.
20. Weber, C. F.; van Eldik, R. *J. Phys. Chem. A* **2002**, *106*, 6904.
21. Hamann, S. D.; le Noble, W. J. *J. Phys. Chem. A* **2004**, *108*, 7121.
22. Firestone, R. A.; Swiss, K. A. *J. Phys. Chem. A* **2002**, *106*, 6909.
23. Firestone, R. A.; Swiss, K. A. *J. Phys. Chem. A* **2004**, *108*, 7124.
24. Kumar, A.; Deshpande, S. S. *J. Org. Chem.* **2003**, *68*, 5411.
25. Berson, J. A.; Hamlet, Z.; Mueller, W. A. *J. Am. Chem. Soc.* **1962**, *84*, 297; Cativiela, C.; Garcia, J. I.; Mayoral, J. A.; Salvatella, L. *J. Chem. Soc., Perkin Trans. 2* **1994**, 847; Ohkata, K.; Tamura, Y.; Shetuni, B. B.; Takagi, R.; Miyanaga, W.; Kojima, S.; Paquette, L. A. *J. Am. Chem. Soc.* **2004**, *126*, 16783.
26. Moha-Ouchane, M.; Boned, C.; Allal, A.; Benseddik, M. *Int. J. Thermophys.* **1998**, *19*, 161.

27. Papaioannou, D.; Bridakis, M.; Panayiotou, C. D. *J. Chem. Eng. Data* **1993**, *38*, 370.
28. Stephan, K.; Lucas, K. *Viscosity of Dense Fluids*; Plenum Press: New York, 1979.
29. Ducoulombier, D.; Zhou, H.; Boned, C.; Peyrelasse, J.; Saint-Guirons, H.; Xans, P. *J. Phys. Chem.* **1986**, *90*, 1692.
30. Klotz, I. *Chemical Thermodynamics*; Prentice-Hall: New York, 1950; pp 330–331.
31. Davies, C. W. *Prog. React. Kin.* **1961**, *1*, 129.
32. Rosenberg, R. C.; Wherland, S.; Holwerda, R. A.; Gray, H. B. *J. Am. Chem. Soc.* **1976**, *98*, 6364.
33. Eigen, M. *Angew. Chem. Int. Ed.* **1964**, *3*, 1.
34. Alberty, W. J.; Bernasconi, C. F.; Kresge, A. J. *J. Phys. Org. Chem.* **1988**, *1*, 29; Bernasconi, C. F.; Ni, J. X. *J. Org. Chem.* **1994**, *59*, 4910; Saunders, W. H., Jr.; Van Vert, J. E. *J. Org. Chem.* **1995**, *60*, 3452.
35. Niu, S.; Hall, M. B. *Chem. Rev.* **2000**, *100*, 353.
36. Ziegler, T. *J. Chem. Soc., Dalton Trans.* **2002**, 642.
37. Poli, R.; Harvey, J. N. *Chem. Soc. Rev.* **2003**, *32*, 1.
38. <http://ccl.osc.edu/ccl/cca.html>
39. Woo, T. K.; Blöchl, P. E.; Ziegler, T. *J. Phys. Chem A* **2000**, *104*, 121; Yang, S.-Y.; Hristov, I.; Fleurat-Lessard, P.; Ziegler, T. *J. Phys. Chem. A* **2005**, *109*, 197.

2

Rate Law and Mechanism

Once the experimental rate law has been established, the next step is to formulate a mechanism that is consistent with the rate law. The rate law will not uniquely define the mechanism but will limit the possibilities. The proposed mechanism will lead to predictions of trends in reactivity and other types of experiments that can be done to test the proposal. These aspects will be described in later chapters for specific types of reactions.

Except for the simplest cases, the development of the rate law from the mechanism can be a messy exercise. The following sections describe some of the assumptions and tricks that can be used. Further discussions can be found in standard textbooks on kinetics.¹⁻³

2.1 QUALITATIVE GUIDELINES

The problem is to determine the most reasonable mechanism(s) which will predict a rate law that is consistent with the observations. Very often this is done by analogy to previous studies on related systems, but there are some general guidelines that can be useful for writing a mechanism that will produce the desired form of the rate law.

The mechanism is composed of elementary reactions whose rate laws are implied from the stoichiometry of each reaction. The elementary mechanistic steps are usually unimolecular or bimolecular reactions; termolecular reactions are very rare because of the improbability of bringing three species together.

The form of the experimental rate law provides some guidelines for the construction of a mechanism. The following generalizations assume that the reaction is monophasic, but they may apply to individual steps in a multiphasic reaction. It also should be remembered that the experimental rate law may be incomplete because of experimental constraints. Then, the predicted rate law may contain terms not observed experimentally, but it should be possible to show that the extra terms are minor contributors under the conditions of the experiment.

For the simplest cases, in which rate = $k_{\text{exp}}[A][B]$ or rate = $k_{\text{exp}}[A]$, the kinetics only requires a one step mechanism involving the species in the rate law. In the second case, the solvent also may be involved because its concentration will be constant and may be included in k_{exp} .

If the rate law has a half-order term, such as $[A]^{1/2}$, then the mechanism probably involves a step in which A is split into two reactive species before the rate-determining step.

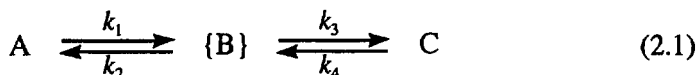
If $\text{rate} = k_{\text{exp}}[A][B][C]^{-1}$, then a mechanism in which C is produced from A and B prior to the rate-determining step will generate such a rate law. If there is a denominator in the rate law that consists of the sum of several terms, then the mechanism may involve consecutive steps that produce reactive intermediates.

If the rate is the sum of several terms, such as $k_{\text{exp}}[A] + k'_{\text{exp}}[A][B]$, then a number of parallel reaction pathways equal to the number of terms in the sum will predict the experimental rate law. This is commonly found for reactions that have pathways catalyzed by acid and/or base.

Once the general outline of the mechanism is established, it is necessary to show that the proposal does give the required rate law. The following sections describe common methods for deriving the rate law from the mechanism.

2.2 STEADY-STATE APPROXIMATION

A mechanism often invokes an unstable intermediate of some defined structure, and a general mechanism might take the form of



where B is an unstable and therefore reactive intermediate. The steady-state approximation assumes that this intermediate will disappear as quickly as it is formed

$$\text{Rate of Appearance of B} = \text{Rate of Disappearance of B} \quad (2.2)$$

so that

$$k_1[A] + k_4[C] = k_2[B] + k_3[B] \quad (2.3)$$

With Eq. (2.3), one can solve for [B] in terms of the reactant and product concentrations, [A] and [C], respectively, to give

$$[B] = \frac{k_1[A] + k_4[C]}{k_2 + k_3} \quad (2.4)$$

The total concentration of reagents can be defined as [T] and will remain constant. Since B is a reactive intermediate, its concentration will always

be small relative to $[A] + [C]$, so that

$$[T] = [A] + [B] + [C] = [A] + [C] \quad (2.5)$$

Substitution for $[C]$ from Eq. (2.5) into Eq. (2.4) gives

$$[B] = \frac{k_1[A] + k_4[T] - k_4[A]}{k_2 + k_3} \quad (2.6)$$

The rate of disappearance of A is given as follows (note that the mechanism has specified that all the steps have first-order or pseudo-first-order rate constants):

$$-\frac{d[A]}{dt} = k_1[A] - k_2[B] = \frac{k_1k_3 + k_2k_4}{k_2 + k_3}[A] - \frac{k_2k_4}{k_2 + k_3}[T] \quad (2.7)$$

where the steady-state expression for $[B]$ has been used to eliminate $[B]$ from the differential equation. This gives a form that can be integrated because $[A]$ is the only concentration variable. However, instead of integrating at this point, it is useful to introduce the equilibrium (final) concentrations, $[A]_e$ and $[C]_e$, through

$$[T] = [A]_e + [C]_e \quad (2.8)$$

and the equilibrium condition

$$K_e = \frac{[C]_e}{[A]_e} = \frac{k_1k_3}{k_2k_4} \quad (2.9)$$

Substitution for $[C]_e$ from Eq. (2.9) into Eq. (2.8) and rearranging gives

$$[T] = \frac{k_1k_3 + k_2k_4}{k_2k_4}[A]_e \quad (2.10)$$

Substitution for $[T]$ from Eq. (2.10) into Eq. (2.7) yields

$$-\frac{d[A]}{dt} = \frac{k_1k_3 + k_2k_4}{k_2 + k_3}([A] - [A]_e) \quad (2.11)$$

which is the mathematical equivalent of the first-order rate law and can be integrated directly to obtain

$$-\ln([A]_e - [A]) + \ln([A]_e - [A]_0) = k_{\text{exp}}t \quad (2.12)$$

where

$$k_{\text{exp}} = \frac{k_1 k_3 + k_2 k_4}{k_2 + k_3} \quad (2.13)$$

Note that the right-hand side of Eq. (2.13) is the same as the coefficient for [A] on the right-hand side of Eq. (2.7). Therefore, it really was not necessary to go through the equilibrium conditions in order to find the expression for k_{exp} . *It is always true that once one has an integratable equation with only one concentration variable in first-order form, then the coefficient of the concentration variable in that equation will be the expression for k_{exp} .*

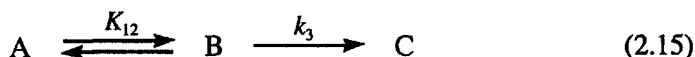
A limiting form of Eq. (2.13) that is often encountered assumes that $k_2 \gg k_3$. Then, the k_{exp} is given by

$$k_{\text{exp}} = \left(\frac{k_1}{k_2}\right)k_3 + k_4 = K_{12}k_3 + k_4 \quad (2.14)$$

The steady-state approximation can be applied to systems with any number of reactive intermediates. King and Altman⁴ have presented a general development for k_{exp} in steady-state systems that is very useful for complex reaction networks.

2.3 RAPID-EQUILIBRIUM ASSUMPTION

The rapid-equilibrium treatment assumes that the reactants are part of a rapidly attained equilibrium that is always maintained during the course of the reaction, as shown by



where B is not a reactive intermediate but a species with a finite concentration. For example, B might be the conjugate base of A, an isomer of A or an ion pair. Either A or B may be the species actually added to start the reaction. Since B may be present at significant concentrations, the total concentration of the species in equilibrium with each other can be defined as [R] and is given by

$$[R] = [A] + [B] \quad (2.16)$$

Since [T] = [A] + [B] + [C], it follows that

$$[R] = [T] - [C] \quad (2.17)$$

Normally, one will know [R] but not [A] or [B], unless K_{12} is known.

The rate of formation of C is easily written down as

$$\frac{d[C]}{dt} = k_3[B] \quad (2.18)$$

and the problem is to express [B] in terms of [C], in order to obtain an equation that can be integrated. A useful trick can be used to get an expression for the concentration of one of the partners in the equilibrium, [B], in terms of the total concentration of the species involved in the equilibrium, [R]. Since $K_{12} = [B]/[A]$, then

$$\frac{1}{K_{12}} + 1 = \frac{[A] + [B]}{[B]} = \frac{[R]}{[B]} \quad (2.19)$$

Rearrangement and substitution for [R] from Eq. (2.17) into Eq. (2.19) gives

$$[B] = \frac{[R]K_{12}}{K_{12} + 1} = \frac{([T] - [C])K_{12}}{K_{12} + 1} \quad (2.20)$$

Substitution for [B] into Eq. (2.18) yields an equation with only [C] as the concentration variable

$$\frac{d[C]}{dt} = \frac{k_3 K_{12}}{K_{12} + 1} ([T] - [C]) \quad (2.21)$$

This equation has the same form as Eq. (2.11) and can be integrated to give an analogous result. But, as noted in the preceding section, it is simpler to recognize that k_{exp} can be obtained directly from the coefficient of [C] as

$$k_{\text{exp}} = \frac{k_3 K_{12}}{K_{12} + 1} \quad (2.22)$$

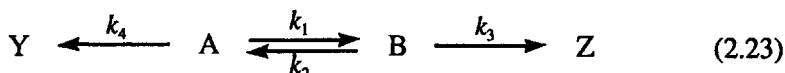
The expression for k_{exp} may be compared to that derived from the steady-state assumption under the condition that $k_2 \gg k_3$. The k_4 is missing in the present example because we have assumed an irreversible model, but otherwise the steady-state and equilibrium models are the same if $K_{12} \ll 1$ (in which case the concentration of B is small).

The preceding discussion can leave the incorrect impression that B is like a particularly stable intermediate on the reaction pathway from A to C. A somewhat different perspective is gained if one views B as the starting material and A as some unreactive form of B. This situation produces the same rate law as Eq. (2.21). The important general lesson is that *all rapid equilibria involving the reactant(s) will enter into the rate law, even if the species involved are not on the net reaction pathway.*

2.4 CURTIN–HAMMETT CONDITIONS

This system has its historical background in physical organic chemistry and the kinetic aspects are the subject of a detailed review by Seeman.⁵ In essence, this is a special application of the rapid-equilibrium assumption. The Curtin–Hammett conditions and their consequences also are relevant to inorganic systems, and this has been recognized especially in the area of stereoselective catalysis.

The system is described in its simplest form by



where the reactants, A and B, are typically structural or optical isomers that react to produce structurally or optically different products, Y and Z. It is assumed that A and B are in rapid equilibrium, which requires that $(k_1 + k_2) \gg k_3$ and k_4 , and that at all times $[B]/[A] = k_1/k_2 = K_{12}$. The interest in these conditions primarily concerns what they predict about the ratio of the product concentrations. The rates of production of the products are given by

$$\frac{d[Z]}{dt} = k_3[B] \quad \text{and} \quad \frac{d[Y]}{dt} = k_4[A] \quad (2.24)$$

If one takes the ratio of these rates and integrates over the limits $[Z]_0 = [Y]_0 = 0$ to $[Z]$ and $[Y]$, respectively, one obtains the product ratio at any time as

$$\frac{[Z]}{[Y]} = \left(\frac{k_3}{k_4}\right) \frac{[B]}{[A]} = \left(\frac{k_3}{k_4}\right) K_{12} \quad (2.25)$$

Thus, the Curtin–Hammett conditions predict that the ratio of the product concentrations is constant at any time during the reaction. However, this ratio does not simply reflect the relative stabilities of the isomeric reactants, as determined by K_{12} , but also depends on k_3/k_4 . Thus, a particular ratio might be obtained when $[A] > [B]$ (i.e. $K_{12} < 1$) and $k_3/k_4 > 1$, or when $[B] > [A]$ (i.e. $K_{12} > 1$) and $k_3/k_4 < 1$.

There is one further important aspect of this system that relates to the species whose free energies control the product ratio. This aspect can be developed in terms of transition-state theory and the reaction coordinate diagram in Figure 2.1.

From transition-state theory (Section 1.6.2), the rate constants k_3 and k_4 are given as

$$k_3 = (k_B T/h) e^{-(G^\ddagger(B^*) - G^\ddagger(B))/RT} \quad \text{and} \quad k_4 = (k_B T/h) e^{-(G^\ddagger(A^*) - G^\ddagger(A))/RT} \quad (2.26)$$

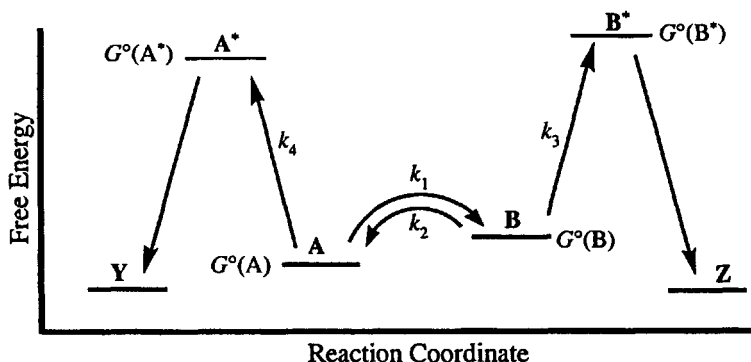


Figure 2.1. A reaction coordinate diagram for the system of two reactants A and B in rapid equilibrium, producing products Y and Z through transition states A^* and B^* , respectively.

and from thermodynamics, K_{12} is given by

$$K_{12} = e^{-(G^\circ(B) - G^\circ(A))/RT} \quad (2.27)$$

Substitution from Eq. (2.26) and Eq. (2.27) into Eq. (2.25) gives

$$\frac{[Z]}{[Y]} = e^{(-G^\circ(B^*) + G^\circ(B) + G^\circ(A^*) - G^\circ(A) - G^\circ(B) + G^\circ(A))/RT} \quad (2.28)$$

which reduces to

$$\frac{[Z]}{[Y]} = e^{(G^\circ(A^*) - G^\circ(B^*))/RT} \quad (2.29)$$

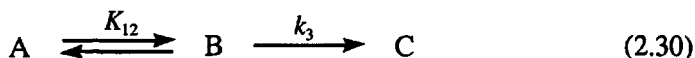
This shows that *the product ratio is only dependent on the difference in the free energies of the transition states* and is independent of the relative free energies of the reactants A and B, as long as the latter are in rapid equilibrium.

2.5 RAPID-EQUILIBRIUM OR STEADY-STATE?

In many cases, the decision as to whether to use the rapid-equilibrium or steady-state conditions will be obvious. If the mechanism proposes some intermediate that is thought to be very reactive, then a steady-state assumption for its concentration is probably appropriate, as long as there is no detectable concentration of the intermediate. Proton transfer reactions between acids and bases are generally treated as equilibria.

For less obvious situations, it is helpful to have some approximate idea of the rate constants involved in the formation and destruction of the

intermediate in order to choose the most appropriate approach. The criteria to use have been the subject of much discussion that is summarized and further delineated in recent work by Viossat and Ben-Aim⁶ and by Gellene.⁷ These authors discuss the following system:



For the steady-state approximation to apply, $k_1 \ll (k_2 + k_3)$ and Gellene notes that the reaction time scale must be such that $t \gg (k_2 + k_3)^{-1}$, whereas for the rapid-equilibrium approximation, $k_3 \ll (k_1 + k_2)$ and $t \gg (k_1 + k_2)^{-1}$. It is noteworthy that the condition $k_3 \ll (k_1 + k_2)$ only requires that either k_1 or k_2 be much larger than k_3 . This results because the rate of attainment of equilibrium is determined by $(k_1 + k_2)$, as shown in Section 1.2.3. In the application of these criteria to real systems, it should be remembered that k_1 , k_2 and k_3 may be pseudo-first-order rate constants that are the product of some species concentration and a specific rate constant.

2.6 NUMERICAL INTEGRATION METHODS

The availability of desktop computers has made numerical integration of differential equations an increasingly popular tool for kinetic analysis. One simply needs to decide on a mechanistic scheme, write the appropriate differential equations for the time dependence of the species, establish initial conditions and then let the computer calculate the species concentrations over a chosen time range. The calculated results can be compared to the experimental ones, visually or by least-squares fitting. The main advantage of such methods is that complex kinetic schemes are easily modeled and that second-order conditions, which might otherwise be impossible to integrate, can be included.

This appears to be an ideal method, since there is no need to do integrations or worry about steady-state or rapid-equilibrium assumptions. However, problems can arise in the numerical analysis. Most of these procedures use the fourth-order Runge-Kutta method in which the integration is done in a series of small time steps. The step size must be small relative to the time dependence of all the concentration variables; this can lead to problems in systems with mechanistic steps of widely different rates, because there is a tendency to shorten the time for calculation by lengthening the step size. Since the rapid-equilibrium and steady-state conditions can cause rapid initial concentration changes, it can be advantageous to apply such assumptions to the differential equations before doing the numerical integration. A problem of numerical significance can also arise for species of very small concentrations, such as steady-state intermediates, unless these are removed from the model by appropriate assumptions.

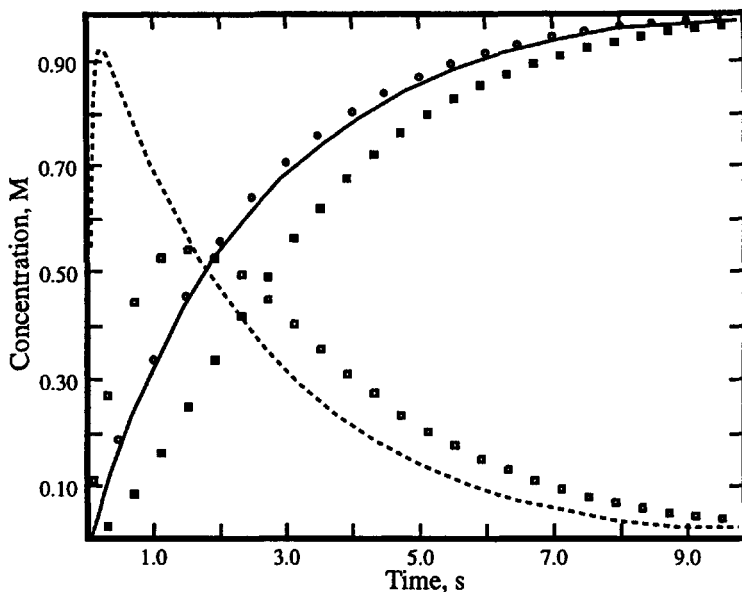


Figure 2.2. The time dependence of the concentrations of species in Eq. (2.30) with $[A]_0 = 1.0$ M: (---) [B] and (—) [C] by numerical integration for $k_1 = 40$, $k_2 = 0.001$, $k_3 = 0.4$ s $^{-1}$ and (◐) [C] calculated from Eq. (2.21); (◑) [B] and (◒) [C] by numerical integration for $k_1 = 1.0$, $k_2 = 0.001$, $k_3 = 0.4$ s $^{-1}$.

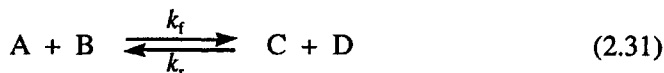
Some examples of numerical integrations for the system in Eq. (2.30) are shown in Figure 2.2 for different relative rates in the rapid-equilibrium model. The dashed and solid lines show the calculated time dependence of [B] and [C], respectively, for relative rate constants that satisfy the rapid-equilibrium conditions and the circles represent [C] for the same conditions, calculated from Eq. (2.21). Note that [B] initially increases rapidly to the equilibrium value; this type of fast initial change can be a problem for numerical integration. The open and closed squares represent [B] and [C], respectively, for rate-constant values that do not satisfy the rapid-equilibrium conditions. These show a slower increase of [B] to a lower maximum value, and a brief initial induction period for [C].

2.7 PRINCIPLE OF DETAILED BALANCING

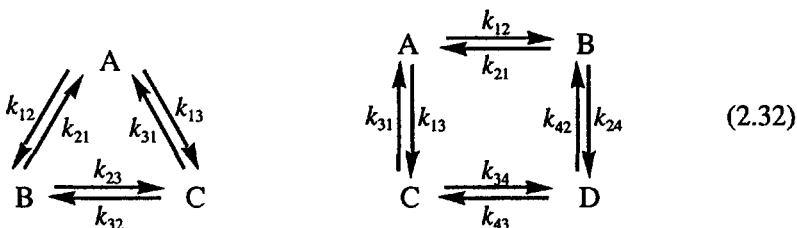
The principle of detailed balancing states that when a system is at equilibrium, the rate in the forward direction equals the rate in the reverse direction for each individual step in the process as well as for the overall reaction.

This can be of use in simple systems because it makes it possible to express one of the rate constants in terms of the others and the overall

equilibrium constant. For the reaction



$K_e = k_f/k_r$, so that $k_r = k_f/K_e$. For cyclic systems, such as



a less obvious consequence is that the product of the rate constants going in one direction around the cycle must equal the product of the rate constants in the other direction. For the three-species system, $k_{12}k_{23}k_{31} = k_{13}k_{32}k_{21}$, so that one needs to know only five of the six rate constants in order to define the system. Similarly, for the four-species system, one obtains $k_{13}k_{34}k_{42}k_{21} = k_{12}k_{24}k_{43}k_{31}$. In systems such as these, Alberty⁸ has noted the anomalies which can occur in numerical integrations if one specifies values for all of the rate constants and ignores the fact that one of the rate constants is defined by the values of the others.

2.8 PRINCIPLE OF MICROSCOPIC REVERSIBILITY

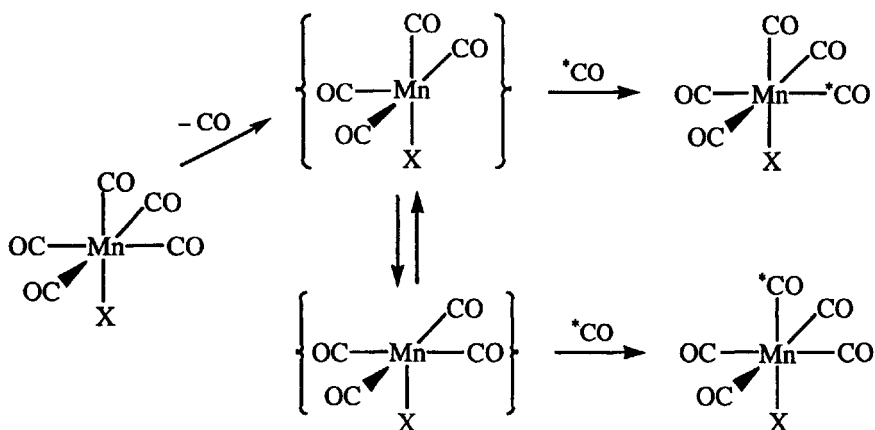
Under the same conditions, the mechanism of the forward and reverse reactions must be the same. This results because *the least energetic pathway in one direction must be the least energetic pathway in the other direction*. The intermediates and transition state must be the same in either direction. One consequence of this is that a catalyst for a forward reaction will be a catalyst for the reverse reaction.

The proper application of the principles of microscopic reversibility and detailed balancing can be helpful in mechanistic assessments, as illustrated by the CO exchange in $Mn(CO)_5X$ systems. Johnson et al.⁹ initially claimed that all the CO ligands were being exchanged at a similar rate and proposed the mechanism in Scheme 2.1.

Brown¹⁰ pointed out that this mechanism violates the principle of microscopic reversibility because, if dissociation of a cis-CO is more favorable kinetically, then addition of a CO to the cis position also must be more favorable.

Subsequent work by Atwood and Brown,¹¹ using IR detection, indicates that the exchange of the cis CO is faster. Jackson¹² has suggested that the more recent analysis transgresses the principle of detailed balancing, but

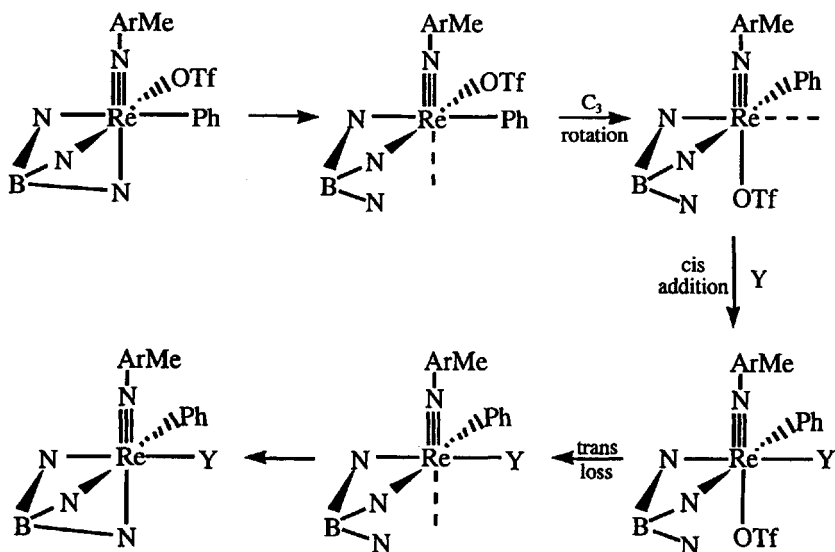
Scheme 2.1



this criticism arises from an incorrect extension of Brown's arguments¹³ by Espenson.¹⁴ The detailed analysis by Jackson, allowing for initial dissociation of both cis- and trans-CO ligands, shows that the ratio of cis to trans products is independent of time if the intermediates are in rapid equilibrium; otherwise the ratio varies with time, unless the two dissociation rates happen to be equal.

A common extension of the principle of microscopic reversibility is illustrated by the mechanism in Scheme 2.2. The reaction involves a ligand substitution on an aryl-Re(V)-imido complex in which OTf is triflate ion, BN_3 is hydrotris(pyrazolyl)borate, Ph is C_6H_5 and ArMe is *p*-tolyl.

Scheme 2.2



McNeil et al.¹⁵ found that the rate of replacement of OTf by Y was first-order in [Y], and a mechanism which is consistent with this is shown in Scheme 2.2. The authors discarded this mechanism because the Y is added at a position cis to the Re≡N and this would suggest that the leaving group, OTf, also should be able to leave from its cis position in the starting material. This invokes an extension of microscopic reversibility in that the principle applies strictly only to degenerate reactions, i.e. when the leaving group and entering group are the same. Another unfavorable aspect of this mechanism is that it requires the rate-controlling step to be the addition of Y to a vacant coordination site, or some following step, because the rate is first-order in [Y].

A subsequent study by Lahti and Espenson¹⁶ on a five-coordinate oxorhenium(V) dithiolate system suggests that the mechanism in Scheme 2.2 might be modified by adding Y to the vacant site after the initial chelate ring opening. This could be followed by rotation about the pseudo-C₃ axis to bring Y into a cis position and OTf to the trans position relative to the ≡N. Lahti and Espenson were able to provide substantial evidence for such a mechanism because the dithiolate consisted of two different S-donors.

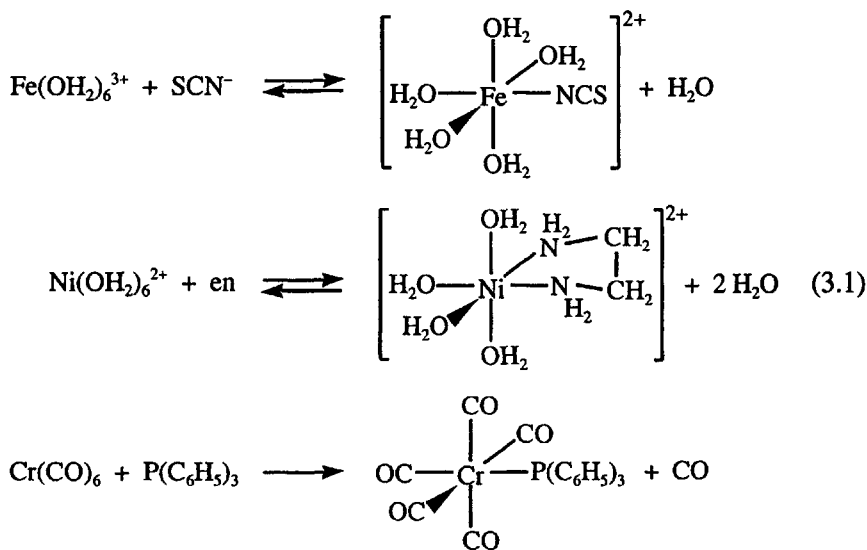
References

1. Moore, J. W.; Pearson, R. G. *Kinetics and Mechanism*, 3rd ed.; Wiley-Interscience: New York, 1980.
2. Espenson, J. H. *Chemical Kinetics and Reaction Mechanisms*; McGraw-Hill: New York, 1981.
3. Laidler, K. J. *Chemical Kinetics*, 3rd ed.; Harper & Row: New York, 1987.
4. King, E. L.; Altman, C. J. *Phys. Chem.* **1956**, *60*, 1375.
5. Seeman, J. I. *Chem. Rev.* **1983**, *83*, 83.
6. Viossat, V.; Ben-Aim, R. I. *J. Chem. Educ.* **1993**, *70*, 732.
7. Gellene, G. I. *J. Chem. Educ.* **1995**, *72*, 196.
8. Alberty, R. A. *J. Chem. Educ.* **2004**, *81*, 1206.
9. Johnson, B. F. G.; Lewis, J.; Miller, J. R.; Robinson, B. H.; Robinson, P. W.; Wojcicki, A. *J. Chem. Soc. A* **1968**, 522.
10. Brown, T. L. *Inorg. Chem.* **1968**, *7*, 2673.
11. Atwood, J. T.; Brown, T. L. *J. Am. Chem. Soc.* **1975**, *97*, 3380.
12. Jackson, W. G. *Inorg. Chem.* **1987**, *26*, 3004.
13. Brown, T. L. *Inorg. Chem.* **1989**, *28*, 3229.
14. Espenson, J. H. *Chemical Kinetics and Reaction Mechanisms*; McGraw-Hill: New York, 1981; pp 128–131.
15. McNeil, W. S.; DuMez, D. D.; Matano, Y.; Lovell, S.; Mayer, J. M. *Organometallics*, **1999**, *18*, 3715.
16. Lahti, D. W.; Espenson, J. H. *J. Am. Chem. Soc.* **2001**, *123*, 6014.

3

Ligand Substitution Reactions

In ligand substitution reactions, one or more ligands around a metal ion are replaced by other ligands. In many ways, all inorganic reactions can be classified as either substitution or oxidation–reduction reactions, so that substitution reactions represent a major type of inorganic process. Some examples of substitution reactions follow:



3.1 OPERATIONAL APPROACH TO CLASSIFICATION OF SUBSTITUTION MECHANISMS

The operational approach was first expounded in 1965 in a monograph by Langford and Gray.¹ It is an attempt to classify reaction mechanisms in relation to the type of information that kinetic studies of various types can provide. It delineates what can be said about the mechanism on the basis of the observations from certain types of experiments. The mechanism is classified by two properties, its stoichiometric character and its intimate character.

Stoichiometric Mechanism

The stoichiometric mechanism can be determined from the kinetic behavior of one system. The classifications are as follows:

1. *Dissociative (D)*: an intermediate of lower coordination number than the reactant can be identified.
2. *Associative (A)*: an intermediate of larger coordination number than the reactant can be identified.
3. *Interchange (I)*: no detectable intermediate can be found.

Intimate Mechanism

The intimate mechanism can be determined from a series of experiments in which the nature of the reactants is changed in a systematic way. The classifications are as follows:

1. *Dissociative activation (d)*: the reaction rate is more sensitive to changes in the leaving group.
2. *Associative activation (a)*: the reaction rate is more sensitive to changes in the entering group.

This terminology has largely replaced the S_N1 , S_N2 and so on type of nomenclature that is still used in physical organic chemistry. These terminologies are compared and further explained as follows:

Dissociative [$D \equiv S_N1$ (limiting)]: there is definite evidence of an intermediate of reduced coordination number. The bond between the metal and the leaving group has been completely broken in the transition state without any bond making to the entering group.

Dissociative interchange ($I_d \equiv S_N1$): there is no definite evidence of an intermediate. In the transition state, there is a large degree of bond breaking to the leaving group and a small amount of bond making to the entering group. The rate is more sensitive to the nature of the leaving group.

Associative interchange ($I_a \equiv S_N2$): there is no definite evidence of an intermediate. In the transition state, there is some bond breaking to the leaving group but much more bond making to the entering group.

Associative [$A \equiv S_N2$ (limiting)]: there is definite evidence of an intermediate of increased coordination number. In the transition state, the bond to the entering group is largely made while the bond to the leaving group is essentially unbroken.

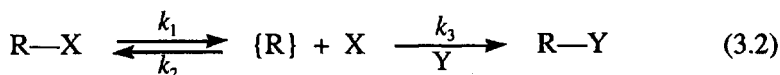
The general goal of a kinetic and mechanistic study of a substitution reaction is to classify the reaction as D , I_d , I_a or A .

3.2 OPERATIONAL TESTS FOR THE STOICHIOMETRIC MECHANISM

According to the original definitions, it should be possible to establish the stoichiometric mechanism on the basis of a study of one system. In practice, this has been expanded in tests for the D mechanism to include studies in which the nature of the leaving group is changed in order to determine if some property of the intermediate is independent of its origin.

3.2.1 Dissociative Mechanism Rate Law

The D mechanism can be described by the following sequence of reactions:



where X and Y are the leaving and entering groups, respectively, and {R} is the intermediate of reduced coordination number.

The k_{exp} for this mechanism can be derived from the previous solution of the system $\text{A} \rightleftharpoons \text{B} \rightleftharpoons \text{C}$ with a steady state for B, by replacing k_2 and k_3 in Eq. (2.13) with $k_2[\text{X}]$ and $k_3[\text{Y}]$, respectively, and setting $k_4 = 0$. Then, if $[\text{X}]$ and $[\text{Y}] \gg [\text{RX}]$, k_{exp} is given by

$$k_{\text{exp}} = \frac{k_1 k_3 [\text{Y}]}{k_2 [\text{X}] + k_3 [\text{Y}]} \quad (3.3)$$

If this rate law is to provide a successful test of the D mechanism, it is necessary for the conditions to be such that $k_2[\text{X}] \approx k_3[\text{Y}]$. Then, for example, if $[\text{X}]$ is held constant and $[\text{Y}]$ is varied in a series of experiments, k_{exp} should change with $[\text{Y}]$, as shown in Figure 3.1. This type of variation is often referred to as "saturation" behavior, and k_{exp} approaches a limiting value of k_1 when $k_3[\text{Y}] \gg k_2[\text{X}]$.

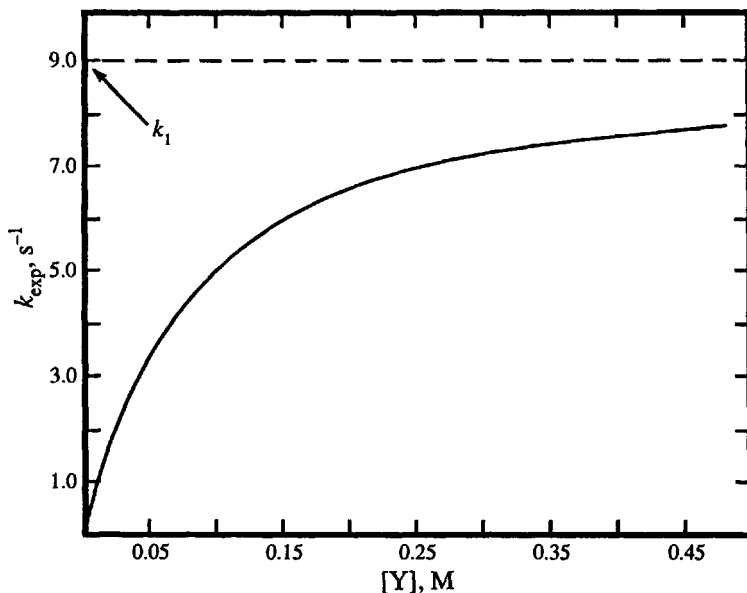


Figure 3.1. Predicted variation of k_{exp} with $[\text{Y}]$ for a D mechanism with $k_1 = 9 \text{ s}^{-1}$ and $k_2[\text{X}]/k_3 = 0.075 \text{ M}$.

It is possible to rearrange Eq. (3.3) to give

$$(k_{\text{exp}})^{-1} = \frac{k_2}{k_1 k_3} \left(\frac{[\text{X}]}{[\text{Y}]} \right) + \frac{1}{k_1} \quad (3.4)$$

Therefore, a plot of $(k_{\text{exp}})^{-1}$ versus $[\text{X}]/[\text{Y}]$ should be linear and k_1 and k_2/k_3 can be determined. It often happens that X is the solvent, S, and a plot of $(k_{\text{exp}})^{-1}$ versus $[\text{Y}]^{-1}$, commonly called a double-reciprocal plot, is used to determine k_1 and $k_2[\text{S}]/k_3$.

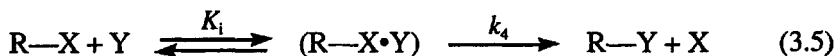
If several different entering groups Y are studied, they should all yield the same value of k_1 as a further condition of a D mechanism.

3.2.2 Ion Pair or Preassociation Problem

The success of the preceding test of a D mechanism depends on the assumption that there are no other reaction sequences that produce the same rate law. Unfortunately, this is *not* true.

Many metal ion complexes are positively charged and many common entering groups are anions. Such oppositely charged species can form association complexes, commonly called ion pairs. The phenomenon of preassociation is not limited to ions and may be appreciable for polar species in nonpolar solvents due to dipole-dipole interactions and hydrogen bonding.

The general process can be described by the following sequence of reactions:



where $(\text{R-X}\cdot\text{Y})$ is the ion pair or preassociation complex formed in a fast pre-equilibrium with an ion pair formation constant, K_i .

The rate law for this type of system was developed in Eq. (2.22) and, if $[\text{Y}] \gg [\text{RX}]$, the pseudo-first-order rate constant is given by

$$k_{\text{exp}} = \frac{k_4 K_i [\text{Y}]}{K_i [\text{Y}] + 1} \quad (3.6)$$

This equation predicts the same type of variation of k_{exp} with $[\text{Y}]$ as that from the D mechanism if $[\text{X}]$ is constant in Eq. (3.3). The latter is often the case because X is the solvent, S. A plot of $(k_{\text{exp}})^{-1}$ versus $[\text{Y}]^{-1}$ should be linear and the slope and intercept can be used to calculate values of k_4 and K_i . The plot also is linear for the D rate law and gives the corresponding values as k_1 and $k_2[\text{S}]/k_3$. It may be possible to distinguish K_i from $k_2[\text{S}]/k_3$ by comparing K_i to known or estimated values from analogous systems. In favorable cases, it may be possible to quantify the extent of ion pairing through its effect on conductivity or charge-transfer bands in the electronic spectrum.

Table 3.1. Calculated Ion Pair Formation Constants ($a = 5 \times 10^{-8}$ cm, $T = 298$ K)

μ (M)	H_2O ($\epsilon = 78.5$)			CH_3OH ($\epsilon = 32$)		CH_2Cl_2 ($\epsilon = 9.1$)
	0.01	0.10	1.0	0.01	0.10	0.01
$z_1 z_2$						
-1	1.08	0.81	0.54	5.1	2.2	1.3×10^3
-2	3.67	2.07	0.93	83	15	5.2×10^6
-3	12.5	5.3	1.6	1400	104	2.1×10^{10}
-4	42.7	13.6	2.7			
-5	146	34.7	4.7			
-6	497	88.9	8.1			

For ion pairs, Fuoss² and Eigen³ developed an equation to estimate K_i based on extended Debye-Hückel theory and a hard-sphere model for the ions. It is given by

$$K_i = \frac{4\pi N a^3}{3000} e^{-U/k_B T} \quad (3.7)$$

where

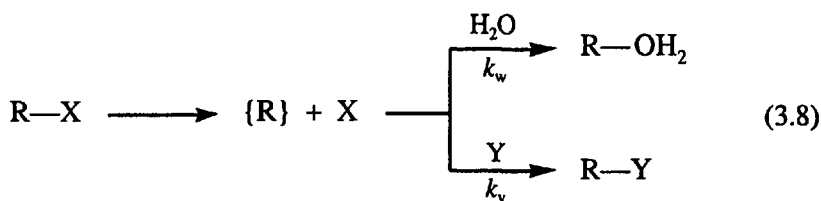
$$U = \frac{z_1 z_2 e^2}{\epsilon} \left(\frac{1}{a(1 + \kappa a)} \right) \quad \text{and} \quad \kappa = \sqrt{\frac{8\pi N e^2 \mu}{1000 \epsilon k_B T}}$$

and N is Avogadro's number, a is the contact distance of the ions in cm, k_B is Boltzmann's constant (1.381×10^{-16} erg K^{-1}), z_1 and z_2 are the ionic charges, e is the electron charge (4.803×10^{-10} esu), ϵ is the solvent dielectric constant and μ is the ionic strength. Some calculated values of K_i are given in Table 3.1 for various charge products, solvents and ionic strengths. Experience indicates that these calculated values are reasonable approximations when compared to the few experimental values. The main point to note is that the value of $K_i[Y]$ can easily be of the same magnitude as 1 for typical charge types and for reasonable concentrations of Y .

3.2.3 Competition Studies for the Intermediate

These studies attempt to test the prediction of a **D** mechanism that a particular metal center should produce the same intermediate, independent of the leaving group. For example, one might study the solvolysis in water of $\text{Co}(\text{NH}_3)_5\text{Cl}^{2+}$ and $\text{Co}(\text{NH}_3)_5(\text{NO}_3)^{2+}$, where Cl^- and NO_3^- are the leaving groups, in the presence of some added nucleophile Y . The object is to get the same product distribution if a common intermediate $\{\text{Co}(\text{NH}_3)_5^{3+}\}$ is formed. The confidence in the conclusions depends on studying a significant range of leaving groups.

The principles of the method are described by the following sequence:



The product ratio $[\text{RY}]/[\text{ROH}_2]$ can be calculated as follows:

$$\begin{aligned}
 \frac{d[\text{RY}]}{dt} &= k_y[\text{R}][\text{Y}] \quad \text{and} \quad \frac{d[\text{ROH}_2]}{dt} = k_w[\text{R}][\text{H}_2\text{O}] \\
 \frac{d[\text{RY}]}{d[\text{ROH}_2]} &= \frac{k_y[\text{Y}]}{k_w[\text{H}_2\text{O}]} = \frac{k_y[\text{Y}]}{k'_w}
 \end{aligned} \quad (3.9)$$

Integration and rearrangement yields

$$\frac{[\text{RY}]}{[\text{ROH}_2][\text{Y}]} = \frac{k_y}{k'_w} \quad (3.10)$$

If a **D** mechanism is operative, the ratio on the left should be a constant for different concentrations of **Y** and for different leaving groups.

A similar analysis can be applied if the product complex has different structural isomers or stereoisomers. Then, the isomers should be produced in a proportion independent of the leaving group.

3.2.4 Constant Thermodynamic Properties for the Intermediate

In this approach, it is hoped to show that the thermodynamic parameters of the intermediate are constant and independent of the leaving group, and thereby establish the independent nature of the intermediate.

The following development is in terms of enthalpy, but the same can be done for free energy, entropy, partial molar volume and so on. The reaction energetics are defined by Figure 3.2, where it should be apparent that

$$\Delta H^* - \Delta H_{\text{stab}} = \Delta H_f^\circ(\text{R}) + \Delta H_f^\circ(\text{X}) - \Delta H_f^\circ(\text{RX}) \quad (3.11)$$

For the overall reaction $\text{RX} + \text{Y} \rightarrow \text{RY} + \text{X}$, the enthalpy change is

$$\Delta H_{\text{rxn}}^\circ = \Delta H_f^\circ(\text{RY}) + \Delta H_f^\circ(\text{X}) - \Delta H_f^\circ(\text{RX}) - \Delta H_f^\circ(\text{Y}) \quad (3.12)$$

Combination of Eqs. (3.11) and (3.12) eliminates $\Delta H_f^\circ(\text{RX})$ and $\Delta H_f^\circ(\text{X})$ to give

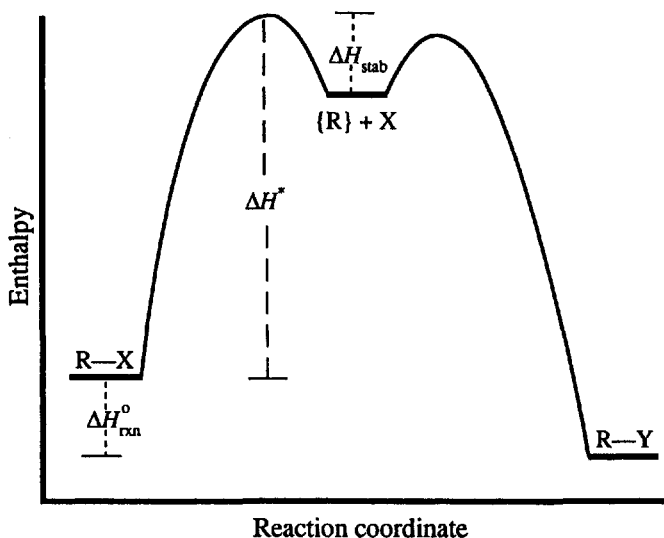


Figure 3.2. Reaction coordinate diagram for a D mechanism.

$$\Delta H_f^\circ(\text{R}) = \Delta H^* - \Delta H_{\text{stab}} - \Delta H_{\text{rxn}}^\circ + \Delta H_f^\circ(\text{RY}) - \Delta H_f^\circ(\text{Y}) \quad (3.13)$$

If a series of leaving groups is examined using the same Y (e.g., the solvent), then

$$\Delta H_f^\circ(\text{R}) = \Delta H^* - \Delta H_{\text{stab}} - \Delta H_{\text{rxn}}^\circ + \text{Constant} \quad (3.14)$$

This equation is not truly independent of X because of ΔH_{stab} , but this term is assumed to be small, so that

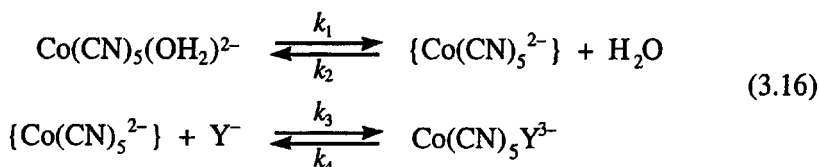
$$\Delta H^* - \Delta H_{\text{rxn}}^\circ \approx \Delta H_f^\circ(\text{R}) - \text{Constant} \quad (3.15)$$

For a D mechanism, $\Delta H^* - \Delta H_{\text{rxn}}^\circ$ is expected to be constant for a particular entering group.

3.3 EXAMPLES OF TESTS FOR A DISSOCIATIVE MECHANISM

3.3.1 Dissociative Rate Law

The first example of the full D rate law was published by Wilmarth and co-workers.^{4,5} They studied the anation of $\text{Co}(\text{CN})_5(\text{OH}_2)^{2-}$ in water with the idea that the negative charge on the metal complex would suppress the ion pair formation and might favor a D mechanism. Their observations were consistent with the following mechanism:



The predicted pseudo-first-order rate constant for this mechanism can be obtained by analogy to Eq. (2.13), to give

$$k_{\text{exp}} = \frac{k_1 k_3 [\text{Y}] + k_2 [\text{H}_2\text{O}] k_4}{k_2 [\text{H}_2\text{O}] + k_3 [\text{Y}]} = \frac{k_1 k_3 [\text{Y}] + k_2' k_4}{k_2' + k_3 [\text{Y}]}
 \tag{3.17}$$

The value of k_4 was determined independently by studying the rate of aquation of $\text{Co(CN)}_5\text{Y}^{3-}$ with $[\text{Y}] \approx 0$, in which case $k_{\text{exp}} = k_4$. If k_4 is subtracted from both sides of Eq. (3.17) and the reciprocal is taken, then one obtains Eq. (3.18) which predicts that a plot of $(k_{\text{exp}} - k_4)^{-1}$ versus $[\text{Y}]^{-1}$ should be linear, allowing one to calculate k_2'/k_3 and k_1 .

$$(k_{\text{exp}} - k_4)^{-1} = (k_1 - k_4)^{-1} + \frac{k_2'}{k_3} (k_1 - k_4)^{-1} [\text{Y}]^{-1}
 \tag{3.18}$$

Wilmarth and co-workers found that their data satisfied this rate law and yielded reasonably constant values of k_1 for a range of Y such as Br^- , NH_3 , I^- , SCN^- and N_3^- . Note that, if Y is H_2O , then $k_{\text{exp}} = k_1$, so that a study of the water exchange rate would provide a further test.

Unfortunately, all of the preceding results have been thrown into serious doubt by recent work. Burnett and Gilfillian⁶ and then Haim⁷ found that the rate law with $\text{Y} = \text{N}_3^-$ has a simple first-order dependence on $[\text{N}_3^-]$. Haim's observations indicate that the early work may be in error because of the presence of $(\text{NC})_5\text{CoO}_2\text{Co(CN)}_5^{6-}$, which has been avoided in the recent studies through modified preparative procedures. The original observations with regard to SCN^- have been confirmed by later work.⁸

The water exchange rate on $\text{Co(CN)}_5(\text{OH}_2)^{2-}$ has been measured by Swaddle and co-workers⁹ who found $k_{\text{exch}} = 5.8 \times 10^{-4} \text{ s}^{-1}$ at 25°C , with $\Delta H^\ddagger = 90.2 \text{ kJ mol}^{-1}$ and $\Delta S^\ddagger = -4 \text{ J mol}^{-1} \text{ K}^{-1}$. This predicts that at 40°C , $k_{\text{exch}} = 3.5 \times 10^{-3} \text{ s}^{-1}$, whereas the results of the substitution studies give $k_1 = 2 \times 10^{-3} \text{ s}^{-1}$ (Haim) or $6 \times 10^{-4} \text{ s}^{-1}$ (Burnett and co-workers).¹⁰ The current status of this system is that it is probably using a dissociative interchange mechanism, I_d , and that there is some preassociation of the metal complex and the entering group despite their unfavorable charge product.

Still, there are systems for which the rate law indicates a **D** mechanism. Some examples of these are $\text{Rh(Cl)}_5(\text{OH}_2)^{2-}$,¹¹ $\text{Co(en)}_2(\text{SO}_3)(\text{OH}_2)^+$,¹² $\text{Co(DMG)}_2(\text{L})\text{X}^{13}$ and $\text{Cr(TPP)}(\text{Cl})\text{X}$,¹⁴ where DMG = dimethylglyoxime and TPP = tetraphenylporphine. Some values of k_3/k_2 are given in Table 3.2. Later work¹⁵ on $\text{Cr(TPP)}(\text{Cl})\text{X}$ systems gave k_3/k_2 values for

Table 3.2. Values of k_3/k_2 for Systems with a D Mechanism Rate Law

Entering Group	Rh(Cl) ₅ (OH) ₂ ²⁻ in Water ^a	Entering Group	Cr(TPP)(Cl)(py) in Toluene
H ₂ O	1.0	Pyridine	1.0 ^b
I ⁻	0.018	PPh ₃	0.0017 ^b
Br ⁻	0.016	P(C ₂ H ₅ CN) ₃	0.0085 ^b
Cl ⁻	0.021	P(OPr) ₃	0.075 ^b
SCN ⁻	0.079	<i>N</i> -Methylimidazole	1.7 ^b , 1.1 ^c
NO ₂ ⁻	0.10	H ₂ O	1.44 ^c
N ₃ ⁻	0.14	3-Methylpyridine	0.93 ^c
		Quinoline	0.0089 ^c

^a Reference 11. ^b Reference 14. ^c Reference 15.

a number of substituted pyridines. The {Cr(TPP)Cl} intermediate has been generated by photolysis¹⁶ and found to react at nearly diffusion controlled rates with the various pyridine entering groups, so that $k_3/k_2 \approx 1$. The small k_3/k_2 values for the phosphines and quinoline may be due to steric hindrance.

3.3.2 Competition Studies for a Dissociative Intermediate

The main limitation for these studies is that the products must be stable enough that their amounts can be accurately determined. The favorite systems for these studies have been cobalt(III) amine complexes, because of their stability and the extensive documentation of their properties.

The early work was done on the hydroxide ion catalyzed hydrolysis of cobalt(III) amines, for which there was evidence that the reaction proceeds by a dissociative conjugate base (DCB) mechanism (S_N1CB in earlier terminology), as shown in Scheme 3.1.

Scheme 3.1

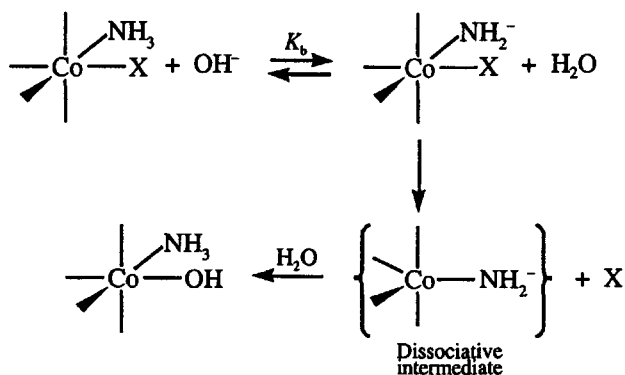


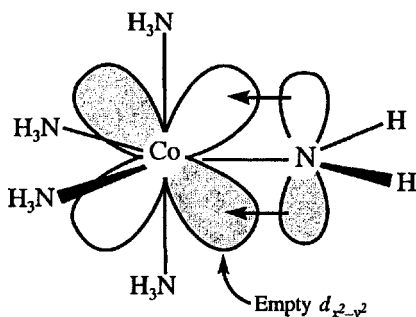
Table 3.3. Product Distribution for *cis*-Co(en)₂(NH₃)X + OH⁻

Leaving Group	% trans	% cis	% Retention	% Racemate
Cl ⁻	22	78	48	30
NO ₃ ⁻	23	77	47	30
Br ⁻	22	78	44	34
(H ₃ C) ₂ SO	23	77	52	25
(H ₃ CO) ₃ PO	23	77	54	23

An analysis of early results on the hydrolysis of *cis* and *trans* isomers of Co(en)₂(L)X complexes by Sargeson and Jordan¹⁷ indicated that if L is the same, then the percentage of *cis* and *trans* isomers in the product Co(en)₂(L)(OH) is fairly constant. Further work by Buckingham et al.¹⁸ on stereoisomers of *cis*-Co(en)₂(NH₃)X is summarized in Table 3.3. The percentage of *cis* and *trans* products is quite constant, but the percentage retention is significantly greater with neutral leaving groups. This can be rationalized if the anionic leaving groups are retained longer within the immediate solvation sheath of the "intermediate" and tend to inhibit entry from the position they have vacated, thereby giving less retention. In the same study, using azide ion as a competing ligand, it was found that neutral leaving groups give about 5% more Co(en)₂(NH₃)(N₃)²⁺ than anionic leaving groups. The preceding rationale also can be used to explain this observation.

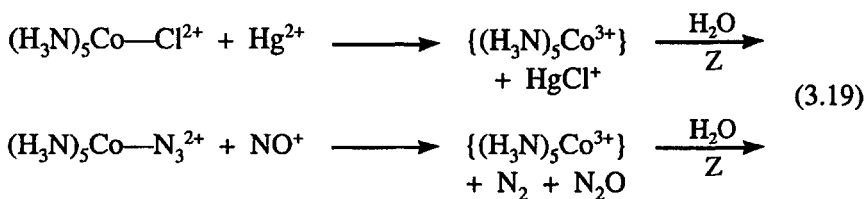
The status of this and related work was summarized by Jackson et al.¹⁹ The earlier observations have been revised and expanded by Buckingham and co-workers,²⁰ especially for the complexes *trans*-Co(NH₃)₄(¹⁵NH₃)X and Co(NH₃)₅(NCS)²⁺. It now appears that an intermediate does form, but that it is very reactive and scavenges its immediate coordination sphere rather than sensing the stoichiometric amounts of various species in the bulk solution. The intermediate may not be truly independent of its source nor of the "inert" ionic medium because it reacts while the leaving group is still in the vicinity, and the products essentially reflect the ionic atmosphere around the reactant. However, the leaving group does not dramatically change the reactivity pattern of the intermediate. In recent reviews, Jackson²¹ has provided an overview of the area, while Baran et al.²² have examined the kinetic effects of the structures of the ground and transition states for various amines in Co(III) complexes of the general type Co(N)₅Cl.

Basolo and Pearson²³ suggested that the {(H₃N)₄Co(NH₂)²⁺} intermediate is stabilized by π back bonding from the NH₂⁻ ligand to the empty $d_{x^2-y^2}$ orbital in these low spin d^6 Co(III) complexes. The intermediate has a trigonal bipyramidal structure with the NH₂⁻ in the trigonal plane, as shown in the following diagram:



Nordmeyer²⁴ suggested that deprotonation of an amine cis to the leaving group could be kinetically more effective because the electron pair in the p -orbital could back bond to the p -orbital on Co(III) being vacated by the leaving group. There is evidence^{25,26} that deprotonation of a *cis*-(*sec*)-NH provides activation, but deprotonation of a *trans*-amine is possible in other systems.²⁷ Nordmeyer also formulated a method to predict the intermediate(s) formed based on the product distribution in *cis*- and *trans*-Co(en)₂(L)X systems.

The competition results for the hydrolysis in acidic aqueous solution (aquation) show a greater sensitivity to the leaving group than those for base-catalyzed hydrolysis. The studies also have involved reactions designed to rapidly produce an intermediate of reduced coordination number, so-called induced aquations. The following are examples of induced aquation reactions:



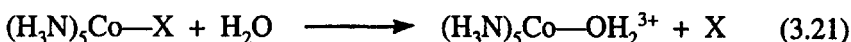
It appears that the $\{(\text{H}_3\text{N})_5\text{Co}^{3+}\}$ intermediate is more reactive than its conjugate base, so that $\{(\text{H}_3\text{N})_5\text{Co}^{3+}\}$ shows a greater dependence of the competition ratios on the leaving group. In the presence of NCS^- , the induced aquation of $\text{Co}(\text{NH}_3)_5(\text{N}_3)^{2+} + \text{NO}^+$ yields 12% $\text{Co}(\text{NH}_3)_5(\text{NCS})^{2+}$, but the simple spontaneous aquation of $\text{Co}(\text{NH}_3)_5(\text{OP}(\text{OCH}_3)_3)^{3+}$ yields 4.6% $\text{Co}(\text{NH}_3)_5(\text{NCS})^{2+}$. However, the distribution of linkage isomers in the product is nearly the same, 60% $(\text{H}_3\text{N})_5\text{Co}-\text{NCS}^{2+}$ and 40% $(\text{H}_3\text{N})_5\text{Co}-\text{SCN}^{2+}$. The status of $\{(\text{H}_3\text{N})_5\text{Co}^{3+}\}$ is still a subject of controversy and is discussed in detail by Jackson and Dutton²⁸ and House and Jackson²⁹ for the reactions with NO^+ and Hg^{2+} , respectively. For spontaneous aquations, differing views have been expressed by Jackson et al.³⁰ and Buckingham and co-workers³¹ on the effect of ion pairing on the NCS^- competitor for the intermediate.

3.3.3 Constant Thermodynamic Parameters

As shown previously, for a **D** mechanism one can expect that

$$\Delta H^* - \Delta H_{\text{rxn}}^\circ = \Delta H_f^\circ(\text{R}) - \Delta H_f^\circ(\text{RY}) + \Delta H_f^\circ(\text{Y}) \quad (3.20)$$

House and Powell³² analyzed enthalpy data for the aquation reaction



and found that $\Delta H^* - \Delta H_{\text{rxn}}^\circ$ (kcal mol⁻¹) varied with X, from 22.2 for SO₄²⁻ to ~25 for Cl⁻, Br⁻ and NO₃⁻, to 27 for H₂O. This variation was taken as evidence against a simple **D** mechanism. On the other hand, for the reaction



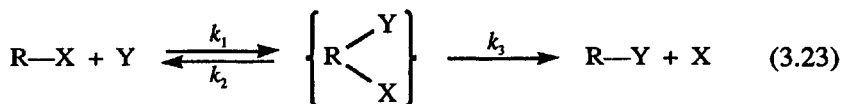
the same enthalpy difference is 32.4±0.5 kcal mol⁻¹ for the same range of leaving groups. This is quite constant and independent of the leaving group, so that it is consistent with a **D** mechanism. This is further evidence in support of the **DCB** mechanism in Scheme 3.1.

The activation volumes, ΔV^* , have been analyzed for the same reactions^{33,34} with similar conclusions. However, the analysis is more complex than was originally anticipated because of solvent electrostriction effects and the effect of the volume of the leaving group on the volume of the reactant.³⁵

3.4 OPERATIONAL TEST FOR AN ASSOCIATIVE MECHANISM

3.4.1 Associative Mechanism Rate Law

The **A** mechanism proceeds by formation of an intermediate with the entering group followed by elimination of the leaving group, as shown by the following sequence:

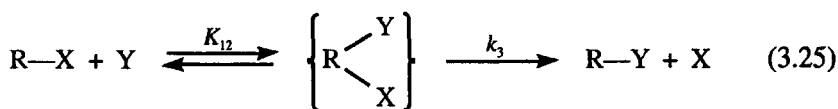


If a steady state is assumed for the intermediate and pseudo-first-order conditions are maintained with $[\text{Y}] \gg [\text{RX}]$, then

$$k_{\text{exp}} = \frac{k_1 k_3 [\text{Y}]}{k_2 + k_3} = \text{Constant} [\text{Y}] \quad (3.24)$$

The rate should always be first-order in [Y], and the rate law contains no information that uniquely defines an A mechanism.

A rather unlikely but feasible possibility is that the intermediate is formed in a rapid pre-equilibrium, as shown in the following:



where, if $[\text{Y}] \gg [\text{RX}]$, then

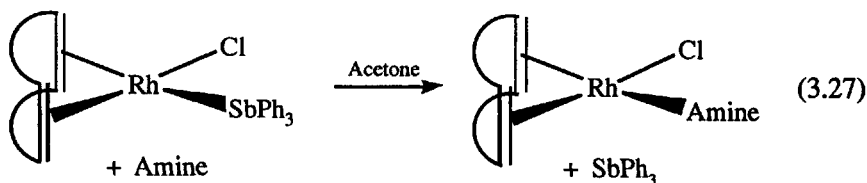
$$k_{\text{exp}} = \frac{k_3 K_{12} [\text{Y}]}{K_{12} [\text{Y}] + 1} \quad (3.26)$$

This expression has the same [Y] dependence as that for the D mechanism and the ion pair pathway. It might be distinguished from the latter by comparing the values of K_{12} to those expected for K_i . In addition, the spectral properties of the intermediate are likely to be much different from those of the reactant, whereas an ion pair is not much different because no bonds have been made or broken in the ion pair. The value of k_3 should depend on the nature of the entering group and thus could be distinguished from its mathematical equivalent k_1 in the D rate law.

3.4.2 Examples of Associative Rate Laws

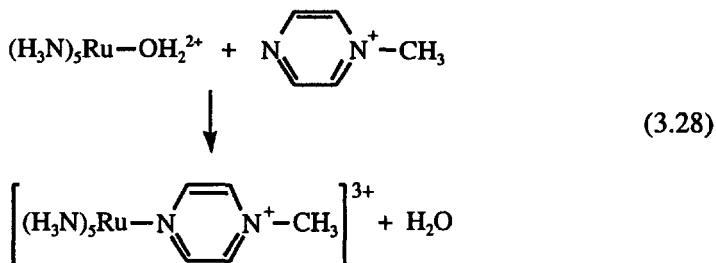
Examples of the complete A rate law in reaction (3.26) are rare because the "intermediate" must be quite stable if $K_{12}[\text{Y}] \geq 1$. Coordinatively unsaturated systems are most likely to satisfy this condition.

One apparent example was reported by Cattalini et al.³⁶ for the following reaction:



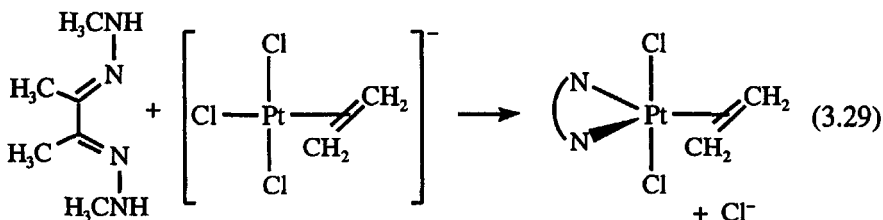
where the diene is cyclooctadiene. The rate is first-order in the Rh complex concentration and independent of the amine concentration. The rate constant varies with the nature of the amine and there is a rapid spectral change on mixing the reactants. If $K_{12}[\text{amine}] \gg 1$, then $k_{\text{exp}} = k_3$ and should depend on the nature of the amine. The values (in acetone at 25°C) of k_{exp} range from $1.58 \times 10^{-2} \text{ s}^{-1}$ for 3-cyanopyridine to $4.57 \times 10^{-2} \text{ s}^{-1}$ for *n*-butylamine and do not show a large variation.

Another apparent example appears in the work of Toma and Malin³⁷ on the reaction

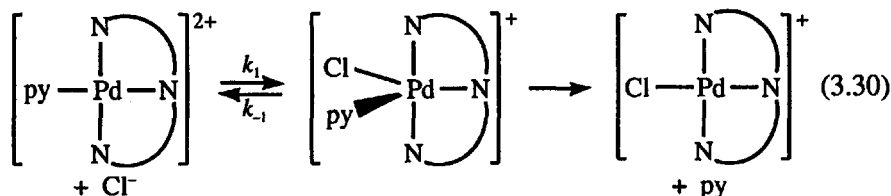


The dependence of k_{exp} on the concentration of methylpyrazinium ion is consistent with the A rate law. The authors argue that this is not due to ion pairing because of the like charges of the reactants. They suggest that the intermediate is a charge-transfer complex due to donation of t_{2g} electrons on Ru(II) to the empty π^* orbitals on the entering group. However, it is debatable whether this should be considered as an intermediate of expanded coordination number.

Species of expanded coordination number have been isolated and structurally characterized by Maresca et al.³⁸ as products of the reaction of Zeise's salt with bis hydrazones, as shown in reaction (3.29). These five-coordinate products slowly lose ethylene in a first-order process.



Tobe and co-workers³⁹ have provided evidence that reaction (3.30) proceeds through a stable intermediate, which may be the five-coordinate species shown or one of its structural isomers.



The intermediate forms reasonably quickly, with a rate that is first-order in $[\text{Cl}^-]$ ($k_1 = 9.3 \times 10^{-2} \text{ M}^{-1} \text{ s}^{-1}$, $k_{-1} = 2.5 \times 10^{-2} \text{ s}^{-1}$ in 1 M NaClO_4 at 25°C), but too slowly to be considered as an ion pair. The ^1H NMR shows that the intermediate has not released pyridine nor undergone ring opening of the dien chelate.

3.5 OPERATIONAL TESTS FOR THE INTIMATE MECHANISM

These tests are concerned with the sensitivity of the reaction rate constant to the chemical nature of the entering and leaving groups for a general reaction, such as



in which there is no definite evidence for an intermediate. Associative activation, *a*, requires more sensitivity to the nature of Y and dissociative activation, *d*, requires more sensitivity to the nature of X.

These effects appear to be easy to test, but there is always a somewhat subjective decision in evaluating the degree of sensitivity to variations in X and Y. For example, in the associative case, since X is still present in the transition state, the rate constant must show some variation with X, but the variation with changes in Y must be greater. A further problem is that X or Y is often the solvent, and it cannot be changed without a major perturbation on the whole system. It is also necessary to ensure that the changes in X or Y have not been so trivial that the interaction with "R" in the transition state would not vary by much. For example, changing from Cl⁻ to Br⁻ would probably not produce much change in the rate constant for either type of activation. In order to avoid such possibilities, scales of nucleophilicity for various ligands are very useful. It is assumed that a better nucleophile will make a stronger bond to "R", so that one should choose entering or leaving groups of significantly different nucleophilicity in testing for the type of activation.

3.5.1 Inorganic Nucleophilicity Scales

Several variables are believed to generally affect nucleophilicity:

1. *Basicity towards H⁺*: the commonly available p*K_a* values of ligands measure this and it seems to parallel the nucleophilicity toward many metal centers.
2. *Polarizability*: a more polarizable ligand should be a better electron donor and therefore a better nucleophile.
3. *Oxidizability*: a more easily oxidized ligand is more willing to give up electrons and therefore is expected to be a better nucleophile. This factor is measured by standard reduction potentials or polarographic half-wave potentials.
4. *Solvation energy*: a ligand that is more strongly solvated in one solvent than another will be a poorer nucleophile when it is more strongly solvated because more solvation energy will be lost during the formation of the metal complex.
5. *Metal at reaction center*: this factor greatly limits the generality of nucleophilicity scales in inorganic chemistry when compared to those in organic chemistry.

3.5.1.1 Edwards Scale

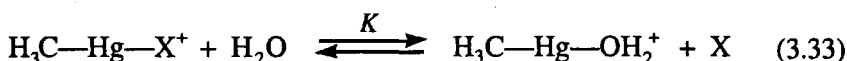
Edwards⁴⁰ proposed that a kinetic nucleophilicity should be correlated by a combination of the factors mentioned earlier for a particular metal center, using the equation

$$\log \left(\frac{k_Y}{k_{\text{solvent}}} \right) = \alpha(-E_{Y_2}^{\circ}) + \beta(\text{p}K_a + 1.74) \quad (3.32)$$

where k_Y and k_{solvent} are rate constants with Y and solvent, respectively, $E_{Y_2}^{\circ}$ is the reduction potential for $Y_2 + 2e^- \rightarrow 2Y^-$ in water and α and β are empirical constants that depend on the reaction. This scale is often mentioned but has limited applicability because of the lack of $E_{Y_2}^{\circ}$ values for all but the halogens and pseudohalogens.

3.5.1.2 Methyl–Mercury(II) Scale

The methyl–mercury(II) scale is based on the equilibrium constant for the reaction⁴¹



and nucleophilicity is taken as proportional to $-\log(K) = \text{p}K$. These $\text{p}K$ values correlate well with the n_{Pt} scale, described in the next section, and they have a similar range of applicability.

3.5.1.3 n_{Pt} Scale

The n_{Pt} scale is a kinetic scale based on the reaction



and the n_{Pt} for Y is related to the rate constant with Y, k_Y , and with the solvent methanol, k_{methanol} , by

$$n_{\text{Pt}} = \log \left(\frac{k_Y}{k_{\text{methanol}}} \right) \quad (3.35)$$

Some typical values⁴² of n_{Pt} are Cl^- (3.04); NH_3 (3.07); N_3^- (3.58), I^- (5.46); CN^- (7.14); PPh_3 (8.93). Clearly, if one is testing for entering group effects in Pt(II) chemistry, one should not choose Cl^- and NH_3 as test nucleophiles because their nucleophilicities are almost identical and one would not see much entering or leaving group effect. This scale works well for Pt(II) reactions, but is at best a qualitative indicator for other metals and not even that for the first-row transition-metal ions.

3.5.1.4 Gutmann Donor Numbers

This scale defines the donor number, DN , of a Lewis base as equal to $-\Delta H_{\text{rxn}}^{\circ}$ (kcal mol⁻¹) for its reaction with 10^{-3} M SbCl_5 in a dichloroethane solution.^{43,44} The larger the DN the stronger the base, therefore the stronger the nucleophile. The scale has been expanded to include acceptor numbers, AN ,⁴⁵ for Lewis acids. Some donor numbers are given in Table 3.4.

This donor number scale is widely referenced in relation to thermodynamic properties,⁴⁶ as well as electron-transfer kinetics⁴⁷ and photochemical properties.⁴⁸ It has been criticized because of the neglect of solvent effects and side reactions that contribute to $\Delta H_{\text{rxn}}^{\circ}$ and because a one-parameter scale can never be entirely adequate. Ambiguities can arise for solvents which have more than one donor site, such as the formamide and sulfoxide derivatives. Recent measurements⁴⁹ with BF_3 as the acid have provided some points of comparison and criticism for the original donor numbers. Recently, Linert et al.^{50,51} have used the solvatochromic shifts of a Cu(II) complex to define donor numbers for anions in dichloromethane. They also have suggested how these values can be converted for use in other solvents through a correlation with the acceptor number of the solvent. Linert et al.⁵² have reviewed the area and provided an extensive compilation of donor numbers from calorimetric and solvatochromic shift measurements. Some anion donor numbers in dichloromethane are included in Table 3.4, and the values for anions in water are ~ 21 kcal mol⁻¹ smaller than those given.

Table 3.4. Donor Numbers (kcal mol⁻¹) for Some Solvents and Anions^a

Solvent	DN	Anion	DN
Dichloromethane	0	$\text{B}(\text{C}_6\text{H}_5)_4^-$	0
Nitromethane	2.7	BF_4^-	6.0
Benzonitrile	11.9	ClO_4^-	8.4
Acetonitrile	14.1	CF_3SO_3^-	16.9
Dioxane	14.8	NO_3^-	21.1
Propylene carbonate	15.1	CN^-	27.1
Acetone	17.0	I^-	28.9
Water	19.5	CH_3O_2^-	29.5
Ether	19.2	SCN^-	31.9
Methanol	19.1	Br^-	33.7
Tetrahydrofuran	20.0	N_3^-	34.3
Dimethylformamide	26.6	OH^-	34.9
Dimethylsulfoxide	29.8	Cl^-	36.2
Pyridine	33.1		
Piperidine	51		

^a In dichloromethane.

3.5.1.5 Drago *E* and *C* Scale

The Drago *E* and *C* scale⁵³ is based on the enthalpy change for the interaction of a Lewis acid (A) and base (B). Each acid and base is characterized by two parameters, E_A and C_A for acids and E_B and C_B for bases, and the enthalpy change for the reaction $A + B \rightarrow (A:B)$ is given by

$$-\Delta H_{\text{rxn}}^{\circ} = E_A E_B + C_A C_B \quad (3.36)$$

The parameters *E* and *C* (kcal mol^{-1})^{1/2} are determined by weighted least-squares fitting of values of $\Delta H_{\text{rxn}}^{\circ}$ for appropriate series of acids and bases. The parameters in current use are based on the reference values for I_2 of $E_A = 0.5$ and $C_A = 2.0$,⁵⁴ and a constant, *W*, that is characteristic of the acid, has been added to Eq. (3.36). The justification for this scale is that it is able to correlate a large number and range of reaction enthalpies. Some recent values of *E* and *C* are given in Table 3.5. The parameters have been expanded to include substituent constants⁵⁵ and a number of phosphines.⁵⁶

Drago has suggested that the *C* parameter is related to the covalent part of the interaction and that *E* is related to the ionic or electrostatic part. Therefore, a strong base that complexes with an acid through a largely ionic interaction will have a large E_B and probably a small C_B . These ideas are potentially useful in selecting appropriate nucleophiles for mechanistic tests, but have not been widely used. There have been applications to heterogeneous adsorption and catalysis,⁵⁷ oxidative-addition kinetics and other organometallic reactions⁵⁸ and to electron-exchange kinetics.⁵⁹

Recently, Hancock and Martell⁶⁰ have developed *E* and *C* values for metal ions and ligands in aqueous solution. These are based on the assumption that aqueous F^- has $E_B = 1.0$ and $C_B = 0$. Values of the logarithm of the first complex formation constant are fitted to a model analogous to Eq. (3.36) with an additional steric term of $-D_A D_B$.

Table 3.5. *E* and *C* Values (kcal mol^{-1})^{1/2} for Representative Acids and Bases

Acid	E_A	C_A	Base	E_B	C_B
I_2	0.50	2.00	NH_3	2.31	2.04
C_6H_5OH	2.27	1.07	$N(CH_3)_3$	1.21	5.61
C_6H_5SH	0.58	0.37	C_3H_5N	1.78	3.54
H_2O	1.31	0.78	$NCCH_3$	1.64	0.71
$B(CH_3)_3$	2.90	3.60	$O=C(C_6H_5)_2$	2.01	0.55
$Al(CH_3)_3$	8.66	3.68	$O=S(CH_3)_2$	2.40	1.47
$Ga(CH_3)_3$	6.95	1.48	$O=P(C_6H_5)_3$	2.59	1.67
$Cu(hfac)_2$	1.82	2.86	$P(CH_3)_3$	0.31	5.51
$[Rh(COD)Cl]_2$	2.43	2.56	$P(C_6H_5)_3$	0.70	3.05

3.5.1.6 Solvent Property Scales

There have been a number of attempts to develop solvent parameter scales that could be used to correlate thermodynamic and kinetic results in terms of these parameters. Gutmann's Donor Numbers, discussed previously, are sometimes used as a solvent property scale. Kamlet and Taft and co-workers⁶¹ developed the solvatochromic parameters, α_1 , β_1 and π^* that are related to the hydrogen bonding acidity, basicity and polarity, respectively, of the solvent. Correlations with these parameters also use the square of the Hildebrand solubility parameter, $(\delta_H)^2$, that gives the solvent cohesive energy density. Parameters for some common solvents are collected in Table 3.6.

A thermochemical scale of hydrogen bond basicity has been proposed based on the differences in the heats of solution, $\delta(\Delta H^\circ)$, of pyrrole, *N*-methylpyrrole, benzene and toluene.⁶² The thermochemical scale correlates well with the β_1 parameter of Kamlet and Taft, with the exception of dioxane and especially of triethylamine. The correlation gives a value for water of $\beta_1 \approx 0.2$, while interpolation of hydrogen abstraction rates⁶³ has given a value of 0.31.

The Reichardt E_T^N scale provides another set of parameters that are related to solvent polarity and basicity.⁶⁴ This parameter has been used to correlate the properties and reactivity of $\text{Co}(\text{CO})_3(\text{L})_2$ systems.⁶⁵

Drago⁶⁶ has proposed a "unified scale of solvent polarities" based on an extension of the *E* and *C* acid and base parameters discussed above. Each solvent is characterized by a parameter *S'*, and the change in some property, $\Delta\chi$, of a probe system is given by $\Delta\chi = PS' + W$, where *P* and *W* are constants for the probe. If the probe is an acceptor (Lewis acid) in a donor solvent, then

$$\Delta\chi = E_A^*E_B + C_A^*C_B + PS' + W \quad (3.37)$$

where E_A^* and C_A^* are constants for the acceptor probe and E_B and C_B are the solvent values, such as those in Table 3.5. If the probe is a donor (Lewis base), then

$$\Delta\chi = E_A'E_B^* + C_A'C_B^* + PS' + W \quad (3.38)$$

where E_A' and C_A' are solvent acid parameters determined by Drago and co-workers, with some examples given in Table 3.6. The E_B^* and C_B^* are determined by fitting $\Delta\chi$ values for the probe system to Eq. (3.38).

The range of applicability and relationships between the various scales are the subject of several publications.^{64,67,68} A meaningful correlation requires that a reasonable range of parameters has been explored. The actual significance of the correlation remains a matter of interpretation which, in turn, depends on the chemical characteristics of the system.

Table 3.6. Measures of Hydrogen Bond Basicity for Some Common Solvents

Solvent	$(\delta_H)^2$	α_1	β_1	π^*	E'_A	C'_A	S'
Benzene	0.838	0	0.1	0.59			1.73
Acetone	1.378	0.08	0.48	0.71			2.58
CCl ₄	0.738	0	0	0.28			1.49
CHCl ₃	0.887	0.44	0	0.58	1.56	0.44	1.74
CH ₂ Cl ₂	0.977	0.30	0	0.82	0.86	0.11	2.08
EtOH	1.621	0.83	0.77	0.54	1.33	1.23	2.80
MeOH	2.052	0.93	0.62	0.60	1.55	1.59	2.87
THF	0.864	0	0.55	0.58			2.08
Et ₂ O	0.562	0	0.47	0.27			1.73
Dioxane	1.00	0	0.37	0.55			1.93
H ₃ CNO ₂	1.585	0.22	0.25	0.85			3.07
DMSO	1.688	0	0.76	1.00			3.0
DMF	1.389	0	0.69	0.88			2.8
DMA	1.166	0	0.76	0.88			2.70
CH ₃ CN	1.378	0.19	0.37	0.75			3.0
C ₆ H ₅ CN	1.229	0	0.37	0.90			2.63
Prop carb				0.83			3.1
H ₂ O	5.49	1.17	0.47	1.09	1.91	1.78	3.53

3.5.1.7 Hard and Soft Acid–Base Theory

This terminology was first proposed by Pearson,⁶⁹ and the basic idea is related to the earlier separation of metal ions into (a) and (b) classes as suggested by Arhland et al.⁷⁰ Acids and bases were qualitatively classified by Pearson as "soft", "hard" or "borderline". Soft acids and bases were suspected of using covalent bonding in their interactions and hard species of using predominantly ionic forces. The rule of thumb is that *hard acids interact most strongly with hard bases and soft acids interact most strongly with soft bases*.

The following selection gives a general idea of the types of hard and soft acids and bases:

Hard Acids: H⁺, Li⁺, Mg²⁺, Cr³⁺, Co³⁺, Fe³⁺

Soft Acids: Cu⁺, Ag⁺, Pd²⁺, Pt²⁺, Hg²⁺, Tl³⁺

Borderline: Mn²⁺, Fe²⁺, Zn²⁺, Pb²⁺

Hard Bases: F⁻, Cl⁻, H₂O, NH₃, OH⁻, H₃CCO₂⁻

Soft Bases: I⁻, CO, P(C₆H₅)₃, C₂H₄, H₅C₂SH

Borderline: N₃⁻, C₅H₅N, NO₂⁻, Br⁻, SO₃²⁻

To answer the criticism that this scale is purely qualitative, Pearson⁷¹ has attempted to establish a quantitative scale of hardness and softness based on ionization potentials, I , and electron affinities, A . The absolute hardness is defined as $\eta = (I - A)/2$, softness as $\sigma = 1/\eta$, and the absolute electronegativity uses Mulliken's definition of $\chi = (I + A)/2$. For an interaction between a Lewis acid (1) and base (2), the strength of the interaction is assumed to be related to the fractional electron transfer, given by $\Delta N = (\chi_1 - \chi_2)/2(\eta_1 + \eta_2)$. These results are too recent to have been tested, except to note that the quantitative scale generally conforms to the ideas of practicing chemists. Pearson has compiled an extensive list of hardness values and a few examples are given in Table 3.7. More recently, Ayers⁷² has analysed the hard/soft approach from first principles and revealed some of the conditions under which it might not work, and the fact that the main driving force is electron transfer from base to acid.

3.5.1.8 Summary

None of these scales has received universal acceptance by inorganic chemists, and it may be that the heterogeneity of the field will defy anyone to establish a truly general scale. As yet, there seems to be nothing as widely applicable as the Hammett and Taft parameters in organic chemistry. Within certain areas and types of applications, one finds one of these scales more often used than others, presumably because it has proven more successful in correlating information.

It has been recognized that a two-parameter scale is necessary, in general, to correlate solvent basicity.^{73,74} The conditions under which a one-parameter correlation may appear to work have been discussed by Drago.⁷⁵

Table 3.7. Absolute Electronegativity, χ , and Hardness, η , Values (eV)

Acid	χ	η	Base	χ	η
Cr ²⁺	23.73	7.23	F ⁻	10.41	7.01
Mn ²⁺	24.66	9.02	Cl ⁻	8.31	4.70
Fe ²⁺	23.42	7.24	Br ⁻	7.60	4.24
Co ²⁺	25.28	8.22	I ⁻	6.76	3.70
Zn ²⁺	28.84	10.88	OH ⁻	7.50	5.67
Fe ³⁺	42.73	12.08	H ₂ O	3.1	9.5
Ru ³⁺	39.2	10.7	NH ₃	2.6	8.2
Os ³⁺	35.2	7.5	C ₅ H ₅ N	4.4	5.0
Co ³⁺	42.4	8.9	CH ₃ CN	4.7	7.5
Cr ³⁺	40.0	9.1	(CH ₃) ₂ O	2.0	8.0
Pd ²⁺	26.18	6.75	(CH ₃) ₃ P	2.8	5.9
Pt ²⁺	27.2	8.0	(CH ₃) ₂ NCHO	3.4	5.8

In mechanistic studies, it is common to fall back on qualitative information relating to the particular metal or nonmetal center. After working with particular types of compounds, a lore develops about what are good, not-so-good and poor nucleophiles. Sometimes, it is recognized that this correlates with one of the basicity scales. It can be of special interest when a particular system or class of ligands fails to follow a reasonably established correlation. This may point to some factor that was overlooked and may provide some mechanistic insight.

3.5.2 Linear Free-Energy Relationships

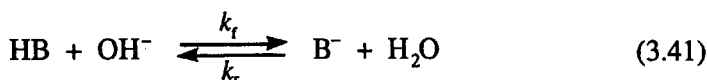
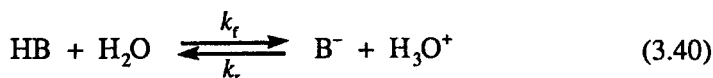
This general area, known as LFER, has been reviewed recently by Linert.⁷⁶ For a simple reaction, the equilibrium constant and the forward and reverse rate constants are related by $K_e = k_f/k_r$, therefore

$$\log(k_f) = \log(K_e) + \log(k_r) \quad (3.39)$$

If a reaction has dissociative activation and one varies the nature of the leaving group X while keeping the entering group Y constant, then k_f should be constant and a plot of $\log(k_f)$ versus $\log(K_e)$ should be linear with a slope of +1. For associative activation, the same type of experiments should have a constant k_r and a plot of $\log(k_r)$ versus $\log(K_e)$ should be linear with a slope of -1.

This type of analysis has been applied to the aquation of $(\text{H}_3\text{N})_5\text{Co}^{\text{III}}\text{—X}$ complexes^{77,78} with the conclusion that the mechanism is I_a . The LFER for $(\text{H}_3\text{N})_5\text{Cr}^{\text{III}}\text{—X}$ and $(\text{H}_2\text{O})_5\text{Cr}^{\text{III}}\text{—X}$ indicates an I_a mechanism.⁷⁹

Proton transfer reactions generally satisfy a LFER. Although they are not directly related to ligand substitution processes, proton transfer steps are often involved and usually treated as rapidly maintained equilibria:



For reactions such as (3.40), the reverse rate constant is essentially diffusion limited so that k_r is fairly constant at $\sim 5 \times 10^{10} \text{ M}^{-1} \text{ s}^{-1}$ (see p 27). However, if there are significant structural and bonding differences between HB and B^- , as with carbon acids, then k_f may be smaller. For a normal acid, with an acid dissociation constant K_a , one can calculate that $k_f \approx 5 \times 10^{10} K_a$. Note that, if K_a is small (e.g., 10^{-10} M), then k_f can be rather modest and could become rate limiting for a subsequent process that consumes B^- . The same analysis applies to reactions such as (3.41), where $k_f \approx 2 \times 10^{10} \text{ M}^{-1} \text{ s}^{-1}$.

3.5.3 Reagent Charge Effects

It is often possible to change the net charge on a metal complex by changing the "nonreacting" ligands (e.g., $\text{Pt}(\text{Cl})_4^{2-}$, $\text{Pt}(\text{NH}_3)(\text{Cl})_3^-$, $\text{Pt}(\text{NH}_3)_2(\text{Cl})_2$, etc.). The variation of substitution rate constant with charge appears to give a clear distinction between associative and dissociative activation. Increasing positive charge on the metal complex should favor bonding to the entering nucleophile and therefore increase the rate of an I_a process, whereas the opposite would be expected for an I_d process.

Unfortunately, when the charge is changed the ligands must change, and these types of studies can be difficult to interpret. For the Pt(II) examples noted above, other evidence indicates an I_a mechanism, but there are only minor differences⁸⁰ in the aquation rates. It can be argued that the increasing positive charge increases the bonding to the entering group but has a similar effect on the leaving group, and the effects tend to cancel.

3.5.4 Solvent Dielectric Constant Effects

In organic systems, an increase of rate with increasing dielectric constant of the solvent is associated with the formation of an electrically polar transition state. The situation is more complex with inorganic systems where the metal complex and the leaving and entering groups are often charged, and one must consider both desolvation of the reactants and solvation of the transition state. The dielectric constant of the solvent also has a substantial influence on the formation of ion pairs that may affect the apparent reactivity. A further complication is that the solvent may be a potential ligand and therefore part of the reacting system, rather than just a reaction medium. As a result, the effect of solvent variation on the rate has not been a generally useful criterion for mechanism. More commonly, such observations are used to assess the solvent effect, when the mechanism is thought to be known, and to test this variation for various theoretical models.

In a study more related to an organic chemistry type of application, Rerek and Basolo⁸¹ attempted to use the variation in rate constant with the dielectric constant of the solvent to differentiate between the following possible rhodium intermediates:

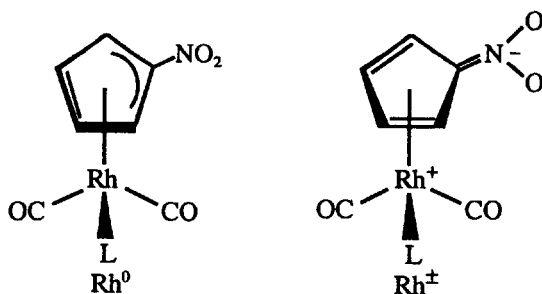


Table 3.8. Variation of the Rate Constant (25°C) with the Dielectric Constant of the Solvent for the Reaction of $\text{Rh}(\eta^5\text{-C}_5\text{H}_4\text{NO}_2)(\text{CO})_2$ with PPh_3

Solvent	ϵ	k ($\text{M}^{-1} \text{s}^{-1}$)	Solvent	ϵ	k ($\text{M}^{-1} \text{s}^{-1}$)
Hexane	1.88	4.44	Dichloromethane	8.93	2.81
Cyclohexane	2.02	3.92	Methanol	32.7	10.4
Toluene	2.38	1.26	Acetonitrile	38.8	9.58
Tetrahydrofuran	7.58	0.963			

Clearly, the Rh^+ intermediate is more polar and should be favored by solvents with higher dielectric constants. The observations are given in Table 3.8. The authors favor the Rh^+ intermediate on the basis of a comparison of the rate constants in THF and methanol. But when the data are presented as in Table 3.8, it could be argued that the solvents in the left-hand column show an inverse dependence of k on ϵ and favor Rh^0 , whereas the solvents in the right-hand column might be going through a solvent-coordinated intermediate with methanol being the most strongly coordinating ligand.

In a system discussed later, Wax and Bergman⁸² used a series of methyl-substituted tetrahydrofurans to test for the involvement of coordinated solvent in the "intermediate" formed after ligand dissociation. These solvents were presumed to have similar dielectric constants so that reactant pre-association would be constant and any kinetic effect would be due to changes in solvent coordination to the intermediate.

As shown in Table 3.1, the solvent dielectric constant can be expected to have a significant effect on reactions involving ion pairing. Tobe and co-workers⁸³ found that $[\text{Pt}(\text{Me}_4\text{en})(\text{DMSO})\text{Cl}]\text{Cl}$ is ~100 times more reactive in CHCl_3 or CH_2Cl_2 than in water or methanol because of complete ion pairing in the former solvents. Moreover, the reactivity is enhanced further if $[\text{Ph}_4\text{As}]\text{Cl}$ is added, due to ion triplet formation. More recently, there have been increasing efforts to determine the structures of ion pairs using NMR.⁸⁴ Brasch et al.⁸⁵ used this method to show that the Cl^- ion is adjacent to the leaving group OH_2 in the $[\text{Co}(\text{tren})(\text{NH}_3)(\text{OH}_2)\cdot\text{Cl}]^{2+}$ ion pair in DMSO.

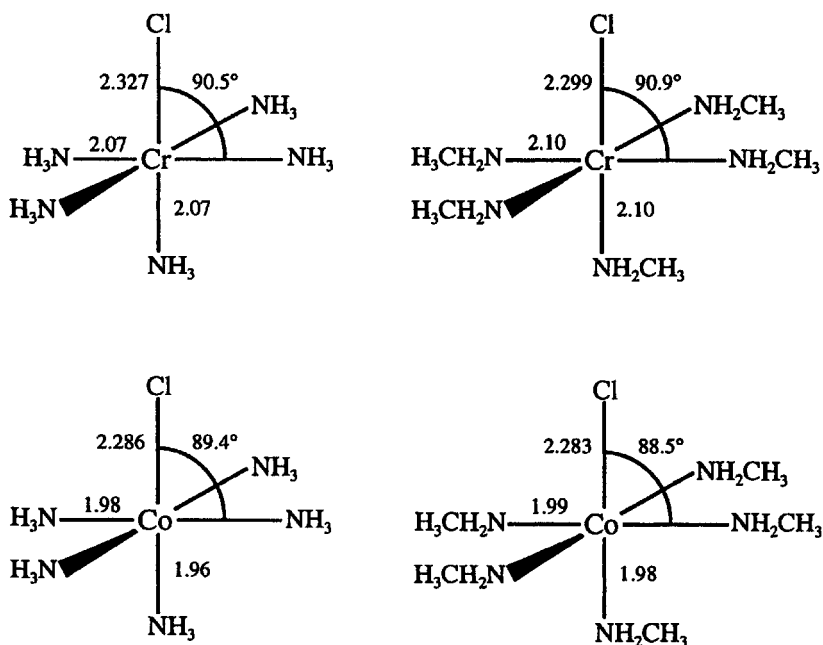
3.5.5 Steric Effects

Changes in the steric bulk of the nonreacting ligands appear to provide a clear distinction between I_d and I_a mechanisms. Increased steric bulk of the ligands should enhance an I_d mechanism by pushing the dissociating ligand away and relieving steric strain. On the other hand, it should make bonding with the entering group more difficult and inhibit an I_a mechanism. This is perhaps the most successful method of distinguishing these mechanisms, but there are some difficulties.

Table 3.9. Rate Constants (25°C) and Activation Parameters for the Aquation of Ammonia and Methylamine Complexes of Co(III) and Cr(III)

	$10^6 \times k$ (s ⁻¹)	ΔH^\ddagger (kJ mol ⁻¹)	ΔS^\ddagger (J mol ⁻¹ K ⁻¹)	ΔV^\ddagger (cm ³ mol ⁻¹)
Co(NH ₃) ₅ Cl ²⁺	1.72	93	-44	-9.9
Co(NH ₂ CH ₃) ₅ Cl ²⁺	39.6	95	-10	-2.3
Cr(NH ₃) ₅ Cl ²⁺	8.70	93	-29	-10.6
Cr(NH ₂ CH ₃) ₅ Cl ²⁺	0.26	110	-2	+0.5

Parris and Wallace⁸⁶ studied the aquation of M(NH₃)₅Cl²⁺ and M(NH₂CH₃)₅Cl²⁺ with M = Co and Cr; the kinetic results of this and later work⁸⁷ by van Eldik and co-workers are summarized in Table 3.9. The original interpretation was that the introduction of the CH₃ group increases *k* for Co(III), consistent with an I_a mechanism, whereas *k* decreases for Cr(III), as expected for an I_a mechanism. This view has persisted for some time and caused many other types of information to be interpreted in a way consistent with this kinetic pattern for these two metal ions. Over the years, structural information has been accumulating and this has been analyzed by Lay.⁸⁸ The structures of the metal complexes are shown in Figure 3.3.

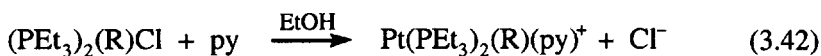
**Figure 3.3.** Structural parameters of some Cr(III) and Co(III) amine complexes.

There are two structural features of note. First, the bond lengths to Co(III) are all shorter than those to Cr(III); this is a general feature and has been part of the rationalization that the mechanisms are different for these two metal ions. Second, the M—Cl bond is actually 0.03 Å shorter in $\text{Cr}(\text{NH}_2\text{CH}_3)_5\text{Cl}^{2+}$ than in $\text{Cr}(\text{NH}_3)_5\text{Cl}^{2+}$; this is opposite to what would have been predicted on steric grounds. Lay's interpretation of the structural and kinetic results is that all these systems are reacting by a common I_d mechanism. The $\text{Cr}(\text{NH}_2\text{CH}_3)_5\text{Cl}^{2+}$ reacts more slowly because of the shorter, and presumably stronger, Cr—Cl bond compared to the NH_3 complex.

Overall, there is little evidence for steric strain in either of the NH_2CH_3 systems, and the nearly 90° bond angles confirm this impression. The $\text{Co}(\text{NH}_2\text{CH}_3)_5\text{Cl}^{2+}$ is more reactive than $\text{Co}(\text{NH}_3)_5\text{Cl}^{2+}$ because the ΔS^\ddagger is larger by $34 \text{ J mol}^{-1} \text{ K}^{-1}$ and not because the ΔH^\ddagger is smaller, as would have been expected if steric effects made the Co—Cl bond weaker in $\text{Co}(\text{NH}_2\text{CH}_3)_5\text{Cl}^{2+}$. Lay has suggested that the entropic difference is due to less effective solvation of the methylamine complex. The general conclusion is that if one is probing steric effects, one must be sure that the expected effects are present in the ground-state reactants if that state is assigned as the source of the reactivity differences.

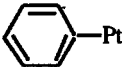
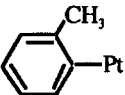
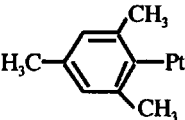
Interest in these systems has continued with the focus on neutral leaving groups, X, in $\text{M}(\text{NH}_2\text{R})_5\text{X}^{3+}$ complexes ($\text{M} = \text{Cr}, \text{Co}, \text{Rh}$; $\text{R} = \text{H}, \text{CH}_3$). The results have been summarized by Gonzalez et al.,⁸⁹ whose mechanistic conclusions are based on the ΔV^\ddagger values rather than on the nonreacting ligand effects. A hint as to the effect of the NH_2CH_3 ligand comes from the work of Benzo et al.⁹⁰ on $\text{Co}(\text{NH}_2\text{CH}_3)(\text{NH}_3)_4(\text{DMF})^{3+}$ complexes with DMF as the leaving group. When compared to $\text{Co}(\text{NH}_3)_5(\text{DMF})^{3+}$, the complex with one *trans*- NH_2CH_3 is 4 times more reactive, while that with one *cis*- NH_2CH_3 is only 1.5 times more reactive. In addition, the ΔV^\ddagger for the *trans* isomer is $10 \text{ cm}^3 \text{ mol}^{-1}$ larger than for the *cis* isomer, suggesting that *trans*- NH_2CH_3 strongly promotes dissociative behavior. The greater effect of the *trans*- NH_2CH_3 is inconsistent with steric arguments and seems more indicative of increased electron donation to Co(III) from NH_2CH_3 compared to NH_3 . The trend towards more dissociative character with NH_2CH_3 present could be ascribed to better stabilization of the intermediate and would be an example of the kinetic *trans* effect, described later in Section 3.6.2.2.

In a somewhat different use of steric effects, Basolo et al.⁹¹ studied reaction (3.42) with various R groups, and the results are shown in Table 3.10.



The trend of decreasing rate constant with increasing steric bulk of R with both isomers is consistent with associative activation on these square

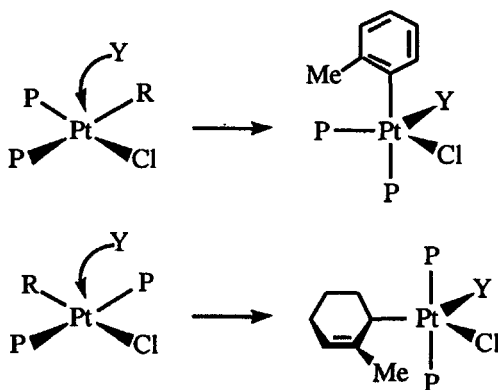
Table 3.10. Rate Constants for Replacement of the Chloro Ligand by Pyridine in Pt(PEt₃)₂(R)Cl

R—Pt	k (M ⁻¹ s ⁻¹)	
	trans (25°C)	cis (0°C)
	1.2×10 ⁻⁴	8×10 ⁻²
	1.7×10 ⁻⁵	2×10 ⁻⁴
	3.4×10 ⁻⁶	1×10 ⁻⁶ (25°C)

planar Pt(II) complexes. However the cis isomer is much more sensitive to the steric effect (note the temperature difference for the last cis entry in Table 3.10).

The larger effect on the cis isomer can be rationalized by a trigonal bipyramidal intermediate, with the entering group Y and the leaving group Cl⁻ occupying equivalent positions in the trigonal plane in order to satisfy microscopic reversibility, as shown in Scheme 3.2, where R is *o*-MeC₆H₅.

Scheme 3.2

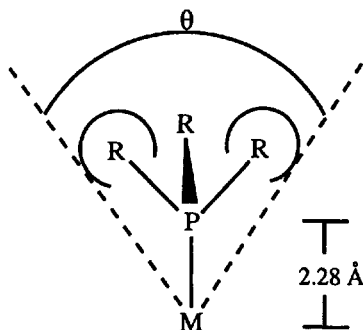


The R group in the axial position in the transition state for the cis isomer will cause more steric crowding than when it is in the equatorial position in the transition state for the trans isomer.

3.5.6 Measures of Ligand Size

The problem in interpreting the "steric" effects in the ammonia and methylamine complexes of Co(III) and Cr(III) might have been avoided if there were some method of estimating the sizes of the ligands and therefore anticipating whether steric effects were really significant in a particular system.

The systematic efforts in this regard originate with the work of Tolman⁹² on phosphine and phosphite ligands. Tolman defined a *cone angle*, θ , for a number of phosphines, PR_3 , based on the following diagram, with the size of the R substituents based on van der Waals radii from CPK models. Seligson and Trogler⁹³ have used the same methodology to determine cone angles for amines.

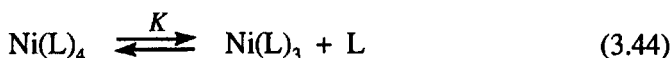


For unsymmetrical ligands $\text{P}(\text{R})(\text{R}')(\text{R}'')$, the angle is calculated by

$$\theta = \frac{2}{3} \sum_{i=1}^3 \frac{\theta_i}{2} \quad (3.43)$$

where θ_i are the cone angles for the symmetrical phosphines.

The original definition chose an M—P distance based on Ni(0) chemistry and applied the steric size of the ligands to correlate equilibrium constant data for the following reaction:



The original definitions have been criticized and examined by DeSanto et al.⁹⁴ Values for ligands with flexible arms, such as $\text{P}(\text{Et})_3$ and $\text{P}(\text{OMe})_3$, have been modified by Stahl et al.⁹⁵ and by Smith et al.⁹⁶ In addition, Maitlis⁹⁷ and Coville et al.⁹⁸ have given cone angles for cyclopentadienyl and arene ligands.

More recently, Brown and co-workers have used molecular mechanics calculations to estimate a steric repulsion energy, E_R , for phosphines and other ligands on $\text{Cr}(\text{CO})_3\text{L}$ ⁹⁹ and $\text{Rh}(\text{Cp})(\text{CO})\text{L}$.¹⁰⁰

Table 3.11. Representative Electronic and Steric Parameters

Ligand	pK_a^a	δ (ppm) ^b	Cone Angle ^c	E_R^c (kcal mol ⁻¹)
P(OMe) ₃	2.6	3.18	107 (117, 130) ^d	52
P(OEt) ₃		3.61	109 (134) ^d	59
PMe ₃	8.65	5.05	118	39
PPhMe ₂	6.5	4.76	122	44
P(OPh) ₃	-2.0	1.69	128	65
PEt ₃	8.69	5.54	132 (137) ^d	61
PPh ₂ Me	4.57	4.53	136	57
PPh ₃	2.73	4.30	145	75
P(CH ₂ Ph) ₃	(6.0)	3.98	165	82
P(C ₆ H ₁₁) ₃	9.7	6.32	171	116
P(C ₆ H ₄ <i>o</i> -Me) ₃	3.08	3.67	194	113
AsMe ₃		4.46	114	27
AsPh ₃		4.16	141	44

^a Reference 104. ^b Reference 103. ^c Reference 100. ^d References 95 and 96.

Some cone angle and E_R values are given in Table 3.11. The strengths and weaknesses of various approaches to steric parameters have been the subject of several reviews.^{101,102}

Since the original application, cone angles have been the basis for many attempts to correlate reactivity and steric effects. A complication in such applications is the separation of the steric and bonding or electronic effects when a ligand is changed. The electronic effect often is assumed to parallel the ligand basicity, as measured by the pK_a or by the effect on the ¹³C NMR chemical shift in Ni(CO)₃L.¹⁰³ Some of these values also are given in Table 3.11. Steric effect studies should involve systems with reasonably constant electronic factors.

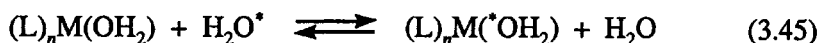
A typical analysis, including electronic effects, is given by Giering and co-workers,¹⁰⁴ who emphasize the fact that steric effects can be minimal below a certain threshold of cone angle. The effects become significant when the sum of the cone angles for two adjacent ligands causes the ligands to come into contact.

3.5.7 Volumes of Activation

This type of information has been discussed with regard to the **D** and **A** mechanisms, and the expectations for **I_d** and **I_a** are qualitatively similar. For the **I_d** mechanism, the prediction is that the activation volume, ΔV^\ddagger , will be positive because the leaving group is being liberated into solution while there has been relatively little bonding to the entering group. On the other hand, for an **I_a** mechanism, the ΔV^\ddagger will be negative because the entering group has been captured from solution while the leaving group is

still bonded to the metal center. Much of the literature bases the mechanistic differentiation on the sign (+ or -) of ΔV^\ddagger . It seems more correct to say that for a family of related reactions, those with a more positive ΔV^\ddagger are more dissociative and those with a more negative ΔV^\ddagger are more associative. Further aspects of ΔV^\ddagger are discussed in section 3.7.3 later in this chapter and in several comprehensive reviews.¹⁰⁵

Values of ΔV^\ddagger for the following exchange reaction with $M = \text{Cr, Co and Rh,}^{106,107} \text{Ru,}^{108,109} \text{Ir}^{110,111}$ and Pt^{112} are given in Table 3.12.



The simplest explanation of this data is that the intimate mechanism involves more bond making to the entering H_2O as the ΔV^\ddagger becomes more negative, but it is *not* necessary that the mechanism changes if the ΔV^\ddagger changes sign. For $\text{Ru}(\text{OH}_2)_6^{2+}$, $\Delta V^\ddagger = -0.4 \text{ cm}^3 \text{ mol}^{-1}$, but the ligand substitution rates are consistent with an I_d mechanism.¹¹³ There is considerable other evidence that substitution on $\text{Pt}(\text{II})$ has an I_a mechanism, but the water exchange reaction may show less bond making than usual because $\text{Pt}(\text{II})$ is a soft acid and water is a hard base. It would be of great value to be able to predict the ΔV^\ddagger for a particular mechanism, but this has proven to be complicated because of solvent electrostriction effects. As the leaving group emerges, polar solvents will constrict around the $(\text{L})_5\text{M}^{3+}$ fragment as its charge density increases and may do likewise around the leaving group if it can be strongly solvated; these factors are difficult to anticipate quantitatively. Such effects might account for the tendency of ΔV^\ddagger to be more negative for the $(\text{L})_5\text{M}^{3+}$ systems when $\text{L} = \text{H}_2\text{O}$. Recent theory¹¹⁴ suggests that the effect is $<2 \text{ cm}^3 \text{ mol}^{-1}$ for water exchange on $\text{Rh}(\text{OH}_2)_6^{3+}$ and $\text{Ir}(\text{OH}_2)_6^{3+}$.

Table 3.12. Volumes and Entropies of Activation for Some Water Exchange Reactions

$(\text{L})_n\text{M}$	$\Delta V^\ddagger (\text{cm}^3 \text{ mol}^{-1})$	$\Delta S^\ddagger (\text{J mol}^{-1} \text{ K}^{-1})$
$(\text{H}_3\text{N})_5\text{Co}^{3+}$	+1.2	28
$(\text{H}_3\text{N})_5\text{Rh}^{3+}$	-4.1	3
$(\text{H}_2\text{O})_6\text{Rh}^{3+}$	-4.2	29
$(\text{H}_3\text{N})_4\text{Ir}^{3+}$	-3.2	11
$(\text{H}_2\text{O})_6\text{Ir}^{3+}$	-5.7	2.1
$(\text{H}_3\text{N})_5\text{Cr}^{3+}$	-5.8	0
$(\text{H}_2\text{O})_6\text{Cr}^{3+}$	-9.6	11.6
$(\text{H}_3\text{N})_5\text{Ru}^{3+}$	-4.0	-7.7
$(\text{H}_2\text{O})_6\text{Ru}^{3+}$	-8.3	-48.3
$(\text{H}_2\text{O})_6\text{Ru}^{2+}$	-0.4	16.1
$(\text{H}_2\text{O})_6\text{Pt}^{2+}$	-4.6	-9

3.5.8 Entropies of Activation

It is generally expected that an I_d mechanism will have a more positive entropy of activation, ΔS^\ddagger , than an I_a mechanism because of the increase in randomness in an I_d transition state, compared to a decrease in randomness in an I_a transition state. This criterion has been used cautiously and only for comparisons of similar reaction types. One reason for caution is the experimental error in ΔS^\ddagger , which is typically ± 8 to $12 \text{ J mol}^{-1} \text{ K}^{-1}$. It was thought that ΔV^\ddagger would have an advantage over ΔS^\ddagger as a mechanistic criterion because of the better accuracy and our better intuitive understanding of volume changes. However, ΔS^\ddagger has a larger range of values than ΔV^\ddagger and this tends to offset the problem of experimental uncertainty. There is some evidence of a correlation between ΔS^\ddagger and ΔV^\ddagger ,¹¹⁵ which could make accurate ΔS^\ddagger values of greater mechanistic importance. There is some indication of such a correlation in Table 3.12 for the systems with $(L)_n = (\text{NH}_3)_5$, but the $(\text{H}_2\text{O})_n$ systems are different, possibly because of the usual scapegoat of solvation differences.

3.6 SOME SPECIAL EFFECTS

3.6.1 Dissociative Conjugate Base Mechanism

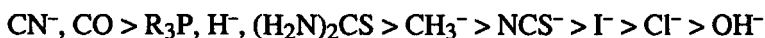
The dissociative conjugate base, DCB, mechanism has been described previously in connection with competition studies for a **D** mechanism (Scheme 3.1). In its original form, it involved the reaction of hydroxide ion with amine complexes of Co(III). It occupies a special place in inorganic mechanistic work because it was the subject of a long controversy during the 1960s between Ingold, Nyholm and Tobe, who favored a simple bimolecular displacement (S_N2) of the leaving group by hydroxide ion, and Basolo and Pearson, who favored the S_N1CB (DCB) mechanism originally proposed by Garrick.¹¹⁶ This controversy stimulated a lot of kinetic work and generated many useful spin-offs in the areas of synthesis, spectroscopy and theory.

In the final analysis, the DCB mechanism has passed every test so far applied and is now the accepted mechanism for these reactions. The results leading to these conclusions are summarized in several articles.^{21,117-119}

The DCB mechanism has received an amount of attention quite out of proportion to its general importance, since it is less effective for amine complexes of M(III) ions other than Co(III). This may be due to the small size of low-spin Co(III) and its ability to stabilize the dissociative intermediate through π bonding. It is interesting to note that a Co(III) complex with no ionizable amine protons has been found to undergo base catalysed hydrolysis by ionization of a methylene group α to pyridine in the chelate backbone. Jackson and co-workers¹²⁰ propose that the negative charge is delocalized to the pyridine N to activate the Co(III).

3.6.2 Trans Effect

It is well documented that the ligand in the position trans to the leaving group has a significant influence on the rate of substitution reactions. This effect has been most thoroughly studied in Pt(II) chemistry, where the ordering of trans labilization is

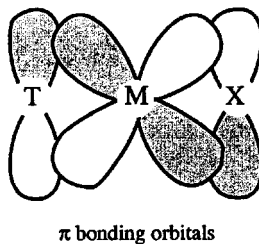
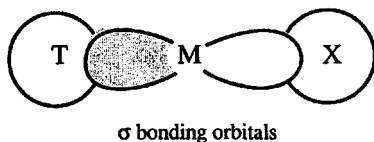


The sources of the trans effect are commonly separated into two factors. The weakening of the bond to the leaving group by the trans ligand in the ground state of the reactant is now called the trans influence, or the thermodynamic trans effect. It can be assessed by structural, spectroscopic and thermodynamic properties of the reactant. The kinetic factor relates to the stabilization of the transition state by the trans ligand and is referred to here as the kinetic trans effect. It is determined from the kinetic properties of the system.

3.6.2.1 Trans Influence or Thermodynamic Trans Effect

Structural evidence for this effect has been summarized in several reviews.¹²¹ The bond length changes generally are not dramatic. For example, the Pt—Cl bond in *cis*-Pt(PR₃)₂(Cl)₂ is 0.08 Å longer than the Pt—Cl bond in *trans*-Pt(PR₃)₂(Cl)₂ although PR₃ is one of the stronger trans labilizing ligands. However, H⁻ causes trans bond lengthening of 0.15 to 0.20 Å.¹²² Evidence for the thermodynamic trans effect was obtained by Chatt et al.¹²³ from the N—H stretching frequencies in T—Pt—NHR₂ systems with various trans ligands, T. The C—O stretching frequencies and NMR chemical shifts also have been used to probe for this effect.

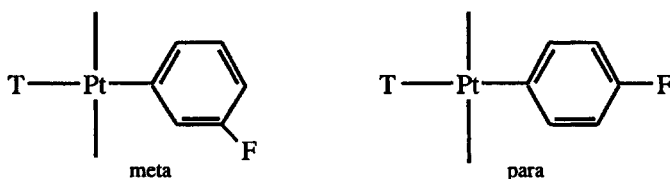
It was recognized at an early stage that, in order to rationalize the order of the ligands in the trans effect series, it would be necessary to invoke both σ - and π -bonding effects. These effects work in the ground state through the metal orbitals shared by the leaving group, X, and the trans ligand, T, as shown in the following diagrams:



The metal σ orbital is empty and both T and X donate electrons into it. If the T ligand is a stronger σ donor, then the σ bond to X will be weaker. The large trans effects of CH₃⁻ and H⁻ are directly attributed to this situation.

The metal π orbital is a filled d_{xy} , d_{xz} or d_{yz} orbital and electrons are being donated from this orbital into empty orbitals on the ligands T and X. These empty orbitals might be π antibonding on CO and CN^- or d orbitals on phosphorus-donor ligands, for example. This "back donation" strengthens the metal–ligand bond and, if T is a better π acceptor (π acid), then its bond to M will be strengthened at the expense of the M–X bond. This effect could explain the positions of CO and PR_3 in the trans effect series, since they are good π acids. However, such systems probably derive most of their reactivity from the kinetic trans effect described in the next section.

In classic studies to separate the σ and π effects, Parshall¹²⁴ studied the ^{19}F NMR chemical shifts for a series of T ligands in the following systems:

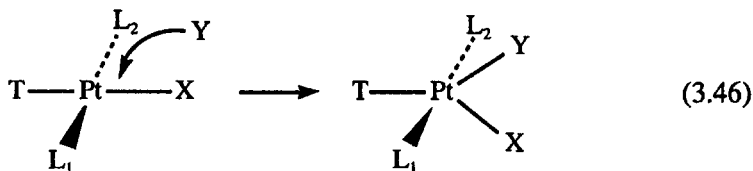


The ^{19}F shift in the meta isomer should only depend on the σ effect, but the shift in the para isomer will be sensitive to both the σ and π effects. Essentially similar NMR methods have been applied to a number of different systems. The results of these studies generally confirm the presence of both types of effects, with magnitudes consistent with expectations for different T ligands. The difficulty is that these observations do not translate easily into a direct measure of the extent of bond weakening in the ground state caused by a trans group; therefore the kinetic consequences are uncertain.

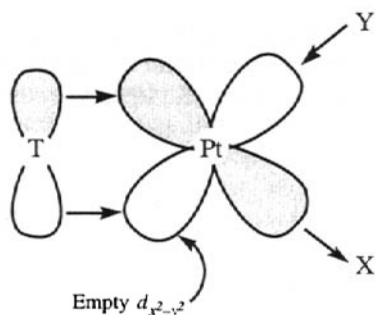
3.6.2.2 Kinetic Trans Effect

The kinetic trans effect is assumed to operate because of better bonding between M and T in the transition state. The effect can be explained pictorially, but there have been attempts at more quantitative quantum mechanical calculations. The contributions have been divided into σ and π effects.

Most explanations have taken square planar Pt(II) complexes as models because the effect is best documented for these systems and the mechanism is taken to be I_2 . The transition state is assumed to be a trigonal bipyramid, formed as follows:



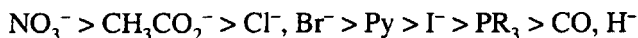
In the transition state, the T ligand is no longer sharing σ or π orbitals with the X ligand, therefore the T ligand can improve its bonding to Pt(II) if it is a good σ donor or π acceptor. This can help to offset the loss in bonding to X. In addition, the transition state can be further stabilized because the empty $d_{x^2-y^2}$ orbital on Pt(II) becomes of π symmetry and can accept π electrons from T if the latter is capable of π donation, as shown in the following diagram:



The earlier theoretical studies¹²⁵⁻¹²⁷ found a trigonal bipyramidal transition state consistent with the above qualitative description, and this has been confirmed by all subsequent calculations. Some conclusions of the recent work are as follows. In 1996, Deeth and Elding¹²⁸ reported that water exchange on $\text{Pt}(\text{OH}_2)_4^{2+}$ and $\text{Pt}(\text{Cl})_2(\text{OH}_2)_2$ proceeds by an I_a mechanism with “relatively extensive bond stretching in the transition state”, and suggested that this stretching explained the rather small ΔV^\ddagger for exchange on $\text{Pt}(\text{OH}_2)_4^{2+}$ (see Table 3.12). Cooper and Ziegler,¹²⁹ in 2002, and Burda et al.,¹³⁰ in 2004, reported that there is very little bond stretching of the nonreacting ligands in a number of reactions, including the aquation of Cl^- from $\text{cis-Pt}(\text{NH}_3)_2(\text{Cl})_2$. The transition state has substantial Pt—Cl bond breaking, and its structure is closer to that of the products. From these three studies, one is left to wonder whether these reactions have quite different mechanisms or if the theory needs further refinement.

3.6.3 Cis Effect

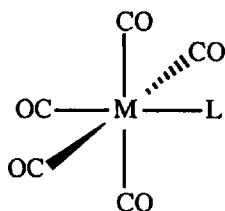
The effect of the cis ligand(s) on substitution rates has been noted especially in the chemistry of octahedral organometallic complexes. In general, the effect is less than the trans effect. The order of cis labilization for various ligands is



This ordering is almost the exact opposite of that for the trans effect. The reaction mechanism also is different in that the systems used as examples show I_a characteristics. Evidence for a ground-state effect is very limited,

as expected, because the cis ligands share only one orbital ($d_{x^2-y^2}$) of minor significance in their σ bonding. Anderson and Orpen¹³¹ have published an analysis of a number of structures which suggests some correlation between the magnitude of the cis and trans influences and the number of d and s valence electrons on the metal. The cis effect normally is attributed to stabilization of the I_d transition state by better bonding with the cis ligand. Davy and Hall¹³² have given a theoretical treatment of the cis effect for $Mn(CO)_5(L^-)$ and $Cr(CO)_5L$ systems. This approach indicates that the π -donor ability of the cis ligand is the most important feature, which is consistent with the ordering of ligands. Ligands such as nitrate and carboxylates may stabilize the intermediate by coordination of the distal oxygen.¹³³

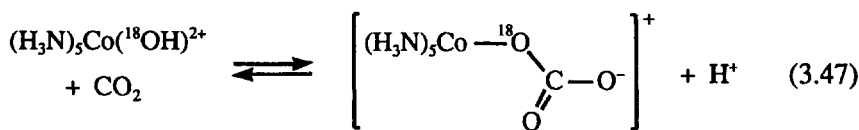
It should be remembered that for systems such as



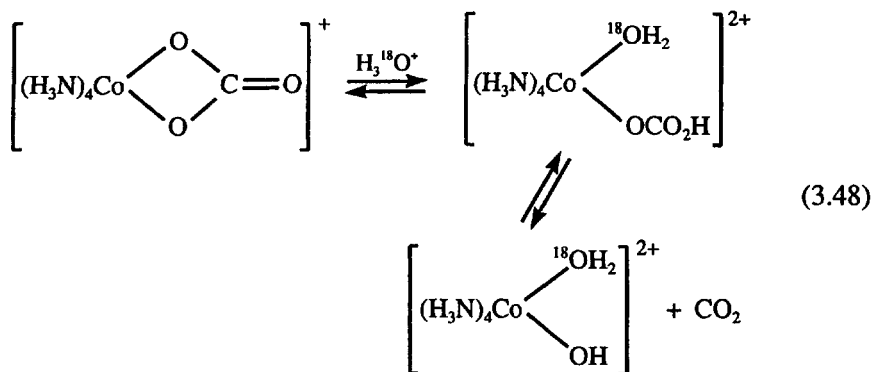
the observation is that the cis-CO ligands exchange, or are replaced more easily, than the trans one. This relative rate difference could be assigned, at least in part, to a *trans-stabilizing* influence of the L group.

3.6.4 Reactions Without Metal-Ligand Bond Breaking

Some reactions of metal complexes that appear to involve substitution may actually occur without breaking a bond to the metal. Since HCO_3^- is in equilibrium with aqueous CO_2 , reaction (3.47) could be a replacement of OH^- by HCO_3^- , but ^{18}O -labeling studies¹³⁴ show that the $Co-O$ bond is retained. The reaction is really electrophilic attack of CO_2 on the coordinated OH^- . Microscopic reversibility requires that the reverse reaction proceeds with $C-O$ bond breaking. This seems to be a general characteristic of CO_2 addition and release from such inert metal complexes. For example, it appears that $W(CO)_5(OH)$ reacts similarly with CO_2 .¹³⁵



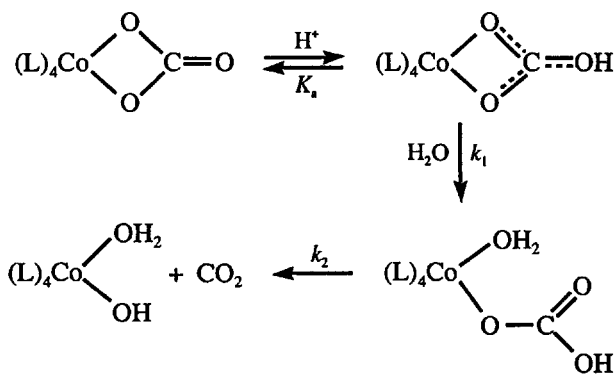
For chelated carbonate complexes, Posey and Taube¹³⁶ found that initial ring opening proceeds with $Co-O$ bond breaking, and then CO_2 is lost by $O-C$ bond breaking, as follows:



There is considerable interest in the reactions of such carbonato complexes because of their possible relevance to the action of carbonic anhydrase, and the area has been reviewed¹³⁷ and reanalysed.¹³⁸

Buckingham and Clark¹³⁹ have used multiwavelength stopped-flow and the $[\text{H}^+]$ dependence of the rate to show that these reactions are biphasic and proceed through a protonated intermediate, as shown in Scheme 3.3.

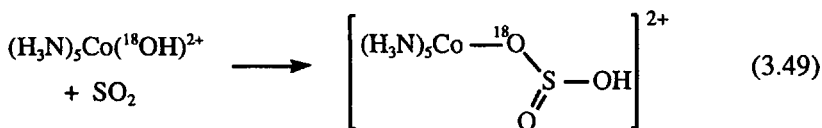
Scheme 3.3



For the various systems that were studied, such as $\text{Co}(\text{NTA})(\text{O}_2\text{CO})^{2-}$, $\text{Co}(\text{gly})_2(\text{O}_2\text{CO})^-$, $\text{Co}(\text{tren})(\text{O}_2\text{CO})^+$ and $\text{Co}(\text{NH}_3)_4(\text{O}_2\text{CO})^+$, it was found that $K_a \sim 1 \text{ M}$ and $k_2 \sim 1 \text{ s}^{-1}$ (25°C , 1.0 M NaClO_4). This insensitivity to the ancillary ligands is consistent with protonation at a site remote from the $\text{Co}(\text{III})$ and for the loss of CO_2 , given by k_2 , proceeding by breaking of the $\text{O}-\text{C}$ rather than the $\text{Co}-\text{O}$ bond. However, k_1 changes by $\sim 10^4 \text{ s}^{-1}$ for the different $(\text{L})_4$ systems and reflects the effect of the $(\text{L})_4$ ligands on breaking a $\text{Co}-\text{O}$ bond. A chelated bicarbonate complex has been characterized by crystallography.¹⁴⁰

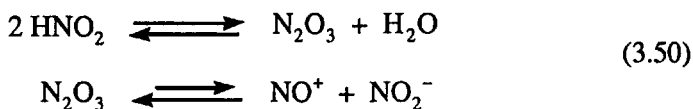
Studies by Harris and co-workers¹⁴¹ indicate that sulfur dioxide reacts in a fashion similar to CO_2 , as shown by the example in reaction (3.49). The

immediate product is the O-bonded sulfito complex, which may undergo linkage isomerism to the S-bonded form or reduce Co(III) to Co(II).



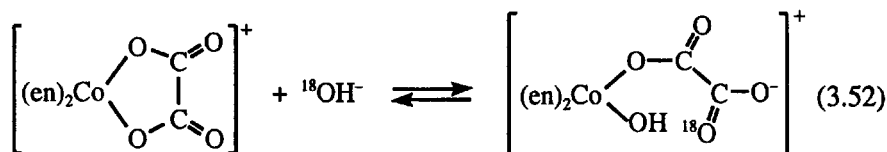
The aliphatic amine complexes of Co(III) react in this way, however the bis(phenanthroline) and bis(bipyridyl) complexes also react with the HSO_3^- and SO_3^{2-} ions.¹⁴²

The reactions with nitrous acid follow a more complicated route, described by



Murmann and Taube¹⁴³ found that the oxygen bonded to Co(III) in the reactant remains in the product, and it was long assumed that this oxygen remained bound to Co(III). Subsequent ^{17}O NMR studies of Jackson et al.¹⁴⁴ confirmed the original observations and showed that the cobalt-bound oxygen is scrambled between the two possible sites in the subsequent linkage isomerism process.

The examples in reactions (3.47), (3.49) and (3.51) can be viewed as intermolecular nucleophilic attack of coordinated OH^- on an electrophile. The same process can occur intramolecularly, as in the case of oxalate chelate ring opening studied by Andrade and Taube,¹⁴⁵ whose isotope tracer results are summarized by

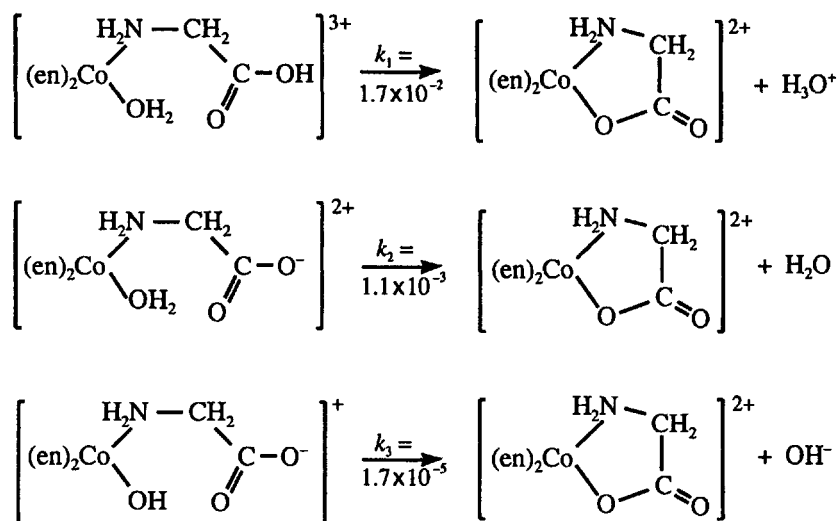


Microscopic reversibility requires that the ring-closing process must occur by O—C bond cleavage after attack of the coordinated OH^- on the uncoordinated end of the oxalate ligand.

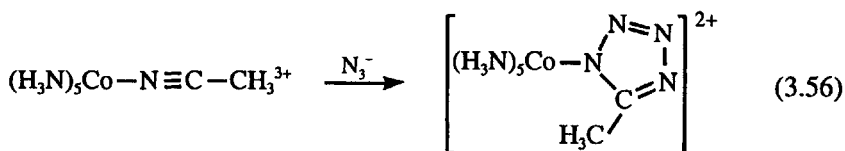
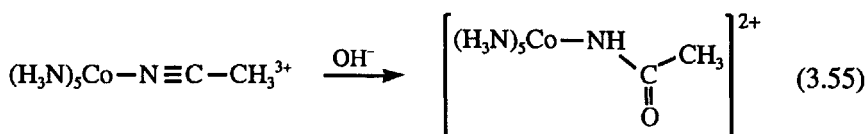
Intramolecular attack by a coordinated OH^- with retention of the M—O bond is now a common feature of biochemical mechanisms. The example in reaction (3.53) illustrates an ester hydrolysis¹⁴⁶ by such a process.

The chelate ring closing of glycine has been the subject of extensive isotope and kinetic studies,¹⁴⁹ and the results are summarized in Scheme 3.5 (k , s^{-1} at 25°C). The reactions proceed with retention of the Co—O bond, and it is noteworthy that coordinated water is an active nucleophile in this intramolecular process. The acidic pathways, given by k_1 and k_2 in Scheme 3.5, show general acid catalysis, which the authors interpret as due to rate-controlling elimination of water from the tetrahedral carbon in a cyclic intermediate.

Scheme 3.5

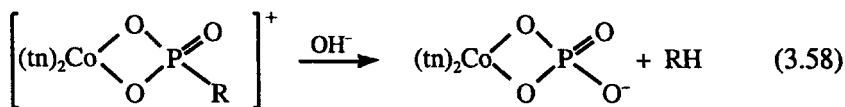


In other cases, coordination to a metal may activate the ligand to nucleophilic attack. The following equations give examples¹⁵⁰⁻¹⁵² of such processes that are generally much slower or not even observed with the free ligand:



It has been found^{153,154} that chelated amino acid esters are activated so that they are useful for peptide synthesis, as shown in reaction (3.57).

chemistry is shown in reaction (3.58), where tn is trimethylenediamine and R is *p*-nitrophenolate.¹⁵⁸ The chelated phosphate ester hydrolyzes about 10⁹ times faster than the free ester. Although chelated phosphate is not common, this observation hints at another mode for activating phosphate monoesters.



Unfortunately, the Co(III) systems are not very active as catalysts because of the kinetic stability of the product and the moderate rates of formation of the phosphate ester complexes of Co(III). Even with the preformed complexes, as in Scheme 3.6, side reactions such as loss of the ester ligand by the DCB mechanism and isomerisation to the inactive trans isomer can present problems.

To overcome some of the above problems, recent work has concentrated on complexes of metal ions which undergo facile substitution and are likely to give stable M(OH₂)(OH) species at pH 7–9. Promising catalysts have been found with complexes of Cu(II),¹⁵⁹ Zn(II),¹⁶⁰ lanthanides¹⁶¹ and Ce(IV).¹⁶² Dinuclear complexes also may be effective by forming phosphate-bridged species analogous to the chelate in reaction (3.58). The area of DNA hydrolysis has been reviewed by Liu et al.¹⁶³

3.7 VARIATION OF SUBSTITUTION RATES WITH METAL ION

The variation in rates of substitution with different metal ions has been an area of interest for many years. This information on the qualitative level is useful for synthetic purposes and for studies on equilibrium properties. It gives an indication of the conditions required for a particular preparative procedure or of how long one must wait for a system to reach equilibrium. The wide range of rates for the transition-metal ions has been of considerable interest, both to rationalize the relative rates and to apply these rationalizations to the probable reaction mechanism. This topic has been the subject of several recent reviews.¹⁶⁴

3.7.1 Water Exchange Rates

Since the pioneering work of Taube and co-workers,¹⁶⁵ shortly followed by Plane and Hunt,¹⁶⁶ and Swift and Connick,¹⁶⁷ one of the most widely studied reactions for transition-metal complexes has been that of water solvent exchange, using either ¹⁸OH₂ or ¹⁷OH₂:

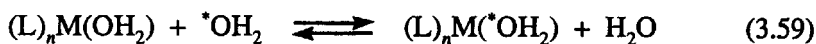


Table 3.13. Water Exchange Rate Constants (25°C) and Activation Parameters

M(L) _n (OH) ₂	<i>k</i> (s ⁻¹)	Δ <i>H</i> [*] (kJ mol ⁻¹)	Δ <i>S</i> [*] (J mol ⁻¹ K ⁻¹)	Δ <i>V</i> [*] (cm ³ mol ⁻¹)	Ref.
Ti(OH) ₂ ³⁺	1.8×10 ⁵	43.4	1.2	-12.1	<i>a</i>
V(OH) ₂ ²⁺	8.7×10 ¹	61.8	-0.4	-4.1	<i>b</i>
V(OH) ₂ ³⁺	5.0×10 ²	49.4	-27.8	-8.9	<i>c</i>
Cr(OH) ₂ ²⁺	>10 ⁸				
Cr(OH) ₂ ³⁺	2.4×10 ⁻⁶	108.6	11.6	-9.6	<i>e</i>
Cr(OH) ₂ (OH) ²⁺	1.8×10 ⁻⁴	111	55.6	2.7	<i>e</i>
Mn(OH) ₂ ²⁺	2.1×10 ⁷	32.9	5.7	-5.4	<i>f</i>
Fe(OH) ₂ ²⁺	4.4×10 ⁶	41.4	21.2	3.8	<i>f</i>
Fe(OH) ₂ ³⁺	1.6×10 ²	63.9	12.1	-5.4	<i>g</i>
Fe(OH) ₂ (OH) ²⁺	1.2×10 ⁵	42.4	5.3	7.0	<i>g</i>
Co(OH) ₂ ²⁺	3.2×10 ⁶	46.9	37.2	6.1	<i>f</i>
Ni(OH) ₂ ²⁺	3.2×10 ⁴	56.9	32.0	7.2	<i>f</i>
Cu(OH) ₂ ²⁺	4.4×10 ⁹	11.5	-21.8	2.0	<i>d</i>
Zn(OH) ₂ ²⁺	>10 ⁷				
Ga(OH) ₂ ³⁺	4.0×10 ²	67.1	30.1	5.0	<i>h</i>
Ru(OH) ₂ ²⁺	1.8×10 ⁻²	87.4	16.1	-0.4	<i>i</i>
Ru(OH) ₂ ³⁺	3.5×10 ⁻⁶	89.8	-48.3	-8.3	<i>i</i>
Ru(OH) ₂ (OH) ²⁺	5.9×10 ⁻⁴	95.8	14.9	0.9	<i>i</i>
Rh(OH) ₂ ³⁺	2.2×10 ⁻⁹	131	29	-4.2	<i>j</i>
Rh(OH) ₂ (OH) ²⁺	4.2×10 ⁻⁵	103		1.5	<i>j</i>
Ir(OH) ₂ ³⁺	1.1×10 ⁻¹⁰	131	2.7	-5.7	<i>k</i>
Ir(OH) ₂ (OH) ²⁺	1.4×10 ⁻¹¹	139	11.5	-0.2	<i>k</i>
Pt(OH) ₂ ²⁺	3.9×10 ⁻⁴	89.7	-9	-4.6	<i>l</i>
Pd(OH) ₂ ²⁺	5.6×10 ²	49.5	-26	-2.2	<i>l</i>
Cr(NH ₃) ₃ (OH) ₂ ³⁺	5.2×10 ⁻⁵	97	0	-5.8	<i>m</i>
Co(NH ₃) ₃ (OH) ₂ ³⁺	5.7×10 ⁻⁶	111	28	1.2	<i>n</i>
Rh(NH ₃) ₃ (OH) ₂ ³⁺	8.4×10 ⁻⁶	103	3	-4.1	<i>m</i>
Ir(NH ₃) ₃ (OH) ₂ ³⁺	6.1×10 ⁻⁸	118	11	-3.2	<i>o</i>

^a Hugi, A. D.; Helm, L.; Merbach, A. E. *Inorg. Chem.* **1987**, *26*, 1763.^b Ducommun, Y.; Zbinden, D.; Merbach, A. E. *Helv. Chim. Acta* **1982**, *65*, 1385.^c Hugi, A. D.; Helm, L.; Merbach, A. E. *Helv. Chim. Acta* **1985**, *68*, 508.^d Powell, D. H.; Helm, L.; Merbach, A. E. *J. Chem. Phys.* **1991**, *95*, 9258; Powell, D. H.; Furrer, P.; Pittet, P.-A.; Merbach, A. E. *J. Phys. Chem.* **1995**, *99*, 16622.^e Xu, F.-C.; Krouse, H. R.; Swaddle, T. W. *Inorg. Chem.* **1985**, *24*, 267.^f Ducommun, Y.; Newman, K. E.; Merbach, A. E. *Inorg. Chem.* **1980**, *19*, 3696.^g Grant, M.; Jordan, R. B. *Inorg. Chem.* **1981**, *20*, 55; Swaddle, T. W.; Merbach, A. E. *Inorg. Chem.* **1981**, *20*, 4212.^h Hugi-Cleary, D.; Helm, L.; Merbach, A. E. *J. Am. Chem. Soc.* **1987**, *109*, 4444.ⁱ Rapaport, I.; Helm, L.; Merbach, A. E.; Bernhard, P.; Ludi, A. *Inorg. Chem.* **1988**, *27*, 873.^j Laurenczy, G.; Rapaport, I.; Zbinden, D.; Merbach, A. E. *Magn. Reson. Chem.* **1991**, *29*, S45.^k Cusanelli, A.; Frey, U.; Richens, D.; Merbach, A. E. *J. Am. Chem. Soc.* **1996**, *118*, 5265.^l Helm, L.; Elding, L. I.; Merbach, A. E. *Inorg. Chem.* **1985**, *24*, 1719.^m Swaddle, T. W.; Stranks, D. R. *J. Am. Chem. Soc.* **1972**, *94*, 8357.ⁿ Hunt, H. R.; Taube, H. *J. Am. Chem. Soc.* **1958**, *80*, 2642.^o Tong, S. B.; Swaddle, T. W. *Inorg. Chem.* **1974**, *13*, 1538.

The results of such studies are summarized in Table 3.13. The NMR studies prior to about 1970 should be viewed with caution, and most of the early work has been repeated with modern instrumentation and methods of analysis. For the $M(OH)_5(OH)^{2+}$ ions, these studies determine kK_h , where K_h is the acid dissociation constant for the parent $M(OH)_6^{3+}$ ion. The ΔH° and ΔV° of K_h often must be approximated, and this produces some uncertainty in the activation parameters for the $M(OH)_5(OH)^{2+}$ ions.

A noteworthy feature of the data in Table 3.13 is the wide range of rate constants: for the 2+ ions, k varies from $3.9 \times 10^{-4} \text{ s}^{-1}$ for Pt(II) to $4.4 \times 10^9 \text{ s}^{-1}$ for Cu(II) and for the 3+ ions, k varies from $1.1 \times 10^{-10} \text{ s}^{-1}$ for Ir(III) to $1.8 \times 10^5 \text{ s}^{-1}$ for Ti(III). The following sections present attempts to explain these variations and their mechanistic implications.

3.7.1.1 Labile and Inert Classification of Taube

Taube¹⁶⁸ was the first to offer an explanation for the variable lability of these metal ions by classifying them qualitatively on the basis of their reactivity.

Labile metal ions react essentially on mixing of the metal ion and ligand solutions, that is, within a few seconds at most. *Inert metal ions* require at least a few minutes for their substitution reactions to be complete. This operational classification provides a useful practical classification that has endured as a qualitative description of the reactivity of a metal ion.

Taube offered a theoretical explanation for the qualitative differences in reactivity in terms of Pauling's valence bond theory, but the same arguments can be framed in terms of crystal field theory for octahedral complexes. The terminology is defined in Figure 3.4. *Labile metal ions* have either an empty low-energy t_{2g} orbital or at least one electron in a high-energy e_g orbital. The rationalization for this is that the empty t_{2g} orbital can be used by the entering group in an A or I_a transition state. Electrons in the e_g orbitals will favor a D or I_d mechanism because the ligand bonds in the ground state will be weaker. *Inert metal ions* must have at least one electron in each t_{2g} orbital and no electrons in the e_g orbitals.

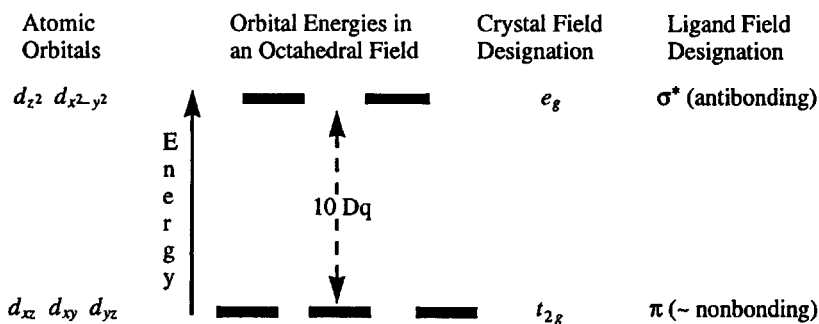


Figure 3.4. Energies and designations of d orbitals in an octahedral complex.

These ideas are consistent with the inertness of the octahedral complexes of Cr(III) (t_{2g}^3), low-spin Co(III) (t_{2g}^6), Fe(II) (t_{2g}^6) and Fe(III) (t_{2g}^5), and the inertness of the complexes of the second- and third-row transition metal ions with more than two d electrons, which are low spin. They also provide a simple explanation for the fact that the complexes of V(III) (t_{2g}^2) are more labile than those of V(II) (t_{2g}^3), whereas the complexes of Cr(III) (t_{2g}^3) are inert and those of Cr(II) ($t_{2g}^3 e_g^1$) are labile.

The predictions of this theory are qualitatively correct but it does not explain the wide range of reactivities, especially of the labile systems. For example, why is the water exchange rate for Ni(II) 10^2 times slower than that for Co(II) and $>10^4$ times slower than that for Cu(II)?

3.7.1.2 Crystal Field Theory Applications

This application of crystal field theory was put forward first in the textbook by Basolo and Pearson¹⁶⁹ in an attempt to explain the finer details of the reactivity differences between various metal ions.

The energies of the valence d orbitals were calculated for various ideal geometries of possible transition states for the substitution reactions. The calculations assume a pure crystal field model (no covalent bonding) and the same bond lengths and crystal field parameter, Dq , as in the ground state of the metal ion complex, with normal bond angles for the various geometries of the intermediates. The crystal field stabilization energy, CFSE, was calculated for the ground state and the intermediate, and the difference between these was defined as the *crystal field activation energy*, CFAE. Differences in reactivity were assigned to the difference in this electronic factor for various numbers of d electrons, with the implication that ΔH^\ddagger dominates the differences in the rate constants.

The energies of the d orbitals in units of Dq are given in Table 3.14. Based on these orbital energies and the d -orbital electronic configuration for the metal ion, one can calculate the CFAE for each of the possible transition states and then predict which transition state is most favorable (the one with the lower CFAE) and the order of reactivity for the different metal ions.

Table 3.14. Energies of d Orbitals for Various Geometries in Units of Dq

Structure	$d_{x^2-y^2}$	d_{z^2}	d_{xy}	d_{xz}	d_{yz}
Octahedron	6.00	6.00	-4.00	-4.00	-4.00
Trigonal bipyramid (T.B.)	-0.82	7.07	-0.82	-2.72	-2.72
Square pyramid (S.P.)	9.14	0.86	-0.86	-4.57	-4.57
Pentagonal bipyramid (P.B.)	2.82	4.93	2.82	-5.28	-5.28
Octahedral wedge (O.W.)	8.79	1.39	-1.51	-2.60	-6.08
Square planar	12.28	-4.28	2.28	-5.14	-5.14

Table 3.15. Crystal Field Activation Energies for Two Transition States with High-Spin Configurations in Units of Dq

No. d Electrons	CFSE			CFAE	
	Octahedron	S. P.	O. W.	S. P.	O. W.
0, 10	0.0	0.0	0.0	0.0	0.0
1, 6	4.00	4.57	6.08	-0.57	-2.08
2, 7	8.00	9.14	8.68	-1.14	-0.68
3, 8	12.00	10.00	10.20	2.00	1.80
4, 9	6.00	9.14	8.79	-3.14	-2.79
5, 10	0.0	0.0	0.0	0.0	0.0

Such calculations are shown in Table 3.15 for the square pyramid and octahedral wedge intermediates. If one disregards differences in Dq for different metal ions, these calculations predict the order of reactivity for a square pyramid transition state as $(d^4, d^9) > (d^2, d^7) > (d^1, d^6) > (d^0, d^5, d^{10}) > (d^3, d^8)$. However, an octahedral wedge gives a more favorable transition state for the (d^1, d^6) and (d^3, d^8) configurations. It also can be shown that a pentagonal bipyramid should be the best transition state for the (d^2, d^7) configurations with a CFAE = $-2.56 Dq$.

Table 3.16 summarizes the predictions and results for the 2+ metal ions of the first transition series. The theory correctly predicts that Ni(II) and V(II) should have the smallest exchange rates and that Cr(II) and Cu(II) should have the largest. The next most labile are predicted to be Co(II) and Fe(II), but they are actually less labile than Mn(II) and probably Zn(II). Only the d^4 and d^9 systems are predicted to use a square pyramid or I_4 transition state.

Table 3.16. Water Exchange Rate Constants (25°C), Activation Parameters and Predicted Crystal Field Activation Energies for First-Row Transition-Metal Ions

		CFAE	k (s ⁻¹)	ΔH^\ddagger (kJ mol ⁻¹)	ΔS^\ddagger (J mol ⁻¹ K ⁻¹)	ΔV^\ddagger (cm ³ mol ⁻¹)
V(OH ₂) ₆ ²⁺	d^3	1.80 (O.W.)	87	61.8	-0.4	-4.1
Cr(OH ₂) ₆ ²⁺	d^4	-3.14 (S.P.)	$>10^8$			
Mn(OH ₂) ₆ ²⁺	d^5	0.0	2.1×10^7	32.9	5.7	-5.4
Fe(OH ₂) ₆ ²⁺	d^6	-2.08 (O.W.)	4.4×10^6	41.4	21.2	3.8
Co(OH ₂) ₆ ²⁺	d^7	-2.56 (P.B.)	3.2×10^6	46.9	37.2	6.1
Ni(OH ₂) ₆ ²⁺	d^8	1.80 (O.W.)	3.2×10^4	56.9	32.0	7.2
Cu(OH ₂) ₆ ²⁺	d^9	-3.14 (S.P.)	$>10^7$			
Zn(OH ₂) ₆ ²⁺	d^{10}	0.0	$>10^7$			

The crystal field predictions of absolute and relative activation energies are less successful. For example, $\text{Ni}(\text{OH}_2)_6^{2+}$ has $Dq = 850 \text{ cm}^{-1}$ (10 kJ) and $\text{V}(\text{OH}_2)_6^{2+}$ has $Dq = 1240 \text{ cm}^{-1}$ (14.8 kJ), so that their ΔH^\ddagger values are calculated to be 18 and 26.6 kJ mol⁻¹, respectively. The differences from the experimental numbers could be ascribed to solvation effects. The predicted difference of 8.6 kJ mol⁻¹ in the ΔH^\ddagger values is larger than the observed value of 5.1 kJ mol⁻¹, but one must allow for an error of $\pm 2 \text{ kJ mol}^{-1}$ in the experimental values. The larger ΔH^\ddagger for the 3+ ions would be attributed to differences in Dq . For Cr(III), the $Dq = 2000 \text{ cm}^{-1}$ (23.7 kJ), so that the calculated $\Delta H^\ddagger = 42.7 \text{ kJ mol}^{-1}$, and the difference between this value and that for Ni(II) is predicted to be 24.7 kJ mol⁻¹ compared to the observed value of 53.1 kJ mol⁻¹. Again, solvation differences with different charge types may explain this discrepancy.

The general impression is that the crystal field approach has pointed out a significant feature for the understanding of the reactivity differences. However, this is not the whole story, and it is probably too crude an approximation in the form used by Basolo and Pearson to be capable of assigning small differences or preferred geometries for transition states.

There have been attempts to refine the theory. Breitschwerdt¹⁷⁰ allowed the effective charge on the metal ion to change with the number of ligands, so that Dq varied between the ground and transition states. The Dq also was decreased by 40% for ligands in the plane of the pentagonal bipyramid compared to the axial ligands. It was found that a square pyramid was the most stable transition state for all the 2+ ions and that all the CFAEs are positive.

Spees et al.¹⁷¹ presented a more extensively parameterized ligand field model and included the possibility of a change of spin state in the "intermediate". Swaddle and co-workers¹⁷² found that this theory was not successful when applied to $\text{M}(\text{NH}_3)_5(\text{OH}_2)^{3+}$ systems. This approach seems to be no more effective than the simpler versions of crystal field theory.

3.7.1.3 Other Theoretical Applications

Burdett¹⁷³ has applied the angular overlap bonding model to this problem. This is essentially an extended Hückel molecular orbital approach. The change in bonding energy between the octahedral ground state and a square pyramid transition state was calculated in terms of the exchange integral, β , and the overlap integral, S . It was also argued that βS^2 would increase with atomic number across the transition series. The energy loss for d^0 to d^3 is $2\beta S^2$, for d^4 to d^8 is $1\beta S^2$ and for d^9 and d^{10} is zero. This predicts the abrupt change in reactivity that is observed between d^3 and d^4 and between d^8 and d^9 , but quantitative predictions are not possible, nor were other transition states considered. The angular overlap model has been applied by Mønsted¹⁷⁴ to the aquation reactions of $\text{Cr}^{\text{III}}(\text{OH}_2)_5\text{X}$ and $\text{Cr}^{\text{III}}(\text{NH}_3)_5\text{X}$ complexes, with the conclusion that an I_a octahedral wedge "transition state" is preferred.

More sophisticated quantum mechanical models began to be applied in the 1980s. Rode et al.¹⁷⁵ calculated the hydration energies of these metal ions by including effects from two hydration shells beyond the first coordination sphere. The stabilization per water molecule in the first coordination sphere, $\Delta E(\text{I})$, and in the second coordination sphere, $\Delta E(\text{II})$, were taken into account. With some rather arbitrary adjustments, these quantities were found to correlate reasonably well with the $\Delta G^\ddagger(25^\circ\text{C})$ for water exchange.

Connick and Alder¹⁷⁶ applied molecular modeling to attempt to understand the nature of the exchange process in the $\text{Ni}(\text{OH}_2)_6^{2+}$ system. Merbach and co-workers¹⁷⁷ used Monte Carlo simulations for lanthanide ions to predict solvation numbers for these ions and found that the calculations predicted a dissociative mechanism for the nine-coordinate ions. Calculations such as these will benefit from the extensive structural information available from EXAFS studies that has been compiled and reviewed by Ohtaki and Radnai.¹⁷⁸

Åkesson et al.¹⁷⁹ have done SCF computations of the gas phase energies for the ions $\text{M}(\text{OH}_2)_n^{3/2+}$ ($n = 5, 6, 7$) of the first transition metal series. They have combined these in a thermochemical cycle with hydration energies, estimated from the Born equation, in order to estimate solvent exchange activation energies for **D** and **I** mechanisms. The results for metal ions with experimentally measured activation energies are given in Table 3.17. For each of the 2+ ions, the smaller of the two calculated ΔH^\ddagger values is $\sim 20 \text{ kJ mol}^{-1}$ larger than the experimental values. For the 3+ ions, the differences between calculated and experimental values are irregular; the

Table 3.17. Experimental and SCF Estimated ΔH^\ddagger for Water Exchange^a

	$\Delta H^\ddagger_{\text{obs}}$	$\Delta H^\ddagger(\text{D})^b$	$\Delta H^\ddagger(\text{I})^c$
$\text{V}(\text{OH}_2)_6^{2+}$	61.8	93 (S.P.)	106
$\text{Mn}(\text{OH}_2)_6^{2+}$	32.9	62 (T.B.)	54
$\text{Fe}(\text{OH}_2)_6^{2+}$	41.4	61 (T.B.)	62
$\text{Co}(\text{OH}_2)_6^{2+}$	46.9	63 (T.B.)	83
$\text{Ni}(\text{OH}_2)_6^{2+}$	56.9	77 (S.P.)	132
$\text{Cu}(\text{OH}_2)_6^{2+}$	11.5	46 (T.B.)	120
$\text{Ti}(\text{OH}_2)_6^{3+}$	43.4	170 (T.B.)	34
$\text{V}(\text{OH}_2)_6^{3+}$	49.4	177 (T.B.)	58
$\text{Cr}(\text{OH}_2)_6^{3+}$	108.6	204 (S.P.)	164
$\text{Fe}(\text{OH}_2)_6^{3+}$	64	169 (T.B.)	85
$\text{Ga}(\text{OH}_2)_6^{3+}$	67.1	150 (T.B.)	155

^a Activation enthalpies in kJ mol^{-1} .

^b For a **D** mechanism with the most stable trigonal bipyramid (T.B.) or square-based pyramid (S.P.) intermediate.

^c For an **I** mechanism with a distorted pentagonal bipyramid (P.B.) intermediate.

calculated ΔH^* is 9 kJ mol⁻¹ smaller than the experimental one for Ti(III) but it is 55 kJ mol⁻¹ larger for Cr(III). The relative values of $\Delta H^*(D)$ and $\Delta H^*(I)$ predict a D mechanism for V(II), Co(II), Ni(II) and Cu(II) and an I mechanism for Ti(III), V(III), Cr(III) and Fe(III), while Ga(III), Fe(II) and possibly Mn(II) are too close to warrant a prediction and might be I_a or I_a. These predictions are consistent with those based on ΔV^* , except for V(II), Mn(II) and Ga(III). It should be noted that in all theoretical studies, the calculation of a ΔH^* involves taking the difference between the calculated total energies of the ground and transition states. The latter are typically on the order of 2–3×10³ kJ mol⁻¹, and therefore much larger than ΔH^* . It is assumed that errors due to assumptions in the calculation of the total energies of the two states will cancel when their difference is taken.

There have been a number of subsequent theoretical analyses of these solvent-exchange reactions using various methodologies and basis sets. These are discussed in reviews by Lincoln¹⁶⁴ and by van Eldik and co-workers.¹⁸⁰ Rotzinger¹⁸¹ has given a comparison of the theoretical methods and come to the conclusion that Hartree–Fock (HF) methods tend to favor the higher coordination number transition states of an I_a mechanism, while Density Functional Theory (DFT) tends to favor I_a transition states.

As might be expected at this stage, there can be disagreements among the theoretical predictions, and a case with Pt(II) reactions already has been mentioned. The aqueous Cu(II) ion presents a case where even the ground-state configuration has been a problem. Pasquarello et al.¹⁸² concluded from neutron scattering and molecular mechanics calculations that this ion is five-coordinate Cu(OH₂)₅²⁺. Persson et al.¹⁸³ questioned this interpretation on the basis of EXAFS and LAXS studies of various salts of Cu(II) in water, and concluded that the ion has a six-coordinate tetragonally distorted structure with four short and two long Cu—O bonds. Rotzinger has suggested that the modeling used by Pasquarello et al. may be an example of the tendency of DFT methods to favor lower coordination numbers, and this is consistent with the results of Schwenk and Rode.¹⁸⁴

3.7.2 Solvent Exchange in Nonaqueous Solvents

Although water is the solvent of most general interest, there has been a great deal of work in other solvents, such as acetonitrile, methanol, dimethylsulfoxide and *N,N*-dimethylformamide. In general, the purpose is to gain some understanding of the effect of ligand size, basicity and so on, on the solvent exchange rate. The main complication is that both the bulk solvent and the exchanging ligand are changed at the same time, so that individual factors affecting the exchange rate are difficult to separate. Some representative results are given in Table 3.18.

The reactivity pattern observed in water generally is maintained in other solvents. For example, Ni(II) always shows substantially smaller exchange rate constants and higher ΔH^* values, and trends in ΔV^* with atomic number are also maintained.

Table 3.18. Nonaqueous Solvent Exchange Rate Constants (25°C), Enthalpies, Entropies and Volumes of Activation^a

Metal	Solvent	k (s ⁻¹)	ΔH^\ddagger (kJ mol ⁻¹)	ΔS^\ddagger (J mol ⁻¹ K ⁻¹)	ΔV^\ddagger (cm ³ mol ⁻¹)
Cr ²⁺	CH ₃ OH	1.2x10 ⁸	31.6	16.6	
Mn ²⁺	CH ₃ OH	3.7x10 ⁵	25.9	-50.2	-5.0
Fe ²⁺	CH ₃ OH	5.0x10 ⁴	50.2	12.6	0.4
Co ²⁺	CH ₃ OH	1.8x10 ⁴	57.7	30.1	8.9
Ni ²⁺	CH ₃ OH	1.0x10 ³	66.1	33.5	11.4
Cu ²⁺	CH ₃ OH	3.1x10 ⁷	17.2	-44.0	8.3
Mn ²⁺	CH ₃ CN	1.4x10 ⁷	29.6	-8.9	-7.0
Fe ²⁺	CH ₃ CN	6.6x10 ⁵	41.4	5.5	3.0
Co ²⁺	CH ₃ CN	2.5x10 ⁵	48.8	22.7	7.7
Ni ²⁺	CH ₃ CN	2.8x10 ³	64.3	37.0	9.6
Co ²⁺	NH ₃	5.0x10 ⁷	45.8	31.2	
Ni ²⁺	NH ₃	7.0x10 ⁴	57.3	40.2	5.9
Mn ²⁺	(CH ₃) ₂ NCHO	2.2x10 ⁶	34.6	-7.4	2.4
Fe ²⁺	(CH ₃) ₂ NCHO	9.7x10 ⁵	43.0	13.8	8.5
Co ²⁺	(CH ₃) ₂ NCHO	3.9x10 ⁵	56.9	52.7	6.7
Ni ²⁺	(CH ₃) ₂ NCHO	3.8x10 ³	62.8	33.5	9.1
Cu ²⁺	(CH ₃) ₂ NCHO	9.1x10 ⁸	24.3	8.1	8.4
Ti ³⁺	(CH ₃) ₂ NCHO	6.6x10 ⁴	23.6	-73.6	-5.7
Fe ³⁺	(CH ₃) ₂ NCHO	6.1x10 ¹	42.3	12.1	-5.4
Cr ³⁺	(CH ₃) ₂ NCHO	3.3x10 ⁻⁷	97.1	-43.5	-6.3
V ³⁺	(CH ₃) ₂ SO	1.3x10 ¹	38.5	-94.5	-10.1
Cr ³⁺	(CH ₃) ₂ SO	3.1x10 ⁻⁸	96.7	-64.5	-11.3
Fe ³⁺	(CH ₃) ₂ SO	9.3	62.5	-16.7	-3.1

^a Original references in reference 164.

There are some disturbing features of the activation parameters with regard to the conventional interpretations of the data in water. For example, the order of Dq values for the solvents is NH₃ > CH₃CN > DMF > H₂O ≈ CH₃OH. If crystal field effects are the determining factor for the ΔH^\ddagger values, then one should expect these to be in the same order for the various solvents. In fact, the order of ΔH^\ddagger values for Ni(II) is CH₃OH > DMF > CH₃CN ≈ NH₃ > H₂O and there seems to be no relationship to the Dq values. The fact that the ΔV^\ddagger values for a particular metal ion are rather insensitive to the solvent will be discussed in the next section.

The general interpretation of these results is that there are specific solvation effects operating in different solvents, and these are not taken into account by any of the simple models. However, it is not widely acknowledged that this greatly weakens all of the more simplistic rationalizations that are used to explain the results of these types of studies.

It was found by Jordan and co-workers¹⁸⁵ that the ΔH^* values can be correlated by Eq. (3.60), which involves a crystal field parameter, a_M , that is fixed for the metal ion and a solvent parameter, b_S , that is a constant for a particular solvent.

$$\Delta H^* = a_M g_M (Dq_{Ni}) + b_S = c_M (Dq_{Ni}) + b_S \quad (3.60)$$

The value of g_M can be obtained from spectroscopic data, which gives the proportionality between the widely available Dq values for Ni(II) and those of the other metal ions.

Since the original correlation in 1978, a number of experimental values have been redetermined. The results of the correlation with the newer values are given in Table 3.19. It should be noted that the parameters are based on the assumption that $c_M = 0$ for Mn(II) because this high-spin d^5 system should not have any crystal field stabilization. In general, if c_M is increased by some amount Δc , then b_S will decrease by $\Delta c \times Dq$.

Overall, the correlation fits the experimental values to within their typical $\pm 10\%$ uncertainty. It remains to be determined whether the Mn(II)–CH₃OH data are in error. Although this correlation seems to have some potential predictive power, there is as yet no rationalization of the b_S values in terms of any property of the solvent. In a study of octahedral–tetrahedral equilibria in Co(II) amine systems, Aizawa and Funahashi¹⁸⁶ suggested that b_S might be related to the spherically symmetrical electric field, ΔE_{spher} , imposed by the ligands. From the electronic spectra of the octahedral and tetrahedral species, the authors were able to do a ligand-field analysis and obtained a value for ΔE_{spher} of 30.1 kJ mol⁻¹ for *n*-propylamine. It is encouraging, but maybe coincidental, that this value is similar to the b_S for NH₃ in Table 3.19.

In these systems, it is difficult to establish mechanistic trends between solvents because the bulk solvent changes in each case. The most common mechanistic criterion now is ΔV^* , as discussed in the next section.

Table 3.19. Correlation of ΔH^* Values (kJ mol⁻¹) for Solvent Exchange^a

Solvent	Dq	b_S	Ni(II)	Co(II)	Fe(II)	Mn(II)
NH ₃	13.0	30.2	57.3 (60.9)	45.8 (49.7)	(42.0)	33.5 (30.2)
CH ₃ CN	12.7	30.1	64.3 (60.2)	48.8 (49.3)	41.4 (41.7)	29.6 (30.1)
DMF	10.5	35.7	62.8 (60.6)	56.9 (51.5)	43.0 (45.3)	34.6 (35.7)
H ₂ O	10.3	32.3	56.9 (56.7)	46.9 (47.8)	41.4 (41.7)	32.9 (32.3)
CH ₃ OH	10.2	41.6	66.1 (65.8)	57.7 (57.0)	50.2 (51.0)	25.9 (41.6) ^b
DMSO	9.41	33.7	54.4 (56.1)	51.1 (47.9)	47.3 (42.4)	31.0 (33.7)
	c_M		2.37	1.51	0.916	0.0

^a Values in parentheses are predicted from the correlation.

^b This value was not used to obtain the correlation parameters.

3.7.3 Volumes of Activation for Solvent Exchange

It has been noted that the ΔV^\ddagger values for the 2+ ions of the first transition series become increasingly positive with atomic number. Merbach and co-workers¹⁸⁷ have suggested that this represents a trend from I_a for $V(OH_2)_6^{2+}$ to I_d for $Ni(OH_2)_6^{2+}$, and that the reason for this is the decreasing size of the metal ion. The values for the $M(OH_2)_5(OH)^{2+}$ ions are more positive than those for the corresponding $M(OH_2)_6^{3+}$ ions ($M = Cr(III), Fe(III), Ru(III)$), suggesting that the former species have more dissociative character. Swaddle¹⁸⁸ has noted that the partial molar volumes of $M(OH_2)_n^{z+}$ ions can be calculated from

$$V_{\text{abs}}^{\circ} = 2.523 \times 10^{-6}(r_M + \Delta r) - 18.07n - \frac{417.5z}{(r_M + \Delta r)} \quad (3.61)$$

where V_{abs}° is the absolute volume of the ion relative to the value of $V_{\text{abs}}^{\circ}(H^+) = -5.4 \text{ cm}^3 \text{ mol}^{-1}$, r_M is the ionic radius of the metal ion, in pm, Δr is the apparent radius of the coordinated water molecule determined empirically and 18.07 is the partial molar volume of water; the last term accounts for solvent electrostriction around the charged ion. Swaddle has used this equation, with appropriately adjusted values of r_M and n , to estimate a limiting value of $\Delta V^\ddagger \approx 13 \text{ cm}^3 \text{ mol}^{-1}$ for a D mechanism and $\Delta V^\ddagger \approx -13 \text{ cm}^3 \text{ mol}^{-1}$ for an A mechanism. This implies that $Ti(OH_2)_6^{3+}$ has a mechanism close to the A limit.

For the nonaqueous systems in Table 3.18, the ΔV^\ddagger values are almost invariant with changes in solvent for a given metal ion. If the mechanism is I_d for Ni(II), as is commonly assumed, then one might expect the ΔV^\ddagger values to parallel the size of the leaving group (solvent), based on an extension of Eq. (3.61) from water to other solvents. Yet the ΔV^\ddagger for DMF is only $2 \text{ cm}^3 \text{ mol}^{-1}$ larger than that for water, although the partial molar volumes of the solvents are 115.4 and $18 \text{ cm}^3 \text{ mol}^{-1}$, respectively.

Tanaka and co-workers¹⁸⁹ observed an insensitivity of ΔV^\ddagger to the volume of the leaving group in a study of the solvent exchange of a series of nitriles on Ni(II). Recently Funahashi and Inada¹⁹⁰ have offered a detailed explanation of these observations that may be generally applicable. Their model proposes that the bulk of a solvent ligand is actually dangling into the second coordination sphere, and that the solvent in the second sphere approaches the metal ion in the spaces between the coordinated solvent molecules. Then, when the solvent ligand is leaving, it is really only the coordinated atom and one or two atoms attached to it which move into the second sphere and affect ΔV^\ddagger . The argument is supported by the ^{14}N NMR relaxation rates of the various solvent molecules in the outer spheres. These rates indicate that the outer-sphere distance of closest approach to Ni(II) is not greatly dependent on the steric bulk of the solvent. This model may not be applicable to water because the second-sphere water molecules may form a highly structured hydrogen-bonded network.¹⁹¹

3.8 LIGAND SUBSTITUTION ON LABILE TRANSITION-METAL IONS

The common complexes of the M(II) and M(III) transition-metal ions of the first transition series are labile, except for Cr(III) and low-spin Co(III), Fe(II) and Fe(III). These labile ions form a wide range of complexes of general chemical and biochemical importance. As a result, there have been many studies of the kinetics and equilibrium constants for reactions of the general form



The majority of this work is in water, but there are an increasing number of studies in nonaqueous solvents. The results have been the subject of several reviews.¹⁹²⁻¹⁹⁴

3.8.1 General Reactivity Trends

The rate constants for these reactions are normally of the same order of magnitude as those for solvent exchange. As a result, the reactions typically have half-times in the microsecond to second range at normal concentrations. Therefore, the experimental techniques are stopped-flow and various relaxation methods pioneered by Eigen (see Chapter 10). The lability of these systems means that one cannot do the type of competition studies that rely on product analysis to yield mechanistic information. Rather, these mechanistic studies are primarily concerned with the evaluation of entering group effects. Since the leaving group is the solvent, it cannot be systematically changed without introducing substantial changes to the solvation energies of the species involved.

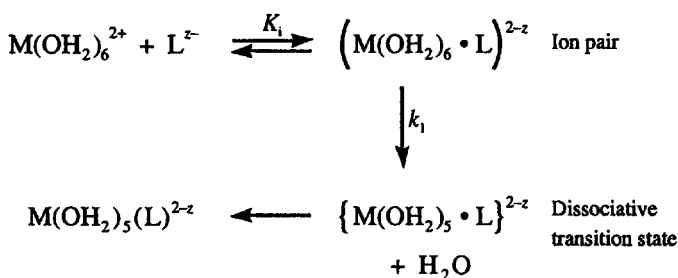
The reactions of Ni(II) are slower than those of the other M(II) ions in this group, and this metal ion has been studied most extensively because the rates fall conveniently in the range of the stopped-flow technique. The substitution kinetic results on $\text{Ni}(\text{OH}_2)_6^{2+}$ have been reviewed by Wilkins.¹⁹³ Some representative results are given in Table 3.20. The first impression of these data is that there are significant entering group effects on the rate constant, so that the mechanism appears to be I_a . However,

Table 3.20. Rate Constants (25°C) for Some Substitution Reactions on $\text{Ni}(\text{OH}_2)_6^{2+}$

Entering Group (L)	$\text{p}K_a$	k ($\text{M}^{-1} \text{s}^{-1}$)
$\text{H}_3\text{CPO}_4^{2-}$	~2	2.9×10^5
F^-	~3	8.0×10^3
NH_3	9.2	4.5×10^3
NH_2CH_3	10	1.3×10^3
$\text{NH}_2(\text{CH}_2)\text{N}(\text{CH}_3)_3^+$	7	4.0×10^2

there is no correlation with the nucleophilicity of L, as judged by the pK_a values of the entering ligands. An analysis of a more extensive set of this type of data led Eigen and Wilkins¹⁹² to suggest that the apparent rate constant was strongly correlated with the charge on L. Within modest limits, the rate constants ($M^{-1} s^{-1}$) are $\sim 3 \times 10^5$ for L^{2-} , $\sim 1 \times 10^4$ for L^- , $\sim 3 \times 10^3$ for L^0 and ~ 500 for L^+ . These observations led Eigen and Wilkins to propose what is now the classic mechanism for this system, called the *Dissociative ion pair mechanism* or the Eigen–Wilkins mechanism; it is formulated in Scheme 3.7.

Scheme 3.7



The rate law for this system with a rapid pre-equilibrium has been developed previously. These studies are usually carried out with total $[M] \gg [L]$, in order to prevent formation of higher complexes such as $M(OH_2)_4(L)_2$; therefore, the experimental pseudo-first-order rate constant is given by

$$k_{\text{exp}} = \frac{k_1 K_i}{1 + K_i [M(OH_2)_6^{2+}]} \quad (3.63)$$

The theoretical expression for K_i , discussed on p. 47, was developed in part to analyze these results. When L is neutral or uninegative, K_i is predicted to be $\leq 1 M^{-1}$, and for most studies total $[M] \approx 10^{-2} M$, so that $K_i [M(OH_2)_6^{2+}] \ll 1$. Under these conditions, the expression for the experimental rate constant in Eq. (3.63) simplifies to

$$k_{\text{exp}} = k_1 K_i \quad (3.64)$$

Since K_i depends on the charge of L, this expression explains the variation of k_{exp} with the charge of the entering group. In many interpretations of experimental results, k_{exp} is divided by a calculated value of K_i in order to obtain k_1 , and then k_1 is compared to the rate constant for solvent exchange, that also is assumed to be dissociatively activated. In many instances, this analysis works well. Since K_i often is of the order of magnitude of $1 M^{-1}$, the value of k_{exp} is quite similar to that for solvent exchange.

For Mn(II), Fe(II) and Co(II), the preceding type of analysis indicates a lack of entering group effects and an I_d mechanism. For $Mn(OH_2)_6^{2+}$, the ΔV^\ddagger values are negative and an I_a mechanism has been suggested.¹⁹⁵ It should be noted that pre-association or ion pairing causes complications in the interpretation of ΔV^\ddagger for complexation. Merbach and co-workers¹⁸⁷ have interpreted the changes in ΔV^\ddagger to indicate that there is a mechanistic trend across the first transition series from I_a for V(II) to I_d for Ni(II).

The best case for an I_a mechanism from entering group effects comes from the results of Chaudhuri and Diebler¹⁹⁶ for $Ti(OH_2)_6^{3+}$, as given in Table 3.21. These results do not correlate simply with the charge of the entering group, but do parallel the nucleophilicity as measured by the pK_a . These reactions are still presumed to proceed through an ion pair, but the rate-controlling step has the entering group dependence expected for an I_a mechanism. Merbach has suggested that the mechanism is A on the basis of the ΔV^\ddagger for the water exchange.¹⁹⁷

Substitution reactions on $V(OH_2)_6^{3+}$ have been of long-standing interest since Taube's prediction that such a d^2 system should be labile with an A mechanism. These studies are difficult because $V(OH_2)_6^{3+}$ is readily oxidized by air and perchlorate ion. The results of several studies, as summarized by Patel and Diebler,¹⁹⁸ are given in Table 3.22. The rate constants vary widely with the entering group and do not show the correlation with charge expected for a dissociative ion pair mechanism. More recently, Merbach and co-workers have studied the reaction of V(III) with NCS^- in water¹⁹⁹ and DMSO.²⁰⁰ For the formation reaction in water, they obtained $\Delta H^\ddagger = 49.1 \text{ kJ mol}^{-1}$, $\Delta S^\ddagger = -39.8 \text{ J mol}^{-1} \text{ K}^{-1}$ and $\Delta V^\ddagger = -9.4 \text{ cm}^3 \text{ mol}^{-1}$. In DMSO, the corresponding values are 44.6, -54.1 and -1.1 , respectively. The rate constant trends and the negative ΔS^\ddagger and ΔV^\ddagger for water exchange and complexation are taken as evidence for an I_a mechanism, confirming Taube's prediction.

Table 3.21. Rate Constants (15°C) for Substitution Reactions on $Ti(OH_2)_6^{3+}$

Entering Group	pK_a	$k_{exp} (\text{M}^{-1} \text{s}^{-1})$
$ClCH_2CO_2H$		6.7×10^2
CH_3CO_2H		9.7×10^2
NCS^-	-1.84	8.0×10^3
$HO_2CCO_2^-$	1.23	3.9×10^5
$Cl_2CHCO_2^-$	1.25	1.1×10^5
$HO_2CCH_2CO_2^-$	2.43	4.2×10^5
$ClCH_2CO_2^-$	2.46	2.1×10^5
$HO_2CCH(CH_3)CO_2^-$	2.62	3.2×10^5
$CH_3CO_2^-$	4.47	1.8×10^6

^a At 8-9°C, Diebler, H. Z. *Phys. Chem.* 1969, 68, 64.

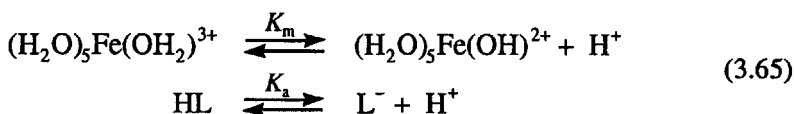
Table 3.22. Rate Constants (25°C) for Substitution Reactions on $V(OH_2)_6^{3+}$

Entering Group	k ($M^{-1} s^{-1}$)
$HC_2O_4^-$	1.3×10^3
SCN^-	1.1×10^2
Br^-	≤ 10
Cl^-	≤ 3
HN_3	0.4
H_2O (in s^{-1})	5.0×10^2

3.8.2 Substitution on Iron(III) and the Proton Ambiguity

Despite its common occurrence and importance, $Fe(OH_2)_6^{3+}$ was the last of the air-stable first-row transition-metal ions to have its water exchange rate determined. The difficulty is the tendency of $Fe(OH_2)_6^{3+}$ to hydrolyze and polymerize in dilute aqueous acid, forming $Fe(OH_2)_5(OH)^{2+}$ and $(H_2O)_4Fe(OH)_2Fe(OH_2)_4^{4+}$, respectively, as the major species. There have been numerous kinetic studies of substitution on $Fe(OH_2)_6^{3+}$, but the results were difficult to interpret because of the lack of a water exchange rate until 1981 and because of the proton ambiguity discussed below.

For the typical system in which the entering group has an ionizable proton, and for Fe(III) concentrations low enough to avoid the hydrolyzed dimer, the rapid equilibria involving the reactants are represented by



where $K_m = 1.6 \times 10^{-3} M$ (25°C). In the following development, the charges of the iron and ligand species have been omitted. The total Fe(III) and ligand concentrations in the reactants are given by

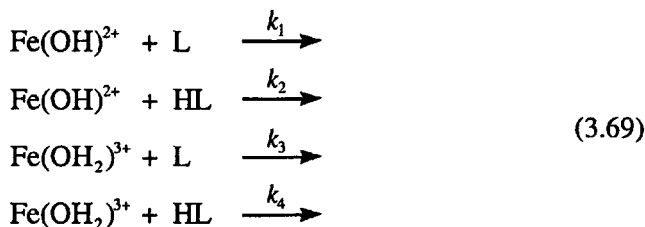
$$[Fe]_{tot} = [FeOH_2] + [FeOH] \quad \text{and} \quad [L]_{tot} = [HL] + [L] \quad (3.66)$$

From reaction (3.65) and Eq. (3.66), the concentrations of the Fe(III) and ligand species in terms of $[Fe]_{tot}$ and $[L]_{tot}$ are given as

$$[FeOH_2] = \frac{[H^+]}{K_m + [H^+]} [Fe]_{tot} \quad \text{and} \quad [FeOH] = \frac{K_m}{K_m + [H^+]} [Fe]_{tot} \quad (3.67)$$

$$[HL] = \frac{[H^+]}{K_a + [H^+]} [L]_{tot} \quad \text{and} \quad [L] = \frac{K_a}{K_a + [H^+]} [L]_{tot} \quad (3.68)$$

The possible substitution reactions in this system are given by



The rate of formation of product, P, is given by Eq. (3.70), so that substitution from Eqs. (3.67–3.68) into Eq. (3.70) leads to Eq. (3.71).

$$\frac{d[\text{P}]}{dt} = (k_1[\text{L}] + k_2[\text{HL}])[\text{FeOH}] + (k_3[\text{L}] + k_4[\text{HL}])[\text{FeOH}_2] \tag{3.70}$$

$$\frac{d[\text{P}]}{dt} = \left(\frac{k_1 K_m K_a + (k_2 K_m + k_3 K_a)[\text{H}^+] + k_4 [\text{H}^+]^2}{(K_m + [\text{H}^+])(K_a + [\text{H}^+)} \right) [\text{Fe}]_{\text{tot}} [\text{L}]_{\text{tot}} \tag{3.71}$$

This can be simplified to

$$\frac{d[\text{P}]}{dt} = k_{\text{exp}} [\text{Fe}]_{\text{tot}} [\text{L}]_{\text{tot}} \tag{3.72}$$

In Eq. (3.72), it has been assumed that the experimental conditions are such that $[\text{H}^+]$ is constant for a particular kinetic run. The overall experimental study involves determining k_{exp} at different $[\text{H}^+]$ and fitting this information to the $[\text{H}^+]$ dependence of k_{exp} predicted by Eq. (3.71).

For most studies, $[\text{H}^+] \gg K_m$ ($= 1.6 \times 10^{-3} \text{ M}$), and two limiting conditions for k_{exp} can be identified depending on the strength of the acid HL.

1. *Strong acid ligands:* $K_a \gg [\text{H}^+]$ and

$$k_{\text{exp}} = \frac{k_1 K_m}{[\text{H}^+]} + \frac{k_2 K_m}{K_a} + k_3 + \frac{k_4 [\text{H}^+]}{K_a} \tag{3.73}$$

2. *Weak acid ligands:* $[\text{H}^+] \gg K_a$ and

$$k_{\text{exp}} = \frac{k_1 K_m K_a}{[\text{H}^+]^2} + \frac{k_2 K_m}{[\text{H}^+]} + \frac{k_3 K_a}{[\text{H}^+]} + k_4 \tag{3.74}$$

The *proton ambiguity* refers to the fact that the $[\text{H}^+]$ dependence of k_{exp} does not allow one to separate $k_2 K_m / K_a$ from k_3 in the first case, or $k_2 K_m$ from $k_3 K_a$ in the second case. This results because the transition states, $\text{Fe(OH)} \cdot \text{HL}$ and $\text{Fe(OH}_2\text{)} \cdot \text{L}$, both contain one ionizable proton that is in different sites. *The kinetics can only give the composition of the transition state, not its structure.*

The experimental pseudo-first-order rate constant for almost all of the substitution reactions on aqueous iron(III) has the general form of

$$k_{\text{exp}} = k' + k''[\text{H}^+]^{-1} \quad (3.75)$$

The specific assignment of k' and k'' can be made by comparison to the theoretical expressions for the appropriate case, except for the proton ambiguity problem.

1. *Strong acid ligands:* ($K_a \gg [\text{H}^+]$). A comparison of Eqs. (3.73) and (3.75) shows that $k'' = k_1 K_m$, and k_1 can be calculated since K_m is known. However, $k' = k_3 + k_2 K_m / K_a$ and cannot be uniquely assigned except for very strong acid ligands, such as Cl^- and Br^- . For such ions, the large K_a ($\approx 10^8 \text{ M}$) makes the second term negligible even if k_2 has a diffusion limiting value of $\sim 10^{10} \text{ M}^{-1} \text{ s}^{-1}$.
2. *Weak acid ligands:* ($[\text{H}^+] \gg K_a$). From Eqs. (3.74) and (3.75), $k' = k_4$ and $k'' = k_2 K_m + k_3 K_a$. If K_a is very small (e.g. $< 10^{-10} \text{ M}$), it may be possible to eliminate the $k_3 K_a$ term again on the grounds that the k_3 would need to be beyond the diffusion-controlled limit.

The usual strategy in this area has been to calculate both k_2 and k_3 in ambiguous cases, and then compare k_1 and k_2 , assuming that they should be similar for a dissociative mechanism, and likewise for k_4 and k_3 . Some results are given in Table 3.23.

Table 3.23. Rate Constants (25°C)^a for Substitution Reactions on Aqueous Iron(III)

Entering Group	$k \text{ (M}^{-1} \text{ s}^{-1}\text{)}$	
	$(\text{H}_2\text{O})_5\text{Fe}(\text{OH})^{2+}$	$\text{Fe}(\text{OH})_6^{3+}$
SO_4^{2-}	1.1×10^5	2.3×10^3
Cl^-	5.5×10^3	4.8
Br^-	2.8×10^3	1.6
NCS^-	5.1×10^3	9.0×10^1
$\text{Cl}_3\text{CCO}_2^-$	7.8×10^3	6.3×10^1
$\text{Cl}_2\text{HCCO}_2^-$	1.9×10^4	1.2×10^2
$\text{ClH}_2\text{CCO}_2^-$	4.1×10^4	1.5×10^3
$\text{H}_3\text{CCO}_2\text{H}$	$\leq 2.8 \times 10^3$	2.7×10^1
$\text{C}_6\text{H}_5\text{OH}$	1.5×10^3	
$\text{C}_{10}\text{H}_{12}(\text{=O})(\text{OH})^b$	6.3×10^3	2.2×10^1
$\text{H}_3\text{CC}(\text{O})\text{NH}(\text{OH})$	2.0×10^3	1.2
H_2O (in s^{-1})	1.2×10^5	1.6×10^2

^a Data from Grant, M.; Jordan, R. B. *Inorg. Chem.* **1981**, *20*, 55, where original references are given.

^b 4-isopropyltropolone, Ishihara, K.; Funahashi, S.; Tanaka, M. *Inorg. Chem.* **1983**, *22*, 194.

Until the water exchange rates were determined, this strategy led to ambiguous mechanistic conclusions.^{201,202} The current interpretation of the data, such as that in Table 3.23, is that the mechanism is I_a for $\text{Fe}(\text{OH}_2)_6^{3+}$ but is I_d for $(\text{H}_2\text{O})_5\text{Fe}(\text{OH})^{2+}$. For the neutral ligand 4-isopropyltropolone, Hipt, the assignment to k_3 was made because the alternative assignment to k_2 ($\text{Fe}(\text{OH})^{2+} + \text{H}_2\text{ipt}^+$) gives a larger value for k_2 than k_1 ($\text{Fe}(\text{OH})^{2+} + \text{Hipt}$) and is contrary to expected charge effects.

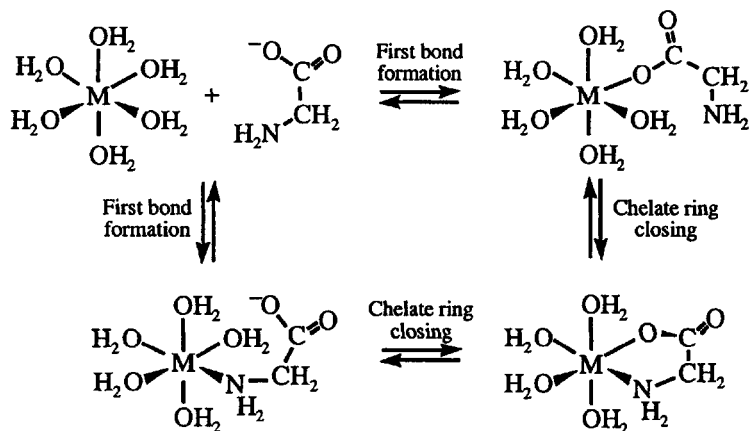
3.9 KINETICS OF CHELATE FORMATION

Complexes containing bidentate, tridentate and so on ligands are very common with metal ions. They are especially important because of their apparently enhanced stability, often referred to as the "chelate effect". Such ligands have two or more potential donor atoms separated by two, three or four other atoms in the molecule. Some common examples are oxalate, glycine, salicylate, ethylenediamine, acetylacetonate, 2,2'-bipyridyl and ethylenediaminetetraacetic acid.

3.9.1 Rate-Controlling Step

The formation of a bidentate chelate from the solvated metal ion involves the displacement of two solvent molecules. The process is unlikely to involve concerted replacement of two solvent ligands, and is rather considered to be a stepwise process, as shown in Scheme 3.8.

Scheme 3.8



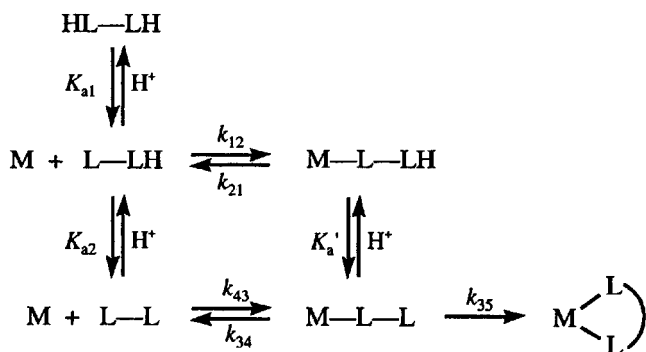
The glycine example in the above Scheme illustrates two mechanistic complications that can occur in chelate formation reactions. First of all, there are two potential rate-controlling steps, either *first bond formation* or *chelate ring closing*. Second, for unsymmetrical chelates, such as glycine,

there is an ambiguity as to which donor group may coordinate first. The latter is not a complication for symmetrical chelates, such as oxalate or ethylenediamine.

Prior to about 1970, it was commonly assumed that the chelate ring-closing step was very fast relative to the first bond formation. The rationale for this assumption was that the free end of the chelate in the monodentate intermediate would have a very high effective concentration in the neighborhood of the metal ion so that ring closing would be fast. However, there is increasing evidence that substitution reactions on the M(II) first-row transition-metal ions have considerable dissociative character, and the dissociative ion pair mechanism has achieved wide acceptance. This is especially true for Ni(II) which is a popular metal ion for mechanistic studies in this area. If the mechanism is dissociative, then the rate-limiting feature is the breaking of the M—OH₂ bond, and the effective concentration of the entering group is no greater than it would be in the ion pair. The idea that first bond formation is always rate limiting still persists in some quarters, perhaps because the experimental rate constants for chelate formation are often quite similar to those for monodentate complex formation with a given metal ion.

A proper consideration of the kinetic situation requires an analysis of the theoretical rate law for such a system. The following analysis is somewhat simplified in that a symmetrical bidentate chelate is assumed and the ring closing is not reversible. A complete version has been given by Letter and Jordan.²⁰³ These reactions are usually done in dilute acid (pH 5–7), so that protonation of the entering group has been included in Scheme 3.9, but charges and coordinated solvent have been omitted.

Scheme 3.9



If the monodentate species (M—L—LH and M—L—L) are assumed to be reactive intermediates, so that the steady-state approximation can be applied to their concentrations, and the usual pseudo-first-order conditions of $[M] \gg [L]_{\text{tot}}$ and constant $[H^+]$ are assumed, then it can be shown that the pseudo-first-order rate constant is given by Eq. (3.76) for $K_{a1} \gg [H^+]$.

$$k_{\text{exp}} = \frac{\left(\frac{k_{12}[\text{H}^+] + k_{43}K_{a2}}{K_{a2} + [\text{H}^+]} \right) k_{35}K'_a}{k_{21}[\text{H}^+] + K'_a(k_{34} + k_{35})} [\text{M}] \quad (3.76)$$

Rearrangement of this equation gives Eq. (3.77), which is of the form often used to analyze data by plotting the left-hand side versus $[\text{H}^+]^{-1}$.

$$\frac{k_{\text{exp}} \left(\frac{K_{a2} + [\text{H}^+]}{[\text{H}^+]} \right)}{[\text{M}]} = \frac{(k_{12} + k_{43}K_{a2}[\text{H}^+]^{-1})k_{35}K'_a}{k_{21}[\text{H}^+] + K'_a(k_{34} + k_{35})} \quad (3.77)$$

In a typical study, such as that of Wilkins and co-workers,²⁰⁴ this plot is linear. The traditional explanation for this is that $k_{35}K'_a \gg k_{21}[\text{H}^+]$ and $k_{35} \gg k_{34}$, so that Eq. (3.77) simplifies to Eq. (3.78), which will give k_{12} as the intercept and $k_{43}K_{a2}$ as the slope.

$$\frac{k_{\text{exp}} \left(\frac{K_{a2} + [\text{H}^+]}{[\text{H}^+]} \right)}{[\text{M}]} = k_{12} + k_{43}K_{a2}[\text{H}^+]^{-1} \quad (3.78)$$

This rate law is consistent with the observations, but there is at least one notable problem. For amino acids such as glycine, $\text{HO}_2\text{CCH}_2\text{NH}_3^+$, it is always found that $k_{12} = 0$ (i.e., there is no significant intercept for the plot). This implies that the zwitterion, $^-\text{O}_2\text{CCH}_2\text{NH}_3^+$, is unreactive. This lack of reactivity always seemed remarkable but was attributed to intramolecular hydrogen bonding between the amino and carboxylate groups. However, monoprotonated ethylenediamine does react, although the charge is less favorable and there is a greater likelihood of hydrogen bonding.

These and other problems caused Letter and Jordan²⁰³ to reconsider the assumptions used to reduce the complete rate law. Is it reasonable that $k_{35}K'_a \gg k_{21}[\text{H}^+]$? If one uses the Ni(II)–glycine system for analysis, then an estimate of $k_{21} \approx 10^4 \text{ s}^{-1}$ can be obtained from the corresponding nickel(II)-acetate system, and $(\text{H}_3\text{N})_5\text{Co}-\text{O}_2\text{CCH}_2\text{NH}_3^+$ can be used to estimate that $K'_a = 3 \times 10^{-10} \text{ M}$. Then, the condition that $k_{35}K'_a \gg k_{21}[\text{H}^+]$ at pH 6 requires that $k_{35} \geq 10^8 \text{ s}^{-1}$. However, $k = 3 \times 10^4 \text{ s}^{-1}$ for water exchange on Ni(II), and all the available evidence indicates an I_d mechanism for substitution on Ni(II). Therefore, if k_{35} is $\geq 10^8 \text{ s}^{-1}$, then the water ligands in the monodentate intermediate must be labilized by about a factor of 10^4 , an effect that is without precedent.

On the other hand, if one assumes that $k_{21}[\text{H}^+] \gg k_{35}K'_a$, then the denominator in the complete rate law, Eq. (3.76), can be rearranged using the principle of detailed balancing, which requires that $K'_a(k_{12}/k_{21}) = K_{a2}(k_{43}/k_{34})$, to yield

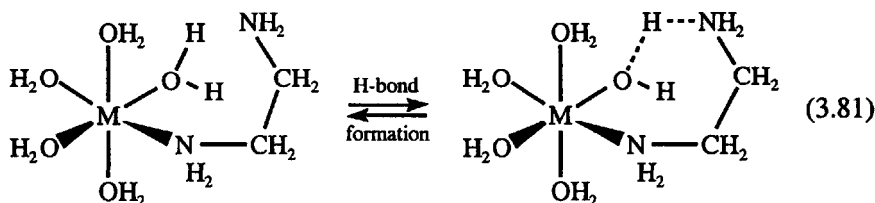
$$k_{21}[\text{H}^+] + K'_a(k_{34} + k_{35}) = \frac{k_{21}[\text{H}^+]}{k_{12}} \left(k_{12} + \frac{k_{43}K_{a2}k_{35}}{k_{34}[\text{H}^+]} \right) \quad (3.79)$$

A comparison of the right- and left-hand sides of Eq. (3.79), combined with the assumed inequality, requires that $k_{12} \gg k_{43}K_{a2}k_{35}/k_{34}[\text{H}^+]$. Then, if $k_{35} \gg k_{34}$, as assumed before, $k_{12} \gg k_{43}K_{a2}/[\text{H}^+]$ and the rearranged version of Eq. (3.76) simplifies to

$$\frac{k_{\text{exp}}(K_{a2} + [\text{H}^+])}{[\text{M}][\text{H}^+]} = \frac{k_{12}k_{35}K_a'}{k_{21}[\text{H}^+]} = \frac{k_{43}k_{35}K_{a2}}{k_{34}[\text{H}^+]} \quad (3.80)$$

This equation is consistent with the experimental observations; a zero intercept is required but does not imply that k_{12} is zero. This rate law corresponds to the condition of a rapid pre-equilibrium formation of the monodentate species, k_{43}/k_{34} , followed by *rate-controlling chelate ring closure*. The values originally associated with k_{43} are actually $k_{43}k_{35}/k_{34}$. Since these are numerically similar to rate constants observed for monodentate systems, it would appear that the ratio k_{35}/k_{34} is of the order of magnitude of 1.

Unusually large experimental rate constants ($\sim 10^7 \text{ M}^{-1} \text{ s}^{-1}$), assigned originally to k_{43} but actually $k_{43}k_{35}/k_{34}$, have been observed for reactions of polyamines, such as ethylenediamine. To explain this, an internal conjugate base, ICB, mechanism was proposed²⁰⁵ in which the free end of the amine forms a hydrogen bond to a coordinated water, giving it some hydroxide character, as shown in reaction (3.81). This is supposed to make the remaining waters more labile to substitution according to the ICB proposal. Strangely, this rate enhancement is not observed with amino acids or with 2-methylaminopyridine.



A reanalysis of these observations for the reaction of ethylenediamine with Ni(II) ²⁰⁶ has shown that $k_{43}k_{35}/k_{34} = 7.2 \times 10^6 \text{ M}^{-1} \text{ s}^{-1}$. One can estimate from the kinetics for the ethylamine reaction that $k_{43} \approx 900 \text{ M}^{-1} \text{ s}^{-1}$ and $k_{34} \approx 15 \text{ s}^{-1}$, so that $k_{35} \approx 1.2 \times 10^5 \text{ s}^{-1}$. This value is about 5 times larger than the rate constant for water exchange on $\text{Ni(OH}_2)_6^{2+}$, but Hunt and co-workers²⁰⁷ found that the water exchange rate constant on $\text{Ni(OH}_2)_5(\text{NH}_3)^{2+}$ is $2.5 \times 10^5 \text{ s}^{-1}$. It is reasonable to expect that the water exchange on the monodentate ethylenediamine complex is similar to that of the NH_3 complex. Therefore, there is no anomalous reactivity for ethylenediamine relative to monodentate models.

The conclusion is that the high reactivity of the polyamines is due to a nonreacting ligand effect in which amines greatly increase the rate of water

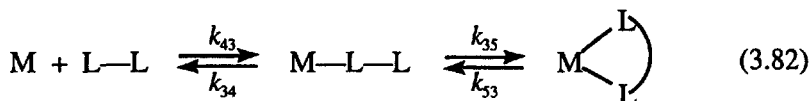
release from Ni(II). The work of Hunt and co-workers also established that a coordinated pyridine or carboxylate group does not have a strong labilizing influence on Ni(II). This explains the normal reactivity of the amino acids and pyridine amines.

Moore and co-workers²⁰⁸ used stopped-flow NMR to measure the rate of first bond formation and chelate ring closing in the reactions of $\text{Al}(\text{DMSO})_6^{3+}$ with 2,2'-bipyridine and 2,2':6',2''-terpyridine systems in nitromethane. They found that the rate constant for first bond formation ($\sim 2 \times 10^3 \text{ M}^{-1} \text{ s}^{-1}$ at 25°C) is much larger than the DMSO exchange rate ($5.3 \times 10^{-2} \text{ s}^{-1}$ at 25°C), presumably because of strong preassociation of the reactants. The chelate ring closing rate constants ($\sim 10^{-2} \text{ s}^{-1}$) are smaller than the solvent exchange rate constant, possibly because of steric hindrance to twisting the second pyridine ring into a conformation suitable for chelation. In the same study, the reaction with 1,10-phenanthroline proceeded in a one-step process to the chelate. This may be because the fused ring of phenanthroline forces the two donor nitrogen atoms to be oriented for chelate formation.

3.9.2 Kinetics and the Chelate Effect

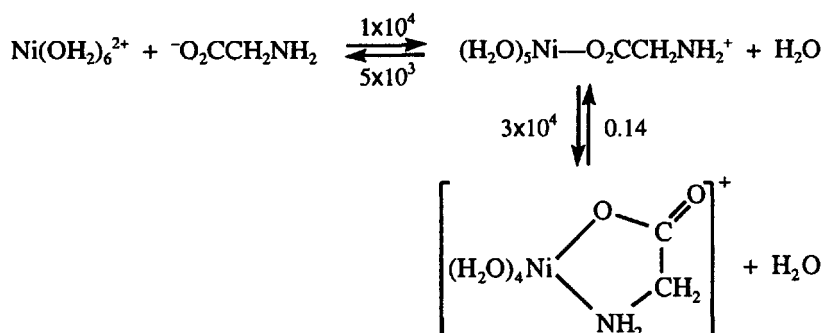
It has been observed many times that the formation constant for a chelate, such as $\text{Ni}(\text{OH}_2)_4(\text{en})^{2+}$ ($K_f = 5 \times 10^7 \text{ M}^{-1}$), is much greater than that for the monodentate analogue, such as $\text{Ni}(\text{OH}_2)_4(\text{NH}_3)_2^{2+}$ ($K_f = \beta_2 = 1.5 \times 10^5 \text{ M}^{-2}$). It should be noted that this is an unfair comparison because the two equilibrium constants have different units. Nevertheless, there is a lot of operational experience to support the greater stability of chelates. There have been several approaches to explaining this effect, such as differences in entropy change due to the different number of particles involved and/or a very large forward rate constant for ring closing because of high local concentration effects in the monodentate intermediates.

It is instructive to consider the chelate formation process from a kinetic analysis of the individual steps, given by



For the ethylenediamine system at 25°C , the analysis in the preceding section gave $k_{43} \approx 900 \text{ M}^{-1} \text{ s}^{-1}$, $k_{34} \approx 15 \text{ s}^{-1}$ and $k_{35} \approx 1.2 \times 10^5 \text{ s}^{-1}$, and by direct measurement of the dissociation kinetics, $k_{53} \approx 0.14 \text{ s}^{-1}$. The small value of k_{53} for chelate ring opening is quite unexpected. From a mechanistic standpoint, one would expect k_{53} to increase relative to k_{34} roughly in proportion to k_{35}/k_{43} , so that it would have a value of $\sim 2 \times 10^3 \text{ s}^{-1}$. But k_{53} is much smaller than k_{34} . A similar conclusion is reached for glycine, for which the rate constants ($\text{M}^{-1} \text{ s}^{-1}$ or s^{-1} at 25°C) are given in Scheme 3.10.

Scheme 3.10



It has been noted that the magnitude of the chelate effect decreases as the chelate ring size increases. For example, the formation constants²⁰⁹ for the aquanickel(II) complexes of ethylenediamine and 1,3-diaminopropane are 2.5×10^7 and $2 \times 10^6 \text{ M}^{-1}$, respectively. The formation constant is about 10 times smaller for the six-membered chelate ring complex, despite the fact that trimethylenediamine is a stronger base toward the proton. This effect has traditionally been assigned to a smaller chelate ring-closing rate constant, k_{35} , for the longer chelate arm in the monodentate intermediate. However, the preceding analysis implies that the effect might lie in a larger rate constant for chelate ring opening, k_{53} , with the larger chelate ring.

Some evidence for this is found for amino-pyridine systems,^{210,211} as shown in Figure 3.5. The rate constant for ring opening of the six-membered chelate is about 10 times larger than that for either of the five-membered rings. A methyl group on the coordinated amine has a more modest effect that could be ascribed to steric acceleration of a dissociative process.

The conclusion is that chelate ring opening, k_{53} , is an unexpectedly slow process, and this accounts for the high formation constants of chelate complexes. It should be noted that this analysis applies for dissociative type substitutions where the rate is insensitive to the entering group.

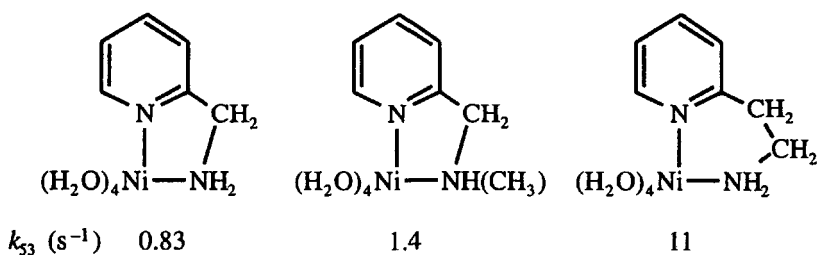


Figure 3.5. Some chelates of $(\text{H}_2\text{O})_4\text{Ni}(\text{amino-pyridine})^{2+}$ and their rate constants for chelate ring opening.

The formation constant for the chelate in Eq. (3.82) is given by

$$K_f = \frac{k_{43}k_{35}}{k_{34}k_{53}} \quad (3.83)$$

The above explanation suggests that K_f is unexpectedly large for a chelate because k_{53} is unexpectedly small relative to the normal lability of the particular metal ion. Previous kinetic explanations have assumed that k_{35} is unusually large. It is somewhat ironic that k_{53} has received very little attention, since kinetic studies in this area have concentrated on entering group effects. Further examples with similar conclusions are provided in a series of papers by Funahashi and co-workers on the exchange of chelating diamines,²¹² and in the work of Clarkson et al.²¹³ on the base hydrolysis of Co(III) macrocycles with NH_3 and en leaving groups.

References

- Langford, C. H.; Gray, H. B. *Ligand Substitution Processes*; Benjamin, Inc.: New York, 1966.
- Fuoss, R. M. *J. Am. Chem. Soc.* **1958**, *80*, 5059.
- Eigen, M. Z. *Electrochem.* **1960**, *64*, 115.
- Haim, A.; Wilmarth, W. K. *Inorg. Chem.* **1962**, *1*, 573, 583.
- Haim, A.; Grassi, R. J.; Wilmarth, W. K. *Adv. Chem. Ser.* **1965**, *49*, 31.
- Burnett, M. G.; Gilfillian, W. M. *J. Chem. Soc., Dalton Trans.* **1981**, 1578.
- Haim, A. *Inorg. Chem.* **1982**, *21*, 2887.
- Abou-El-Wafa, M. H. M.; Burnett, M. G.; McCullagh, J. F. *J. Chem. Soc., Dalton Trans.* **1987**, 2311, and references therein.
- Bradley, S. M.; Doine, H.; Krouse, H. R.; Sisley, M. J.; Swaddle, T. W. *Aust. J. Chem.* **1988**, *41*, 1323.
- Abou-El-Wafa, M. H. M.; Burnett, M. G.; McCullagh, J. F. *J. Chem. Soc., Dalton Trans.* **1986**, 2083.
- Robb, D.; Steyn, M. M. De V.; Kruger, H. *Inorg. Chim. Acta* **1969**, *3*, 383.
- Stranks, D. R.; Yandell, J. K. *Inorg. Chem.* **1970**, *9*, 751.
- Seibles, L.; Deutsch, E. D. *Inorg. Chem.* **1977**, *16*, 2273.
- O'Brien, P.; Sweigart, D. A. *Inorg. Chem.* **1982**, *21*, 2094.
- Inamo, M.; Sumi, T.; Nakagawa, N.; Funahashi, S.; Tanaka, M. *Inorg. Chem.* **1989**, *28*, 2688; Inamo, M.; Sugiura, S.; Fukuyama, H.; Funahashi, S. *Bull. Chem. Soc. Jpn.* **1994**, *67*, 1848.
- Inamo, M.; Hoshino, M.; Nakajima, K.; Aizawa, S.; Funahashi, S. *Bull. Chem. Soc. Jpn.* **1995**, *68*, 2293.
- Sargeson, A. M.; Jordan, R. B. *Inorg. Chem.* **1965**, *4*, 431.
- Buckingham, D. A.; Clark, C. R.; Lewis, T. W. *Inorg. Chem.* **1979**, *18*, 1985.
- Jackson, W. G.; Hookey, C. N. *Inorg. Chem.* **1984**, *23*, 668, 2728; Jackson, W. G.; McGregor, B. C.; Jurisson, S. S. *Inorg. Chem.* **1987**, *26*, 1286.

20. Brasch, N. E.; Buckingham, D. A.; Clark, C. R.; Finnie, K. S. *Inorg. Chem.* **1989**, *28*, 4567.
21. Jackson, W. G. *Inorg. React. Mech.* **2002**, *4*, 1.
22. Baran, Y.; Comba, P.; Lawrance, G. A. *Inorg. React. Mech.* **2002**, *4*, 31.
23. Basolo, F.; Pearson, R. G. *Mechanisms of Inorganic Reactions*, 2nd ed.; Wiley & Sons: New York, 1967.
24. Nordmeyer, F. R. *Inorg. Chem.* **1969**, *8*, 2780.
25. Buckingham, D. A.; Marty, W.; Sargeson, A. M. *Helv. Chim. Acta* **1978**, *61*, 2223.
26. Browne, R. J.; Buckingham, D. A.; Clark, C. R.; McKeon, J. A.; Jackson, W. G. *Helv. Chim. Acta* **2003**, *86*, 13.
27. Buckingham, D. A.; Cresswell, P. J.; Sargeson, A. M. *Inorg. Chem.* **1975**, *14*, 1485; Fabius, B.; Geue, R. J.; Hazell, R. G.; Jackson, W. G.; Larsen, F. K.; Qin, C. J.; Sargeson, A. M. *J. Chem. Soc., Dalton Trans.* **1999**, 3961.
28. Jackson, W. G.; Dutton, B. H. *Inorg. Chem.* **1989**, *28*, 525.
29. House, D. A.; Jackson, W. G. *Inorg. Chim. Acta* **1998**, *274*, 42.
30. Jackson, W. G.; McGregor, B. C.; Jurisson, S. S. *Inorg. Chem.* **1990**, *29*, 4677.
31. Buckingham, D. A.; Clark, C. R.; Liddell, G. F. *Inorg. Chem.* **1992**, *31*, 2909; Brasch, N. E.; Buckingham, D. A.; Clark, C. R.; Simpson, J. *Inorg. Chem.* **1996**, *35*, 7728.
32. House, D. A.; Powell, H. K. J. *Inorg. Chem.* **1971**, *10*, 1583.
33. Lawrance, G. A. *Inorg. Chem.* **1982**, *21*, 3687.
34. Curtis, N. J.; Lawrance, G. A.; van Eldik, R. *Inorg. Chem.* **1989**, *28*, 329.
35. Jordan, R. B. *Inorg. Chem.* **1996**, *35*, 3725.
36. Cattalini, L.; Ugo, R.; Orio, A. *J. Am. Chem. Soc.* **1968**, *90*, 4800.
37. Toma, H.; Malin, J. M. *J. Am. Chem. Soc.* **1972**, *94*, 4039.
38. Maresca, L.; Natile, G.; Calligaris, M.; Delise, P.; Randaccio, L. *J. Chem. Soc., Dalton Trans.* **1976**, 2386.
39. Canovese, L.; Cattalini, L.; Uguagliati, P.; Tobe, M. L. *J. Chem. Soc., Dalton Trans.* **1990**, 867.
40. Edwards, J. O. *J. Am. Chem. Soc.* **1954**, *76*, 1540.
41. Schwarzenbach, G.; Shellenberg, M. *Helv. Chim. Acta* **1965**, *48*, 28.
42. Pearson, R. G.; Sobel, H.; Songstad, J. *J. Am. Chem. Soc.* **1968**, *90*, 319.
43. Mayer, U.; Gutmann, V. *Adv. Inorg. Chem. Radiochem.* **1975**, *17*, 189.
44. Gutmann, V. *Coord. Chem. Rev.* **1976**, *19*, 225; Gutmann, V. *Electrochim. Acta* **1976**, *21*, 661.
45. Mayer, U.; Gutmann, V.; Gerger, W. *Monatsh. Chem.* **1975**, *106*, 1235.
46. Fawcett, W. R. *J. Phys. Chem.* **1993**, *97*, 9540.
47. Mao, W. L.; Qian, Z.; Yen, H. J.; Curtis, J. C. *J. Am. Chem. Soc.* **1996**, *118*, 3247; Neyhart, G. A.; Hupp, J. T.; Curtis, J. C.; Meyer, T. J. *J. Am. Chem. Soc.* **1996**, *118*, 3724; Liard, D. J.; Kleverlaan, C. J.; Vlcek, A., Jr. *Inorg. Chem.* **2003**, *42*, 7995.
48. Friesen, D. A.; Lee, S. H.; Nashiem, R. E.; Mezyk, S. P.; Waltz, W. L. *Inorg. Chem.* **1995**, *34*, 4026.
49. Maria, P.-C.; Gal, J.-F. *J. Phys. Chem.* **1985**, *89*, 1296.

50. Linert, W.; Jameson, R. F.; Taha, A. *J. Chem. Soc., Dalton Trans.* **1993**, 3181.
51. Linert, W.; Camard, A.; Camard, M.; Michot, C. *Coord. Chem. Rev.* **2002**, 226, 137.
52. Linert, W.; Fukuda, Y.; Camard, A. *Coord. Chem. Rev.* **2001**, 218, 113.
53. Drago, R. S. *Coord. Chem. Rev.* **1980**, 33, 251; Drago, R. S.; Wong, N.; Bilgrien, C.; Vogel, G. C. *Inorg. Chem.* **1987**, 26, 9.
54. Drago, R. S.; Dadmun, A. P.; Vogel, G. C. *Inorg. Chem.* **1993**, 32, 2473.
55. Drago, R. S.; Dadmun, A. P. *J. Am. Chem. Soc.* **1994**, 116, 1792; Drago, R. S. *Organometallics* **1995**, 14, 3408.
56. Drago, R. S.; Joerg, S. *J. Am. Chem. Soc.* **1996**, 118, 2654; Joerg, S.; Drago, R. S. *Organometallics* **1998**, 17, 589.
57. Lim, Y. Y.; Drago, R. S.; Babich, M. W.; Wong, N.; Doan, P. E. *J. Am. Chem. Soc.* **1987**, 109, 169.
58. Joerg, S.; Webster, C. E.; Drago, R. S.; Sales, J. *Polyhedron* **1999**, 18, 1097.
59. Drago, R. S.; Ferris, D. C. *J. Phys. Chem.* **1995**, 99, 6563.
60. Hancock, R. D.; Martell, A. E. *Adv. Inorg. Chem.* **1995**, 42, 89; *Ibid. J. Chem. Educ.* **1996**, 73, 654.
61. Abraham, M. H.; Doherty, R. M.; Kamlet, M. J.; Taft, R. W. *Chem. Brit.* **1986**, 22, 551; Abraham, M. H.; Grellier, P. L.; Prior, D. V.; Taft, R. W.; Morris, J. J.; Taylor, P. J.; Laurence, C.; Berthelot, M.; Doherty, R. M.; Kamlet, M. J.; Aboud, J.-L. M.; Sraidi, K.; Guih neuf, G. *J. Am. Chem. Soc.* **1988**, 110, 8534; Marcus, Y.; Kamlet, M. J.; Taft, R. W. *J. Phys. Chem.* **1993**, 22, 409.
62. Catal n, J.; G mez, J.; Couto, A.; Laynez, J. *J. Am. Chem. Soc.* **1990**, 112, 1678.
63. Valgimigli, L.; Ingold, K. U.; Lusztyk, J. *J. Am. Chem. Soc.* **1996**, 118, 3545.
64. Marcus, Y. *J. Solution Chem.* **1984**, 13, 599; Reichardt, E. C. *Solvents and Solvent Effects in Organic Chemistry*, 2nd ed.; VCH Publishers: New York, 1988; Reichardt, E. C. *Chem. Rev.* **1994**, 94, 2319.
65. Schut, D. M.; Keana, K. J.; Tyler, D. R.; Rieger, P. H. *J. Am. Chem. Soc.* **1995**, 117, 8939.
66. Drago, R. S.; Hirsch, M. S.; Ferris, D. C.; Chronister, C. W. *J. Chem. Soc., Perkin Trans. 2* **1994**, 219; George, J. E.; Drago, R. S. *Inorg. Chem.* **1996**, 35, 239.
67. Maria, P.-C.; Gal, J.-F.; Francheschi, J.; Fargin, E. *J. Am. Chem. Soc.* **1987**, 109, 483.
68. Marcus, Y. *Chem. Soc. Rev.* **1993**, 22, 409.
69. Pearson, R. G. *J. Chem. Educ.* **1968**, 45, 643.
70. Arhland, S.; Chatt, J.; Davies, N. R. *Quart. Rev. Chem. Soc.* **1958**, 12, 265.
71. Pearson, R. G. *Inorg. Chem.* **1988**, 27, 734; *Ibid. Coord. Chem. Rev.* **1990**, 100, 403; *Ibid. Inorg. Chim. Acta* **1995**, 240, 93.
72. Ayers, P. W. *J. Chem. Phys.* **2005**, 122, 141102.
73. Doan, P. E.; Drago, R. S. *J. Am. Chem. Soc.* **1984**, 106, 2772.
74. Kamlet, M. J.; Gal, J.-F.; Maria, P.-C.; Taft, R. W. *J. Chem. Soc., Perkin Trans. 2* **1985**, 1583.
75. Drago, R. S. *Inorg. Chem.* **1990**, 29, 1379.

76. Linert, W. *Chem. Soc. Rev.* **1994**, *23*, 429.
77. Langford, C. H. *Inorg. Chem.* **1965**, *4*, 265.
78. Haim, A. *Inorg. Chem.* **1970**, *9*, 426.
79. Swaddle, T. W.; Gustalla, G. *Inorg. Chem.* **1968**, *7*, 1915.
80. Tucker, M. A.; Colvin, C. B.; Martin, D. S., Jr. *Inorg. Chem.* **1964**, *3*, 1373.
81. Rerek, M. E.; Basolo, F. *J. Am. Chem. Soc.* **1984**, *106*, 5908.
82. Wax, M. J.; Bergman, R. G. *J. Am. Chem. Soc.* **1981**, *103*, 7028.
83. Alibrandi, G.; Romeo, R.; Scolaro, L. M.; Tobe, M. L. *Inorg. Chem.* **1992**, *31*, 5061.
84. Macchioni, A.; Zuccaccia, C.; Clot, E.; Gruet, K.; Crabtree, R. H. *Organometallics* **2001**, *20*, 2367; Macchioni, A. *Eur. J. Inorg. Chem.* **2003**, 195.
85. Brasch, N. E.; Buckingham, D. A.; Clark, C. R.; Simpson, J. *Inorg. Chem.* **1996**, *35*, 7728.
86. Parris, M.; Wallace, W. J. *Can. J. Chem.* **1969**, *7*, 2257.
87. Lawrance, G. A.; Schneider, K.; van Eldik, R. *Inorg. Chem.* **1984**, *23*, 3922.
88. Lay, P. A. *Inorg. Chem.* **1987**, *26*, 2144; Lay, P. A. *Coord. Chem. Rev.* **1991**, *110*, 213.
89. Gonzalez, G.; Martinez, M.; Rodriguez, E. *J. Chem. Soc., Dalton Trans.* **1995**, 891.
90. Benzo, F.; Bernhardt, P. V.; Gonzalez, G.; Martinez, M.; Sienna, B. *J. Chem. Soc., Dalton Trans.* **1999**, 3973.
91. Basolo, F.; Chatt, J.; Gray, H. B.; Pearson, R. G.; Shaw, B. L. *J. Chem. Soc.* **1961**, 2207.
92. Tolman, C. A. *Chem. Rev.* **1977**, *77*, 313.
93. Seligson, A. L.; Trogler, W. C. *J. Am. Chem. Soc.* **1991**, *113*, 2520.
94. DeSanto, J. T.; Mosbo, J. A.; Storhoff, B. N.; Bock, P. L.; Bloss, R. E. *Inorg. Chem.* **1980**, *19*, 3086.
95. Stahl, L.; Ernst, R. D. *J. Am. Chem. Soc.* **1987**, *109*, 5673; Stahl, L. S.; Trakarnprul, W.; Freeman, J. W.; Arif, A. M.; Ernst, R. D. *Inorg. Chem.* **1995**, *34*, 1810.
96. Smith, J. M.; Coville, N. J.; Cook, L. M.; Boeyens, C. A. *Organometallics* **2000**, *19*, 5273; Smith, J. M.; Coville, N. J. *Organometallics* **2001**, *20*, 1210.
97. Maitlis, P. *Chem. Soc. Rev.* **1981**, 1.
98. Coville, N. J.; Loonat, M. S.; White, D.; Carlton, L. *Organometallics* **1992**, *11*, 1082.
99. Caffery, M. L.; Brown, T. L. *Inorg. Chem.* **1991**, *30*, 3907; Brown, T. L. *Inorg. Chem.* **1992**, *31*, 1286; Choi, M. G.; White, D.; Brown, T. L. *Inorg. Chem.* **1994**, *33*, 5591.
100. Choi, M. G.; Brown, T. L. *Inorg. Chem.* **1993**, *32*, 5603.
101. Brown, T. L.; Lee, K. J. *Coord. Chem. Rev.* **1993**, *128*, 89.
102. White, D.; Coville, N. J. *Adv. Organomet. Chem.* **1994**, *36*, 95.
103. Bodner, G. M.; May, M. P.; McKinney, L. E. *Inorg. Chem.* **1980**, *19*, 1951.
104. Rahman, Md. M.; Liu, H. Y.; Prock, A.; Giering, W. P. *Organometallics* **1987**, *6*, 650; Lorsbach, B. A.; Bennett, D. M.; Prock, A.; Giering, W. P. *Organometallics* **1995**, *14*, 869.

105. Drljaca, A.; Hubbard, C. D.; van Eldik, R.; Asano, T.; Basilevsky, M. V.; le Noble, W. J. *Chem. Rev.* **1998**, *98*, 2167; van Eldik, R.; Asano, T.; le Noble, W. J. *Chem. Rev.* **1989**, *89*, 549.
106. Swaddle, T. W.; Stranks, D. R. *J. Am. Chem. Soc.* **1972**, *94*, 8357.
107. Laurency, G.; Rapaport, I.; Zbinden, D.; Merbach, A. E. *Magn. Reson. Chem.* **1991**, *29*, S45.
108. Doine, H.; Ishihara, K.; Krouse, H. R.; Swaddle, T. W. *Inorg. Chem.* **1987**, *26*, 3240.
109. Rapaport, I.; Helm, L.; Merbach, A. E.; Bernhard, P.; Ludi, A. *Inorg. Chem.* **1988**, *27*, 873.
110. Tong, S. B.; Swaddle, T. W. *Inorg. Chem.* **1974**, *13*, 1538.
111. Cusanelli, A.; Frey, U.; Richens, D. T.; Merbach, A. E. *J. Am. Chem. Soc.* **1996**, *118*, 5265.
112. Helm, L.; Elding, L. I.; Merbach, A. E. *Inorg. Chem.* **1985**, *24*, 1719.
113. Aebischer, N.; Laurency, G.; Ludi, A.; Merbach, A. E. *Inorg. Chem.* **1993**, *32*, 2810.
114. De Vito, D.; Weber, J.; Merbach, A. E. *Inorg. Chem.* **2004**, *43*, 858.
115. Twigg, M. V. *Inorg. Chim. Acta* **1977**, *24*, L84.
116. Garrick, F. J. *Nature* **1937**, *139*, 507.
117. Tobe, M. L. *Acc. Chem. Res.* **1970**, *3*, 377; Tobe, M. L. *Adv. Inorg. Bioinorg. Mech.* **1983**, *2*, 1.
118. Sargeson, A. M. *Pure Appl. Chem.* **1973**, *33*, 527.
119. Buckingham, D. A.; Clark, C. R.; Lewis, T. W. *Inorg. Chem.* **1979**, *18*, 2041.
120. Dickie, A. J.; Hockless, D. C. R.; Willis, A. C.; McKeon, J. A.; Jackson, W. G. *Inorg. Chem.* **2003**, *42*, 3822; Jackson, W. G.; Dickie, A. J.; McKeon, J. A.; Spiccia, L.; Brudenell, S. J.; Hockless, D. C. R.; Willis, A. C. *Inorg. Chem.* **2005**, *44*, 401.
121. Appleton, T. G.; Clark, H. C.; Manzer, L. E. *Coord. Chem. Rev.* **1973**, *10*, 335; Hartley, F. R. *Chem. Soc. Rev.* **1973**, *2*, 163; Yatsimirskii, K. B. *Pure Appl. Chem.* **1974**, *38*, 341; Coe, B. J.; Glenwright, S. J. *Coord. Chem. Rev.* **2000**, *203*, 5.
122. Coyle, B. A.; Ibers, J. A. *Inorg. Chem.* **1972**, *11*, 1105.
123. Chatt, J.; Duncanson, L.; Shaw, B.; Venanzi, L. *Disc. Faraday Soc.* **1958**, *26*, 131; Adams, D. M.; Chatt, J.; Shaw, B. *J. Chem. Soc.* **1960**, 2047.
124. Parshall, G. W. *J. Am. Chem. Soc.* **1966**, *88*, 704.
125. Zumdahl, S. S.; Drago, R. S. *J. Am. Chem. Soc.* **1970**, *90*, 6669.
126. Armstrong, D. R.; Fortune, R.; Perkins, P. G. *Inorg. Chim. Acta* **1974**, *9*, 9.
127. Lin, Z. Y.; Hall, M. B. *Inorg. Chem.* **1991**, *30*, 646.
128. Deeth, R. J.; Elding, L. I. *Inorg. Chem.* **1996**, *35*, 5019.
129. Cooper, J.; Ziegler, T. *Inorg. Chem.* **2002**, *41*, 6614.
130. Burda, J. V.; Zeizinger, M.; Leszcynski, J. *J. Chem. Phys.* **2004**, *120*, 1253.
131. Anderson, K. M.; Orpen, A. G. *Chem. Commun.* **2001**, 2682.
132. Davy, R. D.; Hall, M. B. *Inorg. Chem.* **1989**, *28*, 3524.
133. Darensbourg, D. J.; Joyce, J. A.; Bischoff, C. J.; Reibenspies, J. H. *Inorg. Chem.* **1991**, *30*, 1137.

134. Hunt, J. P.; Rutenberg, A. C.; Taube, H. *J. Am. Chem. Soc.* **1952**, *74*, 268.
135. Darensbourg, D. J.; Jones, M. L. M.; Reibenspies, J. H. *Inorg. Chem.* **1996**, *35*, 4406.
136. Posey, F. A.; Taube, H. *J. Am. Chem. Soc.* **1953**, *75*, 4099.
137. Palmer, D. A.; van Eldik, R. *Chem. Rev.* **1983**, *83*, 561.
138. Massoud, S.; Jordan, R. B. *Inorg. Chim. Acta* **1994**, *221*, 9.
139. Buckingham, D. A.; Clark, C. R. *Inorg. Chem.* **1994**, *33*, 6171.
140. Baxter, K. E.; Hanton, L. R.; Simpson, J.; Vincent, B. R.; Blackman, A. G. *Inorg. Chem.* **1995**, *34*, 2795.
141. Van Eldik, R.; Harris, G. M. *Inorg. Chem.* **1980**, *19*, 880; Dasgupta, T. P.; Harris, G. M. *Inorg. Chem.* **1984**, *23*, 4398.
142. Joshi, V. K.; van Eldik, R.; Harris, G. M. *Inorg. Chem.* **1986**, *25*, 2229.
143. Murmann, R. K.; Taube, H. *J. Am. Chem. Soc.* **1956**, *78*, 4886.
144. Jackson, W. G.; Lawrance, G. A.; Lay, P. A.; Sargeson, A. M. *J. Chem. Soc., Chem. Commun.* **1982**, 70.
145. Andrade, C.; Taube, H. *J. Am. Chem. Soc.* **1964**, *86*, 1328.
146. Buckingham, D. A.; Foster, D. M.; Sargeson, A. M. *J. Am. Chem. Soc.* **1969**, *91*, 4102.
147. Buckingham, D. A.; Keene, F. R.; Sargeson, A. M. *J. Am. Chem. Soc.* **1974**, *96*, 4981.
148. Buckingham, D. A. In *Biological Aspects of Inorganic Chemistry*; Addison, A. W.; Cullen, W. R.; Dolphin, D.; James, B. R., Eds.; Wiley Interscience: New York, 1977; pp 141–196.
149. Boreham, C. J.; Buckingham, D. A.; Francis, D. J.; Sargeson, A. M.; Warner, L. G. *J. Am. Chem. Soc.* **1981**, *103*, 1975.
150. Pinnel, D.; Wright, G. B.; Jordan, R. B. *J. Am. Chem. Soc.* **1972**, *94*, 6104; Buckingham, D. A.; Keene, F. R.; Sargeson, A. M. *J. Am. Chem. Soc.* **1973**, *95*, 5649.
151. Dixon, N. E.; Fairlie, D. P.; Jackson, W. G.; Sargeson, A. M. *Inorg. Chem.* **1983**, *22*, 4038.
152. Ellis, W. R., Jr.; Purcell, W. L. *Inorg. Chem.* **1982**, *21*, 834.
153. Clark, C. R.; Tasker, R. F.; Buckingham, D. A.; Knighton, D. R.; Harding, D. R. K.; Hancock, W. S. *J. Am. Chem. Soc.* **1981**, *103*, 7023.
154. Sutton, P. A.; Buckingham, D. A. *Acc. Chem. Res.* **1987**, *20*, 357.
155. Hendry, P.; Sargeson, A. M. *Prog. Inorg. Chem.* **1990**, *38*, 201; Kimura, E.; Koike, T. *Adv. Inorg. Chem.* **1997**, *44*, 229; Hegg, E. L.; Burstyn, J. N. *Coord. Chem. Rev.* **1998**, *173*, 133.
156. Jones, D. R.; Lindoy, L. L.; Sargeson, A. M. *J. Am. Chem. Soc.* **1983**, *105*, 7327; Wijesekera, R. D.; Sargeson, A. M. *J. Coord. Chem.* **2005**, *58*, 3.
157. Westheimer, F. H. *Acc. Chem. Res.* **1968**, *1*, 70.
158. Anderson, B.; Milburn, R. M.; MacB. Harrowfield, J.; Robertson, G. B.; Sargeson, A. M. *J. Am. Chem. Soc.* **1977**, *98*, 2652.
159. Deck, K. M.; Tseng, T. A.; Burstyn, J. N. *Inorg. Chem.* **2002**, *41*, 669; Fry, F. H.; Fischmann, A. J.; Belousoff, M. J.; Spiccia, L.; Brügger, J. *Inorg. Chem.* **2005**, *44*, 941.

160. Koike, T.; Kimura, E. *J. Am. Chem. Soc.* **1991**, *113*, 8935; Kimura, E.; Aoki, S.; Koike, T.; Shiro, M. *J. Am. Chem. Soc.* **1997**, *119*, 3068.
161. Roigk, A.; Hettich, R.; Schneider, H. *Inorg. Chem.* **1998**, *37*, 751.
162. Branum, M. E.; Tipton, A. K.; Zhu, S.; Que, L., Jr. *J. Am. Chem. Soc.* **2001**, *123*, 1898.
163. Liu, C.; Wang, M.; Zhang, T.; Sun, H. *Coord. Chem. Rev.* **2004**, *238*, 147.
164. Lincoln, S. F.; Merbach, A. E. *Adv. Inorg. Chem.* **1995**, *42*, 1; Helm, L.; Merbach, A. E. *Coord. Chem. Rev.* **1999**, *187*, 151; Dunand, F. A.; Helm, L.; Merbach, A. E. *Adv. Inorg. Chem.* **2003**, *54*, 1; Lincoln, S. F. *Helv. Chim. Acta* **2005**, *88*, 523.
165. Hunt, J. P.; Taube, H. *J. Chem. Phys.* **1950**, *18*, 757; Friedman, H. L.; Taube, H.; Hunt, J. P. *J. Chem. Phys.* **1950**, *18*, 759; Hunt, J. P.; Taube, H. *J. Chem. Phys.* **1951**, *19*, 602; Rutenberg, A. C.; Taube, H. *J. Chem. Phys.* **1952**, *20*, 825; Baldwin, H. W.; Taube, H. *J. Chem. Phys.* **1960**, *33*, 206; Jackson, J. A.; Lemons, J. F.; Taube, H. *J. Chem. Phys.* **1960**, *32*, 553.
166. Plane, R. A.; Hunt, J. P. *J. Am. Chem. Soc.* **1957**, *79*, 3343.
167. Swift, T. J.; Connick, R. E. *J. Chem. Phys.* **1962**, *37*, 307.
168. Taube, H. *Chem. Rev.* **1952**, *50*, 69.
169. Basolo, F.; Pearson, R. G. *Mechanisms of Inorganic Reactions*, 2nd ed.; Wiley & Sons: New York, 1967; pp 65–80.
170. Breitschwerdt, K. *Ber. Bunsenges. Phys. Chem.* **1968**, *72*, 1046.
171. Spees, S. T., Jr.; Perumareddi, J. R.; Adamson, A. W. *J. Am. Chem. Soc.* **1968**, *90*, 6626.
172. Swaddle, T. W.; Stranks, D. R. *J. Am. Chem. Soc.* **1972**, *94*, 8357; Tong, S. B.; Swaddle, T. W. *Inorg. Chem.* **1974**, *13*, 1538.
173. Burdett, J. K. *Adv. Inorg. Chem. Radiochem.* **1978**, *21*, 113.
174. Mønsted, O. *Acta Chem. Scand.* **1978**, *A32*, 297.
175. Rode, B. M.; Reihnegger, G. J.; Fujiwara, S. *J. Chem. Soc., Faraday Trans. 2* **1980**, *76*, 1268.
176. Connick, R. E.; Alder, B. J. *J. Phys. Chem.* **1983**, *87*, 2764.
177. Galera, S.; Lluch, J. M.; Oliva, A.; Bertran, J.; Foglia, F.; Helm, L.; Merbach, A. E. *New J. Chem.* **1993**, *17*, 773.
178. Ohtaki, H.; Radnai, T. *Chem. Rev.* **1993**, *93*, 1157.
179. Åkesson, R.; Pettersson, L. G. M.; Sandström, M.; Wahlgren, U. *J. Am. Chem. Soc.* **1994**, *116*, 8705.
180. Erras-Hanauer, H.; Clark, T.; van Eldik, R. *Coord. Chem. Rev.* **2003**, *238–239*, 233.
181. Rotzinger, F. P. *J. Phys. Chem.* **2005**, *109*, 1510.
182. Pasquarello, A.; Petri, I.; Salmon, P. S.; Parisel, O.; Car, P.; Tóth, É.; Powell, D. H.; Fischer, H. E.; Helm, L.; Merbach, A. E. *Science*, **2001**, *291*, 856.
183. Persson, I.; Persson, P.; Sandström, M.; Ullström, A.-S. *J. Chem. Soc., Dalton Trans.* **2002**, 1256.
184. Schwenk, C. F.; Rode, B. M. *J. Am. Chem. Soc.* **2004**, *126*, 12786.
185. Rusnak, L. L.; Yang, E. S.; Jordan, R. B. *Inorg. Chem.* **1978**, *17*, 1810.
186. Aizawa, S.; Funahashi, S. *Inorg. Chem.* **2002**, *41*, 4555.

187. Meyer, F. K.; Newman, K. E.; Merbach, A. E. *J. Am. Chem. Soc.* **1979**, *101*, 5588; Ducommun, Y.; Newman, K. E.; Merbach, A. E. *Inorg. Chem.* **1980**, *19*, 3696.
188. Swaddle, T. W. *Inorg. Chem.* **1983**, *22*, 2663.
189. Ishi, M.; Funahashi, S.; Ishihara, K.; Tanaka, M. *Bull. Chem. Soc. Jpn.* **1989**, *62*, 1852.
190. Funahashi, S.; Inada, Y. *Bull. Chem. Soc. Jpn.* **2002**, *75*, 1901.
191. Benmelouka, M.; Messaoudi, S.; Furet, E.; Gautier, R.; Le Fur, E.; Pivan, J.-Y. *J. Phys. Chem. A* **2003**, *107*, 4122.
192. Eigen, M.; Wilkins, R. G. *Adv. Chem. Ser.* **1965**, *49*, 55.
193. Wilkins, R. G. *Acc. Chem. Res.* **1970**, *3*, 407.
194. Kustin, K.; Swinehart, J. *Prog. Inorg. Chem.* **1970**, *13*, 107; Hewkin, D. J.; Prince, R. H. *Coord. Chem. Rev.* **1970**, *5*, 45; Hoffmann, H. *Pure Appl. Chem.* **1975**, *41*, 327. Swaddle, T. W. *Adv. Inorg. Bioinorg. Mech.* **1983**, *2*, 96.
195. Ducommun, Y.; Newman, K. E.; Merbach, A. E. *Inorg. Chem.* **1980**, *19*, 3696.
196. Chaudhuri, P.; Diebler, H. *J. Chem. Soc., Dalton Trans.* **1986**, 1693.
197. Hugi, A. D.; Helm, L.; Merbach, A. E. *Inorg. Chem.* **1987**, *26*, 1763.
198. Patel, R. C.; Diebler, H. *Ber. Bunsenges. Phys. Chem.* **1972**, *76*, 1035.
199. Sauvageat, P.-Y.; Ducommun, Y.; Merbach, A. E. *Helv. Chim. Acta* **1989**, *72*, 1801.
200. Dellavia, I.; Sauvageat, P.-Y.; Helm, L.; Ducommun, Y.; Merbach, A. E. *Inorg. Chem.* **1992**, *31*, 792.
201. Fogg, P. G. T.; Hall, R. J. *J. Chem. Soc. A* **1971**, 1365.
202. Monzyk, B.; Crumblis, A. L. *J. Am. Chem. Soc.* **1979**, *101*, 6203.
203. Letter, J. E., Jr.; Jordan, R. B. *J. Am. Chem. Soc.* **1975**, *97*, 2381.
204. Cassatt, J. C.; Johnson, W. A.; Smith, L. M.; Wilkins, R. G. *J. Am. Chem. Soc.* **1972**, *94*, 8399.
205. Rorabacher, D. B. *Inorg. Chem.* **1966**, *5*, 1891.
206. Jordan, R. B. *Inorg. Chem.* **1976**, *15*, 748.
207. Desai, A. G.; Dodgen, H. W.; Hunt, J. P. *J. Am. Chem. Soc.* **1969**, *91*, 5001; *Ibid.* **1970**, *92*, 798.
208. Brown, A. J.; Howarth, O. W.; Moore, P.; Parr, W. J. E. *J. Chem. Soc., Dalton Trans.* **1978**, 1776.
209. Martell, A. E.; Smith, R. M. *Critical Stability Constants*; Plenum: New York, 1977; Vol. 2.
210. Hubbard, C. D.; Palaitis, W. J. *Coord. Chem.* **1979**, *9*, 107.
211. Jordan, R. B. *J. Coord. Chem.* **1980**, *10*, 239.
212. Aizawa, S.; Ida, S.; Matsuda, K.; Funahashi, S. *Inorg. Chem.* **1996**, *35*, 1338, and references therein.
213. Clarkson, A. J.; Buckingham, D. A.; Rogers, A. J.; Blackman, A. G.; Clark, C. R. *Inorg. Chem.* **2000**, *39*, 4769.

4

Stereochemical Change

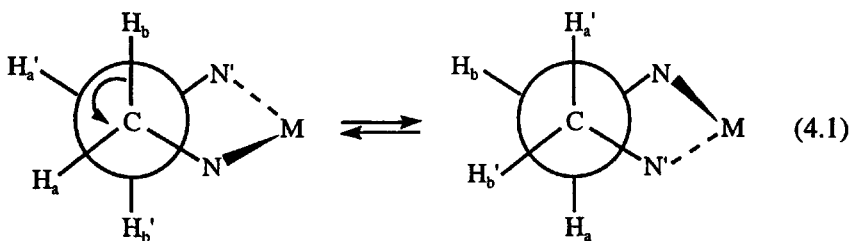
The kinetic and mechanistic aspects of this general area tend to be strongly dependent on the particular system. This makes general treatments and explanations impossible, at least at the current stage of understanding. Various aspects of this area have been summarized in some general reviews.¹⁻⁶

4.1 TYPES OF LIGAND REARRANGEMENTS

Ligands bonded to a metal can undergo a number of structural changes that do not involve complete breaking of the metal–ligand bond(s). Such processes are the subject of the following sections.

4.1.1 Conformational Change

Many chelate ligands have conformers that can interconvert. For example, the conformers of ethylenediamine interchange by rotation about the carbon–carbon bond, as shown in the following structures:



The H_a and H_a' protons are magnetically different from the H_b and H_b' protons, so their interconversion can, in principle, be studied by NMR. These protons may be referred to as exo and endo, respectively. In simple systems, their interconversion is too rapid ($k > 10^6 \text{ s}^{-1}$) for this method. However, if there is some constraint (e.g., CH_3 groups) or if the coordinating atoms are part of a larger chelate system, then interconversion is slow enough to be detected by NMR.⁷ In nonplanar Fe(III)–tetraphenylporphyrinates, the ring inversion rates vary widely, depending on the axial ligand and the substituents on the porphyrin.⁸

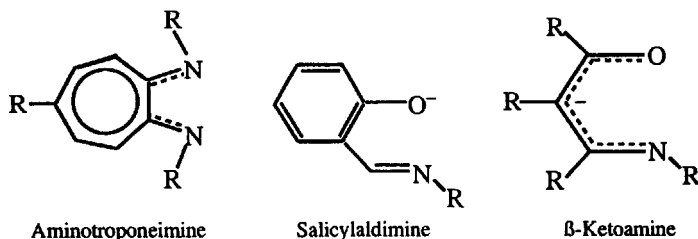
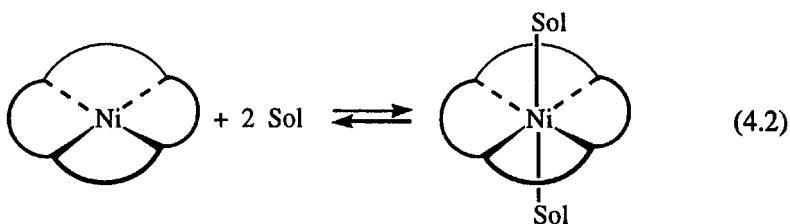


Figure 4.1. Ligands that have paramagnetic tetrahedral and diamagnetic square planar isomers with Ni(II).

4.1.2 Coordination Geometry Change

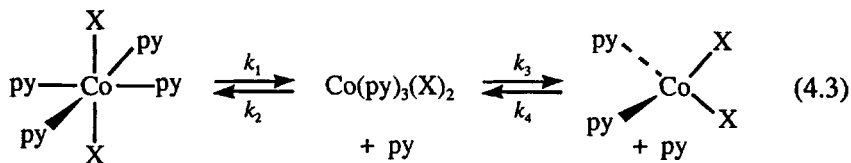
There are several Ni(II) complexes, such as those with the ligands shown in Figure 4.1, which exist as equilibrium mixtures of paramagnetic *tetrahedral* and diamagnetic *square planar* isomers. The planar–tetrahedral interconversions are rapid ($k \approx 10^4\text{--}10^6 \text{ s}^{-1}$, $\Delta H^* \approx 10 \text{ kcal mol}^{-1}$, $\Delta S^* \approx 0$). The mechanism for the transformation is thought to be intramolecular rearrangement with no metal–ligand bond breaking.⁹ A number of equilibria and substitution reactions on such systems have been studied by Elias and co-workers,¹⁰ with the conclusion that substitution does not seem to occur on the tetrahedral form.

Octahedral to square planar transformations have also been observed. These must involve a substitution as well because of the change in coordination number. Again Ni(II) complexes provide the most examples, with systems having a four-coordinate ligand in the square plane and two solvent molecules occupying the other octahedral positions, as shown in the following reaction:



These interconversions are quite rapid and have been studied by laser T-jump¹¹ and ultrasonic relaxation.¹² Kinetic studies¹³ suggest that several nickel(II)-salicylaldimine complexes favor ligand substitution through the square-planar isomer.

A *tetrahedral to octahedral* conversion has been studied by Farina and Swinehart¹⁴ for the following Co(II) complexes, with $X = \text{Cl}^-$ and Br^- , in nitromethane:



The rate was studied by the T-jump method, and the effect of changing the pyridine concentration was found to be consistent with reaction via a five-coordinate intermediate, as shown in reaction (4.3). The authors interpreted the observations to obtain values for k_4 of 8×10^4 and $3.4 \times 10^4 \text{ M}^{-1} \text{ s}^{-1}$ at 25°C from the activation parameters, for Cl^- and Br^- , respectively. The reactions are rapid, as expected for the labile $\text{Co(II)} (d^7)$ ion.

More recently, Funahashi and co-workers studied analogous reactions for $\text{Co}(\text{NH}_2\text{R})_n^{2+}$ complexes, where NH_2R is n-propylamine,¹⁵ n-hexylamine, 2-methoxyethylamine and benzylamine,¹⁶ and the solvent is the respective amine. The equilibrium favors the octahedral complex at low temperature, so that ^{14}N NMR could be used below 5°C to determine the solvent exchange rates for the octahedral complexes of n-propylamine and 2-methoxyethylamine. For the latter amine, the temperature dependence of the species distribution and the NMR relaxation rates are shown in Figure 4.2. The NMR data give $k_{\text{ex}}(25^\circ\text{C}) = 1 \times 10^7 \text{ s}^{-1}$, $\Delta H_{\text{ex}}^* = 46.6 \text{ kJ mol}^{-1}$ and $\Delta S_{\text{ex}}^* = 46 \text{ J mol}^{-1} \text{ K}^{-1}$.

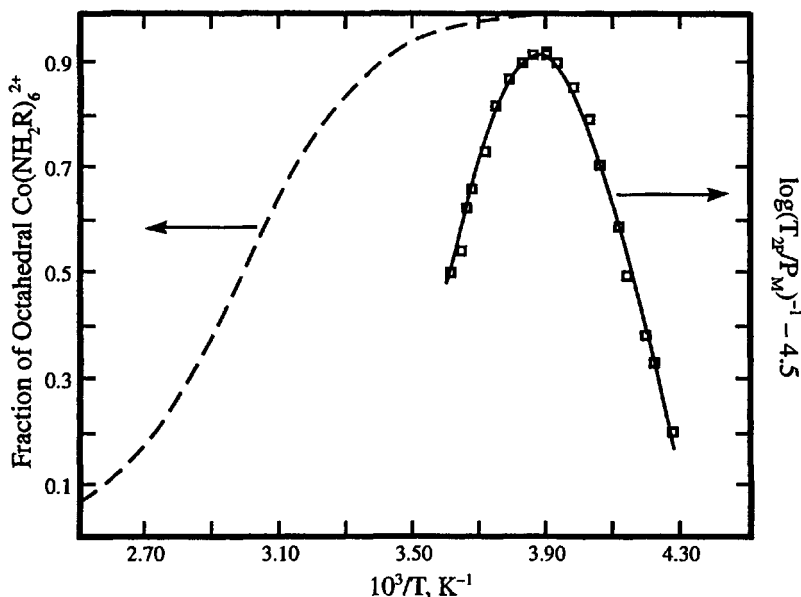
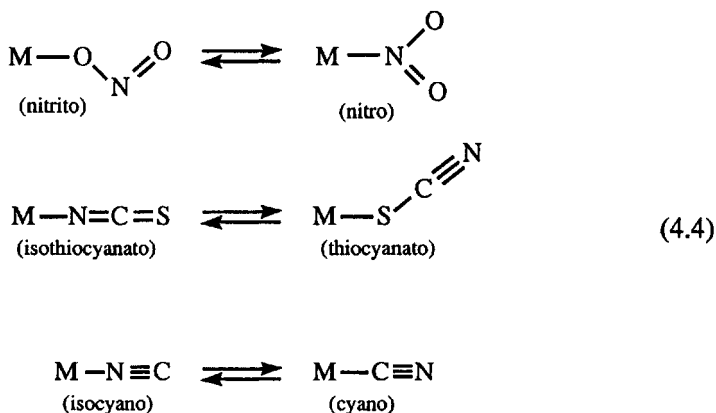


Figure 4.2. The temperature dependence of the fraction of $\text{Co}(\text{NH}_2\text{R})_6^{2+}$ and of the ^{14}N NMR relaxation rate for $\text{NH}_2\text{R} = 2\text{-methoxyethylamine}$.

Evidence discussed in Chapter 3 suggests that octahedral Co(II) reacts by a D mechanism. Therefore, the solvent exchange rate pathway is probably analogous to the k_1 step in reaction (4.3). For the octahedral to tetrahedral equilibrium constant, $\Delta H^\circ = 44.8 \text{ kJ mol}^{-1}$ and $\Delta S^\circ = 134 \text{ J mol}^{-1} \text{ K}^{-1}$.¹⁶ If the five-coordinate species is considered to be the transition state for both the solvent exchange and the isomerization, then one can estimate the activation parameters for addition of the amine to the tetrahedral species which is the equivalent of k_4 in reaction (4.3). The values obtained are $\Delta H_4^* = \Delta H_1^* - \Delta H^\circ = 1.8 \text{ kJ mol}^{-1}$ and similarly $\Delta S_4^* = -88 \text{ J mol}^{-1} \text{ K}^{-1}$. As might be expected for addition of amine to the tetrahedral species, ΔS_4^* has a negative value typical of an I mechanism.

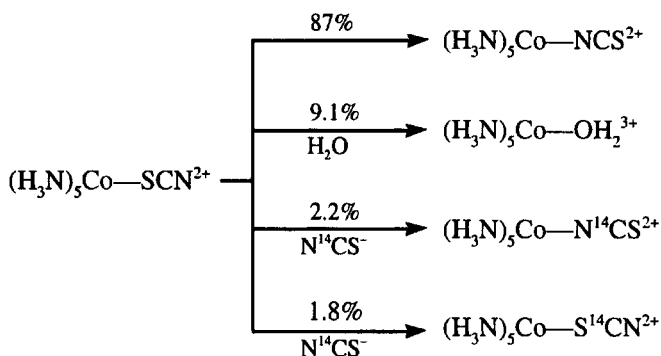
4.1.3 Linkage Isomerism

Linkage isomerism has been studied with inert metal ions and is possible, in principle, for any metal with a ligand that has more than one type of atom with an unshared electron pair. The following reactions are some common examples:^{17,18}



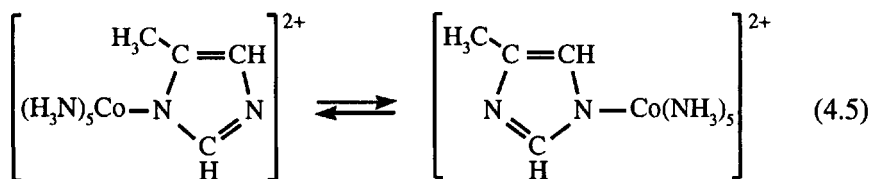
With inert octahedral complexes, these reactions appear to be intramolecular. This can be demonstrated by allowing the reaction to proceed in the presence of the uncomplexed isotopically labeled ligand. A form of linkage isomerism that involves O-atom transfer has been observed in $\text{M}(\text{NO})(\text{NO}_2)$ ¹⁹ and $\text{M}(\text{CO})(\text{CO}_2)$ ²⁰ systems.

The linkage isomerism of $(\text{H}_3\text{N})_5\text{Co}(\text{SCN})^{2+}$ has been extensively studied and recently reviewed.²¹ In water in the presence of N^{14}CS^- , the isomerism was reported²² to occur with ~3% incorporation of N^{14}CS^- into the product, $(\text{H}_3\text{N})_5\text{Co}(\text{NCS})^{2+}$. More recently,²³ it has been found that some N^{14}CS^- enters the coordination sphere during the linkage isomerism; the quantitative results for 1 M NCS^- at 25°C are summarized in Scheme 4.1. It remains unclear whether the intermediate is best considered as a π complex²⁴ or a tight ion pair.

Scheme 4.1

Exchange of free and bound thiocyanate has established that the linkage isomerism of square planar $(\text{Et}_4\text{dien})\text{Pd}(\text{SCN})^+$ occurs by an intermolecular rearrangement. The reaction probably proceeds through a solvent intermediate that reanates to give the isomerized product.²⁵

Data on the linkage isomerization of $(\text{H}_3\text{N})_5\text{Co}(\text{ONO})^{2+}$ in water were given in Chapter 1. The reaction rate has been shown²⁶ to have a significant solvent dependence, which has been interpreted in terms of the Lewis basicity, acidity and polarity of the solvents. The rearrangement of Co(III) complexes of N-bonded carboxamides to their O-bonded isomers have been studied,²⁷ as have analogous processes for thiocarbamates²⁸ and thiosulfenamides.²⁹ The long elusive isocyano complex, $(\text{H}_3\text{N})_5\text{Co}(\text{NC})^{2+}$, has been prepared and found to undergo slow linkage isomerism in water and DMSO, and the reaction is catalysed by Co(II) species.³⁰ The rearrangement of the methyl-imidazole complex is given in the following reaction:

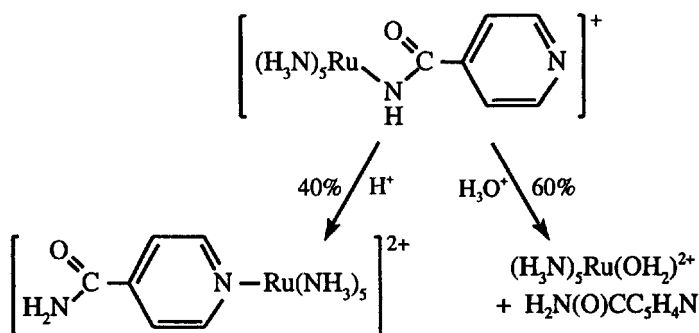


It proceeds intramolecularly with cobalt migration across two of the ring atoms³¹ in a 1,3-shift. The analogous methyltetrazole complexes can undergo 1,2-shifts of $(\text{H}_3\text{N})_5\text{Co}$ between adjacent N atoms.³²

A number of linkage isomerism reactions have been studied for complexes of $(\text{H}_3\text{N})_5\text{Ru}^{\text{II/III}}$. These exploit the fact that Ru(II) favors the softer donor atom and π -acceptor systems, while Ru(III) favors harder donor atoms and does not participate in π bonding. Thus, one isomer of Ru(II) is prepared, then oxidized to Ru(III) by chemical or electrochemical methods and the isomerism is observed. The Ru(III) isomer can be reduced

to Ru(II) and the reverse isomerization observed for the Ru(II) complex. For example, with DMSO, $(\text{H}_3\text{N})_5\text{Ru}-\text{S}(\text{O})(\text{CH}_3)_2^{3+}$ isomerizes to $(\text{H}_3\text{N})_5\text{Ru}-\text{OS}(\text{CH}_3)_2^{3+}$; with acetone, Ru(II) forms an $\eta^2\text{-OC}(\text{CH}_3)_2$ complex that rearranges to the $\eta^1\text{-O}$ bonded isomer in the Ru(III) complex.³⁴ The acrylamide complex reacts analogously.³⁵ Creutz and co-workers³⁶ reduced a Ru(III)-nicotinamide complex to form the Ru(II) isomer and found that the latter undergoes competitive aquation and isomerization by a 1,4-shift with $k = 9.6 \text{ s}^{-1}$, as shown in Scheme 4.2 for $\text{pH} > 6$. The length and speed of the isomerization led the observers to suggest that an $\eta^2\text{-arene}$ intermediate is possible.

Scheme 4.2



There are many analogous reactions in Os(II/III) systems, with the major difference being that Os(II) has a greater tendency for π back bonding than Ru(II). The osmium chemistry has been reviewed recently.³⁷

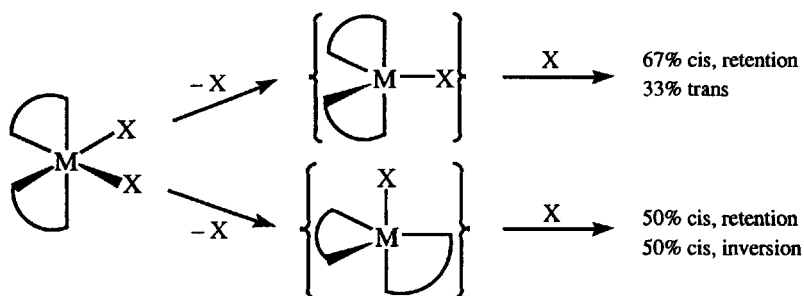
4.2 GEOMETRICAL AND OPTICAL ISOMERISM IN OCTAHEDRAL SYSTEMS

The interconversion of geometrical isomers (*cis*, *trans*, *fac*, *mer*) and the racemization of optical isomers (λ , Δ) can proceed by two general mechanisms, *ligand dissociation* or *intramolecular rearrangement*.

4.2.1 Dissociation Mechanisms

If the complex is an octahedral bis chelate system, $\text{M}(\text{AA})_2(\text{X})_2$, then two trigonal bipyramidal intermediates are possible, as shown in Scheme 4.3. The product distributions in Scheme 4.3 are based on the assumption of a statistical attack along the edges of the trigonal plane of the intermediate. Since the lower intermediate has a plane of symmetry, it must lead to racemization. Similar intermediates can be drawn for tris chelate systems if one end of a chelate dissociates. This is called *one-ended dissociation* and is actually an intramolecular process.

Scheme 4.3



4.2.2 Intramolecular Rearrangement Mechanisms

These mechanisms will be illustrated for chelates of the type $M(AA)_3$ but can be extended to other systems. These rearrangements involve rotating one trigonal face of the octahedron by 120° relative to the opposite trigonal face. The *Bailar* or *trigonal twist* involves rotation about a C_3 axis and the *rhombic* or *Ray-Dutt bend* is rotation about an imaginary C_3 axis. Both of these are shown in Figure 4.3.

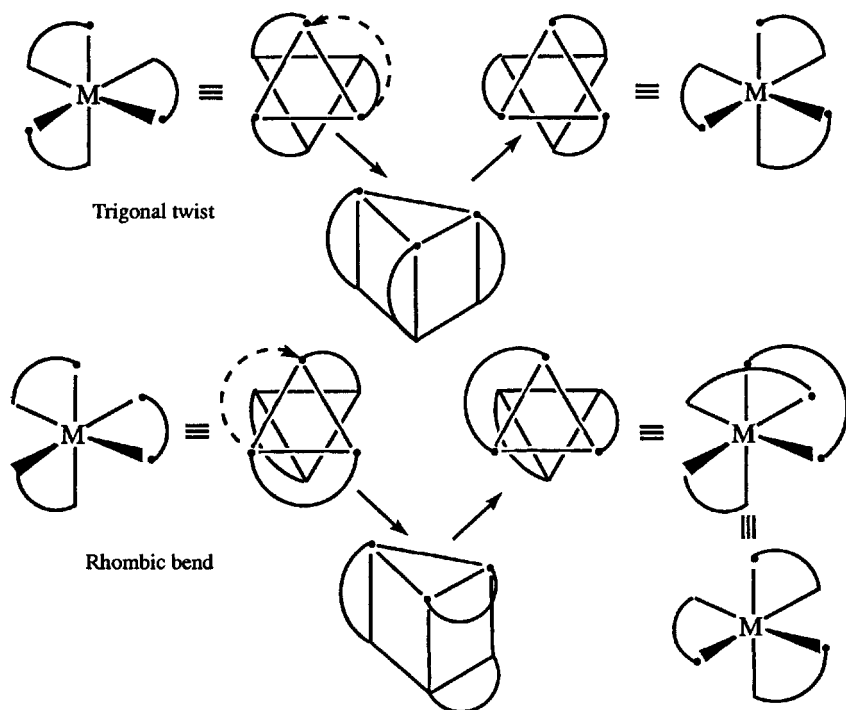


Figure 4.3. Trigonal twist and rhombic bend rearrangements for an unsymmetrical $M(AA)_3$ complex.

4.2.3 Differentiation of Dissociative and Intramolecular Mechanisms

The differentiation of the dissociative and intramolecular mechanisms is usually based on a comparison of the rates of ligand dissociation (exchange or solvolysis) and racemization. If the rates are quite similar, dissociation is assumed, whereas if racemization is much faster, then an intramolecular mechanism is operating. However, this involves the implicit assumption that the initial chelate ring opening step is rate limiting for both processes.

For the tris(oxalato)rhodium(III) ion in water, Damrauer and Milburn³⁸ have studied the kinetics of racemization, aquation and ¹⁸OH₂ exchange of the oxalate oxygens. The racemization and aquation have acid-dependent pseudo-first-order rate constants given by

$$k_{\text{exp}} = k_2[\text{H}^+] + k_3[\text{H}^+]^2 \quad (4.6)$$

The oxygen exchange is first-order in [H⁺] and the inner, coordinated oxygens are exchanged much more slowly than the outer oxygens. The kinetic results are summarized in Table 4.1.

Damrauer and Milburn noted the similarity in the kinetic parameters of *k*₂ for inner oxygen exchange and racemization and suggested that both processes are proceeding through a common intermediate formed by acid-catalyzed one-ended dissociation of oxalate. The crystal structure³⁹ of K₃[Rh(C₂O₄)₃]·4.5H₂O reveals that the O—Rh—O angles are ~83°. This makes it seem more probable that racemization and inner oxygen exchange proceed by a square pyramidal intermediate rather than by a symmetrical trigonal pyramidal one (Scheme 4.3), which requires one O—Rh—O angle of 120°. It is noteworthy that the kinetics of the outer oxygen exchange are similar to those of oxalic acid,⁴⁰ for which *k* (50°C) = 4×10⁻³ s⁻¹, Δ*H*[‡] = 15.1 kcal mol⁻¹ and Δ*S*[‡] = -22.7 cal mol⁻¹ K⁻¹. Palmer and Kelm⁴¹ found that Δ*V*[‡] = -6.3 cm³ mol⁻¹ for the aquation of Rh(C₂O₄)₃³⁻ in 1.0 M H⁺ where *k*₃ dominates.

Table 4.1. Rate Constants (50°C) and Activation Parameters for the Oxygen Exchange, Racemization and Aquation of Rh(C₂O₄)₃³⁻ in 0.54 M NaClO₄/HClO₄

Reaction	<i>k</i> ₂ (M ⁻¹ s ⁻¹)	<i>k</i> ₃ (M ⁻² s ⁻¹)	Δ <i>H</i> [‡] (kcal mol ⁻¹)	Δ <i>S</i> [‡] (cal mol ⁻¹ K ⁻¹)
Outer O exchange	1.1×10 ⁻³		16.9	-20.0
Inner O exchange ^a	3.6×10 ⁻⁵		23.5	-6.4
Racemization ^a	2.0×10 ⁻⁵		23.0	-9.1
		1.1×10 ⁻⁴	27.9	+9.6
Aquation ^a	5.6×10 ⁻⁷		25.6	-8.1
		5.9×10 ⁻⁶	25.7	-3.1

^a Recalculated from the data in Damrauer, L.; Milburn, R. M. *J. Am. Chem. Soc.* **1971**, *93*, 6481.

Tris(oxalato)chromium(III) is much more reactive than its Rh(III) analogue. Odell et al.⁴² indicate that all the oxygens exchange at the same rate ($k = 1.26 \times 10^{-3} \text{ s}^{-1}$, 1.0 M HClO_4 , 25°C) and racemization is about 10 times faster ($k = 1.38 \times 10^{-2} \text{ s}^{-1}$) under the same conditions. The authors conclude that ring opening and closing must be much faster than oxygen exchange; the latter is 2.4 times faster than for free oxalic acid at 25°C. Structures of oxalate complexes of Cr(III)⁴³ indicate O—Cr—O angles of $\sim 83^\circ$ and a square pyramidal intermediate would again seem probable. Lawrance and Stranks⁴⁴ found a very negative value of $\Delta V^\ddagger = -16.3 \text{ cm}^3 \text{ mol}^{-1}$ for racemization of $\text{Cr}(\text{ox})_3^{3-}$ in 0.05 M HCl and rationalized this as mainly due to solvent electrostriction around the $-\text{CO}_2^-$ group in the one-ended dissociation transition state. The authors imply that their results are for an $[\text{H}^+]$ -independent reaction, but the $[\text{H}^+]$ -catalyzed path dominates the kinetics below pH 3. For $\text{Cr}(\text{phen})_2(\text{ox})^+$ and $\text{Cr}(\text{bpy})_2(\text{ox})^+$, the values of ΔV^\ddagger are -1.5 and $-1.0 \text{ cm}^3 \text{ mol}^{-1}$, respectively, and an intramolecular twist is proposed by Lawrance and Stranks.

The racemization of tris(*N,N*-dimethylethylenediamine)nickel(II) seems to proceed by an intramolecular rotation because bond rupture should produce some meso isomer, which is not observed. The kinetic similarity of this and the $\text{Ni}(\text{en})_3^{2+}$ racemization⁴⁵ gives some indication that the latter also is intramolecular. On the other hand, the tris(bipyridyl) and tris(*o*-phenanthroline) complexes of Ni(II)⁴⁶ and Fe(II)⁴⁷ have very similar rates of racemization, ligand exchange and aquation, and therefore are assumed to proceed by dissociation. It seems surprising that these more rigid chelates would choose dissociation, while the more flexible aliphatic diamines go by intramolecular rotation. It should be remembered that the aliphatic amines are much stronger bases than the aromatic amines and thus the former may form stronger bonds to the metal, making dissociation less favorable.

Comparisons of volumes of activation in Table 4.2 from the work of Lawrance and Stranks⁴⁸ provide some further insights. The authors suggest that the small values of ΔV^\ddagger for Ni(II) and Cr(III) imply an intramolecular

Table 4.2. Activation Parameters for the Racemization and Aquation of Some Complexes of Tris(*o*-phenanthroline)

Complex	Reaction	ΔH^\ddagger (kJ mol ⁻¹)	ΔS^\ddagger (J mol ⁻¹ K ⁻¹)	ΔV^\ddagger (cm ³ mol ⁻¹)
$\text{Fe}(\text{phen})_3^{2+}$	Racemization	118 (±3)	89 (±8)	15.6 (±0.3)
	Aquation	135 (±2)	117 (±8)	15.4 (±0.3)
$\text{Ni}(\text{phen})_3^{2+}$	Racemization	105 (±1)	12 (±3)	-1.5 (±0.3)
	Aquation	102 (±2)	3 (±6)	-1.2 (±0.2)
$\text{Cr}(\text{phen})_3^{3+}$	Racemization	94 (±4)	-56 (±3)	3.3 (±0.3)

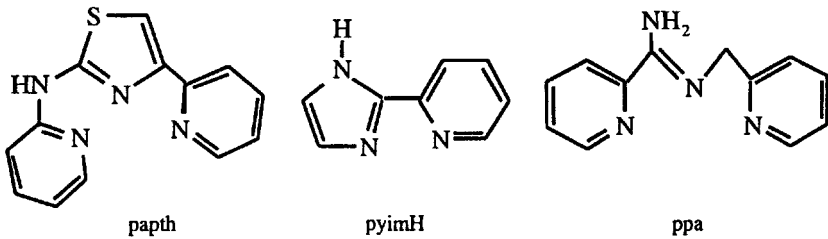
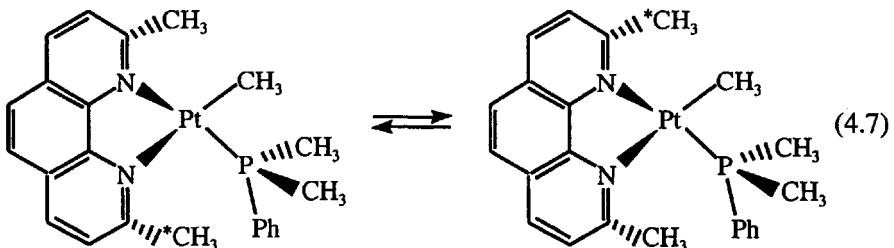


Figure 4.4. Examples of ligands that have Fe(II) complexes with high-spin and low-spin forms.

twist mechanism. To rationalize the large ΔV^\ddagger for Fe(II), they suggest that there is a spin-state change accompanying the intramolecular twist (i.e., the system goes from low-spin d^6 in the ground state to high-spin d^6 in the transition state). This causes the metal-to-ligand bond lengths to increase. Note that the ΔH^\ddagger and ΔS^\ddagger are different for racemization and aquation in the Fe(II) system.

Such spin-state equilibria have been studied for Fe(II) complexes of the ligands shown in Figure 4.4. The $\Delta V^\ddagger = 11 \text{ cm}^3 \text{ mol}^{-1}$ for $\text{Fe}^{\text{II}}(\text{papth})_2$,⁴⁹ and the kinetics for the low-spin to high-spin direction gave values of k (25°C) $= 1.7 \times 10^7 \text{ s}^{-1}$, $\Delta H^\ddagger = 31.7 \text{ kJ mol}^{-1}$ and $\Delta S^\ddagger = 0.37 \text{ J mol}^{-1} \text{ K}^{-1}$. Similar kinetic parameters have been found⁵⁰ for the pyimH and ppa complexes of Fe(II), which have values of ΔV^\ddagger in the 2 to 9 $\text{cm}^3 \text{ mol}^{-1}$ range with a significant solvent dependence.

A somewhat different type of ligand rearrangement has been observed by Romeo and co-workers⁵¹ for Pt(II) complexes with 2,9-dimethyl-1,10-phenanthroline. This is shown in the following reaction, with PMe_2Ph used as an example of one of the phosphines studied.⁵²



In these complexes, the phenanthroline is tilted out of the normal square plane because of the steric effect of the CH_3 substituents, and the latter are below this plane in the structures shown in reaction (4.7). One of these substituents is distinguished by an asterisk to illustrate that they are not equivalent. In the ^1H NMR, the signals from these CH_3 groups coalesce at

temperatures which depend on the nature of the phosphine. The authors attribute this fluxionality to a dissociation of one end of the phenanthroline to give a T-shaped intermediate. The phenanthroline then rotates and closes the chelate ring to exchange the positions of the CH_3 groups. For the complex in reaction (4.7), the diastereotopic CH_3 groups of $\text{P}(\text{CH}_3)_2\text{Ph}$ are observed as one resonance in the ^1H NMR, and the authors attribute this to a more rapid flipping of the phenanthroline without Pt—N bond breaking. The rate constants at 67°C for different phosphines were subjected to a detailed QUALE analysis of electronic and steric effects (see Section 5.1.2). However, since the ΔH^\ddagger values for these reactions show a large variation, from ~ 78 to 41 kJ mol^{-1} , the conclusions of such an analysis may depend on the temperature chosen.

There have been several attempts to provide a theoretical framework for describing geometrical isomerization and racemization. Vanquickenborne and Pierloot⁵³ used ligand field theory to calculate the electronic energies of the intermediates proposed in the dissociative and trigonal twist mechanisms for low-spin d^6 systems.

The d orbital energy diagrams from the analysis of Vanquickenborne and Pierloot for the trigonal twist are shown in Figure 4.5. The values of σ and π are measures of the σ - and π -donor strength of the ligand (e.g., for en, $\sigma = 94.3 \text{ kJ mol}^{-1}$, $\pi = 0$; for H_2O , $\sigma = 78.5 \text{ kJ mol}^{-1}$, $\pi = 12.85 \text{ kJ mol}^{-1}$). The prediction is that these systems should go through a spin-state change to give a more stable transition state.

In order to calculate the ΔH^\ddagger , one must take into account electron repulsion–delocalization factors through the Racah parameters, B and C , in ligand field theory. The diagram gives a change of $6\sigma - 8\pi$ for formation of the transition state and $\Delta H^\ddagger = 6\sigma - 8\pi - 5B - 8C$ for a d^6 system.

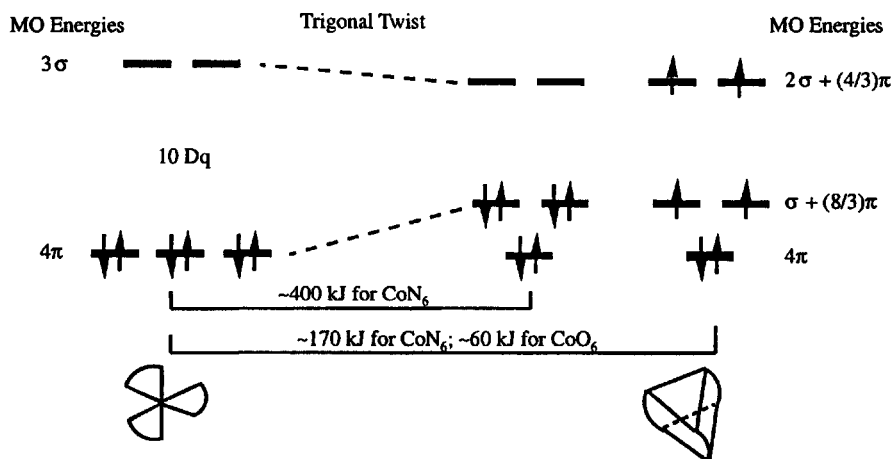


Figure 4.5. Metal d orbital energies for the trigonal twist rearrangement.

For Co(III), $B = 7.14 \text{ kJ mol}^{-1}$, $C = 44 \text{ kJ mol}^{-1}$ and $\Delta H^* \approx 180 \text{ kJ mol}^{-1}$ for Co(en)_3^{3+} going through the high-spin form. This seems an impossibly high barrier. Oxygen donor ligand systems, such as oxalate, have smaller σ values and π values which are >0 . As a result, they are predicted to have much lower barriers of $\sim 60 \text{ kJ mol}^{-1}$ for this intramolecular twist through the high-spin form.

For the dissociative mechanism, it was assumed that a square-based pyramid (C_{4v}) would form first and would rearrange to a trigonal bipyramid (D_{3h}) if some stereochemical change is observed. The orbital energies are given in Figure 4.6. The theory again predicts a spin-state change in the D_{3h} intermediate. As before, the diagram gives a change of $5\sigma - 6.5\pi$ for the high-spin transition state and $\Delta H^* = 5\sigma - 6.5\pi - 5B - 8C \approx 85 \text{ kJ mol}^{-1}$ for the Co(en)_3^{3+} . A comparison of the ΔH^* values from the two mechanisms predicts that the rearrangement should go by a dissociative mechanism through a high-spin transition state.

The theory has been extended to $\text{Co(en)}_2(\text{A})\text{X}$ systems,⁵⁴ but the results are more complex because of the different ligand types. It was concluded by Vanquickenborne that $(\sigma_A - 2\pi_A)$ is the controlling factor, so that better π -donor A ligands will reduce the C_{4v} to D_{3h} energy barrier and therefore give more stereochemical change in a dissociative mechanism. This prediction is consistent with the fact that A ligands, such as CN^- or NH_3 , give hydrolysis with retention. However, if A is Cl^- or OH^- , there is a considerable ($\sim 30\%$) change in the configuration. The theory of Vanquickenborne predicts that the amount of rearrangement should increase with increasing temperature, but this aspect has not been tested experimentally.

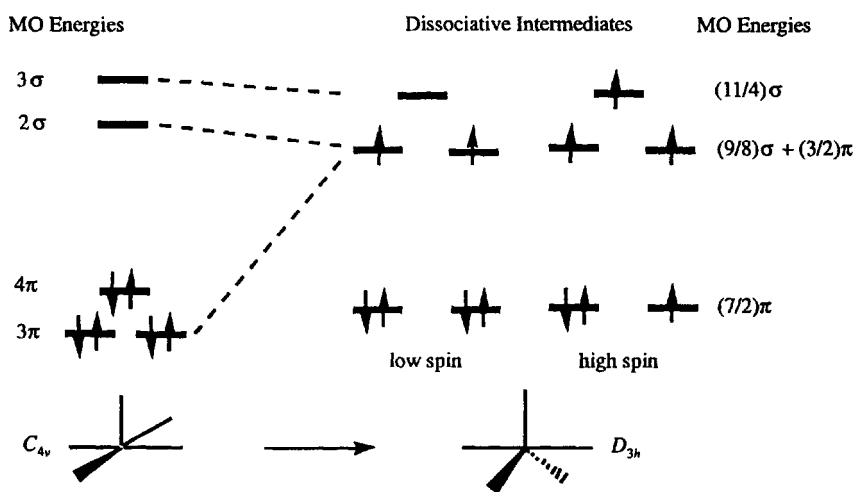
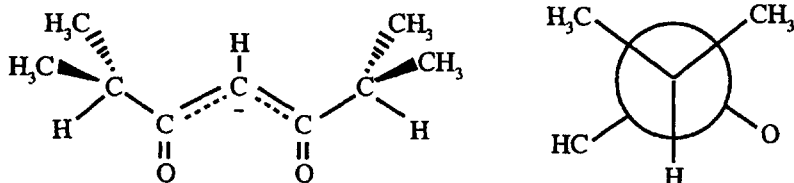
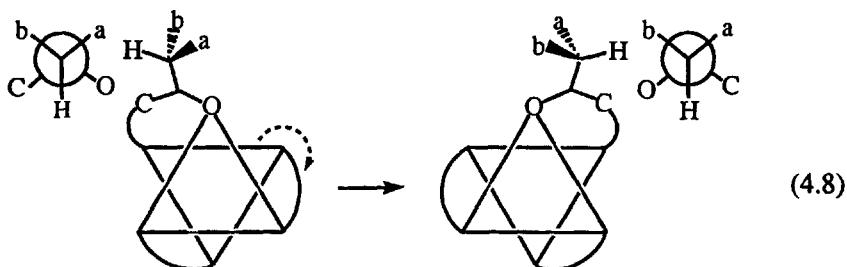


Figure 4.6. Metal d orbital energies for the dissociative rearrangement.

For those interested in studying racemization, a major problem is the need to resolve the optical isomers. It is possible to avoid this problem by using a chelate with a chiral center and studying the system by NMR. An example of such a ligand is diisobutyrylmethanide, where the isopropyl carbon is diastereotopic and the view at the right down the C—C bond shows that the two CH₃ groups can never be magnetically equivalent.



When inversion occurs in a tris chelate of this type, the two CH₃ groups are interchanged and this is observed as a merging of the two NMR signals as the interconversion becomes fast on the NMR time scale; actually, H—H coupling causes four peaks to collapse to two. The process is pictured in the following reaction for one isopropyl group with the CH₃ groups designated as a and b:



4.2.4 Rearrangements in Unsymmetrical Chelates

There are a large number of unsymmetrical chelates which present the feature of having both geometrical and optical isomers, as shown by the examples in Figure 4.7. The fac and mer isomers each have optical isomers; thus, both racemization and geometrical isomerization can be observed in one system. This can serve to eliminate certain rearrangement processes.

For a dissociative mechanism, the different possible **D** transition states give different products, as in the following examples:

- | | |
|-------------------------------|---------------------------------------|
| Axial trigonal bipyramid | → Isomerization + Inversion |
| Equatorial trigonal bipyramid | → Isomerization + Inversion |
| Square-based bipyramid | → Some isomerization + Some inversion |

Further possible products from a dissociative mechanism have been given by Wilkins.⁵⁵

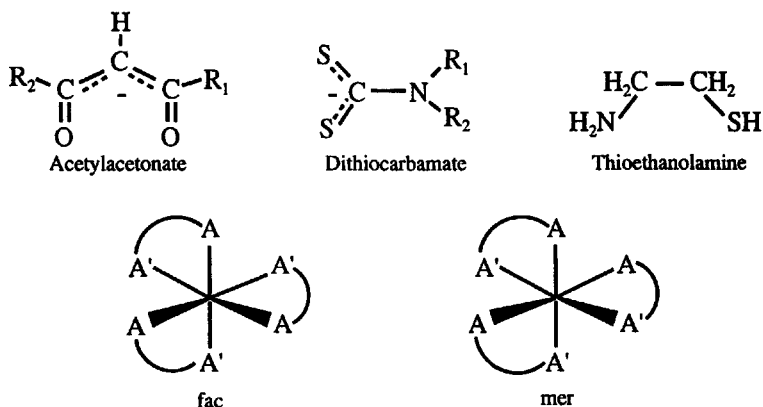


Figure 4.7. Examples of unsymmetrical chelating ligands and their geometrical isomers.

The Al(III) and Ga(III) complexes of the unsymmetrical derivative of acetylacetonate (see Figure 4.7), with $\text{R}_1 = \text{CF}_3$ and $\text{R}_2 = 2\text{-C}_4\text{H}_4\text{S}$, undergo isomerization and racemization by a common pathway.⁵⁶ A dissociative mechanism was suggested from the 10-fold increase in rate on changing the solvent from $(\text{CDCl}_2)_2$ to DMSO. The solvent effect criterion is a subjective one and an 8-fold change in rate between H_2O and DMSO was taken to be minor for a tris-catecholate complex of Ga(III).⁵⁷

The two intramolecular twist mechanisms give different results, as shown in Figure 4.8. The trigonal twist gives inversion without geometrical isomerization, but the rhombic bend gives both. Thus, if the reaction is shown to proceed without dissociation and gives inversion without isomerization, then a trigonal twist mechanism is established.

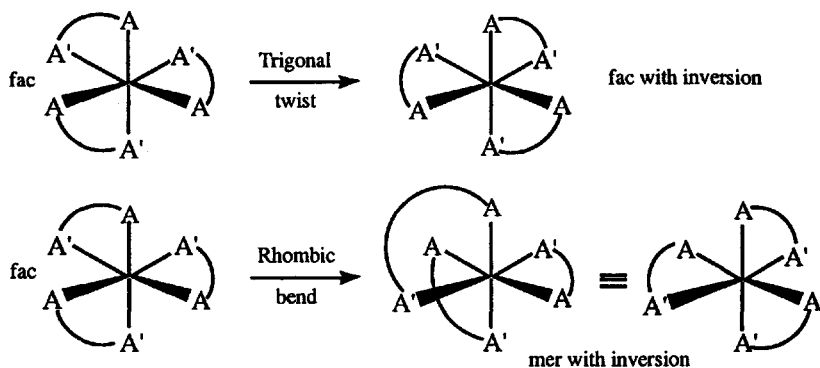
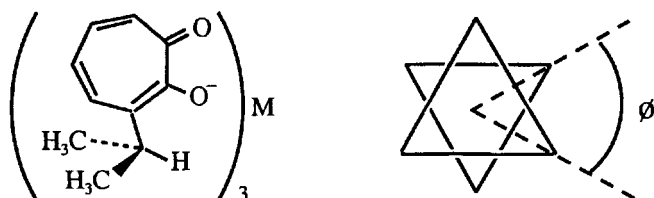


Figure 4.8. Products of the trigonal twist and rhombic bend rearrangements for an unsymmetrical tris chelate.

The trigonal twist is the most restrictive in terms of the rearrangement results. This mechanism has been confirmed for the complexes of Al(III), Ga(III) and Co(III), with the following ligand:



In these systems, the trigonal twist may be favored by ground-state distortions toward the trigonal transition state because of the small bite distance (2.5 Å) of the ligand.⁵⁸ This distortion is measured by the twist angle, \emptyset , which is 60° for an octahedron and 0° for the trigonal transition state. Several Fe(IV), Fe(III) and Ru(III) dithiocarbamates also use the trigonal twist mechanism.⁵⁹ It is fortunate that these systems rearrange by the one process that is established by NMR because it gives inversion without fac-mer rearrangement.

The structural features that may favor the trigonal twist relative to the rhombic bend have been discussed by Rodger and Johnson.⁶⁰ Their approach considers the ligand bite distance, b , and the hard-sphere contact distance, l , of the coordinating atoms, and they conclude that the trigonal twist is favored if b is much smaller than l . Relevant structural information on such systems has been reviewed by Keppert.⁶¹ This approach does not take into account any differences in strain in the chelate backbone.

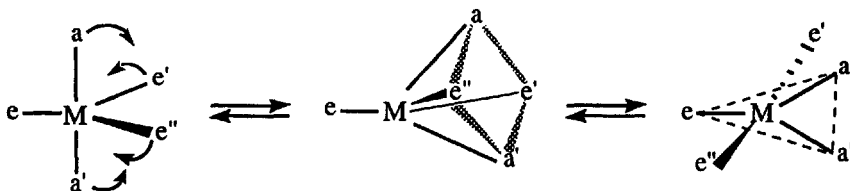
Instead of this mechanistic approach, a pure permutational analysis can be used. The possibilities are given by Holm⁶² and, in more detail, by Eaton et al.⁶³ and Musher.⁶⁴

4.3 STEREOCHEMICAL CHANGE IN FIVE-COORDINATE SYSTEMS

Most of the effort in the area of five-coordinate systems has been on trigonal bipyramid systems, such as PF_5 and $\text{Fe}(\text{CO})_5$. The interconversion is between the axial, a, and equatorial, e, positions. Studies on $\text{Fe}(\text{CO})_5$ are described in section 4.5.1.

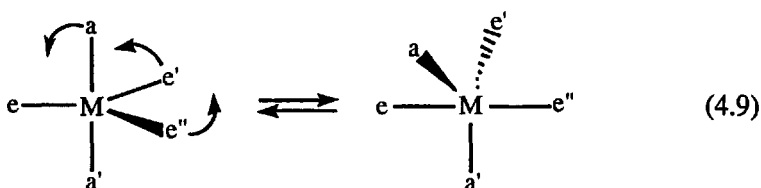
The axial-equatorial conversion is generally quite rapid for $\text{M}(\text{L})_5$ systems, but a series of $\text{M}(\text{P}(\text{OR})_3)_5$ complexes have rates that are accessible on the NMR time scale. Meakin and Jesson⁶⁵ found values for ΔH^\ddagger of 8 to 12 kcal mol⁻¹ and showed that the process required the simultaneous interchange of two axial and two equatorial substituents. The *pseudorotation mechanism* suggested by Berry,⁶⁶ and shown in Scheme 4.4, is consistent with the observations. The equatorial e' and e'' ligands become axial, whereas the axial a and a' become equatorial.

Scheme 4.4



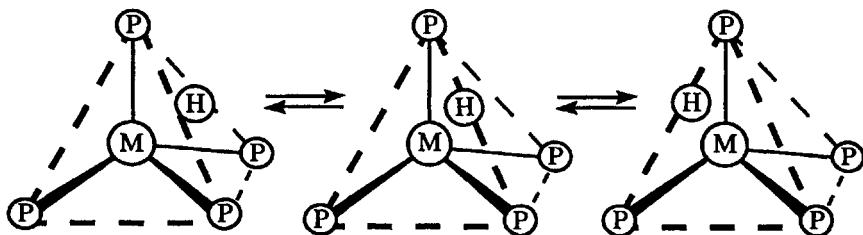
The product appears to be rotated by 90° relative to the starting structure. Note that the intermediate structure is close to a square-based pyramid.

Ugi et al.⁶⁷ have suggested what is called the *turnstile mechanism* which is described in reaction (4.9). This process is also consistent with the observations, because the two mechanisms cannot be distinguished experimentally. Theoretical arguments suggest that the pseudorotation mechanism provides the lower energy pathway for the interconversion.⁶⁸



For some transition-metal hydrides of the type HMP_4 , the ground-state structure is a distorted trigonal bipyramid and can be pictured as a tetrahedral arrangement of the P ligands around M with the H atom on one tetrahedral face. For such hydrides, a *tetrahedral jump mechanism* has been proposed⁶⁹ in which the H atom moves from one tetrahedral face to an edge and then to another face, as shown in Scheme 4.5.

Scheme 4.5



This mechanism is consistent with the NMR observations. If the H and the opposite P are considered as axial, then this process converts the axial P substituent to an equatorial position for each occurrence, and this is not the permutational equivalent of the pseudorotation process.

4.4 ISOMERISM IN SQUARE-PLANAR SYSTEMS

Most examples in this area involve *cis*–*trans* isomerization of Pt(II) complexes. The area was reviewed by Anderson and Cross.⁷⁰ In coordinating solvents, the mechanism usually suggested involves solvolysis of one ligand followed by readdition of that ligand, both proceeding through the five-coordinate associative intermediate that seems consistent with most ligand substitution processes on Pt(II).

For Pt(II) complexes of the type $\text{Pt}(\text{R})_2(\text{L})_2$ and $\text{Pt}(\text{Ar})_2(\text{L})_2$ in non-coordinating solvents, a dissociative mechanism involving a 14-electron T-shaped intermediate has been suggested.⁷¹ This pathway typically has a positive ΔS^\ddagger and the rate is retarded by free L in solution.

The anticancer agent cisplatin, *cis*- $\text{Pt}(\text{NH}_3)_2(\text{Cl})_2$, has been extensively studied.^{72,73} Theoretical explanations have been offered for the kinetic preference for the cross-linking of guanine bases by this drug⁷⁴ and for the lack of binding to thiol groups of peptides in the natural system.⁷⁵ A metabolite of cisplatin is the bis-L-methionine complex, $\text{Pt}(\text{L-Met-S,N})_2$, which forms an equilibrium mixture of *cis* and *trans* isomers in water. The *trans* to *cis* isomerization has $\Delta H^\ddagger = 95 \text{ kJ mol}^{-1}$ and $\Delta S^\ddagger = -18 \text{ J mol}^{-1} \text{ K}^{-1}$, and an intramolecular twist through a tetrahedral intermediate has been suggested.⁷⁶

4.5 FLUXIONAL ORGANOMETALLIC COMPOUNDS

The mechanisms of geometrical and optical isomerization already discussed also apply to organometallic compounds, but these show some additional unique rearrangement processes. This area has been reviewed by Mann.^{77,78}

4.5.1 Iron Pentacarbonyl

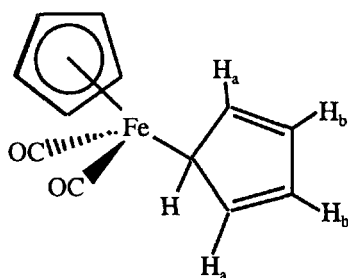
Iron pentacarbonyl is an $\text{M}(\text{L})_5$ complex for which the rearrangement mechanisms have been discussed in Section 4.3. $\text{Fe}(\text{CO})_5$ deserves special mention because of the amount of attention it has received. The structure is known to be a trigonal bipyramid in the solid⁷⁹ and in the gas.⁸⁰ The axial and equatorial bond lengths are similar, but the structure in the gas phase suggests that the axial bonds are $\sim 0.03 \text{ \AA}$ shorter, while in the solid they are $\sim 0.01 \text{ \AA}$ longer. Rose-Petruk and co-workers⁸¹ have studied solutions of $\text{Fe}(\text{CO})_5$ using FTIR, XANES and EXAFS. The observations indicate that there are significant amounts of square pyramidal $\text{Fe}(\text{CO})_5$ in solvents, such as C_6H_6 , $\text{C}_6\text{H}_5\text{F}$ and $\text{C}_6\text{F}_5\text{H}$, which hydrogen bond to Fe from the base of the pyramid.

Thus far, the equatorial–axial exchange has proven to be too fast to measure by ^{13}C NMR, even down to -120°C .^{69,82} This conclusion assumes that there is a significant chemical shift difference between the axial and equatorial ^{13}C nuclei; this has been questioned by Mahnke et al.⁸³ A solid-

state NMR study⁸⁴ down to 100 K indicated some fluxional behavior with an energy barrier of ~ 1 kcal mol⁻¹. More recent solid state ¹³C NMR results⁸⁵ indicate a shift difference of 182 Hz at 22.53 MHz and an interchange rate of $<10^2$ s⁻¹ at -38°C . A study⁸⁶ of the polarized UV spectrum in a CO matrix at 20 K shows that there is slow interconversion at that temperature. Theoretical studies⁸⁷ of the fluxionality of Fe(CO)₅ are consistent in predicting a low barrier of ~ 2 kcal mol⁻¹ for the Berry pseudorotation pathway. This seems consistent with the observation that even hydrogen bonding to benzene is capable of converting the structure to one similar to the pseudorotation intermediate.

4.5.2 Fluxional Ring Systems

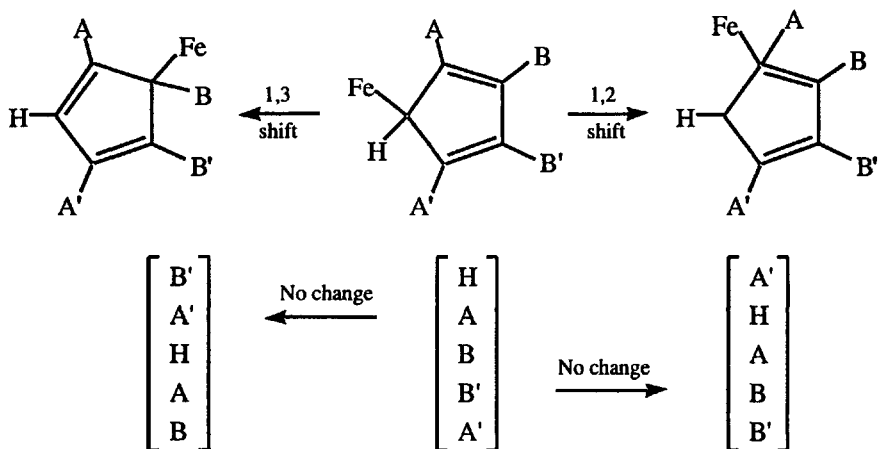
The term *ring whizzers* was coined by Cotton to describe the phenomenon that was first studied quantitatively by Bennett et al.⁸⁸ in the compound Fe(η^5 -C₅H₅)(η^1 -C₅H₅)(CO)₂, which has the following structure:



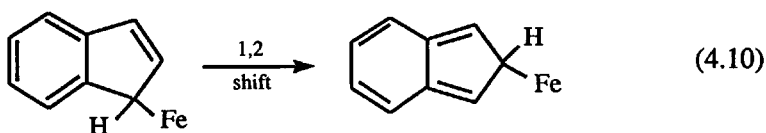
The ¹H NMR for this compound at 30°C in CS₂ shows only two peaks, one typical of the η^5 -C₅H₅ hydrogens and one for all of the η^1 -C₅H₅ hydrogens. If the latter is static, then it should show two peaks (due to a and b protons in the structure) plus the unique H on the same C as the Fe. At -100°C , the two peaks (+ coupling features) expected for the a and b sets become resolved. In addition, it was observed that the peak at lower field collapses more rapidly than the other one as the temperature is increased from -100°C .

These observations are consistent with the Fe moving around the C₅H₅⁻ ring or the ring whizzing around the Fe, depending on your point of view. The mechanism could be a series of either 1,2 or 1,3 shifts of the Fe about the η^1 -C₅H₅. If the shift were a random process, then all the peaks should collapse at the same rate. The two shift mechanisms are shown in Scheme 4.6, which starts at the center and goes through a 1,3 shift to the left and a 1,2 shift to the right. The change in magnetic type of the original H atoms is shown in Scheme 4.6 for each type of shift. For the 1,2 shift, the B' becomes a magnetically equivalent B, whereas for the 1,3 shift, the A becomes a magnetically equivalent A'. Therefore, the mechanism is a 1,2 shift if the B resonance is collapsing more slowly and a 1,3 shift if the A resonance is the one collapsing more slowly.

Scheme 4.6



By analogy to other systems, Bennett et al. assigned the more slowly collapsing resonance to the B and B' hydrogens and concluded that the mechanism involved a 1,2 shift. However, the spectral assignment remained somewhat uncertain, and it is a common feature in this type of work that *the mechanism will rely directly on the validity of the spectral assignments for the low-temperature, nonexchanging state of the system*. To test their assignment of the spectrum and mechanism, Cotton et al.⁸⁹ prepared $\text{Fe}(\eta^5\text{-C}_5\text{H}_5)(\eta^1\text{-indenyl})(\text{CO})_2$. They anticipated that a 1,2 shift, as shown in reaction (4.10), would be unfavorable in this system because of the loss of aromatic resonance energy in the product.



The compound shows no fluxional behavior and all the expected ^1H resonances are observed in the room-temperature NMR spectrum.

4.5.3 Symmetry Rules for Sigmatropic Shifts

As a result of the above and other work through the 1970s, it appeared that these fluxional processes prefer the 1,2 shift mechanism; this led to what has been termed "the principle of least motion" as being a major factor in determining the shift mechanism. Recent work has examined these processes in more detail and emphasized the orbital symmetry involved, following the Woodward-Hoffmann rules⁹⁰ for sigmatropic shifts in organic chemistry. The adaptation of these rules to inorganic transition-metal systems has had some success, but the inorganic systems have

several potential complications that weaken the predictive power of the rules. The main problem is that p and d orbitals may be involved and their symmetry gives predictions opposite to those derived from organic systems where only sigma symmetry orbitals are needed. Another problem is that the inorganic systems may proceed by dissociation, so that the process is not concerted, as required for the extended Woodward–Hoffmann rules. The latter complication arises because C—H and C—C bonds are much stronger than metal–carbon bonds, so that dissociation is unlikely in the organic systems. Nevertheless, the current organometallic studies generally attempt to interpret results in terms of symmetry rules and focus on agreement and apparent exceptions to the rules.

A process is symmetry allowed if the migrating group can maintain proper overlap as it moves from the original position to make a new bond with an appropriate empty antibonding orbital, which produces the new species. In addition, the movement must be suprafacial, meaning that the migrating group must stay on the same side of the molecule, rather than antarafacial. Several examples are described in the following paragraphs.

A *1,3 sigmatropic shift* is symmetry allowed but occurs *antarafacially*, because the migrating group must move from one side of the molecule to the other, as shown by the orbital picture in Figure 4.9. The orbital diagram on the left in Figure 4.9 shows the unoccupied antibonding π^* orbital, which becomes the bonding π orbital in the product. To maintain proper symmetry overlap during the migration, the σ orbital must move antarafacially from the top to the bottom of the molecule. This movement is viewed as unlikely for organometallic systems and the 1,3 process is not expected to be favorable. It might appear from Figure 4.9 that a 1,2 shift would be allowed, but this would produce a species that would violate normal valence rules for carbon.

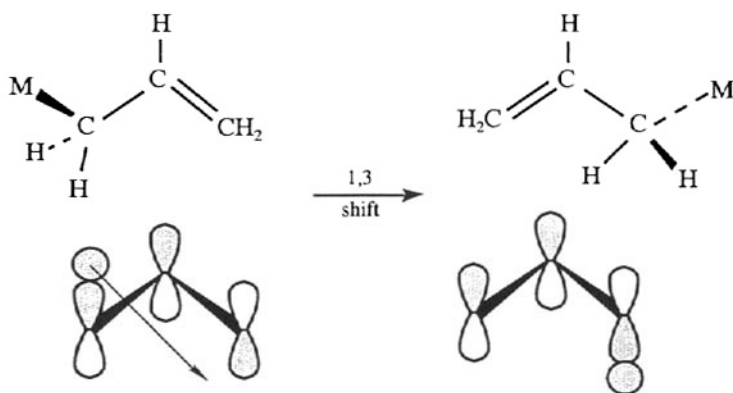


Figure 4.9. Structural and orbital representations of a 1,3 antarafacial sigmatropic shift.

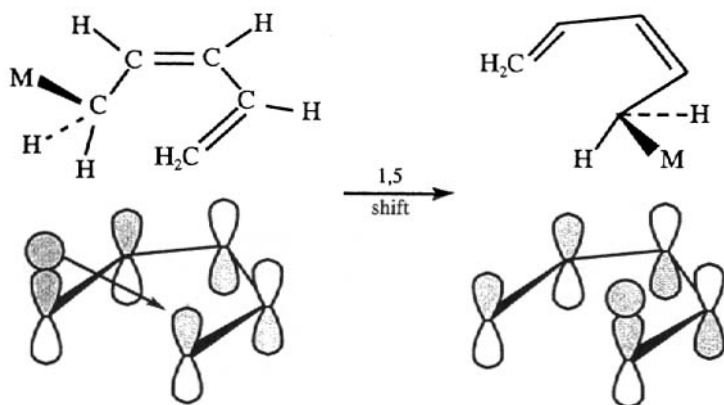
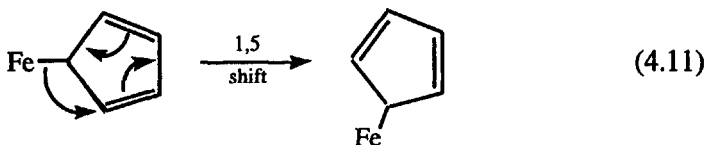


Figure 4.10. Structural and orbital representations of a 1,5 suprafacial sigmatropic shift.

A *1,5 sigmatropic shift* is symmetry allowed and occurs *suprafacially* with the migrating group staying on the same side of the molecule, as shown in Figure 4.10. This process should be facile. Extensions to larger systems follow in an obvious way and predict that *1,7 shifts should be antarafacial and 1,9 shifts suprafacial*.

Mingos⁹¹ extended these ideas to π -bonded cyclic systems by using a simple valence bond approach that greatly expanded the applicability of these rules in organometallic systems. Essentially, one draws the valence bond structure and moves electron pairs in the standard way of organic chemistry to obtain the product. If the rearrangement is symmetry allowed and suprafacial, then the fluxional process is expected to have a low energy barrier. For example, with the $\text{Fe}(\eta^1\text{-C}_5\text{H}_5)$ system discussed on page 131, the process is shown by the following reaction:



Note that this corresponds to a 1,5 shift and would be predicted to be of low energy. We called this a 1,2 shift previously, but that is the same as a 1,5 shift for a C_5 ring.

An unexplained exception to the predictions is the $\text{Re}(\eta^1\text{-C}_7\text{H}_7)(\text{CO})_5$ system,⁹² which shows 1,2 (= 1,7) shifts with an energy barrier of $\sim 80 \text{ kJ mol}^{-1}$. The symmetry rules predict that a 1,5 shift should be allowed, as shown in Figure 4.11. Only a minor 1,5 pathway has been observed with $\text{Re}(\eta^1\text{-C}_7\text{H}_7)(\eta^5\text{-C}_5\text{H}_5)(\text{CO})_2$. Mann⁷⁸ has suggested that the reaction may

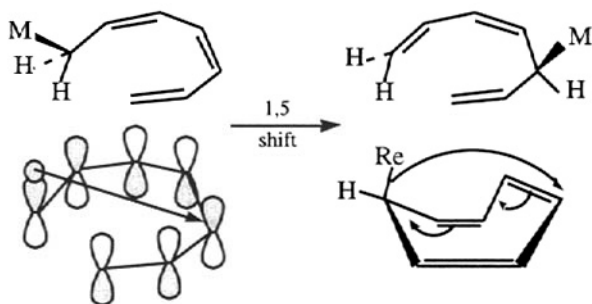
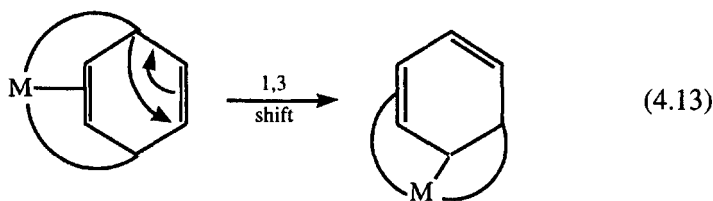
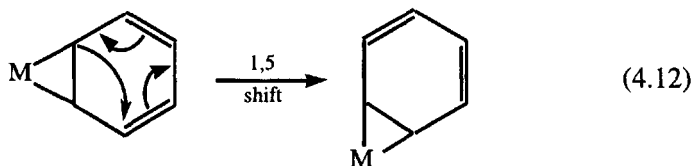


Figure 4.11. The predicted allowed shift for an $\eta^1\text{-C}_7\text{H}_7$ system.

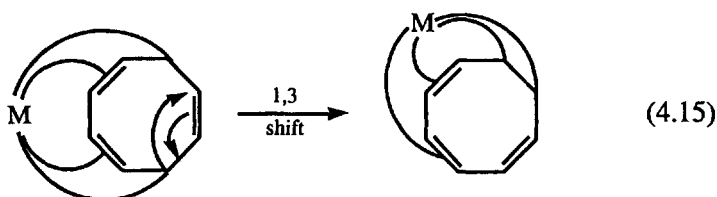
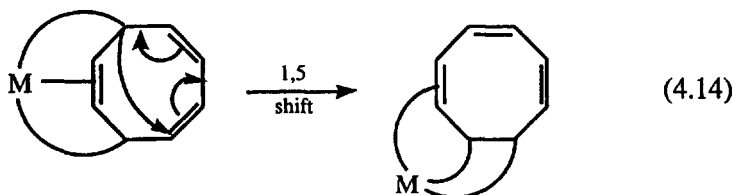
involve homolytic fission of the Re—C bond, or that the rules break down because of participation of metal *p* or *d* orbitals. Takats and McClung and co-workers⁹³ have come to the latter conclusion in their detailed study of several $\eta^3\text{-C}_7\text{H}_7$ and $\eta^5\text{-C}_7\text{H}_7$ systems. They note that the latter undergo facile 1,2-shifts which are symmetry forbidden.

The delicate balance between dissociation and intramolecular pathways can be seen in the, albeit somewhat different, $\eta^3\text{-C}_7\text{H}_6$ complex of $\text{Pt}(\text{PPh}_3)_2$. In the initial study,⁹⁴ it was determined from saturation transfer and observation of scrambling of Pt isotopomers that the fluxionality was due to dissociation of $\text{Pt}(\text{PPh}_3)_2$ from the ring with $\Delta H^\ddagger = 26.8 \text{ kcal mol}^{-1}$ and $\Delta S^\ddagger = 15.1 \text{ cal mol}^{-1} \text{ K}^{-1}$, determined from 60°C to 80°C. Subsequent work⁹⁵ has confirmed the observations at 80°C, but shown that the process is entirely intramolecular at 60°C, possibly via a carbene intermediate. This study also showed that the bimetallic derivative $(\text{OC})_3\text{Mo}(\text{C}_7\text{H}_6)\text{Pt}(\text{PPh}_3)_2$ shows fluxionality at lower temperature and proceeds by an intramolecular shift of $\text{Pt}(\text{PPh}_3)_2$.

The approach of Mingos can be used for higher levels of "hapticity". For example, $\eta^2\text{-C}_6\text{H}_6$ systems undergo a favorable 1,5 shift, but $\eta^4\text{-C}_6\text{H}_6$ systems have an unfavorable 1,3 shift, as shown in the following reactions:



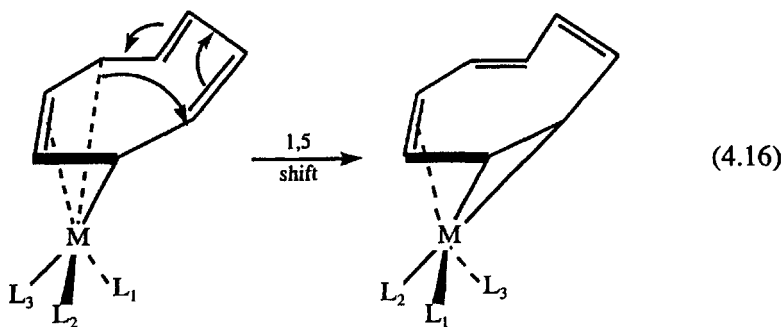
For cyclooctatetraene systems, the prediction is that $\eta^2\text{-C}_8\text{H}_8$ systems should be static because a 1,7 shift is required. The $\eta^4\text{-C}_8\text{H}_8$ systems should be fluxional by a 1,5 shift, but $\eta^6\text{-C}_8\text{H}_8$ systems should be static because a 1,3 shift is required, as shown in the following reactions:



The $\eta^6\text{-C}_8\text{H}_8$ systems that have been studied,⁹⁶ $\text{M}(\eta^6\text{-C}_8\text{H}_8)(\text{CO})_3$ ($\text{M} = \text{Cr}, \text{W}$), are fluxional, but with barriers $>60 \text{ kJ mol}^{-1}$ and with a mixture of shift types. This behavior has been attributed to formation of an $\eta^4\text{-C}_8\text{H}_8$ intermediate. Recently, a 1,5 shift has been identified in $\text{Os}(\eta^6\text{-C}_8\text{H}_8)(\eta^4\text{-1,5-cyclooctadiene})$.⁹⁷

The general experimental observations are that the neutral complexes of $\eta^2\text{-C}_6\text{R}_6$, $\eta^3\text{-C}_7\text{H}_7$ and $\eta^4\text{-C}_8\text{H}_8$ are highly fluxional, but those of $\eta^4\text{-C}_6\text{R}_6$, $\eta^5\text{-C}_7\text{H}_7$, $\eta^2\text{-C}_8\text{H}_8$ and $\eta^6\text{-C}_8\text{H}_8$ are usually static or have quite high barriers ($>80 \text{ kJ mol}^{-1}$).

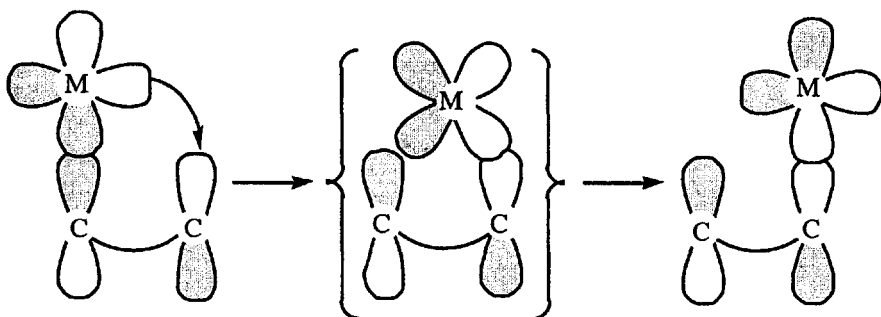
The 1,5 shift in $\eta^4\text{-C}_8\text{H}_8$ systems predicts specific movements of the remaining ligands on the metal, as follows:



These predictions have been tested for $\text{Fe}(\eta^4\text{-C}_8\text{H}_8)(\text{CO})_2(i\text{-PrNC})$ and are claimed to be confirmed.⁹⁸ The system is complicated by the fact that there are two stable structural isomers with $i\text{-PrNC}$ in positions L_1 or L_2 in

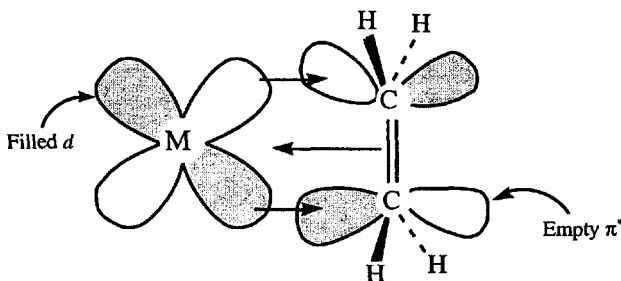
the left-hand structure. However, for $\text{Os}(\eta^3\text{-C}_7\text{H}_7)(\text{CO})_3(\text{SnPh}_3)$, a similar test is not consistent with the predictions and the observations indicate that 1,2 shifts predominate.⁹⁹ The latter results seem more consistent with a slip mechanism, possibly involving a p orbital on the metal. One version of the slip mechanism is pictured in Scheme 4.7.

Scheme 4.7



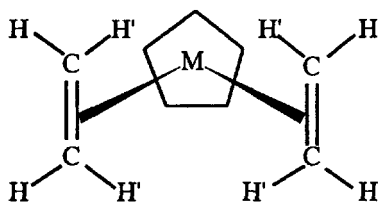
4.5.4 Rotations of π -Bonded Olefins

The bonding in π -bonded olefins consists of donation from the olefin π orbital to a metal σ orbital and back donation from a metal d to the olefin π^* orbital. The latter type of bonding is shown in the following diagram:



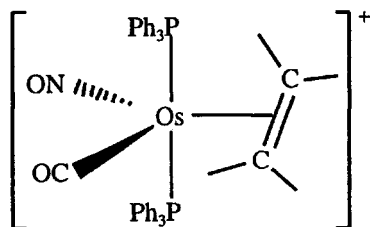
This results in at least a partial double bond between M and the olefin and some restricted rotation of the olefin relative to the metal might be expected. Rotation could be about the M -olefin bond or about the $C=C$ axis. The $M(L)_3(\text{olefin})$ compounds normally have the $C=C$ axis perpendicular to the plane of the $M(L)_3$ unit, while $M(L)_4(\text{olefin})$ compounds have the olefin in the trigonal plane with the $C=C$ axis parallel to the trigonal plane. The theoretical analysis of Hoffmann and co-workers¹⁰⁰ suggests that the orientation of the olefin in the square planar complexes is controlled by steric factors, while the trigonal bipyramidal complexes prefer ethylene in the trigonal xy plane to give better overlap with the hybridized d_{xy} orbital compared to the unhybridized d_{xz} orbital.

Cramer et al.¹⁰¹ observed ethylene rotation in $M(\eta^5\text{-C}_5\text{H}_5)(\text{C}_2\text{H}_4)_2$ ($M = \text{Rh, Ir}$) complexes with the following structure:



For $M = \text{Rh}$, the H and H' can be observed separately in the NMR spectrum at -20°C , but the peaks collapse to one at 57°C . The analogous C_2F_4 compound shows no collapse of the ^{19}F spectrum up to 100°C . The rotational barrier also is increased by CH_3 groups on the cyclopentadiene ring and by changing from Rh to Ir. These differences can be explained by steric and better π back bonding factors, but they do not determine whether rotation is about the metal–olefin or C=C bond.

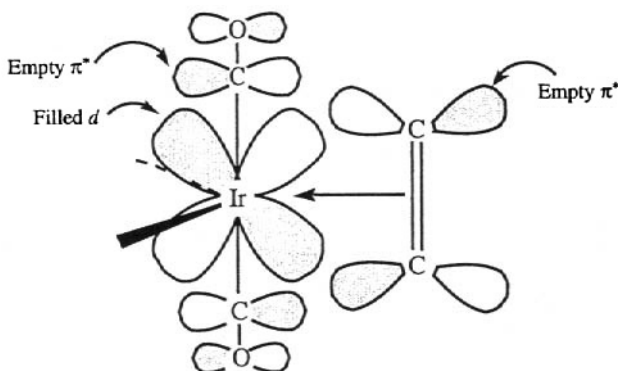
Rotation about the metal–olefin bond has been observed¹⁰² in $\text{Os}(\text{PPh}_3)_2(\text{CO})(\text{NO})(\text{C}_2\text{H}_4)$, shown in the following diagram:



The two ends of the ethylene are different and the ^{13}C NMR spectrum shows that they are static at -80°C , but interconvert rapidly at 20°C . Since the $^1\text{H}\text{-}^{31}\text{P}$ coupling is retained, the reaction does not involve dissociation of ethylene. Similar behavior has been reported for the essentially square-pyramidal $\text{Os}(\text{tBu}_2\text{Me})_2(\text{Cl})(\text{H})(\text{C}_2\text{H}_4)$ system.¹⁰³

A π -electron-donating substituent on an unsymmetrical olefin causes a shift towards η^1 -bonding at the unsubstituted carbon.¹⁰⁴ For a range of para-substituents, X, in $\text{CpFe}(\text{CO})_2(\eta^2\text{-CH}_2\text{C}(\text{H})\text{NH}(\text{C}_6\text{H}_5\text{X}))$, increased electron donation by X causes a lowering of ΔH^\ddagger by about 10 kJ mol^{-1} .¹⁰⁵ This presumably results from a weakening of the π back bonding.

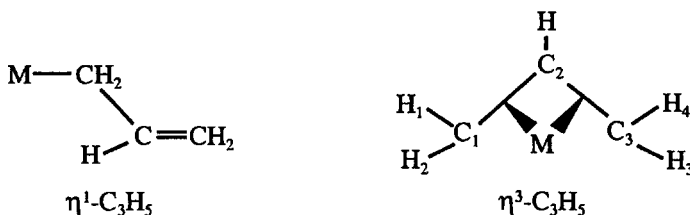
The theoretical work of Hoffmann suggests that the $(\text{L})_4\text{M}$ –ethylene systems should rearrange by a pseudorotation mechanism with the ethylene remaining in the trigonal plane. The $\text{M}(\text{CO})_4(\text{ethylene})$ compounds ($M = \text{Fe, Ru, Os}$) show axial–equatorial CO interchange.¹⁰⁶ Caulton and co-workers¹⁰⁷ have suggested that ethylene rotation may be facilitated by interaction with π^* orbitals of axial CO ligands in a transition state, such as that in the following diagram:



This is used to rationalize the nonfluxional character of systems without a CO ligand, such as $\text{Ir}(\text{PPhMe}_2)_4(\text{C}_2\text{H}_4)^+$, $\text{Ir}(\text{PPhMe}_2)_3(\text{CH}_3\text{CN})(\text{C}_2\text{H}_4)^+$ and $\text{Ir}(\text{PPhMe}_2)_3(\text{CH}_3)(\text{C}_2\text{H}_4)$.

4.5.5 Fluxional Allyl Complexes

The allyl group, $-\text{C}_3\text{H}_5^-$, can be bonded to a metal either as $\eta^1-\text{C}_3\text{H}_5$ or as $\eta^3-\text{C}_3\text{H}_5$, as shown in the following diagrams:

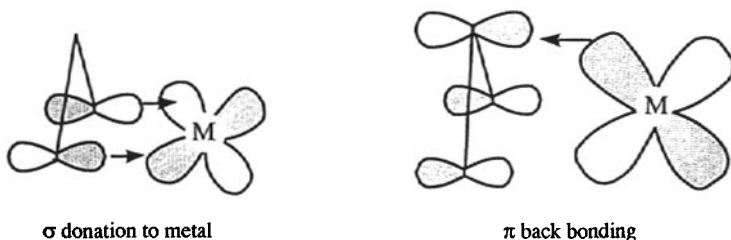


The former is normally observed with nontransition metals and the latter is the predominant form with transition metals, but both forms have been isolated in some systems.¹⁰⁸

In the $\eta^1-\text{C}_3\text{H}_5$ complexes, fluxional behavior involves movement of the metal from one end of the allyl ligand to the other. In $\eta^3-\text{C}_3\text{H}_5$ systems, the syn protons (H_1 , H_4) and anti protons (H_2 , H_3) may interchange and the C_1 and C_3 may be observed to interchange if other ligands make the two sides of the complex different. The bonding¹⁰⁹ and fluxional aspects¹¹⁰ of these systems have been reviewed.

The $\eta^1-\text{C}_3\text{H}_5$ systems are predicted to be static by the symmetry rules, and this is the case for $\text{Mn}(\text{CO})_5(\eta^1-\text{C}_3\text{H}_5)$. However, if the metal is coordinatively unsaturated (<18 valence electrons), then the systems are highly fluxional and are thought to proceed through an $\eta^3-\text{C}_3\text{H}_5$ intermediate, as in the cases of $\text{Pd}(\text{PPhMe}_2)(\text{NC}_5\text{H}_4\text{CO}_2)(\eta^1-\text{C}_3\text{H}_5)$ and $\text{Ti}(\text{NMe}_2)_2(\eta^1-\text{C}_3\text{H}_5)$. A similar state can be attained by reversible loss of another ligand. Heterolytic bond cleavage also has been proposed for an Fe complex.¹¹¹

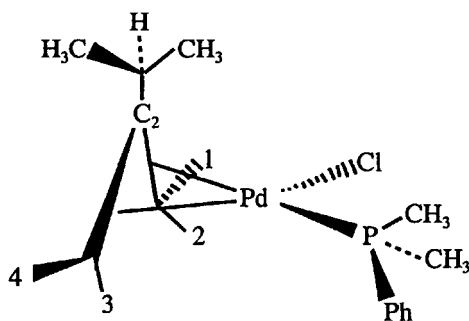
The reason for restricted rotation in the $\eta^3\text{-C}_3\text{H}_5$ complexes can be understood from the following bonding pictures that depict the "sigma" donation from the ligand on the left and the back donation from the metal to the π^* orbital of the ligand on the right. Recent theoretical studies have examined the structures and reactions of these systems.¹¹²



Three processes have been suggested for the fluxionality observed in the $\eta^3\text{-C}_3\text{H}_5$ systems:

1. In the olefin rotation mechanism, the intermediate has a bond only with the $\text{C}_1\text{-C}_2$ end, and the C_3 is free to rotate and interchange the syn and anti protons.
2. In the allyl flip mechanism, the intermediate is bonded only at C_1 and C_3 , and the C_2 does an end-over flip. The syn and anti protons will interchange at both ends of the allyl ligand.
3. In the $\pi\text{-}\sigma\text{-}\pi$ mechanism, the intermediate is $\eta^1\text{-}\sigma$ bonded at one end (e.g., C_1), and the ligand is free to rotate about the $\text{C}_1\text{-C}_2$ bond. Each event causes syn-anti exchange at one end of the ligand.

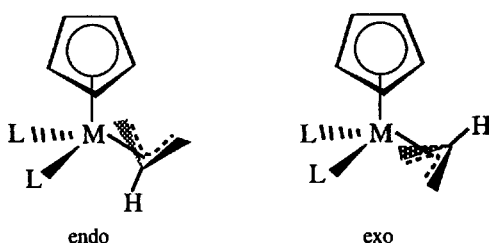
The " $\pi\text{-}\sigma\text{-}\pi$ " mechanism is now commonly accepted. Some of the evidence is from observations on the following system:¹¹³



The 3 and 4 protons interchange at the same rate as the methyl protons on the phosphine and the methyl protons of the 2-isopropyl group. This is expected if the C_2 is moving above and below the P-Pd-Cl plane as in the " $\pi\text{-}\sigma\text{-}\pi$ " mechanism.

With a suitably unsymmetrical arrangement of the other ligands in the system, the orientation of the η^3 -allyl group can produce endo and exo

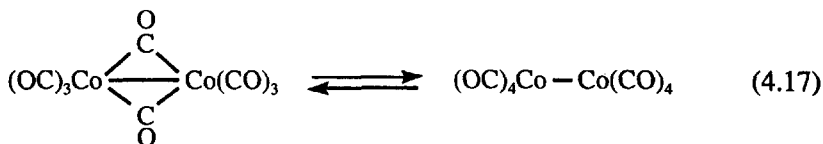
isomers. These are shown for an $(\eta^5\text{-C}_5\text{H}_5)\text{M}(\text{L})_2(\eta^3\text{-allyl})$ complex in the following structures:



The interconversion of these isomers can occur by rotation about the M—allyl axis, in which case the syn and anti protons do not exchange, as was observed for $\text{CpMo}(\text{CO})_2(\eta^3\text{-C}_3\text{H}_4\text{R})$ ($\text{R} = \text{H}, \text{CH}_3$).¹¹⁴ On the other hand, if an η^1 intermediate is involved, then the syn and anti protons should exchange, as was found for $\text{CpM}(\text{CO})(\eta^3\text{-C}_3\text{H}_5)$ ($\text{M} = \text{Fe},^{115} \text{Ru}^{116}$). An electronic explanation for the difference between the formally d^2 Mo and the d^6 Fe and Ru systems was given originally in terms of frontier molecular orbitals by Fish et al.¹¹⁵ This has been amplified recently by Ariaifard et al.¹¹⁷ using density functional theory. Lin and co-workers¹¹⁸ studied the endo–exo reaction in $(\text{Ph}_3\text{P})_2(\text{CO})\text{ClRu}(\eta^3\text{-CH}_2\text{CHCMe}_2)$ and discussed the factors affecting the relative stabilities of the isomers.

4.5.6 Bridge–Terminal Carbonyl Exchange

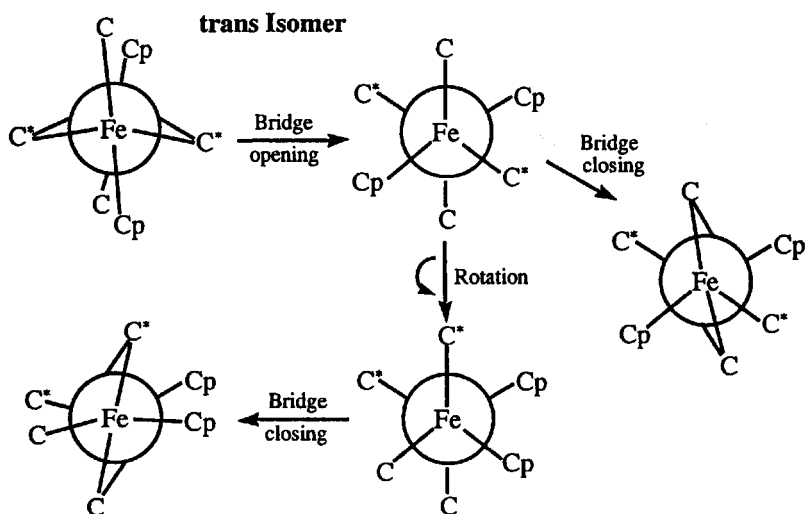
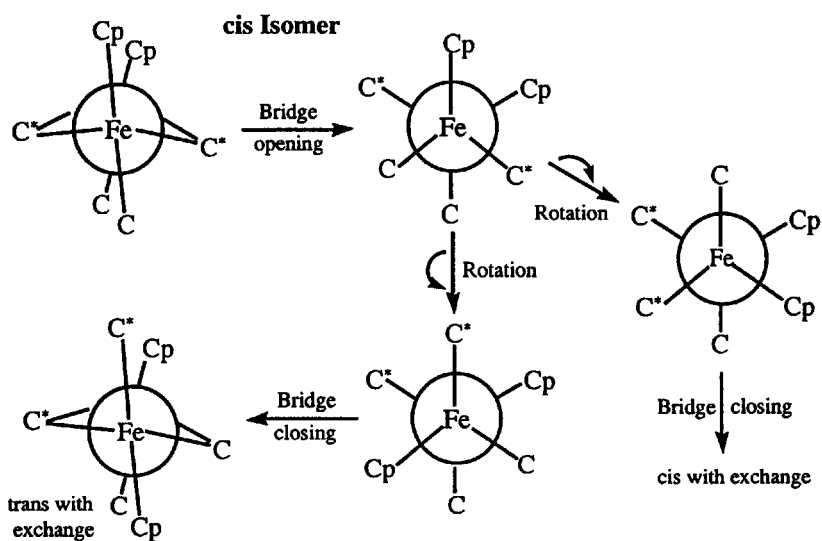
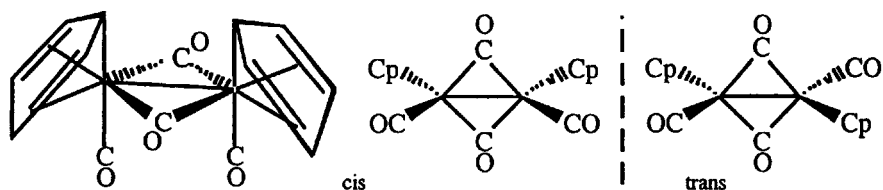
The phenomenon of bridge–terminal carbonyl exchange can occur in any dimetal system that can exist in CO-bridged and metal–metal bonded forms, such as $\text{Co}_2(\text{CO})_8$:



Another example¹¹⁹ is $(\text{Ru}(\eta^5\text{-C}_5\text{H}_5)(\text{CO})_2)_2$, where exchange is rapid on the NMR time scale down to -100°C .

A more complex and informative process has been observed with $(\text{Fe}(\eta^5\text{-C}_5\text{H}_5)(\text{CO})_2)_2$, which has bridging and terminal CO ligands and cis and trans isomers. The temperature dependence of the cis–trans equilibrium adds a complication to the NMR analysis. Several detailed studies¹²⁰ have shown that the bridge–terminal CO exchange has a lower activation energy in the trans isomer. Furthermore, bridge–terminal exchange in the cis isomer occurs at the same rate as the cis–trans isomerization. These observations have been explained by Adams and Cotton¹²¹ by the mechanism depicted in Scheme 4.8.

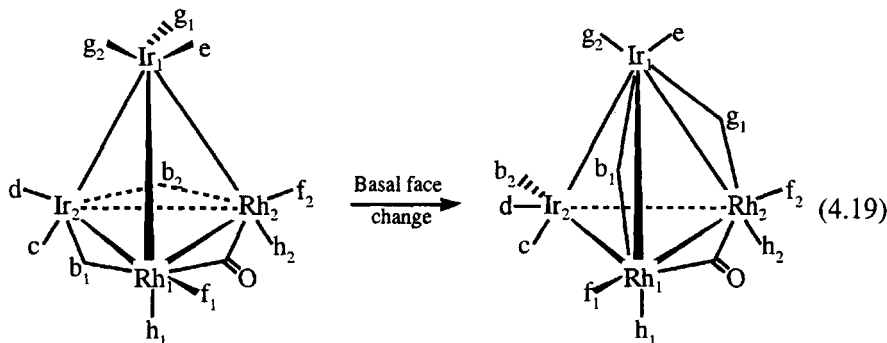
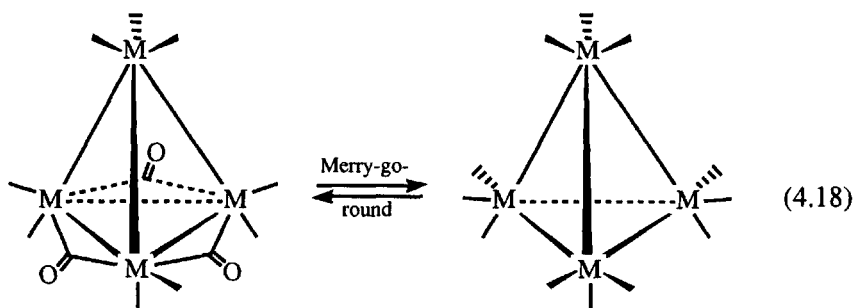
Scheme 4.8



The basis of the mechanism is a nonbridged intermediate, which in the *cis* case must undergo rotation to cause bridge-terminal exchange and isomerization. But the *trans* isomer can undergo exchange without rotation. It is necessary to remember that ring closing can only occur with two CO ligands on opposite sides of the molecule. This general mechanism seems to be consistent with observations on other systems. Thus, the same rate is observed for the *cis*-*trans* isomerization and bridge-terminal exchange in $\text{Fe}_2(\eta^5\text{-C}_5\text{H}_5)_2(\text{P}(\text{OPh})_3)(\text{CO})_3$ because the phosphite ligand cannot occupy a bridging position.¹²² Other systems, such as $\text{Mn}_2(\eta^5\text{-C}_5\text{H}_5)_2(\text{NO})_2(\text{CO})_2$, $\text{Cr}_2(\eta^5\text{-C}_5\text{H}_5)_2(\text{NO})_4$ ¹²³ and $\text{Pt}_2(\eta^5\text{-C}_5\text{H}_5)_2(\text{CO})_2$,¹²⁴ provide further examples of this type of fluxionality.

The fluxionality of $\text{M}_3(\text{CO})_{12}$ systems ($\text{M} = \text{Fe}, \text{Ru}, \text{Os}$) and their derivatives has been extensively examined. The structures typically have a $(\mu\text{-CO})_2$ bridge, but the unbridged or D_3 structure seems to be close in energy and has been characterized at 173 K in $\text{FeRu}_2(\text{CO})_{12}$ by Braga et al.¹²⁵ Mann and co-workers¹²⁶ describe the fluxionality by a low energy concerted bridge-opening bridge-closing mechanism around the Fe_3 plane and a higher energy merry-go-round¹²⁷ in which the bridge opens and closes on different COs. Johnson and co-workers¹²⁸ consider the process in terms of rotation of the $(\text{CO})_{12}$ icosahedron and the M_3 plane.

In $\text{M}_4(\text{CO})_{12}$ systems, the merry-go-round¹²⁹ and basal face change¹³⁰ mechanisms, shown in reactions (4.18) and (4.19), have been identified. In the first case the unbridged intermediate is shown. For the second case, the



product of one rearrangement of $\text{Ir}_2\text{Rh}_2(\text{CO})_9(\mu\text{-CO})_3$ is given, and the bridging CO which is unaffected is uniquely designated. In the example given, the “base of the pyramid” shifts from $(\text{Ir}_2\text{-Rh}_1\text{-Rh}_2)$ to $(\text{Ir}_1\text{-Rh}_1\text{-Rh}_2)$.

Roulet and co-workers¹³¹ have determined ΔV^\ddagger for two systems which interchange CO's by the merry-go-round process; the values are -6 and $-7.7 \text{ cm}^3 \text{ mol}^{-1}$ for $\text{Rh}_4(\text{CO})_{12}$ and $\text{IrRh}_3(\text{CO})_{12}$, respectively. It was suggested that the ΔV^\ddagger is negative because of shorter M—M bonds in the unbridged species. This has been justified on the basis of known structures¹³² and density functional calculations. In a separate study¹³³ of systems using the basal face change process, positive values of 7.9 and $15.1 \text{ cm}^3 \text{ mol}^{-1}$ were found for $\text{Ir}_2\text{Rh}_2(\text{CO})_9(\mu\text{-CO})_3$ and $\text{Ir}_4(\text{CO})_{11}(\mu\text{-SO}_2)$, respectively. On this basis, the authors have suggested that ΔV^\ddagger could be used to distinguish between these two fluxional pathways. Finally, it should be mentioned that Allian and Garland¹³⁴ have used FTIR to detect unbridged $\text{M}_4(\text{CO})_{12}$ in hexane, and determined the thermodynamic parameters for its equilibrium with $\text{Rh}_4(\text{CO})_9(\mu\text{-CO})_3$.

References

1. Basolo, F.; Pearson, R. G. *Mechanisms of Inorganic Reactions*, 2nd ed.; Wiley: New York, 1967.
2. Holm, R. H.; O'Connor, M. J. *Prog. Inorg. Chem.* **1971**, *14*, 241.
3. Serpone, N.; Bickley, D. G. *Prog. Inorg. Chem.* **1972**, *17*, 391.
4. Wilkins, R. G. *The Study of Kinetics and Mechanism of Reactions of Transition Metal Complexes*; Allyn and Bacon: Boston, 1974; Chapter 7.
5. *Dynamic Nuclear Magnetic Resonance Spectroscopy*; Jackman, L. M.; Cotton, F. A., Eds.; Academic Press: New York, 1975; Chapters 8–12.
6. Rotzinger, F. P. *Chem. Rev.* **2005**, *105*, 2003.
7. Beattie, J. K. *Acc. Chem. Res.* **1971**, *4*, 253.
8. Yatsunyk, L. A.; Ogura, H.; Walker, F. A. *Inorg. Chem.* **2005**, *44*, 2867.
9. McGarvey, J. J.; Wilson, J. J. *Am. Chem. Soc.* **1975**, *97*, 2531.
10. Knoch, R.; Elias, H.; Paulus, H. *Inorg. Chem.* **1995**, *34*, 4032, and references therein.
11. Ivin, K. J.; Jamison, R.; McGarvey, J. J. *J. Am. Chem. Soc.* **1972**, *94*, 1763; Campbell, L.; McGarvey, J. J.; Samman, N. G. *Inorg. Chem.* **1978**, *17*, 3378.
12. Beattie, J. K.; Moody, W. E. *J. Coord. Chem.* **1994**, *32*, 155.
13. Haus, A.; Raidt, M.; Link, T. A.; Elias, H. *Inorg. Chem.* **2000**, *39*, 5111.
14. Farina, R. D.; Swinehart, J. H. *Inorg. Chem.* **1972**, *11*, 645.
15. Aizawa, S.; Iida, S.; Matsuda, K.; Funahashi, S. *Inorg. Chem.* **1996**, *35*, 1338.
16. Aizawa, S.; Funahashi, S. *Inorg. Chem.* **2002**, *41*, 4555.
17. Balahura, R. J.; Lewis, N. A. *Coord. Chem. Rev.* **1976**, *20*, 109.
18. Burmeister, J. L. *Coord. Chem. Rev.* **1968**, *3*, 225.
19. Hubbard, J. L.; Zoch, C. R.; Elcesser, W. L. *Inorg. Chem.* **1993**, *32*, 3333.
20. Maher, J. M.; Lee, G. R.; Cooper, N. J. *J. Am. Chem. Soc.* **1982**, *104*, 6797.

21. Buckingham, D. A. *Coord. Chem. Rev.* **1994**, *135*, 587.
22. Buckingham, D. A.; Creaser, I. I.; Sargeson, A. M. *Inorg. Chem.* **1970**, *9*, 655.
23. Buckingham, D. A.; Clark, C. R.; Liddel, G. F. *Inorg. Chem.* **1992**, *31*, 2909.
24. Palmer, D. A.; van Eldik, R.; Kelm, H. *Inorg. Chim. Acta* **1978**, *30*, 83.
25. Basolo, F.; Baddley, W. H.; Weidenbaum, K. J. *J. Am. Chem. Soc.* **1966**, *88*, 1576.
26. Jackson, W. G.; Lawrance, G. A.; Lay, P. A.; Sargeson, A. M. *Aust. J. Chem.* **1982**, *35*, 1562.
27. Fairlie, D. P.; Angus, P. M.; Fenn, M. D.; Jackson, W. G. *Inorg. Chem.* **1991**, *30*, 1564.
28. Jackson, W. G.; McKeon, J. A.; Balahura, R. J. *Inorg. Chem.* **2004**, *43*, 4889.
29. Sisley, M. J.; McDonald, R.; Jordan, R. B. *Inorg. Chem.* **2004**, *43*, 5339.
30. Jackson, W. G.; Rahman, A. F. M. M. *Inorg. Chem.* **1990**, *29*, 3247.
31. Blackman, A. G.; Buckingham, D. A.; Clark, C. R.; Simpson, J. *J. Chem. Soc., Dalton Trans.* **1991**, 3031.
32. Hubinger, S.; Hall, J. H.; Purcell, W. L. *Inorg. Chem.* **1993**, *32*, 2394; Jackson, W. G.; Cortez, S. *Inorg. Chem.* **1994**, *33*, 1921.
33. Yeh, A.; Scott, N.; Taube, H. *Inorg. Chem.* **1982**, *21*, 2542.
34. Powell, D. W.; Lay, P. A. *Inorg. Chem.* **1992**, *31*, 3542.
35. Katz, N. E.; Fagalde, F. *Inorg. Chem.* **1993**, *32*, 5391.
36. Chou, M. H.; Brunshwig, B. S.; Creutz, C.; Sutin, N.; Yeh, A.; Chang, R. C.; Lin, C.-T. *Inorg. Chem.* **1992**, *31*, 5347.
37. Lay, P. A.; Harman, W. D. *Adv. Inorg. Chem.* **1991**, *37*, 219.
38. Damrauer, L.; Milburn, R. M. *J. Am. Chem. Soc.* **1971**, *93*, 6481.
39. Dalzell, B. C.; Eriks, K. *J. Am. Chem. Soc.* **1971**, *93*, 4298.
40. Gamsjäger, H.; Murmann, R. K. *Adv. Inorg. Bioinorg. Mech.* **1983**, *2*, 317.
41. Palmer, D. A.; Kelm, H. *J. Inorg. Nucl. Chem.* **1978**, *40*, 1095.
42. Odell, A. L.; Olliff, R. W.; Rands, D. B. *J. Chem. Soc., Dalton Trans.* **1972**, 752.
43. Lethbridge, J. W.; Glasser, L. S. D.; Taylor, H. F. W. *J. Chem. Soc. A* **1970**, 1862.
44. Lawrance, G. A.; Stranks, D. R. *Inorg. Chem.* **1977**, *16*, 929.
45. Ho, F. F.-L.; Reilley, C. N. *Anal. Chem.* **1969**, *41*, 1835; Evilia, R. F.; Young, D. C.; Reilley, C. N. *Inorg. Chem.* **1971**, *10*, 433.
46. Wilkins, R. G.; Williams, M. J. G. *J. Chem. Soc.* **1957**, 1763.
47. Basolo, F.; Hayes, J. C.; Neumann, H. M. *J. Am. Chem. Soc.* **1954**, *76*, 3807.
48. Lawrance, G. A.; Stranks, D. R. *Inorg. Chem.* **1977**, *16*, 929; *Ibid.* **1978**, *17*, 1804.
49. Beattie, J. K.; Binstead, R. A.; West, R. J. *J. Am. Chem. Soc.* **1978**, *100*, 3046.
50. McGarvey, J. J.; Lawthers, I.; Heremans, K.; Toftlund, H. *Inorg. Chem.* **1990**, *29*, 252.
51. Romeo, R.; Fenech, L.; Monsù Solarno, L.; Albinati, A.; Macchioni, A.; Zuccaccia, C. *Inorg. Chem.* **2001**, *40*, 3293; Romeo, R.; Fenech, L.; Carnabuci, S.; Plutino, M. R.; Romeo, A. *Inorg. Chem.* **2002**, *41*, 2839.
52. Romeo, R.; Carnabuci, S.; Plutino, M. R.; Romeo, A.; Rizzato, S.; Albinati, A. *Inorg. Chem.* **2005**, *44*, 1248.

53. Vanquickenborne, L. G.; Pierloot, K. *Inorg. Chem.* **1981**, *20*, 3673.
54. Vanquickenborne, L. G.; Pierloot, K. *Inorg. Chem.* **1984**, *23*, 1471.
55. Wilkins, R. G. *The Study of Kinetics and Mechanism of Reactions of Transition Metal Complexes*; Allyn and Bacon: Boston, 1974; p 350.
56. Kite, K.; Orrell, K. G.; Sik, V. *Polyhedron*, **1995**, *14*, 2711.
57. Kersting, B.; Telford, J. R.; Meyer, M.; Raymond, K. N. *J. Am. Chem. Soc.* **1996**, *118*, 5712.
58. Eaton, S. S.; Eaton, G. R.; Holm, R. H. *J. Am. Chem. Soc.* **1973**, *95*, 1116.
59. Pignolet, L. H.; Duffy, D. J.; Que, L., Jr. *J. Am. Chem. Soc.* **1973**, *95*, 295; Palazzotto, M. C.; Duffy, D. J.; Edgar, B. L.; Que, L., Jr.; Pignolet, L. H. *J. Am. Chem. Soc.* **1973**, *95*, 4537.
60. Rodger, A.; Johnson, B. F. G. *Inorg. Chem.* **1988**, *27*, 3061.
61. Keppert, D. *Prog. Inorg. Chem.* **1977**, *23*, 1.
62. Holm, R. H. In *Dynamic Nuclear Magnetic Resonance Spectroscopy*; Jackman, L. M.; Cotton, F. A., Eds.; Academic Press: New York, 1975; p 317.
63. Eaton, S. S.; Hutchinson, J. R.; Holm, R. H. *J. Am. Chem. Soc.* **1972**, *94*, 6411.
64. Musher, J. I. *J. Chem. Educ.* **1974**, *51*, 94.
65. Meakin, P.; Jesson, J. P. *J. Am. Chem. Soc.* **1973**, *95*, 7272.
66. Berry, R. S. *J. Chem. Phys.* **1960**, *32*, 933.
67. Ugi, I.; Marquarding, D.; Klusacek, H.; Gillespie, P. *Acc. Chem. Res.* **1971**, *4*, 288.
68. Strich, A. *Inorg. Chem.* **1978**, *17*, 942; Merx, H.; Brickmann, J. *Zeit. Physik. Chemie* **2004**, *218*, 155.
69. Meakin, P.; Muettterties, E. L.; Jesson, J. P. *J. Am. Chem. Soc.* **1972**, *94*, 5271.
70. Anderson, G. K.; Cross, R. J. *Chem. Soc. Rev.* **1980**, *9*, 185.
71. Alibrandi, G.; Scolaro, L. M.; Romeo, R. *Inorg. Chem.* **1991**, *30*, 4007; Minnitti, D. *Inorg. Chem.* **1994**, *33*, 2631.
72. Appleton, T. G.; Hall, J. R.; Ralph, S. F.; Thompson, C. S. M. *Inorg. Chem.* **1989**, *28*, 1989; Miller, S. E.; Gerard, K. J.; House, D. A. *Inorg. Chim. Acta* **1991**, *190*, 135; Mikola, M.; Arpalahiti, J. *Inorg. Chem.* **1994**, *33*, 4439.
73. Wong, E.; Giandomenico, C. M. *Chem. Rev.* **1999**, *99*, 2451; Reedjik, J. *Proc. Natl. Acad. Sci. U.S.A.* **2003**, *100*, 3611.
74. Baik, M.-H.; Friesner, R. A.; Lippard, S. J. *J. Am. Chem. Soc.* **2003**, *125*, 14082.
75. Deubel, D. V. *J. Am. Chem. Soc.* **2004**, *126*, 5999.
76. Murdoch, P. S.; Ranford, J. D.; Sadler, P. J.; Berners-Price, S. J. *Inorg. Chem.* **1993**, *32*, 2249.
77. Mann, B. E. In *Comprehensive Organometallic Chemistry*; Abel, E. W.; Stone, F. G. A.; Wilkinson, G., Eds.; Pergamon Press: London, 1982; Vol. 3, p 89.
78. Mann, B. E. *Chem. Soc. Rev.* **1986**, *15*, 167.
79. Braga, D.; Grepion, F.; Orpen, A. G. *Organometallics* **1993**, *12*, 1481.
80. McClellad, B. W.; Robiette, A. G.; Hedberg, L.; Hedberg, K. *Inorg. Chem.* **2001**, *40*, 1358.

81. Lee, T.; Benesch, F.; Jiang, Y.; Rose-Petruk, C. G. *Chem. Phys.* **2004**, *299*, 233; Lee, T.; Welch, E.; Rose-Petruk, C. G. *J. Phys. Chem. A* **2004**, *108*, 11768, and references therein.
82. Sheline, R. K.; Mahnke, H. *Angew. Chem. Int. Ed.* **1975**, *14*, 314.
83. Mahnke, H.; Clark, R. J.; Rosanske, R.; Sheline, R. K. *J. Chem. Phys.* **1973**, *60*, 2997.
84. Speiss, H. W.; Grosescu, R.; Haerberlen, U. *Chem. Phys.* **1974**, *6*, 226.
85. Hanson, B. E.; Whitmire, K. H. *J. Am. Chem. Soc.* **1990**, *112*, 974.
86. Burdett, J. K.; Gryzbowski, J. M.; Poliakov, M.; Turner, J. J. *J. Am. Chem. Soc.* **1976**, *98*, 5728.
87. Blyholder, G.; Springs, J. *Inorg. Chem.* **1985**, *24*, 224; Jang, J. H.; Lee, J. G.; Lee, H.; Xie, Y.; Schaffer, H. F., III. *J. Phys. Chem. A* **1998**, *102*, 5298.
88. Piper, T. S.; Wilkinson, G. *J. Inorg. Nucl. Chem.* **1956**, *3*, 104; Bennett, M. J.; Cotton, F. A.; Davison, A.; Faller, J. W.; Lippard, S. J.; Morehouse, S. M. *J. Am. Chem. Soc.* **1966**, *88*, 4371.
89. Cotton, F. A.; Musco, A.; Yagupsky, G. *J. Am. Chem. Soc.* **1967**, *89*, 6136.
90. Woodward, R. B.; Hoffmann, R. *J. Am. Chem. Soc.* **1965**, *87*, 2511.
91. Mingos, D. M. P. *J. Chem. Soc., Dalton Trans.* **1977**, 602.
92. Heinekey, D. M.; Graham, W. A. G. *J. Am. Chem. Soc.* **1979**, *101*, 6115; *Ibid.* **1982**, *104*, 915; *J. Organomet. Chem.* **1982**, *232*, 335.
93. Muhandiram, D. R.; Kiel, G.-Y.; Aarts, G. H. M.; Saez, I. M.; Reuvers, J. G. A.; Heinekey, D. M.; Graham, W. A. G.; Takats, J.; McClung, R. E. D. *Organometallics* **2002**, *21*, 2687.
94. Lu, Z.; Jones, W. M.; Winchester, W. R. *Organometallics*, **1993**, *12*, 1344.
95. Klosin, J.; Zheng, X.; Jones, W. M. *Organometallics*, **1996**, *15*, 3788.
96. Gibson, J. A.; Mann, B. E. *J. Chem. Soc., Dalton Trans.* **1979**, 1021.
97. Grassi, M.; Mann, B. E.; Spencer, C. M. *J. Chem. Soc., Chem. Commun.* **1985**, 1169.
98. Hails, M. J.; Mann, B. E.; Spencer, C. M. *J. Chem. Soc., Dalton Trans.* **1985**, 693.
99. Takats, J.; Kiel, G.-Y. *Organometallics* **1987**, *6*, 2009.
100. Albright, T. A.; Hoffmann, R.; Thibeault, J. C.; Thorn, D. L. *J. Am. Chem. Soc.* **1979**, *101*, 3801.
101. Cramer, R.; Kline, J. B.; Roberts, J. D. *J. Am. Chem. Soc.* **1969**, *91*, 2519.
102. Segal, J. A.; Johnson, B. F. G. *J. Chem. Soc., Dalton Trans.* **1975**, 677.
103. Ferrando, G.; Gérard, H.; Spivak, G. J.; Coalter, III, J. N.; Huffman, J. C.; Eisenstein, O.; Caulton, K. G. *Inorg. Chem.* **2001**, *40*, 6610.
104. Watson, L. A.; Franzman, B.; Bollinger, J. C.; Caulton, K. G. *New J. Chem.* **2003**, *27*, 1769.
105. Matchett, S. A.; Zhang, G.; Frattarelli, D. *Organometallics* **2004**, *23*, 5440.
106. Takats, J.; Burke, M. R. *J. Am. Chem. Soc.* **1983**, *105*, 4092.
107. Lundquist, E. G.; Folting, K.; Streig, W. E.; Huffman, J. C.; Eisenstein, O.; Caulton, K. G. *J. Am. Chem. Soc.* **1990**, *112*, 855.
108. Ramdeehul, S.; Barloy, L.; Osborn, J. A. *Organometallics* **1996**, *15*, 5442; Werner, H.; Kühn, A.; Burschka, C. *Chem. Ber.* **1980**, *113*, 2291.

109. Mingos, D. M. P. In *Comprehensive Organometallic Chemistry*; Abel, E. W.; Stone, F. G. A.; Wilkinson, G., Eds.; Pergamon Press: London, 1982; Vol. 3, pp 60–61.
110. Vrieze, K.; van Leeuwen, P. W. N. M. *Prog. Inorg. Chem.* **1971**, *14*, 1; Clarke, H. L. *J. Organomet. Chem.* **1974**, *80*, 155; Tsutsui, M.; Courtney, A. *Adv. Organomet. Chem.* **1977**, *16*, 241; Anderson, G. K.; Cross, R. J. *Chem. Soc. Rev.* **1980**, *9*, 185.
111. Rosenblum, M.; Waterman, P. J. *Organomet. Chem.* **1981**, *206*, 197.
112. Norrby, P. O.; Åkermark, B.; Haefner, F.; Hansen, S.; Blomberg, M. *J. Am. Chem. Soc.* **1993**, *115*, 4859; Sakai, S.; Satoh, H.; Shono, H.; Ujino, Y.; *Organometallics* **1996**, *15*, 1713; Solin, N.; Szabó, K. *J. Organometallics* **2001**, *20*, 5464.
113. van Leeuwen, P. W. N. M.; Praat, N. A. P.; van Diepen, M. *J. Organomet. Chem.* **1971**, *29*, 433.
114. Davison, A.; Rode, W. C. *Inorg. Chem.* **1967**, *6*, 2124; Fallor, J. W.; Incorvia, M. J. *Inorg. Chem.* **1968**, *4*, 840.
115. Fish, R. W.; Giering, W. P.; Marten, D.; Rosenblum, M. *J. Organomet. Chem.* **1976**, *105*, 101.
116. Gibson, D. H.; Hsu, W.-L.; Steinmetz, A. L.; Johnson, B. V. *J. Organomet. Chem.* **1981**, *208*, 89.
117. Ariafard, A.; Bi, S.; Lin, Z. *Organometallics* **2005**, *24*, 2241.
118. Xue, P.; Bi, S.; Sung, H. H. Y.; Williams, I. D.; Lin, Z.; Jia, G. *Organometallics*, **2004**, *23*, 4753.
119. Bullitt, J. G.; Cotton, F. A.; Marks, T. J. *J. Am. Chem. Soc.* **1970**, *92*, 2155.
120. Gansow, O. A.; Burke, A. R.; Vernon, W. D. *J. Am. Chem. Soc.* **1972**, *94*, 2550; Adams, R. D.; Cotton, F. A. *J. Am. Chem. Soc.* **1973**, *95*, 6589.
121. Adams, R. D.; Cotton, F. A. In *Dynamic Nuclear Magnetic Resonance Spectroscopy*, Jackman, L. M.; Cotton, F. A., Eds.; Academic Press: New York, 1975; Chapter 12.
122. Cotton, F. A.; Kruczynski, L.; White, A. J. *Inorg. Chem.* **1974**, *13*, 1402.
123. Kirchner, R. M.; Marks, T. J.; Kristoff, J. S.; Ibers, J. A. *J. Am. Chem. Soc.* **1973**, *95*, 6602.
124. Boag, N. M.; Goodfellow, R. J.; Green, M.; Hessner, B.; Howard, J. A. K.; Stone, F. G. A. *J. Chem. Soc., Dalton Trans.* **1983**, 2585.
125. Braga, D.; Farrugia, L. J.; Gillion, A. L.; Greponi, F.; Tedesco, E. *Organometallics*, **1996**, *15*, 4684.
126. Adams, H.; Bailey, N. A.; Bentley, G. W.; Mann, B. E. *J. Chem. Soc., Dalton Trans.* **1989**, 1931; Adams, H.; Carr, A. G.; Mann, B. E.; Melling, R. *Polyhedron* **1995**, *14*, 2771.
127. Cotton, F. A.; Hunter, D. L. *Inorg. Chim. Acta* **1974**, *11*, L9.
128. Johnson, B. F. G.; Parisini, E.; Roberts, Y. V. *Organometallics* **1993**, *12*, 233; Johnson, B. F. G.; Roberts, Y. V. *J. Chem. Soc., Dalton Trans.* **1993**, 2945.
129. Cotton, F. A. *Inorg. Chem.* **1966**, *5*, 1083.
130. Braga, D.; Ros, R.; Roulet, R. *J. Organomet. Chem.* **1985**, 286, C8.

131. Besancon, K.; Laurency, G.; Lumini, T.; Roulet, R.; Bruyndonckx, R.; Daul, C. *Inorg. Chem.* **1998**, *37*, 5634.
132. Braga, D.; Grepioni, F.; Byrne, J. J.; Calhorda, M. J. *J. Chem. Soc., Dalton Trans.* **1995**, 3287.
133. Beni, Z.; Guidoni, L.; Laurency, G.; Roethlisberger, U.; Roulet, R. *Dalton Trans.* **2005**, 310.
134. Allian, A. D.; Garland, M. *Dalton Trans.* **2005**, 1957.

5

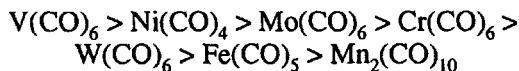
Reaction Mechanisms of Organometallic Systems

5.1 LIGAND SUBSTITUTION REACTIONS

The general principles discussed in Chapter 3 also apply to reactions of organometallic complexes. Because these systems do not have a wide range of structurally similar complexes with different metal atoms for comparative studies across the Periodic Table, comparisons are usually made down a particular group. However, there is a wide range of ligands available for studies of entering and leaving group effects. This area has been the subject of several recent reviews.¹⁻³ A major difference from the systems discussed in Chapter 3 is that many of these complexes are soluble in organic solvents, including hydrocarbons. This can minimize the complicating factor of solvent coordination, but these solvents often have quite low dielectric constants so that various types of preassociation are more probable.

5.1.1 Metal Carbonyls

The metal carbonyl family of compounds is typical of the range of structures and reactivities of organometallic complexes. The rate of CO exchange was examined in early studies, and this work is the subject of a recent review.⁴ The order of reaction rates is as follows:



Where the rate law has been determined, the reaction is first-order in $[\text{M(CO)}_n]$ and zero-order in $[\text{CO}]$. This implies a **D** mechanism, since a solvent intermediate is unlikely for the "noncoordinating" solvents. This mechanism also is probable for other ligand substitutions.

The main mechanistic exception to the above generalizations is V(CO)_6 , which has an **I_a** mechanism for PR_3 substitution reactions.⁵ This compound is unique in that it is the only 17-electron metal carbonyl and also is by far the most labile. Some kinetic results for substitution on V(CO)_6 in hexane are given in Table 5.1.

Table 5.1. Rate Constants (25°C) and Activation Parameters for PR₃ Substitution on V(CO)₆ in Hexane

Entering Group	Cone Angle	<i>k</i> (M ⁻¹ s ⁻¹)	ΔH^* (kcal mol ⁻¹)	ΔS^* (cal mol ⁻¹ K ⁻¹)
PMe ₃	118	132	7.6	-23.4
P(<i>n</i> -Bu) ₃	132	50.2	7.6	-25.2
P(OMe) ₃	107	0.70	10.9	-22.6
PPh ₃	145	0.25	10.0	-27.8

The substitution rates have rather low ΔH^* values, and the negative ΔS^* values are typical of an associative process. The rates for various entering groups correlate with the basicity rather than the size, as measured by the cone angle. It has been suggested that formation of a 19-electron associative intermediate from a 17-electron reactant is much more favorable than a 20-electron intermediate from an 18-electron reactant.

Quantitative studies of CO exchange have been rather limited because of experimental difficulties, especially the low solubility of CO in most solvents. This is illustrated by work on Ni(CO)₄. The original study was incorrect because much of the exchange was occurring in the gas phase, where it is faster than in solution. Subsequent work⁶ showed that the CO exchange and PPh₃ substitution occur at the same rate as expected for a **D** mechanism ($k = 2.1 \times 10^{-2} \text{ M}^{-1} \text{ s}^{-1}$ (30°C), $\Delta H^* = 24 \text{ kcal mol}^{-1}$, $\Delta S^* = 13.1 \text{ cal mol}^{-1} \text{ K}^{-1}$). Theoretical estimates⁷ of the first bond dissociation energy of Ni(CO)₄ are in reasonable agreement with the measured ΔH^* . It seems surprising that a species, such as Ni(CO)₄, with an initially small coordination number would react by a **D** mechanism, but it appears that 20-electron associative intermediates or transition states are less stable than 16-electron dissociative ones because the extra electron pair must go into an antibonding orbital.

The exchange of CO on Fe(CO)₅ was originally reported to show two rates attributed to the axial and equatorial CO ligands. Of course, this is inconsistent with the very rapid fluxionality of Fe(CO)₅ discussed in Chapter 4. Later studies report⁸ only one observable rate of CO exchange. The CO exchange on Fe(CO)₅ is too slow to measure relative to thermal decomposition. However, Basolo and co-workers⁹ have estimated the rate for this exchange based on measured rates for PR₃ substitution in Os(CO)₅ and Ru(CO)₅.¹⁰ The results are given in Table 5.2. The reactivity pattern down the group is similar to that for Group 6, discussed later, but Fe(CO)₅ is still surprisingly unreactive. Basolo has suggested that this could be because the {Fe(CO)₄} dissociative intermediate is high-spin, consistent with observations of Poliakoff and Turner,¹¹ and therefore the process is spin-forbidden. However, a spin-allowed dissociation to the higher energy spin-paired species is possible.

Table 5.2. Rate Constants (50°C) and Activation Parameters for PR₃ Substitution on Group 5 Metal Carbonyls in Decalin

Compound	k (s ⁻¹)	ΔH^\ddagger (kcal mol ⁻¹)	ΔS^\ddagger (cal mol ⁻¹ K ⁻¹)
Fe(CO) ₅	(6×10 ⁻¹¹)	40	18
Ru(CO) ₅	3.0×10 ⁻³	27.6	15.2
Os(CO) ₅	4.9×10 ⁻⁸	30.6	1.33

Theoretical studies by Ziegler and co-workers¹² and by Ehlers and Frenking¹³ have given first bond dissociation energies of 46, 33, 35 and 41, 28, 31 kcal mol⁻¹, respectively, for the Fe, Ru and Os systems. These values are impressively similar to the ΔH^\ddagger values in Table 5.2, especially when one recognizes that they are the difference between the calculated energies of the M(CO)₅ ground state and the M(CO)₄ + CO products. The results of Ziegler indicate that the triplet state of Fe(CO)₄ is ~2 kcal mol⁻¹ lower than the singlet, but both Ziegler and co-workers and Ehlers and Frenking assumed that dissociation occurred by the spin-allowed pathway to the singlet state. Ehlers and Frenking suggested that Os(CO)₅ proceeds by an I_a mechanism, but this is not consistent with the fact that the rate is independent of CO concentration.

Ziegler indicates that relativistic effects contribute about 3 and 10 kcal mol⁻¹ to strengthen the bonds in Ru(CO)₅ and Os(CO)₅, respectively, and this difference largely accounts for the lower reactivity of Os(CO)₅. There is an implication that the relativistic effects are somewhat less important in the M(CO)₄ product than in the M(CO)₅ reactant.

The Group 6 M(CO)₆ compounds have been most widely studied with regard to CO exchange and substitution. The substitution reactions usually have the following two-term pseudo-first-order rate constant:

$$k_{\text{exp}} = k_1 + k_2[\text{L}] \quad (5.1)$$

The k_1 term is assigned to a D mechanism and the k_2 term to an I_a mechanism. Some results for CO exchange and P(*n*-C₄H₉)₃ substitution are given in Table 5.3. Clearly, the kinetic parameters for exchange and k_1 are quite similar, as expected if CO dissociation is rate controlling for both reactions. The parallel between $f_{\text{M-C}}$ and ΔH^\ddagger and ΔH_1^\ddagger is expected for a dissociative process.

Any explanation for the lack of a smooth trend in ΔH^\ddagger down the group first requires a decision as to which member is out of line. It was argued by King¹⁴ that W(CO)₆ has an especially strong M—C bond because the lanthanide contraction makes the covalent radius of W smaller than expected (Cr, 1.25 Å; Mo, 1.36 Å; W, 1.37 Å), with the result that the 5*d* and maybe 4*f* orbitals give much better π back bonding. More recent theoretical studies^{12,13} indicate that this argument is overly simplistic.

Table 5.3. Activation Parameters for CO Exchange and P(*n*-C₄H₉)₃ Substitution on M(CO)₆ in Decalin^a

Compound	Exchange		Substitution				<i>f</i> _{M-C} ^b
	ΔH^*	ΔS^*	ΔH_1^*	ΔS_1^*	ΔH_2^*	ΔS_2^*	
Cr(CO) ₆	38.7	18.5	40.2	22.6	25.5	-14.6	2.08
Mo(CO) ₆	30.2	-0.4	31.7	6.7	21.7	-14.9	1.96
W(CO) ₆	39.8	11.0	39.9	13.8	29.2	-6.9	2.36

^a Activation enthalpies and entropies in kcal mol⁻¹ and cal mol⁻¹ K⁻¹, respectively; original sources are given in reference 12.

^b Force constant for the M—C bond in m dyn Å⁻¹.

According to Ziegler and co-workers, the π back bonding is more effective because relativistic effects raise the energy of the 5*d* π -type orbitals and reduce the energy gap with the π^* orbitals of CO so that back bonding is enhanced with W. Grimme and co-workers¹⁵ have explored the strengths and weaknesses of various theoretical approaches to calculating CO dissociation energies from several first-row transition metal carbonyls with quantitative results similar to those from the earlier studies.

For phosphine substitution,¹⁶ $\Delta V_1^* = 15 \text{ cm}^3 \text{ mol}^{-1}$ for Cr(CO)₆ in cyclohexane and $10 \text{ cm}^3 \text{ mol}^{-1}$ for Mo(CO)₆ in isoctane. The values are positive, as expected for a dissociative process. For W(CO)₆, the ΔV_2^* of $-10 \text{ cm}^3 \text{ mol}^{-1}$ is negative, as expected for an associative process. The negative values of ΔS_2^* in Table 5.3 also are consistent with an associative activation. The parallel between ΔH_1^* and ΔH_2^* indicates a significant amount of bond breaking in the associative transition state. Calculations by Ziegler and co-workers¹² for an associative pathway indicate that this is only slightly less favorable than the dissociative one for Cr and Mo and is more favorable for W.

5.1.2 Substituted Metal Carbonyls, M_m(CO)_n(X)_x

The CO exchange and substitution reactions on these systems are usually discussed in terms of the *cis* and *trans* effects of the heteroligand X and steric factors. The rate laws are similar to that described for the M(CO)₆ systems given in Eq. (5.1) but, depending on the system, the *k*₁ or *k*₂ path may dominate.

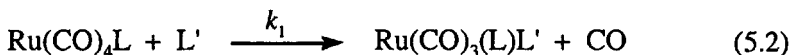
The Mn(CO)₅X (X = Cl, Br) systems have been the subject of a number of studies. Wojcicki and Basolo¹⁷ originally reported that *cis*-CO exchange was much faster than *trans*-CO exchange. Later work¹⁸ indicated that the two rates were within a factor of less than two of each other. However, Atwood and Brown¹⁹ found that *cis*-CO exchange is more than 10 times faster than *trans*-CO exchange in Mn(CO)₅Br and Re(CO)₅Br. Exchange

into the trans position is proposed to occur subsequent to cis exchange by a fluxional process in the intermediate, as described in Chapter 1 with regard to the principle of microscopic reversibility.

Theoretical work on $\text{Mn}(\text{CO})_5\text{X}$ systems by Lichtenberger and Brown²⁰ and by Davy and Hall²¹ showed that the labilization of the cis-CO could result from both ground-state and transition-state effects of the X ligand. It also was suggested that the initial square-based pyramid resulting from CO loss could relax to varying extents towards a trigonal bipyramid, with the latter being favored by π -donor X ligands. Wilms et al.²² calculated that the most stable form of $\{\text{Mn}(\text{CO})_4\text{Cl}\}$ is a distorted trigonal bipyramid with an equatorial Cl. Macgregor and MacQueen²³ examined the isoelectronic $\text{M}(\text{CO})_5\text{X}^-$ ions ($\text{M} = \text{Cr}, \text{Mo}, \text{W}$; $\text{X} = \text{NH}_2, \text{OH}, \text{F}, \text{Cl}, \text{Br}, \text{I}, \text{CH}_3, \text{H}$) and found similar behavior. They note that π donors tend to both destabilize the 18-electron ground state and stabilize the 16-electron transition state.

A recurrent problem in this area and for other substitution reactions is the separation of the electronic and steric effects of the nonreacting ligands. In organometallic systems, the steric effect is usually measured by the Tolman cone angle, θ ,²⁴ but the electronic effect is a mixture of the σ -donor and π -acceptor abilities of the nonreacting ligands. These features have been discussed previously in Section 3.5.6.

Chen and Poë²⁵ studied the reaction



and used the ^{13}C NMR chemical shift, δ , in $\text{Ni}(\text{CO})_3\text{L}$ as a measure of the electronic factor for L to correlate the results with

$$\log k_1 = \alpha + \beta_L\delta + \gamma_L\theta \quad (5.3)$$

They also found that this approach correlates substitution kinetics for several other substituted metal carbonyls and for a methyl migration reaction. Giering and co-workers²⁶ have analysed steric and electronic effects for a large number of systems and coined the expression "Qualitative Analysis of Ligand Effects", QUALE, for such studies. These studies measured the electronic effect by the parameter, χ , derived from IR data for $\text{Ni}(\text{CO})_3\text{L}$,²⁷ and the steric effect by the cone angles, θ . More recently, this approach has been further parameterized by using χ_d for σ -donicity, π_p for π -acidity and E_{ar} for the "aryl effect".²⁸ Recent studies,²⁹ including further work on reaction (5.2),³⁰ illustrate the application of this type of analysis. The QUALE methodology has been criticized by Drago and co-workers³¹ and defended by Giering and co-workers.³²

Since steric effects are so widely used either to protect or activate a metal center, it is not surprising that there have been attempts to refine or improve the venerable cone angles. It is difficult to define a cone angle for

ligands with conformationally flexible substituents, such as $P(\text{Et})_3$, $P(\text{iPr})_3$ and $P(\text{OR})_3$, and Tolman's values seem to have been based on the most compact conformation. The ligand repulsive energies, E_R , calculated by Brown and co-workers,³³ suggested that the original θ values for $P(\text{OMe})_3$ and $P(\text{OEt})_3$ should be increased by $\sim 20^\circ$. This was confirmed by Ernst and co-workers³⁴ from a correlation of ΔH versus θ . Coville and co-workers³⁵ have analyzed a number of crystal structures with $P(\text{OR})_3$ ligands and found that $P(\text{OMe})_3$ tends to have θ values of 117° and 130° , while $P(\text{OEt})_3$ shows values of 119° , 124° and 132° . The multiple values are attributed to the different conformers.

In addition to θ and E_R , other measures of ligand size have been proposed but are not as widely used as θ . White et al.³⁶ have advocated the use of solid angles, Ω_C , which are essentially the three-dimensional cone angle, but their use may be limited by the complexity of the calculation. For $P(\text{RR}'\text{R}'')$ ligands, Orpen and co-workers³⁷ suggested the symmetric deformation coordinate, S_4' , which is the sum of the three $\text{M}-\text{P}-\text{R}$ angles minus the sum of the three $\text{R}-\text{P}-\text{R}$ angles. This is simple to determine from a known or calculated structure, but it has been noted that angles obtained from crystal structures may be subject to distortion by crystal packing forces.³⁸ The S_4' scale has been updated recently by Cundari and co-workers,³⁹ whose results suggest that it causes phosphites to appear much smaller than indicated by the revised values of θ .³⁵

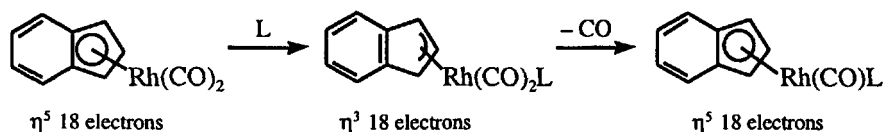
Much of the theoretical and experimental background on the problem of separating σ -donor and π -acceptor effects in rationalizing the influence of nonreacting ligands, especially with phosphines, has been summarized by Woska et al.⁴⁰ The latter have used available data to estimate the QUALE parameters, χ_d and π_p , for PF_3 , PCl_3 and PH_3 , and conclude that the first two are good π acceptors. Frenking et al.⁴¹ have come to the same conclusion from a theoretical analysis of $\text{M}(\text{CO})_5(\text{PX}_3)$ systems ($\text{M} = \text{Cr}, \text{Mo}, \text{W}$; $\text{X} = \text{H}, \text{Me}, \text{F}, \text{Cl}$). They add the cautionary note that π -acceptor strength can be expected to depend on both the donor and acceptor, so that there need not be a unique π -acceptor strength for a ligand. They also provide an example of the lack of correlation between bond length and bond strength; PMe_3 has both the longest and the strongest bond in all the systems they examined.

The nonreacting ligand can have special properties that influence the substitution lability and mechanism. For example, $\text{Cr}(\eta^6\text{-arene})(\text{CO})_3$ ⁴² and $\text{M}(\eta^5\text{-C}_5\text{H}_5)(\text{CO})_2$ compounds ($\text{M} = \text{Co}, \text{Rh}, \text{Ir}$) react by an I_a mechanism.⁴³ This has been explained⁴⁴ as "slippage" of the $\eta^5\text{-C}_5\text{H}_5$ to an $\eta^3\text{-C}_5\text{H}_5$ form in the transition state, thereby liberating a metal orbital to accept an electron pair from the entering group.⁴⁵ In a study of the reaction of various phosphines with $\text{Ru}(\eta^5\text{-C}_5\text{H}_5)(\eta^4\text{-C}_5\text{H}_4\text{O})\text{L}^+$ systems, Wherland and co-workers⁴⁶ identified one reaction pathway as proceeding through a phosphine- $\eta^3\text{-C}_5\text{H}_5$ intermediate. The rates and activation parameters for formation of this intermediate are rather insensitive to the basicity of the

phosphine and the authors suggest that slippage occurs before significant formation of the Ru—P bond. A reverse form of slippage was suggested in a theoretical study of chromium-based catalysts which produce 1-hexene from ethylene.⁴⁷ An initially η^1 -N-bonded pyrrole is proposed to stabilize unsaturated intermediates by slippage to form η^3 - and η^5 -pyrrole.

An especially favorable form of slippage has been used by Basolo and co-workers⁴⁸ to explain the unusually high associative substitution lability of $\text{Rh}(\eta^5\text{-indenyl})(\text{CO})_2$, which is about 10^8 times more reactive than the ($\eta^5\text{-C}_5\text{H}_5$) analogue. This has come to be known as the *indenyl effect*. It is proposed that the intermediate formed by slippage is stabilized by the gain in resonance energy in the six-membered ring, as shown in Scheme 5.1.

Scheme 5.1



Similar rate enhancements and associative pathways were observed for indenyl complexes of manganese,⁴⁹ rhenium⁵⁰ and iridium.⁵¹ However, substitutions on $\text{Fe}(\eta^5\text{-indenyl})(\text{CO})_2\text{I}$ ⁵² and $\text{RuCl}(\eta^5\text{-indenyl})(\text{PPh}_3)_2$ ⁵³ have *D* mechanisms. The same mechanism is shown by the 19-electron radical $\text{Fe}(\eta^5\text{-indenyl})(\text{CO})_3$, which is 10^3 times less reactive than its $\eta^5\text{-C}_5\text{H}_5$ analogue.⁵⁴ It seems that factors other than slippage are contributing to the indenyl effect and the variation of the indenyl donor ability with ancillary ligands has been suggested in theoretical studies.^{55,56} The electrochemical studies on bis(η^5 -indenyl)Fe derivatives⁵⁷ and $\text{RuCl}(\eta^5\text{-indenyl})(\text{PPh}_3)_2$ ⁵³ and their ($\eta^5\text{-C}_5\text{H}_5$) analogues indicate that the indenyl group is a better donor than the cyclopentadienyl group. To add to the mechanistic possibilities for these systems, it should be noted that Chirik and co-workers⁵⁸ have reported an η^9 -indenyl derivative and the system has been the subject of a theoretical study.⁵⁹

The danger in making generalizations in these systems also is shown by CO exchange studies⁶⁰ on $\text{V}(\eta^5\text{-C}_5\text{R}_n)_2(\text{CO})$ compounds. As expected, $\text{V}(\eta^5\text{-indenyl})_2(\text{CO})$ and $\text{V}(\eta^5\text{-C}_5\text{Me}_5)_2(\text{CO})$ are quite labile and react by an *I_a* mechanism, k_2 . This is consistent with either the 17- to 19-electron intermediate formation or slippage of the ring. The unexpected fact is that derivatives of $\text{V}(\eta^5\text{-C}_5\text{H}_7)_2(\text{CO})$ are much more inert and show a significant dissociative reaction pathway, k_1 . Some data for such systems are given in Table 5.4. It seems surprising that the mixed complex $\text{V}(\eta^5\text{-C}_5\text{H}_5)(\eta^5\text{-C}_5\text{H}_7)(\text{CO})$ is just slightly more reactive than $\text{V}(\eta^5\text{-C}_5\text{H}_7)_2(\text{CO})$ and quite different from $\text{V}(\eta^5\text{-C}_5\text{H}_5)_2(\text{CO})$. The authors attributed this great difference in reactivity to electronic factors related to the poorer donation of electrons to the metal from $\eta^5\text{-C}_5\text{H}_7$, than from $\eta^5\text{-C}_5\text{H}_5$. This argument is supported by the CO stretching frequencies, ν_{CO} .

Table 5.4. Rate Constants (60°C) and Activation Parameters for CO Exchange on $V(\eta^5-C_5R_n)_2(CO)$ Systems in Decalin^a

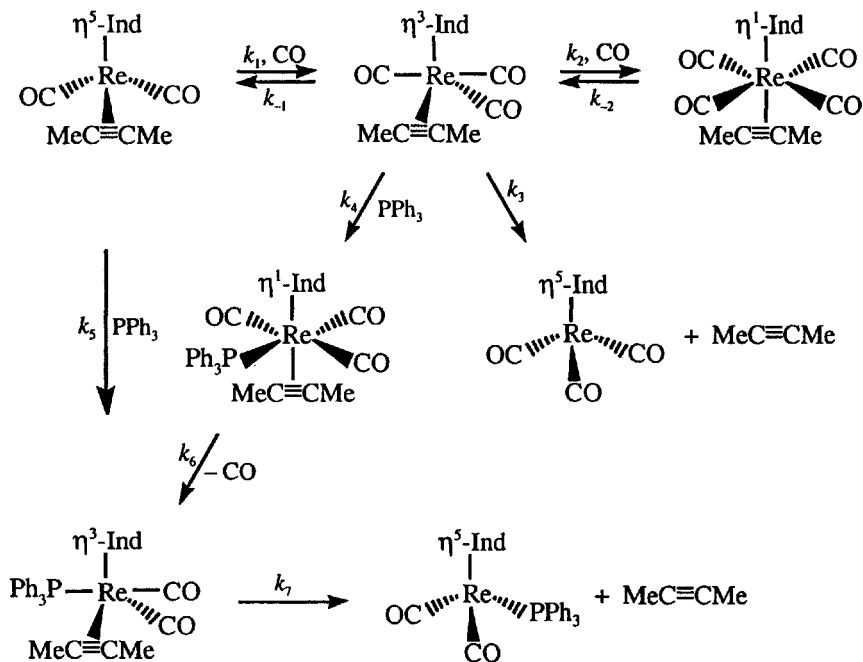
Compound	k_1	ΔH_1^\ddagger	ΔS_1^\ddagger	k_2	ΔH_2^\ddagger	ΔS_2^\ddagger
$V(\eta^5-C_5H_5)_2(CO)$	$\sim 10^{-4}$			8.0×10^2	~ -6	~ -30
$V(\eta^5-C_5Me_5)_2(CO)$	$\sim 10^{-4}$			2.6×10^2	8.9	-21
$V(\eta^5-C_5H_5)(\eta^5-C_5H_7)(CO)$	3×10^{-4}			5.7×10^{-3}		
$V(\eta^5-C_5H_7)_2(CO)$	8×10^{-6}	28.1	2	3.8×10^{-3}	22.7	-2

^a k_1 (s^{-1}), k_2 ($M^{-1} s^{-1}$), ΔH^\ddagger ($kcal\ mol^{-1}$) and ΔS^\ddagger ($cal\ mol^{-1}\ K^{-1}$).

which are $1959\ cm^{-1}$ in the former and $1881\ cm^{-1}$ in the latter. The lower value indicates more back donation into the π^* orbital of CO and a stronger M—C bond. In any case, it is fair to say that these reactivity differences were quite unexpected.

A detailed kinetic study by Casey et al.⁶¹ has shown that the η^5 -indenyl system, shown in Scheme 5.2, undergoes CO exchange and reaction with PPh_3 much faster than its $\eta^5-C_5H_5$ or *cis*-MeHC=CHMe analogues.

Scheme 5.2



Primarily as a result of the dependence of the rate on CO pressure, the major reaction pathways and products shown in Scheme 5.2 have been identified. Extensive ^{13}CO labeling studies, not shown in the Scheme, also

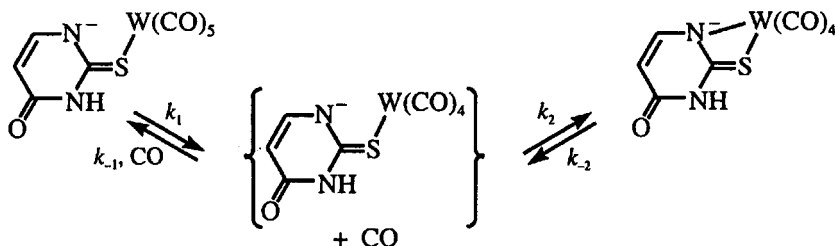
have elucidated the stereochemistry of the CO addition. The latter seems to be assisted both by slippage of the η^5 -indenyl ligand and by the alkyne. The reaction with PPh_3 is catalysed by CO and this has been attributed to the pathway involving k_1 , k_4 and k_6 being more favorable than the direct route via k_5 .

Nitrosyl ligands tend to favor associative activation. For example, $\text{Co}(\text{NO})(\text{CO})_3$ and $\text{Fe}(\text{NO})_2(\text{CO})_2$ are isoelectronic with $\text{Ni}(\text{CO})_4$ but have associative substitution mechanisms.⁶² Basolo has suggested that if the NO is formally regarded as NO^+ , then its stronger π -acceptor ability relative to CO can be rationalized and NO^+ will withdraw more electron density from the metal, favoring associative activation.

5.1.2.1 Cis-Labilizing Effect

The cis-labilizing effect has been discussed previously, and the order of cis-labilizing influence is opposite to that of the trans effect, with π -donor ligands being the most cis-labilizing. The work of Darensbourg and co-workers⁶³ indicates that oxygen-donor ligands are especially effective for the cis labilization of CO ligands, and the use of phosphine oxides and acetate ion in the synthesis of specifically labeled metal carbonyls has been especially useful. They also have demonstrated⁶⁴ the cis effect in $\text{W}(\text{CO})_5\text{F}$ and found that 1,2-substituted benzene ligands can stabilize the coordinatively unsaturated species to the extent that they can be fully characterized.⁶⁵ For the thiouracilate system, shown in Scheme 5.3, both the penta- and tetra-carbonyl derivatives can be isolated.⁶⁶ The kinetics of their interconversion in acetonitrile was determined by controlling the pressure of CO and are consistent with the dissociative mechanism shown.

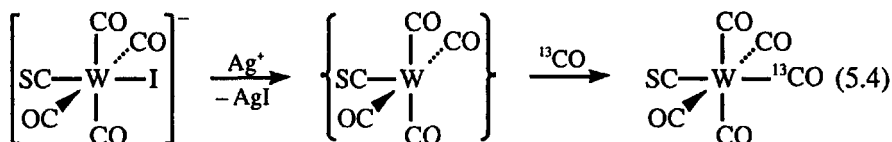
Scheme 5.3



In the corresponding uracilate system,⁶⁷ only the $\text{W}(\text{CO})_5$ derivative bonded through the N^- could be identified. The *cis*-CO exchange rate is ~ 8 times faster in the thiouracilate system, indicating that it is a better *cis* activator.

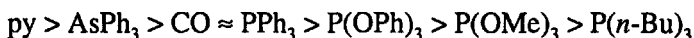
Rossi and Hoffmann⁶⁸ suggested that poor or non π acceptors prefer the equatorial site in a d^6 square pyramidal dissociative intermediate. The same conclusion was reached by Lichtenberger and Brown⁶⁹ for $\text{Mn}(\text{CO})_5\text{X}$ systems. This prediction has been used in stereoselective labeling work,

since it predicts that such heteroligands will minimize the amount of scrambling due to fluxionality in the intermediate. On the other hand, if the heteroligand is a better σ donor and π acceptor than CO, then the heteroligand should favor the axial position in the square pyramid and should minimize fluxionality. For example, this approach has been exploited⁷⁰ with CS as the heteroligand for the following synthesis:



5.1.2.2 Heteroligand Replacement

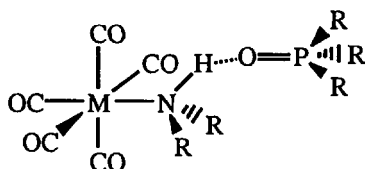
For $\text{M}(\text{CO})_5\text{L}$ systems, the kinetic order for replacement of the leaving group, L, in a first-order process is generally as follows:



High reactivity may be associated with poor π -acceptor ability, as for py and AsPh_3 , or with poor σ -donor ability, as for CO. The phosphites are considered to be better π acceptors than the phosphines, but steric effects enter as a compensating factor. This type of dichotomy pervades the interpretation of reactivity patterns for these systems.

For *cis*- $\text{Mo}(\text{CO})_4(\text{L})_2$ complexes, steric effects seem to dominate the substitution reactions. For $\text{L} = \text{PPh}_3$, the rate of L displacement by CO is ~ 200 times larger than that for $\text{L} = \text{PMePh}_2$. The ground-state structures⁷¹ show that the $\text{P}-\text{Mo}-\text{P}$ angle is distorted from 90° to 104.6° in the former and only to 92.5° in the latter. The distortion of the structure is relieved in the dissociative transition state. It should be noted that the $\text{Mo}-\text{P}$ bond lengths are very similar, 2.577 Å for PPh_3 and 2.555 Å for PMePh_2 .

The replacement of the amine by phosphines in $\text{M}(\text{CO})_5(\text{NHR}_2)$ is catalyzed by phosphine oxides. This has been ascribed⁷² to a preassociation phenomenon involving hydrogen bonding of the phosphine oxide to the amine hydrogen, thereby weakening the $\text{M}-\text{N}$ bond. With $\text{OP}(n\text{-Bu})_3$ and for $\text{M} = \text{Mo}$ and $\text{R} = \text{NHC}_5\text{H}_{10}$, the kinetics show a saturation effect with the concentration of oxide. In hexane at 34.5°C , the equilibrium constant for formation of the adduct is 600 M^{-1} and the following structure was proposed:



This is a particular case of general Lewis base catalysis of a substitution reaction. It may be troublesome for other studies because of the ease with which some phosphines are oxidized to phosphine oxides. This type of preassociation and catalysis is favored by the low-polarity solvents used in this area and may be unobserved in more polar and hydroxylic solvents.

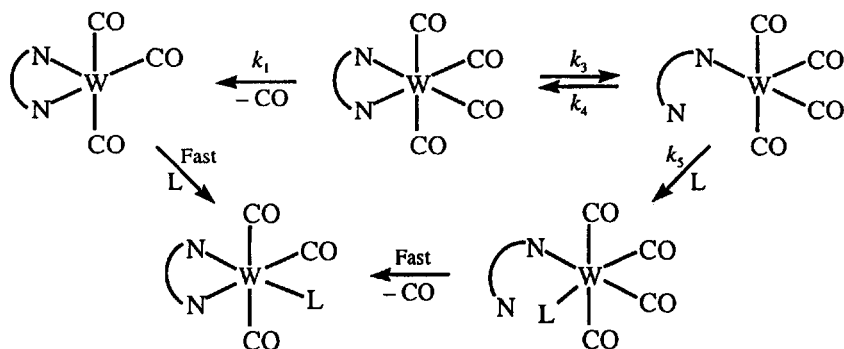
A coordinatively unsaturated species,⁷³ $W(CO)_3(PCy_3)_2$, has been found to undergo very rapid substitution,⁷⁴ with rate constants in the range of 10^3 to 10^6 $M^{-1} s^{-1}$, depending on the steric bulk of the entering group. The reactant is stabilized by an "agostic bond" to an H from a Cy ring. If these H atoms are replaced by D atoms, the rate of substitution of $P(OMe)_3$ increases by a factor of 1.15 at 25°C in toluene.

Chelate ring-opening processes also have been studied in these systems. Graham and Angelici⁷⁵ studied the reaction of $W(CO)_4(bpy)$ with phosphites and found that the pseudo-first-order rate constant is given by

$$k_{\text{exp}} = k_1 + k_2[\text{phosphite}] \quad (5.5)$$

Memering and Dobson⁷⁶ noted that the values of k_1 given by Graham and Angelici were not the same for different phosphites, and this is not consistent with a D mechanism for the k_1 path. They suggested that the reaction was proceeding through a ring-opened intermediate, as shown in Scheme 5.4, and that the apparent k_1 values are a composite of these two processes that resulted from an incomplete rate law in the original work. The A mechanism of the k_2 path is not shown in Scheme 5.4.

Scheme 5.4



The experimental rate constant predicted from Scheme 5.4 is given by

$$k_{\text{exp}} = k_1 + k_2[L] + \frac{k_2 k_5 [L]}{k_4 + k_5 [L]} \quad (5.6)$$

A detailed analysis confirmed this rate law and gave consistent k_1 values. Dobson and co-workers⁷⁷ also studied other chelates and systems in which the chelate is actually displaced. These reactions generally conform to the

preceding mechanism. The volumes of activation have been measured⁷⁸ for displacement of sulfur-bonding chelates from $\text{Cr}(\text{CO})_4(\text{S}\overline{\text{S}})$ and the values of $14 \text{ cm}^3 \text{ mol}^{-1}$ are consistent with the **D** ring-opening process.

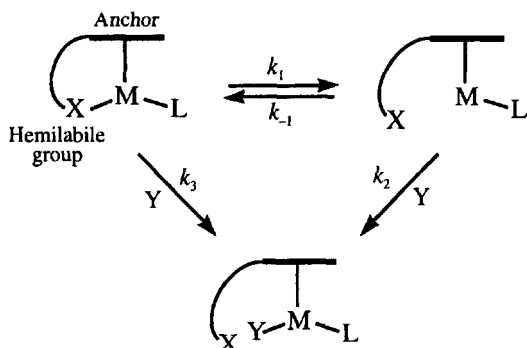
The mechanism of chelate ring closure in such systems bears directly on the ring-opening process because of microscopic reversibility. Eyring, van Eldik and co-workers⁷⁹ have studied a number of such reactions of Group 6 metal carbonyls. They examined ring-closing reactions of $\text{Mo}(\text{CO})_5(\text{phen})$ and substituted phenanthrolines and found rate constants varying from 10^4 to 10^{-2} s^{-1} . They concluded from ΔV^\ddagger values that slower reactions with bulky and less basic phenanthroline derivatives are controlled by release of CO, but the mechanism changes to **I_a** as the steric constraints are removed and the phenanthroline becomes more basic. Later studies by Grevels et al.⁸⁰ suggested that the photochemical process used to generate the monodentate reactants was not as clean as originally thought. Photolysis of $\text{M}(\text{CO})_6$ in the presence of a potential chelate L-L can generate $(\text{OC})_5\text{M}(\text{L-L})\text{M}(\text{CO})_5$ and $\text{M}(\text{CO})_4(\text{L-L})_2$ as well as the desired $\text{M}(\text{CO})_5(\text{L-L})$. Then, van Eldik and co-workers⁸¹ examined the ring closure in several $\text{Cr}(\text{CO})_5(\text{N-N})$ systems prepared by both thermal and photochemical methods. They found values of ΔV^\ddagger in the range of 12 to $18 \text{ cm}^3 \text{ mol}^{-1}$ and suggested a dissociative mechanism for the ring closing. However, the photochemically produced reactant always gave ΔV^\ddagger values at the low end of the range and substantially smaller values of ΔH^\ddagger and ΔS^\ddagger .

The kinetics of ring closing in $\text{M}(\text{CO})_5(\text{R}_2\text{P-PR}_2)$ systems ($\text{M} = \text{Cr}, \text{Mo}$) was assessed by Connor and Riley⁸² to be a largely dissociative process because it shows acceleration with increasing steric bulk of the R groups. Poë and co-workers⁸³ studied a number of systems of the general type $\text{Ru}(\text{CO})_4(\text{R}_2\text{P-PR}_2)$, where the monodentate diphosphine is in the axial position of the basic trigonal-bipyramidal structure. By comparison of the ΔS^\ddagger values to those for dissociatively activated substitution on $\text{Ru}(\text{CO})_4\text{L}$ systems,²⁵ they also concluded that bulky R groups favor an **I_a** mechanism. In other cases with smaller ΔS^\ddagger values, the authors suggested some associative character, but this does not vary much with the basicity of the diphosphine because greater donation from the coordinated end works against the greater nucleophilicity of the free end of the diphosphine. In square-planar Pt(II) systems of the general type *cis*-(Ph)₂Pt(CO)(X-X), Romeo et al.⁸⁴ have concluded that ring closing with loss of CO proceeds by an **I_a** mechanism which is typical for substitution on Pt(II) complexes.

5.1.3 Hemilabile Ligand Systems

Hemilabile ligands are multidentate ligands in which one arm is thought to be capable of easily decreasing its denticity in order to accommodate an entering substrate. There has been a great deal of interest in the synthesis of such systems and their application to catalysis.⁸⁵ Scheme 5.5 shows a generic hemilabile complex as the reactant and the reaction pathways that have been proposed for the initial substitution of the substrate Y.

Scheme 5.5



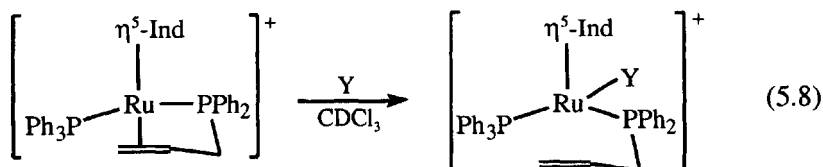
The anchor is some kinetically inert ligand to which side-chain functions can be attached. Common anchors are η^5 -indenyl or η^5 -cyclopentadienyl groups with an alkyl side-chain to the hemilabile X group. For the latter, groups such as NR_2 ,⁸⁶ OR ,⁸⁷ PR_2 and SR ⁸⁸ have been used, as well as C=C and aryl groups. It should be noted that, in addition to providing a pathway for entry of substrate, the hemilabile group may serve to protect unsaturated intermediates from side reactions in a catalytic process and may provide some activation through simpler nonreacting ligand effects.

There have been relatively few kinetic studies on such systems and they are largely confined to the initial substrate binding, as shown in Scheme 5.5. For conditions of $[\text{Y}] \gg [\text{M}]$, the predicted pseudo-first-order rate constant is given by

$$k_{\text{obsd}} = \frac{k_1[\text{Y}]}{(k_{-1}/k_2) + [\text{Y}]} + k_3[\text{Y}] \quad (5.7)$$

The first term has two limiting forms: if $k_{-1}/k_2 \ll [\text{Y}]$, then it reduces to k_1 ; if $k_{-1}/k_2 \gg [\text{Y}]$, then it becomes $(k_1/k_{-1})k_2[\text{Y}]$ which corresponds to the ring-opening step being a rapid equilibrium. In the latter case, the two terms in Eq. (5.7) have the same dependence on $[\text{Y}]$ and cannot be distinguished by the kinetics.

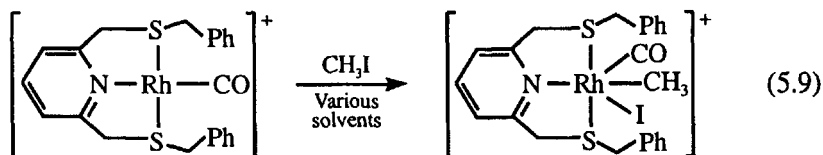
Bassetti and co-workers⁸⁹ have studied the following reaction:



For $\text{Y} = \text{CH}_3\text{CN}$, $\text{C}_6\text{H}_5\text{C}\equiv\text{CH}$ and $4\text{-ClC}_6\text{H}_4\text{C}\equiv\text{CH}$, they found a two-term rate law with one term independent of $[\text{Y}]$ and one first-order in $[\text{Y}]$. They assigned the first term to k_1 and the second one to k_3 . The magnitude of k_1

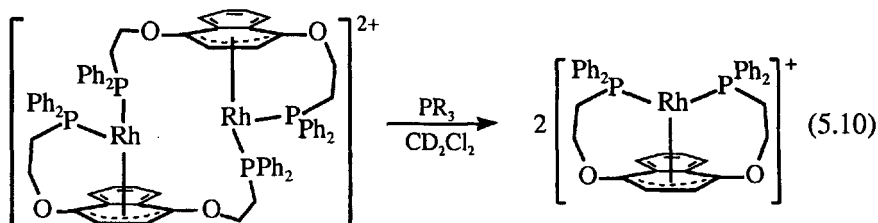
is the same, within experimental error, for all the Y. The authors argue that this pathway is not due to slippage of the η^5 -indenyl group because this process normally would be first-order in [Y]. In any case, the k_1 path is a relatively minor component for the range of [Y] studied.

The following oxidative addition with a potentially hemilabile —SPh has been studied in several solvents:⁹⁰



Such reactions normally proceed by backside nucleophilic attack of the electron-rich metal on the CH_3I . In CH_3CN , CH_2Cl_2 and $(\text{H}_3\text{C})_2\text{CO}$, a two-term rate law was found with one term independent and the other first-order in $[\text{CH}_3\text{I}]$. The first term was assigned to k_1 on the basis that its magnitude, $(0.7\text{--}1.7)\times 10^{-5} \text{ s}^{-1}$, was rather independent of the solvent. However, in CH_3OH , kinetic saturation was observed as the $[\text{CH}_3\text{I}]$ increased and this was attributed to the first term in Eq. (5.7), with $k_1 = 1.7\times 10^{-4} \text{ s}^{-1}$ and $k_{-1}/k_2 = 1.8 \text{ M}$.

A somewhat different example is the phosphine catalysed dissociation of a dimer, studied by Mirkin and co-workers⁹¹ and shown in reaction (5.10).



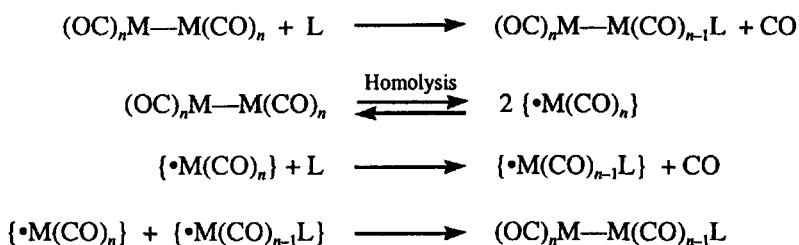
The rate is first-order in $[\text{PR}_3]$, decreases with increasing steric bulk of the phosphine and has a quite negative ΔS^\ddagger of $-158 \text{ kJ mol}^{-1} \text{ K}^{-1}$. The authors concluded that the rate-controlling step is associative attack of the phosphine accompanied by slippage of the arene ring from η^4 to η^2 to maintain a 16-electron count on the $\text{Rh}(\text{I})$. Hemilability of the PPh_2 group is not a factor.

A hemilabile phenyl group has been observed⁹² to be advantageous in catalysts of the general type $(\eta^5\text{-C}_5\text{H}_4\text{C}(\text{CH}_3)_2\text{C}_6\text{H}_5)\text{Ti}(\text{CH}_3)_2^+$ for the conversion of ethylene to 1-hexene. The only kinetic information is that the amount of product seems to have a first-order dependence on the ethylene pressure, and it was noted that methyl substituents on the phenyl group are detrimental to the activity of the catalyst. A theoretical study⁹³ suggests that the initial displacement of the phenyl group by ethylene is an important kinetic factor and that the phenyl group helps to stabilize the transition state for a β -hydride transfer step during chain growth.

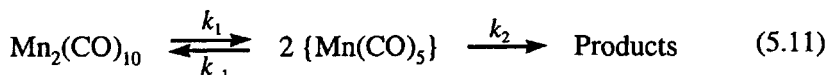
5.1.4 Metal–Metal Bonded Carbonyls and Clusters

Metal–metal bonded carbonyl systems have received considerable attention and have been the subject of some controversy. The reactions may proceed by a normal substitution reaction or by homolytic cleavage of the M—M bond, as shown in Scheme 5.6, to give radicals that then undergo rapid substitution before recombining to form the products. The homolysis is a possibility because of the weakness of the M—M bonds.

Scheme 5.6



The first study on $\text{Mn}_2(\text{CO})_{10}$ by Wawersik and Basolo⁹⁴ indicated a D mechanism for PR_3 substitution because the rate was inhibited by free CO. However, later work by Poë and co-workers⁹⁵ claimed to find no CO inhibition and the homolytic cleavage mechanism in Scheme 5.6 was proposed. It is important to note that these were primarily studies of the decomposition of $\text{Mn}_2(\text{CO})_{10}$, either in the absence or presence of O_2 and mainly in decalin, at temperatures of 115–180°C. Poë and co-workers found that the rate is half-order in $[\text{Mn}_2(\text{CO})_{10}]$ under an argon atmosphere and proposed that the reaction proceeds by homolysis of the Mn—Mn bond, as shown in the following reaction:



If the dimetal and monometal species are represented by M_2 and M , respectively, and a steady state is assumed for M , then the rate law can be developed as follows:

$$2k_1[\text{M}_2] - 2k_{-1}[\text{M}]^2 - k_2[\text{M}] = 0 \quad (5.12)$$

and

$$-\frac{d[\text{M}_2]}{dt} = k_1[\text{M}_2] - k_{-1}[\text{M}]^2 = \frac{k_2[\text{M}]}{2} \quad (5.13)$$

The first equation is a quadratic in $[\text{M}]$ can be solved for $[\text{M}]$ in terms of $[\text{M}_2]$ to give the following expression:

$$\begin{aligned}
 [\text{M}] &= \frac{k_2}{4k_{-1}} \left[-1 \pm \left(1 + \frac{16k_{-1}k_1}{(k_2)^2} [\text{M}_2] \right)^{1/2} \right] \\
 &= \frac{k_2}{4k_{-1}} [-1 + (1+a)^{1/2}]
 \end{aligned}
 \tag{5.14}$$

where a is defined by comparison of expressions in Eq. (5.14) and the positive root is chosen because $[\text{M}]$ must be positive. If the term $1 + (1+a)^{1/2}$ is multiplied and divided into Eq. (5.14), then one obtains

$$[\text{M}] = \frac{k_2}{4k_{-1}} \left(\frac{a}{1 + (1+a)^{1/2}} \right)
 \tag{5.15}$$

Substitution for $[\text{M}]$ in Eq. (5.13) gives

$$-\frac{d[\text{M}_2]}{dt} = \frac{(k_2)^2}{8k_{-1}} \left(\frac{a}{1 + (1+a)^{1/2}} \right)
 \tag{5.16}$$

If $a^{1/2} \gg 1$, which requires that $a \gg 1$, then Eq. (5.16) yields

$$-\frac{d[\text{M}_2]}{dt} = \frac{(k_2)^2}{8k_{-1}} (a)^{1/2} = \frac{k_2}{2} \left(\frac{k_1[\text{M}_2]}{k_{-1}} \right)^{1/2}
 \tag{5.17}$$

Therefore, the rate predicted by this mechanism can be half-order in $[\text{M}_2]$. It remains questionable as to whether the assumption about the magnitude of a is reasonable. More recent work⁹⁶ has shown that the recombination is nearly diffusion controlled ($k_{-1} \approx 10^9 \text{ M}^{-1} \text{ s}^{-1}$).

Later studies have questioned the observations of Poë and co-workers and especially their relevance to the mechanism for CO substitution on $\text{Mn}_2(\text{CO})_{10}$. Sonnenberger and Atwood⁹⁷ studied the reaction of PR_3 with $(\text{OC})_5\text{Mn}-\text{Re}(\text{CO})_5$ in decane and did not find any $\text{Mn}_2(\text{CO})_9(\text{PR}_3)$ or $\text{Re}_2(\text{CO})_9(\text{PR}_3)$ products. They expected the latter to form by radical recombination, but this expectation has been questioned by Poë on the basis of probable lifetimes and reactivities of the $\{\bullet\text{M}(\text{CO})_5\}$ intermediate. Atwood argued that the time dependence of the product distribution also is inconsistent with a radical mechanism, since $(\text{OC})_5\text{Mn}-\text{Re}(\text{CO})_4(\text{PR}_3)$ and $(\text{R}_3\text{P})(\text{OC})_4\text{Mn}-\text{Re}(\text{CO})_5$ increase in concentration and then decay as the disubstituted species is formed. Muetterties and co-workers⁹⁸ found that $^{185}\text{Re}_2(\text{CO})_{10}$ does not give isotopic scrambling with $^{187}\text{Re}_2(\text{CO})_{10}$ under thermal decomposition conditions, even when CO is added to suppress the decomposition. They also found that $\text{Mn}_2(^{12}\text{CO})_{10}$ and $\text{Mn}_2(^{13}\text{CO})_{10}$ show no CO scrambling in octane at 120°C over time periods in which there is substantial exchange with free CO. In addition, the half-times for CO exchange and PPh_3 substitution are 45 and 46 min, respectively, indicative of the same rate-controlling process for both reactions. The various details

of this problem are discussed in an exchange of notes between Poë⁹⁹ and Atwood.¹⁰⁰

There have been a number of studies of substitution reactions on derivatives of metal carbonyl clusters of the general form $M_m(\text{CO})_n(\text{L})_p$. These include examples of Ir_4 ,¹⁰¹ Co_4 ,¹⁰² Rh_4 ,¹⁰³ Os_3 ,¹⁰⁴ and Ru_3 .¹⁰⁵ The substitution reactions generally have the two-term rate law given by Eq. (5.1). Studies of the derivatives indicate that the dissociative pathway, k_1 , is enhanced by the number and steric bulk of the L hetero-ligand. Brodie and Poë¹⁰⁶ correlated such reactions for $\text{Ru}_3(\text{CO})_{11}\text{L}$ and $\text{Ru}_3(\text{CO})_{10}(\text{L})_2$ systems by Eq. (5.3) and found a strong correlation of $\log k_1$ with the cone angle of the spectator ligand L. Shen and Basolo¹⁰⁷ have studied activation by an anionic ligand in $\text{Os}_3(\text{CO})_{11}\text{X}^-$ systems ($\text{X} = \text{Cl}, \text{Br}, \text{I}, \text{NCO}$) and concluded that the k_1 pathway is facilitated by rearrangement to a bridging X intermediate prior to substitution.

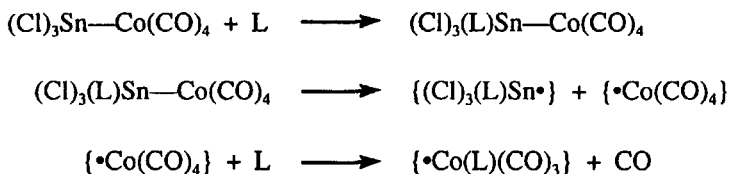
The associative pathway, k_2 , has been extensively studied and analysed for CO substitution on $\text{Os}_3(\mu_2\text{-H})_2(\text{CO})_{10}$.¹⁰⁸ The rate constant shows a steric threshold of $\sim 147^\circ$ and decreases for cone angles above this value. The ΔV^\ddagger values are negative and correlate with the cone angle function, $\tan^2(\theta/2)$, because the latter is related to the ligand volume. More recently, the reactions of $\text{Ru}_3(\text{CO})_{12}$ ¹⁰⁹ and $\text{Ru}_4(\text{CO})_{12}$ ¹¹⁰ with phosphines have been subjected to detailed QUALE analyses. Basolo and co-workers¹¹¹ have observed adduct intermediates with $\text{Ru}_3(\mu_3\text{-}\eta^2\text{-(2-PhNpy)})(\text{CO})_9^+$ which they ascribe to the opening of the μ_3 bridge to a μ_1 form. The reactivities of $\text{Ru}_6\text{C}(\text{CO})_{17}$ ¹¹² and $\text{Ru}_5\text{C}(\text{CO})_{15}$ ¹¹³ have been correlated to entering group size and nucleophilicity, and the latter system shows adduct formation for ligands with $\theta \leq 133^\circ$. Poë and co-workers have proposed that the reaction of $\text{Os}_3(\text{CO})_9(\mu\text{-C}_4\text{Ph}_4)$ with phosphines proceeds through two different cluster intermediates. For phosphines with $\theta \leq 143^\circ$, the cluster opens and forms an adduct which eliminates CO and closes to give the substitution product. When $\theta \geq 145^\circ$, a higher energy and more rigid intermediate is required to accommodate the phosphine and the adduct of this intermediate undergoes fragmentation of the cluster. These conclusions are based on the differences in products and differences in the QUALE parameters. It also was suggested that the same mechanism may apply to $\text{Ru}_5\text{C}(\text{CO})_{15}$.

5.1.5 Radical Pathways for Ligand Substitution

Although the question of radical pathways in the metal-metal bonded systems remains doubtful, there are examples of organometallic radical reactions, and they may be more prevalent than originally expected. Rates that are sensitive to O_2 and irreproducible are hints of radical pathways.

Absi-Halabi and Brown¹¹⁴ found that substitution on $\text{Cl}_3\text{Sn-CO}(\text{CO})_4$ shows properties characteristic of a radical process. The reaction is catalyzed by light and inhibited by radical traps, such as O_2 and galvinoxyl. The proposed process is given in Scheme 5.7, followed by an assortment of radical recombination reactions and electron transfers to the reactant.

Scheme 5.7



Byers and Brown¹¹⁵ observed that $\text{Re(CO)}_5\text{H}$ is inert toward phosphine substitution at 60°C in hexane in the dark under an N_2 atmosphere. However, any sort of radical initiator gave complete substitution in a few hours, and the reactive species was proposed to be $\{\cdot\text{Re(CO)}_5\}$. On the other hand, $\text{Mn(CO)}_5\text{H}$ appears to undergo normal substitution¹¹⁶ without evidence for a radical process. However, Sweany and Halpern¹¹⁷ reported that the hydrogenation of $\text{PhMeC}=\text{CH}_2$ by $\text{Mn(CO)}_5\text{H}$ proceeds by a radical pathway, on the basis of the observation of chemically induced dynamic nuclear polarization, CIDNP, in the proton NMR of the methyl styrene. The radicals initially formed by hydrogen atom abstraction by methyl styrene from $\text{Mn(CO)}_5\text{H}$ can either recombine or diffuse apart and undergo further reaction. Bullock and Samsel¹¹⁸ have suggested a similar mechanism for the reactions of several metal carbonyl hydrides with α -cyclopropylstyrene. This work also provides relative rates for H-atom abstraction and cyclopropyl ring opening by the organic radical.

The mechanism of substitution on the 17-electron radical species has been the subject of several studies. For $\{\cdot\text{Mn(CO)}_5\}$, Herrinton and Brown¹¹⁹ have shown that the substitution is a bimolecular process, with the rate constants for different entering groups given in Table 5.5. It also was concluded from this study that decomposition of $\{\cdot\text{Mn(CO)}_5\}$ by loss of CO must have a rate constant $<90 \text{ s}^{-1}$. The reactions of CO with the substituted radicals $\{\cdot\text{Mn(CO)}_3(\text{PR}_3)_2\}$ are second-order, with rate constant values of 42 and $0.32 \text{ M}^{-1} \text{ s}^{-1}$ (24°C in hexane)¹²⁰ for $\text{R} = n\text{-Bu}$ and $i\text{-Bu}$, respectively. Poř and co-workers¹²¹ studied the reactions of PPh_3 and P^nBu_3 with $\{\cdot\text{Re(CO)}_5\}$ in competition with $\text{Cl}\cdot$ abstraction from CCl_4 . The rate of phosphine substitution is first-order in the phosphine concentration, but shows minor changes with the nature of the phosphine. The authors concluded that the substitution is associative and that the insensitivity to the nature of the phosphine reflects the high reactivity of $\{\cdot\text{Re(CO)}_5\}$. The relative rates of substitution to $\text{Cl}\cdot$ abstraction is ~ 30 in C_6H_{12} .

Trogler and co-workers¹²² studied the reactions of $\{\cdot\text{Fe(CO)}_3(\text{PR}_3)_2^+\}$ radicals and found that CO substitution is a second-order process whose rate depends on the steric bulk of the entering group. The rate constants correlate with the pK_a of the pyridine nucleophiles. For pyridine reacting with $\{\cdot\text{Fe(CO)}_3(\text{PPh}_3)_2^+\}$ (25°C in CH_2Cl_2), the parameters are $k = 13.6 \text{ M}^{-1} \text{ s}^{-1}$, $\Delta H^\ddagger = 9.8 \text{ kcal mol}^{-1}$ and $\Delta S^\ddagger = -21 \text{ cal mol}^{-1} \text{ K}^{-1}$; these values are typical of the other systems.

Table 5.5. Rate Constants (24°C) for the Reaction of $\{\bullet\text{Mn}(\text{CO})_5\}$ with Various Entering Groups in Hexane

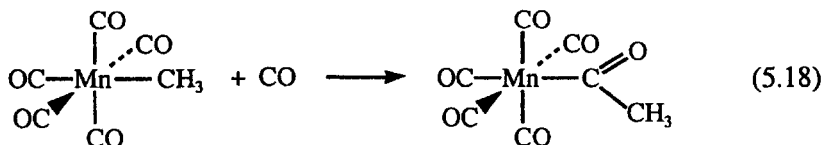
Entering Group	k ($\text{M}^{-1} \text{s}^{-1}$)
PPh_3	1.7×10^7
AsPh_3	6.5×10^4
$\text{P}(n\text{-Bu})_3$	1.0×10^9
$\text{P}(i\text{-Pr})_3$	6.7×10^7
$\text{P}(\text{O}-i\text{-Pr})_3$	3.1×10^7

Theoretical aspects of the substitution on 17-electron systems, including an analysis of the geometries of the radicals and the direction of nucleophilic attack, have been discussed by Therien and Trogler.¹²³ The prevalence of associative attack is consistent with the observations of Basolo and co-workers⁵ on various 17-electron V(0) species.

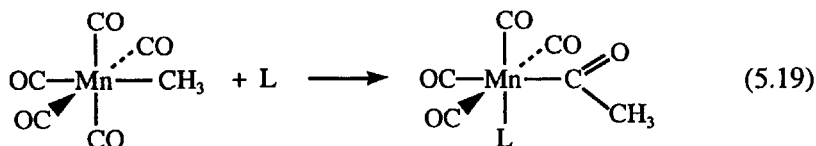
5.2 INSERTION REACTIONS

5.2.1 CO "Insertion"

The classic example of a CO insertion reaction is



The CO insertion can be an important step in carbon-carbon bond-forming reactions that are catalyzed by organometallic complexes. At first sight, this appears to be an insertion of the entering CO into the Mn-CH₃ bond and the name "insertion" has continued to be used. However, phosphines and other nucleophiles, L, bring about an analogous transformation, as shown in the following reaction:

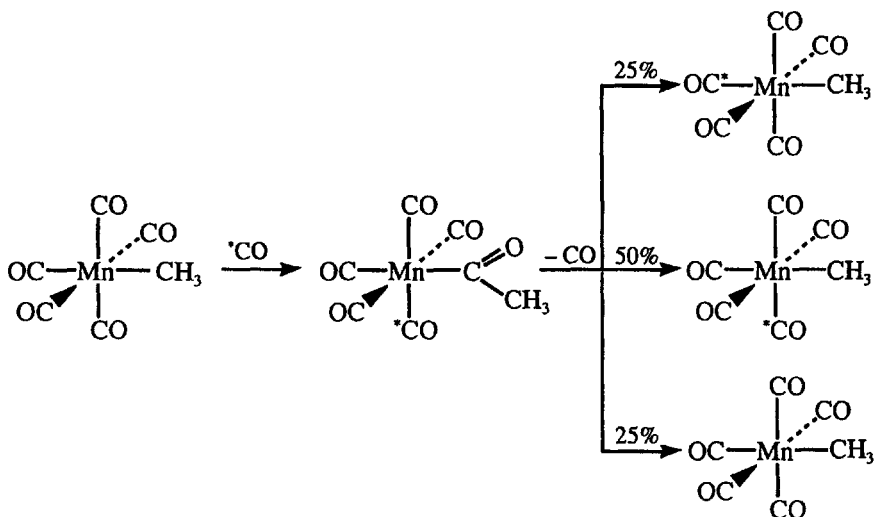


This could still be an insertion of a coordinated CO into the M-CH₃ bond, but it might also be migration of the CH₃ to a coordinated CO. The classic IR study of Noack and Calderazzo¹²⁴ using ¹³C-labeled CO showed that the

reaction is actually $-\text{CH}_3$ migration. The original work has been confirmed by the ^{13}C NMR studies of Flood et al.¹²⁵

The basis of the mechanistic conclusion for this system relies on the product distribution from the reverse reaction (decarbonylation of CO), as shown in Scheme 5.8. If the mechanism is CH_3 migration, then the products should be 25% with the labeled CO trans to CH_3 , 50% with the labeled CO cis to the CH_3 and 25% with no label, as shown in the diagram. If the reaction goes by insertion of a coordinated CO, then the products should be 75% with labeled CO in the cis position and 25% with no label. The results of both studies give a *product distribution consistent with CH_3 migration*.

Scheme 5.8

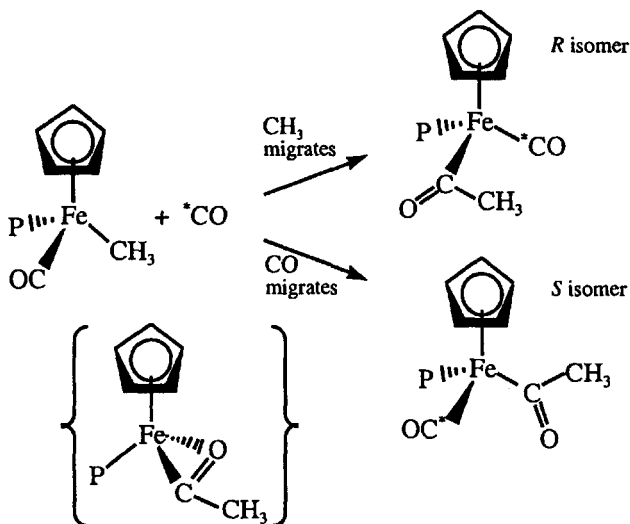


For many other metal carbonyls the mechanistic details are not known, and it is assumed that they are also proceeding by the methyl migration mechanism. The results of Wright and Baird¹²⁶ on the reaction of ^{13}CO with $\text{Fe}(\text{CO})_2(\text{PMe}_3)(\text{CH}_3)\text{I}$ are consistent with methyl migration, but the interpretation is complicated by I^- dissociation. Jablonski et al.¹²⁷ found, from the ^{13}C NMR spectrum at 203 K, that $\text{Fe}(\text{CO})_2(\text{PPh}_2\text{Me})(\text{CH}_3)\text{I}$ exists in equilibrium with the η^2 -acyl form, and the temperature dependence of its formation gave values of $\Delta H^\circ = -5.4 \text{ kJ mol}^{-1}$ and $\Delta S^\circ = -6.5 \text{ J mol}^{-1} \text{ K}^{-1}$. Saturation transfer NMR experiments at 223 K showed that the acyl carbon migrated specifically into the site cis to the CH_3 of its isomer.

The CO insertion in optically active $\text{Fe}(\eta^5\text{-C}_5\text{H}_5)(\text{CO})(\text{PR}_3)(\text{CH}_3)$ was studied by Flood and Campbell,¹²⁸ who expected the products to reflect which group migrates, as shown in Scheme 5.9. The results indicated that in nitromethane and acetonitrile the products are consistent with methyl migration, while in dimethylsulfoxide, *N,N*-dimethylformamide, propylene

carbonate and hexamethylphosphoramide, the products imply CO migration. However, the possible intervention of the η^2 -acyl intermediate, shown in curled brackets in Scheme 5.9, makes the interpretation less than definitive with regard to the migrating group.

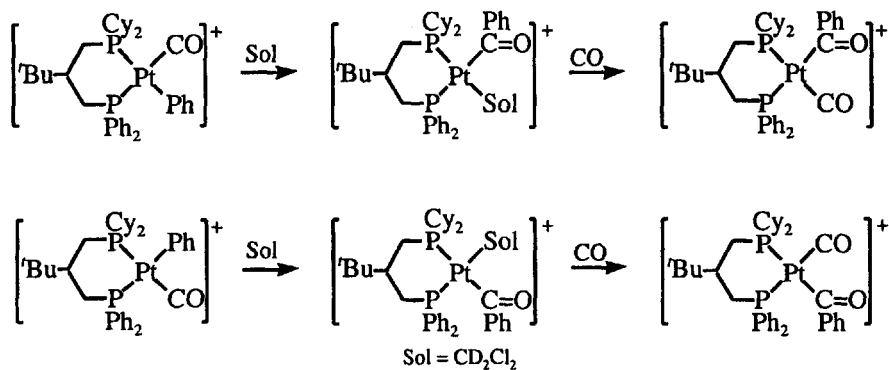
Scheme 5.9



Brunner et al.¹²⁹ have shown that methyl migration occurs in the system studied by Flood if the reaction is catalyzed by BF_3 . This catalysis is consistent with BF_3 complexing with the oxygen of CO, thereby decreasing the electron density on the C and promoting CH_3 migration.

By using an unsymmetrical phosphine chelate on Pt(II) and ^{31}P NMR, it has been shown¹³⁰ that Ph migration occurs through identification of the isomers of the insertion products, as given in Scheme 5.10.

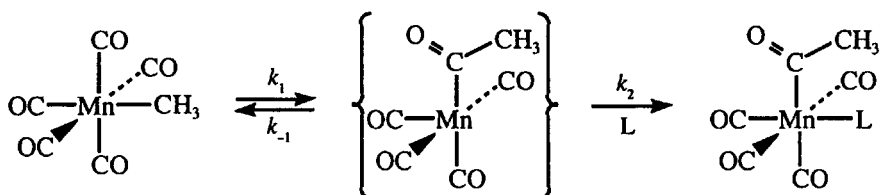
Scheme 5.10



For the analogous CH_3 derivative of Pd(II) , CH_3 migration was found. Qualitative rate observations indicated that the least stable isomer, based on the trans effect, is the most reactive in these systems.

The kinetics for these reactions with $\text{Mn(CO)}_5(\text{CH}_3)$ are consistent with a **D** mechanism through formation of an unsaturated intermediate, as shown in Scheme 5.11. The intermediate may be stabilized by coordination of the solvent, by an η^2 -acyl interaction and/or by an agostic interaction with an H of the migrating group.

Scheme 5.11



The pseudo-first-order rate constant ($[\text{L}] \gg [\text{Mn}]$) is given by

$$k_{\text{exp}} = \frac{k_1 k_2 [\text{L}]}{k_{-1} + k_2 [\text{L}]} \quad (5.20)$$

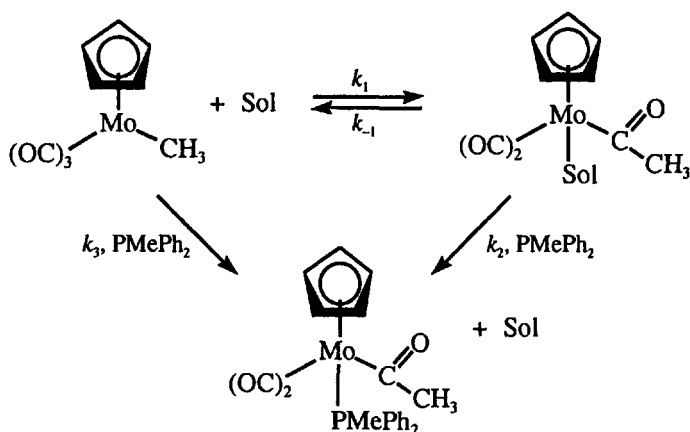
If L is CO, it is found that k_{exp} shows a direct dependence on $[\text{CO}]$. This is interpreted to mean that $k_2 [\text{CO}] \ll k_{-1}$ because of the small CO concentration imposed by the low solubility of CO in most solvents. If L is pyridine,¹³¹ then $k_{\text{exp}} = k_1$, apparently because $k_2 [\text{L}] \gg k_{-1}$.

The reaction rate shows a substantial dependence on the nature of the solvent,¹³² with faster reactions occurring in more polar solvents. The solvent effect could be due either to better solvation of the polar intermediate or to direct coordination of the solvent.

Boese and Ford¹³³ have studied the photolysis of $\text{Mn(CO)}_5(\text{C(O)CH}_3)$ to generate the intermediate shown in Scheme 5.11. They reasoned that the photochemical and thermal reaction intermediates are the same because, for $\text{L} = \text{P(OMe)}_3$ at 25°C in THF, they give the same values of k_{-1}/k_2 of $6.6 \pm 1.4 \times 10^{-3}$ and $5.5 \pm 1.5 \times 10^{-3}$ M, respectively. In C_6H_{12} , the reaction is first-order in $[\text{P(OMe)}_3]$, but this is not consistent with the condition in Eq. (5.20) that $k_2 [\text{L}] \gg k_{-1}$, because the measured values are $k_{-1} = 9 \text{ s}^{-1}$ and $k_2 = 1.4 \times 10^6 \text{ M}^{-1} \text{ s}^{-1}$. The authors suggest that there is another pathway involving direct attack of L on Mn in alkane solvents, analogous to the example discussed in the next paragraph.

For $\text{Mo(Cp)(CO)}_3(\text{CH}_3)$ ¹³⁴ reacting with PPh_3 , the rate is first-order in $[\text{PPh}_3]$ in benzene but independent of $[\text{PPh}_3]$ in tetrahydrofuran. Recently, Wax and Bergman¹³⁵ have studied this system in a series of methyl-substituted tetrahydrofuran solvents that were chosen because of their similar polarities. Their results are consistent with the following Scheme:

Scheme 5.12

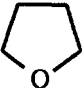
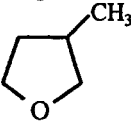
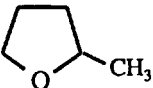
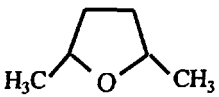


The pseudo-first-order rate constant is given by

$$k_{\text{exp}} = \frac{k_1[PMePh_2]}{\frac{k_{-1}}{k_2} + [PMePh_2]} + k_3[PMePh_2] \quad (5.21)$$

In THF and 3-MeTHF, the kinetics show saturation, and one can calculate k_{-1}/k_2 ; but in 2-MeTHF and 2,5-Me₂THF saturation is not observed, presumably because k_2 is larger in more weakly coordinating solvents, so that k_{-1}/k_2 is smaller. The kinetic results are summarized in Table 5.6.

Table 5.6. Methyl Migration Rate Constants (59.9°C) for Mo(Cp)(CO)₃(CH₃) in Various Solvents

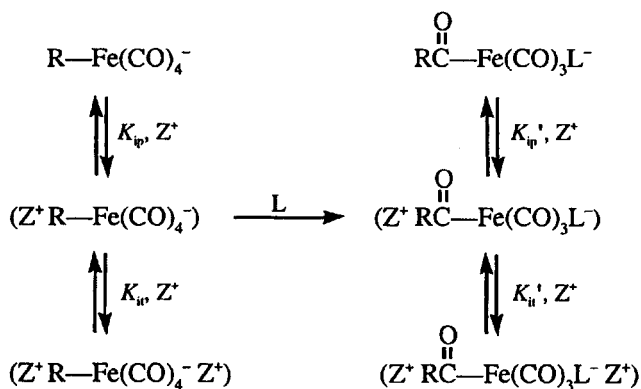
Solvent	$10^4 \times k_1$ (s ⁻¹)	k_{-1}/k_2 (M)	$10^4 \times k_3$ (M ⁻¹ s ⁻¹)
	7.78	1.04×10^{-2}	1.73
	6.46	0.82×10^{-2}	1.86
	1.48		1.95
	0.23		1.67

Studies in mixed THF and 2,5-Me₂THF also show that the k_1 path is first-order in [THF], as expected. The k_1 and k_2 steps appear to be associative because of the first-order dependence on the concentration of the entering group. This might be caused by slippage of the η^5 -C₅H₅ to an η^3 -C₅H₅ form to allow for coordination of the entering group. It may be noted that the k_1 values show the trend expected for steric inhibition of the entering group with associative activation. The k_3 values are relatively constant, as expected if the general solvent effects are not large. The earlier work of Butler et al.¹³⁴ found the rate with PPh₃ in THF to be independent of [PPh₃], which implies that k_3 and k_2 are much smaller with this phosphine. This is consistent with a steric effect of the entering group.

Photolytic dissociation of CO from $(\eta^5\text{-C}_5\text{H}_5)\text{Fe}(\text{CO})(\text{COCH}_3)$ was used by Ford and co-workers to produce the unsaturated acyl intermediate and its reactions were monitored by time-resolved infrared spectroscopy. The solvent dependence of the rates of methyl migration to Fe and capture of the intermediate by P(OCH₃)₃¹³⁶ and CO¹³⁷ suggest that the intermediate is stabilized by solvent coordination in THF and acetonitrile. In cyclohexane, the ΔH^\ddagger and ΔS^\ddagger for CO capture are 34 kJ mol⁻¹ and -28 J mol⁻¹ K⁻¹, respectively, while the corresponding values for migration of the methyl group are 44 kJ mol⁻¹ and -5 J mol⁻¹ K⁻¹. In the thermal reactions of phosphines with $(\eta^5\text{-C}_5\text{H}_5)\text{Fe}(\text{CO})_2(\text{CH}_3)$ and $(\eta^5\text{-C}_9\text{H}_7)\text{Fe}(\text{CO})_2(\text{CH}_3)$, the kinetics show a saturation effect. Bassetti and co-workers¹³⁸ suggested that this is due to a charge-transfer adduct in which the metal acts as an electron donor to the phosphine. The indenyl system gives stronger adducts and reacts ~10 times faster, but adduct formation is not attributed to slippage in either system.

Insertion reactions on R—Fe(CO)₄⁻ have been studied kinetically by Collman et al.¹³⁹ This work shows the importance of ion pairs when charged species are involved. The system can be described by Scheme 5.13, which includes ion pairs and ion triplets with the reactant and product and where Z⁺ = Na⁺, Li⁺ or (Ph₃P)₂N⁺.

Scheme 5.13

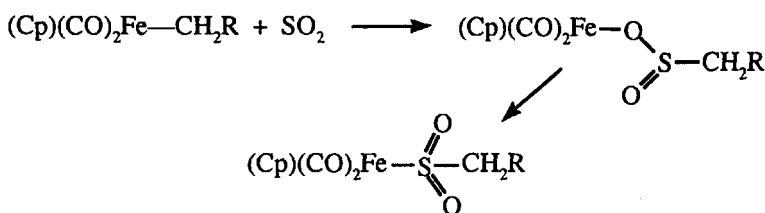


The respective values of K_{ip} , K_{ip}' , K_{it} and K_{it}' are 1.1×10^4 , 2×10^6 , 1.7×10^2 and $1 \times 10^2 \text{ M}^{-1}$, for Na^+ in THF. The rate is first-order in $[\text{L}]$ and in the reactant ion pair concentration. An increase in the solvent polarity reduces the rate, presumably because of less ion pair formation. The ion pair may be the more reactive species because of cation interaction with the CO ligands ($\text{Fe}-\text{CO} \cdots \text{Na}^+$), which will favor methyl migration.

5.2.2 Sulfur Dioxide Insertion

Sulfur dioxide insertion has been found to proceed via the O-bonded sulfinato intermediate, which rearranges to the S-bonded product,¹⁴⁰ as shown in Scheme 5.14.

Scheme 5.14

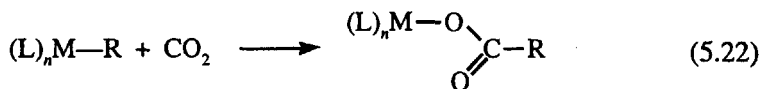


It has been observed¹⁴¹ that this reaction proceeds with inversion at the alkyl carbon bonded to Fe, and the mechanism is believed to involve electrophilic attack of SO_2 at this C followed by rearrangement to the O-bonded isomer. An analogous pathway has been found¹⁴² for SO_2 insertion into $\text{W}(\text{CO})_5(\text{Y}(\text{CH}_3)_3)^-$, where Y = Si or Sn.

Sulfur dioxide also has been found to insert into $\text{Pd}^{\text{II}}-\text{OR}$ bonds, where R is H or various alkyl groups. The isolated products are S-bonded sulfito complexes¹⁴³ or an O-bonded dimer.¹⁴⁴ The reactions are rapid under mild conditions but have not been kinetically characterized. Van Koten and co-workers¹⁴⁵ have identified an SO_2 adduct of the Pt(II) complex $\text{Pt}(\text{NCN})\text{I}$, where NCN is tridentate 2,6-(Me_2CH_2) $_2\text{C}_6\text{H}_3^-$. The SO_2 is acting as a Lewis acid in the adduct and undergoes rapid exchange with free SO_2 in $\text{C}_2\text{F}_4\text{Br}_2$ at a rate which is independent of $[\text{SO}_2]$. Although it does not undergo insertion, this adduct may represent a model for one mode of attack of SO_2 on electron-rich metal centers.

5.2.3 Carbon Dioxide Insertion

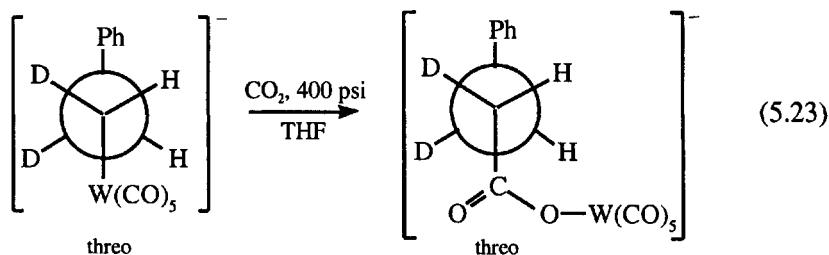
Carbon dioxide is an abundant industrial raw material,¹⁴⁶ and the carbon dioxide insertion, shown in (5.22), is a potentially important C—C bond-forming reaction.¹⁴⁷



Sakakai and Musashi¹⁴⁸ have reported a theoretical analysis of such a reaction for the $\text{Cu}(\text{PH}_3)_2\text{R} + \text{CO}_2$ system ($\text{R} = \text{H}, \text{CH}_3, \text{OH}$).

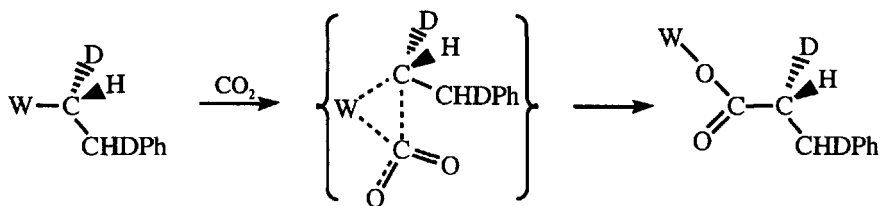
The kinetics and stereochemistry of CO_2 insertion reactions have been investigated by Darensbourg and co-workers.¹⁴⁹ The rate is increased by more electron-rich metal complexes and shows much less sensitivity to the nature of the carbon center than the CO insertions. The reactions of $\text{W}(\text{CO})_4(\text{L})\text{R}^-$ ($\text{L} = \text{CO}$, phosphine, phosphite; $\text{R} = \text{Me}, \text{Et}, \text{Ph}$) have been studied in THF. The kinetics for $\text{W}(\text{CO})_5(\text{CH}_3)^-$ show a first-order dependence on $[\text{CO}_2]$ and $[\text{W}(\text{CO})_5(\text{CH}_3)^-]$. The rate is increased by addition of Na^+ , presumably due to ion pair formation. The kinetic work used $(\text{Ph}_3\text{P})_2\text{N}^+$ as the counter ion, which should at least minimize ion pair effects because of the size and charge delocalization in this cation. For $\text{W}(\text{CO})_4(\text{P}(\text{OMe})_3)(\text{CH}_3)^-$, the activation-parameter values are $\Delta H^\ddagger = 42.7 \text{ kJ mol}^{-1}$ and $\Delta S^\ddagger = -181 \text{ J mol}^{-1} \text{ K}^{-1}$.

The stereochemistry at the carbon bonded to W was investigated using the threo-ligand isomer of $(\text{OC})_5\text{W}-\text{CHD}-\text{CHDPh}^-$ and was found to proceed with retention of stereochemistry at the α carbon, as shown by

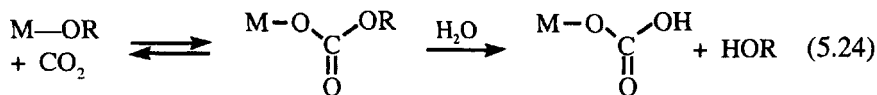


A mechanism consistent with the observations is shown in Scheme 5.15.

Scheme 5.15



Carbon dioxide also can undergo insertion into metal—heteroatom bonds. The following shows the reversible reaction with alkoxides:^{150,151}

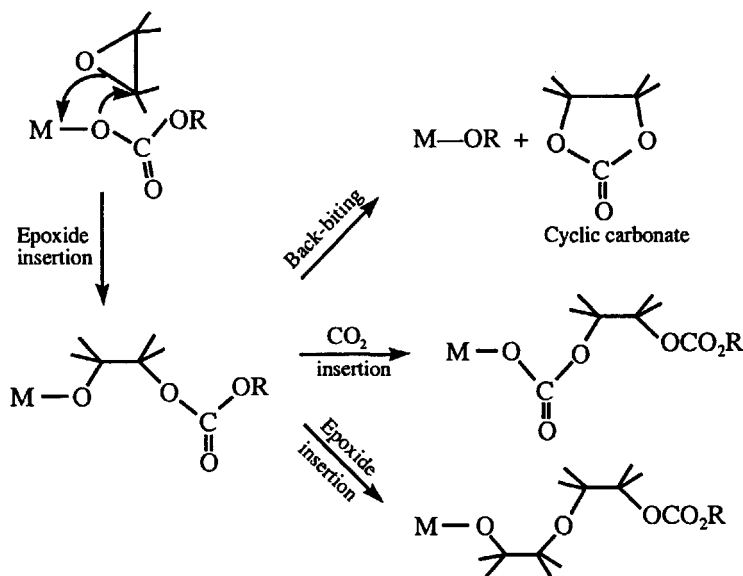


The carbonate ester product is easily hydrolyzed to the carbonate and

sometimes to further metal derivatives because of the cis-labilizing and chelating ability of the carbonate ligand. The $M-NHR$ species react to give the O-bonded amide. It is generally believed that these reactions occur by electrophilic attack of CO_2 on the atom coordinated to the metal.

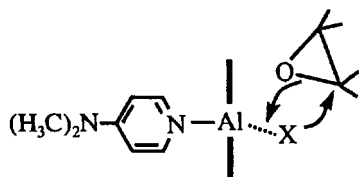
The polymerization of epoxides, such as propylene oxide and cyclohexene oxide, in the presence of CO_2 to produce polycarbonates has been an area of considerable interest and has been reviewed recently.¹⁵² A number of metal ion complexes have been found to catalyze the process. A general outline of the possible reactions is shown in Scheme 5.16, where the initial reactant is the result of CO_2 insertion into an alkoxide, as shown in reaction (5.24). This Scheme does not show the many stereochemical possibilities if the epoxide is chiral.

Scheme 5.16

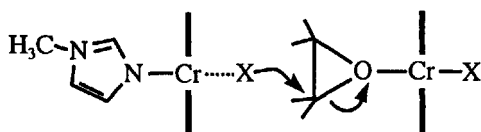


The so-called back-biting produces a cyclic carbonate which may be of interest but leads to no further polymerization. The CO_2 insertion step, followed by another epoxide insertion and so on, leads to polycarbonate. The epoxide insertion leads to an ether-linked polyoxide. Clearly, the product will depend on the relative rates of the insertions and back-biting.

Many of the metal ion complexes which catalyze these reactions have the metal coordinated to a planar N-donor ligand, such as a substituted porphyrin or salen, (N,N' -bis(salicylidene)-1,2-ethylene-diimine, and no alkoxide is initially present. These systems also require a co-catalyst which often is an imidazole or pyridine derivative. The rate of epoxide opening is found to be either first-order or second-order in the concentration of the catalyst for different systems. For a first-order system, the ring opening can be pictured as shown in the following diagram:



This example is taken from the study of Chisholm and Zhou,¹⁵³ and represents an Al(III)–tetraphenylporphyrin complex, with X = Cl⁻. The co-catalyst serves to weaken the M–X bond to facilitate the transfer of X to the epoxide in the initiation process. Jacobsen and co-workers¹⁵⁴ studied a system in which initiation is second-order in the the concentration of catalyst and suggested that the two metal centers are involved in the following activation process:

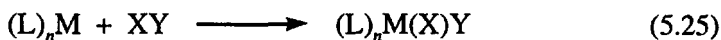


where X = N₃⁻ and the catalyst is a Cr(III)–salen complex. Darensbourg and co-workers¹⁵⁵ have explored the CO₂ dependence of the rate for such a system. A second-order dependence also can result from the catalyst being present in a dimeric form, as found in the Zn system studied by Coates and co-workers.¹⁵⁶ Ready and Jacobsen¹⁵⁷ designed binuclear Co catalysts to exploit their added reactivity and enantioselectivity.

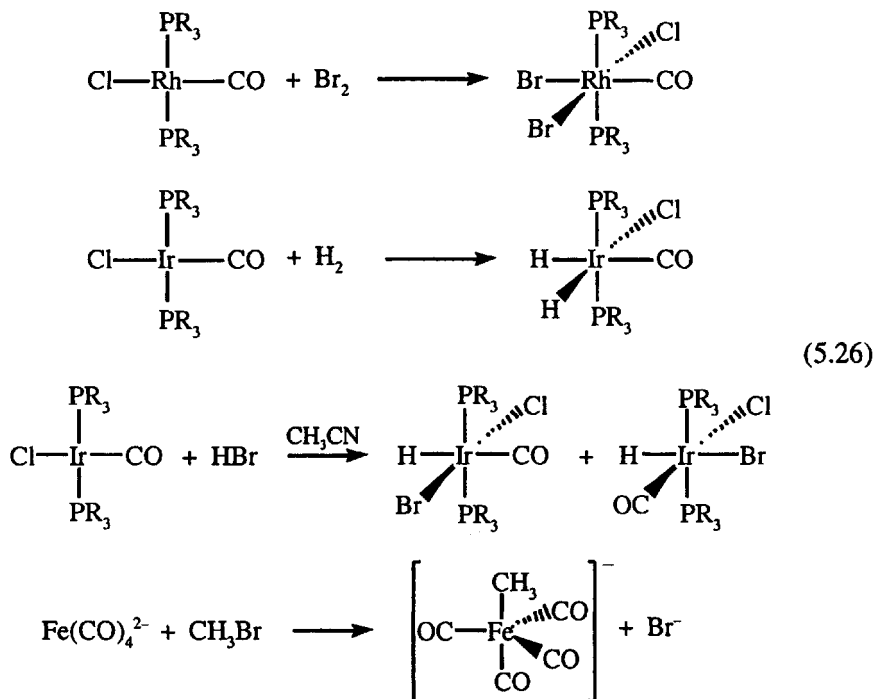
5.3 OXIDATIVE ADDITION REACTIONS

5.3.1 General Considerations and Mechanisms

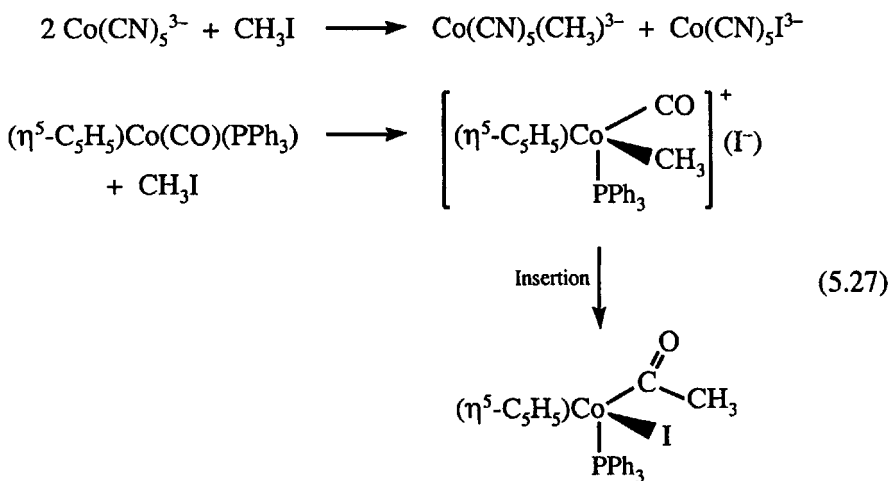
Oxidative addition reactions usually involve a coordinatively unsaturated 16-electron metal complex or a five-coordinate 18-electron species, and take the following general form:



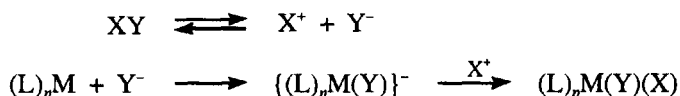
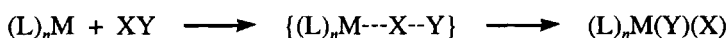
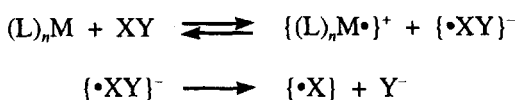
If the X and Y ligands in the product are considered to be formally –1, then the metal center has increased its formal oxidation state by +2, and this is the origin of the name *oxidative addition*. The reverse reaction is called *reductive elimination*. The various mechanisms have been reviewed by Rendina and Puddephat,¹⁵⁸ with special reference to Pt(II) systems. The following reactions are examples of various types of oxidative additions. The stereochemistry of the products can be controlled by subsequent isomerization reactions and is not always indicative of the immediate oxidative addition product.



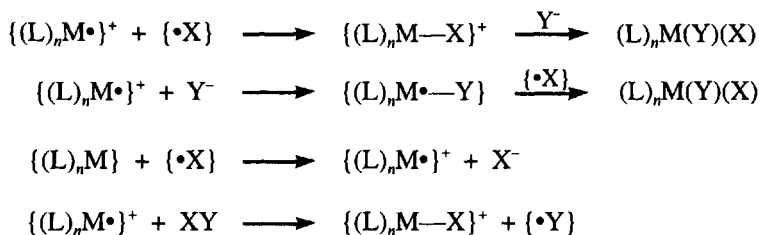
Oxidative addition reactions can also produce less obvious products, as shown in the following examples:



The rate law for these reactions is usually first-order in the metal complex and XY concentrations. The reaction mechanism depends on the nature of XY and can be broken into three generally recognized categories, as shown in Scheme 5.17.

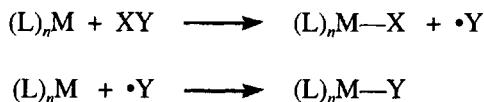
Scheme 5.17*Ionic**Nucleophilic Attack (S_N2)**Free Radical (Single Electron Transfer, SET)*

Possible Free Radical Termination



For species that are known to ionize, such as HI and HBr (and less obvious examples, such as SnCl₄ and acyl halides), the ionic mechanism is the most probable and will be especially favored in more polar solvents. The nucleophilic mechanism occurs with many organic halides and requires the availability of an unshared electron pair on the (L)_nM species. The free radical electron-transfer mechanism is an obvious candidate when XY is an oxidizing agent, such as Cl₂ and Br₂. The other possible reactions, noted in Scheme 5.17 for the radical path, take account of the fact that the concentration conditions are such as to favor reaction of the radicals with reagents rather than with other radicals, unless the latter are reasonably persistent.

A fourth alternative, not widely encountered in organometallic systems, is the atom-transfer mechanism in Scheme 5.18.

Scheme 5.18*Atom Transfer*

If $(L)_nM-X$ and $(L)_nM-Y$ are stable products, the implication is that $(L)_nM$ is an odd-electron (e.g., 17-electron) organometallic complex. This mechanism is observed for bis(dimethylglyoxime)cobalt(II) and $Co(CN)_5^{3-}$ reacting with organic halides, but only the products are true organometallic complexes.

5.3.2 Oxidative Addition of H_2

In view of the fact that the H—H bond energy is $105 \text{ kcal mol}^{-1}$, this reaction is unexpectedly facile with 16-electron complexes. There has been a great deal of interest in this reaction because of its importance in catalytic hydrogenation reactions. The values of ΔH^\ddagger and ΔS^\ddagger are typically in the range of 5 to 10 kcal mol^{-1} and -20 to $-50 \text{ cal mol}^{-1} \text{ K}^{-1}$, respectively. The reaction has always been observed to give the *cis*-dihydride product. The rate is increased by more electron-donating ligands on the metal. Some typical data are given in Table 5.7. The reaction shows a relatively modest deuterium isotope effect of ~ 1.2 , which indicates that the H—H bond is largely intact in the transition state. A theoretical analysis¹⁵⁹ of the addition of H_2 to $Ir(CO)(PH_3)_2X$ indicates that π -acceptor X ligands give more stable oxidative addition products. Crabtree and co-workers¹⁶⁰ discussed the effect of the ancillary ligands on the stereochemistry of the product for the addition of H_2 to such d^8 complexes.

The above discussion refers to what are now called classical hydrides. In 1984, Kubas and co-workers¹⁶¹ reported the first nonclassical hydride complexes containing η^2-H_2 . The first examples were $W(\overline{CO})_3(PR_3)_2(H_2)$, which have a pentagonal bipyramidal structure with an H—H bond length of 0.82 \AA compared to 0.74 \AA in gaseous H_2 . Since then, many examples have been identified with a range of H—H bond lengths. They are now qualitatively classified by the H—H distance as: nonclassical ($0.8\text{--}1.1 \text{ \AA}$);

Table 5.7. Rate Constants (30°C) and Activation Parameters for the Oxidative Addition of H_2 to $Ir(CO)(PR_3)_2X$ in Benzene

X	R	k ($M^{-1} s^{-1}$)	ΔH^\ddagger (kcal mol^{-1})	ΔS^\ddagger ($\text{cal mol}^{-1} \text{ K}^{-1}$)
Cl	Ph	0.93^a	10.8	-23
Br	Ph	14.3^a	12.0	-14
I	Ph	$>100^a$		
Cl	<i>p</i> -OCH ₃ Ph	0.66^b	6.0	-39
Cl	<i>p</i> -CH ₃ Ph	0.53^b	4.3	-45
Cl	<i>p</i> -ClPh	0.16^b	9.8	-28
Cl	<i>p</i> -FPh	0.25^b	11.6	-22

^a Halpern, J.; Chock, P. B. *J. Am. Chem. Soc.* **1966**, *88*, 3511.

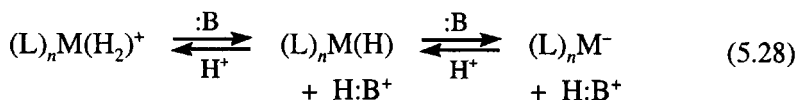
^b Ugo, R.; Pasini, A.; Fusi, A.; Cenini, S. *J. Am. Chem. Soc.* **1972**, *94*, 7364.

stretched dihydrogen (1.1–1.2 Å); compressed dihydride (1.2–1.6 Å); classical dihydride (>1.6 Å). Structural trends from neutron diffraction studies have been summarized and discussed by Bau and co-workers.¹⁶² The field has been reviewed extensively.¹⁶³ The bonding of $\eta^2\text{-H}_2$ to M in the nonclassical systems is generally attributed to donation from the σ bonding orbital of H_2 and back donation from M to the σ^* antibonding orbital of H_2 . If the latter is favored by the ancilliary ligands, then a trend towards the dihydride is favored since occupation of the σ^* orbital weakens the H—H bond. The theoretical aspects of the bonding were discussed by Saillard and Hoffmann¹⁶⁴ and by Hay¹⁶⁵ and reviewed more recently by Maseras et al.¹⁶⁶ The analysis of Frenking¹⁶⁷ and co-workers provides some insight into the relative contributions to the bonding of the donor and acceptor properties of H_2 and the effects of the same properties of other ligands in the system.

The dihydrides, $\text{M}(\text{P}(\text{OR})_3)_5(\text{H})_2$ (M = Cr, W),^{168,169} have been found to be readily fluxional and this seems to be a general property of many dihydride and hydride- $\eta^2\text{-H}_2$ systems. The nature and mechanisms of this fluxionality have been discussed in, for example, $\text{Ir}(\text{P}^i\text{Pr}_3)_2(\text{H})_2(\text{H}_2)\text{X}$,¹⁷⁰ $\text{Ir}(\text{Cp}^*)(\text{PR}_3)(\text{H})_3^+$,¹⁷¹ and $\text{Os}(\text{BH}_4)(\text{PR}_3)_2(\text{H})_3$.¹⁷² A theoretical study by Albright and co-workers¹⁷³ suggests that $\text{M}(\text{L})_4(\text{H})_2$ systems may rearrange through a dihydrogen species, which is consistent with the observations of Duckett and co-workers¹⁷⁴ on $\text{Ru}(\text{CO})_2(\text{L})_2(\text{H})_2$ systems. The $\eta^2\text{-H}_2$ ligand normally undergoes rotation with a low energy barrier of <3 kcal mol⁻¹ in d^6 systems,¹⁷⁵ but several d^2 Nb(III) and Ta(III) cationic species have barriers of ~ 10 kcal mol⁻¹. Theory indicates that the barrier is high because of the loss of back donation as the H_2 rotates.¹⁷⁶ Several $(\text{L})_n\text{M}(\text{H})(\text{H}_2)$ systems undergo rapid intramolecular exchange of the H atoms.¹⁷⁷

A few systems¹⁷⁸ form an equilibrium mixture of the dihydride and $\eta^2\text{-H}_2$ complexes and their interconversion occurs on the NMR time scale. The process may not be exceptionally fast because the formation of $\text{M}(\text{H})_2$ from $\text{M}(\text{H}_2)$ requires an additional coordination site on M and some rearrangement of the geometry of the other ligands on M. Stopped-flow¹⁷⁹ and NMR studies¹⁸⁰ have found that the dihydrogen complex formed by $\text{W}(\text{CO})_3(\text{PR}_3)_2$ converts to the dihydride with a rate constant in the range of 10 to 20 s⁻¹ at 25°C for R = cyclohexyl and isopropyl.

The hydrides and dihydrogen complexes are protic acids with widely varying acidities that depend on the metal, its oxidation state and the other ligands in the complex. The acid–base equilibria with some base, :B, and an unspecified source of H^+ are illustrated by the following system:



These and other reactions of such systems were exhaustively reviewed by

Jessop and Morris¹⁸¹ and acidity scales have been described recently by Morris and co-workers.¹⁸² It seems to be true generally that the nonclassical H₂ compounds react with an appropriate base to cleave the H₂ heterolytically to yield a metal hydride and the conjugate acid of the base. Even in (L)_nM(H)(H₂) systems, the H₂ is deprotonated in preference to the hydride ligand. Conversely, protonation of a metal hydride yields an η²-H₂ complex as the kinetic product.¹⁸³ This has allowed the preparation of metastable η²-H₂ complexes by carrying out the protonation at low temperature.¹⁸⁴ There appears to be one exception to this in that protonation of (C₅H₅)Fe(CO)(PEt₃)H yields the dihydride.¹⁸⁵ Norton and co-workers¹⁸⁶ studied the kinetics of deprotonation of a number of hydrides in H₃CCN using para-substituted anilines as the bases. The deprotonation reactions have a wide range of rate constants and show a good correlation of log *k* with log *K* for a particular hydride. It should be noted that these reactions inevitably involve ionic species and are often done in solvents of low dielectric constant, so that ion pairing and hydrogen bonding can complicate the speciation and interpretation.^{183,187}

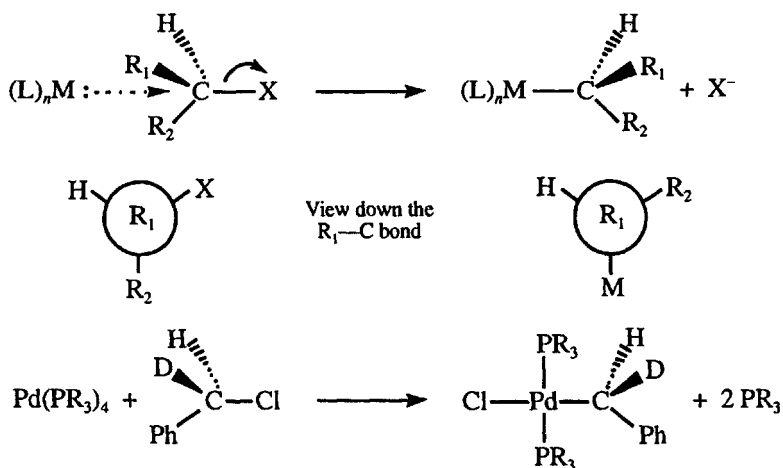
The above discussion suggests a general pathway for oxidative addition of H₂ to coordinatively saturated systems. The latter could lose a ligand to form an unsaturated intermediate which would react to form the η²-H₂ complex and then isomerize to the dihydride. The study by Hoff and co-workers¹⁷⁹ suggests that this is the mechanism for the W(CO)₃(PR₃)₂ systems first found by Kubas,¹⁶¹ but these are somewhat unusual in that the unsaturated species is strongly stabilized by an agostic interaction. The same is true for the (⁴Bu₂PhP)₂Ir(X)(H)₂ system studied by Hauger et al.¹⁸⁸ In the complex (η³-Tp)Ir(PPh₃)(C₂H₄), where Tp = a tris(pyrazolyl)borate, Oldham and Heinekey¹⁸⁹ found that the displacement of C₂H₄ by H₂ proceeds through a 16-electron η²-Tp species which binds the H₂ and then ring-closes to displace C₂H₄. The final product is a dihydride. More generally, one can infer the oxidative addition mechanism from studies of the displacement of η²-H₂ by nucleophiles. Results for such reactions have been summarized and discussed by Basallote et al.¹⁹⁰ The general picture which emerges is that the process may be dissociative loss of the η²-H₂ or dissociation of one end of a chelate to allow the nucleophile to enter, followed by the chelate-ring closing to eliminate the η²-H₂. The former mechanism was found for *trans*-(R₂P(CH₂)₂PR₂)₂Fe(H)(H₂)⁺ with R = Me or Et,¹⁹¹ but with R = Ph,¹⁹² the latter was observed.

The reaction of H₂ with Wilkinson's compound, Rh(PPh₃)₃Cl, is of special significance because of the applications of this complex as a catalyst and is discussed in Section 5.6.2.

5.3.3 Oxidative Addition of Aliphatic Halides

The available evidence indicates that oxidative addition of organic halides quite often proceeds by nucleophilic attack of the metal center on the halogen-bearing carbon, as shown in Scheme 5.19.¹⁹³

Scheme 5.19



In several examples, it has been shown that the reaction proceeds with inversion of configuration at C, as predicted by the mechanism. The general example implies that addition of X⁻ is a subsequent process and is usually too fast to be observed. The fact that these reactions are not stereoselective is consistent with this. In the example in Scheme 5.19, the alkyl group and Cl⁻ are in a trans configuration in the product. This would be difficult to rationalize if the addition were a concerted process.

The reaction rates are first-order in the concentrations of each reactant, and some kinetic data for Ir(CO)(PR₃)₂Cl are given in Table 5.8. The rate is more affected by the ligand environment than is H₂ addition, and increases with increasing polarity of the solvent. Decreasing the ligand basicity or increasing the steric bulk decreases the rate.¹⁹⁴ The order of reactivity for various halides is generally: CH₃ > CH₂CH₃ > CH(R)₂ > cyclohexyl > adamantyl.

Table 5.8. Rate Constants^a (25°C) and Activation Parameters for the Reaction of Ir(CO)(PR₃)₂Cl + CH₃I in Benzene

R	<i>k</i> (M ⁻¹ s ⁻¹)	Δ <i>H</i> [‡] (kcal mol ⁻¹)	Δ <i>S</i> [‡] (cal mol ⁻¹ K ⁻¹)
Ph	3.3×10 ⁻³	7.0	-47
EtPh ₂	1.2×10 ⁻²	9.8	-34
<i>p</i> -CH ₃ Ph	3.3×10 ⁻²	13.8	-20
<i>p</i> -FPh	1.5×10 ⁻⁴	17.0	-20
<i>p</i> -ClPh	3.7×10 ⁻⁵	14.9	-28

^a Chock, P. B.; Halpern, J. *J. Am. Chem. Soc.* **1966**, *88*, 3511; Ugo, R.; Pasini, A.; Fusi, A.; Cenini, S. *J. Am. Chem. Soc.* **1972**, *94*, 7364.

The S_N2 mechanism usually is observed with methyl, benzyl and allyl halides, and α -haloethers. But other saturated alkyl halides, vinyl and aryl halides and α -haloesters show characteristics of a radical pathway with $\text{Ir}(\text{CO})(\text{PMe}_3)_2\text{Cl}$.¹⁹⁵ For the reaction with $\text{Ir}(\text{CO})_2(\text{I})_2^-$, Maitlis and co-workers¹⁹⁶ observed normal behavior for methyl iodide, but ethyl and *n*-propyl iodides were more complex above 30°C unless the radical scavenger duroquinone was added. Direct EPR evidence has been obtained for radicals in the reaction of $(\eta^5\text{-C}_5\text{H}_5)_2\text{Zr}(\text{PMePh}_2)$ with butyl chlorides.¹⁹⁷ The reaction of a Au(I) dimer, $(\text{Au}(\text{CH}_2)_2\text{PPh}_2)_2$, has been suggested¹⁹⁸ to proceed by a single electron transfer, SET, mechanism, based on the parallel between the rates and the reducibility of the organic halide. The reaction of alkyl halides with $\text{Pt}(\text{PPh}_3)_2$ is proposed to proceed by a halogen atom abstraction mechanism.¹⁹⁹

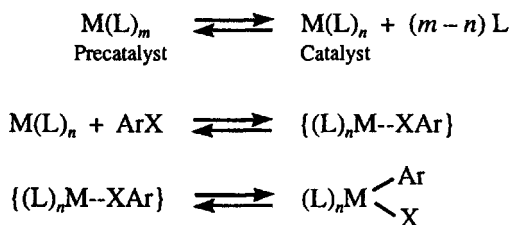
There have been suggestions that an alternative concerted mechanism in which the C—X bond of the halide is oriented side-on to the metal might operate in some instances. This mechanism was found to be the more favorable in a theoretical study by Kinnunen and Laasonen²⁰⁰ for oxidative addition to $\text{Rh}(\text{CO})_2(\text{PX}_3)_2^+$ systems. The same authors found that the S_N2 mechanism was favored for the reaction with $\text{Rh}(\text{CO})_2(\text{I})_2^-$.²⁰¹ They concluded that the poorer nucleophilicity of the cation caused the change in mechanism. There have been several studies of the solvent dependence of the oxidative addition of CH_3I to various d^8 systems which might differentiate the side-on and S_N2 mechanisms if one assumes that the latter has a more polar transition state. However, the rate constant typically increases only about 10-fold as the solvent is changed from benzene to nitromethane, for example. In an early study, Jawad and Puddephatt²⁰² found a correlation of the rate constant with Reichardt's solvent polarity parameter, E_T , for a Pt(II) system. Van Eldik and co-workers²⁰³ suggested a side-on transition state based on the small dependence of ΔV^\ddagger on the dielectric constant of the solvent for the reaction with $\text{Rh}(\text{LL}')(\text{CO})(\text{PPh}_3)$, where $\text{LL}' = \text{H}_3\text{C}(\text{S})\text{CHC}(\text{O})\text{CH}_3^-$. Recently, Theron et al.²⁰⁴ have reported a correlation of ΔV^\ddagger with the pressure dependence of the dielectric constant of the solvent for the reaction of an Ir(I) complex and concluded that there was no change in mechanism of this system for the range of solvents studied by van Eldik and co-workers. The insensitivity of the rate constant to solvent changes and the activation parameters from the latter two studies suggest that there is some compensation between ΔH^\ddagger and ΔS^\ddagger . This might be due to a trend from an early to a late S_N2 transition state as the polarity and solvating properties of the solvent change.

5.3.4 Oxidative Addition of Aromatic Halides

The oxidative addition of aromatic halides, ArX , has received a great deal of attention because it is an important step in various synthetic reactions involving aryl group transfer to another reagent. The catalysts are typically phosphine complexes of d^{10} Pd(0) and a key step is believed to be oxidative

addition of ArX to the catalyst. The initial reactant or precatalyst can be either a tetrahedral $M(L)_4$ or a linear $M(L)_2$ species. In the synthetic work, a Pd(II) salt is often used for convenience and it is assumed that some component of the system, possibly the phosphine, reduces the Pd(II) to Pd(0). A very generic mechanism for the oxidative addition is outlined in Scheme 5.20.

Scheme 5.20



The mechanism starts with some Pd(0) precatalyst which loses some phosphine ligand(s) to form the active catalyst. As a reference point for future discussion, the next step is shown to produce an intermediate for the oxidative addition, but this may be a concerted process leading to the final product. For generality, the reactions are shown to be reversible, but this is a condition that depends on the particular system.

In most cases, the catalyst is a bis-phosphine complex with either two monodentate or one bidentate phosphine ligand. An exception is the Pd(P(*o*-tolyl)₃)₂ system, in which the rate of oxidative addition is inverse-first-order in the phosphine concentration, indicating that Pd(P(*o*-tolyl)₃) is the catalyst. Hartwig and Paul²⁰⁵ suggested that the steric bulk of the phosphine makes the bis-complex less reactive. Jutand and co-workers²⁰⁶ found the same rate law with L = P(Cy)(^tBu)₂ and P(^tBu)₃ and identified the product as (Ph)(L)Pd(μ-X)₂Pd(L)(Ph) with one L per Pd. For the bidentate systems, the rate of dissociation of the bidentate ligand from the Pd(P∩P)₂ precatalyst can be rate determining. Under such circumstances, the rate is expected to be independent of [ArX] and inversely dependent on [P∩P]. Blackmond and Buchwald and co-workers²⁰⁷ have shown that the kinetics can be more complicated in such cases, especially when the oxidative-addition product is coupled to some other substrate in a subsequent process. The rate of this process may appear to increase with time as more of the active catalyst is produced. Even for simple oxidative addition, some catalyst may form during the time required to bring the system to the reaction temperature. At low [PhX], the oxidative addition may be competitive with catalyst formation and produce more complex kinetic behavior. For PhI and PhBr, Alcazar-Roman and Hartwig²⁰⁸ observed a pathway first-order in [PhX] for concentrations >1 M. They attribute this to direct coordination of PhX to a Pd(P∩P)₂ species in which one end of the chelate has dissociated. Although this might be some

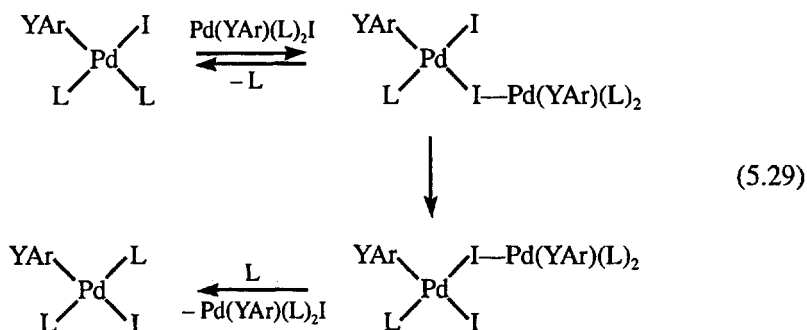
general solvent effect, the authors note that it does not appear when $X = \text{triflate}$. It should be noted that the $\text{Pd}(\text{P}\curvearrowright\text{P})$ systems cannot adopt the linear geometry preferred by monodentate $\text{Pd}(\text{P})_2$ complexes. The theoretical analysis by Senn and Ziegler²⁰⁹ of several $\text{Pd}(\text{P}\curvearrowright\text{P})_2$ systems indicates that chelate dissociation to form $\text{Pd}(\text{P}\curvearrowright\text{P})$ is always rate-limiting, but they did not consider a monodentate chelate in their analysis.

The oxidative addition step in Scheme 5.20 is generally viewed as being concerted; the kinetics only give the composition but not the structure of any intermediates or the transition state shown in braces. Several theoretical analyses of this step have some common features but also some differences which leave room for further study. Thiel and co-workers²¹⁰ analysed the $(\text{Me}_3\text{P})_2\text{Pd}(\text{O}_2\text{CCH}_3)^-$ system and found an initially formed $\text{Pd}\rightarrow\text{IPh}$ adduct in which the PhI acts as an electron acceptor from the $\text{Pd}(0)$ anion and the phosphine ligands have a trans orientation. This adduct goes through a series of reorientations involving $\eta^2\text{-PhI}$ species to produce either *cis*- $(\text{Me}_3\text{P})_2\text{Pd}(\text{Ph})(\text{O}_2\text{CCH}_3)$ or *cis*- $(\text{Me}_3\text{P})_2\text{Pd}(\text{PhI})$. Thiel notes that formation of the adduct is consistent with earlier observations of Jutand and co-workers.²¹¹ An analogous adduct was found with PhBr and when acetate was replaced by chloride ion. The study of Senn and Ziegler²⁰⁹ involved bidentate phosphines with no anions added. They found initial formation of a three-coordinate $(\text{P}\curvearrowright\text{P})\text{Pd}(\eta^2\text{-PhX})$ species which rearranged to the final product. Shaik and co-workers²¹² simplified the model by using monodentate and chelate PH_n ligands, and also added chloride ion to examine the differences between neutral and anionic $\text{Pd}(0)$ species. For both the neutral and anionic $\text{Pd}(0)$ complexes, the reaction proceeds through a series of $\eta^2\text{-PhI}$ species analogous to those found by Senn and Ziegler.

The interest in anionic $\text{Pd}(0)$ complexes stems from the observation that the addition of anions often increases the rate of oxidative addition. One standard synthetic recipe starts with reduction of $\text{Pd}(\text{II})$ acetate with PPh_3 . It is known²¹¹ that acetate forms $(\text{Ph}_3\text{P})_2\text{Pd}(\text{O}_2\text{CCH}_3)^-$ which is the active reactant in the subsequent oxidative addition. Chloride and bromide ions can have a similar effect and the reactivity of the anionic complexes is attributed to their greater nucleophilicity. Roy and Hartwig²¹³ explored the effect of such additives with $\text{Pd}(\text{P}(o\text{-tolyl})_3)_2$ and a bidentate phosphine, both of which are sterically crowded. They found that the linear species $\text{XPd}(\text{P}(o\text{-tolyl})_3)^-$ is more reactive than $\text{Pd}(\text{P}(o\text{-tolyl})_3)_2$, but the Y-shaped $\text{XPd}(\text{P}\curvearrowright\text{P})^-$ is less reactive than $\text{Pd}(\text{P}\curvearrowright\text{P})$. Oxidative addition to the latter is accelerated by addition of NBu_4PF_6 and $\text{N}(\text{octyl})\text{Br}$, but this was ascribed to an ionic medium effect since PF_6^- is considered to have a low affinity for coordination to $\text{Pd}(0)$. Possibly, the $(\text{Ph}_3\text{P})_2\text{PdX}^-$ systems are reactive because of less steric crowding and/or more geometrical flexibility than the chelate.

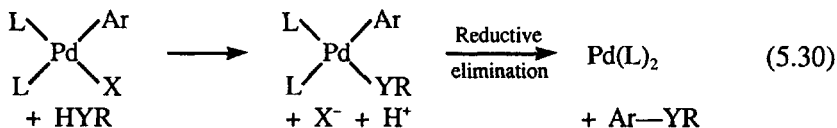
The *cis*-isomer is the desired product for aryl-transfer applications and the product predicted by theory. However, the *trans*-isomer is by far the

most commonly isolated product, and is expected to be the more stable because of the strong trans effect of the Ar⁻ ligand. It is generally assumed that cis to trans isomerization is fast enough to explain the isolated product. Casado and Espinet²¹⁴ studied the isomerization of the oxidative addition product, *cis*-Pd(YAr)(PPh₃)₂I, where YAr = 3,5-dichlorofluorophenyl. In THF, they found, in addition to pathways normal for isomerization in square-planar complexes, two pathways that were catalysed by both the reactant and the product. Their proposal for the pathway that is inhibited by PPh₃ is shown in the following reaction, where L = PPh₃:



The authors were able to determine that the rate constant for the second step is 1.4×10^{-5} times smaller than that for reaction with PPh₃ to form the reactant. There is a parallel pathway in which the initial dinuclear species is formed from a solvento complex. Furthermore, there is another pathway that is catalysed by the reactant but is not inhibited by PPh₃. This pathway was assigned to associative formation of a dinuclear complex, without loss of PPh₃, followed by intramolecular rearrangement to yield the product.

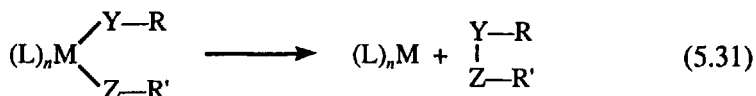
The products of the oxidative addition of aryl halides have an important use in coupling reactions, as shown in the following general reaction, where HYR may be an amine, alcohol or thiol and a strong base is added to remove the protons:



Clearly, the *cis*-isomer is needed for the coupling to occur in a concerted fashion. The inorganic product of the final reductive elimination step is the initial Pd(0) complex so that the overall process is catalytic in Pd(0). The kinetics of product formation can be complicated because of the multiple potential rate-controlling steps.²⁰⁷ In addition, the nature of the catalyst may change due to complexation by X⁻ as the reaction proceeds, and the strong base may complex with Pd(0) or Pd(II)²¹⁵ to further complicate matters.

5.4 REDUCTIVE ELIMINATION REACTIONS

This process is the reverse of oxidative addition and results when two ligands couple and are eliminated from the metal center with a decrease of two units in the formal oxidation state of the metal. A general example is shown in the following reaction:



The initially coordinated atoms, Y and Z, may be of the same or different type. The reaction is often a late stage in a catalytic process to produce the coupled product, as in the aryl coupling described in the previous section.

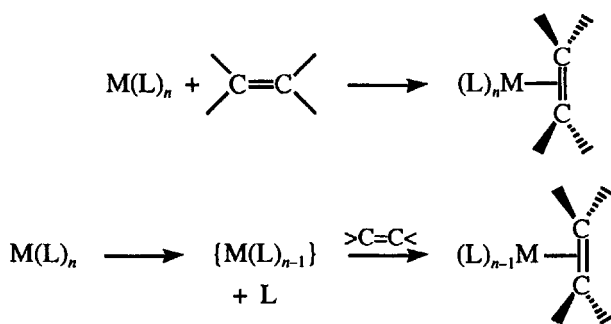
The rate of the reaction increases with the electron donating power and steric bulk of the spectator ligands, L. If the latter are chelates, then reaction is favored by chelates with a larger bite angle. Reductive elimination is more favorable for 4*d* than for 5*d* metals, other factors being equal; thus Pd(II) is more reactive than Pt(II) and reductive elimination is not rate-limiting in the systems described in the previous section.

The influence of groups to be coupled has been discussed recently from a theoretical standpoint by Morokuma and co-workers,²¹⁶ and van Leeuwen and co-workers.²¹⁷ Shekar and Hartwig²¹⁸ have examined the effect of substituents in several systems. For two para-substituted phenyl groups on a Pt(II) complex, the coupling is faster with electron-donating substituents, but even better if one group has electron-donating and the other electron-withdrawing substituents. For the coupling of *p*-C₆H₄CF₃ to substituted amines on a Pd(II) complex, electron-donating groups on the amine gave faster elimination.²¹⁹ For coupling of aryl groups to thiolates in Pd(II) systems, elimination was favored by electron-deficient aryl groups and electron-rich thiolates.²²⁰ These observations by Hartwig and co-workers suggest that the amine and thiolate can be viewed as nucleophiles attacking the aryl group during the coupling reaction.

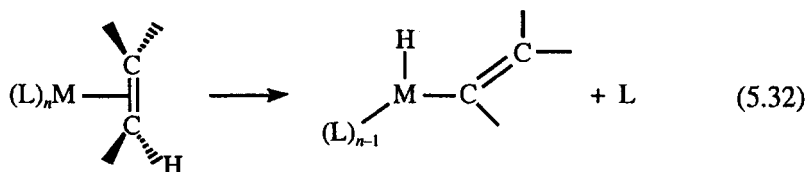
5.5 REACTIONS OF ALKENES

Alkenes and alkynes are capable of normal substitution reactions like other nucleophiles, but this is rarely an associative process with 18-electron systems because alkenes and alkynes are poor nucleophiles. Such systems require prior dissociation of a ligand to allow coordination of the alkene, which can then form strong complexes because of the π back bonding from the metal to the π^* orbital of the C—C multiple bond. The bonding π electrons have relatively low nucleophilicity. However, in coordinatively unsaturated systems, prior dissociation is not a problem. The expected initial reactions are shown in Scheme 5.21.

Scheme 5.21

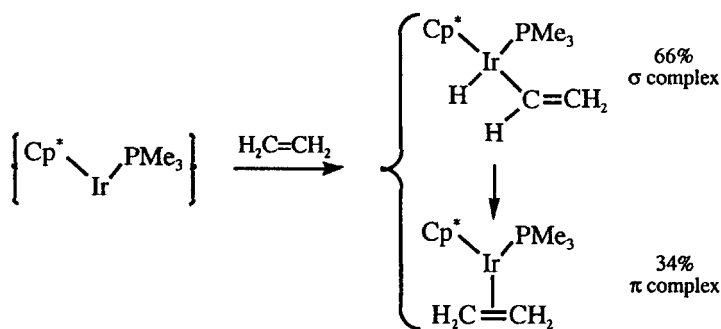


These reactions may be followed by rearrangement with H-atom migration to a σ -bonded form:



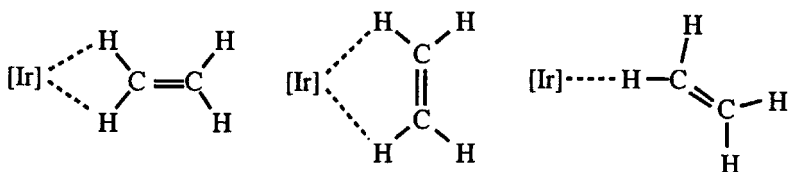
The latter process would seem to be a straightforward rearrangement subsequent to π -complex formation, but the work of Stoutland and Bergman²²¹ indicates that the process is more complex. The thermolysis of $(\eta^5\text{-C}_5\text{Me}_5)\text{Ir}(\text{PMe}_3)(\text{C}_6\text{H}_{11})\text{H}$ yields C_6H_{12} and the unsaturated reactive species $(\eta^5\text{-C}_5\text{Me}_5)\text{Ir}(\text{PMe}_3)$, which reacts with ethylene to give the kinetic products shown in Scheme 5.22.

Scheme 5.22



The σ complex will isomerize to the thermodynamically more stable π complex ($\Delta H^* = 34.6 \text{ kcal mol}^{-1}$, $\Delta S^* = 2.6 \text{ cal mol}^{-1} \text{ K}^{-1}$), but the latter is the minor kinetic product. The implication is that the two products are forming directly from two slightly different transition states. Stoutland and

Bergman suggested the possible transition states which involve initial bonding between the metal and hydrogen substituents on the ethylene, as shown by the following structures:



A perplexing feature of the observations is that the same product ratio is obtained from $\text{H}_2\text{C}=\text{CD}_2$ and *cis*-(HD) $\text{C}=\text{C}(\text{HD})$. It was expected that an isotope effect acting on the proposed transition states would cause a change in product distribution for the deuterated reactants.

A combination of calorimetric measurements and bond energy estimates leads to the reaction coordinate diagram in Figure 5.1. This diagram is different from the normal one in that the reaction starts at the high-energy intermediate; this will then react to give the two products in amounts that depend on the relative heights of the energy barriers to the left and right. It should be noted that the difference in energy barriers must be less than 1 kcal mol^{-1} in order to explain the approximately 2:1 product distribution. The difference is exaggerated in Figure 5.1, in order to show that the barrier leading to the π complex must be higher to account for the product distribution.

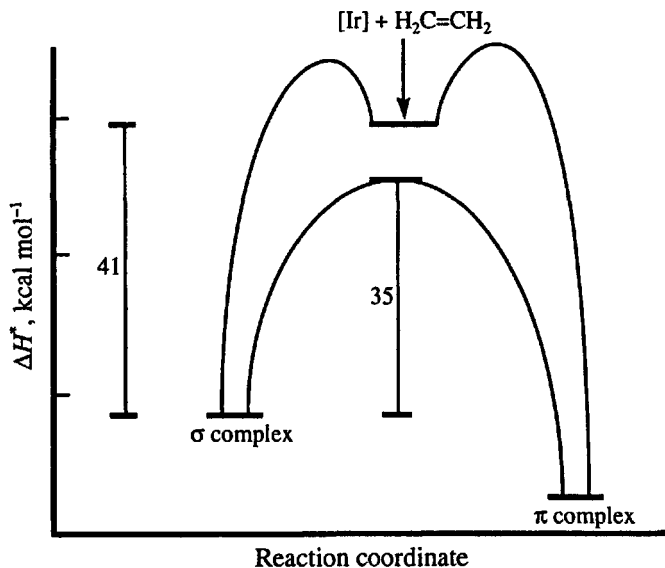
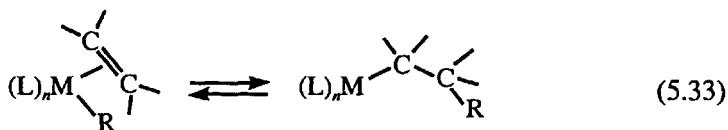


Figure 5.1. Reaction coordinate diagram for the addition of ethylene to coordinatively unsaturated iridium.

Baker and Field²²² have observed rather similar behavior with $\text{Fe}(\text{P}_2(\text{CH}_2)_2(\text{R})_4)_2(\text{H})_2$, for which photolysis in the presence of ethylene gives mainly the cis σ complex. The cis σ complex isomerizes to trans and eventually yields the more stable π complex. Graham and co-workers²²³ have observed that the trifluoromethylpyrazolylborate, HBPF_3 , π complex of iridium, $\text{Ir}(\eta^2\text{-HBPF}_3)(\text{CO})(\eta^2\text{-C}_2\text{H}_4)$, converts to the more stable σ complex, $\text{Ir}(\eta^2\text{-HBPF}_3)(\text{CO})(\text{H})(\text{-C}_2\text{H}_3)$, at 100°C. However, the σ complex of rhodium isomerizes to the more stable π complex at 25°C. Clearly, there is a delicate balance between the stabilities of these species.

Grant and co-workers²²⁴ studied the dissociation of ethylene from $\text{Cr}(\text{CO})_5(\text{C}_2\text{H}_4)$ in the gas phase in the presence of CO and C_2H_4 . The rate of formation of $\text{Cr}(\text{CO})_6$ has the usual dissociative rate law, with a competition ratio of 1.1/1 for $\text{C}_2\text{H}_4/\text{CO}$. The activation parameters for the dissociation are $\Delta H^\ddagger = 24 \text{ kcal mol}^{-1}$ and $\Delta S^\ddagger = 15 \text{ cal mol}^{-1} \text{ K}^{-1}$. The ΔH^\ddagger indicates the magnitude of the $\text{Cr}-(\text{C}_2\text{H}_4)$ bond energy.

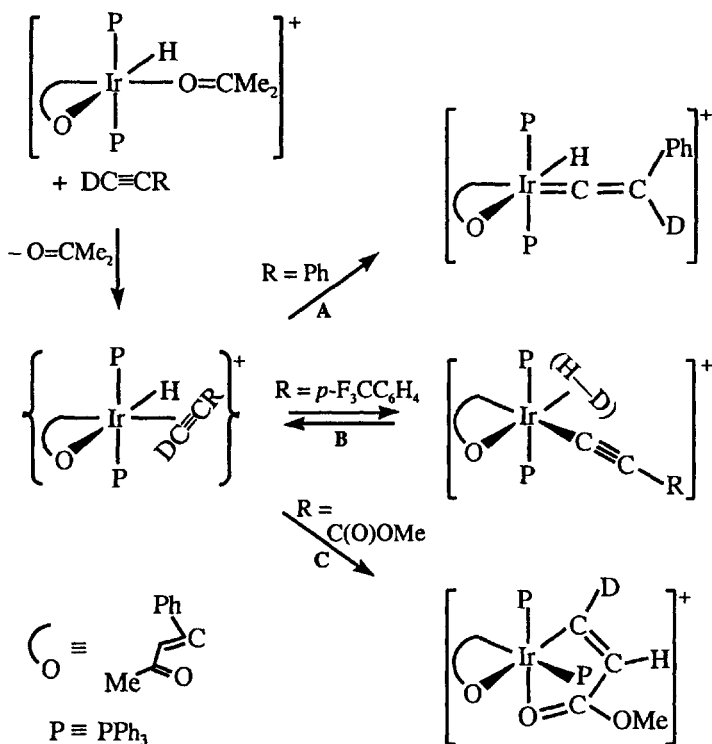
In complexes with an η^2 -alkene and H or alkyl ligands, the following migratory-insertion reaction can occur:



When $\text{R} = \text{H}$, the reverse reaction is called β -hydride elimination. The insertion produces an unsaturated metal which can be stabilized by agostic interactions with H substituents on the alkyl group. Casey et al.²²⁵ have discussed the factors affecting the relative strengths of these interactions with various substituents along the alkyl chain. Wadepohl et al.²²⁶ recently summarized earlier kinetic results on the migratory insertions with $\text{R} = \text{H}$ or CH_3 , and studied the kinetics for $((\text{H}_3\text{C})_3\text{P})_3\text{Co}(\text{H})(\text{C}_2\text{H}_4)$. The authors concluded that this electron-rich system has very little agostic interaction and that a more electropositive metal center will give a lower energy barrier for migration because of agostic assistance. The migratory insertion reaction is a key step in olefin polymerization. The product in reaction (5.33) is coordinatively unsaturated and can react with another olefin molecule and then undergo migratory insertion to begin the polymerization process. There is a great deal of interest in these processes and the work is summarized in the theoretical papers of Ziegler and co-workers²²⁷ and Morokuma and co-workers.²²⁸

The reaction of an alkyne, $\text{HC}\equiv\text{CR}$, with a metal hydride can proceed in several ways. It may proceed by insertion into the $\text{M}-\text{H}$ bond to form $\text{M}-\text{CH}=\text{CHR}$, or transfer of an H to the hydride to give $(\text{H}_2)\text{M}-\text{C}\equiv\text{CR}$ or formation of a vinylidene hydride, $(\text{H})\text{M}=\text{C}=\text{CHR}$. A study by Crabtree and co-workers²²⁹ shows the variation with the substituent R for the reaction of one metal hydride with different alkynes, as shown in the following Scheme:

Scheme 5.23



In all cases, the initial η^2 -alkyne shown in Scheme 5.23 was not seen and the pathways were deduced from deuterium labelling. In paths A and B, the final products are η^2 -butadienyl derivatives that result from addition of a second alkyne and a second migratory insertion. In path A, the D atom undergoes a 1,2-shift, and this was explained by formation of the vinylidene species shown. In path B, the electron-withdrawing group on the alkyne, causes the D and H atoms to be scrambled, and this can be rationalized by the reversible oxidative addition and rapid rotation of the η^2 -(HD). In path C, with a polar group on the alkyne, the product is the one expected for direct insertion into the Ir—H bond; the authors suggested a rearrangement process that leads to the rather unusual cis orientation of the phosphines in the product. Strangely, the *o*-F₃C derivative went by path A rather than B.

Becker and Bergman²³⁰ studied the following unusual reaction:

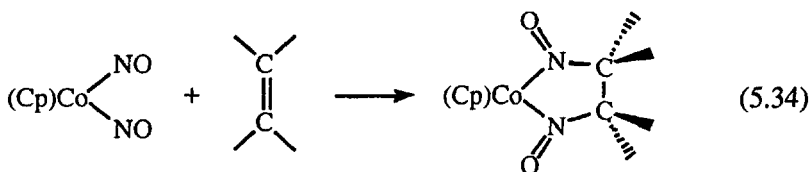


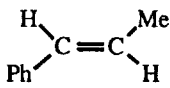
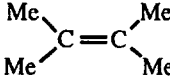


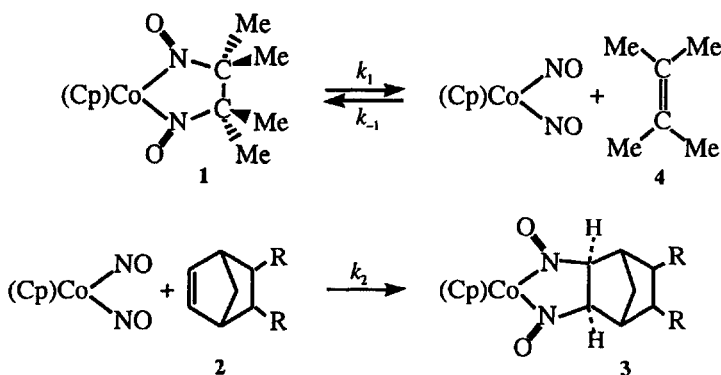
Table 5.9. Rate Constants (20°C) for the Reaction of Olefins with $\text{Co}(\text{Cp})(\text{NO})_2$ in Cyclohexane

Olefin	k_2 ($\text{M}^{-1} \text{s}^{-1}$)
	130
	3.9
	0.84
	0.25

The direct reaction is first-order in the concentrations of the metal complex and the olefin and the second-order rate constant depends on the nature of olefin, as indicated by some of the data in Table 5.9. Strain in the olefin appears to increase its reactivity, as shown for norbornene and cyclopentene. There may be some steric effects of olefin substituents, but these effects may be attenuated by better electron donation from the substituents. It was found also that the reaction rate with 2,3-dimethyl-2-butene was insensitive to the polarity of the solvent, with relative values of 1:0.6:0.8 in cyclohexane, THF and methanol, respectively. This seems to rule out an ionic or polar transition state or intermediate, and the authors favor a concerted cycloaddition mechanism.

The exchange of one olefin adduct with another has reaction kinetics that are consistent with the pathway shown in Scheme 5.24.

Scheme 5.24



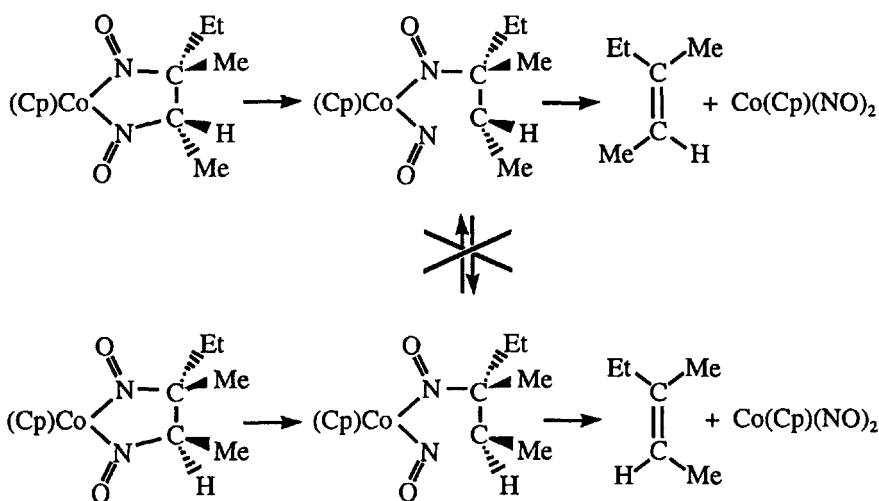
If a steady-state condition is applied to $(\text{Cp})\text{Co}(\text{NO})_2$, then the experimental second-order rate constant is given by

$$k_{\text{exp}} = \frac{k_1[1][2]}{\left(\frac{k_{-1}}{k_2}\right)[4] + [2]} \quad (5.35)$$

The kinetic results give values of $k_1 = 4.3 \times 10^{-4} \text{ s}^{-1}$ ($E_a = 29.4 \text{ kcal mol}^{-1}$) and $k_2/k_{-1} = 115$ for $\text{R} = \text{CO}_2\text{Me}$ at 75°C in toluene.

The exchange of one olefin for another is stereospecific, with no isomerization of the olefin. This observation indicates that the exchange does not proceed through an intermediate with a C—C single bond, or at least that such an intermediate is not persistent enough to allow rotation about the C—C bond, as indicated in Scheme 5.25. This also would be consistent with a concerted mechanism (no intermediate) for the addition and dissociation reactions.

Scheme 5.25



Since $(\text{Cp})\text{Co}(\text{NO})_2$ can achieve an 18-electron configuration by considering one NO as a three-electron donor and the other as a one-electron donor, this reaction could be considered as a formal analogue of 1,3-dipolar cycloadditions in organic chemistry. It is also possible for the NO to switch from a three- to a one-electron donor in the transition state, thereby leaving the Co unsaturated and able to form a transient π complex before rearranging to the observed product. Slippage of the C_5 ring is another possibility, but the rate only decreases by a factor of about three when the C_5 is changed from C_5H_5 to $\text{C}_5(\text{Me})_5$ and is essentially unchanged by $\text{C}_5\text{H}_4\text{CO}_2\text{Me}$.

5.6 CATALYTIC HYDROGENATION OF ALKENES

The addition of H_2 to a $>C=C<$ system is thermodynamically favorable but generally difficult to achieve. In the laboratory, chemists use catalysts such as platinum black and Raney nickel to make the reaction proceed at a reasonable rate. The kinetic barrier for this reaction can be understood in terms of simple orbital symmetry diagrams, shown in Figure 5.2. The basic principle is that in the activated state the electrons must flow in such a way as to make and break the appropriate bonds. In the case of hydrogenation, the electron flow must break the $H-H$ σ and $C-C$ π bonds and make two $C-H$ bonds. The electrons must flow from an occupied orbital on one molecule to an unoccupied orbital on the other, that is, from the highest occupied molecular orbital, HOMO, on one species to the lowest unoccupied molecular orbital, LUMO, on the other.

For H_2 , the HOMO is the σ -bonding orbital and the LUMO is the corresponding σ -antibonding orbital. For an alkene, the HOMO is the π -bonding orbital and the LUMO is the corresponding π -antibonding orbital. To stabilize the activated complex, the appropriate HOMO and LUMO must produce good overlap; that is, the signs of the radial parts of the wave functions should be the same in the overlap region. In addition, electron flow from HOMO to LUMO should break and make the required bonds. The first diagram in Figure 5.2 shows that the overlap is correct for the two HOMO orbitals in this system, but there can be no useful electron flow between two occupied orbitals. The second and third diagrams show the HOMO-LUMO combinations that would give the appropriate electron flow, but these do not produce net overlap; thus, the transition state will not be stabilized. Such a reaction is said to be *symmetry forbidden*.

A catalyst must somehow overcome this symmetry restriction. As already discussed, H_2 can add to organometallic species to make a metal hydride. If one can make an olefin complex of the metal hydride, then the electrons can flow from the $M-H$ σ bond to the π antibonding orbital of the olefin to initiate the process of breaking the $C=C$ bond and making a $C-H$ bond.

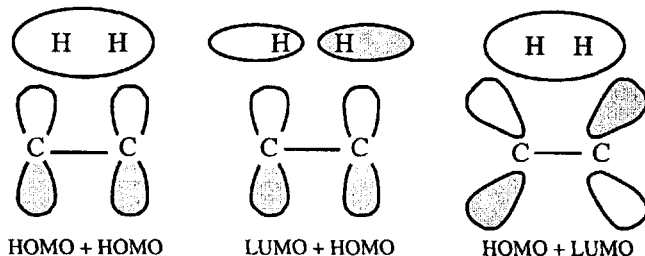
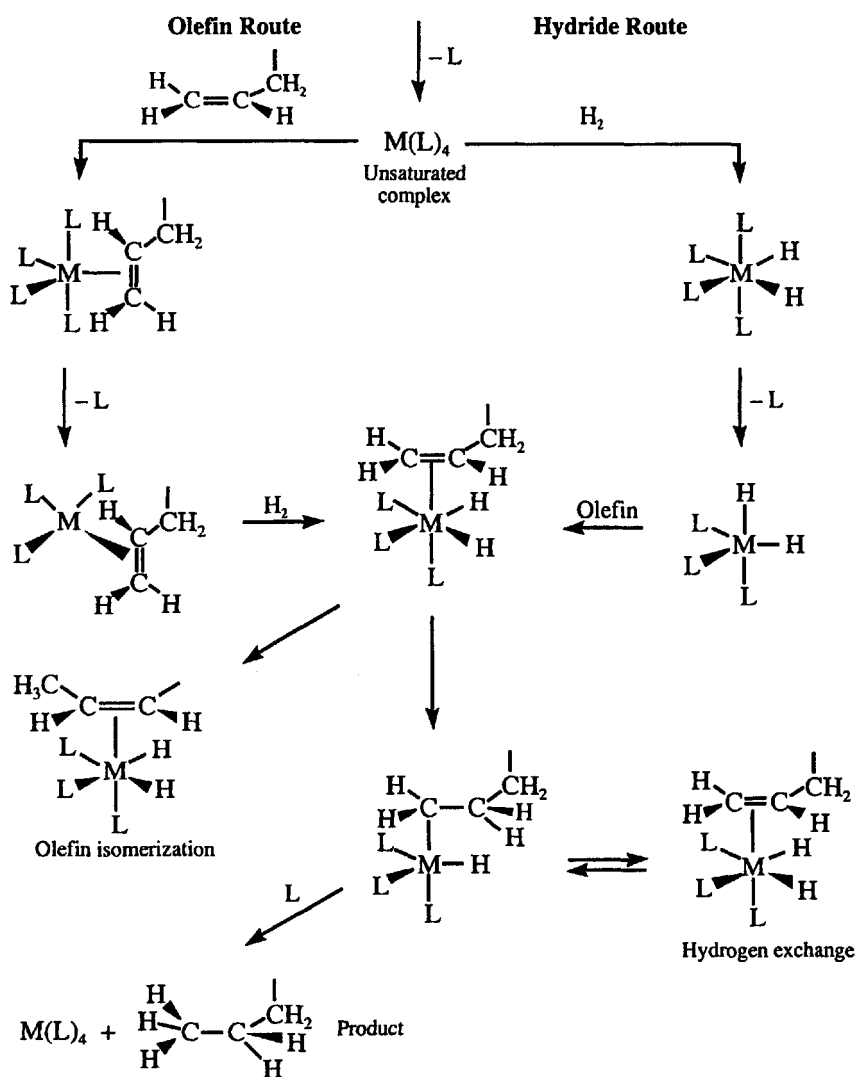


Figure 5.2. The highest occupied molecular orbitals and their combinations with the lowest unoccupied molecular orbitals in H_2 and $CH_2=CH_2$.

5.6.1 General Mechanisms

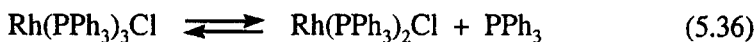
The two generally recognized routes by which an organometallic complex can catalyze the hydrogenation of alkenes are referred to as the *olefin* or *unsaturated route* and the *hydride route*, as shown in Scheme 5.26. Both pathways start from a coordinatively unsaturated (16-electron) metal complex, $M(L)_4$, which might be formed by ligand dissociation, as shown. The two routes differ in the first step which is olefin complexation or oxidative addition of H_2 . Both routes lead to the key dihydride-olefin species in the center of the Scheme.

Scheme 5.26

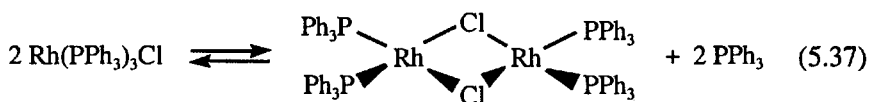


5.6.2 Hydrogenation by Wilkinson's Catalyst: $\text{Rh}(\text{PPh}_3)_3\text{Cl}$

The catalytic properties of $\text{Rh}(\text{PPh}_3)_3\text{Cl}$ were first reported by Wilkinson and co-workers.²³¹ The nature of the species present in hydrocarbon solvents was the subject of controversy until the work of Arai and Halpern,²³² which indicated some PPh_3 dissociation, shown by

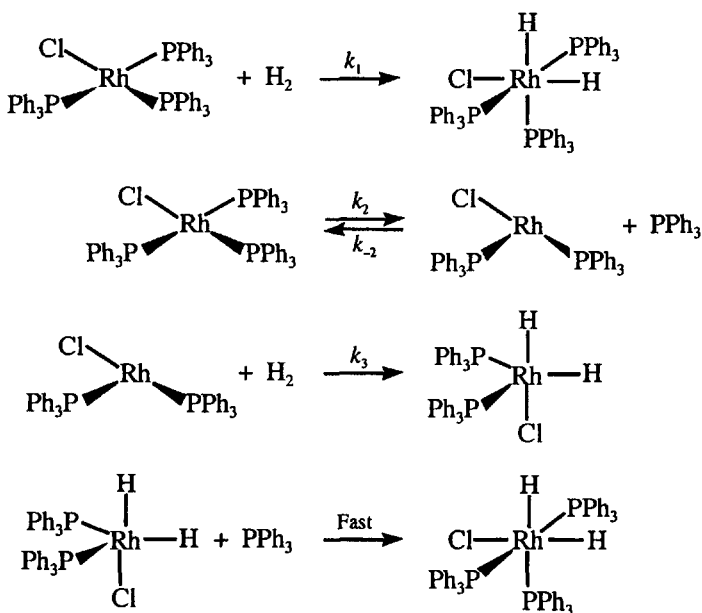


However, Tolman and co-workers²³³ found that phosphine liberation was accompanied by dimer formation, which has $K = 2.4 \times 10^4 \text{ M}$ in benzene at 25°C . The reaction and suggested structure for the dimeric product are given by



Halpern and Wong²³⁴ acknowledged the correctness of Tolman's interpretation and studied the kinetics of the hydrogenation of $\text{Rh}(\text{PPh}_3)_3\text{Cl}$ in the presence of excess PPh_3 to suppress the formation of dimer, with the conclusions that the reaction pathways are as shown in Scheme 5.27.

Scheme 5.27



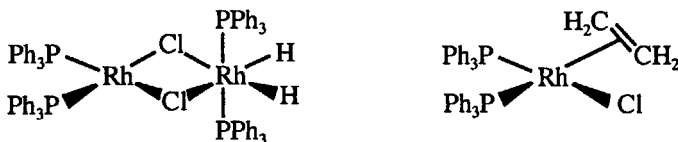
With $[\text{H}_2]$ and $[\text{PPh}_3] \gg [\text{Rh}]$ at 25°C in benzene, the kinetics indicate that the reaction proceeds by parallel paths involving oxidative addition to

Wilkinson's catalyst and to the species with one phosphine dissociated, as shown in Scheme 5.27. If a steady state is assumed for $\text{Rh}(\text{PPh}_3)_2\text{Cl}$, the rate for the system in Scheme 5.27 is given by the following expression:

$$\text{Rate} = \left(k_1 + \frac{k_2 k_3}{k_{-2}[\text{PPh}_3] + k_3[\text{H}_2]} \right) [\text{H}_2][\text{Rh}(\text{PPh}_3)_3\text{Cl}] \quad (5.38)$$

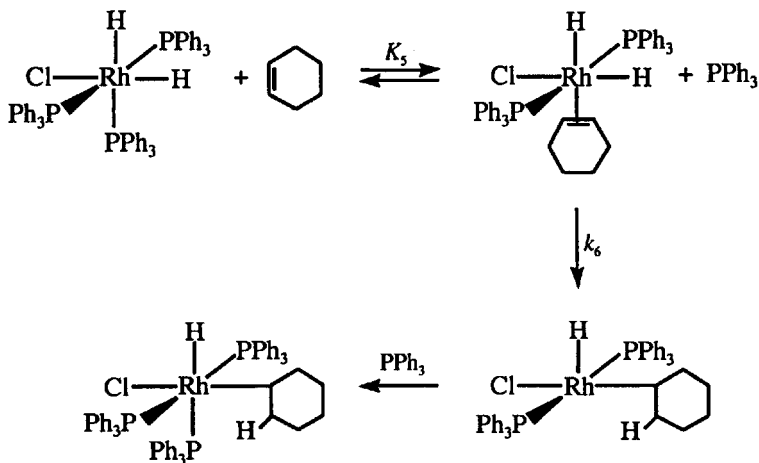
Values of $k_1 = 4.8 \text{ M}^{-1} \text{ s}^{-1}$, $k_2 = 0.71 \text{ s}^{-1}$ and $k_{-2}/k_3 = 1.1$ (25°C in benzene) were determined from the dependence of the rate on $[\text{PPh}_3]$ and $[\text{H}_2]$. At low $[\text{PPh}_3]$, the pseudo-first-order rate constant $k_{\text{exp}} = k_1[\text{H}_2] + k_2$, and for typical H_2 concentrations of $\sim 2 \times 10^{-3} \text{ M}$ (at 1 atm), the k_2 path is dominant. Subsequent work, based on modeling,²³⁵ *para*- H_2 induced polarization²³⁶ and a crystal structure of the $\text{P}(\text{tBu})_3$ analogue,²³⁷ suggest that the product of the k_3 path actually has a *trans* arrangement of the phosphines with equivalent hydride ligands.

Separate studies on the dimer gave a rate that is first-order in [dimer] and $[\text{H}_2]$ and independent of $[\text{PPh}_3]$, with $k = 5.4 \text{ M}^{-1} \text{ s}^{-1}$. Tolman et al.²³⁸ showed that the dimer reacts with H_2 and with ethylene to give the following dihydride and ethylene complexes, but it does not react with cyclohexene.



Halpern et al.²³⁹ found that the kinetics of the hydrogenation of cyclohexene by the rhodium dihydride are consistent with Scheme 5.28, with $K_5 = 3.4 \times 10^{-4}$ and $k_6 = 0.2 \text{ s}^{-1}$ at 25°C in benzene.

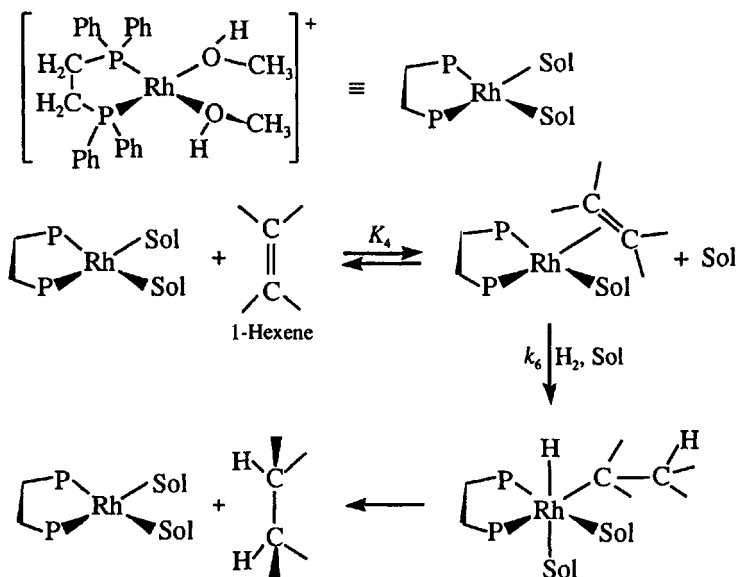
Scheme 5.28



The above examples are considered to be consistent with the hydride route for hydrogenation with Wilkinson's catalyst.

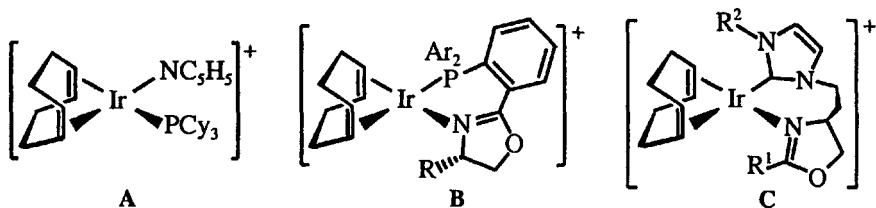
However, the hydride route is not universally observed, even for closely related catalysts. Halpern et al.²⁴⁰ studied the diphos system and found that the kinetics were consistent with the reaction sequence in Scheme 5.29.

Scheme 5.29



The reaction follows the "olefin route" (Scheme 5.26), and the kinetics give $K_4 = 1.6 \text{ M}^{-1}$ and $k_6 = 0.18 \text{ atm}^{-1} \text{ s}^{-1}$ at 25°C . Halpern has rationalized the difference caused by using a chelating phosphine as due to the instability of the dihydride that forms by oxidative addition of H_2 . The trans configuration of the hydride and phosphine ligands is thought to be unstable because of the trans effect of the phosphine. With a related diphosphine chelate, Osborn and co-workers²⁴¹ have suggested that the mechanism in methanol changes from the olefin route to the hydride route as the pressure of H_2 is increased above $\sim 30 \text{ atm}$.

Another important group of hydrogenation catalysts is derived from the Ir(I) complexes shown in the following structures:



These have the advantage that the catalyst precursors are quite stable and the systems are able to hydrogenate substituted alkenes. Crabtree and co-workers²⁴² first developed catalyst **A**. Twenty years later, the groups of Pfaltz²⁴³ and then Burgess²⁴⁴ developed catalysts based on **B** and **C**, respectively. The latter two systems are potential catalysts for asymmetric hydrogenation, as discussed in the following Section.

Kinetic and mechanistic information on these systems is still rather sparse. They all contain the 1,5-cyclooctadiene ligand, COD, and the concept is that this will be hydrogenated under the reaction conditions and dissociate to form an Ir(I) species which can add H₂ and alkene. In a system related to **A**, with two PMePh₂ ligands, Crabtree et al.²⁴⁵ found initial coordination of H₂, but the liberation of COD was about 5 times slower than hydrogenation of ethylene. Thus, in the initial stages, the two processes are occurring. In the same paper, a tentative mechanism was proposed in which the resting state of the catalyst is a *bis*-alkene complex that oxidatively adds H₂ and transfers hydrogens to one of the alkenes. It also was noted that the usual solvent, CH₂Cl₂, may play a crucial role in stabilizing unsaturated intermediates while being easily displaced by alkene or H₂.

Pfaltz and co-workers²⁴⁶ reported some kinetic results for catalysts based on **B** with various Ar and R groups. They noted that the catalyst is deactivated by formation of polyhydride species,²⁴⁷ a phenomenon also seen by Crabtree for **A**. The Pfaltz group studied anion effects and found that the deactivation process was dramatically reduced with fluorinated tetraphenylborate salts, compared to the more commonly used BF₄⁻ and PF₆⁻. Since the reactions were typically over in <1 min, the authors suggest that the rates are diffusion limited and do not yield information about the rate law. Subsequently, Pfaltz and co-workers²⁴⁸ studied the hydrogenation of (*E*)-1,2-diphenyl-1-propene with **B** (Ar = *o*-tolyl, R = *t*-butyl) at 4°C and with lower catalyst concentrations. It was noted that 0.05% water by volume completely deactivates the PF₆⁻ salt, while the rate only changes by 6% with the B(C₆F₅)₄⁻ salt. Although the kinetics are complicated by an induction period, it appears that the rate law also varies with the salt. The rate is close to first-order in the alkene concentration (0.074–0.26 M) for the PF₆⁻ salt, but close to zero-order for the B(3,5-F₃CC₆H₄)₄⁻ salt. The rate is first-order in [H₂] for the latter, but ~1.5-order for the former. The dependence on the catalyst concentration is complicated by competitive deactivation processes. For concentrations between 0.036 to 3.6 mM, the maximum rate tends to become independent of the catalyst concentration at ~0.05 mM.

Brandt and co-workers²⁴⁹ studied the kinetics of the hydrogenation of 1,2-diphenylpropene by **B** (Ar = Ph, R = ^tBu), as the B(3,5-F₃CC₆H₄)₄⁻ salt apparently. They found the rate to be first-order in the concentrations of both H₂ and catalyst. These authors also did a theoretical study of a modified system with Ar = R = Me and with ethylene as the substrate. The

analysis started with a disolvated dihydride of Ir(III) which adds ethylene and then H₂ by displacement of the solvent ligands. In the rate-limiting step, migratory insertion and oxidative addition produces an Ir(V) trihydride–ethyl species which undergoes migratory insertion to an Ir(III) dihydride–ethane complex. The latter dissociates ethane and adds solvent to return to the starting point. However, the theory did not consider the resting state as the *bis*-alkene complex suggested by Crabtree et al., although this would seem reasonable since the concentration of alkene is much larger than that of H₂ under typical experimental conditions. Dietiker and Chen²⁵⁰ used electrospray mass spectrometry to examine the hydrogenation of styrene by **B** (Ar = Ph, R = isopropyl) and concluded that the reaction was going by an Ir(I)/Ir(III) cycle, rather than the Ir(III)/Ir(V) cycle suggested by the calculations of Brandt and co-workers.

For the **C** type catalysts, there are no full kinetic studies, but some inferences can be drawn from the dependence of the products on the reaction conditions. Burgess and co-workers²⁴⁴ noted one case where one stereoisomer predominated under 1 bar of H₂ at 25–40°C, but the opposite isomer is the major product under 85–90 bar at –15 or –30°C. This could reflect a change in the rate-controlling step with temperature or H₂ concentration, or a temperature-dependent change in the conformation of the alkene adduct with the catalyst. Cui and Burgess²⁵¹ studied the reaction of 2,3-diphenylbutadiene with **C** (R¹ = adamantyl, R² = 2,6-*i*-PrC₆H₃) under 1 atm of H₂ at 25°C. They observed a brief induction period during which the COD was released. The products at this stage were complex unless the alkene was present. The hydrogenation of the first C=C bond proceeded with a zero-order dependence on the concentration of the substrate and was followed by a faster and more stereoselective hydrogenation of the second C=C bond. The authors suggest that, during the first stage, the diene acts as an η⁴-donor and cycles between Ir(I) and Ir(III), analogous to the proposal of Crabtree²⁴⁵ with two monoalkenes coordinated. Burgess and co-workers later favored an Ir(III)/Ir(V) cycle, based on theoretical calculations.²⁵²

5.6.3 Asymmetric Hydrogenation

The field of asymmetric hydrogenation continues to evolve rapidly as new catalysts are developed. The area has been the subject of several books²⁵³ and reviews.^{254–257} The Nobel lectures of Knowles²⁵⁸ and Noyori²⁵⁹ provide background perspectives on developments in the field. Much of the interest is related to the need for highly stereoselective syntheses for medical applications.²⁶⁰

To understand the literature in this field, several terms need to be defined. An important practical property of these systems is their stereoselectivity or enantioselectivity, which is their ability to produce one enantiomer in preference to the other. This property is commonly given as the percent enantiomeric excess, ee, determined from an analysis of the products. If *R* and *S* are the percentages of the major and minor

enantiomers, respectively, then $ee = R - S$, and since $R + S = 100$, then $R = (100 + ee)/2$. In the absence of a detailed kinetic study, the efficiency of the catalyst is often expressed by the turnover frequency, TOF, which is the moles of product produced per mole of catalyst in some unit time. When the TOF values of different catalysts are compared, it is implicitly assumed that the rate is first-order in the amount of catalyst. The often quoted turnover number, TON, must be treated cautiously because of variability in the definition. It may be either the moles of desired product or total product or substrate consumed, divided by the moles of catalyst for specified conditions of time and temperature, etc. An excellent catalyst would have a high TOF, such as 10^6 h^{-1} , and an ee of $>90\%$.

5.6.3.1 Asymmetric Hydrogenation of C=C Bonds

An important commercial application of these types of catalysts is in the production of L-dopa for the treatment of Parkinson's disease. The key to this application is the stereoselectivity shown by the phosphine chelate, (2*S*,3*S*)-bis(diphenylphosphino)butane, called chiraphos. In a benchmark study, Halpern and co-workers²⁶¹ found that the Rh system is unusual in that the most stable olefin adduct does not lead to the major or desired product. This mechanistic pathway has been termed the anti-lock-and-key mechanism to contrast it with the lock-and-key mechanism often proposed for enzyme catalysis. In the latter, it is assumed that the best fit of substrate and enzyme will give the most effective catalysis.

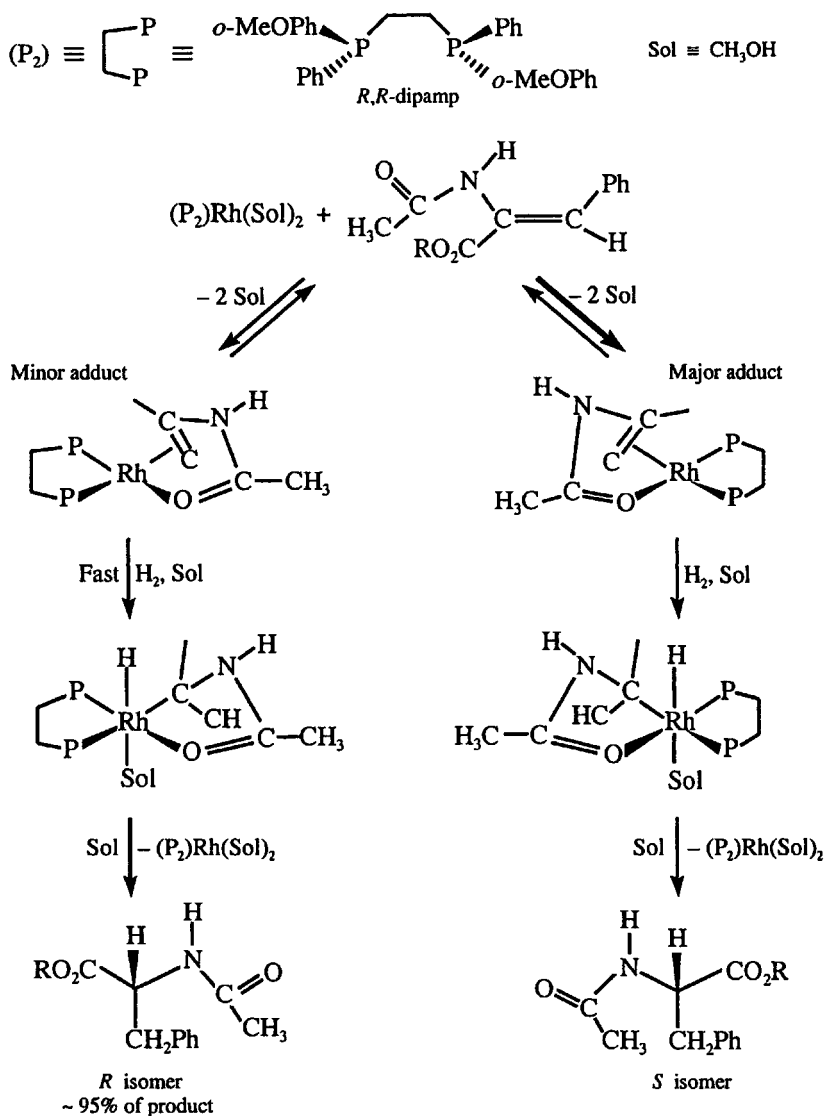
The hydrogenation follows the olefin route like the chelate in Scheme 5.29, and Landis and Halpern²⁶² later reported a detailed kinetic study of the system, shown in Scheme 5.30. The chiral diphosphine, *R,R*-dipamp, has the advantage of giving the major and minor catalyst-substrate adducts in detectable amounts. Again, it was concluded that the minor species generates the major portion of the product because of its greater reactivity with H_2 .

At 25°C , the minor species reacts $\sim 5 \times 10^2$ times faster with H_2 , primarily due to a 3 kcal mol^{-1} more favorable ΔH^\ddagger . The stereoselectivity decreases with increasing H_2 pressure, i.e. less *R* and more *S* product is produced. This was attributed to addition of H_2 becoming competitive with conversion of the major to the minor species so that more product was coming from the major species.

It has been noted²⁶³ that the H_2 pressure dependence of the rate and products in such systems may be affected by rate-limiting transfer of H_2 between the gas and solution phases. It seems unlikely that this was a problem in the study of Landis and Halpern because of the slowness of the reaction. This problem is discussed in more detail in Chapter 9.

The theoretical analysis of Feldgus and Landis,²⁶⁴ using DuPHOS²⁶⁵ for the diphosphine and α -formamidacrylonitrile for the substrate, has provided support for the mechanism. They also have given a detailed rationale for the higher reactivity of the minor species with H_2 .²⁶⁶

Scheme 5.30



More recently, Heller and co-workers²⁶⁷ have determined the structure of the major species with $\text{Rh}(\text{dipamp})^+$ and an analogue of the substrate used by Landis and Halpern. The Rh-substrate complex has the expected structure.

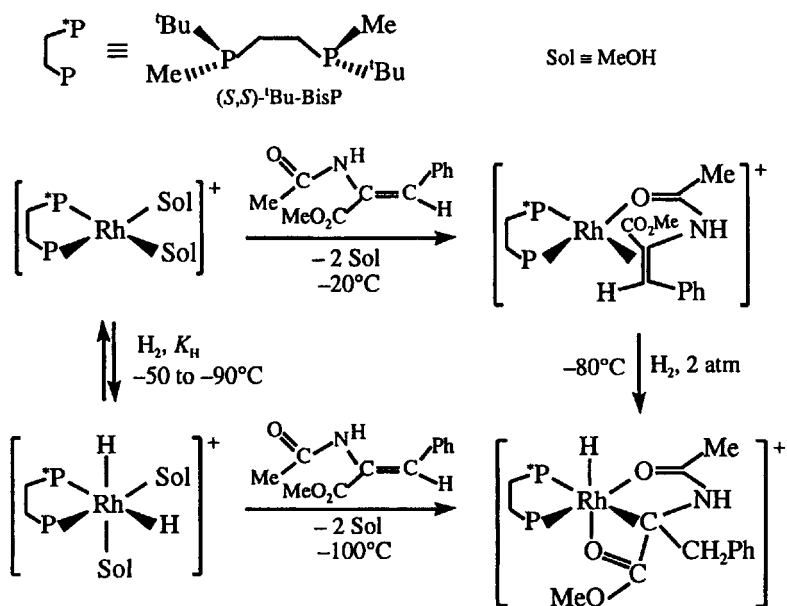
The Heller group also has studied the hydrogenation of β -amino acid precursors, and determined the structure of the dominant one.²⁶⁸ In this study, they note that, although the mechanism is believed to be analogous to that in Scheme 5.30, now the dominant complex is the more reactive one

and gives the *S* enantiomer as the major product. An earlier kinetic study²⁶⁹ explored the reactivity with various diphosphines and the effect of H₂ pressure and temperature on the rate and stereochemistry of the products. It should be noted that these substrates have *E* and *Z* isomers which show different reactivity but yield the same dominant enantiomer of the product.

It also has been found that chiral monodentate phosphine derivatives can be used in place of the diphosphine. Reetz et al.²⁷⁰ studied the kinetics of a Rh(I) system with chiral phosphite ligands. The rate is first-order in H₂ pressure and is optimum for a 2:1 ratio of phosphite:Rh. These authors suggest that the reaction follows the olefin route, with the rate-limiting step being the oxidative addition of H₂, and that the active catalyst retains two phosphite ligands. The *R* configuration of the phosphite produces mainly the *R*-enantiomer from itaconic acid dimethyl ester. Calculations indicate that this comes from the major catalyst–substrate complex.

A somewhat different approach to these systems has been taken by the group of Gridnev and Imamoto.²⁵⁵ They have used more electron-rich diphosphines, such as Me(^tBu)P(CH₂)₂P(^tBu)Me, which should favor oxidative addition of H₂ and the hydride route. They have used low temperature NMR to characterize the species present under close to stoichiometric conditions of substrate and catalyst. This methodology can yield interesting chemical information, but one also needs to establish the relevance of the observations to the catalytic conditions where the substrate is in large excess. The following Scheme outlines the dominant species observed in a study²⁷¹ with the same substrate as in Scheme 5.30.

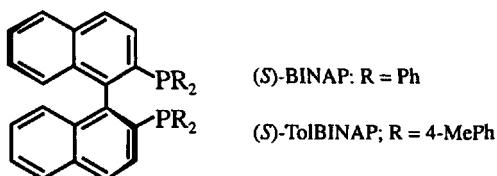
Scheme 5.31



In the absence of substrate, the catalyst precursor reacts with H_2 to give two isomeric dihydrides, with the dominant one shown. The equilibrium constant K_H was determined in methanol between -50 and $-95^\circ C$ to obtain values for ΔH° and ΔS° of $-6.3 \text{ kcal mol}^{-1}$ and $-23.7 \text{ cal mol}^{-1} \text{ K}^{-1}$, respectively. These parameters predict a value for K_H of $\sim 0.25 \text{ M}^{-1}$ at $25^\circ C$. This suggests that there will be little of these species present at $25^\circ C$ where the solubility of H_2 is $4 \times 10^{-3} \text{ M}$ under 1 atm of H_2 . The formation of the catalyst-substrate complex was apparently complete with a 2:1 ratio of substrate to catalyst ($\sim 0.1 \text{ M}:0.05 \text{ M}$), suggesting that formation of this complex will dominate over the dihydride. The authors note that the structure of the dominant isomer of this complex, shown in Scheme 5.31, would not lead to the observed *R*-enantiomer of the product. Therefore, if the reaction proceeds by the olefin route, the product would appear to form from the minor isomer, as observed for the system in Scheme 5.30. It was observed that the interconversion of the major and minor isomers may be fast enough at $-80^\circ C$ to be consistent with reaction via the minor isomer. Although the dihydride does form in the absence of substrate, there is nothing in the observations which requires that it is the active catalyst.

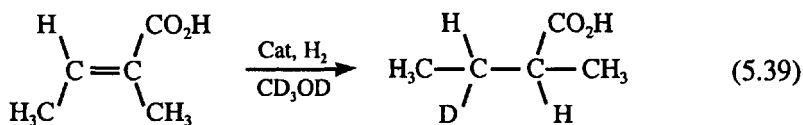
In a later study by Gridnev et al.²⁷² with ethenephosphonate substrates, the observations were analogous to those described above. However, it was found that reaction of the dihydride with substrate at $-100^\circ C$ gave better enantioselectivity than reaction of the catalyst-substrate complex under 2 atm of H_2 at $-30^\circ C$. The optical yield under normal catalytic conditions (substrate:catalyst = 100, under 4 atm H_2 , for 18h and presumably at ambient temperature) fell between those of the other two experiments. The authors suggest that this may indicate a mixed hydride/olefin mechanism.

A major step in this area was the development of a Ru(II) based asymmetric catalysts. The area has been reviewed by Genet.²⁵⁵ Noyori and co-workers reported procedures for the hydrogenation of a wide range of alkenes²⁷³ and β -keto esters²⁷⁴ using the chiral BINAP ligand, one isomer of which is shown in the following diagram:

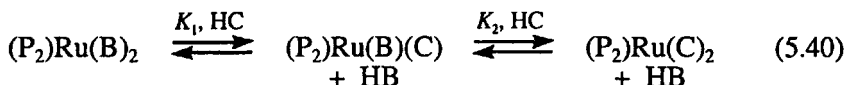


The BINAP ligand derives its asymmetry from the steric interaction of the two naphthalene rings, which forces them not to be coplanar. The development of BINAP type ligands has been reviewed by Berthod et al.²⁷⁵

Ashby and Halpern²⁷⁶ have studied the hydrogenation of several α,β -unsaturated carboxylic acids catalysed by $(R\text{-BINAP})Ru(O_2CCH_3)_2$ in methanol. The kinetics of the hydrogenation of tiglic acid was studied in detail and the major product from the reaction in deuterated methanol is shown in the following reaction:



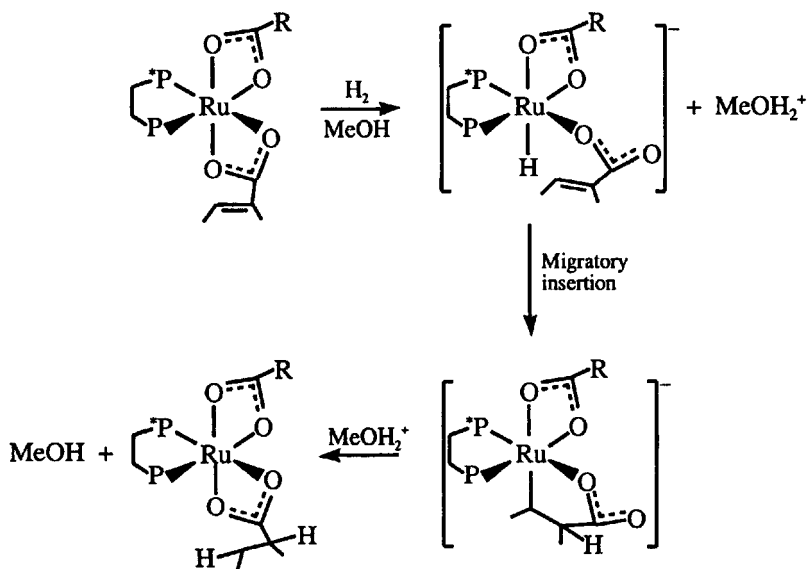
Clearly, the deuterium on the β -carbon is derived from the solvent and neither the olefin nor the hydride route mechanisms are operative because they deliver both hydrogens from H_2 . Ashby and Halpern also measured the equilibrium constants for the following reactions:



where P_2 is BINAP, B is the substrate anion and C is the product anion for reaction (5.39). There is a slight preference for complexing of the B and C species compared to acetate but, since the latter only comes from the catalyst, $[\text{B}] + [\text{C}] \gg [\text{acetate}]$ throughout the reaction and acetate complexes can be ignored. The similarity of NMR spectra of the complexes with both alkene and aliphatic substituents suggests that coordination always is through the carboxylate group. The rate of consumption of H_2 was found to be first-order in the concentration of the catalyst and pressure of H_2 (0.44 to 1.5 atm) and inverse first-order in the sum of the substrate and product concentrations.

The main features of the mechanism are shown in the following Scheme, where $\text{P}-\text{P}^*$ is BINAP:

Scheme 5.32



The rate-limiting step is the initial heterolytic addition of H_2 to give a monohydride and a solvated proton. This is followed by migratory insertion to give an alkyl complex that is protonated to form the product. The sources of the H atoms added are consistent with reaction (5.39) and, with a few numerical simplifications, the authors showed that the mechanism is consistent with the rate law.

The heterolytic cleavage of H_2 seems to be typical of these Ru(II) hydrogenation catalysts. Another common feature is interference from untreated Pyrex glassware. Ashby and Halpern used quartz, while stainless steel and teflon-coated Pyrex vessels often are used now.

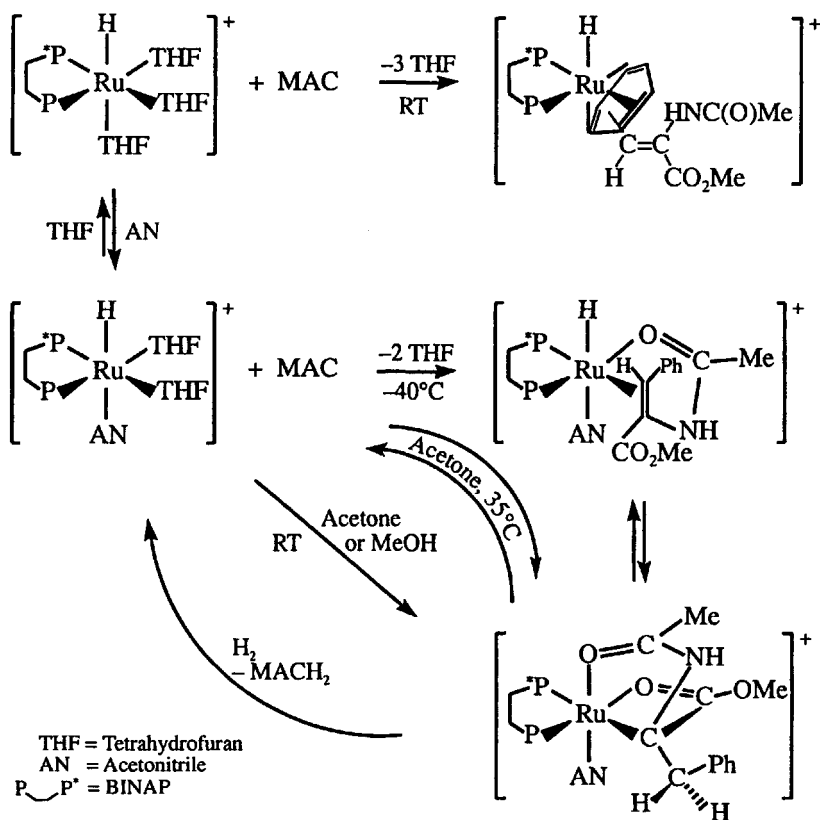
Other studies with unsaturated carboxylic acids are consistent with the mechanism of Ashby and Halpern. Ohta et al.²⁷⁷ hydrogenated several such substrates with D_2 in MeOH or H_2 in MeOD and found a labeling pattern predicted by the mechanism. They, as well as Chan et al.,²⁷⁸ found that β,γ -unsaturated carboxylic acids give labeling consistent with formation of a five-membered ring for the Ru-alkyl intermediate. It should be noted, however, that different patterns have been observed with different catalyst precursors, such as (BINAP)Ru(acac)⁺, used by Brown et al.²⁷⁹ and (BINAP)₂Ru(H)⁺, used by Saburi et al.²⁸⁰ It is not clear if these represent chemical complications due to gas/solvent isotope exchange or mechanistic differences. Ashby and Halpern, and Ohta et al. examined qualitatively the MeOH/ D_2 exchange catalyzed by their ruthenium hydride complexes.

It was noted by Ohta et al. that the amount of isotope from the gas phase species increased as the pressure changed from 4 to 145 atm. This might be due to isotope exchange between the gas and solvent, but the authors also suggested an additional pathway involving heterolytic addition of H_2 to the Ru-alkyl intermediate. Chan et al. advocated this proposal to explain a substantial increase in the enantioselectivity for the hydrogenation of 2-(6-methoxy-2-naphthyl)acrylic acid between 1 and 34 atm at 25°C in methanol, although the effect was much less at 11°C. Dong and Erkey²⁸¹ gave the same explanation for a decrease in enantioselectivity between 3 and 95 atm for the reaction with tiglic acid, also at 25°C in methanol.

When the substrate is changed from a carboxylic acid to a species with no acidic protons, the system changes in a subtle but possibly important way. Addition of such a substrate to (BINAP)Ru(O₂CCH₃)₂ liberates acetate ion, and heterolytic addition of H_2 will yield acetic acid rather than a solvated proton. The acetic acid may not be strong enough in methanol to bring about the protolysis of the Ru—C bond, shown as the last step in Scheme 5.32.

One of the most thoroughly studied such substrates is the ester, methyl (*Z*)- α -(acetamido)cinnamate, MAC, whose Rh catalyzed hydrogenation is described in Scheme 5.30. In several reports, Wiles and Bergens used a solvated (BINAP)Ru precatalyst and low temperature NMR to study the (BINAP)Ru—MAC system largely under stoichiometric conditions. Their observations are summarized in the following Scheme:

Scheme 5.33



The solvated species, $(\text{THF})_3$, is observed only in the absence of AN, while in the presence of AN, the $(\text{THF})_2(\text{AN})$ and $(\text{THF})(\text{AN})_2$ complexes have been identified. It is suspected that the latter is not active because it must dissociate an AN to give a bidentate MAC complex. The tris-THF species reacts with a stoichiometric amount of MAC to give the η^6 -aryl complex shown and therefore also is thought not to be active.²⁸² The speciation in acetone and methanol is not known but is presumed to be similar. The $[(\text{BINAP})\text{Ru}(\text{H})(\text{AN})(\text{MAC})]^+$ ion has been characterized by NMR in solution at -40°C .²⁸² It also has been shown that the main Ru complex present under catalytic conditions (excess MAC) is the Ru—C species in the lower right of the Scheme, and it has been characterized by X-ray crystallography.²⁸³ This species undergoes facile exchange with MAC at 35°C in acetone.²⁸⁴ The details of the interconversion of the olefin and Ru—C complexes are unknown, but it may be envisaged as hydride transfer and rotation about the Ru—C bond. In the same study, isotopic labeling showed that liberation of the hydrogenated product, MACH_2 , occurs primarily by hydrogenolysis, as indicated in the Scheme. Although

the details of this rate-limiting step are not known, dissociation of AN and formation of an $\eta^2\text{-H}_2$ intermediate seems reasonable and consistent with the observation that the rate is inhibited by addition of AN in acetone. However, this inhibition is not observed in methanol and the authors suggest that, in a subsequent step, this solvent may protonate the metal in the Ru—C species as a pathway to form MACH_2 ; presumably the MeO^- would then promote heterolysis of a subsequently formed $\eta^2\text{-H}_2$ complex and form MeOH.

Subsequently, Kitamura et al.²⁸⁵ studied the kinetics of the hydrogenation of MAC and some of its analogues catalyzed by the standard catalyst $(\text{BINAP})\text{Ru}(\text{O}_2\text{CCH}_3)_2$ in methanol. The reaction was monitored by the change in intensity of the carbonyl stretching band of the product at 1750 cm^{-1} . The data were analysed by first-order plots of $\ln [\text{MAC}]$ versus time which appeared linear for H_2 pressures between 0.7 and 1.2 atm. Deviations at 0.3 atm were attributed to mass transfer limitations and an initial rate was used. This limitation seems unusual because the rate is slower at lower pressures and the fraction of gas transferred to the liquid phase is independent of the partial pressure of the gas, as shown in Chapter 9. At pressures >1.5 atm, the plots were not linear and a change of mechanism was suggested. Under 7 atm of H_2 , the reaction is said to be zero-order in $[\text{MAC}]$. The kinetic analysis was limited to the 0.3–1.2 atm region where it was determined that the rate was first-order in the catalyst's concentration (0.1–1.0 mM) and the pressure of H_2 and independent of added acetic acid (0–11 mM).

The most surprising fact is that the first-order rate constant decreases as the initial concentration, $[\text{MAC}]_0$, increases from 0.10 to 0.40 M, and shows a saturation effect for $[\text{MAC}]_0 > 0.20$ M. Nevertheless, Kitamura et al. maintain that the reaction follows first-order kinetics in $[\text{MAC}]$, apparently because of the linearity of the $\ln [\text{MAC}]$ versus time plots. How can these observations be reconciled? A simple rate law that might be consistent with the observations is given by the following:

$$-\frac{d[\text{MAC}]}{dt} = \frac{b}{[\text{MAC}] + c} \quad (5.41)$$

After rearrangement and integration over the limits of $t = 0$ to t and $[\text{MAC}] = [\text{MAC}]_0$ to $[\text{MAC}]_t$, one obtains

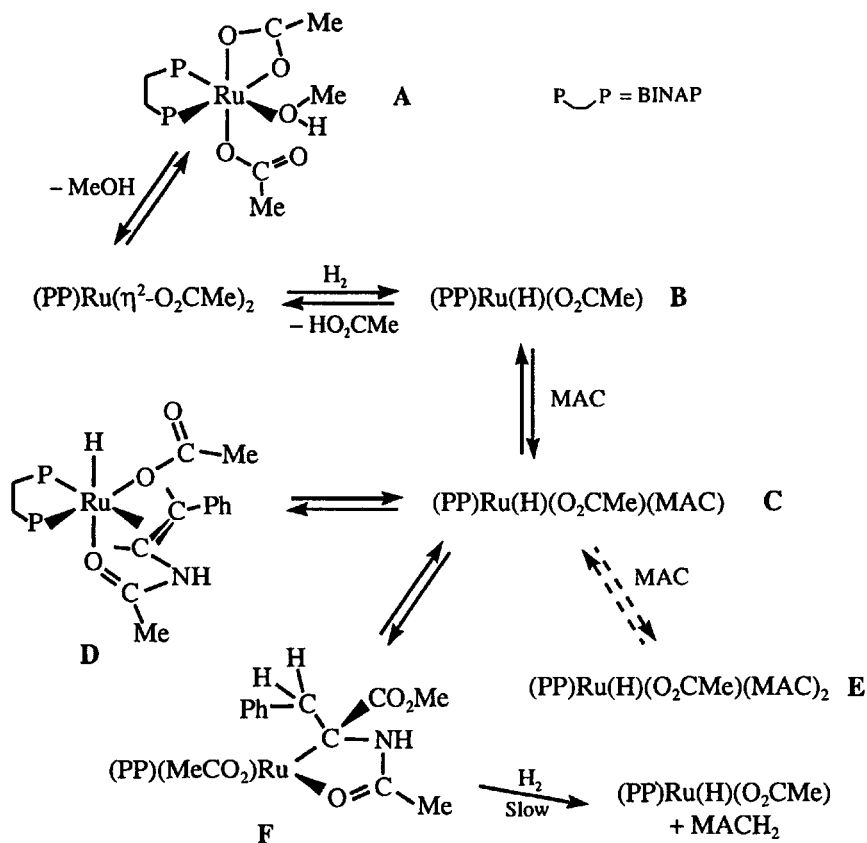
$$[\text{MAC}]_t^2 - [\text{MAC}]_0^2 + 2c([\text{MAC}]_t - [\text{MAC}]_0) = -2bt \quad (5.42)$$

This equation gives an excellent fit of all of the published $[\text{MAC}]$ versus time data between 0.10 and 0.40 M with $b = 4.5 \times 10^{-4}\text{ M}^2\text{ min}^{-1}$ and $c = 0.70$ M. The lesson to be learned here is that *first-order plots which appear linear are not definitive proof of a first-order concentration dependence in the reagent being monitored*. Fortunately, in this case, the

concentration of the reagent was varied so that the actual rate law could be revealed. The form of Eq. (5.41) might indicate the formation of an inactive bis-complex of the catalyst with MAC and implies that formation of the mono-complex is essentially complete during the ~75% of the reaction actually followed. If the reaction were inhibited by the product, MACH_2 , then Eq. (5.41) can be modified by replacing $[\text{MAC}]$ by $[\text{MACH}_2] = [\text{MAC}]_0 - [\text{MAC}]_t$. Integration gives a solution similar in form to Eq. (5.42) which also fits the data of Kitamura et al., but they have done other runs with added MACH_2 which show that it is not the inhibitor.

The major features of the mechanism deduced from the observations of Kitamura et al. are summarized in the following Scheme:

Scheme 5.34

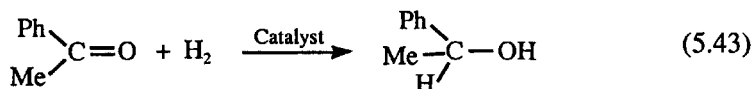


To fit the rate law, the complexation of a second MAC from C to E has been added. The rate law would be consistent with complexation of the starting material, but the ^{31}P NMR of $(\text{PP})\text{Ru}(\text{O}_2\text{CMe})_2$ is not changed in the presence of 0.015 M MAC at -60°C . Although these conditions are

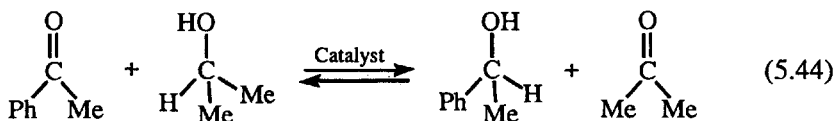
rather far from the typical catalytic conditions of 0.15 M MAC and 30°C, the second addition of MAC to species C has been adopted here. Species A was detected by NMR under catalytic conditions and was isolated and structurally characterized. The structure of species D was suggested from its ^{31}P NMR at -60°C ; the failure to observe coupling between the amide carbon and P was used to place the amide trans to the H ligand. An unfavorable perpendicular alignment of the Ru—H and C=C bonds was used to suggest that species D is not on the direct pathway to product. Species F was not observed but is suggested on the basis of some of the systems discussed previously. Based on deuterium labeling experiments, the authors proposed that F is converted to product about 85% by hydrogenolysis, as shown in the Scheme, and about 15% by methanolysis, analogous to that suggested by Wiles and Bergens.²⁸⁴ The observations of Kitamura et al. indicate that 11 mM acetic acid in methanol does not compete with H_2 for the conversion of F to product.

5.6.3.2 Asymmetric Hydrogenation of C=O Bonds

The conversion of an aldehyde or a ketone to an alcohol is an important transformation in organic synthesis. There are several efficient organometallic catalysts for this process which corresponds to the hydrogenation of a C=O bond, as shown in the following reaction:



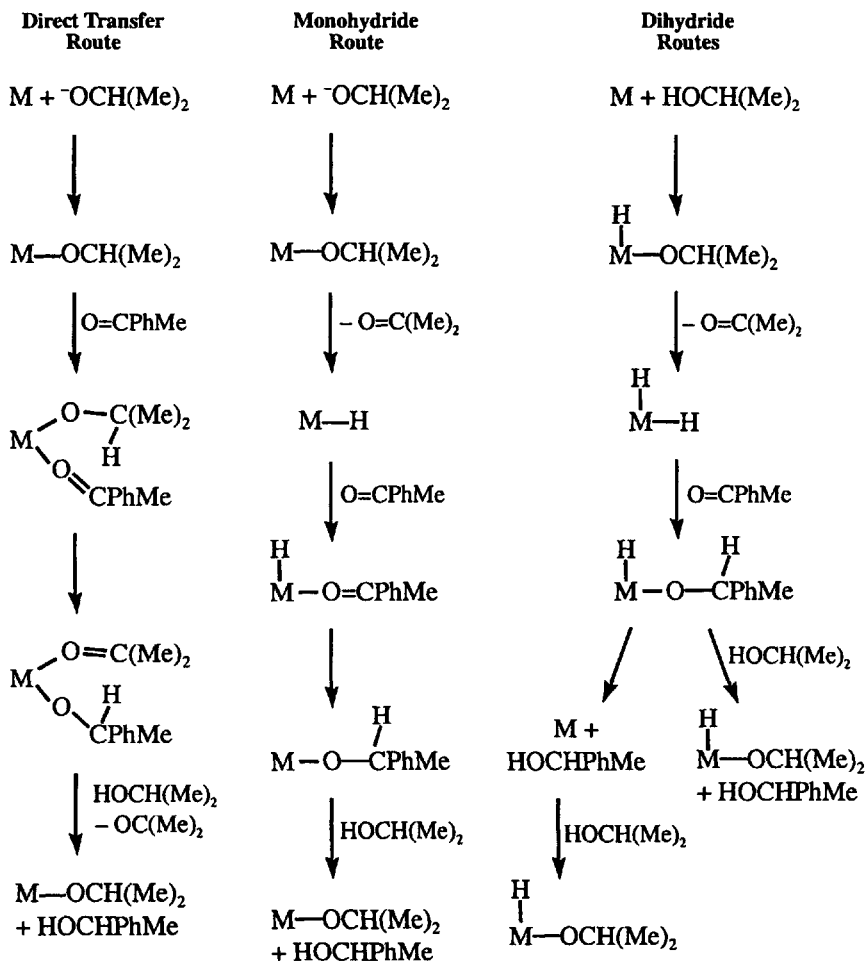
The discussion here will focus on the stereoselective hydrogenation of ketones. Since these reactions are normally done in an alcohol solvent, there is another possible pathway, commonly called transfer hydrogenation, which is illustrated by the following example:



A particular catalyst may promote both of these processes to differing extents. The contribution by transfer hydrogenation can be determined by carrying out the reaction in the absence of H_2 or by comparing the amount of H_2 consumed to the amount of reactant consumed or product formed. The processes also may be distinguished, in principle, by deuterium labeling, but the interpretation can be complicated by isotope scrambling between H_2 and the alcohol. For the purposes of designing an enantioselective catalyst, it can be important to know the contributions of the two paths because they may have different selectivities.

A number of mechanisms have been proposed for transfer hydrogenation and these are described in several reviews.^{257,286} Because of recent developments, the present discussion will concentrate on reactions under basic conditions in which the alkoxide ion of the alcohol is present. Proposed mechanisms under these conditions are summarized in the following Scheme:

Scheme 5.35



For the sake of generality, the metal involved, its oxidation state and its ancillary ligands are not specified. It also should be noted that, in many cases, these reactions do not proceed to completion; the reverse reactions are omitted from the Scheme. Two alternative last steps are shown for the dihydride mechanism. The one on the right is the more conventional protonation of the coordinated alkoxide by solvent; the one on the left

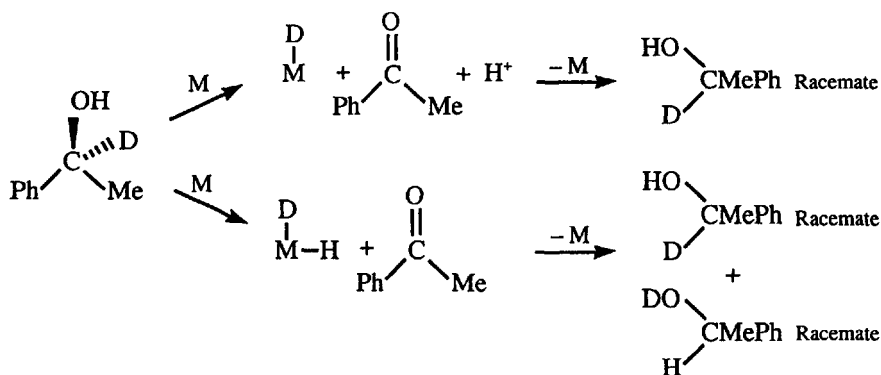
involves reductive elimination of the alkoxide and was proposed by Pàmies and Bäckvall for a Ru catalyst.²⁸⁷

The kinetics of reaction (5.44) have been studied by De Bellefon and Tanchoux²⁸⁸ using a catalyst prepared by the reaction of $(\text{Rh}(1,5\text{-COD})\text{Cl})_2$ and $(1S,2S)\text{-N,N'dimethyl-1,2-diphenyl-1,2-ethanediamine}$. The available evidence suggests that the catalyst is $(1,5\text{-COD})\text{Rh}(\text{NPhCH}_2\text{CH}_2\text{---})_2^+$.²⁸⁹ The initial rates at 25°C in isopropanol were studied as a function of the concentrations of water, acetone and acetophenone. The rate is inhibited by water (0–2.2 M) and by acetone (0.02–0.9 M) and shows saturation behavior with acetophenone above ~0.05 M. The results were considered to be consistent with the direct transfer route since there was no kinetic evidence for hydride intermediates. Theoretical studies on analogous but greatly simplified systems have suggested a monohydride mechanism coupled with dissociation of one end of the diamine ligand,²⁹⁰ however, a later report²⁹¹ supports a mechanism analogous to that discussed later in this section.

For the achiral $\text{Ru}(\text{Cl})_2(\text{PPh}_3)_3$ system, Bäckvall and co-workers²⁹² have concluded that the active catalyst is the dihydride, $\text{Ru}(\text{PPh}_3)_3(\text{H})_2$. The latter is formed from $\text{Ru}(\text{Cl})_2(\text{PPh}_3)_3$ in isopropanol with added base and was identified by ³¹P NMR. The dihydride gave immediate reaction between cyclopentanol and acetone in the presence of K_2CO_3 , while $\text{Ru}(\text{Cl})_2(\text{PPh}_3)_3$ and $\text{Ru}(\text{H})(\text{Cl})(\text{PPh}_3)_3$ were slower to react and showed induction periods.

It was proposed by Laxmi and Bäckvall²⁹³ that the mono- and dihydride pathways could be distinguished by studying the racemization of deuterated (*S*)- α -phenylethanol, as described in the following Scheme, where M represents some metal complex catalyst:

Scheme 5.36

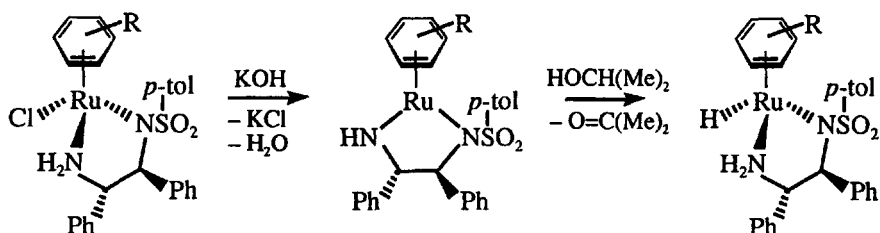


For the monohydride pathway, microscopic reversibility requires that the D transferred from the α -carbon to the catalyst will be returned to the same position in the racemic product and the racemate should have the same D composition as the reactant. This assumes no exchange between M—H and

H⁺. However, if the H and D in the dihydride are chemically equivalent or become scrambled, then the racemate will have 50% of the D on the α -carbon. In practice, the deuterium content of the product is always somewhat less than predicted. For the Ru(PPh)₃(H)₂ catalyst described in the previous paragraph, 37% of the expected D was found on the α -carbon. Pàmies and Bäckvall applied this method to a number of catalysts and found that many Rh and Ir catalysts gave >90% retention of D on the α -carbon, suggesting a monohydride pathway. The same was true for most of the Ru systems tested, except for the case mentioned above and for (Ph₃P)₂Ru(Cl)₂(η^2 -NH₂CH₂CH₂NH₂).

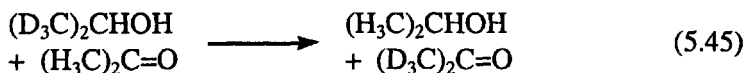
Prior to 1995, most transfer hydrogenation catalysts showed modest activity and enantioselectivity and required somewhat elevated temperatures for convenient reaction times. Then, the situation changed dramatically with the report by Noyori and co-workers²⁹⁴ of a catalytic system with good reactivity and excellent enantioselectivity at ambient temperature. The catalytic system, shown in Scheme 5.37, is a Ru(II) complex with (1*S*,2*S*)-*N*-*p*-toluenesulfonyl-1,2-diphenylethylenediamine, (*S,S*)-TsDPEN, and an η^6 -arene as crucial ligands.

Scheme 5.37



The catalyst precursor reacts with one equivalent of KOH to eliminate KCl and H₂O and form a deprotonated 16-electron species. The latter reacts rapidly with isopropanol to form an 18-electron hydride. All of these species were characterized by X-ray crystallography.

Noyori and co-workers²⁹⁵ used ¹H NMR at 23°C, with the 16-electron species as the initial form of the catalyst, to study the initial rates of the isotope exchange reaction between isopropanol and acetone, as shown in the following reaction, with d₆-isopropanol as the solvent:



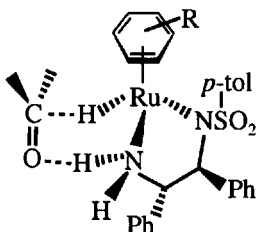
They found that the rate of loss of (H₃C)₂CO is first-order in the concentration of acetone at low concentrations, but becomes independent of the acetone concentration for values >0.4 M. With (D₃C)₂CO as the solvent, they found that the rate of loss of (H₃C)₂CHOH was first-order in

the concentrations of isopropanol and the catalyst. With the assumption that these orders also apply in isopropanol, one can deduce the full rate law as the following:

$$-\frac{d[(\text{H}_3\text{C})_2\text{CHOH}]}{dt} = \frac{k[(\text{H}_3\text{C})_2\text{CHOH}][(\text{H}_3\text{C})_2\text{CO}][\text{Ru}]}{Q + [(\text{H}_3\text{C})_2\text{CO}]} \quad (5.46)$$

where $Q = 0.55 \text{ M}$ and $k = 4.6 \times 10^{-3} \text{ M}^{-1} \text{ s}^{-1}$, if $[(\text{D}_3\text{C})_2\text{CHOH}] = 13.1 \text{ M}$ in pure isopropanol. In acetone, the pseudo-first-order rate constants given by the authors yield $k \approx 2.4 \times 10^{-3} \text{ M}^{-1} \text{ s}^{-1}$.

A mechanism for this type of system based on the classical proposals given in Scheme 5.35 has a problem with the formation of a ketone complex with the 18-electron hydride. Slippage of the η^6 -arene ring or dissociation of one end of the diamine are possibilities, but they seem unlikely because of the speed of the reaction and the weak coordinating power of the carbonyl oxygen in most ketones. The answer to this problem came from the proposal by Noyori and Hashiguchi²⁹⁶ of the following type of intermediate:



In this species, there is no direct coordination of the ketone to the Ru, but rather an outer-sphere association with an orientation of the ketone such that two H atoms can be transferred from the 18-electron hydride, one coming from the hydridic H and the other from the NH_2 group. This nonclassical mechanistic pathway is now widely accepted for this class of catalysts and is referred to as metal–ligand bifunctional catalysis. Theoretical work of Andersson and co-workers²⁹⁷ and Noyori et al.²⁹⁸ provided support for the mechanism and further details are discussed in a review by Noyori et al.²⁹⁹

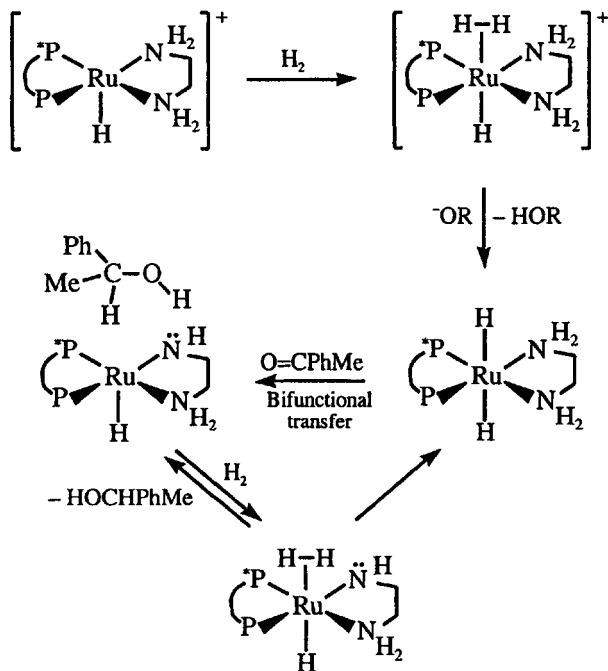
For other metals with analogous ligand sets, the situation remains uncertain, with most of the mechanistic inferences coming from theory. Results for Rh have been discussed already. Meijer and co-workers³⁰⁰ have done a theoretical comparison of $(\eta^6\text{-arene})\text{Ru}$ and $(1,5\text{-COD})\text{Ir}$ systems with amino alcohol and amino thiol chelates. They concluded that the Ru system uses the bifunctional mechanism, but the Ir system proceeds by direct transfer with chelate ring opening to accommodate the alcohol and ketone ligands and no formation of a hydride.

Also in 1995, Noyori and co-workers³⁰¹ reported that the hydrogenation of ketones is catalysed by ruthenium–diamine complexes, such as the

complex with (*S*)-BINAP and (*S,S*)-1,2-diphenylethylenediamine, (*S,S*)-DPEN. The reaction proceeds smoothly at 28°C in isopropanol under 4 atm of H₂ with the addition of 2 equivalents of KOH. Several reviews by Noyori and co-workers²⁵⁴ summarize subsequent work which has shown that the reaction is highly selective for C=O over C=C bonds and that higher concentrations of base, up to ~10 mM, impart greater reactivity.³⁰² Hartmann and Chen³⁰³ reported that the hydrogenation of acetophenone with the precatalyst (BINAP)Ru(Cl)₂(DPEN) is assisted by K⁺ ions and proposed that its association with the catalyst promotes heterolytic cleavage of η²-H₂. Later observations from Noyori's group,³⁰² using a phosphazene base and added M(BPh₄) salts, suggest that the cations are helpful but not essential. Noyori and co-workers reported that the amine must have at least one N—H bond, while others have found lower reactivity and poor stereoselectivity in the absence of an N—H bond.³⁰⁴ Noyori and co-workers reported recently that the replacement of DPEN by 2-aminomethylpyridine imparts good reactivity towards sterically hindered ketones, however, the enantioselectivity is poor with acetophenone.³⁰⁵

There is general agreement that these systems also are proceeding via metal–ligand bifunctional catalysis, but the details of the reactive species remain somewhat obscure. A somewhat simplified version of the proposal by Noyori and co-workers³⁰² for the system under basic conditions is shown in the following Scheme:

Scheme 5.38

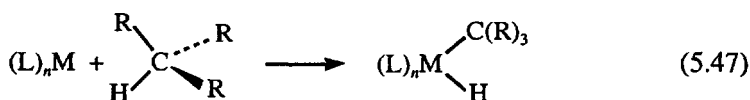


This proposal is based on observations with TolBINAP and DPEN as the ligands, but none of the intermediate species were identified. Morris and co-workers³⁰⁶ studied a system with tetramethylethylenediamine as the chelating amine and found that the dihydride species is a catalyst in benzene with no base added. Bergens and co-workers³⁰⁷ have prepared the $\eta^2\text{-H}_2$ species with BINAP and DPEN and shown that it is not a catalyst unless activated by base or BH_4^- . Noyori and co-workers³⁰² suggested that the excess base is needed to convert the $\eta^2\text{-H}_2$ species to the dihydride. Hartmann and Chen³⁰⁸ have studied the effect of H_2 pressure on the kinetics of H_2 consumption and modeled the observations to a three-species catalytic cycle. They conclude that the rate-limiting step changes from $\eta^2\text{-H}_2$ cleavage to hydrogen transfer as the pressure increases from 2 to 5 atm. They also note that the high rate of the reaction poses potential problems for mass transfer of H_2 between the gas and liquid phases.

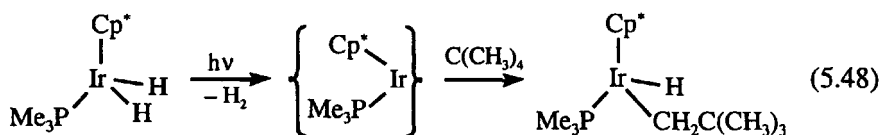
Although the bifunctional mechanism is widely accepted, it seems unusual that alkoxide species are not more involved since RO^- is typically present at the 5–20 mM level in the actual catalytic system. It is of interest to note that Noyori and co-workers have suggested recently that the species *cis*-Ru(H)(OR)((*S*)-TolBINAP)(aminomethylpyridine) is the reactive form for the reduction of *tert*-alkyl ketones.³⁰⁵ There also have been periodic proposals that the alcohol solvent is important for cleavage of $\eta^2\text{-H}_2$.³⁰⁹

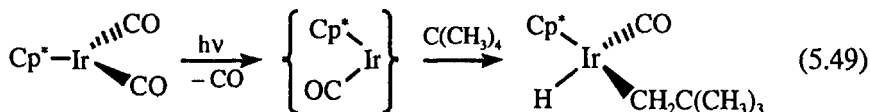
5.6.4 Carbon–Hydrogen Bond Activation

Carbon–hydrogen bond activation is formally the oxidative addition of a hydrocarbon to a metal complex, as shown in reaction (5.47). It is a potentially important reaction because it represents the initial step in a possible route to functionalize hydrocarbons.



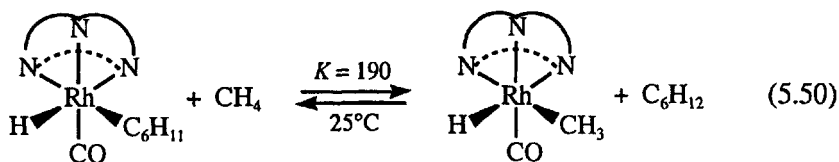
Until the discovery of this process in 1982,^{310,311} it was thought to be difficult at best, and perhaps impossible under moderate conditions, because of the low reactivity of hydrocarbons and the high strength (95–100 kcal mol⁻¹) of the C–H bond. The latter limitation could be overcome by sufficiently strong M–H and M–C bonds. The first observations of this type of reaction indicated that it could occur by photochemical activation of the metal center at room temperature, as shown in the following examples:





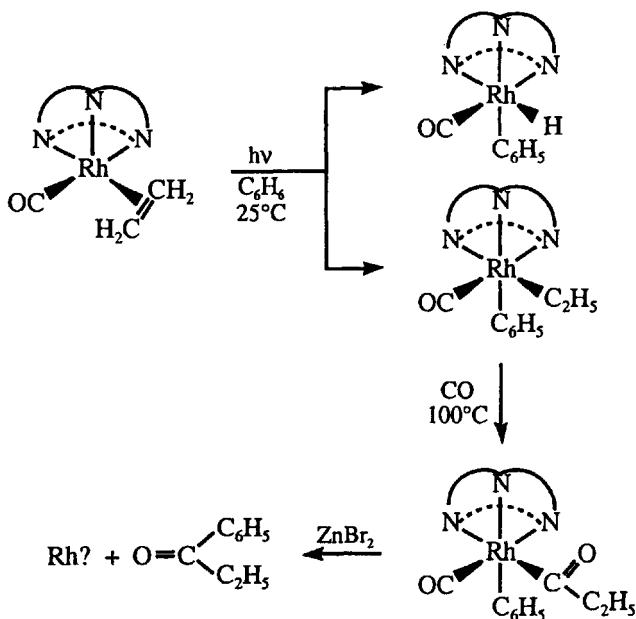
In both cases, a highly reactive unsaturated species is assumed to be generated by photolysis and reacts with the neopentane solvent, as shown. Cyclohexane reacted similarly in both cases. Since the original discovery, many metal complexes have been found to undergo oxidative addition of hydrocarbons,³¹²⁻³¹⁵ and the area has been reviewed recently.³¹⁶⁻³¹⁸

Ghosh and Graham³¹⁹ have shown that $\text{Rh}(\text{HBPz}^*_3)(\text{CO})_2$, where HBPz^*_3 is tris(dimethylpyrazolyl)borato, photolyzes under mild conditions with elimination of CO and oxidative addition of hydrocarbons. In this system, the cyclohexyl hydride complex exchanges with methane, as shown in (5.50), to give the methyl hydride complex.



Ghosh and Graham³²⁰ used $\text{Rh}(\text{HBPz}^*_3)(\text{CO})(\text{C}_2\text{H}_4)$ to prepare the first generation of functionalized products from such reactions, as shown in Scheme 5.39.

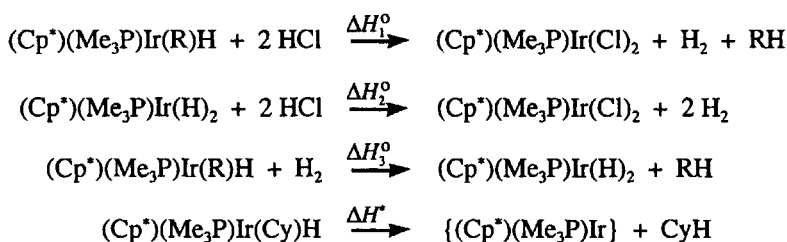
Scheme 5.39



Tanaka and co-workers³²¹ have found that the irradiation of $\text{Rh}(\text{PR}_3)_2(\text{CO})\text{Cl}$ in hydrocarbon solvents under 1 atm of CO can yield aldehyde and alcohol derivatives of the hydrocarbon in a photoassisted catalytic reaction. They attribute the reaction to photochemical dissociation of CO followed by C—H activation and then CO insertion. The observation that the catalysis is improved if the irradiation wavelength is below the absorbance maximum of $\text{Rh}(\text{PR}_3)_2(\text{CO})\text{Cl}$ indicates that photochemistry may be involved in other steps in addition to the decarbonylation. This system has been the subject of a theoretical study.³²²

The energetics of the C—H activation process have been of concern since its discovery. Calorimetric, equilibrium constant and kinetic information have been used to obtain estimates of the M—C and M—H bond energies. In general, these bonds have been found to be stronger than originally anticipated. Nolan et al.³²³ used a combination of calorimetric and kinetic data to estimate these bond enthalpies from the reactions in the following Scheme:

Scheme 5.40



The enthalpy change was measured for the first two reactions in toluene, with $\text{R} = \text{Cy}$ and Ph . When these equations are combined, one obtains the third equation, so that $\Delta H_3^\circ = \Delta H_1^\circ - \Delta H_2^\circ$. With the standard assumptions that the bond energies in the $(\text{Cp}^*)(\text{Me}_3\text{P})\text{Ir}$ fragment are the same in all the species and that the Ir—H bond energy is independent of the other ligands, ΔH_3° is related to the bond dissociation energies, D , by

$$\Delta H_3^\circ = D(\text{H—H}) + D(\text{Ir—R}) - D(\text{Ir—H}) - D(\text{R—H}) \quad (5.51)$$

With experimental values of ΔH_3° and known values for $D(\text{H—H})$, $D(\text{Cy—H})$ and $D(\text{Ph—H})$ of 104, 96 and 110 kcal mol⁻¹, respectively, it is possible to calculate that the bond energy differences, $D(\text{Ir—R}) - D(\text{Ir—H})$, for $\text{R} = \text{Cy}$ and Ph are -23.4 and 6.4 kcal mol⁻¹, respectively. Therefore, the Ir—Ph bond is ~30 kcal mol⁻¹ stronger than the Ir—Cy bond.

In order to estimate the bond energies, Nolan et al. used the ΔH^* for the thermal dissociation of $(\text{Cp}^*)(\text{Me}_3\text{P})\text{Ir}(\text{Cy})\text{H}$, previously determined by Bergman and co-workers.³²⁴ If it is assumed that the transition state is close in energy to the species shown in braces in Scheme 5.40, then

$$\Delta H^* = D(\text{Ir—H}) + D(\text{Ir—Cy}) - D(\text{Cy—H}) \quad (5.52)$$

From the known values of ΔH^* and $D(\text{Cy—H})$ of 36 and 96 kcal mol⁻¹, respectively, one can estimate that the sum of the Ir—H and Ir—Cy bond energies is ~132 kcal mol⁻¹. This sum can be used, along with the difference determined above, to estimated values for $D(\text{Ir—H})$, $D(\text{Ir—Cy})$ and $D(\text{Ir—Ph})$ of 78, 55 and 84 kcal mol⁻¹, respectively. It should be noted that, aside from the other assumptions, these values are upper limits and would be reduced by whatever amount the assumed transition state in Scheme 5.40 is actually stabilized relative to the true transition state. Bergman and co-workers estimated that this stabilization is ≤ 5 kcal mol⁻¹.

The above estimates illustrate that the M—C and M—H bond energies can be large enough to overcome the strength of the C—H bond, so that the oxidative addition of hydrocarbons can be exothermic. General aspects of the bond energies in organometallic species have been reviewed by Simoes and Beachamp and by Hoff.³²⁵ More recent developments, especially for early transition metals, have been discussed by Marks and co-workers.³²⁶

Mechanistic studies on the actual oxidative addition of RH have been limited because of the necessity to generate the unsaturated metal center photochemically. The need for an appropriate "inert" solvent also is a problem.

Marx and Lees³²⁷ studied quantum yields, Φ , for the photochemical reaction of $(\text{Cp})\text{Ir}(\text{CO})_2$ with C_6H_6 in hexafluorobenzene at 20°C and found that Φ shows a saturation effect with increasing $[\text{C}_6\text{H}_6]$ and is independent of $[\text{CO}]$. They concluded that the rate-controlling process is not CO dissociation and suggest that it is an η^5 to η^3 slippage, which then allows complexation of benzene prior to oxidative addition. Drolet and Lees³²⁸ proposed a similar slippage mechanism for the photolysis of $(\text{Cp})\text{Rh}(\text{CO})_2$ in the presence of PPh_3 in decalin at 10°C. Their conclusion is based on the observation that the quantum yield for CO replacement is first-order in $[\text{PPh}_3]$ and unaffected by 9×10^{-3} M CO.

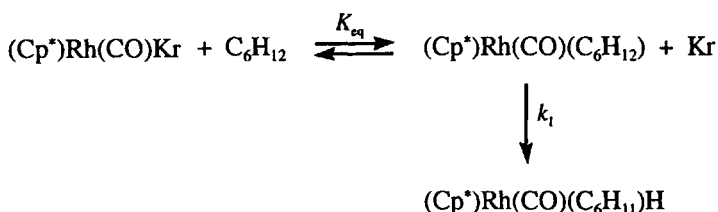
Bergman and co-workers³²⁹ studied the reaction of $(\text{Cp}^*)\text{Rh}(\text{CO})_2$ with C_6H_{12} by IR laser flash kinetics in inert gas solvents. Their conclusions are different from those of Lees and co-workers. At -31°C in xenon, irradiation gives a new species that Bergman and co-workers assign as $(\text{Cp}^*)\text{Rh}(\text{CO})$ or its solvated form, $(\text{Cp}^*)\text{Rh}(\text{CO})\text{Xe}$. A similar but more reactive species is observed in krypton, and when cyclohexane is added to the solution, the $(\text{Cp}^*)\text{Rh}(\text{CO})\text{Kr}$ undergoes oxidative addition with a rate that shows saturation behavior described by

$$k_{\text{exp}} = \frac{\alpha[\text{C}_6\text{H}_{12}]}{[\text{C}_6\text{H}_{12}] + \beta} \quad (5.53)$$

If the mechanism involves rate-controlling dissociation of the solvent followed by cyclohexane addition, then α should be independent of the

nature of the alkane. However, if C_6D_{12} is used, α decreases by a factor of about 20. Therefore, Bergman and co-workers have proposed the mechanism in Scheme 5.41.

Scheme 5.41



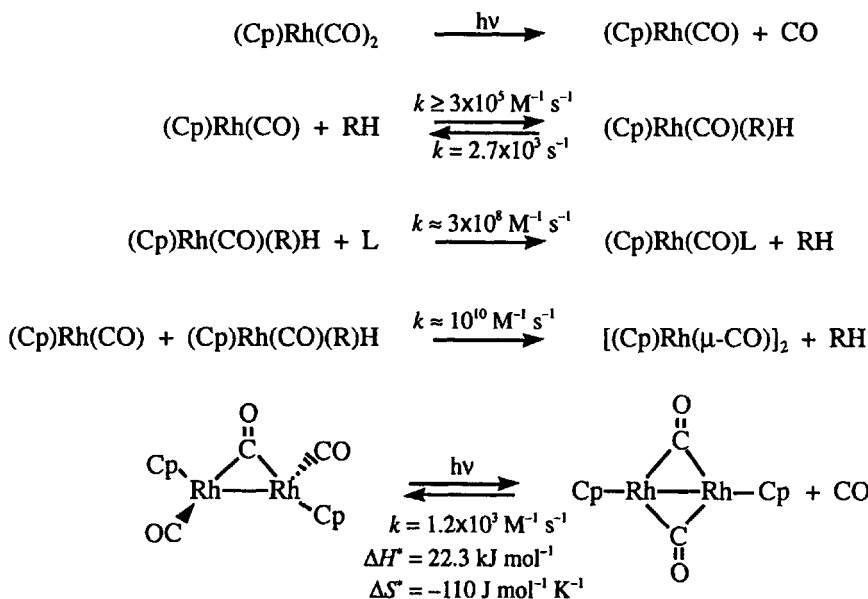
From the preceding expression for k_{exp} , $\alpha = k_1$ and $\beta = [Kr]/K_{eq}$. The nature of the cyclohexane precursor complex is uncertain, but studies with neopentane have allowed the IR spectra of the krypton and neopentane complexes to be resolved.³³⁰

Bergman and co-workers³³¹ analyzed the energy profile for the gas-phase reaction of methane and $(Cp)Rh(CO)$. It was estimated that the formation of the precursor, $(Cp)Rh(CO) \cdot HCH_3$, is exothermic by ~ 10 kcal mol⁻¹, the C—H activation energy is ~ 4.5 kcal mol⁻¹ and the overall exothermicity is ~ 15 kcal mol⁻¹. It also has been found³³² that $(Cp)Co(CO)$ gives no C—H activation and does not even form a precursor complex, but reacts with its parent to give $Co_2(Cp)_2(CO)_3$. The earlier theoretical studies of these systems³³³ have been extended and compared by Siegbahn.³³⁴ This analysis indicates that $(Cp)Co(CO)$ is different and unreactive because it has a triplet ground state that cannot easily cross to the singlet state due to the substantial differences in bond lengths in the two states.

The differences in reactivity of the $M(R_2P(CH_2)_2PR_2)_2$ species, where M is Fe or Ru, generated by photolysis of the corresponding dihydride,³³⁵ might originate from the spin-state factors described by Siegbahn. The Fe derivative has a significantly different electronic spectrum and shows a much greater range of reactivities with nucleophiles, compared to the Ru analogue. This is not a problem for all first-row transition metals because photolysis of $(Cp)Mn(CO)_3$ forms a complex with n-heptane.³³⁶ The authors estimated the Mn—heptane interaction energy to be in the range of 8 to 9 kcal mol⁻¹.

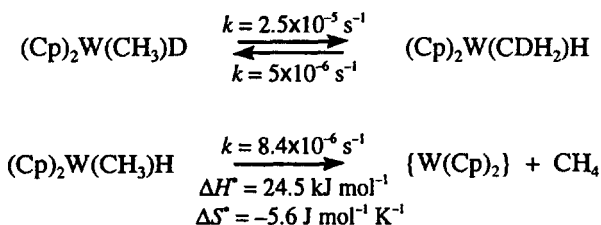
Perutz and co-workers³³⁷ observed the time-resolved photochemistry of $(Cp)Rh(CO)_2$ and $(Rh(Cp)(CO))_2(\mu-CO)$ in the 300-nm region. The results are summarized in Scheme 5.42, where RH is a solvent such as C_6H_{12} or C_6H_6 . The structure of $((Cp)Rh(\mu-CO))_2$ was assigned as shown on the basis of its polarized IR spectrum. The unusual aspects of these observations are the high dimerization rate and the rapid formation of the hydride species of cyclohexane within 400 ns (the product with benzene could be $\eta^2-C_6H_6$).

Scheme 5.42



Studies of the reverse reaction, reductive elimination, have also been used to shed light on the overall reaction mechanism. Norton and co-workers³³⁸ studied the reductive elimination of methane from $(\text{Cp})_2\text{W}(\text{CH}_3)\text{H}$ and found that H exchange into the CH_3 group occurs more rapidly than CH_4 elimination. Such exchange has been observed in other systems, and some rate constants at 48°C in 10% CD_3CN –90% C_6D_6 are given in Scheme 5.43. The CD_3CN serves to trap the $\text{W}(\text{Cp})_2$ as $(\text{Cp})_2\text{W}(\eta^2\text{-CD}_3\text{CN})$, but the kinetics are unaffected by the concentration of CD_3CN .

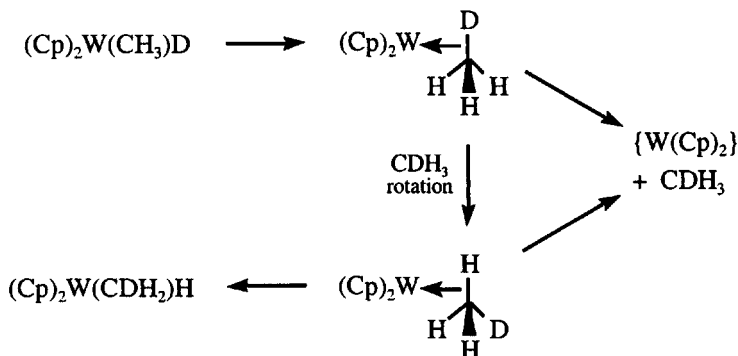
Scheme 5.43



Reductive elimination has an inverse isotope effect, H/D, of 0.75 at 72.6°C . The authors propose that the exchange and reductive elimination proceed through a σ complex that may revert to reactant with exchange or give elimination, as shown in Scheme 5.44. The isotope effect was ascribed

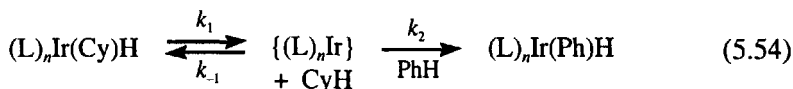
to greater stability of the deuterio σ complex, $(\text{Cp})_2\text{W}(\text{D}-\text{CH}_3)$, compared to $(\text{Cp})_2\text{W}(\text{H}-\text{CH}_3)$ in a preequilibrium before elimination of methane.

Scheme 5.44



A theoretical study by Green and Jardine³³⁹ suggests that the elimination of CH_4 proceeds through an $\eta^2\text{-H,H}$ σ complex. In a later paper, Green et al.³⁴⁰ examined the theoretical aspects of analogous W and Mo systems and the consequences of the fact that the $\text{M}(\text{Cp})_2$ species have triplet electronic ground states.

As already mentioned, Bergman and co-workers³²⁴ studied the kinetics of the following reaction in which $(\text{L})_n$ represents $(\text{Cp}^*)(\text{Me}_3\text{P})$:



The thermolysis was studied over the range of 100 to 140°C in mixtures of benzene and cyclohexane. It was found that the reaction rate is inhibited by added cyclohexane, but unaffected by added PMe_3 . The pseudo-first-order rate constant is given by

$$k_{\text{exp}} = \frac{k_1[\text{C}_6\text{H}_6]}{\left(\frac{k_{-1}}{k_2}\right)[\text{C}_6\text{H}_{12}] + [\text{C}_6\text{H}_6]} \quad (5.55)$$

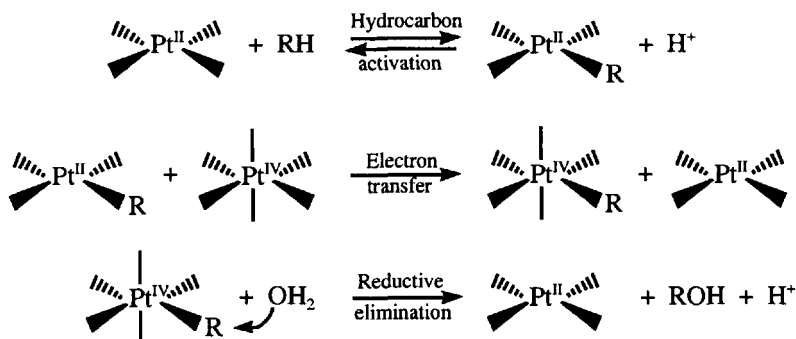
The variation of the pseudo-first-order rate constant with the ratio of $[\text{C}_6\text{H}_6]/[\text{C}_6\text{H}_{12}]$ at 130°C yields values of k_1 and k_2/k_{-1} of $6.6 \times 10^{-5} \text{ s}^{-1}$ and 2.2, respectively. For k_1 , the values of ΔH^\ddagger and ΔS^\ddagger are $35.6 \text{ kcal mol}^{-1}$ and $10 \text{ cal mol}^{-1} \text{ K}^{-1}$, respectively. Isotope labeling showed that the reaction does not involve H transfer to Cp^* and that it is intramolecular because $(\text{L})_n\text{Ir}(\text{C}_6\text{H}_{11})\text{H} + \text{C}_6\text{D}_6$ yields only C_6H_{12} with no isotope scrambling. This seems to eliminate radical mechanisms involving Ir—C bond homolysis. Ring slippage is compatible with the rate law only if the oxidative addition

of C_6H_{12} to the intermediate is competitive with the η^3 to η^5 change to give product; Bergman and co-workers believe that this is unlikely. Isotope exchange was observed in $(L)_nIr(C_6H_{11})D$, with the α position of C_6H_{11} becoming deuterated. Although the value of k_2/k_{-1} may be affected by the change in solvent composition, there is not the marked preference for C_6H_6 which might be expected if an $\eta^2-C_6H_6$ intermediate was formed. Overall, the observations are similar to those of Norton and co-workers, and an analogous σ complex would explain the results.

Oxidative addition normally is favored for metals in low oxidation states. However, it has become increasingly clear that C—H activation also can be observed with M(II) and M(III) species. Probably the first observation of this was the report by Shilov and co-workers³⁴¹ that substitutionally inert aqueous Pt(II) activates alkanes to form alcohols. However, this case was not clearly recognized because of mechanistic uncertainties. Subsequent to much of the detailed work with low oxidation states, examples of oxidative additions to Ir(III)³⁴² and Rh(III)³⁴³ have been documented.

In 1972, Shilov and co-workers³⁴⁴ reported that $PtCl_4^{2-}$ catalysed the oxidation of methane to methanol by $PtCl_6^{2-}$ in aqueous solution at 120°C in the presence of air. This system eventually attracted a great deal of attention due to the simplicity of the conditions. However, mechanistic work came much later, possibly because Pt metal is also formed during the reaction and might be acting as a heterogeneous catalyst. This changed greatly in the 1990s and much of the work has been summarized in a number of reviews on the activation of hydrocarbons by Pt(II).³⁴⁵ The current view is that the main reaction pathway is the one proposed by Shilov and co-workers in 1983,³⁴⁶ as outlined in the following Scheme:

Scheme 5.45



The mechanistic details of each step have been left unspecified. The hydrocarbon activation is believed to proceed through a σ complex. This may undergo oxidative addition to a Pt(IV) alkyl hydride which undergoes reductive elimination of H⁺ to give the Pt(II)—R species. Alternatively, the process has been viewed as a concerted electrophilic addition with transfer

of H^+ to solvent or an anion present in the system. In model studies of the reverse reaction, it has been shown that $Pt(II)-R$ species can protonate on Pt and then release RH . A (diimine) $Pt(CH_3)_2$ model has been studied in detail by Tilset and co-workers.³⁴⁷ It has been argued that microscopic reversibility then requires that the activation step follows the reverse of the protonation process. However, the model studies are done with different ancillary ligands and under different conditions of solvent and temperature than the catalytic process.

The electron-transfer step may follow an inner-sphere or outer-sphere mechanism, as discussed in the next chapter. The main interest here has been to find more economical oxidants than $Pt(IV)$. The trick is to find a species which will oxidize $Pt(II)-R$ but not the $Pt(II)$ catalyst itself.

The final reductive elimination results from nucleophilic attack of H_2O on the coordinated CH_2 of the hydrocarbon. Some of the best evidence for this comes from the findings of Bercaw and co-workers³⁴⁸ that the reaction proceeds with inversion as expected for an S_N2 mechanism.

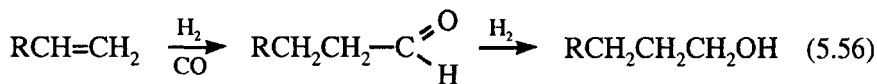
There have been a number of theoretical studies of these types of systems. The reviews noted above may be consulted for details. In general, theory has been equivocal, especially about the activation process. It seems possible that the relative energetics of the oxidative addition and electrophilic substitution pathways depend significantly on the ancillary ligands, the solvent and the other anions present.

5.7 HOMOGENEOUS CATALYSIS BY ORGANOMETALLIC COMPOUNDS

There are a number of processes that appear to be catalyzed by organometallic complexes. The reactions generally involve $C-C$ bond formation and often involve CO and H_2 . In the industrial application,³⁴⁹ the catalyst is often added as a metal salt, and it is assumed that this is transformed to active organometallic species under the reducing conditions of the process. In most cases, there may be several organometallic species present, and the nature of the catalytic mechanism is inferred from the known chemistry of simpler systems and the overall rate law.

5.7.1 Hydroformylation or "Oxo" Reaction

The overall process is described by

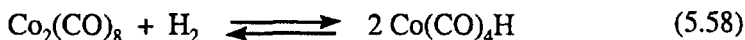


In 1938, Roelen discovered that the reaction is catalyzed by cobalt salts, and, more recently, rhodium catalysts have been developed. The main commercial product is *n*-butanol from propylene, and the major problems

are to avoid branched-chain alcohols and alkanes. The reaction was reviewed by Pruett.³⁵⁰ With a cobalt catalyst, the reaction is done at 100°C to 200°C and at 100 to 500 psi of H₂ + CO. Linear product is favored by lower CO pressures and by "modified cobalt catalysts" that contain phosphines in the reaction mixture. The rate law is given by

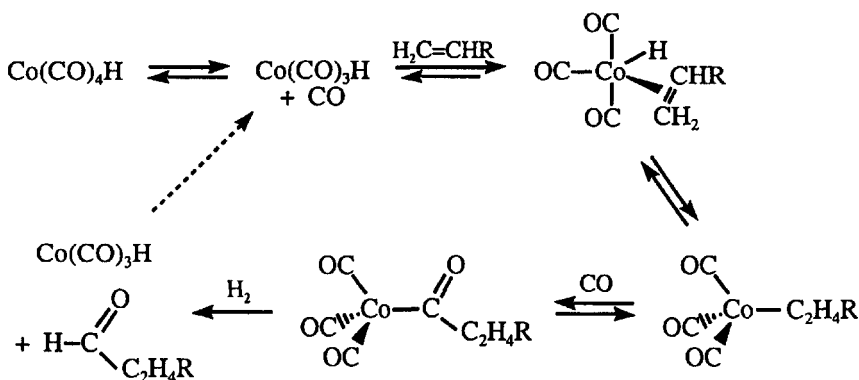
$$\text{Rate} = k[\text{Co}][\text{Alkene}][\text{H}_2][\text{CO}]^{-1} \quad (5.57)$$

It is accepted generally that the important cobalt species is Co(CO)₄H, formed by the following reaction:



The mechanism in Scheme 5.46 was first proposed by Heck and Breslow³⁵¹ and is still thought to be essentially correct. The speciation studies, using high-pressure NMR, of Dwyer et al.,³⁵² and *para*-H₂ results of Duckett and co-workers³⁵³ have provided recent support. The hydride shift in the third step, followed by CO "insertion", are common steps proposed in many such processes. The first dissociation of CO is assumed to be the source of the [CO]⁻¹ term in the rate law.

Scheme 5.46



Under the catalytic conditions, the aldehyde product shown is further reduced to the alcohol. The hydrogenation of the alkene reactant and insertion at the internal CHR group are two undesired side reactions. Modified catalysts, in which a phosphine is added, give better stability, better selectivity to insertion at the terminal H₂C and higher reactivity for aldehyde reduction, but are less reactive and give more hydrogenation of the alkene.

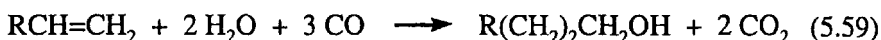
Wilkinson and co-workers³⁵⁴ discovered that rhodium catalysts are effective in this reaction. It is thought that the key intermediate may be

$\text{Rh}(\text{PPh}_3)_2(\text{CO})_2\text{H}$, which may react by dissociative loss of PPh_3 or by direct formation of a π -olefin complex. The reaction could proceed by a hydride route, as proposed in some hydrogenation processes.

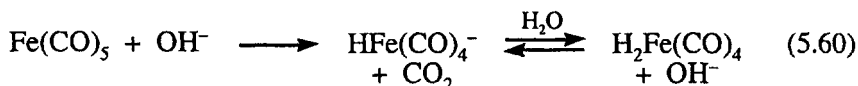
The recent reviews by Damoense et al.³⁵⁵ and Kramer et al.³⁵⁶ give further information on these and related hydroformylation catalytic systems. Stereoselective hydroformylations have been reviewed by Breit.³⁵⁷ There have been many theoretical studies of these systems and much of this work is described, along with new results, in a series of papers by Jiao and co-workers.³⁵⁸

5.7.2 Reppe Synthesis

The Reppe synthesis, shown in reaction (5.59), has a formal resemblance to hydroformylation, with H_2 replaced by H_2O .



The most effective catalysts for the reaction are iron species, often derived from $\text{Fe}(\text{CO})_5$. Pettit and co-workers³⁵⁹ found that the catalyst is most effective at $\text{pH} > 11$. This has been rationalized by the known reactions shown in (5.60) and assuming that $\text{H}_2\text{Fe}(\text{CO})_4$ is the active species that interacts with alkenes.



A quite different process, called Reppe carbonylation, has been used to convert acetylene to acrylic acid esters. The catalysts are carbonyls of iron, cobalt or nickel and the hydrogen source is a hydrogen halide, HX . The process is thought to involve oxidative addition of HX to the metal carbonyl, followed by coordination and insertion of alkyne into the $\text{M}-\text{H}$ bond and insertion of CO into the $\text{M}-\text{C}$ bond. The resulting acyl complex is cleaved by alcohol to produce the ester and the metal hydride catalyst. De Angelis et al.³⁶⁰ have reported a theoretical analysis of the $\text{Ni}(\text{CO})_4$ system.

5.7.3 Fischer-Tropsch Reaction

The Fischer-Tropsch reaction involves the conversion of carbon from coal to hydrocarbons as follows:



The reaction is attractive because of the conversion of cheap materials, coal and water, into valuable hydrocarbons. The process was developed by

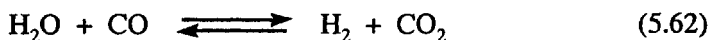
Fischer and Tropsch in 1923 using heterogeneous iron catalysts, and catalyst improvements have continued in a rather unsystematic way ever since. The reaction became uneconomical with the advent of cheap oil after World War II but came into vogue again in the late 1970s as oil prices rose. Only South Africa has operating plants using the process, with the industrial conditions being 200–300°C and a total pressure of ~25 atm.

It was found by Muetterties³⁶¹ and Ford³⁶² and their co-workers that polynuclear carbonyls, such as $\text{Os}_3(\text{CO})_{12}$, $\text{Ru}_3(\text{CO})_{12}$ and $\text{Ir}_4(\text{CO})_{12}$, are effective homogeneous catalysts. The early work was reviewed by Herrmann,³⁶³ and a mechanism involving a metal carbene, $\text{M}=\text{CH}_2$, and $\eta^2\text{-CO}$ was suggested by Masters.³⁶⁴ The $\eta^2\text{-CO}$ was proposed to weaken the CO triple bond and make it susceptible to reduction.

Maitlis³⁶⁵ has reviewed the homogeneous and heterogeneous systems and noted that the former produce mainly oxygenated products, such as alcohols and esters. Most of the recent work on the Fischer–Tropsch reaction has focused on heterogeneous catalysts. The mechanism(s) of the later are mainly inferred from isotope labeling and product distributions. The observations and mechanistic proposals of the Sheffield group have been summarized by Maitlis.³⁶⁶ However, there is still some controversy about the heterogeneous pathways.^{367,368}

5.7.4 Water Gas Shift Reaction

The water gas shift reaction involves the following process:

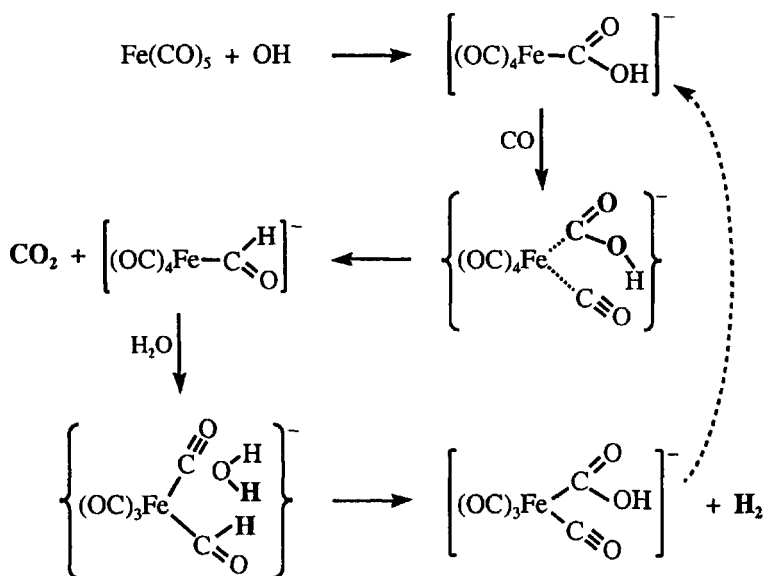


The reaction increases the H_2 content of syngas, $\text{CO} + \text{H}_2$ mixtures, and can be used in conjunction with the Fischer–Tropsch process. There has been renewed interest in this reaction as a source of H_2 for fuel cells. Metal carbonyls of Fe, Ru and Rh, under either acidic or basic conditions, are effective homogeneous catalysts.³⁶⁹ Fachinetti and co-workers have investigated the speciation and reactivity of $\text{Rh}_4(\text{CO})_{12}$ ³⁷⁰ and $\text{Ru}_3(\text{CO})_{12}$ ³⁷¹ under acidic conditions. These systems are complicated by reactions such as disproportionation and complexation of the catalyst by the conjugate base of the acid.

The theoretical study by Torrent et al.³⁷² led to a mechanistic energy profile that seems inconsistent with a first-order dependence of the rate on the pressure of CO. This and other theoretical aspects are discussed in a review by the same authors.³⁷³ The classic mechanism³⁷⁴ involves attack of OH^- on coordinated CO to give $\text{M}-\text{CO}_2\text{H}^-$, which is protonated by H_2O and loses CO_2 to form $\text{M}(\text{H})_2$. Then, H_2 is reductively eliminated, and CO added to return the catalyst. More recently, a theoretical analysis of the alkaline $\text{Fe}(\text{CO})_5$ system by Barrows³⁷⁵ has led to the mechanism shown in Scheme 5.47. In this Scheme, the species in braces show the composition

of the proposed transition states and atoms in bold are proceeding to the products, also shown in bold.

Scheme 5.47



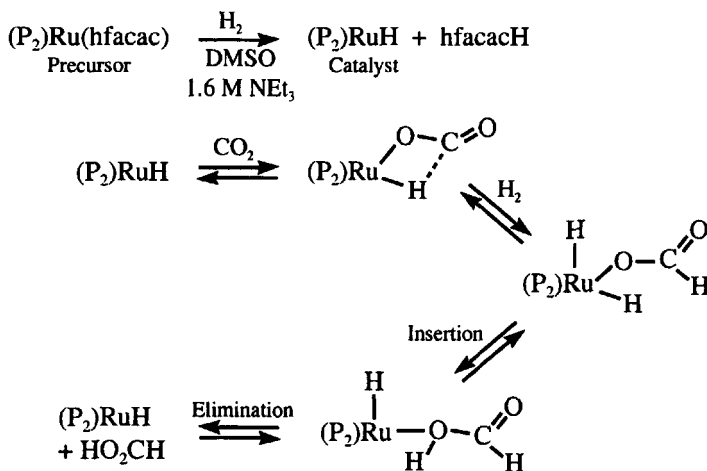
The last step, which involves addition of H_2O and elimination of H_2 , is calculated to be the rate-limiting one, so that the rate will be first-order in the concentration of CO .

A related reaction of interest is the hydrogenation of CO_2 to form formic acid. Thermodynamics dictates that the reaction will not go to completion under normal conditions, but is much more favorable in basic solution where formate ion is the product. The review by Jessop et al.³⁷⁶ documents a number of the catalytic systems and the possible mechanisms. Noyori and co-workers³⁷⁷ described a particularly reactive system using $(\text{Me}_3\text{P})_4\text{Ru}(\text{H})_2$ in supercritical CO_2 . Sakaki and co-workers have presented theoretical analyses of the system with PH_3 ³⁷⁸ and PMe_3 ³⁷⁹ as the phosphine ligands. It should be noted that the calculated energy profiles for these systems appear strange because the intermediates and transition states are all lower in energy than either the reactants or the products. The authors conclude that the rate determining step is insertion of CO_2 into the $\text{Ru}(\text{II})\text{—H}$ bond, but it actually appears to be the elimination of HCO_2H to form the products.

Leitner and co-workers³⁸⁰ studied the reaction in DMSO with the base NEt_3 and the precatalyst $(\text{P})_2\text{Ru}(\text{hfacac})$, where $(\text{P})_2 = \text{Ph}_2\text{P}(\text{CH}_2)_3\text{PPh}_2$ and $\text{hfacac} = \text{HC}(\text{C}(\text{O})\text{CF}_3)_2^-$. The authors also did a theoretical analysis of the reaction in which the phosphine chelate was replaced by *cis*- $(\text{PH}_3)_2$. The initial rate measurements indicate that the reaction is first-order in the concentrations of catalyst, CO_2 and H_2 , but shows saturation behavior for

all of these reagents. The latter may be due to mass transfer limitations at the higher concentrations. The authors suggested the reaction sequence shown in the following Scheme, where approximate structures derived from their theoretical analysis also are shown:

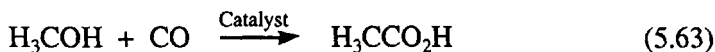
Scheme 5.48



The sequence of reactions with $(\text{P}_2)\text{RuH}$, i.e. CO_2 addition, H_2 addition, insertion and elimination, is analogous to that calculated by Sakaki and co-workers for the *cis*- $(\text{Me}_3\text{P})_3\text{Ru}(\text{H})_2$ system, and the calculated structures of the various intermediates have some clear similarities. Leitner and co-workers also noted that the rate decreases with decreasing concentration and basicity of the amine and with its increasing steric bulk. In the same study, Hutschka and Dedieu suggested, on the basis of theory, that the amine assists in the H-transfer of the insertion step.

5.7.5 Methanol Carbonylation

The major source of the world's acetic acid is the homogeneously metal-catalysed carbonylation of methanol.



The Monsanto process, which was commercialized in 1970, uses a rhodium catalyst, while the more recent Cativa process uses an iridium one. Iodide complexes and methyl iodide are key players in both processes, and the essential features of the catalytic cycles are the same. The reaction pathways for the rhodium system were elucidated by Forster³⁸¹ and have been summarized in several reviews.³⁸² Maitlis and co-workers have studied the iridium system in detail and the major pathways deduced from a recent study³⁸³ are outlined in the following Scheme:

The iridium and rhodium catalytic cycles are similar, but the former undergoes $\sim 10^2$ times faster oxidative addition, while the latter undergoes $\sim 10^6$ times faster migration of the methyl group. The numerous theoretical studies of these systems are summarized in recent reports by Cheong and Ziegler,¹⁹³ and by Bo and co-workers.³⁸⁶ There is general agreement that this involves nucleophilic attack of the metal complex on the methyl group. Cheong and Ziegler conclude that the lower barrier with iridium is largely due to relativistic stabilization of the Ir—CH₃ bond.

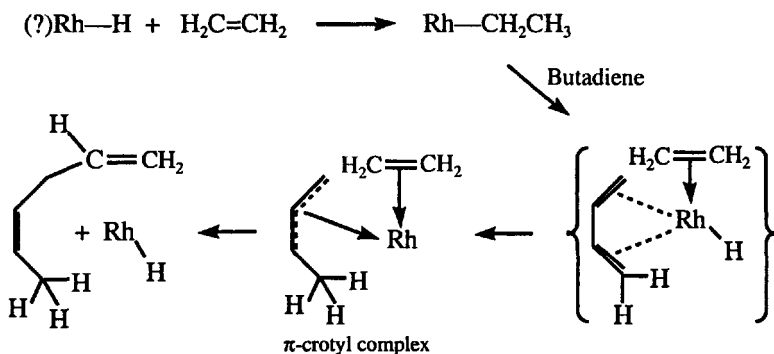
5.7.6 Olefin Codimerization and Metathesis

The purpose of the ethylene–butadiene codimerization process is to produce *trans*-1,4-hexadiene from ethylene and butadiene, as shown in reaction (5.65). The product is an important monomer in synthetic rubber production.



The reaction is catalyzed in the presence of RhCl₃ in aqueous HCl and has been studied kinetically by Cramer.³⁸⁷ It is proposed that under the reducing influence of the ethylene, an unspecified rhodium hydride species (Rh(Cl)₂H ?) forms as the catalyst and reacts with the ethylene to give an η^1 -ethyl complex that may be converted to the η^2 -ethyl complex by complexing with butadiene. This is followed by H transfer to give a π -crotyl complex and finally the desired product, as shown in Scheme 5.50.

Scheme 5.50



Tolman³⁸⁸ found that $\text{Ni}(\text{P}(\text{OEt})_3)_4\text{H}^+$ also is a good catalyst for this reaction, and showed that it reacts by dissociation of a phosphite ligand to form a π -crotyl complex with butadiene. Then, another phosphite is lost and the π -ethylene + π -crotyl complex forms and rearranges similarly to the Rh system in Scheme 5.50. The area of organometallic catalysis of ethylene dimerization and polyolefin formation has been reviewed recently

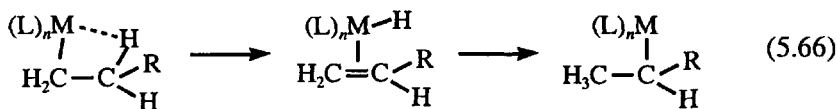
controlled hydrolysis of $\text{Al}(\text{CH}_3)_3$.³⁹¹ Two mechanisms are shown for the initiation step. The Cossee mechanism is essentially an insertion into the $\text{M}-\text{CH}_3$ bond and may proceed through an η^2 -olefin complex. Lavery and Rooney³⁹³ and Brookhart and Green³⁹⁴ modified this mechanism by adding an α -agostic interaction, which Brintzinger and co-workers³⁹⁵ have suggested would assist the insertion and improve the stereoselectivity. Grubbs and Coates³⁹⁶ have questioned the effectiveness of this interaction. The Trigger mechanism³⁹⁷ suggests that a second olefin monomer is involved to assist the insertion.

The propagation step is another olefin insertion, but it should be noted that it might insert at the CH_2R center and introduce irregularity into the polymer chain. Two of many possible termination steps are shown. The first is a β -hydride shift that yields a terminal olefin product. The second can result when H_2 is introduced into the system for the purpose of shortening the polymer length and yields an alkane.

The kinetic behavior of these systems can be quite varied, with brief induction periods and decreasing reactivity with time often being observed. Ion pairing effects also have been observed. Much of this work is summarized in detail by Resconi et al.³⁹⁰ One notable feature is that the rate often is between first- and second-order in the concentration of the monomer.³⁹⁸ This is not expected from the simple Cossee mechanism if initiation is the rate-controlling step, but it is consistent with the Trigger mechanism. Brintzinger and co-workers³⁹⁹ have provided some theoretical justification for the Trigger mechanism, but it is more often ignored. The greater than first-order dependence also has been explained by more complex kinetic models involving ion pairing,⁴⁰⁰ mixed single and double monomer coordination⁴⁰¹ or a two-state catalyst.⁴⁰²

There have been many theoretical approaches to these systems and the results have been summarized in recent papers.^{403,404} Unfortunately, these studies generally assume that the rate is first-order in the concentration of the monomer, which seems to be the exception rather than the rule.³⁹⁰

There has been increasing interest in polymerization catalysis by complexes of the late transition metals, such as nickel and palladium.^{389,405,406} The chain propagation mechanism is similar to that in Scheme 5.51, but there are other mechanistic differences. The η^2 -olefin complexes are more stable and tend to be the resting state and the migratory insertion is the rate-limiting step. There also is a greater tendency to reversible β -hydride transfer and movement of the metal along the polymer chain, as shown in the following reaction:

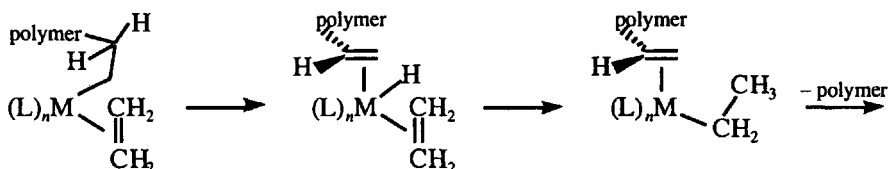


The result of this movement is a more branched-chain polymer. This can

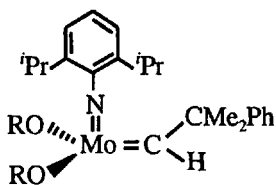
be overcome by increasing the monomer concentration so that it complexes with the reactant in reaction (5.66) competitively with the β -hydride transfer.

The termination step for these systems can be displacement of the η^2 -olefin chain in the middle species in reaction (5.66) by a monomer. An alternative, suggested by theory, is that the resting state undergoes β -hydride transfer from the polymer chain and then β -hydride transfer to the monomer and loss of the polymer, as shown in the following Scheme:

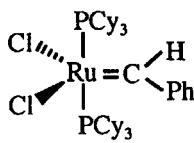
Scheme 5.52



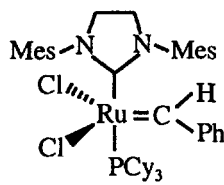
In recent years, several organometallic complexes have generated a great deal of activity in the general area of olefin coupling reactions. The predominant examples of the systems are shown below, where Mes is 1,3,5-trimethylbenzene:



A



B

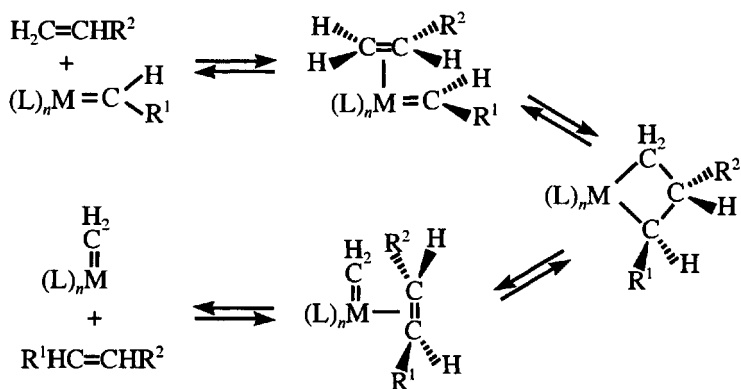


C

The examples shown are more common variants of species with a range of organic substituents, but they are all metal-carbenes. The molybdenum systems, **A**, were developed by Schrock and co-workers,⁴⁰⁷ while the ruthenium systems were developed by Grubbs and co-workers and are commonly known as first-generation, **B**,⁴⁰⁸ and second-generation, **C**,⁴⁰⁹ Grubbs' catalysts. The N-heterocyclic carbene, NHC, ligand in the latter imparts much greater reactivity. The molybdenum systems show high reactivity, even toward sterically crowded olefins, but are sensitive to O₂, moisture, and protic and polar functional groups. The ruthenium compounds are much more stable and more tolerant of functional groups, and the second generation systems rival the activity of the molybdenum complexes. Forman et al.⁴¹⁰ have reported that the activity and selectivity of the **B** and **C** systems are greatly improved by the addition of phenol.

The simplest reaction brought about by these species is olefin metathesis, as illustrated in a general way in the following Scheme:

Scheme 5.53



The reaction pathway shown is the widely accepted Chauvin mechanism⁴¹¹ which involves a metalacycle formed by C—C bond formation within an η^2 -olefin-carbene complex. It should be noted that the metal complex is not really a catalyst, but rather a promoter, because it is transformed into a new carbene. Theory suggests⁴¹² that the carbene fragment and the olefin should be parallel, as shown in the Scheme, for the C—C bond to form. It also suggests that a great deal of the added reactivity of the C systems is derived from the NHC enforcing this orientation on the carbene through steric interactions.

With regard to the mechanisms, several theoretical studies⁴¹³ indicate that for the A systems, the formation of the metalacycle has a low energy barrier. However, for B and C, initial dissociation of the PCy_3 must occur before coordination of the olefin. Grubbs and co-workers⁴¹⁴ have described the various kinetic scenarios that can result when phosphine dissociation is slow or when its recoordination is competitive with binding of the olefin.

Finally, it should be noted that the metathesis reaction in Scheme 5.53 is not a synthetic miracle. However, there are a number of very useful synthetic applications of these species, including ring-closing metathesis, RCM, and ring-opening metathesis polymerization, ROMP. These have been well documented in a recent review by Nicolau et al.⁴¹⁵

References

1. Darensbourg, D. J. *Adv. Organomet. Chem.* **1982**, *21*, 113.
2. Basolo, F. *Coord. Chem. Rev.* **1982**, *49*, 7.
3. Howell, J. A. S.; Burkinshaw, P. M. *Chem. Rev.* **1983**, *83*, 557.
4. Basolo, F. *J. Organomet. Chem.* **1990**, *383*, 579.
5. Shi, Q.-Z.; Richmond, T. G.; Trogler, W. C.; Basolo, F. *J. Am. Chem. Soc.* **1984**, *106*, 71.
6. Day, J. P.; Basolo, F.; Pearson, R. G. *J. Am. Chem. Soc.* **1968**, *90*, 6927.

7. Bernardi, F.; Bottoni, A.; Nicasastro, M.; Rossi, I. *Organometallics* **2000**, *19*, 2170; Bottoni, A.; Miscione, G. P.; Novoa, J. J.; Prat-Resina, X. *J. Am. Chem. Soc.* **2003**, *125*, 10412.
8. Noack, K.; Ruch, M. *J. Organomet. Chem.* **1969**, *17*, 309.
9. Shen, J.-K.; Gao, Y.-C.; Shi, Q.-Z.; Basolo, F. *Inorg. Chem.* **1989**, *28*, 4304.
10. Huq, R.; Pöe, A. J.; Chawla, S. *Inorg. Chim. Acta* **1980**, *38*, 121.
11. Poliakoff, M.; Turner, J. J. *J. Chem. Soc., Faraday Trans. 2* **1974**, *70*, 93.
12. Li, J.; Schreckenbach, G.; Ziegler, T. *J. Am. Chem. Soc.* **1995**, *117*, 486.
13. Ehlers, A. W.; Frenking, G. *Organometallics* **1995**, *14*, 423.
14. King, R. B. *J. Inorg. Nucl. Chem.* **1969**, *5*, 906.
15. Hyla-Krispin, I.; Grimme, S. *Organometallics* **2004**, *23*, 5581; Diedrich, C.; Lüchow, A.; Grimme, S. *J. Chem. Phys.* **2005**, *122*, 021101.
16. Brower, K. R.; Chen, T.-S. *Inorg. Chem.* **1973**, *12*, 2198.
17. Wojcicki, A.; Basolo, F. *J. Am. Chem. Soc.* **1961**, *83*, 527.
18. Kaesz, H. D.; Bau, R.; Hendrikson, D.; Smith, M. *J. Am. Chem. Soc.* **1967**, *89*, 2844; Johnson, B. F. G.; Lewis, J.; Meiser, J. R.; Robinson, B. H.; Robinson, P. W.; Wojcicki, A. *J. Chem. Soc. A* **1968**, 522; Robinson, P. W.; Cohen, M. A.; Wojcicki, A. *Inorg. Chem.* **1971**, *10*, 2081; Berry, A.; Brown, T. L. *Inorg. Chem.* **1972**, *11*, 1165.
19. Atwood, J. D.; Brown, T. L. *J. Am. Chem. Soc.* **1975**, *97*, 3380.
20. Lichtenberger, D. L.; Brown, T. L. *J. Am. Chem. Soc.* **1975**, *97*, 3380.
21. Davy, R. D.; Hall, M. B. *Inorg. Chem.* **1989**, *28*, 3524.
22. Wilms, M. P.; Baerends, E. J.; Rosa, A.; Stufkens, D. J. *Inorg. Chem.* **1997**, *36*, 1541.
23. Macgregor, S. A.; MacQueen, D. *Inorg. Chem.* **1999**, *38*, 4868.
24. Tolman, C. A. *Chem. Rev.* **1977**, *77*, 313.
25. Chen, L.; Poë, A. J. *Inorg. Chem.* **1989**, *28*, 3641.
26. Wilson, M. R.; Liu, H.; Prock, A.; Giering, W. P. *Organometallics* **1993**, *12*, 2044, and references therein; Lorsbach, B. A.; Bennett, D. M.; Prock, A.; Giering, W. P. *Organometallics* **1995**, *14*, 869.
27. Bartik, T.; Himmler, T.; Schulte, H.-G.; Seevogel, K. *J. Organomet. Chem.* **1984**, *272*, 29.
28. Fernandez, A. L.; Reyes, C.; Prock, A.; Giering, W. P. *J. Chem. Soc., Perkin Trans. 2* **2000**, 1033.
29. Romeo, R.; Carnabuci, S.; Plutino, M. R.; Romeo, A.; Rizzato, S.; Albinati, A. *Inorg. Chem.* **2005**, *44*, 1248; Buntén, K. A.; Moreno, C.; Pöe, A. J. *Dalton Trans.* **2005**, 1416; Buntén, K. A.; Pöe, A. J.; Stomnova, T. A. *Dalton Trans.* **2005**, 3780.
30. Babij, C.; Chen, L.; Koshevoy, I. O.; Pöe, A. J. *Dalton Trans.* **2004**, 833.
31. Joerg, S.; Drago, R. S.; Sales, J. *Organometallics* **1998**, *17*, 589, and references therein.
32. Fernandez, A. L.; Tsung, Y.-L.; Reyes, C.; Prock, A.; Giering, W. P. *Organometallics* **1998**, *17*, 3169.
33. Brown, T. L.; Lee, K. J. *Coord. Chem. Rev.* **1993**, *128*, 89, and references therein.

34. Stahl, L.; Trakarnpruk, W.; Freeman, J. W.; Arif, A. M.; Ernst, R. D. *Inorg. Chem.* **1995**, *34*, 1810.
35. Smith, J. M.; Coville, N. J.; Cook, L. M.; Boeyens, J. C. A. *Organometallics* **2000**, *19*, 5273; Smith, J. M.; Coville, N. J. *Organometallics* **2001**, *20*, 1210.
36. White, D.; Taverner, B. C.; Leach, P. G. L.; Coville, N. J. *J. Compt. Chem.* **1993**, *36*, 1042.
37. Dunne, B. J.; Morris, R. B.; Orpen, A. G. *J. Chem. Soc., Dalton Trans.* **1991**, 653.
38. Matín, A.; Orpen, A. G. *J. Am. Chem. Soc.* **1996**, *118*, 1464.
39. Cooney, K. D.; Cundari, T. R.; Hoffman, N. W.; Pittard, K. A.; Temple, M. D.; Zhao, Y. *J. Am. Chem. Soc.* **2003**, *125*, 4318.
40. Woska, D.; Prock, A.; Giering, W. P. *Organometallics* **2000**, *19*, 4629.
41. Frenking, G.; Wichman, K.; Fröhlich, N.; Grobe, J.; Golla, W.; Van, D. L.; Krebs, B.; Läge, M. *Organometallics* **2002**, *21*, 2921.
42. Zhang, S.; Shen, J. K.; Basolo, F.; Ju, T. D.; Lang, R. F.; Kiss, G.; Hoff, C. D. *Organometallics* **1994**, *13*, 3692.
43. Schuster-Woldan, H. G.; Basolo, F. *J. Am. Chem. Soc.* **1966**, *88*, 1657.
44. Cramer, R.; Seiwel, L. P. *J. Organomet. Chem.* **1975**, *92*, 245; Bleeke, J. R.; Peng, W. J. *Organometallics* **1986**, *5*, 635.
45. O'Connor, J. M.; Casey, C. P. *Chem. Rev.* **1987**, *87*, 307.
46. Simanko, W.; Tesch, W.; Sapunov, V. N.; Mereiter, K.; Schmid, R.; Kirchner, K.; Coddington, J.; Wherland, S. *Organometallics* **1998**, *17*, 5674.
47. Van Rensburg, W. J.; Grové, C.; Steynberg, J. P.; Stark, K. L.; Huyser, J. J.; Steynberg, P. J. *Organometallics* **2004**, *23*, 1207.
48. Rerek, M. E.; Ji, L.-N.; Basolo, F. *J. Chem. Soc., Chem. Commun.* **1983**, 1208.
49. Ji, L.-N.; Rerek, M. E.; Basolo, F. *Organometallics* **1984**, *3*, 740.
50. Casey, C. P.; O'Connor, J. M. *Organometallics* **1985**, *4*, 384; Bang, H.; Lynch, T. J.; Basolo, F. *Organometallics* **1992**, *11*, 40.
51. Habib, A.; Tanke, R. S.; Holt, E. M.; Crabtree, R. H. *Organometallics* **1989**, *8*, 1225.
52. Jones, D. J.; Mawby, R. J. *Inorg. Chim. Acta* **1972**, *6*, 157.
53. Gamasa, M. P.; Gimeno, J.; Gonzalez-Bernardo, C.; Martin-Vaca, B. M.; Monti, D.; Bassetti, M. *Organometallics* **1996**, *15*, 302.
54. Pevear, K. A.; Banaszak Holl, M. M.; Carpenter, G. B.; Rieger, A. L.; Sweigart, D. A. *Organometallics* **1995**, *14*, 512.
55. Bonifaci, C.; Cecon, A.; Santi, S.; Mealli, C.; Zoellner, R. W. *Inorg. Chim. Acta* **1995**, *240*, 541.
56. Calhorda, M. J.; Gamella, C. A.; Gonçalves, I. S.; Herdweck, E.; Romao, C. C.; Veiros, L. F. *Organometallics* **1998**, *17*, 2597.
57. Bradley, C. A.; Flores-Torres, S.; Lobkovsky, E.; Abruna, H. D.; Chirik, P. J. *Organometallics* **2004**, *23*, 5332.
58. Bradley, C. A.; Keresztes, I.; Lobkovsky, E.; Young, V. G.; Chirik, P. J. *J. Am. Chem. Soc.* **2004**, *126*, 16937.
59. Veiros, L. F. *Chem. Eur. J.* **2005**, *11*, 2505.

60. Kowaleski, R. M.; Basolo, F.; Trogler, W. C.; Ernst, R. D. *J. Am. Chem. Soc.* **1986**, *108*, 6046; Kowaleski, R. M.; Basolo, F.; Trogler, W. C.; Gedridge, R. W.; Newbound, T. D.; Ernst, R. D. *J. Am. Chem. Soc.* **1987**, *109*, 4860.
61. Casey, C. P.; Vos, T. E.; Brady, J. T.; Hayashi, R. K. *Organometallics* **2003**, *22*, 1183.
62. Morris, D. E.; Basolo, F. *J. Am. Chem. Soc.* **1968**, *90*, 2531.
63. Darensbourg, D. J.; Darensbourg, M. Y.; Walker, N. *Inorg. Chem.* **1981**, *20*, 1918; Cotton, F. A.; Darensbourg, D. J.; Kolthammer, B. W. S.; Kudasroski, R. *Inorg. Chem.* **1982**, *21*, 1656.
64. Darensbourg, D. J.; Klausmeyer, K. K.; Reibenspies, J. H. *Inorg. Chem.* **1995**, *34*, 4933.
65. Darensbourg, D. J.; Klausmeyer, K. K.; Reibenspies, J. H. *Inorg. Chem.* **1996**, *35*, 1529; *Ibid.* **1996**, *35*, 1535.
66. Darensbourg, D. J.; Frost, B. J.; Derecskei-Kovacs, A.; Reibenspies, J. H. *Inorg. Chem.* **1999**, *38*, 4715.
67. Darensbourg, D. J.; Draper, J. D.; Larkins, D. L.; Frost, B. J.; Reibenspies, J. H. *Inorg. Chem.* **1998**, *37*, 2538.
68. Rossi, A. G.; Hoffmann, R. *Inorg. Chem.* **1975**, *14*, 365.
69. Lichtenberger, D. L.; Brown, T. L. *J. Am. Chem. Soc.* **1978**, *100*, 366.
70. Poliakoff, M. *Inorg. Chem.* **1976**, *15*, 2892.
71. Cotton, F. A.; Darensbourg, D. J.; Klein, S.; Kolthammer, B. W. S. *Inorg. Chem.* **1982**, *21*, 294.
72. Ewen, J. E.; Darensbourg, D. J. *J. Am. Chem. Soc.* **1975**, *97*, 6874.
73. Kubas, G. J. *Acc. Chem. Res.* **1988**, *21*, 120.
74. Gonzalez, A. A.; Zhang, K.; Hoff, C. D. *Inorg. Chem.* **1989**, *28*, 4285.
75. Graham, J. R.; Angelici, R. J. *Inorg. Chem.* **1967**, *6*, 992.
76. Memering, M. N.; Dobson, G. R. *Inorg. Chem.* **1973**, *12*, 2490.
77. Halverson, D. E.; Reisner, G. M.; Dobson, G. R.; Bernal, I.; Mulcahy, T. L. *Inorg. Chem.* **1982**, *21*, 4285.
78. Macholdt, H.-T.; van Eldik, R.; Dobson, G. R. *Inorg. Chem.* **1986**, *25*, 1914.
79. Cao, S.; Reddy, K. B.; Eyring, E. M.; van Eldik, R. *Organometallics* **1994**, *13*, 91.
80. Grevels, F.-W.; Kayran, C.; Özkar, S. *Organometallics* **1994**, *13*, 2937, and references therein.
81. Dücker-Benfer, C.; Grevels, F.-W.; van Eldik, R. *Organometallics* **1998**, *17*, 1669.
82. Connor, J. A.; Riley, P. I. *J. Organomet. Chem.* **1975**, *94*, 55.
83. Bunten, K. A.; Farrar, D. H.; Poč, A. J.; Lough, A. J. *Organometallics* **2000**, *19*, 3674.
84. Romeo, R.; Monsu' Scolaro, L.; Plutino, M. R.; Romeo, A.; Nicolo, F.; Del Zotto, A. *Eur. J. Inorg. Chem.* **2002**, 629, and references therein.
85. Slone, C. S.; Weimberg, D. A.; Mirkin, C. A. *Prog. Inorg. Chem.* **1999**, *48*, 233; Müller, C.; Vos, D.; Jutzi, P. *J. Organomet. Chem.* **2000**, *600*, 127.
86. Jutzi, P. *Eur. J. Inorg. Chem.* **1998**, 663.
87. Siemling, U. *Chem. Rev.* **2000**, *100*, 1495.

88. Butenschoen, H. *Chem. Rev.* **2000**, *100*, 1527.
89. Alvarez, P.; Lastra, E.; Gimeno, J.; Brana, P.; Sordo, J. A.; Gomez, J.; Falvello, L. R.; Bassetti, M. *Organometallics* **2004**, *23*, 2956; Bassetti, M.; Alvarez, P.; Gimeno, J.; Lastra, E. *Organometallics* **2004**, *23*, 5127.
90. Bassetti, M.; Capone, A.; Mastrofrancesco, L.; Salamone, M. *Organometallics* **2003**, *22*, 2535; Bassetti, M.; Capone, A.; Salamone, M. *Organometallics* **2004**, *23*, 247.
91. Holliday, B. J.; Jeon, Y.-M.; Mirkin, C. A.; Stern, C. L.; Incarvito, C. D.; Zakharov, L. N.; Sommer, R. D.; Rheingold, A. L. *Organometallics* **2002**, *21*, 5713.
92. Deckers, P. J. W.; Hessen, B.; Teuben, J. H. *Organometallics* **2002**, *21*, 5122.
93. Tobisch, S.; Ziegler, T. *Organometallics* **2004**, *23*, 4077.
94. Wawersik, H.; Basolo, F. *Inorg. Chim. Acta* **1969**, *3*, 113.
95. Fawcett, J. P.; Poë, A.; Sharma, K. R. *J. Am. Chem. Soc.* **1976**, *98*, 1401; Fawcett, J. P.; Poë, A. *J. Chem. Soc., Dalton Trans.* **1977**, 1302.
96. Wegman, R. W.; Olsen, R. J.; Gard, D. R.; Faulkner, L. R.; Brown, T. L. *J. Am. Chem. Soc.* **1981**, *103*, 6089.
97. Sonnenberger, D.; Atwood, J. D. *J. Am. Chem. Soc.* **1980**, *102*, 3484.
98. Coville, N. J.; Stolzenberg, A. M.; Muettterties, E. L. *J. Am. Chem. Soc.* **1983**, *105*, 2499.
99. Poë, A. *Inorg. Chem.* **1981**, *20*, 4029, 4032.
100. Atwood, J. D. *Inorg. Chem.* **1981**, *20*, 4031.
101. Sonnenberger, D. C.; Atwood, J. D. *J. Am. Chem. Soc.* **1982**, *104*, 2113; Darensbourg, D. J.; Baldwin-Zuschke, B. J. *J. Am. Chem. Soc.* **1982**, *104*, 3906.
102. Darensbourg, D. J.; Zalewski, D. J.; Delford, T. *Organometallics* **1984**, *3*, 1210.
103. Kennedy, J. R.; Basolo, F.; Trogler, W. C. *Inorg. Chim. Acta* **1988**, *146*, 75.
104. Poë, A. J.; Sekhar, V. C. *Inorg. Chem.* **1985**, *24*, 4376.
105. Chen, L.; Poë, A. J. *Can. J. Chem.* **1989**, *67*, 1924.
106. Brodie, M. J.; Poë, A. J. *Can. J. Chem.* **1995**, *73*, 1187.
107. Shen, J.-K.; Basolo, F. *Organometallics* **1993**, *12*, 2942.
108. Neubrand, A.; Poë, A. J.; van Eldik, R. *Organometallics* **1995**, *14*, 3249.
109. Babij, C.; Chen, H.; Chen, L.; Poë, A. J. *Dalton Trans.* **2003**, 3184.
110. Bunten, K. A.; Farrar, D. H.; Poë, A. J. *Organometallics* **2003**, *22*, 3448.
111. Shen, J.-K.; Basolo, F.; Nombel, P.; Lugan, N.; Lavigne, G. *Inorg. Chem.* **1996**, *35*, 755.
112. Poë, A. J.; Farrar, D. H.; Zheng, Y. *J. Am. Chem. Soc.* **1992**, *114*, 5146.
113. Farrar, D. H.; Poë, A. J.; Zheng, Y. *J. Am. Chem. Soc.* **1994**, *116*, 6252.
114. Absi-Halabi, M.; Brown, T. L. *J. Am. Chem. Soc.* **1977**, *99*, 2983.
115. Byers, B. H.; Brown, T. L. *J. Am. Chem. Soc.* **1977**, *99*, 2527.
116. Byers, B. H.; Brown, T. L. *J. Organomet. Chem.* **1977**, *127*, 181.
117. Sweany, R. L.; Halpern, J. *J. Am. Chem. Soc.* **1977**, *99*, 8335.
118. Bullock, R. M.; Samsel, E. G. *J. Am. Chem. Soc.* **1991**, *112*, 6886.
119. Herrinton, T. R.; Brown, T. L. *J. Am. Chem. Soc.* **1985**, *107*, 5700.

120. McCullen, S. B.; Walker, H. W.; Brown, T. L. *J. Am. Chem. Soc.* **1982**, *104*, 4007.
121. Fox, A.; Malito, J.; Poë, A. *J. Chem. Soc., Chem. Commun.* **1981**, 1052.
122. Therien, M. J.; Ni, C.-L.; Anson, F. C.; Osteryoung, J. G.; Trogler, W. C. *J. Am. Chem. Soc.* **1986**, *108*, 4037.
123. Therien, M. J.; Trogler, W. C. *J. Am. Chem. Soc.* **1988**, *110*, 4942.
124. Noack, K.; Calderazzo, F. *J. Organomet. Chem.* **1967**, *10*, 101.
125. Flood, T. C.; Jensen, J. E.; Statler, J. A. *J. Am. Chem. Soc.* **1981**, *103*, 4410.
126. Wright, S. C.; Baird, M. C. *J. Am. Chem. Soc.* **1985**, *107*, 6899.
127. Jablonski, C.; Bellachioma, G.; Cardacci, G.; Reichenbach, G. *J. Am. Chem. Soc.* **1990**, *112*, 1632.
128. Flood, T. C.; Campbell, K. D. *J. Am. Chem. Soc.* **1984**, *106*, 2853.
129. Brunner, H.; Hammer, B.; Bernal, I.; Draux, M. *Organometallics* **1983**, *2*, 1595.
130. van Leeuwen, P. W. N. M.; Roobeek, C. F.; van der Heijden, H. *J. Am. Chem. Soc.* **1994**, *116*, 12117.
131. Mawby, R. J.; Basolo, F.; Pearson, R. G. *J. Am. Chem. Soc.* **1964**, *86*, 3994.
132. Mawby, R. J.; Basolo, F.; Pearson, R. G. *J. Am. Chem. Soc.* **1964**, *86*, 5043.
133. Boese, W. T.; Ford, P. C. *J. Am. Chem. Soc.* **1995**, *117*, 8381.
134. Butler, I. S.; Basolo, F.; Pearson, R. G. *Inorg. Chem.* **1967**, *6*, 2074.
135. Wax, M. J.; Bergman, R. G. *J. Am. Chem. Soc.* **1981**, *103*, 7028.
136. McFarlane, K.; Lee, B.; Fu, W. F.; van Eldik, R.; Ford, P. C. *Organometallics* **1998**, *17*, 1826.
137. Massik, S. M.; Ford, P. C. *Organometallics* **1999**, *18*, 4632.
138. Bassetti, M.; Mannina, L.; Monti, D. *Organometallics* **1994**, *13*, 3293; Allevi, M.; Bassetti, M.; LoSterzo, C.; Monti, D. *J. Chem. Soc., Dalton Trans.* **1996**, 3527.
139. Collman, J. P.; Finke, R. G.; Cawse, J. N.; Brauman, J. I. *J. Am. Chem. Soc.* **1978**, *100*, 4766.
140. Wojcicki, A. *Adv. Organomet. Chem.* **1974**, *12*, 31.
141. Whitesides, G. M.; Boschetto, D. J. *J. Am. Chem. Soc.* **1971**, *93*, 1529.
142. Darensbourg, D. J.; Bauch, C. G.; Reibenspies, J. H.; Rheingold, A. L. *Inorg. Chem.* **1988**, *27*, 4203.
143. Ruiz, J.; Martinez, M. T.; Florenciano, F.; Rodriguez, V.; Lopez, G.; Perez, J.; Chaloner, P. A.; Hitchcock, P. B. *Dalton Trans.* **2004**, 929.
144. Gates, D. P.; White, P. S.; Brookhart, M. *Chem. Commun.* **2000**, 47.
145. Albrecht, M.; Gossage, R. A.; Frey, U.; Ehlers, A. W.; Baerends, E. J.; Merbach, A. E.; van Koten, G. *Inorg. Chem.* **2001**, *40*, 850.
146. Leitner, W. *Angew. Chem. Int. Ed.* **1995**, *34*, 2207.
147. Braunstein, P.; Matt, D.; Nobel, D. *Chem. Rev.* **1988**, *88*, 747; Culter, A. R.; Hanna, P. K.; Vites, J. C. *Chem. Rev.* **1988**, *88*, 1363.
148. Sakaki, S.; Musashi, Y. *Inorg. Chem.* **1995**, *34*, 1914.
149. Darensbourg, D. J.; Hanckel, R. K.; Bauch, C. G.; Pala, M.; Simmons, D.; White, J. N. *J. Am. Chem. Soc.* **1985**, *107*, 7463; Darensbourg, D. J.; Grötsch, G. *J. Am. Chem. Soc.* **1985**, *107*, 7473.

150. Darensbourg, D. J.; Sanchez, K. M.; Reibenspies, J. H.; Rheingold, A. L. *J. Am. Chem. Soc.* **1989**, *111*, 7094.
151. Simpson, R. D.; Bergman, R. G. *Organometallics* **1992**, *11*, 4306.
152. Jacobsen, E. N. *Acc. Chem. Res.* **2000**, *33*, 421; Coates, G. W.; Moore, D. R. *Angew. Chem. Int. Ed.* **2004**, *43*, 6618.
153. Chisholm, M. H.; Zhou, Z. *J. Am. Chem. Soc.* **2004**, *126*, 11030.
154. Hansen, K. B.; Leighton, J. L.; Jacobsen, E. N. *J. Am. Chem. Soc.* **1996**, *118*, 10924.
155. Darensbourg, D. J.; Mackiewicz, R. M.; Rodgers, J. L.; Fang, C. C.; Billodeaux, D. R.; Reibenspies, J. H. *Inorg. Chem.* **2004**, *43*, 6024.
156. Moore, D. R.; Cheng, M.; Lobkovsky, E. B.; Coates, G. W. *J. Am. Chem. Soc.* **2003**, *125*, 11911, and references therein.
157. Ready, J. M.; Jacobsen, E. N. *Angew. Chem. Int. Ed.* **2002**, *41*, 1374.
158. Rendina, L. M.; Puddephat, R. *J. Chem. Rev.* **1997**, *97*, 1735.
159. Abu-Hasanayan, F.; Goldman, A. S.; Krogh-Jespersen, K. *Inorg. Chem.* **1994**, *33*, 5122.
160. Burk, M. J.; McGrath, M. P.; Wheeler, R.; Crabtree, R. H. *J. Am. Chem. Soc.* **1988**, *110*, 5034.
161. Kubas, G. J.; Ryan, R. R.; Swanson, B. I.; Vergamini, P. J.; Wasserman, H. *J. Am. Chem. Soc.* **1984**, *106*, 451; Kubas, G. J. *Acc. Chem. Res.* **1988**, *21*, 120, and references therein.
162. Yousufuddin, M.; Wen, T. B.; Mason, S. A.; McIntyre, G. J.; Jia, G. Bau, R. *Angew. Chem. Int. Ed.* **2005**, *44*, 7227.
163. Kubas, G. J. *J. Organomet. Chem.* **2001**, *635*, 37; Custoean, R.; Jackson, J. E. *Chem. Rev.* **2001**, *101*, 1963; McGrady, G. S.; Guilera, G. *Chem. Soc. Rev.* **2003**, *32*, 383; Heinekey, D. M.; Lledós, A.; Lluch, J. M. *Chem. Soc. Rev.* **2004**, *33*, 175; Bakhmutov, V. I. *Eur. J. Inorg. Chem.* **2005**, 245.
164. Saillard, J.-Y.; Hoffmann, R. *J. Am. Chem. Soc.* **1984**, *106*, 2006.
165. Hay, P. J. *J. Am. Chem. Soc.* **1987**, *109*, 705.
166. Maseras, F.; Lledós, A.; Clot, E.; Eisenstein, O. *Chem. Rev.* **2000**, *100*, 601.
167. Nemcsok, D. S.; Kovács, A.; Rayón, V. M.; Frenking, G. *Organometallics* **2002**, *21*, 5803, and references therein.
168. Choi, H. W.; Muetterties, E. L. *J. Am. Chem. Soc.* **1982**, *104*, 153.
169. Van-Catledge, F. A.; Ittel, S. D.; Jesson, J. P. *Organometallics* **1985**, *4*, 18.
170. Eckert, J.; Jensen, C. M.; Koetzle, T. F.; Husebo, T. L.; Nicol, J.; Wu, P. J. *J. Am. Chem. Soc.* **1995**, *117*, 7271.
171. Heinekey, D. M.; Hinkle, A. S.; Close, J. D. *J. Am. Chem. Soc.* **1996**, *118*, 5353.
172. Demachy, I.; Esteruelas, M. A.; Jean, Y.; Lledós, A.; Maseras, F.; Oro, L. A.; Valero, C.; Volatron, F. *J. Am. Chem. Soc.* **1996**, *118*, 8388.
173. Soubra, C.; Oishi, Y.; Albright, T. A.; Fujimoto, H. *Inorg. Chem.* **2001**, *40*, 620.
174. Schott, D.; Sleight, C. J.; Lowe, J. P.; Duckett, S. B.; Mawby, R. J. *Inorg. Chem.* **2002**, *41*, 2960.
175. Clot, E.; Eckert, J. *J. Am. Chem. Soc.* **1999**, *121*, 8855.

176. Sabo-Etienne, S.; Rodriguez, V.; Donnadiou, B.; Chaudret, B.; el Markarim, H. A.; Barthelat, J.-C.; Ulrich, S.; Limbach, H.-H.; Moïse, C. *New J. Chem.* **2001**, *25*, 55, and references therein.
177. Heinekey, D. M.; Mellows, H.; Pratum, T. *J. Am. Chem. Soc.* **2000**, *122*, 6498; Pons, V.; Conway, S. L. J.; Green, M. L. H.; Green, J. C.; Herbert, B. J.; Heinekey, D. M. *Inorg. Chem.* **2004**, *43*, 3475.
178. Khalsa, G. R. K.; Kubas, G. J.; Unkefer, C. J.; Van Der Sluys, L. S.; Kubat-Martin, K. A. *J. Am. Chem. Soc.* **1990**, *112*, 3855; Chinn, M. S.; Heinekey, D. M. *J. Am. Chem. Soc.* **1990**, *112*, 5166; Luo, X.-L.; Michos, D.; Crabtree, R. H. *Organometallics* **1992**, *11*, 237.
179. Zhang, K.; Gonzalez, A. A.; Hoff, C. D. *J. Am. Chem. Soc.* **1989**, *111*, 3627.
180. Khalsa, G. R. K.; Kubas, G. J.; Unkefer, C. J.; Van Der Sluys, L. S.; Kubat-Martin, K. A. *J. Am. Chem. Soc.* **1990**, *112*, 3855.
181. Jessop, P. G.; Morris, R. H. *Coord. Chem. Rev.* **1992**, *121*, 155.
182. Abdur-Rashid, K.; Fong, T. P.; Greaves, B.; Gusev, D. G.; Hinman, J. G.; Landau, S. E.; Lough, A. J.; Morris, R. H. *J. Am. Chem. Soc.* **2000**, *122*, 9155.
183. Papish, E. T.; Rix, F. C.; Spetseris, N.; Norton, J. R.; Williams, R. D. *J. Am. Chem. Soc.* **2000**, *122*, 12235, and references therein.
184. Chinn, M. S.; Heinekey, D. M. *J. Am. Chem. Soc.* **1990**, *112*, 5166; Jia, G.; Lough, A. J.; Morris, R. H. *Organometallics* **1992**, *11*, 161.
185. Scharrer, E.; Chang, S.; Brookhart, M. *Organometallics* **1995**, *14*, 5686.
186. Edidin, R. T.; Sullivan, J. M.; Norton, J. R. *J. Am. Chem. Soc.* **1987**, *109*, 3945.
187. Epstein, L. M.; Shubina, E. S. *Coord. Chem. Rev.* **2002**, *231*, 165; Basallote, M. G.; Besora, M.; Durán, J.; Fernandez-Trujillo, M. J.; Lledós, A.; Máñez, M. A.; Maseras, F. *J. Am. Chem. Soc.* **2004**, *126*, 2320.
188. Hauger, B. E.; Gusev, D.; Caulton, K. G. *J. Am. Chem. Soc.* **1994**, *116*, 208.
189. Oldham, W. J.; Heinekey, D. M. *Organometallics* **1997**, *16*, 467.
190. Basallote, M. G.; Durán, J.; Fernandez-Trujillo, M. J.; Máñez, M. A. *J. Organomet. Chem.* **2000**, *609*, 29.
191. Hellenen, C. A.; Henderson, R. A.; Leigh, G. J. *J. Chem. Soc., Dalton Trans.* **1999**, 1213.
192. Basallote, M. G.; Durán, J.; Fernandez-Trujillo, M. J.; González, G.; Máñez, M. A.; Martínez, M. *Inorg. Chem.* **1998**, *37*, 1623.
193. Griffin, T. R.; Cook, D. B.; Haynes, A.; Pearson, J. M.; Monti, D.; Morris, G. E. *J. Am. Chem. Soc.* **1996**, *118*, 3029; Ivanova, E. A.; Gisdakis, P.; Nasluzov, V. A.; Rubailo, A. I.; Rösch, N. *Organometallics* **2001**, *20*, 1161; Cheong, M.; Ziegler, T. *Organometallics* **2005**, *24*, 3053.
194. Shaw, B. L.; Stainbank, R. E. *J. Chem. Soc., Dalton Trans.* **1972**, 223; Miller, E. M.; Shaw, B. L. *J. Chem. Soc., Dalton Trans.* **1974**, 480.
195. Labinger, J. A.; Osborn, J. A. *Inorg. Chem.* **1980**, *19*, 3230; Labinger, J. A.; Osborn, J. A.; Coville, N. J. *Inorg. Chem.* **1980**, *19*, 3236.
196. Ellis, P. R.; Pearson, J. M.; Haynes, A.; Adams, H.; Bailey, N. A.; Maitlis, P. M. *Organometallics* **1994**, *13*, 3215.

197. Williams, G. M.; Schwartz, J. *J. Am. Chem. Soc.* **1982**, *104*, 1122.
198. Basil, J. D.; Murray, H. H.; Fackler, J. P., Jr.; Tocher, J.; Mazany, A. M.; Trzcinska-Bancroft, B.; Knachel, H.; Dudis, D.; Delord, T. J.; Marler, D. O. *J. Am. Chem. Soc.* **1985**, *107*, 6908.
199. Kramer, A. V.; Labinger, J. A.; Bradley, J. S.; Osborn, J. A. *J. Am. Chem. Soc.* **1974**, *96*, 7145; Kramer, A. V.; Osborn, J. A. *J. Am. Chem. Soc.* **1974**, *96*, 7832.
200. Kinnunen, T.; Laasonen, K. *J. Organomet. Chem.* **2003**, *665*, 150.
201. Kinnunen, T.; Laasonen, K. *J. Mol. Struct. (Theochem)* **2001**, *542*, 273.
202. Jawad, J. K.; Puddephatt, R. J. *J. Organomet. Chem.* **1976**, *117*, 297.
203. Venter, J. A.; Leipoldt, J. G.; van Eldik, R. *Inorg. Chem.* **1991**, *30*, 2207.
204. Theron, M.; Grobelaar, E.; Purcell, W.; Basson, S. S. *Inorg. Chim. Acta* **2005**, *358*, 2457.
205. Hartwig, J. F.; Paul, F. *J. Am. Chem. Soc.* **1995**, *117*, 5373.
206. Galardon, E.; Ramdeehul, S.; Brown, J. M.; Cowley, A.; Hii, K. K.; Jutand, A. *Angew. Chem. Int. Ed.* **2002**, *41*, 1760.
207. Singh, U. K.; Stieter, E. R.; Blackmond, D. G.; Buchwald, S. L. *J. Am. Chem. Soc.* **2002**, *124*, 14104.
208. Alcazar-Roman, L. M.; Hartwig, J. F. *Organometallics* **2002**, *21*, 491.
209. Senn, H. M.; Ziegler, T. *Organometallics* **2004**, *23*, 2980.
210. Goossen, L. J.; Koley, D.; Hermann, H. L.; Thiel, W. *Organometallics* **2005**, *24*, 2398.
211. Amatore, C.; Jutand, A. *Acc. Chem. Res.* **2000**, *33*, 314.
212. Kozuch, S.; Amatore, C.; Jutand, A.; Shaik, S. *Organometallics* **2005**, *24*, 2319.
213. Roy, A. H.; Hartwig, J. F. *Organometallics* **2004**, *23*, 194.
214. Casado, A. L.; Espinet, P. *Organometallics* **1998**, *17*, 954.
215. Alcazar-Roman, L. M.; Hartwig, J. F. *J. Am. Chem. Soc.* **2001**, *123*, 12905.
216. Ananikov, V. P.; Musaev, D. G.; Morokuma, K. *Organometallics* **2005**, *24*, 715.
217. Freixa, Z.; van Leeuwen, P. W. N. M. *Dalton Trans.* **2003**, 1890; Zuidema, E.; van Leeuwen, P. W. N. M.; Bo, C. *Organometallics* **2005**, *24*, 3703.
218. Shekhar, S.; Hartwig, J. F. *J. Am. Chem. Soc.* **2004**, *126*, 13016.
219. Yamashita, M.; Cuevas Vicario, J. V.; Hartwig, J. F. *J. Am. Chem. Soc.* **2003**, *125*, 16347.
220. Mann, G.; Baranano, D.; Hartwig, J. F.; Rheingold, A. L.; Guzei, I. A. *J. Am. Chem. Soc.* **1998**, *120*, 9205.
221. Stoutland, P. O.; Bergman, R. G. *J. Am. Chem. Soc.* **1988**, *110*, 5732.
222. Baker, M. V.; Field, L. D. *J. Am. Chem. Soc.* **1986**, *108*, 7436.
223. Ghosh, C. K.; Hoyano, J. K.; Krentz, R.; Graham, W. A. G. *J. Am. Chem. Soc.* **1989**, *111*, 5480.
224. McNamara, B.; Becher, D. M.; Towns, M. H.; Grant, E. R. *J. Phys. Chem.* **1994**, *98*, 4622.
225. Casey, C. P.; Tunge, J. A.; Lee, T.-Y.; Fagan, M. *J. Am. Chem. Soc.* **2003**, *125*, 2641.

226. Wadepohl, H.; Kohl, U.; Bittner, M.; Köppel, H. *Organometallics* **2005**, *24*, 2097.
227. Deng, L.; Woo, T. K.; Cavallo, L.; Margl, P. M.; Ziegler, T. *J. Am. Chem. Soc.* **1997**, *119*, 6177, and references therein.
228. Froese, R. D. J.; Musaev, D. G.; Morokuma, K. *J. Am. Chem. Soc.* **1998**, *120*, 1581.
229. Li, X.; Vogel, T.; Incarvito, C. D.; Crabtree, R. H. *Organometallics* **2005**, *24*, 62.
230. Becker, P. N.; Bergman, R. G. *J. Am. Chem. Soc.* **1983**, *105*, 2985.
231. Osborn, J. A.; Jardine, F. H.; Young, J. F.; Wilkinson, G. *J. Chem. Soc. A* **1966**, 1711; Jardine, F. H.; Osborn, J. A.; Wilkinson, G. *J. Chem. Soc. A* **1967**, 1574; Montelatici, S.; van der Ent, A.; Osborn, J. A.; Wilkinson, G. *J. Chem. Soc. A* **1968**, 1054.
232. Arai, H.; Halpern, J. *J. Chem. Soc., Chem. Commun.* **1971**, 1571.
233. Meakin, P.; Jesson, J. P.; Tolman, C. A. *J. Am. Chem. Soc.* **1972**, *94*, 3240.
234. Halpern, J.; Wong, S. W. *J. Chem. Soc., Chem. Commun.* **1973**, 629.
235. Brown, J. M.; Evans, P. L.; Lucy, A. R. *J. Chem. Soc., Perkin Trans II* **1987**, 1590.
236. Duckett, B.; Newell, C. L.; Eisenberg, R. *J. Am. Chem. Soc.* **1994**, *116*, 10548; *Ibid.* **1997**, *119*, 2068.
237. Yoshida, T.; Otsuka, S.; Matsumoto, M.; Nakatsu, K. *Inorg. Chim. Acta* **1978**, *29*, L257.
238. Tolman, C. A.; Meakin, P. Z.; Lindner, D. L.; Jesson, J. P. *J. Am. Chem. Soc.* **1974**, *96*, 2762.
239. Halpern, J.; Okamoto, T.; Zakhariiev, A. *J. Mol. Catal.* **1977**, *2*, 65.
240. Halpern, J.; Riley, D. P.; Chan, A. S. C.; Pluth, J. J. *J. Am. Chem. Soc.* **1977**, *99*, 8055.
241. Buriak, J. M.; Klein, J. C.; Herrington, D. C.; Osborn, J. A. *Chem. Eur. J.* **2000**, *6*, 139.
242. Crabtree, R. H.; Felkin, H.; Morris, G. E. *J. Chem. Soc., Chem. Commun.* **1976**, 716; Crabtree, R. *Acc. Chem. Res.* **1979**, *12*, 331, and references therein.
243. Pfaltz, A.; Blankenstein, J.; Hilgraf, R.; Hörmann, E.; McIntyre, S.; Menges, F.; Schönleber, M.; Smidt, S. P.; Wüstenberg, B.; Zimmermann, N. *Adv. Synth. Catal.* **2003**, *345*, 33, and references therein.
244. Perry, M. C.; Cui, X.; Powell, M. T.; Hou, D.-R.; Reibenspies, J. H.; Burgess, K. *J. Am. Chem. Soc.* **2003**, *125*, 113.
245. Crabtree, R. H.; Demon, P. C.; Erden, D.; Mihelcic, J. M.; Parnell, C. A.; Quirk, J. M.; Morris, G. E. *J. Am. Chem. Soc.* **1982**, *104*, 6994.
246. Blackmond, D. G.; Lightfoot, A.; Pfaltz, A.; Rosner, T.; Schnider, P.; Zimmermann, N. *Chirality* **2000**, *12*, 442.
247. Smidt, S. P.; Pfaltz, A.; Martinez-Vincente, E.; Pregosin, P. S.; Albinati, A. *Organometallics* **2003**, *22*, 1000.
248. Smidt, S. P.; Zimmermann, N.; Studer, M.; Pfaltz, A. *Chem. Eur. J.* **2004**, *10*, 4685.

249. Brandt, P.; Hedberg, C.; Anderson, P. G. *Chem. Eur. J.* **2003**, *9*, 339.
250. Dietiker, R.; Chen, P. *Angew. Chem. Int. Ed.* **2004**, *43*, 5513.
251. Cui, X.; Burgess, K. *J. Am. Chem. Soc.* **2003**, *125*, 14212.
252. Cui, X.; Fan, Y.; Hall, M. B.; Burgess, K. *Chem. Eur. J.* **2005**, *11*, 6859.
253. *Comprehensive Asymmetric Catalysis*, Eds. Jacobsen, E. N.; Pfaltz, A.; Yamamoto, H., Springer, Berlin, 1999; *Catalytic Asymmetric Synthesis*, 2nd ed., Ed. Ojima, I., Wiley-VCH, New York, 2000; Noyori, R. *Asymmetric Catalysis in Organic Synthesis*, Wiley, New York, 1994.
254. Noyori, R.; Ohkuma, T. *Angew. Chem. Int. Ed.* **2001**, *40*, 40; Noyori, R.; Kitamura, M.; Ohkuma, T. *Proc. Nat. Acad. Sci. U.S.A.* **2004**, *101*, 5356.
255. Genet, J.-P. *Acc. Chem. Res.* **2003**, *36*, 908.
256. Gridnev, I. L.; Imamoto, T. *Acc. Chem. Res.* **2004**, *37*, 633.
257. Clapham, S. E.; Hadzovic, A.; Morris, R. H. *Coord. Chem. Rev.* **2004**, *248*, 2201.
258. Knowles, W. S. *Angew. Chem. Int. Ed.* **2004**, *21*, 1998.
259. Noyori, R. *Angew. Chem. Int. Ed.* **2004**, *21*, 2008.
260. Drexler, H.-J.; You, J.; Zhang, S.; Fischer, C.; Baumann, W.; Spannenberg, A.; Heller, D. *Org. Process Res. Dev.* **2003**, *7*, 355; Blaser, H.-U.; Malan, C.; Pugin, B.; Spindler, F.; Steiner, H.; Studer, M. *Adv. Synth. Catal.* **2003**, *345*, 103.
261. Chan, A. S. C.; Pluth, J. J.; Halpern, J. *J. Am. Chem. Soc.* **1980**, *102*, 5952.
262. Landis, C. R.; Halpern, J. *J. Am. Chem. Soc.* **1987**, *109*, 1746.
263. Sun, Y.; Landau, R. N.; Wang, J.; LeBlond, C.; Blackmond, D. G. *J. Am. Chem. Soc.* **1996**, *118*, 1348.
264. Feldgus, S.; Landis, C. R. *J. Am. Chem. Soc.* **2000**, *122*, 12714.
265. Burk, M. J.; Feaster, J. E.; Nugent, W. A.; Harlow, R. L. *J. Am. Chem. Soc.* **1993**, *115*, 10125.
266. Landis, C. R.; Feldgus, S. *Angew. Chem. Int. Ed.* **2000**, *39*, 2863.
267. Schmidt, T.; Baumann, W.; Drexler, H.-J.; Arrieta, A.; Heller, D.; Buschmann, H. *Organometallics* **2005**, *24*, 3842.
268. Drexler, H.-J.; Baumann, W.; Schmidt, T.; Zhang, S.; Sun, A.; Spannenberg, A.; Fischer, C.; Buschmann, H.; Heller, D. *Angew. Chem. Int. Ed.* **2005**, *44*, 1184.
269. Heller, D.; Drexler, H.-J.; You, J.; Baumann, W.; Drauz, K.; Krimmer, H.-P.; Börner, A. *Chem. Eur. J.* **2002**, *8*, 5196.
270. Reetz, M.; Meiswinkel, A.; Mehler, G.; Angermund, K.; Graf, M.; Thiel, W.; Mynott, R.; Blackmond, D. G. *J. Am. Chem. Soc.* **2005**, *127*, 10305.
271. Gridnev, I. D.; Higashi, N.; Asakura, K.; Imamoto, T. *J. Am. Chem. Soc.* **2000**, *122*, 7183.
272. Gridnev, I. D.; Yasutake, M.; Imamoto, T.; Beletskaya, I. P. *Proc. Nat. Acad. Sci. U.S.A.* **2004**, *101*, 5385.
273. Noyori, R.; Ohta, M.; Hsiao, Y.; Kitamura, M.; Ohta, T.; Takaya, H. *J. Am. Chem. Soc.* **1986**, *108*, 7117.
274. Noyori, R.; Ohkuma, T.; Kitamura, M.; Takaya, H.; Sayo, N.; Kumobayashi, H.; Akutagawa, S. *J. Am. Chem. Soc.* **1987**, *109*, 5856.

275. Berthod, M.; Migani, G.; Woodward, G.; Lemaire, M. *Chem. Rev.* **2005**, *105*, 1801.
276. Ashby, M. T.; Halpern, J. *J. Am. Chem. Soc.* **1991**, *113*, 589.
277. Ohta, T.; Takaya, H.; Noyori, R. *Tetrahedron Lett.* **1990**, *31*, 7189.
278. Chan, A. S. C.; Chen, C. C.; Yang, T. K.; Huang, J. H.; Lin, Y. C. *Inorg. Chim. Acta* **1995**, *234*, 95.
279. Brown, J. M.; Rose, M.; Knight, F. I.; Wienand, A. *Recl. Trav. Chim. Pays-Bas* **1995**, *114*, 242.
280. Saburi, M.; Takeuchi, H.; Ogasawara, M.; Tsukahara, T.; Ishii, Y.; Ikariya, T.; Takahashi, T.; Uchida, Y. *J. Organomet. Chem.* **1992**, *428*, 155.
281. Dong, X.; Erkey, C. *J. Mol. Cat. A* **2004**, *211*, 73.
282. Wiles, J. A.; Bergens, S. H. *Organometallics* **1999**, *18*, 370.
283. Wiles, J. A.; Bergens, S. H. *J. Am. Chem. Soc.* **1997**, *119*, 2940.
284. Wiles, J. A.; Bergens, S. H. *Organometallics* **1998**, *17*, 2228.
285. Kitamura, M.; Tsukamoto, M.; Bessho, Y.; Yoshimura, M.; Kobs, U.; Widhalm, M.; Noyori, R. *J. Am. Chem. Soc.* **2002**, *124*, 6649.
286. Zassinovich, G.; Mestroni, G.; Gladiali, S. *Chem. Rev.* **1992**, *92*, 1061; Naota, H.; Hashiguchi, S. *Chem. Rev.* **1998**, *98*, 2599.
287. Pàmies, O.; Bäckvall, J.-E. *Chem. Eur. J.* **2001**, *7*, 5052.
288. De Bellefon, C.; Tanchoux, N. *Tetrahedron: Asymmetry* **1998**, *9*, 3677.
289. Bernard, M.; Guiral, V.; Delbecq, F.; Fache, F.; Sautet, P.; Lemaire, M. *J. Am. Chem. Soc.* **1998**, *120*, 1441.
290. Guiral, V.; Delbecq, F.; Sautet, P. *Organometallics* **2000**, *19*, 1589, and references therein.
291. Guiral, V.; Delbecq, F.; Sautet, P. *Organometallics* **2001**, *209*, 2207.
292. Bäckvall, J.-E. *J. Organomet. Chem.* **2002**, *652*, 105, and references therein.
293. Laxmi, Y. R. S.; Bäckvall, J.-E. *Chem. Commun.* **2000**, 611.
294. Hashiguchi, S.; Fujii, A.; Takehara, J.; Ikariya, T.; Noyori, R. *J. Am. Chem. Soc.* **1995**, *117*, 7562.
295. Haack, K.-J.; Hashiguchi, S.; Fujii, A.; Ikariya, T.; Noyori, R. *Angew. Chem. Int. Ed. Engl.* **1997**, *36*, 285.
296. Noyori, R.; Hashiguchi, S. *Acc. Chem. Res.* **1997**, *30*, 97.
297. Alonso, D. A.; Brandt, P.; Nordin, S. J. M.; Andersson, P. G. *J. Am. Chem. Soc.* **1999**, *121*, 9580.
298. Yamakawa, M.; Ito, H.; Noyori, R. *J. Am. Chem. Soc.* **2000**, *122*, 1466.
299. Noyori, R.; Yamakawa, M.; Hashiguchi, S. *J. Org. Chem.* **2001**, *66*, 7931.
300. Handgraaf, J.-H.; Reek, J. N. H.; Meijer, E. *J. Organometallics* **2003**, *22*, 3150.
301. Ohkuma, T.; Ooka, H.; Hashiguchi, S.; Ikariya, T.; Noyori, R. *J. Am. Chem. Soc.* **1995**, *117*, 2675.
302. Sandoval, C. A.; Ohkuma, T.; Muñiz, K.; Noyori, R. *J. Am. Chem. Soc.* **2003**, *123*, 13490.
303. Hartmann, R.; Chen, P. *Angew. Chem. Int. Ed.* **2001**, *40*, 3581.
304. Jiang, Y.; Jiang, Q.; Zhang, X. *J. Am. Chem. Soc.* **1998**, *120*, 3817; Leong, C. G.; Akosti, O. M.; Ferguson, M. J.; Bergens, S. H. *Chem. Commun.* **2003**, 750, and erratum.

305. Ohkuma, T.; Sandoval, C. A.; Srinivasan, R.; Lin, Q.; Wei, Y.; Muñiz, K.; Noyori, R. *J. Am. Chem. Soc.* **2005**, *127*, 8288.
306. Abdur-Rashid, K.; Clapham, S. E.; Hadzovic, A.; Harvey, J. N.; Lough, A. J.; Morris, R. J. *J. Am. Chem. Soc.* **2002**, *124*, 15104.
307. Hamilton, R. J.; Leong, C. G.; Bigam, G.; Miskolzie, M.; Bergens, S. H. *J. Am. Chem. Soc.* **2005**, *127*, 4152.
308. Hartmann, R.; Chen, P. *Adv. Synth. Catal.* **2003**, *345*, 1353.
309. Hedberg, C.; Källström, K.; Arvidsson, P. I.; Brandt, P.; Andersson, P. G. *J. Am. Chem. Soc.* **2005**, *127*, 15083, and references therein.
310. Janowicz, A. H.; Bergman, R. G. *J. Am. Chem. Soc.* **1982**, *104*, 352.
311. Hoyano, J. K.; Graham, W. A. G. *J. Am. Chem. Soc.* **1982**, *104*, 3723.
312. Thompson, M. E.; Bercaw, J. E. *Pure Appl. Chem.* **1984**, *56*, 1.
313. Crabtree, R. H. *Chem. Rev.* **1985**, *85*, 245.
314. Brookhart, M.; Green, M. L. H.; Wong, L.-L. *Prog. Inorg. Chem.* **1988**, *36*, 1.
315. Rothwell, I. P. *Acc. Chem. Res.* **1988**, *21*, 153.
316. Perutz, R. N. *Chem. Soc. Rev.* **1993**, 361.
317. Arndtsen, B. A.; Bergman, R. G.; Mobley, T. A.; Peterson, T. H. *Acc. Chem. Res.* **1995**, *28*, 154.
318. Crabtree, R. H. *J. Organomet. Chem.* **2004**, *689*, 4083.
319. Ghosh, C. K.; Graham, W. A. G. *J. Am. Chem. Soc.* **1987**, *109*, 4726.
320. Ghosh, C. K.; Graham, W. A. G. *J. Am. Chem. Soc.* **1989**, *111*, 375.
321. Sakakura, T.; Sodeyama, T.; Sasaki, K.; Wada, K.; Tanaka, M. *J. Am. Chem. Soc.* **1990**, *112*, 7221.
322. Margl, P.; Ziegler, T.; Blöchl, P. E. *J. Am. Chem. Soc.* **1996**, *118*, 5412.
323. Nolan, S. P.; Hoff, C. D.; Stoutland, P. D.; Newman, L. J.; Buchanan, J. M.; Bergman, R. G.; Yang, G. K.; Peters, K. S. *J. Am. Chem. Soc.* **1987**, *109*, 3143.
324. Buchanan, J. M.; Stryker, J. M.; Bergman, R. G. *J. Am. Chem. Soc.* **1986**, *108*, 1537.
325. Simoes, M.; Beachamp, J. L. *Chem. Rev.* **1990**, *90*, 629; Hoff, C. D. *Prog. Inorg. Chem.* **1992**, *40*, 503.
326. King, W. A.; Di Bella, S.; Gulino, A.; Lanza, G.; Fragalà, I. L.; Stern, C. L.; Marks, T. J. *J. Am. Chem. Soc.* **1999**, *121*, 355.
327. Marx, D. E.; Lees, A. J. *Inorg. Chem.* **1988**, *27*, 1121.
328. Drolet, D. P.; Lees, A. J. *J. Am. Chem. Soc.* **1990**, *112*, 5878.
329. Weiller, B. H.; Wasserman, E. P.; Bergman, R. G.; Moore, C. B.; Pimentel, G. C. *J. Am. Chem. Soc.* **1989**, *111*, 8288; Schulz, R. H.; Bengali, A. A.; Tauber, M. J.; Wasserman, E. P.; Weiller, B. H.; Kyle, K. R.; Moore, C. B.; Bergman, R. G. *J. Am. Chem. Soc.* **1994**, *116*, 7369.
330. Bengali, A. A.; Schultz, R. H.; Moore, C. B.; Bergman, R. G. *J. Am. Chem. Soc.* **1994**, *116*, 9585.
331. Wasserman, E. P.; Morse, C. B.; Bergman, R. G. *Science* **1992**, *255*, 315.
332. Bengali, A. A.; Bergman, R. G.; Moore, C. B. *J. Am. Chem. Soc.* **1995**, *117*, 3879.
333. Ziegler, T.; Tschinke, V.; Fan, L.; Becke, A. D. *J. Am. Chem. Soc.* **1989**, *111*, 9177; Song, J.; Hall, M. B. *Organometallics* **1993**, *12*, 3118; Musaev, D. G.; Morokuma, K. *J. Am. Chem. Soc.* **1995**, *117*, 799.

334. Siegbahn, P. E. M. *J. Am. Chem. Soc.* **1996**, *118*, 1487.
335. Whittlesey, M. K.; Mawby, R. J.; Osman, R.; Perutz, R. N.; Field, L. D.; Wilkinson, M. P.; George, M. W. *J. Am. Chem. Soc.* **1993**, *115*, 8627; Cronin, L.; Nicasio, C.; Perutz, R. N.; Peters, R. G.; Roddick, D. M.; Whittlesey, M. K. *J. Am. Chem. Soc.* **1995**, *117*, 10047.
336. Klassen, J. K.; Selke, M.; Sorensen, A. A.; Yang, G. K. *J. Am. Chem. Soc.* **1990**, *112*, 1267.
337. Belt, S. T.; Grevels, F.-W.; Klotzbücher, W. E.; McCamley, A.; Perutz, R. N. *J. Am. Chem. Soc.* **1989**, *111*, 8373.
338. Bullock, R. M.; Headford, C. E. L.; Hennessy, K. M.; Kegley, S. E.; Norton, J. R. *J. Am. Chem. Soc.* **1989**, *111*, 3897.
339. Green, J. C.; Jardine, C. N. *J. Chem. Soc., Dalton Trans.* **1998**, 1057.
340. Green, J. C.; Harvey, J. N.; Poli, R. *J. Chem. Soc., Dalton Trans.* **2002**, 1861.
341. Gol'dshleger, N. F.; Tyabin, M. B.; Shilov, A. E.; Shteinman, A. A. *Zh. Fiz. Khim. (Engl. Trans.)* **1969**, *43*, 1222; Shilov, A. E.; Shulpin, G. B. *Chem. Rev.* **1997**, *97*, 2879.
342. Baudry, D.; Eohritikhine, M.; Felkin, H.; Zakrewski, J. *Tetrahedron Lett.* **1984**, *25*, 1283; Burk, M. J.; Crabtree, R. H. *J. Am. Chem. Soc.* **1987**, *109*, 8025; Klei, S. R.; Tilley, D.; Bergman, R. H. *J. Am. Chem. Soc.* **2000**, *122*, 1816.
343. Corkey, B. K.; Taw, F. L.; Bergman, R. G.; Brookhart, M. *Polyhedron* **2004**, *23*, 2943.
344. Gol'dschleger, N. F.; Eskova, V. V.; Shilov, A. E.; Shteinman, A. A. *Zh. Fiz. Khim. (Engl. Trans.)* **1972**, *46*, 785.
345. Sen, A. *Acc. Chem. Res.* **1998**, *31*, 550; Stahl, S. S.; Labinger, J. A.; Bercaw, J. E. *Angew. Chem. Int. Ed.* **1998**, *37*, 2180; Fekl, U.; Goldberg, K. I. *Adv. Inorg. Chem.* **2003**, *54*, 259; Lersch, M.; Tilset, M. *Chem. Rev.* **2005**, *105*, 2471.
346. Kushch, L. A.; Lavrushko, V. V.; Misharin, Y. S.; Moravsky, A. P.; Shilov, A. E. *Nouv. J. Chim.* **1983**, *7*, 729.
347. Johansson, L.; Tilset, M. *J. Am. Chem. Soc.* **2001**, *123*, 739; Wik, B. J.; Lersch, M.; Tilset, M. *J. Am. Chem. Soc.* **2002**, *124*, 12116.
348. Luinistra, G. A.; Labinger, J. A.; Bercaw, J. E. *J. Am. Chem. Soc.* **1993**, *115*, 3004; Luinistra, G. A.; Wang, L.; Stahl, S. S.; Labinger, J. A.; Bercaw, J. E. *J. Organomet. Chem.* **1995**, *504*, 75.
349. Cornils, B.; Herrmann, W. A. *Applied Homogeneous Catalysis with Organometallic Compounds*; VCH: Weinheim, 1996.
350. Pruet, R. L. *Adv. Organomet. Chem.* **1979**, *17*, 1.
351. Heck, R. F.; Breslow, D. S. *J. Am. Chem. Soc.* **1961**, *83*, 4023.
352. Dwyer, C. A.; Assumption, H.; Coetzee, J.; Crause, C.; Damoense, L.; Kirk, M. *Coord. Chem. Rev.* **2004**, *248*, 653.
353. Goddard, C.; Duckett, S. B.; Polas, S.; Tooze, R.; Whitwood, A. C. *J. Am. Chem. Soc.* **2005**, *127*, 4994.
354. Yagupsky, G.; Brown, C. K.; Wilkinson, G. *J. Chem. Soc. A* **1970**, 1392; Brown, C. K.; Wilkinson, G. *J. Chem. Soc. A* **1970**, 2753.
355. Damoense, L.; Datt, M.; Green, M.; Steenkamp, C. *Coord. Chem. Rev.* **2004**, *248*, 2393.

356. Kamer, P. C. J.; van Rooy, A.; Schoemaker, G. C.; van Leeuwen, P. W. N. *M. Coord. Chem. Rev.* **2004**, *248*, 2409.
357. Breit, B. *Acc. Chem. Res.* **2003**, *36*, 264.
358. Huo, C.-F.; Li, Y.-W.; Beller, M.; Jiao, H. *Organometallics* **2003**, *22*, 4665; *Ibid.* **2004**, *23*, 765; *Ibid.* **2005**, *24*, 3634.
359. Kang, H.; Mauldin, C. H.; Cole, T.; Slegeir, W.; Cann, K.; Pettit, R. *J. Am. Chem. Soc.* **1977**, *99*, 8323.
360. De Angelis, F.; Sgamellotti, A.; Re, N. *Organometallics* **2000**, *19*, 4104.
361. Thomas, M. G.; Beier, B. F.; Muetterties, E. L. *J. Am. Chem. Soc.* **1976**, *98*, 1296; Demitras, G. C.; Muetterties, E. L. *J. Am. Chem. Soc.* **1977**, *99*, 2796.
362. Laine, R. M.; Rinker, R. G.; Ford, P. C. *J. Am. Chem. Soc.* **1977**, *99*, 252.
363. Herrmann, W. A. *Adv. Organomet. Chem.* **1982**, *20*, 159; *Angew. Chem. Int. Ed. Engl.* **1982**, *21*, 117.
364. Masters, C. *Adv. Organomet. Chem.* **1979**, *17*, 61.
365. Maitlis, P. M. *J. Mol. Catal. A* **2003**, *204–205*, 55.
366. Maitlis, P. M. *J. Organomet. Chem.* **2004**, *689*, 4366.
367. Shi, B.; Davis, B. H. *Catal. Today* **2001**, *65*, 95, and references therein.
368. Ndlova, S. B.; Phala, N. S.; Hearshaw-Timme, M.; Beagly, P.; Moss, J. R.; Claeys, M.; van Steen, E. *Catal. Today* **2002**, *71*, 343.
369. Ford, P. C.; Rinker, R. G.; Ungermann, C.; Laine, R. M.; Landis, V.; Moya, S. A. *J. Am. Chem. Soc.* **1978**, *100*, 4595.
370. Fachinetti, G.; Fochi, G.; Funaioli, T. *Inorg. Chem.* **1994**, *33*, 1719.
371. Fachinetti, G.; Funaioli, T.; Lecci, L.; Marchetti, F. *Inorg. Chem.* **1996**, *35*, 7217.
372. Torrent, M.; Sola, M.; Frenking, G. *Organometallics* **1999**, *18*, 2801.
373. Torrent, M.; Sola, M.; Frenking, G. *Chem. Rev.* **2000**, *100*, 439.
374. Ungermann, C.; Landis, V.; Moya, S. A.; Cohen, H.; Walker, H.; Pearson, R. G.; Rinker, R. G.; Ford, P. C. *J. Am. Chem. Soc.* **1979**, *101*, 5922.
375. Barrows, S. E. *Inorg. Chem.* **2004**, *43*, 8236.
376. Jessop, P. G.; Ikariya, T.; Noyori, R. *Chem. Rev.* **1995**, *95*, 259.
377. Jessop, P. G.; Hsiao, Y.; Ikariya, T.; Noyori, R. *J. Am. Chem. Soc.* **1996**, *118*, 344.
378. Musashi, Y.; Sakaki, S. *J. Am. Chem. Soc.* **2002**, *124*, 7588.
379. Ohnishi, Y.; Matsunaga, T.; Nakao, Y.; Sato, H.; Sakaki, S. *J. Am. Chem. Soc.* **2005**, *127*, 4021.
380. Hutschka, F.; Dedieu, A.; Eichberger, M.; Fornika, R.; Leitner, W. *J. Am. Chem. Soc.* **1997**, *119*, 4432.
381. Forster, D. *J. Chem. Soc., Dalton Trans.* **1979**, 1639.
382. Sunley, G. J.; Watson, D. J. *Catal. Today* **2000**, *58*, 293; Haynes, A. *Educ. Chem.* **2001**, *38*, 99.
383. Haynes, A.; Maitlis, P. M.; Morris, G. E.; Sunley, G. J.; Adams, H.; Badger, P. W.; Bowers, C. M.; Cook, D. B.; Elliot, P. I. P.; Ghaffar, T.; Green, H.; Griffin, T. R.; Payne, M.; Pearson, J. M.; Taylor, M. J.; Vickers, P. W.; Watt, R. J. *J. Am. Chem. Soc.* **2004**, *126*, 2847.

384. Maitlis, P. M.; Haynes, A.; James, B. R.; Catellani, M.; Chiusoli, G. P. *Dalton Trans.* **2004**, 3409.
385. Gautron, S.; Giordano, R.; Le Berre, C.; Jaud, J.; Daran, J.-C.; Serp, P.; Kalck, P. *Inorg. Chem.* **2003**, *42*, 5523.
386. Feliz, M.; Freixa, Z.; van Leeuwen, P. W. N. M.; Bo, C. *Organometallics* **2005**, *24*, 5718.
387. Cramer, R. *Acc. Chem. Res.* **1968**, *1*, 186.
388. Tolman, C. A. *Chem. Rev.* **1977**, *77*, 313.
389. Speiser, F.; Braunstein, P.; Saussine, L. *Acc. Chem. Res.* **2005**, *38*, 784.
390. Resconi, L.; Cavallo, L.; Fait, A.; Piemontesi, F. *Chem. Rev.* **2000**, *100*, 1253.
391. Chen, E. Y.-X.; Marks, T. J. *Chem. Rev.* **2000**, *100*, 1391.
392. Corradini, P.; Guerra, G.; Cavallo, L. *Acc. Chem. Res.* **2004**, *37*, 231.
393. Lavery, D. T.; Rooney, J. J. *J. Chem. Soc., Faraday Trans. I* **1983**, *79*, 869.
394. Brookhart, M.; Green, M. L. H. *J. Organomet. Chem.* **1983**, *250*, 395.
395. Prosenc, M.-H.; Janiak, C.; Brintzinger, H.-H. *Organometallics* **1992**, *11*, 4036.
396. Grubbs, R. H.; Coates, G. W. *Acc. Chem. Res.* **1996**, *29*, 85.
397. Ystenes, M. *Makromol. Chem., Macromol. Symp.* **1993**, *66*, 71.
398. Dornik, H. P.; Luft, G.; Rau, A.; Wieczorek, T. *Macromol. Mater. Eng.* **2003**, *288*, 558.
399. Prosenc, M.-H.; Schaper, F.; Brintzinger, H.-H. In *Metalorganic Catalysts for Synthesis and Polymerization*; Kaminsky, W., Ed.; Springer-Verlag: Berlin, 1999; p 223.
400. Richarson, D. E.; Alameddin, N. G.; Ryan, M. F.; Hayes, T.; Eyler, J. R.; Siedle, A. R. *J. Am. Chem. Soc.* **1996**, *118*, 11244.
401. Marques, M. M.; Dias, A. R.; Costa, C.; Lemos, F.; Ramoa Ribiero, F. *Polym. Int.* **1997**, *43*, 77.
402. Fait, A.; Resconi, L.; Guerra, G.; Corradini, P. *Macromolecules* **1999**, *32*, 2104.
403. Vanka, K.; Xu, Z.; Ziegler, T. *Organometallics* **2004**, *23*, 2900.
404. Silanes, I.; Ugalde, J. M. *Organometallics* **2005**, *24*, 3233.
405. Ittel, S. D.; Johnson, L. K.; Brookhart, M. *Chem. Rev.* **2000**, *100*, 1169.
406. Gibson, V. C.; Spitzmesser, S. K. *Chem. Rev.* **2003**, *103*, 283.
407. Schrock, R. R.; Murdzek, J. S.; Bazan, G. C.; Robbins, J.; DiMare, M.; O'Reagan, M. *J. Am. Chem. Soc.* **1990**, *112*, 3875; Schrock, R. R. *Acc. Chem. Res.* **1990**, *23*, 158.
408. Schwab, P.; Grubbs, R. H.; Ziller, J. W. *J. Am. Chem. Soc.* **1996**, *118*, 100; Trnka, T. M.; Grubbs, R. H. *Acc. Chem. Res.* **2001**, *34*, 18, and references therein.
409. Bielawski, C. W.; Grubbs, R. H. *Angew. Chem. Int. Ed.* **2000**, *39*, 2903.
410. Forman, G. S.; McConnell, A. E.; Tooze, R. P.; van Rensburg, W. J.; Meyer, W. H.; Kirk, M. M.; Dwyer, C. L.; Serfontein, W. W. *Organometallics* **2005**, *24*, 4528.
411. Hérisson, J.-L.; Chauvin, Y. *Makromol. Chem.* **1971**, *141*, 161.

412. Straub, B. F. *Angew. Chem. Int. Ed.* **2005**, *44*, 5974.
413. Goumans, T. P. M.; Ehlers, A. W.; Lammertsma, K. *Organometallics* **2005**, *24*, 3200, and references therein.
414. Sanford, M. S.; Love, J. A.; Grubbs, R. H. *J. Am. Chem. Soc.* **2001**, *123*, 6543.
415. Nicolau, K. C.; Bulger, P. G.; Sarlah, D. *Angew. Chem. Int. Ed.* **2005**, *44*, 4490.

6

Oxidation–Reduction Reactions

For most purposes, inorganic reactions can be classified as either substitution reactions or oxidation–reduction reactions. The latter involve the transfer of at least one electron from the reducing agent to the oxidizing agent. Such reactions are widely used in analytical procedures and are important in many biological processes. One of the mechanistic types in this area is unique in having a fairly simple theoretical basis for predicting rate constants in solution from measurable input parameters.

6.1 CLASSIFICATION OF REACTIONS

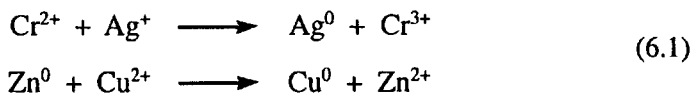
Oxidation–reduction reactions have been classified in two general ways; the first, historically, is by stoichiometry and the second is by mechanism.

6.1.1 Stoichiometric Classification

The stoichiometric classification only requires a knowledge of the reaction stoichiometry but has limited kinetic applicability.

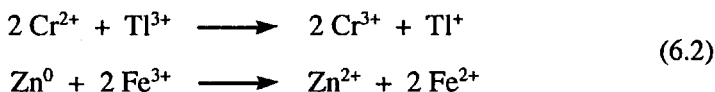
6.1.1.1 Complementary Reactions

The change in oxidation state of the reducing agent is the same as the change in oxidation state of the oxidizing agent. Some examples are

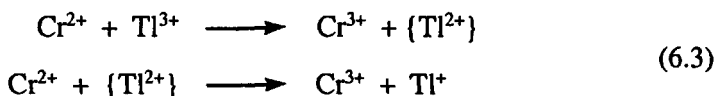


6.1.1.2 Noncomplementary Reactions

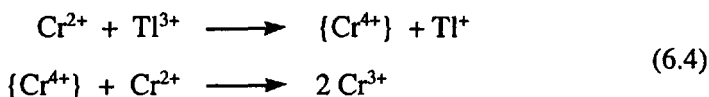
The oxidizing agent and the reducing agent undergo different net changes in oxidation state. Some examples are



This classification has no direct mechanistic implications. However, it is a qualitative observation that complementary reactions are faster than noncomplementary reactions. This "rule" can be useful in designing analytical and preparative procedures, but it is by no means universal. The mechanistic rationale for this qualitative kinetic observation is based on the assumption that the reactions occur in bimolecular steps. Therefore, noncomplementary reactions must normally proceed through an unstable oxidation state of one of the reactants, as in the following examples:



or



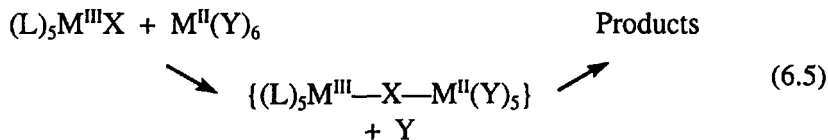
For the sequence of reactions in (6.3), Tl^{2+} is an unstable oxidation state of thallium and in reactions (6.4), Cr^{4+} is an unstable state for chromium. These unstable states may present an energy barrier for the reaction.

6.1.2 Mechanistic Classification

The mechanistic classification obviously requires a knowledge of the reaction mechanism. A major theme of this area is the elucidation of the kinetic features that allow one to determine the type of mechanism.

6.1.2.1 Inner-Sphere Electron Transfer

At least one ligand is shared in the first coordination sphere of the oxidant and reductant in the transition state for the electron-transfer process:



The formation of the transition state involves a substitution reaction on one of the metal centers, M^{II} in this example, in order to form the intermediate or transition state with the bridging ligand $-\text{X}-$ in reaction (6.5). Then, electron transfer occurs, possibly via the bridging ligand, and the final products are determined by the substitution lability of the metal centers.

This mechanism was first demonstrated by Taube and co-workers¹ in a system that exploited the ideas of substitution lability and inertness that Taube was developing at the same time. The experiment involved

approach can be used to anticipate the rates of these reactions. To date, this is one of the few areas in which theory has provided useful guidelines for mechanistic studies. A mechanistic decision between the inner- and outer-sphere possibilities is often based on whether or not the reaction rate corresponds reasonably to the predictions of the outer-sphere theory.

6.2 OUTER-SPHERE ELECTRON-TRANSFER THEORY

The outer-sphere theory has been developed using an electrostatic approach to calculate the energy necessary to bring reactants together, to reorganize the solvent around the transition state and to prepare the metal centers for electron transfer.

In North America the theory is associated with the name of Marcus and referred to as the Marcus theory.² However, Hush³ in Australia and Levitch⁴ and Dogonadze⁵ in the U.S.S.R. have made original contributions. Marcus started from the transition-state theory for ionic reactions, Hush from solid-state electron-transfer theory and Levitch from a consideration of reactions at electrodes. All arrived at essentially the same result, although using different terminologies. More recently, Tachiya and co-workers⁶ have developed a model based on the electrostatic interaction of the reactants with a polar solvent which also reduces to the same result under certain conditions. The version of the theory developed by Marcus has remained predominant for kinetic studies because it is framed in more familiar terminology and yields relationships that appear simple to test by experiment.

The Franck-Condon principle is fundamental to the theory. This principle states that electron movement is much faster than nuclear motion; thus, internuclear distances do not change during the instant of electron transfer. Therefore, it is assumed that on approaching the transition state, the bond lengths of the reactants will adjust to approach those of the products.

The electron transfer is assumed to be an *adiabatic process in the Ehrenfest sense* so that the transmission coefficient, κ , in the transition-state theory expression (Section 1.6.2), Eq. (6.7), is equal to one.

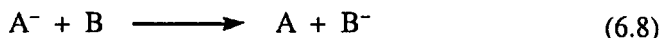
$$k = \kappa \frac{k_B T}{h} e^{-(\Delta H^\ddagger - T\Delta S^\ddagger)/RT} \quad (6.7)$$

This implies that there is enough interaction between reactants in the transition state to make the probability of electron transfer equal to one, although normal bonding forces are assumed to be much weaker than electrostatic ones. There are occasions when the interaction is thought to be so weak that $\kappa > 1$ and the effect of "nonadiabaticity" on the reaction rate is sometimes used as a rationale for differences between observed and predicted rate constants.

6.2.1 Marcus Cross Relationship from Thermodynamics

One of the most important results to evolve from the theoretical treatment of Marcus is now referred to as the Marcus cross relationship. This important relationship was developed later by Ratner and Levine⁷ from a thermodynamic perspective, and this formulation provides a simple basis for understanding some of the concepts and assumptions in the more microscopic molecular theory of Marcus that is described later.

The electron-transfer reaction between a reductant, A^- , and an oxidant, B , is given by the following net reaction:



It is assumed that the reactants come together to form a precursor complex $(A^-)(B^*)$; then, electron transfer occurs to give the successor complex $(A^*)(B^-)$, which decomposes to products, as shown in Figure 6.1.

Ratner and Levine assumed that in the precursor and successor complexes, one can define thermodynamic properties for the individual partners, (A^-) , (B^*) , (A^*) and (B^-) . This amounts to assuming that there is no significant bonding between the partners in the precursor and successor complexes. For such a condition, it was shown earlier by Levine⁸ that detailed balance requires that the free energies of the precursor and successor complexes must be equal, so that

$$G^0(A^-) + G^0(B^*) = G^0(A^*) + G^0(B^-) \quad (6.9)$$

and this is shown by the horizontal dashed line between the activated complexes in Figure 6.1.

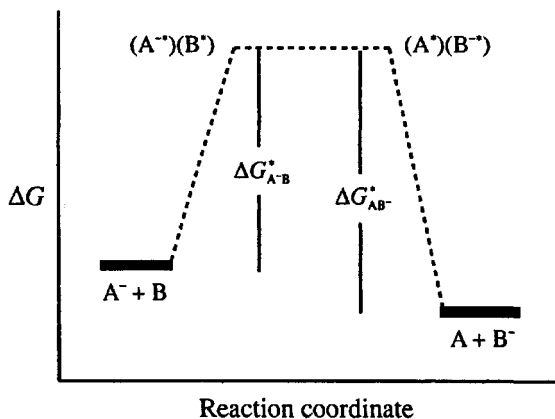
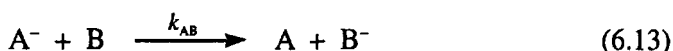
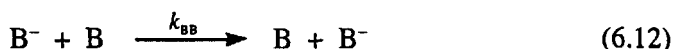


Figure 6.1. Reaction coordinate diagram for an outer-sphere electron-transfer reaction.

The net free energy change for the reaction is

$$\Delta G_{A^-B}^{\circ} = G^{\circ}(A) + G^{\circ}(B^-) - G^{\circ}(A^-) - G^{\circ}(B) \quad (6.10)$$

The cross relationship involves the relationship between the free energies or rate constants for the following reactions, where (6.11) and (6.12) are called self-exchange reactions and (6.13) is called the cross reaction:



It is assumed that the free energies of the individual partners in the self-exchange reactions are the same as in the cross reaction; therefore

$$\Delta G_{AA}^* = G^{\circ}(A^{-*}) + G^{\circ}(A^*) - G^{\circ}(A^-) - G^{\circ}(A) \quad (6.14)$$

$$\Delta G_{BB}^* = G^{\circ}(B^{-*}) + G^{\circ}(B^*) - G^{\circ}(B^-) - G^{\circ}(B) \quad (6.15)$$

$$\Delta G_{AB}^* = G^{\circ}(A^{-*}) + G^{\circ}(B^*) - G^{\circ}(A^-) - G^{\circ}(B) \quad (6.16)$$

If Eq. (6.16) is multiplied by 2 and substitution is made from Eq. (6.9), one obtains

$$2\Delta G_{AB}^* = G^{\circ}(A^{-*}) + G^{\circ}(B^*) + G^{\circ}(A^*) + G^{\circ}(B^{-*}) - 2G^{\circ}(A^-) - 2G^{\circ}(B) \quad (6.17)$$

Then, substitution from Eq. (6.10), rearrangement and substitution from Eqs. (6.14) and (6.15) gives

$$\Delta G_{AB}^* = 1/2(\Delta G_{AA}^* + \Delta G_{BB}^* + \Delta G_{A^-B}^{\circ}) \quad (6.18)$$

This is the Marcus cross relationship in terms of free energies.

The thermodynamic development of the cross relationship depends on the *assumptions* that:

1. The activation process for A^- and B is independent of the other reactant.
2. The activated species are the same for the self-exchange and the cross reaction.

Clearly, these assumptions are not valid for an inner-sphere mechanism. They also will be invalid if there are special attractive or repulsive forces between A^- and B that are not present between A and A^- or B and B^- .

From the transition-state theory, the free energy of activation and the rate constant are related by

$$k_{ij} = Z_{ij} e^{-\Delta G_{ij}^{\ddagger}/RT} \quad (6.19)$$

where Z_{ij} is the collision frequency. If this expression and the thermodynamic relationship $\Delta G_{A-B}^{\ddagger} = -RT(\ln K_{AB})$ are substituted into Eq. (6.18), then one obtains

$$\begin{aligned} k_{AB} &= \left(k_{AA} k_{BB} K_{AB} \frac{Z_{AB}^2}{Z_{AA} Z_{BB}} \right)^{1/2} \\ &= (k_{AA} k_{BB} K_{AB} F_{AB})^{1/2} \end{aligned} \quad (6.20)$$

This is the cross relationship in terms of rate constants. There is often reason to believe (or need to assume) that $F_{AB} \approx 1$, and then Eq. (6.20) reduces to what is often called the simplified Marcus cross relationship. This is particularly useful because a knowledge of any three of the values, k_{AB} , k_{AA} , k_{BB} or K_{AB} allows one to predict the fourth.

The assumption that $F_{AB} \approx 1$ means that $Z_{AB}^2 \approx Z_{AA} Z_{BB}$. For ionic reactants, this would seem quite reasonable if the reaction has charge symmetry (e.g., $A^{2+} + B^{3+} \rightarrow A^{3+} + B^{2+}$) since the charges of the species in the self-exchange reactions are the same as those in the net reaction. The assumption is somewhat less valid if the species are of the same charge type but the reaction lacks charge symmetry (e.g., $A^{2+} + B^{3+} \rightarrow A^{1+} + B^{4+}$). In this example, Z_{AA} for $A^{2+} + A^{1+}$ will be larger than Z_{BB} for $B^{3+} + B^{4+}$, but Z_{AB} for $A^{2+} + B^{3+}$ may be intermediate between the two, and it may still be true that $Z_{AB}^2 \approx Z_{AA} Z_{BB}$ within a factor of 10. However, if the reactants are of opposite charge type, such as $A^{2-} + B^{3+} \rightarrow A^{3-} + B^{2+}$, then the attractive force between the ions of opposite charge will make Z_{AB} larger than either Z_{AA} or Z_{BB} and F_{AB} will be much larger than 1.

The preceding development illustrates the assumptions that are necessary to develop the cross relationship. The more detailed theory that follows provides further understanding in terms of the molecular properties of the reactants and solvent.

6.2.2 Marcus Theory Details

The details of the Marcus theory have been described in several reviews⁹⁻¹⁵ and in books by Reynolds and Lumry¹⁶ and Cannon.¹⁷ The following discussion will simply outline the features of the theory and give the physical factors that are predicted to be important in determining the rates of outer-sphere electron-transfer reactions.

The reactants are considered to be two hard spheres of charge z_1 and z_2 and radii a_1 and a_2 . This and later assumptions may be easier to justify by noting that many of the systems are of the general type $M(L)_n^{z+}$. Work will

be required to bring the reactants together to a separation of $r = a_1 + a_2$, which is taken to be the reactant separation in the transition state. Simple electrostatics give this contribution to the free energy of activation as

$$\Delta G_{\text{coul}}^* = \left(\frac{Nz_1z_2e^2}{4\pi\epsilon_0} \right) \left(\frac{1}{\epsilon_s r} \right) \quad (6.21)$$

where N is Avogadro's number, e is the charge on the electron, ϵ_0 is the vacuum permittivity and ϵ_s is the bulk dielectric constant of the solvent. In more recent treatments, the formation of the precursor complex has been considered as a diffusion-controlled equilibrium reaction, with the equilibrium constant, K_{os} , equal to the ratio of the forward and reverse rate constants and given by

$$K_{\text{os}} = \frac{4\pi Nr^3}{3000} e^{U/(1+B\mu^{1/2})} \quad (6.22)$$

where

$$U = \frac{z_1z_2e^2}{4\pi\epsilon_0\epsilon_srk_{\text{B}}T}$$

and the terms in U have been defined previously in Eq. (1.79). The B is the Debye–Hückel factor discussed in Eq. (1.78) and μ is the ionic strength. The latter terms obviously are introduced in an attempt to correct for ionic strength variations. Alternative approaches to the ionic strength effect have been described in Chapter 1 and by Tembe et al.¹⁸ In the transition state theory equation, either ΔG_{coul}^* is a contribution to the overall ΔG^* or K_{os} is a pre-exponential factor.

When the reactants come together, they are considered to form a spherical transition state of diameter r . The solvent molecules will reorganize around the transition state, and this solvent or outer-sphere reorganization contribution to the overall ΔG^* is given by

$$\Delta G_{\text{solv}}^* = (\Delta q)^2 \left(\frac{Ne^2}{16\pi\epsilon_0} \right) \left(\frac{1}{2a_1} + \frac{1}{2a_2} - \frac{1}{r} \right) \left(\frac{1}{n_s^2} - \frac{1}{\epsilon_s} \right) \quad (6.23)$$

where Δq is the number of electrons transferred ($\Delta q = 1$ for the majority of reactions), n_s is the refractive index of the solvent (n_s^2 is the high-frequency dielectric constant of the solvent).

In order to satisfy the Franck–Condon principle, the ligands around the metal ions will adjust their bond lengths in the transition state toward the lengths they will have in the products. This factor is the inner-sphere reorganization energy contribution to the overall ΔG^* and is given by

$$\Delta G_{\text{is}}^* = N \left(\frac{nf_1}{2} (d_1^o - d_1^*)^2 + \frac{nf_2}{2} (d_2^o - d_2^*)^2 \right) \quad (6.24)$$

where n is the number of ligands, f_1 and f_2 are the force constants for the symmetrical breathing vibrational mode, which is assumed to generate the appropriate bond lengthening or shortening, and d_i^0 and d_i^* are the ground-state and transition-state metal-ligand bond lengths, respectively. The ΔG_{is}^* is the most difficult term to calculate because d_i^* is unknown and the force constants require an assignment of the vibrational spectrum in the difficult region of ~ 200 to 800 cm^{-1} . One approach is to let $d^* = d_1^* = d_2^*$ and then solve for d^* when ΔG_{is}^* is a minimum (i.e., when $d(\Delta G_{is}^*)/d(d^*) = 0$). Then

$$d^* = \frac{f_1 d_1^0 + f_2 d_2^0}{f_1 + f_2} \quad (6.25)$$

and

$$\Delta G_{is}^* = N \left(\frac{n f_1 f_2}{2(f_1 + f_2)} \right) (d_2^0 - d_1^0)^2 \quad (6.26)$$

To determine the force constants, f_i , the appropriate potential energy function, U , should be used to calculate $f = d^2(U)/d^2(d)$. A simple harmonic diatomic oscillator is often assumed, so that $f_i = (2\pi\nu_i c)^2 m_r$, where ν_i is the vibrational frequency in cm^{-1} , c is the speed of light in cm s^{-1} and m_r is the reduced mass of the metal-ligand fragment in kg.

Nuclear tunneling has also been included as a pre-exponential factor, Γ_n , in the rate constant expression. It is given by $\Gamma_n = 3 \times 10^{10} \nu_n$, where ν_n is the nuclear vibrational frequency of the reactants and

$$\nu_n^2 = \frac{\nu_{\text{solv}}^2 \Delta G_{\text{solv}}^* + \nu_{\text{is}}^2 \Delta G_{\text{is}}^*}{\Delta G_{\text{solv}}^* + \Delta G_{\text{is}}^*} \approx \frac{\nu_{\text{is}}^2 \Delta G_{\text{is}}^*}{\Delta G_{\text{solv}}^* + \Delta G_{\text{is}}^*} \quad (6.27)$$

where it is assumed that the frequency for the outer-sphere solvent molecules, $\nu_{\text{solv}} \sim 30\text{ cm}^{-1}$, is more than 10 times smaller than the inner-sphere frequency, $\nu_{\text{is}} \sim 400\text{ cm}^{-1}$, and $\Delta G_{\text{is}}^* \approx \Delta G_{\text{solv}}^*$. The value of ν_{is} is taken as the average of the breathing-mode frequencies of the two reactants, ν_1 and ν_2 , as calculated from

$$\nu_{\text{is}}^2 = \frac{2\nu_1^2 \nu_2^2}{\nu_1^2 + \nu_2^2} \quad (6.28)$$

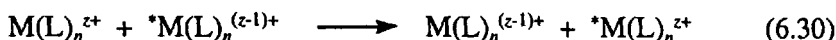
The final feature to be considered as a pre-exponential factor is the electronic transmission coefficient, κ_{el} , which is equal to one if the electron-transfer step is adiabatic and is smaller otherwise.

All of the pre-exponential factors and contributions to the overall ΔG^* are incorporated into the transition state theory equation to obtain the calculated outer-sphere rate constant as

$$k_{\text{calc}} = \kappa_{\text{el}} \Gamma_n K_{\text{os}} e^{-(\Delta G_{\text{solv}}^* + \Delta G_{\text{is}}^*)/RT} \quad (6.29)$$

6.2.3 Tests of Marcus Theory Predictions

The next step is to compare rate constants calculated from Eq. (6.29) to some experimental results. Because of their overall symmetry, it is easier to do this for electron-exchange reactions such as (6.30), where M and L are the same and only the oxidation state is different in the two reactants:



Results for some such systems are given in Table 6.1. The calculated and observed values agree very well for $Fe(OH_2)_6^{2/3+}$ and $Co(NH_3)_6^{2/3+}$, less well but acceptably for $Ru(NH_3)_6^{2/3+}$ and poorly for $Ru(OH_2)_6^{2/3+}$. The main feature controlling the relative rates for different metal ions is the difference in ΔG_{is}^* , which is in turn controlled by the difference in bond lengths between the two oxidation states. This is critical because ΔG_{is}^* depends on the square of this difference. For example, the observed and calculated values for $Ru(OH_2)_6^{2/3+}$ agree if the size difference is 0.125 Å instead of 0.09 Å and a change from 0.04 Å to 0.095 Å gives agreement for $Ru(NH_3)_6^{2/3+}$. Errors in the force constants will be somewhat self-compensating, as can be seen from Eq. (6.26). A detailed analysis of the $Ru(OH_2)_6^{2/3+}$ system by Bernhard and Ludi¹⁹ yielded force constants of 191 and 298 N m⁻¹ for the II and III oxidation states, respectively, while the simple model based on a harmonic oscillator gives 190 and 300 N m⁻¹, respectively. This factor does not seem to be a major source of concern.

Table 6.1. Comparison of Relevant Parameters and Calculated and Observed Self-Exchange Rate Constants for $M(L)_n^{2/3+}$ Systems

Parameter	$Fe(OH_2)_6^{2/3+}$	$Ru(OH_2)_6^{2/3+}$	$Ru(NH_3)_6^{2/3+}$	$Co(NH_3)_6^{2/3+}$
a_1, a_2 (Å)	3.33, 3.19	3.32, 3.23	3.37, 3.33	3.41, 3.19
ν_1, ν_2 (cm ⁻¹)	390, 490	424, 532	442, 500	357, 394
ν_n (cm ⁻¹)	319	286	151	347
$10^{-12} \chi \Gamma_n$ (s ⁻¹)	9.6	8.6	4.5	10.4
μ (M)	0.55	5.0	0.10	2.5
K_{os} (M ⁻¹)	0.055	0.23	0.017	0.093
ΔG_{solv}^* (kJ mol ⁻¹)	29.3	29.2	28.5	29.0
ΔG_{is}^* (kJ mol ⁻¹)	35.0	17.1	3.2	73.4
k_{calc} (M ⁻¹ s ⁻¹ , 25°C)	2.8	1.5×10^5	2.2×10^5	1.1×10^{-6}
k_{obsd} (M ⁻¹ s ⁻¹ , 25°C)	4.2 ^a	20 ^b	6.7×10^3 ^c	8×10^{-6} ^d

^a Brunshwig, B. S.; Creutz, C.; Macartney, D. H.; Sham, T.-K.; Sutin, N. *Disc. Faraday Soc.* **1982**, 74, 113; Jolley, W. H.; Stranks, D. R.; Swaddle, T. W. *Inorg. Chem.* **1990**, 29, 1948.

^b Bernhard, P.; Helm, L.; Ludi, A.; Merbach, A. E. *J. Am. Chem. Soc.* **1985**, 107, 312.

^c Extrapolated with $\Delta H^\ddagger = 5$ kcal mol⁻¹ from measurements at 4°C of Smolenaers, P. J.; Beattie, J. K. *Inorg. Chem.* **1986**, 25, 2259.

^d Hammershoi, A.; Geselowitz, D.; Taube, H. *Inorg. Chem.* **1984**, 23, 979, at 40°C.

In general, the most common scapegoat for disagreement between k_{calc} and k_{obsd} is the electronic transmission coefficient, κ_{el} . Since calculated values are usually higher than observed, nonadiabaticity is invoked so that $\kappa_{\text{el}} < 1$. Values in the range of 0.1 to 10^{-3} often bring the observed and calculated values into agreement.

There has been much discussion of the solvent dependence of the self-exchange rates.²⁰ The theory is based on a solvent dielectric continuum model and predicts a variation in rate constant with the properties of the solvent due to the $(n_s^{-2} - \epsilon_s^{-1})$ dependence of ΔG_{solv}^* . More sophisticated approaches have been developed by adding solvent dynamics to the model.^{21,22} However, these are difficult to test experimentally and have not been widely used in the analysis.

Chan and Wahl²³ found that the continuum prediction was followed for the tris(hexafluoroacetylacetonato)ruthenium(II)/(III) system. Later studies²⁴ on the $\text{Fe}(\text{C}_5\text{H}_5)_2^{0/+}$ system also showed the expected general trend, although the correlation is not perfect. Further studies²⁵ on other metallocenes led to the suggestion of a correlation with "solvent friction", as measured by solvent NMR relaxation times. Drago and Ferris²⁶ criticized the solvent friction model and analyzed the results in terms of the S' parameter of the "united solvation model" and the E_{B} and C_{B} values of the solvents. Abbott and Rusling²⁷ found a correlation with the Kamlet-Taft solvent parameters. Lay et al.²⁸ studied the effect of solvent on the reduction potentials of several Co(III) complexes and found a correlation with hydrogen-bonding basicities. Curtis and co-workers²⁹ have studied several Ru(II/III) ammine systems and found a correlation of the self-exchange rates with the Gutmann donor number of the solvent. They suggest that this results from hydrogen bonding between the ammine complex and the solvent. These correlations indicate the limitations of the conventional continuum model for solvent effects. A similar conclusion might be drawn from Swaddle's detailed analysis³⁰ of the solvent effects on the volumes of activation for electron-exchange reactions. However, more recent work³¹ indicates that the ΔV^* values are consistent with the Marcus model. Overall, these studies are of value in pointing out that the solvent continuum model has limitations when there are specific solvent-solute interactions.

There have been several recent attempts to estimate self-exchange rate constants using quantum mechanics and molecular modeling methods. The $\text{M}(\text{OH}_2)_6^{2/3+}$ systems, with $\text{M} = \text{V}, \text{Cr}, \text{Mn}, \text{Fe}$ and Co , have been examined by Rosso and co-workers^{32,33} and by Zhang and Liu,³⁴ although the latter only considered the inner-sphere rearrangement process. Earlier, Zhang et al.³⁵ presented a more complete analysis of the cobalt system. It should be noted that all of these studies seem to have treated $\text{Co}(\text{OH}_2)_6^{3+}$ as a high-spin system, but it is actually low-spin. The Fe system has been analyzed by Bu³⁶ and by Rustad et al.³⁷ The latter also considered hydrolyzed Fe(III) species but did not consider an inner-sphere mechanism with the

$\text{Fe}(\text{OH}_2)_5(\text{OH})^{2+}$ ion. Rosso et al.³⁸ did parallel calculations on the Fe and Mn systems and concluded that transfer of a t_{2g} electron from $\text{Fe}(\text{OH}_2)_6^{2+}$ is more favorable than transfer of an e_g electron from $\text{Mn}(\text{OH}_2)_6^{2+}$. The calculations also suggest that the high-spin Mn(III) d^4 and Fe(II) d^6 ions undergo a Jahn–Teller distortion with shortening of two M—OH₂ bonds.

Theoretical aspects of the $\text{Co}(\text{NH}_3)_6^{2/3+}$ system have been described recently by Endres et al.³⁹ They considered the involvement of various possible spin states of Co(III) and Co(II) and concluded that the most favorable exchange occurs between the ground state of Co(III), t_{2g}^6 , and a spin-excited state of Co(II), $t_{2g}^6 e_g^1$. They find that the latter is stabilized by Jahn–Teller distortion, a factor which was not considered in earlier work⁴⁰ where it was concluded that the reactants were electronic ground states for both oxidation states. The issue of spin-state effects in other cobalt complexes is discussed below. Endres et al. also have provided a brief summary of the weaknesses of Density Functional Theory when applied to such systems. If the spin-state change prediction is correct, then the agreement between calculated and observed values for the $\text{Co}(\text{NH}_3)_6^{2/3+}$ system in Table 6.1 could be fortuitous.

The reduction potentials and kinetic parameters for self-exchange for several systems of the same charge type are given in Table 6.2. For the $\text{M}(\text{OH}_2)_6^{2/3+}$ systems, the rate law has a term with an $[\text{H}^+]^{-1}$ dependence assigned to the reaction of $\text{M}(\text{OH}_2)_6^{2+}$ with $\text{M}(\text{OH}_2)(\text{OH})_5^{2+}$ and a term independent of $[\text{H}^+]$ assigned to the reaction of $\text{M}(\text{OH}_2)_6^{2+}$ with $\text{M}(\text{OH}_2)_6^{3+}$. The tabulated results are for the latter pathway, which is widely assumed to proceed by an outer-sphere mechanism. It should be noted that, for all of these systems studied except $\text{Ru}(\text{OH}_2)_6^{2/3+}$, one of the partners is labile toward substitution so that an inner-sphere mechanism would be possible. However, evidence discussed in Section 6.4 and the theory described above indicate that H₂O is a very poor bridging group.

Amongst the $\text{M}(\text{OH}_2)_6^{2/3+}$ systems, the k_{AA} values fall in the range of 0.01 to 20 $\text{M}^{-1} \text{s}^{-1}$, except for $\text{Cr}(\text{OH}_2)_6^{2/3+}$ which has a value of $<10^{-5} \text{M}^{-1} \text{s}^{-1}$. This may be attributed to the fact that Cr(II), with the formal $t_{2g}^3 e_g^1$ configuration, must transfer an e_g electron and has a Jahn–Teller distorted octahedral geometry so that the inner-sphere rearrangement energy is larger. The same rationalizations might be used for the $\text{Mn}(\text{OH}_2)_6^{2/3+}$ system which has been inferred to have a small k_{AA} from an analysis of cross reactions,⁴¹ as described in the following section. Similar reasons may account for the slow exchange between the distorted octahedral d^9 $\text{Cu}(\text{OH}_2)_6^{2+}$ ion and what is probably the tetrahedral d^{10} $\text{Cu}(\text{OH}_2)_4^+$ ion.⁴²

It should be noted that electronic configuration and geometrical rearrangement factors also would predict slow exchange for the $\text{Co}(\text{OH}_2)_6^{2/3+}$ system, but this system does not appear unusually slow. One escape from this logical inconsistency would be to suppose that the spin-state change requires less energy for $\text{Co}(\text{OH}_2)_6^{2/3+}$ than for $\text{Co}(\text{NH}_3)_6^{2/3+}$ because of the smaller $10Dq$ of the former.

Table 6.2. Reduction Potentials and Kinetic Parameters for Self-Exchange Rates (25°C) for Selected Reagents in H₂O

Redox Couple	$E^{\circ a}$ (V)	μ^b (M)	k_{AA} (M ⁻¹ s ⁻¹)	ΔH^\ddagger (kcal mol ⁻¹)	ΔS^\ddagger (cal mol ⁻¹ K ⁻¹)	ΔV^\ddagger (cm ³ mol ⁻¹)
V(OH) ₂ ²³⁺	-0.24 ^c	0.5 NaClO ₄	1x10 ^{-2 d}	12.6	-24.9	
Cr(OH) ₂ ²³⁺	-0.40	1.0 HClO ₄	≤1x10 ^{-5 a}			
Fe(OH) ₂ ²³⁺	+0.74	0.1 NaClO ₄	1.2 ^e	11.1	-21.1	
Fe(OH) ₂ ²³⁺		0.5 NaClO ₄	4.5 ^f	9.9	-22.2	-11.1 ^g
Fe(phen) ₃ ²³⁺	1.00 ^h	0.4 H ₂ SO ₄	1.5x10 ^{7 i}	0.4	-24.4	-2.2
Co(OH) ₂ ²³⁺	+1.85 ^j	0.5 NaClO ₄	2.4 ^k	10.7	-20.9	
Co(OH) ₂ ²³⁺		1.0 NaClO ₄	4.8 ^k	13.3	-10.9	
Co(sep) ²³⁺	-0.26 ^l	0.2 NaCl	5.1 ^m	9.4	-23.7	
Co(sep) ²³⁺		0.2 NaCl	5.1 ⁿ	9.9	-22.2	-6.4
Co(phen) ₃ ²³⁺	+0.37	0.1 NaCl	4.9 ^o	8.4	-27.0	-17.6 ^p
Co(phen) ₃ ²³⁺		0.1 NaNO ₃	9.3 ^o	4.9	-37.3	
Co(en) ₃ ²³⁺	-0.17 ^l	0.98 KCl	7.7x10 ^{-5 q}	13.9	-30.8	-15.5 ^p
Co(NH ₃) ₆ ²³⁺	-0.02 ^l	2.5 KTrf	8x10 ^{-6 r}			
Ru(OH) ₂ ²³⁺	-0.22	5 NaTrf	2.0x10 ^{1 s}	11.0	-15.7	
Ru(NH ₃) ₆ ²³⁺	+0.10 ^l	0.01 DTrf	8.2x10 ^{2 t}	10.3	-11.0	
Ru(NH ₃) ₆ ²³⁺	+0.051	0.1 DTrf	3.2x10 ^{3 u}	(4.5)	(-27)	
Ru(en) ₃ ²³⁺	+0.19	0.25 NaTrf	2.4x10 ^{4 v}	6.0	-18.2	-15.1
Ru(bpy) ₃ ²³⁺	+1.26	0.1 HClO ₄	4.2x10 ^{8 w}	7.7	-6.6	

^a Chou, M.; Creutz, C.; Sutin, N. *J. Am. Chem. Soc.* **1977**, *99*, 5615, and references therein unless otherwise indicated.

^b Ionic medium for the kinetic results; Trf = trifluoromethanesulfonate.

^c Fiore, M.; Orecchio, S.; Romano, V.; Zingales, R. *J. Chem. Soc., Dalton Trans.* **1993**, 799.

^d Krishnamurty, K. V.; Wahl, A. C. *J. Am. Chem. Soc.* **1958**, *80*, 5921.

^e Brunshwig, B. S.; Creutz, C.; Macartney, D. H.; Sham, T.-K.; Sutin, N. *Faraday Discuss., Chem. Soc.* **1982**, *74*, 113.

^f Silverman, J.; Dodson, R. W. *J. Phys. Chem.* **1952**, *56*, 846.

^g Jolley, W. H.; Stranks, D. R.; Swaddle, T. W. *Inorg. Chem.* **1990**, *29*, 1948.

^h Macartney, D. H.; Sutin, N. *Inorg. Chem.* **1985**, *24*, 3403.

ⁱ Doine, H.; Swaddle, T. W. *Can J. Chem.* **1988**, *66*, 2763.

^j Warnqvist, B. *Inorg. Chem.* **1970**, *9*, 682; Rosseinsky, D. R.; Jauregui, G. A. *J. Chem. Soc., Faraday Trans. 1* **1979**, 473; Mowforth, C. W.; Rosseinsky, D. R.; Stead, K. *Ibid.* **1979**, 1268.

^k Habib, H. S.; Hunt, J. P. *J. Am. Chem. Soc.* **1966**, *88*, 1668.

^l Comba, P.; Sickmüller, A. F. *Inorg. Chem.* **1997**, *36*, 4500, and references therein.

^m Creaser, I. I.; Sargeson, A. M.; Zanella, A. W. *Inorg. Chem.* **1983**, *22*, 4022.

ⁿ Doine, H.; Swaddle, T. W. *Inorg. Chem.* **1991**, *30*, 1858.

^o Warren, R. M. L.; Lappin, A. G.; Mehta, B. D.; Neumann, H. M. *Inorg. Chem.* **1990**, *29*, 4185.

^p Shalders, R. D.; Swaddle, T. W. *Inorg. Chem.* **1995**, *34*, 4815, and references therein.

^q Dwyer, F. P.; Sargeson, A. M. *J. Phys. Chem.* **1961**, *65*, 1892.

^r Hammershoi, A.; Geselowitz, D.; Taube, H. *Inorg. Chem.* **1984**, *23*, 979, at 40°C.

^s Bernhard, P.; Helm, L.; Ludi, A.; Merbach, A. E. *J. Am. Chem. Soc.* **1985**, *107*, 312.

^t Meyer, T. J.; Taube, H. *Inorg. Chem.* **1968**, *7*, 2369.

^u Brown, G. M.; Sutin, N. *J. Am. Chem. Soc.* **1979**, *101*, 883; ΔH^\ddagger and ΔS^\ddagger calculated from theory.

^v Metelski, P. D.; Fu, Y.; Khan, K.; Swaddle, T. W. *Inorg. Chem.* **1999**, *38*, 3103.

^w Young, R. C.; Keene, F. R.; Meyer, T. J. *J. Am. Chem. Soc.* **1977**, *99*, 2468.

The results in Table 6.2 also show that the k_{AA} values for the cobalt complexes are much more sensitive to the ligand environment than their ruthenium analogues. Since the latter are low-spin in both oxidation states, a spin-state change is very improbable and a spin-state change with cobalt might account for the difference in sensitivity to the ligands. The systems also are electronically different because a t_{2g} electron is transferred between Ru(II), t_{2g}^5 , and Ru(III), t_{2g}^6 , without any electronic excitation.

The spin-state change argument seems to falter for the $\text{Co}^{\text{III/II}}(\text{N})_6$ cage complexes, such as $\text{Co}(\text{sep})^{2/3+}$. Their k_{AA} values are much larger than those of noncaged analogues such as $\text{Co}(\text{NH}_3)_6^{2/3+}$ and $\text{Co}(\text{en})_3^{2/3+}$. Sargeson and co-workers⁴³ have attributed the high reactivity to ring-strain in the cage ligands. For example, in the case of $\text{Co}(\text{sep})^{2/3+}$, the Co(III) is a bit too small to fit into the cage and the Co(II) is a bit too large.⁴⁴ As a result, bond length distortion toward the transition state is particularly favorable. Similar factors may apply to $\text{Co}(\text{tacn})_2^{2/3+}$ (an N_3 macrocycle) with $k_{AA} = 0.18 \text{ M}^{-1} \text{ s}^{-1}$, compared to $\text{Ru}(\text{tacn})_2^{2/3+}$ with $k_{AA} = 5 \times 10^4 \text{ M}^{-1} \text{ s}^{-1}$.⁴⁵ For $\text{Co}(\text{ttacn})_2^{2/3+}$ (an S-donor chelate) and $\text{Co}(\text{azacpten})^{2/3+}$ (an S_3N_3 cage), the bond lengths are almost the same in the two oxidation states because the Co(II) is low-spin and the rate constants are 1.3×10^4 and $4.5 \times 10^3 \text{ M}^{-1} \text{ s}^{-1}$, respectively.^{46,47} For further support, calculated ring-strain energies show some correlation with electron exchange rate constants for a range of systems.⁴⁸ For such systems, analysis of electrochemical thermodynamics by Turner and Schultz⁴⁹ and ΔV^* values by Shalders and Swaddle⁵⁰ both indicate that the spin-state change pathway is most consistent with the observations.

For $\text{M}(\text{phen})_3^{2/3+}$ and $\text{M}(\text{bipy})_3^{2/3+}$ systems, the k_{AA} values are typically large and approach the diffusion-controlled limit for most M, except Co. The large values of k_{AA} are attributed to electron transfer occurring through the conjugated ring system. This provides a low energy pathway and allows electron transfer at a greater separation between the metal centers than is possible with smaller, saturated ligands. In addition, these systems are usually low-spin in both oxidation states, so that bond length changes are smaller than would otherwise be the case, and inner-sphere reorganization requires less energy. The $\text{Co}(\text{phen})_3^{2/3+}$ system is different in two ways: the Co(II) complex is high-spin⁵¹ and the system may be going by the spin-state change pathway.

If counter ions have an effect on the electron-transfer rates, then Marcus theory would have a problem because these ions are not included in the theory. For most cationic reactants, such as those in Table 6.2, anions affect the rate through normal ionic strength effects and ion pairing. The latter has been observed generally to inhibit reaction in nonaqueous solvents.⁵² The $\text{Co}(\text{phen})_3^{2/3+}$ system is somewhat unusual in that NO_3^- seems to have some catalytic effect. For anionic reactants the situation is quite different and cations often provide significant catalysis. One of the most widely studied of these is the $\text{Fe}(\text{CN})_6^{3/4-}$ system for which Wahl and

co-workers⁵³ studied the effect of many cations and estimated the value of k_{AA} by extrapolation to zero cation concentration. More recently, Swaddle and co-workers⁵⁴ have shown that the K^+ ion can be complexed by crypt-2.2.2 to give a cation that is not a catalyst. At an ionic strength of ~ 0.2 M and 25°C , they found $k_{AA} = 2.4 \times 10^2 \text{ M}^{-1} \text{ s}^{-1}$ with $\Delta H^\ddagger = 5.0 \text{ kcal mol}^{-1}$, $\Delta S^\ddagger = -31 \text{ cal mol}^{-1} \text{ K}^{-1}$ and $\Delta V^\ddagger = -11.3 \text{ cm}^3 \text{ mol}^{-1}$. For both cationic and anionic reactants, the counter ion may provide some decrease of the electrostatic repulsion between the reactants. The greater effectiveness of cations has led to the suggestion⁵⁵ that they may provide a pathway of positive potential for electron exchange between the anionic reactants.

The significance and uses of ΔV^\ddagger values in this area will be discussed at the end of the following section.

6.2.4 Applications of the Marcus Cross Relationship

From the detailed theory, Marcus recognized certain simplifications that led to a cross relationship of the same form as that developed by Ratner and Levine. In Marcus' terms, this relationship is given by

$$k_{AB} = (k_{AA}k_{BB}K_{AB}f_{AB})^{1/2} \quad (6.31)$$

where

$$\log f_{AB} = \frac{(\log K_{AB})^2}{4 \log \left(\frac{k_{AA}k_{BB}}{Z^2} \right)}$$

and Z is the collision number for the ions in solution ($\approx 10^{11} \text{ M}^{-1} \text{ s}^{-1}$). The f_{AB} factor is analogous to the F_{AB} in the Ratner and Levine development and $f_{AB} \approx 1$ unless K_{AB} is large. If $f_{AB} \approx 1$, then Eq. (6.31) reduces to Eq. (6.32), called the simplified Marcus equation:

$$k_{AB} = (k_{AA}k_{BB}K_{AB})^{1/2} \quad (6.32)$$

For a one-electron transfer at 25°C , the logarithmic form of this equation is given by

$$\log k_{AB} = 0.5(\log k_{AA} + \log k_{BB} + 16.9\Delta E^\circ) \quad (6.33)$$

where ΔE° is the reduction potential in volts. Sutin and co-workers⁵⁶ tested this equation using a series of $\text{Fe}(\text{phenX})_3^{2/3+}$ complexes, for which k_{BB} is expected to be constant, reacting with aqueous $\text{Fe}(\text{II})$ and $\text{Ce}(\text{IV})$. They found that plots of $\log k_{AB}$ versus ΔE° have close to the expected slope, but the intercepts are smaller than predicted.

This equation can be applied to calculate one of the self-exchange rate constants, k_{AA} or k_{BB} , or to calculate k_{AB} , in order to compare it to an

experimental value. These applications have been reviewed by Sutin and co-workers,⁵⁷ who conclude that k_{AB} can be predicted to within a factor of about 25 if the reaction is outer-sphere. Since the self-exchange rate constant depends on the square of k_{AB} , one could expect to predict k_{AA} or k_{BB} to within 25². Some typical results from the cross relationship are given in Table 6.3. The first three examples are typical of the type of agreement that is generally viewed as acceptable. However, the calculations involving the Fe(II/III) couple, with $k_{AA} = 4 \text{ M}^{-1} \text{ s}^{-1}$, consistently give predicted values that are larger than the experimental values and seem more consistent with a value of k_{AA} that is $\sim 10^3$ smaller than the measured value. This effect will be discussed further with regard to the results in Table 6.4.

Bernhard and Sargeson⁵⁸ have applied Eq. (6.31) to determine the self-exchange rates of some encapsulated ruthenium, manganese, iron and nickel complexes. They used five reagents with known self-exchange rates and studied 19 cross reactions in order to determine five new self-exchange rates by using a least-squares fit of the data to Eq. (6.31). Some representative results are given in Table 6.4. The authors allowed Z to be a fitting variable and obtained a best-fit value five times smaller than that of $10^{11} \text{ M}^{-1} \text{ s}^{-1}$ commonly assumed, but this is not a major influence on the fit because f_{AB} is near unity for most systems. Bernhard and Sargeson found that the measured self-exchange rate for the $\text{Fe}(\text{OH}_2)_6^{2/3+}$ system does not fit the results and treated this as a variable to obtain a self-consistent value of $6.2 \times 10^{-3} \text{ M}^{-1} \text{ s}^{-1}$. Deviations such as this were noted by Sutin et al.⁵⁷ and were examined further by Hupp and Weaver,⁵⁹ who suggested that a value of $\sim 10^{-3} \text{ M}^{-1} \text{ s}^{-1}$ is more consistent for a number of reactions.

The standard explanation for this deviation is that the $\text{Fe}(\text{OH}_2)_6^{2/3+}$ exchange is inner-sphere with a bridging water molecule. It has been suggested⁶⁰ that the self-exchange rate of $20 \text{ M}^{-1} \text{ s}^{-1}$ for the system $\text{Ru}(\text{OH}_2)_6^{2/3+}$ also implies a much smaller value for $\text{Fe}(\text{OH}_2)_6^{2/3+}$ because the inner-sphere rearrangement is greater for Fe than for Ru (see Table 6.1). In a similar vein, it should be noted that the difference in ionic radii of V(II) and V(III) is very similar to that of Fe(II) and Fe(III), so that the $\text{Fe}(\text{OH}_2)_6^{2/3+}$ exchange rate might be expected to be $\sim 0.01 \text{ M}^{-1} \text{ s}^{-1}$. On the

Table 6.3. Comparison of Some Observed Rate Constants ($\text{M}^{-1} \text{ s}^{-1}$, 25°C) with Those Calculated from the Marcus Cross Relationship

Reactants	$\log K_{AB}$	$k_{AB \text{ obsd}}$	$k_{AB \text{ calc}}$
$\text{Ru}(\text{NH}_3)_6^{2+} + \text{Co}(\text{phen})_3^{3+}$	6.25	1.5×10^4	3.5×10^5
$\text{V}(\text{OH}_2)_6^{2+} + \text{Co}(\text{en})_3^{3+}$	2.12	5.8×10^{-4}	3.1×10^{-3}
$\text{V}(\text{OH}_2)_6^{2+} + \text{Ru}(\text{NH}_3)_6^{3+}$	5.19	1.3×10^3	2.2×10^3
$\text{V}(\text{OH}_2)_6^{2+} + \text{Fe}(\text{OH}_2)_6^{3+}$	16.9	1.8×10^4	1.6×10^6
$\text{Ru}(\text{NH}_3)_6^{2+} + \text{Fe}(\text{OH}_2)_6^{3+}$	11.7	3.4×10^5	1.2×10^7
$\text{Fe}(\text{OH}_2)_6^{2+} + \text{Ru}(\text{bpy})_3^{3+}$	8.81	7.2×10^5	3.6×10^8

Table 6.4. Self-Exchange Rate Constants ($M^{-1} s^{-1}$, $25^{\circ}C$) Obtained by Fitting to the Marcus Cross Relationship

Reagent		E_A (V)	E_B (V)	$k_{AA}^{a,b}$	$k_{BB}^{a,c}$	$10^{-4} \times k^a$	
A	B					obsd	calc
Ru(sar) ²⁺	Ru(NH ₃) ₅ (py) ³⁺	0.29	0.302	1.2×10^5	1.1×10^5	10.5	14
Ru(sar) ²⁺	Ru(NH ₃) ₅ (nic) ³⁺	0.29	0.362	1.2×10^5	1.1×10^5	28	44
Ru(sar) ²⁺	Ru(NH ₃) ₅ (isn) ³⁺	0.29	0.384	1.2×10^5	1.1×10^5	52	66
Ru(sar) ²⁺	Ru(tacn) ³⁺	0.29	0.366	1.2×10^5	5.4×10^4	73	34
Ru(sar) ²⁺	Mn(sar) ³⁺	0.29	0.519	1.2×10^5	1.7×10^1	17	9
Ru(sar) ²⁺	Fe(OH ₂) ₆ ³⁺	0.29	0.74	1.2×10^5	6.2×10^{-3b}	7.2	6.7
Mn(sar) ³⁺	Ru(NH ₃) ₅ (py) ²⁺	0.519	0.302	1.7×10^1	1.1×10^5	3.7	7.2
Mn(sar) ³⁺	Ru(NH ₃) ₅ (isn) ²⁺	0.519	0.384	1.7×10^1	1.1×10^5	1.4	1.7
Mn(sar) ³⁺	Ru(tacn) ²⁺	0.519	0.366	1.7×10^1	1.2×10^5	2.9	1.6
Mn(sar) ³⁺	Fe(OH ₂) ₆ ³⁺	0.519	0.74	1.7×10^1	6.2×10^{-3b}	1.2 ^d	2.0 ^d

^a $\mu = 0.1$ M, selected from Ref. 58, where structures of the ligands are given.

^b Determined from a least-squares fit to Eq. (6.31) with $Z = 1.9 \times 10^{10} M^{-1} s^{-1}$.

^c Fixed values known independently unless otherwise indicated.

^d Values of $10^{-1} \times k$.

other hand, for the Fe(OH₂)₆^{2/3+} exchange⁶¹, the ΔV^* of $-11 \text{ cm}^3 \text{ mol}^{-1}$ has been taken as evidence for an outer-sphere mechanism, especially by comparison to the value of $0.8 \text{ cm}^3 \text{ mol}^{-1}$ for Fe(OH₂)₅OH^{2+/Fe(OH₂)₆²⁺ which is believed to be an inner-sphere reaction. It is somewhat ironic that the mechanism for one of the most studied and analyzed reactions remains controversial.}

The cross relationship can also be used to estimate self-exchange rates when these rates cannot be measured directly. If the least-squares analysis of Bernhard and Sargeson is not used, then the calculation is somewhat cyclical because k_{BB} also appears in f_{AB} , but f_{AB} is often ~ 1 and not strongly dependent on k_{BB} . Macartney and Sutin⁶² applied this method to various ascorbate radicals and their parents and calculated the following self-exchange rate constants ($M^{-1} s^{-1}$, $25^{\circ}C$): 2×10^3 for H₂A/H₂A^{•+}; 1×10^5 for HA/HA[•]; $\sim 2 \times 10^5$ for A²⁻/A^{•-}.

Confidence in such applications is tempered by attempts to calculate the self-exchange rate constant for the dioxygen/superoxide, O₂/O₂⁻, couple. Taube and co-workers⁶³ studied the oxidation of three Ru(II) ammine complexes and analyzed the results, using Eq. (6.31) to obtain a reasonably self-consistent self-exchange rate constant of $1 \times 10^3 M^{-1} s^{-1}$ for O₂/O₂⁻. Espenson and co-workers⁶⁴ expanded the earlier study with more reducing agents and refined the analysis by including so-called work terms that attempt to correct for asymmetries in the charge and size of the species involved. The work term corrections are given by the following equations:⁶⁵

$$k_{AB} = (k_{AA}k_{BB}K_{AB}f_{AB})^{1/2}W_{AB} \quad (6.34)$$

where f_{AB} and W_{AB} are given by

$$\ln f_{AB} = \frac{(\ln K_{AB} + (w_{AB} - w_{BA})/RT)^2}{4 \ln(k_{AA}k_{BB}/Z^2) + (w_{AA} + w_{BB})/RT}$$

$$\ln W_{AB} = -(w_{AB} + w_{BA} - w_{AA} - w_{BB})/2RT$$

The individual work terms are calculated from

$$w_{ij} = \frac{4.225 \times 10^3 z_A z_B}{r(1 + 0.329 r \mu^{1/2})} \quad (6.35)$$

where r is the sum of the radii of the reaction partners in Å, μ is the ionic strength, the numerical constants are for water at 25°C and the w_{ij} are in cal mol⁻¹. Some of these results are given in Table 6.5. The O₂ reductions give values of k_{BB} that are consistent within the accepted limits, but the O₂⁻ oxidations give quite different and divergent values. Finally, the self-exchange rate constant has been measured⁶⁶ by oxygen isotope exchange and found to be (4.5 ± 1.6) × 10² M⁻¹ s⁻¹ (0.3 M 2-propanol, 0.02 M NaOH). Several rationalizations for the discrepancy between the direct and Marcus relationship values may be offered. The direct O₂/O₂⁻ reaction may not be truly outer-sphere in that there might be some bonding interaction during the encounter of the reactants. In that case, the Marcus relationship might be giving the true outer-sphere rate constant by an argument analogous to that used for the Fe(OH₂)₆^{2/3+} system. The small values obtained for the reductions by O₂⁻ present the unanswered problem of whether they represent the true outer-sphere rate constant or are due to some unexpected chemical problem. However, it may be that the Marcus formulation is not entirely justified for small and possibly strongly solvated and hydrogen-bonded species such as aqueous O₂⁻. On the other hand, theoretical studies,³³ based on an outer-sphere model, give a predicted rate constant in good agreement with experiment. The theory suggests rapid transfer of an electron between the π* orbitals of the donor and acceptor.

The results in Table 6.5 show that the corrections due to W_{AB} can be substantial because k_{BB} depends on W_{AB}^2 . The small f_{AB} values for the O₂⁻ reactions result mainly from the large equilibrium constants for these reactions, which produce small values of f_{AB} because the denominator in the $\ln f_{AB}$ equation is negative.

This cross relationship is often applied to metalloenzyme systems to determine their self-exchange rates, because techniques are seldom available to measure the values directly. These applications have variable success and the difficulties usually are attributed to varying points of attack on the enzyme and induced conformational changes in the enzyme.

Table 6.5. Self-Exchange Rate Constants (25°C) for Various Reactions of O_2/O_2^- Calculated from the Marcus Cross Relationship^a

Reactants	k_{AB} ($M^{-1} s^{-1}$)	a_{ML} ^b (Å)	W_{AB}	f_{AB}	k_{BB} ^c ($M^{-1} s^{-1}$)
$Cr(bpy)_3^{2+} + O_2$	6×10^5	6.8	4.0	0.78	0.6
$Cr(phen)_3^{2+} + O_2$	1.5×10^6	6.8	4.0	0.72	1.9
$Ru(NH_3)_6^{2+} + O_2$	6.3×10^1	3.4	29.0	0.84	3.1
$Ru(en)_3^{2+} + O_2$	3.6×10^1	4.0	15.9	0.44	2.7×10^2
$Co(sep)^{2+} + O_2$	4.3×10^1	4.5	11.3	0.82	7.0×10^{-2}
$Fe(CN)_6^{3-} + O_2^-$	3×10^2	4.5	3.65	0.090	1.5×10^{-8}
$Fe(C_5H_5)_2^+ + O_2^-$	8.6×10^6	5.0	1.4	0.016	5.7×10^{-4}

^a Further data and original references given in Zahir, K.; Espenson, J. H.; Bakac, A. *J. Am. Chem. Soc.* **1988**, *110*, 5059.

^b The radii of O_2 and O_2^- used are 1.21 and 1.33 Å, respectively; a_{ML} is for the reduced complex and a value 0.05 Å smaller was used for the oxidized form, except for equal values for Ru complexes.

^c $Z = 1 \times 10^{11} M^{-1} s^{-1}$ is used for all reactions.

Volumes of activation have been studied for a number of exchange reactions and for fewer cross reactions. The area of pressure effects on homogeneous exchange reactions and electrochemical reactions has been reviewed recently by Swaddle.⁶⁷ Interest in the electrochemical process stems, at least in part, from the observation of Swaddle and co-workers⁶⁸ of a correlation between the ΔV for the electrode reaction and the ΔV^* for the homogeneous electron-exchange reaction. Later work has shown that this only applies in water, apparently because the nonaqueous electrode reactions are diffusion limited and are affected by changes in viscosity with pressure that do not affect the homogeneous reaction. The viscosity of water happens to be relatively insensitive to pressure. Swaddle also has revised earlier suggestions and noted there that the ΔV^* values do not distinguish between adiabatic and nonadiabatic reactions, and that the ΔV^* data are consistent with the spin-change mechanism for Co(II/III) self-exchange reactions. The fact that ΔV^* for $Fe(OH_2)_5(OH)^{2+} + Fe(OH_2)_6^{3+}$ exchange is $\sim 12 \text{ cm}^3 \text{ mol}^{-1}$ more positive than for $Fe(OH_2)_6^{2/3+}$ is consistent with the former reaction proceeding by an inner-sphere mechanism. One anomaly in Table 6.2 is that $Co(en)_3^{2/3+}$ and $Ru(en)_3^{2/3+}$ have almost the same ΔV^* . The latter would be expected to have a much smaller ΔV^* because both oxidation states of ruthenium are low-spin and bond length differences should be much less.

For cross reactions, Swaddle and co-workers⁶⁹ have shown that the ΔV analogue of Eq. (6.18) should apply for adiabatic reactions of modest driving force. They found that agreement between experimental and predicted values of ΔV^* is good for $Fe(OH_2)_6^{3+} + Co([9]aneS_3)_2^{2+}$ but poor for $Fe(OH_2)_6^{3+} + Co(sep)^{2+}$. They suggest that the larger driving force for the latter causes the simple cross relationship to fail.

6.2.5 Further Predictions of Marcus Theory

There are several other predictions from Marcus theory which are less widely applied but still serve as tests for the theory. Marcus and Sutin⁷⁰ have shown that, if Eq. (6.31) is expressed in terms of ΔG values, then appropriate derivatives with respect to T can be used to obtain expressions for ΔH_{AB}^\ddagger and ΔS_{AB}^\ddagger in terms of the values for the overall and cross reactions. Marcus and Sutin used these expressions to explain the negative values of ΔH_{AB}^\ddagger obtained in previous work by Meyer and co-workers.⁷¹ Brown and Sutin⁷² used this approach to calculate the activation parameters for the $\text{Ru}(\text{NH}_3)_6^{2/3+}$ system given in Table 6.2. Weaver and Yee⁷³ applied a somewhat modified version of this approach to a wider range of reactions and found fair agreement as long as the overall ΔG_{AB}° was not too large. In a recent review,¹⁵ Newton concluded that the enthalpy and entropy values are not well accounted for by this approach, but compensating effects give satisfactory free energies.

It was recognized early in the development of the theory⁷⁴ that Eq. (6.31) predicts that as $-\Delta G_{AB}^\circ$, i.e. ΔE_{AB}° , increases k_{AB} should go through a maximum when $\log K_{AB} = 2 \log (Z^2/k_{AA}k_{BB})$. The predicted behavior is illustrated in Figure 6.2, where the predicted maximum value of $k_{AB} = Z$ has been restricted to a value of $3 \times 10^9 \text{ M}^{-1} \text{ s}^{-1}$ which is a typical diffusion controlled limit in water at 25°C. The so-called "inverted region" is evident at the right for the conditions of the dashed curve.

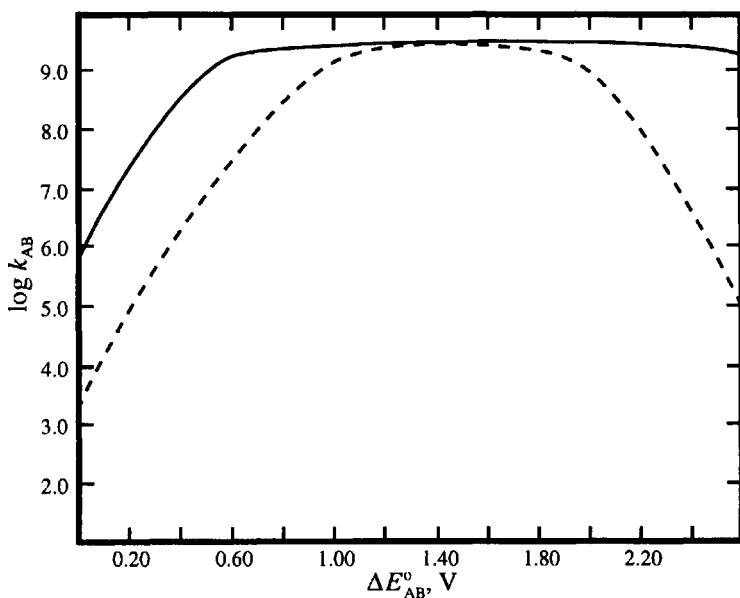


Figure 6.2. Predicted dependence of $\log k_{AB}$ on ΔE_{AB}° for $k_{AA}k_{BB} = 3 \times 10^6 \text{ M}^{-2} \text{ s}^{-2}$ (—) and $k_{AA}k_{BB} = 3 \times 10^{11} \text{ M}^{-2} \text{ s}^{-2}$ (- -) with $Z = 10^{11}$ in both cases.

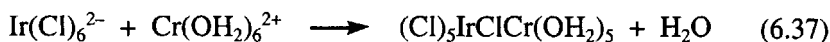
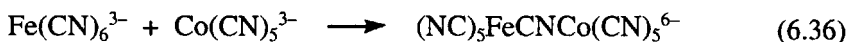
The counterintuitive nature of the predicted inverted region has generated considerable theoretical and experimental interest. More detailed theory⁷⁵⁻⁷⁸ has confirmed the basic phenomenon but modified several details. An examination of Figure 6.2 reveals that it will be difficult to observe the inverted region for a bimolecular reaction because it requires a high value of $k_{AA}k_{BB}$ and a $\Delta E_{AB}^0 \geq 2$ V. Otherwise, at high ΔE_{AB}^0 , one will observe the diffusion limited value of k_{AB} , as shown by the solid curve in Figure 6.2. As a result, the most definitive observations^{79,80} of the inverted region have come from unimolecular systems in which the oxidant and reductant are part of one species. Then, the rate is not limited by bimolecular diffusion but by faster processes such as reorganization of the solvent and vibrational relaxation.

A hint of the inverted region was suggested by Creutz and Sutin⁸¹ for the bimolecular electron transfer between photo-excited $\text{Ru}(\text{bpy})_3^{2+}$ and $\text{M}(\text{bpy})_3^{3+}$ complexes, where $\text{M} = \text{Cr}, \text{Os}$ and Ru . However, all of the rate constants are within a factor of two of the diffusion-limited value. Marcus and Siders⁷⁵ have given a more detailed analysis of these results.

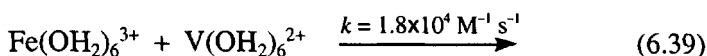
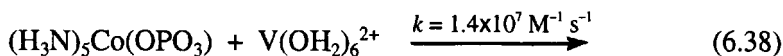
6.3 DIFFERENTIATION OF INNER-SPHERE AND OUTER-SPHERE MECHANISMS

Several criteria can be used to differentiate the two mechanisms:

1. The best method is to identify a product to which the bridging group has been transferred, as in the classic study by Taube and co-workers discussed earlier. Unfortunately, the appropriate combination of labile and inert metals is seldom available. Aside from $\text{Cr}(\text{II})$, other reagents, such as $\text{Co}(\text{CN})_5^{3-}$ and bis(dimethylglyoxime)cobalt(II), can be used. Sometimes, both metal centers in the product are inert and the dimeric product can be identified, as in the following examples.^{82,83}



2. If the rate constant for the oxidation-reduction reaction is larger than the rate of ligand substitution on either metal, then an outer-sphere mechanism is required. For example, $\text{V}(\text{OH}_2)_6^{2+}$ has a water exchange rate of 90 s^{-1} and substitution is by an I_a mechanism, so that the substitution rate constants should be $<100 \text{ M}^{-1} \text{ s}^{-1}$. For the following reactions, the rate constant is much larger than this.

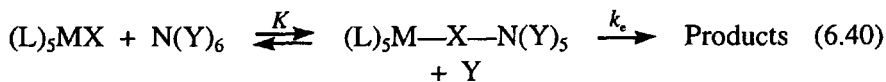


In the last example, substitution might occur on $\text{Fe}(\text{OH}_2)_6^{3+}$, but it has a water exchange rate of $\sim 150 \text{ s}^{-1}$ and the rate of the oxidation–reduction is too fast for this pathway. Therefore, both reactions must be using an outer-sphere mechanism. Clearly, if both reactants are quite inert to substitution, an outer-sphere mechanism is almost certain. For this reason, complexes with metals from the second and third transition series often are chosen for outer-sphere studies because they are low-spin and inert.

3. If all the ligands on both reactants have no unshared electron pairs, it will not be possible to form a bridged intermediate. For the chelates, one must be certain that ring opening does not precede electron transfer for this criterion to guarantee an outer-sphere mechanism. Fused-ring chelates and cages often are suitable choices. More commonly, complexes of phenanthroline and bipyridyl derivatives are used although, as noted above, they may transfer the electron through the conjugated π -system of the ligand.
4. If the reaction(s) obey the predictions of the Marcus theory, then an outer-sphere mechanism is often assumed. This is a dangerous criterion, because it has been observed that inner-sphere reaction rates^{84,85} also show a correlation with the overall ΔG° of the reaction that is predicted by the Marcus theory for outer-sphere reactions. Murdoch⁸⁶ has shown that such linear free-energy correlations may be more general than might originally have been expected.

6.4 BRIDGING LIGAND EFFECTS IN INNER-SPHERE REACTIONS

An inner-sphere mechanism consists of two processes, precursor complex formation and electron transfer, as shown in the following reaction:



where k_e is the rate constant for electron transfer between the two metal centers. To form the precursor complex, the bridging group, X, must have unshared pairs to share with both M and N. If the precursor formation is assumed to be a rapid pre-equilibrium, then the experimental second-order rate constant is given by

$$k_{\text{exp}} = Kk_e \quad (6.41)$$

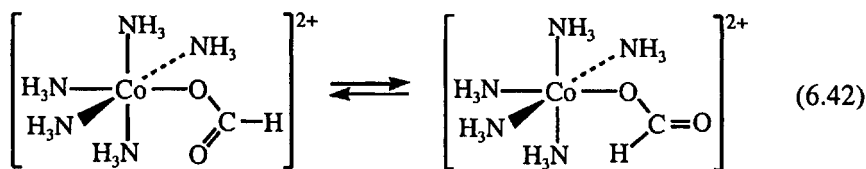
For many systems K is not known, so that the variation of k_{exp} with the nature of the bridging ligand may reflect changes in either or both K and k_e . Rate constants for some inner-sphere reactions with different bridging ligands are given in Table 6.6.

Table 6.6. Rate Constants (25°C) for the Reduction of Some $\text{Co}^{\text{III}}(\text{NH}_3)_5\text{X}$ Complexes by Cr^{2+} at $\mu = 1.0 \text{ M}$

X	k ($\text{M}^{-1} \text{ s}^{-1}$)	ΔH^\ddagger (kcal mol^{-1})	ΔS^\ddagger ($\text{cal mol}^{-1} \text{ K}^{-1}$)
F^- ^a	2.5×10^5		
Cl^- ^a	6×10^5		
Br^- ^b	1.4×10^6		
HCO_2^- ^c	7.2	8.3	-27
H_3CCO_2^- ^c	3.5×10^{-1}	8.2	-33
$\text{Cl}_2\text{HCO}_2^-$ ^c	7.5×10^{-2}	8.1	-36
F_3CCO_2^- ^c	1.7×10^{-2}	9.3	-35
$(\text{H}_3\text{C})_3\text{CCO}_2^-$ ^c	7.0×10^{-3}	11.1	-31
$\text{HO}_2\text{CCO}_2^-$ ^d	1.0×10^2		
$^- \text{O}_2\text{CCO}_2^-$ ^d	4.6×10^4	2.3	-20
$\text{H}_3\text{CC}(=\text{O})\text{CO}_2^-$ ^d	1.1×10^4	5.8	-21
$\text{H}_3\text{CC}(\text{OH})_2\text{CO}_2^-$ ^e	2.6×10^1		

^a Candlin, J. P.; Halpern, J. *Inorg. Chem.* **1965**, *4*, 766.^b Moore, M. C.; Keller, R. N. *Inorg. Chem.* **1971**, *10*, 747, at $\mu = 0.1 \text{ M}$.^c Barrett, M. B.; Swinehart, J. H.; Taube, H. *Inorg. Chem.* **1971**, *10*, 1983.^d Price, H. J.; Taube, H. *Inorg. Chem.* **1968**, *7*, 1.^e Sisley, M. J.; Jordan, R. B. *Inorg. Chem.* **1989**, *28*, 2714.

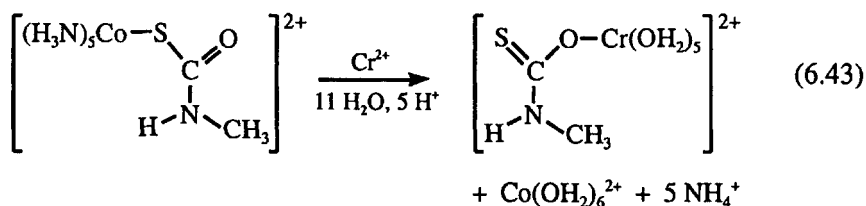
Several kinetic trends have been interpreted as largely reflecting changes in K . When $\text{Co}(\text{NH}_3)_5\text{X}^{2+}$ complexes with $\text{X} = \text{F}^-$, Cl^- and Br^- are reduced by Cr^{2+} , the order of reactivity is $\text{Br}^- > \text{Cl}^- > \text{F}^-$, but the opposite order is observed when Eu^{2+} is the reducing agent. This is rationalized from the knowledge that Eu^{2+} is a harder acid and forms stronger complexes with F^- than with Br^- , whereas Cr^{2+} forms stronger complexes with Br^- . If X is a carboxylate anion, then the order of reactivity in Table 6.6 is $\text{HCO}_2^- > \text{H}_3\text{CCO}_2^- > \text{Cl}_2\text{HCO}_2^- > \text{F}_3\text{CCO}_2^- > (\text{H}_3\text{C})_3\text{CCO}_2^-$. This order is interpreted as a combination of steric and electron-withdrawing effects, causing K to decrease. The high reactivity of the formate complex has been attributed⁸⁷ to its ability to form the more sterically accessible conformer on the right in reaction (6.42), thereby giving a larger K than expected.



The much higher rates for the oxalato and keto form of pyruvato complexes⁸⁸ are attributed to stabilization of the bridged intermediate by

chelation. The same effect may be operating, but less effectively, for the pyruvate hydrate complex.⁸⁹

The kinetic product⁹⁰ shown in reaction (6.43) indicates that the simple carboxylate ions probably use the β -oxygen in bridging.



The O-bonded Cr(III) complex isomerizes to the stable S-bonded form. It was also shown that the O-bonded Co(III) complex produces the S-bonded Cr(III) product.

With Cr(II) as the reducing agent, the Cr(III) product provides evidence of an inner-sphere mechanism, but in a more general sense it would be useful to know the necessary properties for a bridging ligand. The minimum requirement is two electron pairs, one to bond to the oxidizing agent and the other to the reducing agent. Jordan and Balahura⁹¹ have suggested that in ligands more complex than the halides and hydroxide, two metal centers are unlikely to bond to the same atom and must be bonded to atoms that are part of a conjugated system. Then, the electron may transfer through the π or π^* orbital of the conjugated system. The evidence for this was based on observations of the Cr(III) products from the Cr(II) reductions of the Co(III) complexes in Figure 6.3.

The observation that $\text{Co}(\text{NH}_3)_5(\text{OH}_2)^{3+}$ is reduced very slowly by Cr(II)⁹² indicates that water is not an effective bridging ligand. However, OH^- is an effective bridge in the same system.

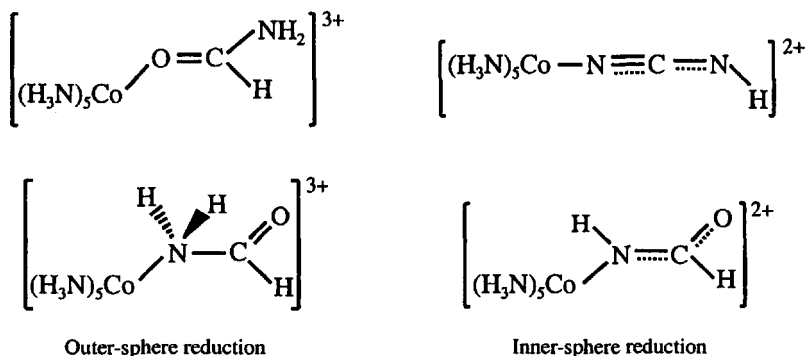


Figure 6.3. Cobalt(III) complexes whose chromium(II) reduction products show the reaction mechanism and the properties needed for a bridging ligand.

Table 6.7. Rate Constants (25°C) for Reduction by Remote Attack of Cr²⁺

X:Co(NH ₃) ₅	<i>k</i> (M ⁻¹ s ⁻¹)
	17.4
	2.5x10 ⁵
	6x10 ³
	0.28

The isonicotinamide system⁹⁶ gives an initial product with Cr(III) bonded to the oxygen of the amide group and provides clear evidence for a remote attack mechanism. The meta isomer, nicotinamide, reacts about 500 times slower and gives about 70% Cr(III)-amide complex. The smaller rate of the *m*-acetylcyanobenzene complex compared to the *p*-acetyl isomer⁹⁷ also reflects the importance of conjugation between the remote group and the lead-in group at cobalt. These observations have led to the suggestion that such systems may proceed by a *chemical mechanism* in which the electron is transferred to the bridging group to form a radical intermediate.

In the case of the *p*-formylbenzoato complex, the rate law has a [H⁺]-dependent path that is consistent with the mechanism in Scheme 6.3.⁹⁸

Scheme 6.3

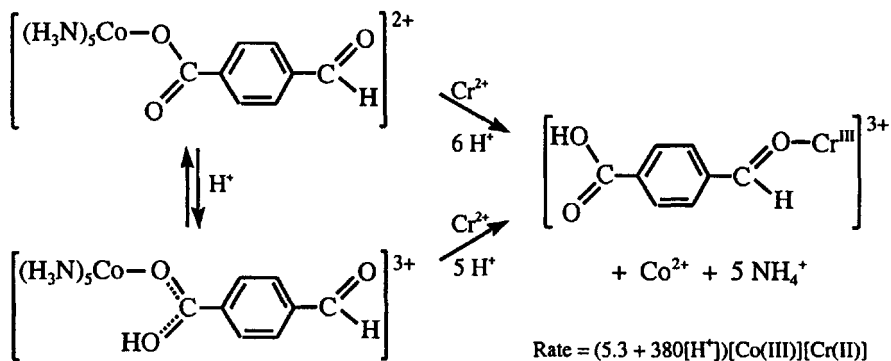
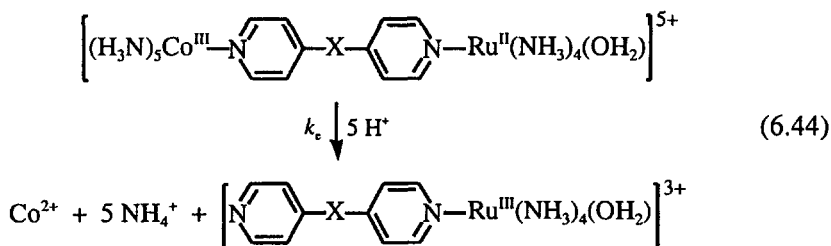


Table 6.8. Rate Constants (25°C) for the Reduction of Some Nitrobenzoate Radicals Coordinated to $\text{Co}^{\text{III}}(\text{NH}_3)_5$

X (isomer)	k_e (s^{-1})	X (isomer)	k_e (s^{-1})
- (<i>o</i>)	4.0×10^5	CH=CH (<i>o</i>)	1.7×10^3
- (<i>m</i>)	1.5×10^2	CH=CH (<i>m</i>)	3.1
- (<i>p</i>)	2.6×10^3	CH=CH (<i>p</i>)	4.8×10^2
CH_2 (<i>o</i>)	3.5×10^4	$\text{CH}_2\text{CH}_2\text{CH}_2$ (<i>p</i>)	1.5×10^2
CH_2 (<i>m</i>)	1.0×10^2	$\text{OC}(\text{NH})\text{CH}_2$ (<i>p</i>)	5.8
CH_2 (<i>p</i>)	3.9×10^2		

group is introduced. The meta isomers are least reactive because of poor conjugation. The moderate reactivity of the saturated $\text{CH}_2\text{CH}_2\text{CH}_2$ derivative is ascribed to the "outer-sphere" path allowed by the flexibility of the $\text{CH}_2\text{CH}_2\text{CH}_2$ chain. The $\text{OC}(\text{NH})\text{CH}_2$ derivative is less reactive because of the rigidity imposed by the planar $\text{OC}(\text{NH})$ group.

Another potential method of separating the K and k_e effects on electron-transfer rates is actually to prepare the bridged complex using inert oxidizing and reducing centers. For example, Taube and co-workers¹⁰² studied the following system:

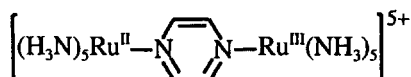


The values of k_e are rather insensitive to X ($\text{CH}_2\text{-CH}_2$, CH=CH) and small (0.1×10^{-2} to $4 \times 10^{-2} \text{ s}^{-1}$, 25°C) when compared to the value of $3 \text{ M}^{-1} \text{ s}^{-1}$ for the reaction of $\text{Co}(\text{NH}_3)_5(\text{OH}_2)^{3+}$ with $\text{Ru}(\text{NH}_3)_6^{2+}$. It was suggested that the reactions are slow because of inner-sphere reorganization analogous to that proposed for outer-sphere reactions of Co(III) complexes.

A similar study by Haim and co-workers,¹⁰³ has been done on the analogous $(\text{H}_3\text{N})_5\text{Co-L-Fe}(\text{CN})_5$ system. The values of k_e are all in the range of 1.5×10^{-3} to $5 \times 10^{-3} \text{ s}^{-1}$, except for much smaller values when X = CH_2 or CO. The rate constants are similar to the values for the outer-sphere reactions of $\text{Co}(\text{NH}_3)_5(\text{L}')^{3+} + \text{Fe}(\text{CN})_5\text{L}^{3-}$, where L and L' are pyridine derivatives. These reactions proceed through a strong ion pair ($K_{\text{ip}} \approx 900 \text{ M}^{-1}$) so that k_e in the ion pair is measured.¹⁰⁴ The implication is that the binuclear systems with more flexible X, such as $(\text{CH}_2)_2$ and $(\text{CH}_2)_3$, use a bridged outer-sphere mechanism.

6.5 INTERVALLENCE ELECTRON TRANSFER

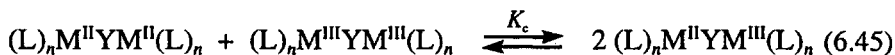
There has been intense interest in the process referred to as intervalence electron transfer in mixed-valence (oxidation state) species ever since the initial preparation¹⁰⁵ of the Taube-Creutz compound:



The intervalence electron transfer involves electron exchange between the two metal centers that are in different oxidation states. This process is typified by transitions in the near-IR region of the electronic spectra of such species. For the preceding ion in water, this band occurs at 1,560 nm ($6,400 \text{ cm}^{-1}$). These transitions are variously referred to as metal to metal charge transfer, MMCT, intervalence charge transfer, IVCT, or intervalence transfer, IT. It was realized that these systems presented the possibility of studying fundamental aspects of bridged electron transfer, and that they might be prototypes for molecular devices. A great deal of experimental and theoretical work has explored these possibilities.

In discussions of these systems, reference is often made to the qualitative classification system of Robin and Day.¹⁰⁶ The species are placed in one of three classes: Class I is completely localized with no electronic interaction (coupling) between the metals; Class II is somewhat delocalized with a measurable interaction between the metals; Class III is fully delocalized. Not surprisingly, some systems seem to fall between classes, as discussed in a review by Meyer and co-workers.¹⁰⁷

There are several ways of classifying the extent of delocalization. The simplest is on the basis of the comproportionation constant, K_c , as defined by the following reaction;



If there is no interaction between the metals in the mixed valence product, then statistics predicts that $K_c = 4$. However, if the product is stabilized by electronic coupling between M^{II} and M^{III} , then K_c should be larger. For the Taube-Creutz compound $K_c = 3 \times 10^6$. This method has been used in a review by Ward¹⁰⁸ where values in the range of 10^{10} – 10^{13} suggest a strong interaction and values $< 10^2$ indicate a weak one. Cautions about this method have been expressed by D'Alessandro and Keene¹⁰⁹ and by LeSuer and Geiger.¹¹⁰

Another method to assess delocalization is based on the measurement of the electric dipole change associated with the intervalence transition. This is done by electroabsorption spectroscopy which measures the effect of an electric field on the spectrum of the sample in a glassy matrix.¹¹¹ In a weakly coupled system, the dipole change should be large as the electron is

essentially transferred from one end of the species to the other, while there is no such displacement in a fully delocalized system.

There is some debate as to whether the localized- or trapped-valence description of the Taube–Creutz ion is correct or whether a delocalized picture is more appropriate. A theoretical study indicates that it is a delocalized, Class III system.¹¹² Meyer and co-workers¹⁰⁷ have summarized the structural and spectroscopic evidence and placed it between Class II and Class III. The trapped-valence model seems correct¹¹³ for the complex in which the bridging ligand is 4,4'-bipyridine, since the two pyridine rings are not planar and therefore are not in full conjugation.

The unique electronic absorbance observed in these mixed-valence systems is usually assigned as a metal–metal charge transfer band, MMCT. Hupp and Meyer¹¹⁴ have noted that it should not be a single band because of the lower than O_h symmetry and spin-orbit coupling in Ru. The t_{2g} level will split into three nondegenerate levels so that three closely spaced bands may actually be observed. Since the MMCT process is equivalent to electron transfer from one metal to another, the interest in these systems has centered on the energetics of the MMCT process. Hush¹¹⁵ suggested that the energy of the MMCT band would be the sum of the inner- and outer-sphere reorganization energies, $\Delta G_{is}^* + \Delta G_{solv}^*$, and therefore presents a way of studying these features. Calculations by Creutz¹¹³ indicate that ΔG_{is}^* is $\sim 1,400 \text{ cm}^{-1}$ for Ru(II)/(III), so that ΔG_{solv}^* seems to be dominant, since the MMCT energies are in the 6,000 to 12,000 cm^{-1} range.

Hupp and Meyer measured the MMCT energy, E_{OP} , as a function of solvent for the 4,4'-bipyridine dimer, in order to test the prediction of Hush that E_{OP} should be given by

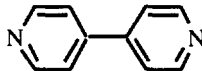
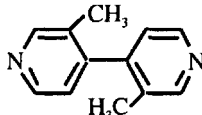
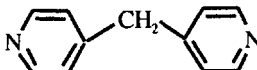
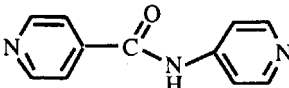
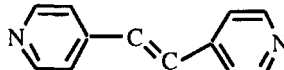




$$E_{OP} = \Delta G_{is}^* + \frac{Ne^2}{16\pi\epsilon_0} \left(\frac{1}{a} - \frac{1}{r} \right) \left(\frac{1}{n_s^2} - \frac{1}{\epsilon_s} \right) \quad (6.46)$$

where it is assumed that $a_1 = a_2 = a$ in Eq. (6.23). The variation of E_{OP} with $(n_s^{-2} - \epsilon_s^{-1})$ is linear, but the slope of 78,100 cm^{-1} is much larger than the one predicted, 22,500 cm^{-1} ($a = 3.5 \text{ \AA}$, $r = 11.3 \text{ \AA}$), and the intercept of 4,820 cm^{-1} is rather far from the one expected, 1,400 cm^{-1} . The authors offered several explanations for these discrepancies, including the band multiplicity problem mentioned earlier.

Later, Meyer and co-workers¹¹⁶ correlated the solvent dependence of the reduction potentials and electronic spectra with the Gutmann donor number for $(\text{bpy})_2(\text{Cl})\text{Os}(\text{L})\text{Ru}(\text{NH}_3)_5^{4+}$ systems, where L = 4,4'-bipyridine or pyrazine. They find that the two metal centers respond differently to the solvent so that the oxidation states are $\text{Os}^{\text{III}}\text{--Ru}^{\text{II}}$ for $DN < 14$ and $\text{Os}^{\text{II}}\text{--Ru}^{\text{III}}$ for $DN > 15$. They also conclude that intramolecular electron transfer involves coupled electronic and nuclear motions and has no simple relationship to thermal electron transfer. Medium effects on various types of charge transfer bands have been reviewed by Chen and Meyer.¹¹⁷

The variation of E_{OP} with the structure of the bridging ligand has been the subject of several studies. Some results are given in Table 6.9 from studies by Sutton and Taube¹¹⁸ and Spangler and co-workers^{119,120} on the pyridine derivatives, and by Stein et al.¹²¹ on the thiospiranes. Further examples and details are given in reviews by Crutchley¹²² and more recently by Isied and co-workers.¹²³ The systems in Table 6.9 fall into two broad categories: if the molar absorption coefficient, ϵ , is $>150 \text{ M}^{-1} \text{ cm}^{-1}$, the metal centers show significant coupling; if $\epsilon < 100 \text{ M}^{-1} \text{ cm}^{-1}$, the metal centers show weak coupling. The electron transfer may be considered as being adiabatic for the first case, but probably is nonadiabatic for the second case. Various aspects of this area are the subject of several recent reviews.¹²⁴

Table 6.9. Intervalence Absorption Energies for Some Complexes of the Type $(\text{H}_3\text{N})_5\text{Ru}^{\text{III}}-\text{L}-\text{Ru}^{\text{II}}(\text{NH}_3)_5^{5+}$

L	d (Å)	$10^{-3} \times E_{OP}$ (cm ⁻¹)	ϵ (M ⁻¹ cm ⁻¹)
	11.3	9.71	920
	11.3	11.24	165
	10.5	12.35	30
	13.7	12.40	50
	13.8	10.42	760
	15.8	9.615	1430
	11.3	10.99	43
	14.4	12.30	9
	17.6	14.50	2.3

The substituents in the bridge clearly affect the coupling between the metal centers in a rational way that is reflected in the ϵ values. The two CH_3 substituents twist the pyridine rings further out of conjugation and reduce the coupling and the ϵ value, as does the saturated $-\text{CH}_2-$ bridge. The amide bridge provides poor coupling although there is conjugation, at least in principle in the $\text{C}(\text{O})\text{NH}$ group. The conjugated $-\text{CH}_2=\text{CH}_2-$ bridge allows conjugation between rings and increases ϵ . It should be noted that the earlier results of Spangler and co-workers¹¹⁹ were reanalyzed by Reimers and Hush,¹²⁵ who have corrected the energies for band overlap and these corrections have been incorporated in later work. Recently, it has been found that ferrocene linked by $-\text{CH}_2=\text{CH}_2-$ bridges behaves similarly to the $\text{Ru}(\text{NH}_3)_5$ analogues.¹²⁶

For the pyridine systems, there is no correlation of the properties of the intervalence band and the $\text{Ru}-\text{Ru}$ distance. However, for the thiospiranes, the ϵ decreases and the E_{OP} increases as the $\text{Ru}-\text{Ru}$ distance increases. Both of these trends indicate reduced coupling as the distance increases, and are expected for coupling through space or through σ bonds.

The nature of the relationship between intervalence electronic bands and electron-transfer processes remains an open question. There appears to be a relationship between E_{OP} and ΔG_{soln}^* , but the quantitative interpretation in terms of the Hush equation is less than satisfactory, as noted by Hupp and Meyer.¹¹⁴ A correlation between the ΔG^* for electron transfer and the metal-metal separation has been noted by Haim¹²⁷ for the systems $(\text{H}_3\text{N})_5\text{Co}-\text{L}-\text{Fe}(\text{CN})_5$ and $(\text{H}_3\text{N})_5\text{Co}-\text{L}-\text{Ru}(\text{NH}_3)_4(\text{OH}_2)$. For the $(\text{H}_3\text{N})_5\text{Ru}^{\text{II}}-\text{L}-\text{M}^{\text{III}}(\text{NH}_3)_5$ systems, Geselowitz¹²⁸ found that E_{OP} for $\text{M} = \text{Ru}$ correlates with ΔG^* for electron transfer for $\text{M} = \text{Co}$. He concluded that such systems have adiabatic electron transfer and the correlation works because E_{OP} is related to ΔG_{soln}^* when L gives reasonable coupling between metal centers. The suggestion of a complex relationship by Meyer and co-workers¹¹⁶ was noted above.

The standard interpretation for weakly coupled systems has assumed that the inner- and outer-sphere rearrangement energies are not dependent on the separation between the metal centers and that the distance dependence of E_{OP} and ΔG^* for electron transfer is due to the decrease in electronic coupling between the centers with increasing distance. This electronic factor will affect the probability of electron transfer and therefore is lumped together with ΔS^* in transition-state theory interpretations. The dependence of the electronic factor, κ_e , on distance is taken to be related to that of the exchange integral, H_{AB} , between the metal centers, and quantum mechanics predicts that

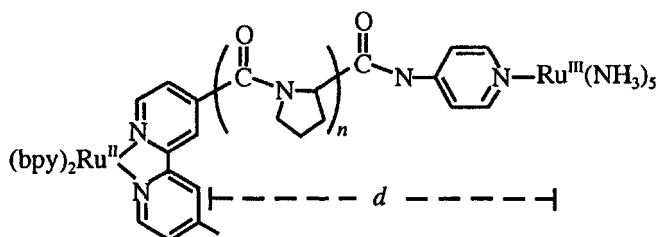
$$\kappa_e = \kappa_{e0} e^{-\beta(r-r_0)} \quad (6.47)$$

where $\beta \approx 1 \text{ \AA}^{-1}$ (values of 0.9 to 1.2 are often used), r is the metal-metal separation in the system under study and r_0 is the separation at which the

transfer will be adiabatic (when $\kappa_e = \kappa_{eo}$). The value of r_o is not known and is sometimes taken to be 0, although 3 to 4 Å might be more reasonable. The electron-transfer rate should have an exponential dependence on the metal-metal separation if other factors are constant.

Sutin and co-workers¹²⁹ have questioned the assumption that the nuclear factors, $\Delta G_{is}^* + \Delta G_{sol}^*$, are independent of the M—M separation. They find a correlation between separation and E_{OP} for $Ru^{II}-L-Ru^{III}$ systems and the same correlation between the separation and ΔH^* for electron transfer in $Os^{II}-iso(Pro)_n-Ru^{III}$ systems, where $iso(Pro)_n$ is a polyproline bridge. This implies that the ΔH^* is dependent on distance and that it is not valid to assume that separation affects only the probability of electron transfer through the electronic factor.

In more recent work, Isied and co-workers¹³⁰ have studied the electron transfer kinetics in the following proline oligomer systems:



The $Ru(II)$ reductant was either a photoactivated excited state or a bpy based radical produced by pulse radiolysis. The value of n ranged from 0 to 9 and d was estimated to change from 8.7 to 32 Å. The rate constants decreased as d increased, as expected from Eq. (6.46) with $d \approx r - r_o$, but the change was slower for $n > 4$. The authors proposed that there is mainly a direct or superexchange mechanism for $n < 4$, and a hopping mechanism for $n > 4$. In the latter mechanism, the electron steps from one proline unit to the next as it moves from the reductant to the oxidant. Meyer and co-workers¹³¹ studied an analogous system with n from 2 to 5 but the results were equivocal with regard to any mechanistic change.

6.6 ELECTRON TRANSFER IN METALLOPROTEINS

The metalloproteins consist of a metal complex imbedded in and bonded to a protein net of covalently bonded amino acids. The most commonly studied systems are the myoglobins and cytochromes, which contain $Fe(II)$ or $Fe(III)$ in a porphyrin complex, or the copper blue proteins, which have $Cu(II)$ or $Cu(I)$ complexed most often by histidine nitrogens and cysteine and methionine sulfurs from the protein. Metalloproteins can be oxidized or reduced by standard transition-metal complex reagents, and the latter usually are chosen to ensure outer-sphere electron transfer. This area has been the subject of numerous reviews.¹³²⁻¹⁴²

In these systems, the oxidant and reductant typically are linked by a largely saturated protein chain, with chain lengths of 10 to 20 Å. Thus, the systems have an analogy to the weakly coupled bimetal systems discussed in the previous section. The distance dependence of the rate of electron transfer has been investigated using modified proteins in which, typically, $\text{Ru}^{\text{III}}(\text{NH}_3)_5$ is attached at a specific site; then, it is reduced to $\text{Ru}(\text{II})$ and the rate of electron transfer from the latter to the metal in the protein is measured.¹⁴³

The interpretation of the kinetic results on these systems has revolved around the distance dependence, as discussed in the previous section. Dutton and co-workers¹⁴⁴ first noted a correlation with the distance, r Å, between donor and acceptor, of the following form:

$$k(\text{s}^{-1}) = 10^{13}e^{-1.4(r-3.6)} \quad (6.48)$$

However, a study¹⁴⁵ of Ru-modified myoglobins gave the following smaller dependence on distance:

$$k(\text{s}^{-1}) = 7.8 \times 10^8 e^{-0.91(r-3)} \quad (6.49)$$

Theoretical work indicates that such interpretations may be overly simplistic. The theory proposed by Hopfield and co-workers¹⁴⁶ suggests that the electron transfers through the σ bonds in the protein by a tunneling mechanism. The rate is then related to the most favorable electron-transfer path that can be found from a reagent at a particular site on the metalloprotein to its metal center. The theory has been applied¹⁴⁷ and found to be consistent with the relative rate constants observed for Ru-modified cytochrome *c*, but the simple-distance theory is also consistent with these observations. Beratan and Onuchic and co-workers¹⁴⁸ have surveyed several ruthenated proteins and devised methods for predicting the most favorable electron-transfer pathway. This approach has undergone several more recent refinements.^{149,150} Ulstrup and co-workers¹⁵¹ have given an extended Hückel theory analysis of the electron-transfer routes along different amino acid sequences in platocyanins.

Jay-Gerin and co-workers¹⁵² surveyed many such systems and proposed a model based on through-space coupling of donor and acceptor. The coupling depends on the energy of the protein's orbitals relative to those of the donor and acceptor, the associated bandwidth and the density of nonhydrogen sites in the protein. They suggest that the distance dependence is strongly dependent on the energy of the protein's orbitals and can be variable for different proteins.

At present, there is still debate about the importance of the hopping and direct or superexchange mechanisms for these systems. The model of Beratan and Onuchic suggests that hydrogen bonding within the peptide chain facilitates the superexchange pathway, but observations by

McLendon and co-workers¹⁵³ indicate that hydrogen bonding is not a major factor. Recently evidence has been presented for a hopping mechanism in an oligoproline system,¹⁵⁴ and against this mechanism for a peptide chain of α -aminoisobutyric acid homooligomers.¹⁵⁵ Of course, it is quite possible that different peptides will have different mechanisms, or even a mixture of mechanisms if there are different peptides in the chain.

References

1. Taube, H.; Myers, H.; Rich, R. L. *J. Am. Chem. Soc.* **1953**, *75*, 4118; Taube, H.; Myers, H. *J. Am. Chem. Soc.* **1954**, *76*, 2103.
2. Marcus, R. A. *Annu. Rev. Phys. Chem.* **1964**, *15*, 155; *Ibid. J. Chem. Phys.* **1965**, *43*, 679.
3. Hush, N. S. *Trans. Faraday Soc.* **1961**, *57*, 557; *Ibid. Prog. Inorg. Chem.* **1967**, *8*, 391; *Ibid. Electrochim. Acta* **1968**, *13*, 1005.
4. Levitch, V. G. *Adv. Electrochem. Eng.* **1966**, *4*, 249.
5. Dogonadze, R. R. In *Reactions of Molecules at Electrodes*; Hush, N. S., Ed.; Wiley-Interscience: New York, 1971, Ch. 3.
6. Tachiya, M. *J. Phys. Chem.* **1993**, *97*, 5911; Seki, K.; Traytak, S. D.; Tachiya, M. *J. Chem. Phys.* **2003**, *118*, 669, and references therein.
7. Ratner, M. A.; Levine, R. D. *J. Am. Chem. Soc.* **1980**, *102*, 4898.
8. Levine, R. D. *J. Phys. Chem.* **1979**, *83*, 159.
9. Sutin, N. *Acc. Chem. Res.* **1968**, *1*, 225.
10. Newton, T. W. *J. Chem. Educ.* **1968**, *45*, 571.
11. Sutin, N. *Prog. Inorg. Chem.* **1983**, *30*, 441.
12. Marcus, R. A.; Sutin, N. *Biochim. Biophys. Acta* **1985**, *811*, 265.
13. Creutz, C.; Newton, M. D.; Sutin, N. *J. Photochem. Photobiol. A: Chem.* **1994**, *82*, 4.
14. Brunschwig, B. S.; Sutin, N. *Coord. Chem. Rev.* **1999**, *187*, 233.
15. Newton, M. D. *Coord. Chem. Rev.* **2003**, *238-239*, 167.
16. Reynolds, W. L.; Lumry, R. W. *Mechanisms of Electron Transfer*; Ronald Press: New York, 1966.
17. Cannon, R. D. *Electron Transfer Reactions*; Butterworths: London, 1980.
18. Tembe, B. L.; Friedman, H. L.; Newton, M. J. *J. Chem. Phys.* **1982**, *76*, 1490.
19. Bernhard, P.; Ludi, A. *Inorg. Chem.* **1984**, *23*, 870.
20. Wherland, S. *Coord. Chem. Rev.* **1993**, *123*, 169.
21. Leontyev, I. V.; Basilevsky, M. V.; Newton, M. D. *Theor. Chem. Acc.* **2004**, *111*, 110, and references therein.
22. Swaddle, T. W. *Chem. Rev.* **2005**, *105*, 2573, and references therein.
23. Chan, M.-S.; Wahl, A. C. *J. Chem. Phys.* **1982**, *86*, 126.
24. Nielson, R. M.; McManis, G. E.; Safford, L. K.; Weaver, M. J. *J. Chem. Phys.* **1989**, *93*, 2152.
25. Weaver, M. J. *Chem. Rev.* **1992**, *92*, 463.
26. Drago, R. S.; Ferris, D. C. *J. Phys. Chem.* **1995**, *99*, 6563.
27. Abbott, A. P.; Rusling, J. F. *J. Phys. Chem.* **1990**, *94*, 8910.

28. Lay, P. A.; McAlpine, N. S.; Hupp, J. T.; Weaver, M. J.; Sargeson, A. M. *Inorg. Chem.* **1990**, *29*, 4322.
29. Mao, W.; Qian, Z.; Yen, H.-J.; Curtis, J. C. *J. Am. Chem. Soc.* **1996**, *118*, 3247.
30. Swaddle, T. W. *Inorg. Chem.* **1990**, *29*, 5017.
31. Zahl, A.; van Eldik, R.; Matsumoto, M.; Swaddle, T. W. *Inorg. Chem.* **2003**, *42*, 3718.
32. Rosso, K. M.; Rustad, J. R. *J. Phys. Chem. A* **2000**, *104*, 6718.
33. Rosso, K. M.; Morgan, J. J. *Geochim. Cosmochim. Acta* **2002**, *66*, 4223.
34. Zhang, D.; Liu, C. *New J. Chem.* **2002**, *26*, 361.
35. Zhang, D.; Hu, H.; Liu, Y.; Bu, Y.; Liu, C. *J. Mol. Struct. (Theochem)* **2001**, *543*, 177.
36. Bu, Y. *J. Mol. Struct. (Theochem)* **2001**, *540*, 193.
37. Rustad, J. R.; Rosso, K. M.; Felmy, A. R. *J. Chem. Phys.* **2004**, *120*, 7607.
38. Rosso, K. M.; Smith, D. M. A.; Dupuis, M. *J. Phys. Chem. A* **2004**, *108*, 5242.
39. Endres, R. G.; LaBute, M. X.; Cox, D. L. *J. Chem. Phys.* **2003**, *118*, 8706.
40. Buhks, E.; Bixon, M.; Jortner, J.; Navon, G. *Inorg. Chem.* **1979**, *18*, 2014; Newton, M. D. *J. Phys. Chem.* **1991**, *95*, 30.
41. Macartney, D. H.; Sutin, N. *Inorg. Chem.* **1985**, *24*, 3403.
42. Sisley, M. J.; Jordan, R. B. *Inorg. Chem.* **1992**, *31*, 2880.
43. Creaser, I. I.; Geue, R. J.; Harrowfield, J. MacB.; Herlt, A. J.; Sargeson, A. M.; Snow, M. R.; Springborg, J. *J. Am. Chem. Soc.* **1982**, *104*, 6016; Geue, R. J.; McCarthy, M. G.; Sargeson, A. M. *J. Am. Chem. Soc.* **1984**, *106*, 8282.
44. Geselowitz, D. *Inorg. Chem.* **1981**, *20*, 4457.
45. Bernhard, P.; Sargeson, A. M. *Inorg. Chem.* **1988**, *27*, 2582.
46. Dubs, R. V.; Gahan, L. R.; Sargeson, A. M. *Inorg. Chem.* **1983**, *22*, 2523.
47. Küppers, H.-J.; Neves, A.; Pomp, C.; Ventur, D.; Wiegardt, K.; Nuber, B.; Weiss, J. *Inorg. Chem.* **1986**, *25*, 2400.
48. Comba, P.; Sickmüller, A. F. *Inorg. Chem.* **1997**, *36*, 4500, and references therein.
49. Turner, J. W.; Schultz, F. A. *Coord. Chem. Rev.* **2001**, *219-221*, 81.
50. Shalders, R. D.; Swaddle, T. W. *Inorg. Chem.* **1995**, *34*, 4815.
51. Grace, M. R.; Swaddle, T. W. *Inorg. Chem.* **1993**, *32*, 5597.
52. Pfeiffer, J.; Kirchner, K.; Wherland, S. *Inorg. Chim. Acta* **2001**, *313*, 37, and references therein.
53. Campion, R. J.; Deck, C. F.; King, P., Jr.; Wahl, A. C. *Inorg. Chem.* **1967**, *6*, 672.
54. Zahl, A.; van Eldik, R.; Swaddle, T. W. *Inorg. Chem.* **2002**, *41*, 757.
55. Takagi, H.; Swaddle, T. W. *Inorg. Chem.* **1992**, *31*, 4669.
56. Ford-Smith, M. H.; Sutin, N. *J. Am. Chem. Soc.* **1961**, *83*, 1830; Dulz, G.; Sutin, N. *Inorg. Chem.* **1963**, *2*, 917.
57. Chou, M.; Creutz, C.; Sutin, N. *J. Am. Chem. Soc.* **1977**, *99*, 5615.
58. Bernhard, P.; Sargeson, A. M. *Inorg. Chem.* **1987**, *26*, 4122.
59. Hupp, J. T.; Weaver, M. J. *Inorg. Chem.* **1983**, *22*, 2557.
60. Bernhard, P.; Helm, L.; Ludi, A.; Merbach, A. E. *J. Am. Chem. Soc.* **1985**, *107*, 312.

61. Jolley, W. H.; Stranks, D. R.; Swaddle, T. W. *Inorg. Chem.* **1990**, *29*, 1948.
62. Macartney, D. H.; Sutin, N. *Inorg. Chim. Acta* **1983**, *74*, 221.
63. Stanbury, D. M.; Haas, O.; Taube, H. *Inorg. Chem.* **1980**, *19*, 518.
64. Zahir, K.; Espenson, J. H.; Bakac, A. *J. Am. Chem. Soc.* **1988**, *110*, 5059.
65. Sutin, N. *Acc. Chem. Res.* **1982**, *15*, 275.
66. Lind, J.; Shen, X.; Merényi, G.; Jonsson, B. O. *J. Am. Chem. Soc.* **1989**, *111*, 7655.
67. Swaddle, T. W. *Chem. Rev.* **2005**, *105*, 2573.
68. Metelski, P. D.; Fu, Y.; Khan, K.; Swaddle, T. W. *Inorg. Chem.* **1999**, *38*, 3103, and references therein.
69. Grace, M. R.; Takagi, H.; Swaddle, T. W. *Inorg. Chem.* **1994**, *33*, 1915.
70. Marcus, R. A.; Sutin, N. *Inorg. Chem.* **1975**, *14*, 213.
71. Braddock, J. N.; Meyer, T. J.; *J. Am. Chem. Soc.* **1973**, *95*, 3158; Cramer, J. L.; Meyer, T. J. *Inorg. Chem.* **1974**, *13*, 1250.
72. Brown, G. M.; Sutin, N. *J. Am. Chem. Soc.* **1979**, *101*, 883.
73. Weaver, M. J.; Yee, E. L. *Inorg. Chem.* **1980**, *19*, 1936.
74. Marcus, R. A. *Discuss. Faraday Soc.* **1960**, *29*, 21; *Ibid. J. Chem. Phys.* **1965**, *43*, 2654.
75. Marcus, R. A.; Siders, P. *J. Phys. Chem.* **1982**, *86*, 622.
76. Jortner, J.; Bixon, M. *J. Chem. Phys.* **1988**, *88*, 167.
77. Cao, J.; Jung, Y. *J. Chem. Phys.* **2000**, *112*, 4716.
78. Gladkikh, V.; Burshtein, A. I.; Rips, I. *J. Phys. Chem. A* **2005**, *109*, 4983.
79. Closs, G. L.; Miller, J. R. *Science* **1988**, *240*, 440, and references therein.
80. Chen, P.; Duesing, R.; Graff, D. K.; Meyer, T. J. *J. Phys. Chem.* **1991**, *95*, 5850.
81. Creutz, C.; Sutin, N. *J. Am. Chem. Soc.* **1977**, *99*, 241.
82. Haim, A.; Wilmarth, W. K. *J. Am. Chem. Soc.* **1961**, *83*, 509.
83. Sykes, A. G.; Thorneley, R. N. F. *J. Chem. Soc. A* **1970**, 232.
84. Hua, L. H.-C.; Balahura, R. J.; Fanchiang, Y.-T.; Gould, E. S. *Inorg. Chem.* **1978**, *17*, 3692.
85. Linck, R. G. *Inorg. React. Methods* **1986**, *15*, 68.
86. Murdoch, J. R. *J. Am. Chem. Soc.* **1972**, *94*, 4410.
87. Balahura, R. J.; Jordan, R. B. *Inorg. Chem.* **1973**, *12*, 1438.
88. Price, H. J.; Taube, H. *Inorg. Chem.* **1968**, *7*, 1.
89. Sisley, M. J.; Jordan, R. B. *Inorg. Chem.* **1989**, *28*, 2714.
90. Balahura, R. J.; Johnson, M. D.; Black, T. *Inorg. Chem.* **1989**, *28*, 3933.
91. Jordan, R. B.; Balahura, R. J. *J. Am. Chem. Soc.* **1971**, *93*, 625.
92. Toppen, D. L.; Linck, R. G. *Inorg. Chem.* **1971**, *10*, 2635.
93. Shea, C.; Haim, A. *J. Am. Chem. Soc.* **1971**, *93*, 3055.
94. Schwarz, C. I.; Endicott, J. F. *Inorg. Chem.* **1995**, *34*, 4572.
95. Kupferschmidt, W. C.; Jordan, R. B. *Inorg. Chem.* **1981**, *20*, 3469.
96. Nordmeyer, F.; Taube, H. *J. Am. Chem. Soc.* **1968**, *90*, 1162.
97. Balahura, R. J.; Purcell, W. L. *J. Am. Chem. Soc.* **1976**, *98*, 4457.
98. Zannella, A.; Taube, H. *J. Am. Chem. Soc.* **1972**, *94*, 6403.
99. Barrett, M. B.; Swinchart, J. H.; Taube, H. *Inorg. Chem.* **1971**, *10*, 1983.

100. Tsukahara, K.; Wilkins, R. G. *Inorg. Chem.* **1989**, *28*, 1605.
101. Whitburn, K. D.; Hoffman, M. Z.; Simic, M. G.; Brezniak, N. V. *Inorg. Chem.* **1980**, *19*, 3180; Whitburn, K. D.; Hoffman, M. Z.; Brezniak, N. V.; Simic, M. G. *Inorg. Chem.* **1986**, *25*, 3037.
102. Fischer, H.; Tom, G. M.; Taube, H. *J. Am. Chem. Soc.* **1976**, *98*, 5512.
103. Jwo, J.-J.; Gaus, P. L.; Haim, A. *J. Am. Chem. Soc.* **1979**, *101*, 6189.
104. Gaus, P. L.; Villanueva, J. L. *J. Am. Chem. Soc.* **1980**, *102*, 1934.
105. Creutz, C.; Taube, H. *J. Am. Chem. Soc.* **1969**, *91*, 3988; *Ibid.* **1973**, *95*, 1086.
106. Robin, M. B.; Day, P. *Adv. Inorg. Chem. Radiochem.* **1967**, *10*, 247.
107. Demadis, K. D.; Hartshorn, C. M.; Meyer, T. *J. Chem. Rev.* **2001**, *101*, 2655.
108. Ward, M. D. *Chem Soc. Rev.* **1995**, *24*, 121.
109. D'Alessandro, D. M.; Keene, F. R. *Dalton Trans.* **2004**, 3950.
110. LeSuer, R.; Geiger, W. E. *Angew. Chem. Int. Ed.* **2000**, *39*, 248.
111. Brunschwig, B. S.; Creutz, C.; Sutin, N. *Coord. Chem. Rev.* **1998**, *177*, 61, and references therein.
112. Bencini, A.; Ciofini, I.; Daul, C. A.; Ferretti, A. *J. Am. Chem. Soc.* **1999**, *121*, 11418.
113. Creutz, C. *Inorg. Chem.* **1978**, *17*, 3723.
114. Hupp, J. T.; Meyer, T. *J. Inorg. Chem.* **1987**, *26*, 2332.
115. Hush, N. S. *Inorg. Chem.* **1967**, *8*, 391.
116. Neyhart, G. A.; Hupp, J. T.; Curtis, J. C.; Timpson, C. J.; Meyer, T. *J. Am. Chem. Soc.* **1996**, *118*, 3724; Neyhart, G. A.; Timpson, C. J.; Bates, W. D.; Meyer, T. *J. Am. Chem. Soc.* **1996**, *118*, 3730.
117. Chen, P.; Meyer, T. *J. Chem. Rev.* **1998**, *98*, 1439.
118. Sutton, J. E.; Taube, H. *Inorg. Chem.* **1981**, *20*, 3125.
119. Woitellier, S.; Launay, J. P.; Spangler, C. W. *Inorg. Chem.* **1989**, *28*, 758.
120. Ribou, A.-C.; Launay, J.-P.; Takahashi, K.; Nihira, T.; Tarutani, S.; Spangler, C. W. *Inorg. Chem.* **1994**, *33*, 1325.
121. Stein, C. A.; Lewis, N. A.; Seitz, G. *J. Am. Chem. Soc.* **1982**, *104*, 2596.
122. Crutchley, R. J. *Adv. Inorg. Chem.* **1994**, *41*, 273.
123. Distefano, A. J.; Wishart, J. F.; Isied, S. S. *Coord. Chem. Rev.* **2005**, *249*, 507.
124. Brunschwig, B. S.; Creutz, C.; Sutin, N. *Chem. Soc. Rev.* **2002**, *31*, 168; Endicott, J. F.; Chen, Y.-J.; Xie, P. *Coord. Chem. Rev.* **2005**, *249*, 343; Bernhardt, P. V.; Bozoglián, F.; Macpherson, B. P.; Martinez, M. *Coord. Chem. Rev.* **2005**, *249*, 1902.
125. Reimers, J. R.; Hush, N. S. *Inorg. Chem.* **1990**, *29*, 4510.
126. Ribou, A.-C.; Launay, J.-P.; Sachtleben, M. L.; Li, H.; Spangler, C. W. *Inorg. Chem.* **1996**, *35*, 3735.
127. Haim, A. *Pure Appl. Chem.* **1983**, *55*, 89.
128. Geselowitz, D. *Inorg. Chem.* **1987**, *26*, 4135.
129. Isied, S. S.; Vassilian, A.; Wishart, J. F.; Creutz, C.; Schwarz, H. A.; Sutin, N. *J. Am. Chem. Soc.* **1988**, *110*, 635.
130. Malak, R. A.; Gao, Z.; Wishart, J. F.; Isied, S. S. *J. Am. Chem. Soc.* **2004**, *126*, 13888.

131. Serron, S. A.; Aldridge, S. III; Fleming, C. N.; Danell, R. M.; Baik, M.-H.; Sykora, M.; Dattelbaum, D. M.; Meyer, T. J. *J. Am. Chem. Soc.* **2004**, *126*, 14506.
132. Isied, S. S. *Prog. Inorg. Chem.* **1984**, *32*, 443.
133. Sykes, A. G. *Chem. Soc. Rev.* **1985**, *14*, 283.
134. McLendon, G.; Guarr, T.; McGuire, M.; Simolo, K.; Strauch, S.; Taylor, K. *Coord. Chem. Rev.* **1985**, *64*, 113.
135. Marcus, R. A.; Sutin, N. *Biochim. Biophys. Acta* **1985**, *811*, 265.
136. Gray, H. B. *Chem. Soc. Rev.* **1986**, *15*, 17.
137. McLendon, G. *Acc. Chem. Res.* **1988**, *21*, 160.
138. Isied, S. S.; Ogawa, M. Y.; Wishart, J. F. *Chem. Rev.* **1992**, *92*, 381.
139. Piotrowiak, P. *Chem. Soc. Rev.* **1999**, *28*, 143.
140. Brunori, M.; Giuffrè, A.; Sarti, P. *J. Inorg. Biochem.* **2005**, *99*, 324.
141. Long, Y.-T.; Abu-Irhayem, E.; Kraatz, H.-B. *Chem. Eur. J.* **2005**, *11*, 5186.
142. Simonneaux, G.; Bondon, A. *Chem. Rev.* **2005**, *105*, 2627.
143. Scott, R. A.; Mauk, A. G.; Gray, H. B. *J. Chem. Educ.* **1985**, *62*, 932; Karas, J. L.; Lieber, C. M.; Gray, H. B. *J. Am. Chem. Soc.* **1988**, *110*, 599.
144. Moser, C. C.; Keske, J. M.; Warncke, K.; Faird, R. S.; Dutton, P. L. *Nature* **1992**, *355*, 796.
145. Axup, A. W.; Albin, M.; Mayo, S. L.; Crutchley, R. J.; Gray, H. B. *J. Am. Chem. Soc.* **1988**, *110*, 435.
146. Beratan, D. N.; Onuchic, J. N.; Hopfield, J. J. *J. Chem. Phys.* **1987**, *86*, 4488; Cowan, J. A.; Upmacis, R. K.; Beratan, D. N.; Onuchic, J. N.; Gray, H. B. *Ann. N. Y. Acad. Sci.* **1989**, *550*, 68.
147. Bowler, B. E.; Meade, T. J.; Mayo, S. L.; Richards, J. H.; Gray, H. B. *J. Am. Chem. Soc.* **1989**, *111*, 8757.
148. Beratan, D. N.; Onuchic, J. N.; Betts, J. N.; Bowler, B. E.; Gray, H. B. *J. Am. Chem. Soc.* **1990**, *112*, 7915; Betts, J. N.; Beratan, D. N.; Onuchic, J. N. *J. Am. Chem. Soc.* **1992**, *114*, 4043; Skourtis, S. S.; Regan, J. J.; Onuchic, J. N. *J. Phys. Chem.* **1994**, *98*, 3379.
149. Kobayashi, C.; Baldrige, K.; Onuchic, J. N. *J. Chem. Phys.* **2003**, *119*, 3550, and references therein.
150. Shin, Y. K.; Newton, M. D.; Isied, S. S. *J. Am. Chem. Soc.* **2003**, *125*, 3722.
151. Christensen, H. E. M.; Conrad, L. S.; Mikkelsen, K. V.; Nielsen, M. K.; Ulstrup, J. *Inorg. Chem.* **1990**, *29*, 2808.
152. Lopez-Castillo, J.-M.; Filali-Mouhim, A.; Plante, I. L.; Jay-Gerin, J.-P. *J. Phys. Chem.* **1995**, *99*, 6864; Lopez-Castillo, J.-M.; Filali-Mouhim, A.; Van Binh-Otten, E. N.; Jay-Gerin, J.-P. *J. Am. Chem. Soc.* **1997**, *119*, 1978.
153. Zheng, Y.; Case, M. A.; Wishart, J. F.; McLendon, G. L. *J. Phys. Chem. B* **2003**, *107*, 7288.
154. Giese, B.; Napp, M.; Jacques, O.; Boudebous, H.; Taylor, A. M.; Wirz, J. *Angew. Chem. Int. Ed.* **2005**, *44*, 4073.
155. Polo, F.; Antonello, S.; Formaggio, F.; Toniolo, C.; Maran, F. *J. Am. Chem. Soc.* **2005**, *127*, 492.

Inorganic Photochemistry

Electromagnetic radiation in the form of UV and visible light has long been used as a reactant in inorganic reactions. The energy of light in the 200- to 800-nm region varies between 143 and 36 kcal mol⁻¹, so it is not surprising that chemical bonds can be affected when a system absorbs light in this readily accessible region. Systematic mechanistic studies in this area have benefited greatly from the development of lasers that provided intense monochromatic light sources and from improvements in actinometers to measure the light intensity. Prior to the laser era, it was necessary to use filters to limit the energy of the light used to a moderately narrow region or to just cut off light below a certain wavelength. Pulsed-laser systems also allow much faster monitoring of the early stages of the reaction and the detection of primary photolysis intermediates.

The systems discussed in this chapter have been chosen because of their relationship to substitution reaction systems discussed previously. For a broader assessment of this area, various books¹⁻⁵ and review articles⁶⁻¹² should be consulted.

7.1 BASIC TERMINOLOGY

Mechanistic photochemistry incorporates features of both electron-transfer and substitution reactions, but the field has some of its own terminology,¹³ which is summarized as follows:

Quantum Yield

The quantum yield, Φ , is the number of defined events, in terms of reactant or product, that occur per photon absorbed by the system. An einstein, E , is defined as a mole of photons, and if n is the moles of reactant consumed or product formed, then $\Phi = n/E$. For simple reactions $\Phi \leq 1$ but can be >1 for chain reactions.

Actinometer

An actinometer is a device used to measure the number of einsteins emitted at a particular wavelength by a particular light source. Photon-counting devices are now available and secondary chemical actinometers have been developed, such as that based on the Reineckate ion,¹⁴ $\text{Cr}(\text{NH}_3)_2(\text{NCS})_4^-$, as

well as the traditional iron(III)–oxalate and uranyl–oxalate actinometers. An early problem in this field was the lack of an actinometer covering the 450- to 600-nm range and the Reineckate actinometer solved this problem.

Reactant Photolyzed

The number of moles, n , of reactant photolyzed is determined by appropriate analytical techniques. A combination of spectrophotometry and chromatography is commonly used. This is not a trivial problem because photochemical studies typically follow only the first 5–15% of the reaction, so that the change in reactant concentration is small, as is the amount of product formed.

Internal Filtration

If the reaction products absorb light at the wavelength being used, then the quantum yield will decrease as the reaction proceeds because reactants are not absorbing all the light. This is called internal filtration. To minimize the problem, only the initial stages of the photochemical process are studied.

Secondary Photolysis

Secondary photolysis refers to the photolysis of the initial products to give secondary products. Again, only the initial part of the primary reaction is followed to minimize this problem.

Stern–Volmer Plots

Stern–Volmer plots are used to test the dependence of the quantum yield on the concentration of reactants. The form of the plot depends on the photochemical mechanism proposed.

Fluorescence

Fluorescence refers to the emission of light when an electronic excited state decays to another state of the same spin multiplicity. The emission is usually very fast.

Phosphorescence

Phosphorescence refers to the emission of light when an electronic excited state decays to another state of different spin multiplicity. This process is usually slower than fluorescence and is typically on the millisecond to microsecond time scale for transition-metal complexes.

Sensitizer

A sensitizer is a substance that makes a reaction more sensitive to photolysis. Sensitizers absorb light more strongly than the reactant and then transfer the absorbed energy to the reactant. The sensitizer must have an electronic excited state that is sufficiently long-lived to allow for the energy transfer to the reactant, and the energy of this state must be similar to that of the acceptor state of the reactant.

Quencher

A quencher is a substance that reduces the quantum yield of a process by accepting energy from the photoexcited state(s) of the reactant. The energy of the excited state of the quencher must be similar to that of the reactant.

Photostationary State

A photostationary state can occur in a kinetically labile system, initially at equilibrium, in which only the forward reaction is promoted by light. Under photochemical conditions, more reactant will be converted to product and a new equilibrium condition will be established in which the forward and reverse rates are the same; this is referred to as a photostationary state. If the light source is removed, the system will return to the thermodynamic equilibrium position.

Intersystem Crossing

Intersystem crossing refers to the process whereby an electronic excited state may be converted to another excited state of similar or lower energy. Back intersystem crossing refers to the reverse process.

7.2 KINETIC FACTORS AFFECTING QUANTUM YIELDS

Most photochemical systems have some common features that affect the lifetime of the photoexcited states and thereby the quantum yields. Figure 7.1 describes a general system with a ground state, **G**, which absorbs a photon at a rate of dE/dt to produce an excited state, **I**. Excited vibrational levels have been omitted for simplicity.

The excited state can undergo intersystem crossing to produce the photoactive state **A** which decays to products **P** or back to the ground state. It is normal to assume a steady state for the excited states, **A** and **I**, and

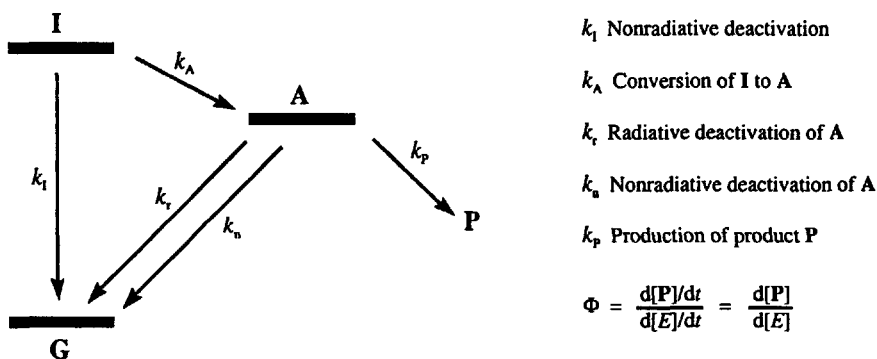


Figure 7.1. A general photochemical system with a ground state **G**, an initially activated state **I**, a photoactive state **A** and products **P**.

their steady-state concentrations are given by

$$[\text{A}] = \frac{k_{\text{A}}[\text{I}]}{(k_{\text{p}} + k_{\text{r}} + k_{\text{n}})} \quad (7.1)$$

$$[\text{I}] = \frac{1}{k_{\text{A}} + k_{\text{I}}} \left(\frac{dE}{dt} \right) \quad (7.2)$$

The substitution for [I] from Eq. (7.2) into Eq. (7.1) gives

$$[\text{A}] = \frac{k_{\text{A}}}{(k_{\text{A}} + k_{\text{I}})(k_{\text{p}} + k_{\text{r}} + k_{\text{n}})} \left(\frac{dE}{dt} \right) \quad (7.3)$$

The rate of formation of product is given by

$$\frac{d[\text{P}]}{dt} = k_{\text{p}}[\text{A}] \quad (7.4)$$

and substitution for [A] from Eq. (7.3) gives

$$\frac{d[\text{P}]}{dt} = \frac{k_{\text{p}}k_{\text{A}}}{(k_{\text{A}} + k_{\text{I}})(k_{\text{p}} + k_{\text{r}} + k_{\text{n}})} \left(\frac{dE}{dt} \right) \quad (7.5)$$

From its definition, and substitution from Eq. (7.5), the quantum yield is

$$\Phi = \frac{d[\text{P}]}{dt} \left(\frac{dE}{dt} \right)^{-1} = \frac{k_{\text{p}}k_{\text{A}}}{(k_{\text{A}} + k_{\text{I}})(k_{\text{p}} + k_{\text{r}} + k_{\text{n}})} \quad (7.6)$$

This development shows that several factors in addition to k_{p} can affect the quantum yield. It is not uncommon in this area to study the effect of changing ligand substituents and solvents on Φ and to use the results to infer the mechanism of the k_{p} step. But such changes in conditions may affect k_{A} , k_{I} , k_{r} and/or k_{n} and thereby make any mechanistic conclusions very tenuous. Similar ambiguities can arise when the solvent is changed.

The system in Figure 7.1 could be expanded to include formation of products from the initially populated state I or from other photoactive states produced from I or A. Furthermore, there could be back intersystem crossing from A to I. It is also possible to have the simpler case in which I is the only photoactive state.

7.3 PHOTOCHEMISTRY OF COBALT(III) COMPLEXES

Cobalt(III) forms a wide range of substitution-inert (low-spin d^6) complexes whose thermal aquation and anation reactions have been thoroughly studied. These provide useful comparisons for photochemical

work. In addition, the substitution inertness of the products is an advantage for product studies.

7.3.1 $\text{Co}^{\text{III}}\text{L}_6$ Complexes

The electronic spectroscopy of $\text{Co}^{\text{III}}\text{L}_6$ systems is well understood and described by ligand field theory. The electronic states which involve the d orbitals are shown in Figure 7.2. The electronic spectra generally show two absorptions in the visible region, ${}^1\text{A}_{1g} \rightarrow {}^1\text{T}_{1g}$ (~ 500 nm) and ${}^1\text{A}_{1g} \rightarrow {}^1\text{T}_{2g}$ (~ 350 nm). The spin-forbidden transitions to the ${}^3\text{T}_{1g}$ and ${}^5\text{T}_{2g}$ states are normally too weak to be observed. In addition, there often is a ligand-to-metal charge-transfer band in the UV region.

The diagram at the right in Figure 7.2 shows the potential energy surfaces for four of these levels in $\text{Co}(\text{NH}_3)_6^{3+}$, as suggested by the low-temperature spectroscopic study of Wilson and Solomon.¹⁵ The Co—N bond lengths change by Δ from the ground-state values. The photoaquation of $\text{Co}(\text{NH}_3)_6^{3+}$ has a very low quantum yield of 3.1×10^{-4} mol einstein⁻¹ for wavelengths in the visible region. It is usually assumed that the ${}^3\text{T}_{1g}$ state is photoactive and is populated by intersystem crossing from the ${}^1\text{T}_{1g}$ and ${}^1\text{T}_{2g}$ states. Radiationless deactivation of these states could account for the low quantum yield.

Wilson and Solomon suggest that the ${}^3\text{T}_{1g}$ may decay to the ${}^5\text{T}_{2g}$ state,

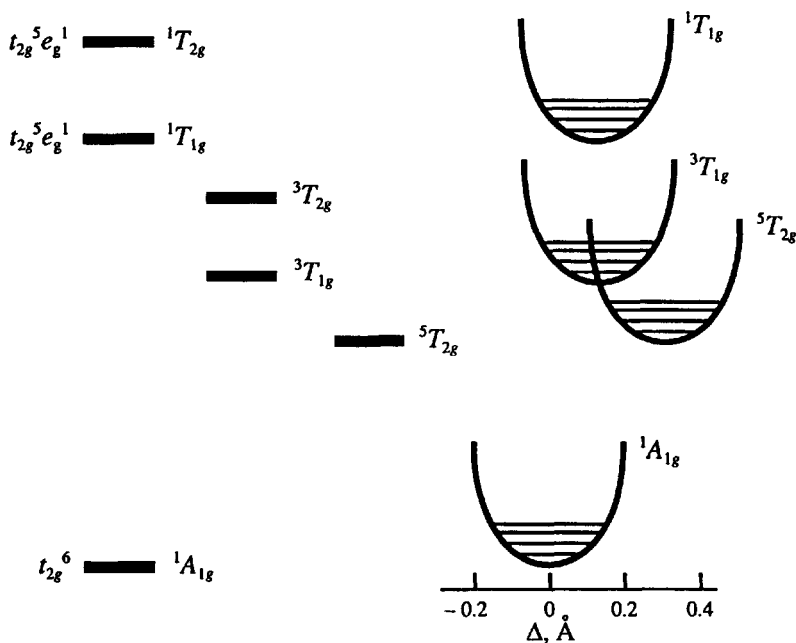


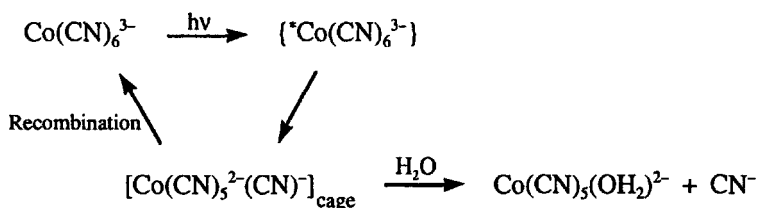
Figure 7.2. The ligand field electronic state energies and potential energy surfaces for octahedral $\text{Co}(\text{III})$.

which then decays efficiently to the ground state because of the overlap of the potential energy surfaces.

According to studies by Scandola et al.¹⁶ and Nishazawa and Ford,¹⁷ the photoaquation of $\text{Co}(\text{CN})_6^{3-}$ is much more efficient ($\Phi = 0.31$) for wavelengths in the visible region. Wilson and Solomon have suggested that the ${}^5T_{2g}$ state is at higher energy than the ${}^3T_{1g}$ state in this system because the Dq of CN^- is much larger than that of NH_3 . As a result, deactivation through the quintet state is not effective in $\text{Co}(\text{CN})_6^{3-}$.

Scandola et al. studied the solvent dependence of the quantum yield in water–glycerol solutions and found that Φ decreases from 0.31 to 0.1 with increasing amounts of glycerol. They interpreted this as a viscosity effect on a cage intermediate, shown in Scheme 7.1.

Scheme 7.1



It was suggested that increasing viscosity inhibited CN^- release from the cage and therefore favored recombination to give a lower quantum yield. This type of explanation is not uncommon in photochemical studies, but it is now recognized that solvent changes can also affect the lifetimes of the photoactive states by changing the efficiency of the various decay mechanisms, and meaningful interpretations require information about excited-state lifetimes in the solvent mixtures. In the case of $\text{Co}(\text{CN})_6^{3-}$, Wong and Kirk¹⁸ found that $\text{Co}(\text{CN})_5(\text{glycerol})^{2-}$ is actually formed.

Tyler and co-workers¹⁹ have discussed the theory and some experimental observations on solvent and other effects on the lifetimes of caged species.

7.3.2 $\text{Co}^{\text{III}}(\text{L})_5\text{Y}$ Complexes

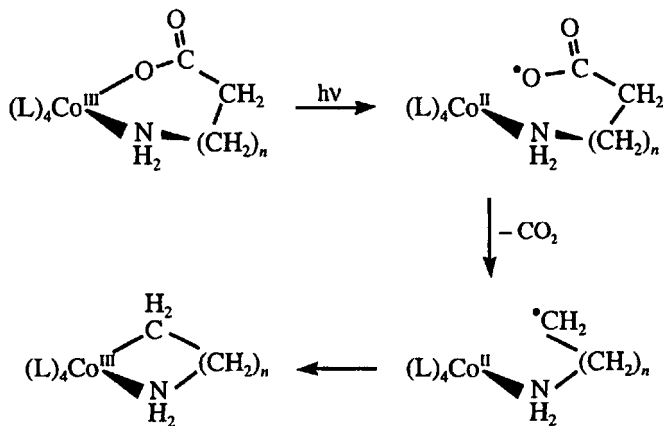
The $\text{Co}^{\text{III}}(\text{CN})_5\text{X}$ complexes photoaquate cleanly to $\text{Co}^{\text{III}}(\text{CN})_5(\text{OH}_2)^{2-}$ with quantum yields in the range of 0.05 to 0.3, depending on X. Kirk and Kneeland²⁰ studied the competition of SCN^- with H_2O to compare the thermal and photochemical reactions of $\text{Co}^{\text{III}}(\text{CN})_5\text{X}^{3-}$ complexes. The ratio of the two linkage isomers, $\text{Co}^{\text{III}}(\text{CN})_5(\text{SCN})^{3-}$ and $\text{Co}^{\text{III}}(\text{CN})_5(\text{NCS})^{3-}$, is independent of the leaving group X, but the ratio is different for the thermal and photochemical reactions, as shown in Table 7.1. The conclusion is that the transition states for the two processes are different because they give different isomer ratios, but both appear to be dissociative because the ratio is reasonably independent of the leaving group. Kirk and Kneeland suggested that the photoactive state, possibly ${}^3T_{1g}$, has a more

This process was studied extensively by Endicott and co-workers²² for the $\text{Co}^{\text{III}}(\text{NH}_3)_5\text{X}$ complexes, and by Weit and Kutal²³ for the systems $\text{Co}^{\text{III}}(\text{NH}_2\text{CH}_3)_5\text{X}$ with $\text{X} = \text{Cl}^-$ and Br^- . The NH_3 and NH_2CH_3 systems are more different than might be expected from the rather simple addition of a methyl group. The electronic spectral properties indicate that species A will be favored by higher energy irradiation compared to species B. The NH_3 systems appear to undergo internal conversion to B or react with solvent, based on the solvent sensitivity of the reaction, and do not form any amine-type radicals. The NH_2R systems are different in that they show a wavelength dependence of the quantum yield, a different solvent variation in glycerol–water and an increase in quantum yield in the presence of O_2 . Weit and Kutal interpret these differences as due to shielding of the complex from the solvent by the CH_3 group so that reaction from A is observed. The O_2 effect is ascribed to scavenging of the $\bullet\text{NH}_2\text{R}^+$ radicals by O_2 . Following earlier observations of Hennig and co-workers,²⁴ Wang and Kutal²⁵ found that these photoredox reactions are sensitized by ion pairing with BPh_4^- in CH_3OH and $\text{CH}_3\text{OH}:\text{CH}_2\text{Cl}_2$, with significant quantum yields even at 436 nm. Kutal²⁶ has reviewed the use of these types of reactions as photoinitiators for polymerization, where either the radical X^\bullet or the base NH_2R can be the initiator.

The photolysis of $\text{Co}(\text{NH}_3)_4(\text{OCO}_2)^+$ at 254 nm yields a mixture of $\text{Co}(\text{II})$ and $\text{Co}(\text{NH}_3)_4(\text{OH}_2)(\text{OCO}_2\text{H})^{2+}$.²⁷ A recent flash photolysis study²⁸ suggests that the initial species formed is $\text{Co}^{\text{II}}(\text{NH}_3)_4(\text{OCO}_2^\bullet)^+$ and that it undergoes chelate ring opening followed by competitive loss of NH_3 and OCO_2^\bullet and back electron transfer to give the various products.

Poznyak et al.²⁹ have shown that aminocarboxylate complexes of $\text{Co}(\text{III})$ undergo photolysis by UV light to produce products with stable $\text{Co}-\text{C}$ bonds. The observations can be understood by the reaction sequence in Scheme 7.3.

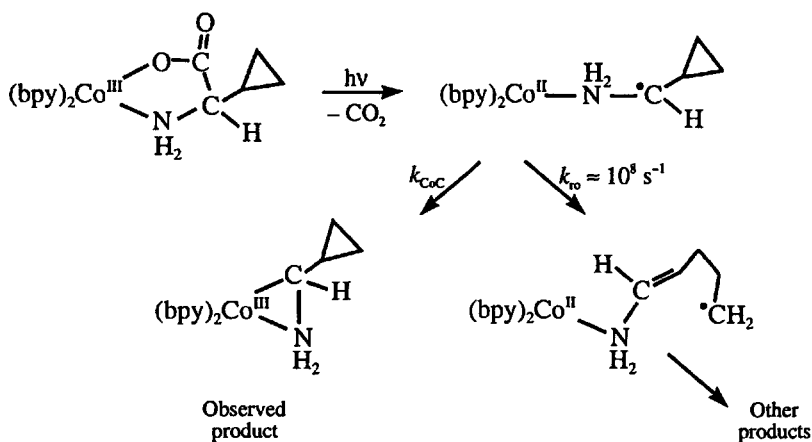
Scheme 7.3



Studies by Kawaguchi et al.³⁰ with various isomers have shown that the reaction does not always go with retention, probably due to fluxionality in the Co(II) intermediate(s).

The $(\text{bpy})_2\text{Co}(\text{glycinate})^{2+}$ complex yields a particularly stable product whose structure has been determined.³¹ This complex also was studied by flash photolysis³² and the Co—C bonded product was found to form with a rate constant of $\sim 4 \times 10^3 \text{ s}^{-1}$ which was independent of pH in the range of 1 to 6.2. In this study, the rate-controlling step was assigned to the Co—C bond formation. More recently, Hartshorn and Telfer³³ suggested that this assignment might be incorrect because intermolecular reactions of Co(III) complexes with methyl radicals typically have k values $> 10^7 \text{ M}^{-1} \text{ s}^{-1}$. Hartshorn and Telfer performed the "radical clock" experiment with a cyclopropyl derivative of glycine, as described in Scheme 7.4.

Scheme 7.4



If the rate constant for ring opening, k_{ro} , is known, then the relative amounts of the unchanged and ring-opened products can be used to determine k_{CoC} . Substantial background information in the organic literature³⁴ indicates that $k_{\text{ro}} \approx 10^8 \text{ s}^{-1}$ for the $\text{H}_2\text{C}^{\cdot}-\text{C}_3\text{H}_5$ radical, and that the process is rather independent of substituents on the radical. Hartshorn and Telfer found no evidence for any ring opening and suggested that k_{CoC} must be larger than the value of $4 \times 10^3 \text{ s}^{-1}$ inferred from the flash photolysis study. Organic experience suggests that loss of CO_2 from RCO_2^{\cdot} radicals is a very fast process and seems unlikely to be the rate limiting step.³⁵ The original authors suggested that the radical clock results might be explained by an ionic mechanism with further electron transfer giving Co(I) and a coordinated $\text{RHC}-\text{NH}_2^+$ intermediate. It should be noted that further work by these authors, with the amino acid incorporated in a macrocyclic ring, gave more stable products and confirmed the lack of ring opening in the cyclopropyl ring.³⁶

Table 7.2. Quantum Yields (25°C) for the Loss of X and NH₃ for Complexes of the Type Co^{III}(NH₃)₅X

X	Φ_X	Φ_{NH_3}
F ⁻ ^a	5.5x10 ⁻⁴	2.0x10 ⁻³
Cl ⁻ ^a	1.7x10 ⁻³	5.1x10 ⁻³
Br ⁻ ^b	2.0x10 ⁻³	5.1x10 ⁻⁴

^a Zribush, R. A.; Poon, C. K.; Bruce, C. M.; Adamson, A. W. *J. Am. Chem. Soc.* **1974**, *96*, 3027, at pH 2, 488 nm; Langford, C. H.; Malkhasian, Y. S. *J. Am. Chem. Soc.* **1987**, *109*, 2682 give λ dependence with X = Cl⁻.

^b Zanella, A. W.; Ford, K. H.; Ford, P. C. *Inorg. Chem.* **1978**, *17*, 1051, at pH 3.4, 546 nm.

If a Co^{III}(NH₃)₅X complex is photolysed by irradiation into the *d-d* bands (wavelength ≥ 450 nm), then photoaquation is observed with low quantum yields in the range of 1x10⁻² to 1x10⁻³. These reactions show a significant *antithermal pathway* in which NH₃ is released to yield Co(NH₃)₄(OH₂)X²⁺ mainly as the trans isomer. Some examples of quantum yields for the two paths are given in Table 7.2.

7.4 PHOTOCHEMISTRY OF RHODIUM(III) COMPLEXES

Rhodium(III) systems are formally analogous to cobalt(III) in that both are *d⁶* systems. The larger *Dq* values for second-row transition metals makes all the Rh(III) complexes more analogous to the cyano complexes of Co(III). Studies with Rh(III) have the advantage that the rate of decay of the photoexcited states can be measured. The area was reviewed by Mønsted and Mønsted³⁷ and by Skibsted.³⁸ The photoactive state appears to be the ³T_{1g} (³E for Rh(L)₅X symmetry), and the rate constants, *k_n*, for phosphorescent decay from this state in the solids at 77 K are given in Table 7.3.³⁹ A more recent and extensive compilation has been given in a review by Forster.⁴⁰ Some values of *k_n* in representative solvents are given in Table 7.4.

Table 7.3. Rate Constants (77 K) for Decay of the Triplet State for Some Rh(III) Complexes

Complex	<i>k_n</i> (s ⁻¹)
Rh(NH ₃) ₅ (OH ₂) ³⁺	2.9x10 ⁵
Rh(NH ₃) ₅ Cl ²⁺	8.2x10 ⁴
Rh(NH ₃) ₅ (NH ₃) ³⁺	5.1x10 ⁴
Rh(ND ₃) ₅ (ND ₃) ³⁺	0.8x10 ⁴

Table 7.4. Photolysis (25°C) of $\text{Rh}(\text{NH}_3)_5\text{Cl}^{2+}$ in Various Solvents

Solvent	Φ_{Cl^-}	Φ_{NH_3}	k_n (s^{-1})
Water	0.18	0.02	7.0×10^7
Formamide	0.057	<0.011	4.5×10^7
Dimethylsulfoxide	<0.006	0.029	2.8×10^7
Methanol	0.008	0.11	$<5 \times 10^7$
Dimethylformamide	0.004	0.070	3.1×10^7

The dramatic effect of changing hydrogen for deuterium in the hexaammine complex indicates that the energy of the excited state is dissipated to ligand vibrational modes. This is probably a common feature for many complexes.

Solvent effects have been investigated⁴¹ for the photolysis of $\text{Rh}(\text{NH}_3)_5\text{Cl}^{2+}$. The reaction proceeds with loss of either NH_3 or Cl^- in proportions that vary with the solvent, as shown by the quantum yields given in Table 7.4. The quantum yields do not correlate with the lifetime of the excited state, and the chloride loss process is especially sensitive to the solvent. A complicating feature may be the increasing recombination with Cl^- in the solvent cage when solvation of the chloride ion is less favorable.

The volumes of activation for the photoaquation of $\text{Rh}(\text{NH}_3)_5\text{Cl}^{2+}$ have been determined⁴² as -8.6 and $9.3 \text{ cm}^3 \text{ mol}^{-1}$ for the production of $\text{Rh}(\text{NH}_3)_5(\text{OH}_2)^{3+}$ and *trans*- $\text{Rh}(\text{NH}_3)_4(\text{OH}_2)\text{Cl}^{2+}$, respectively. The large difference in these values implies that leaving group solvation is an important factor, but the analysis is complicated by the uncertain volumes of the electronic excited state(s). The photoaquation of *cis*- $\text{Rh}(\text{bpy})_2(\text{Cl})_2^+$ to *cis*- $\text{Rh}(\text{bpy})_2(\text{OH}_2)\text{Cl}^{2+}$ has a $\Delta V^\ddagger = -9.7 \text{ cm}^3 \text{ mol}^{-1}$. The two negative activation volumes for Cl^- release pose a problem for rationalizations⁴³ in terms of a dissociative mechanism. DiBenedetto and Ford have reviewed the general problem of interpreting photochemical volumes of activation.⁴⁴

Studies of the photoaquation of *cis* and *trans* isomers of $\text{Rh}^{\text{III}}(\text{N})_4(\text{L})\text{X}$ systems present the possibility of obtaining mechanistic information from the product distribution. Some results of such studies are collected in Table 7.5.^{37,38} For the first four entries, the ratio $\Phi_{\text{trans}}/\Phi_{\text{cis}}$ is nearly the same and Skibsted⁴⁵ suggested that this could be rationalized by two isomers of the dissociative intermediate $\{\text{Rh}(\text{NH}_3)_4\text{Cl}^{2+}\}$ that are in thermal equilibrium. The capture of H_2O by these intermediates would lead to the same product distribution from the different starting complexes. Subsequent work, illustrated by the next four entries, indicates that this explanation does not hold for a $\{\text{Rh}(\text{en})_2(\text{NH}_3)^{3+}\}$ intermediate, nor for a $\{\text{Rh}(\text{NH}_3)_4(\text{OH}_2)^{3+}\}$ intermediate from the last two entries. It was suggested that ion pairing might influence the latter, more highly charged intermediates, but the original evidence now seems to be more coincidental than informative.

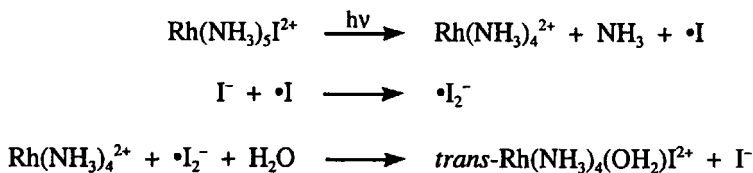
Table 7.5. Quantum Yields of Geometrical Isomers Produced by Photoaquation of X from $\text{Rh}^{\text{III}}(\text{N})_4(\text{L})\text{X}$ Complexes

Complex	X	Φ_{trans}	Φ_{cis}	$\Phi_{\text{trans}}/\Phi_{\text{cis}}$
<i>trans</i> -Rh(NH ₃) ₄ (Cl)Cl ⁺	Cl ⁻	0.122	0.025	4.9
<i>cis</i> -Rh(NH ₃) ₄ (Cl)Cl ⁺	Cl ⁻	0.328	0.063	5.2
<i>trans</i> -Rh(NH ₃) ₄ (Cl)(OH ₂) ²⁺	OH ₂	0.33	0.074	4.5
<i>cis</i> -Rh(NH ₃) ₄ (Cl)(OH ₂) ²⁺	OH ₂	0.543	0.12	4.5
<i>trans</i> -Rh(en) ₂ (NH ₃)Cl ²⁺	Cl ⁻	0	0.075	0
<i>cis</i> -Rh(en) ₂ (NH ₃)Cl ²⁺	Cl ⁻	0.004	0.071	0.06
<i>trans</i> -Rh(en) ₂ (NH ₃)(OH ₂) ³⁺	OH ₂	0.05	0.276	0.18
<i>cis</i> -Rh(en) ₂ (NH ₃)(OH ₂) ³⁺	OH ₂	0.113	0.33	0.34
<i>trans</i> -Rh(NH ₃) ₄ (OH ₂)(OH ₂) ³⁺	OH ₂	0.014	0.011	1.3
<i>cis</i> -Rh(NH ₃) ₄ (OH ₂)(OH ₂) ³⁺	OH ₂	0.102	0.041	2.5

Morrison and co-workers⁴⁶ have studied the photochemically activated reaction of *cis*-Rh(phen)₂(Cl)₂⁺ with deoxyadenosine, deoxyguanosine and uric acid. Based on the variation of products in the presence or absence of dioxygen, they suggest that the photoactivated *cis*-Rh(phen)₂(Cl)₂⁺ is reduced by deoxyguanosine to Rh^{II}(phen)₂Cl⁺ and by uric acid to Rh^I(phen)₂⁺. In the absence of dioxygen, the latter reacts with the oxidized form of uric acid to give a Rh—uric acid adduct. This work has evolved into the development of phototoxic reagents that can bind and nick DNA.⁴⁷

Irradiation of the ligand-to-metal charge-transfer bands of Rh(NH₃)₅I²⁺ gives *trans*-Rh(NH₃)₄(OH₂)I²⁺ with a quantum yield about half of that for irradiation of the lower energy *d-d* bands.⁴⁸ This indicates that deactivation of the charge-transfer states is very competitive with intersystem crossing to the lower energy states. Flash photolysis studies in the presence of traces of I⁻ reveal the presence of transient $\bullet\text{I}_2^-$ and the redox mechanism that was proposed is shown in Scheme 7.5.

Scheme 7.5



This behavior is quite different from that of the cobalt complexes in the preceding section, possibly because Rh(II) remains in the low-spin state, while Co(II) goes to the labile high-spin state. Photoredox chemistry also has been reported for *trans*-Rh(NH₃)₄(SO₃)₂⁻.⁴⁹

7.5 PHOTOCHEMISTRY OF CHROMIUM(III) COMPLEXES

Chromium(III) systems have long been the prototype for inorganic photochemical studies. They have the same chemical advantages as cobalt(III) systems, but the quantum yields are much larger, the bands in the electronic spectra are well separated and there is no photoredox process. Some general observations can be made:

1. Quantum yields are typically 0.1 to 0.8.
2. The quantum yield is independent of the incident light energy.
3. The reactions often appear to be antithermal.

For example, photolysis⁵⁰ of $\text{Cr}(\text{NH}_3)_5(\text{NCS})^{2+}$ gives $\Phi_{\text{NH}_3} = 0.46$ and $\Phi_{\text{NCS}} = 0.03$ at 373 nm, and $\Phi_{\text{NH}_3} = 0.47$ and $\Phi_{\text{NCS}} = 0.021$ at 492 nm. Ammonia loss is the dominant photochemical process, but it is not observed thermally.

7.5.1 Homoleptic $\text{Cr}^{\text{III}}(\text{L})_6$ Complexes

The electronic states involving the valence d orbitals in $\text{Cr}^{\text{III}}\text{L}_6$ complexes are shown in Figure 7.3. Electronic transitions to the ${}^4T_{2g}$ and ${}^4T_{1g}$ states are observed at 550 to 600 nm and 350 to 400 nm, respectively. Weak spin-forbidden transitions to the ${}^2T_{1g}$ and 2E_g states can sometimes be observed in the 600-nm region.

There has long been a controversy about the photoactive state(s) in these complexes, primarily concerning the ${}^4T_{2g}$ and doublet states (${}^2T_{1g}$, 2E_g). Some evidence favoring the quartet state was consistent with the idea that population of the e_g orbital would promote a dissociative mechanism, but the empty t_{2g} orbital would be expected to favor an associative mechanism.

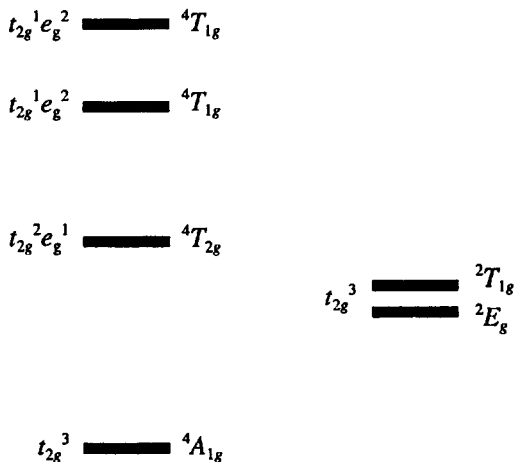
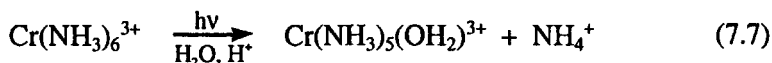


Figure 7.3. The d orbital electronic states for $\text{Cr}^{\text{III}}(\text{L})_6$ complexes.

In the doublet states, the metal ligand bonds would not be weakened much compared to the ground state, but the empty t_{2g} orbital could favor an associative substitution mechanism. The lack of wavelength dependence of the quantum yield is most easily rationalized by intersystem crossing always producing photoactive doublet states. However, back-intersystem crossing, BISC, from the doublets, although energetically unfavorable, could produce a more reactive $^4T_{2g}$ state. A useful property of these systems is that the doublets have lifetimes of the order of microseconds so that suitable quenchers can be used to shorten their lifetimes and the effect of such quenchers on the quantum yield can be determined.

Waltz and Lillie⁵¹ have used pulsed-laser techniques to measure the phosphorescent lifetimes of $\text{Cr}(\text{NH}_3)_6^{3+}$ and conductivity to monitor the following photoaquation reaction:



They observed an initial fast decrease in conductivity ($t_{1/2} \approx 1 \times 10^{-6}$ s) followed by a slower change ($t_{1/2} \approx 10 \times 10^{-6}$ s). The major process (>67%) is the slower one and it has the same rate as the phosphorescent decay, which is from a doublet state. They suggested that the fast conductivity change is due to photoaquation from the quartet state and the slower and dominant decay is from the doublet state. The implication is that both doublet and quartet states can be photoactive, with their relative amounts depending on the efficiency of the intersystem crossing between these states, which in turn will depend on the ligands on the Cr(III).

Later, Waltz and co-workers⁵² studied the temperature, pressure and solvent dependencies of the emission lifetimes and the pressure dependence of the quantum yields for reaction (7.7). The lifetimes increase with increasing donor number of the solvent. In water, the emission has an activation energy, E_a , of 43 kJ mol^{-1} and a ΔV^\ddagger of $4.3 \text{ cm}^{-3} \text{ mol}^{-1}$. The quantum yield for solvolysis is relatively unaffected by the change in solvent and has values of E_a^{53} and ΔV^\ddagger of 44 kJ mol^{-1} and $-6 \text{ cm}^{-3} \text{ mol}^{-1}$, respectively. The authors suggested that the 2E_g state decays mainly by BISC to the $^4T_{2g}$ state. The very similar values of E_a for emission and solvolysis suggest that BISC may be rate-limiting for both processes.

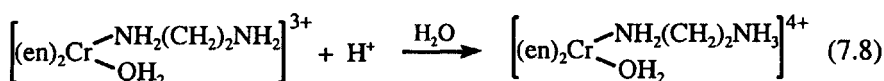
For $\text{Cr}(\text{CN})_6^{3-}$, Wasgestian⁵⁴ found that the emission lifetime of the doublet state(s) is very solvent dependent in mixtures of water with *N,N*-dimethylformamide, but the quantum yield for aquation (0.11) is unaffected by the solvent composition. This shows that reactivity is not from the doublet state(s) and suggests that the quartet state is photoactive. From the activation volume⁵⁵ for photoaquation of $2.7 \text{ cm}^{-3} \text{ mol}^{-1}$ (15°C , 364.5 nm), an I_d mechanism was suggested. In the related complex, $\text{Cr}(\text{CN})_5(\text{NH}_3)^{2-}$, quartet state activity also is indicated⁵⁶ since $\text{Co}(\text{sep})^{3+}$ quenches the phosphorescence in dimethylsulfoxide but does not change the quantum yields.

7.5.2 Homoleptic Cr^{III}(LL)₃ Chelates

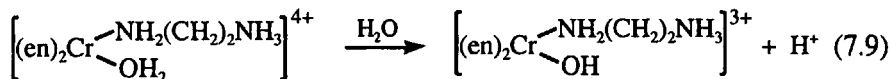
These systems can undergo both photochemical racemization and ligand substitution. For chelates, the latter process can be complicated by intermediates that result from one-ended dissociation. The N-bonded amine chelates typically undergo substitution in a manner analogous to Cr(NH₃)₆³⁺, with ~25% as a prompt reaction directly from the quartet state and ~75% as a slow process involving the doublet state. However, as described below, the pH dependence for the chelates can be more complicated.

Photoracemization of Cr(en)₃³⁺ was found by Linck and co-workers⁵⁷ to have a quantum yield of 0.015 which was independent of [H⁺] in the range of 0.08 to 1.0 M. Based on the latter observation, the authors concluded that the reaction was not going by one-ended dissociation because the free amine end would be rapidly protonated and this should inhibit ring closure.

Photoaquation of Cr(en)₃³⁺ in acidic solution has a quantum yield of ~0.4, independent of wavelength between 365 and 685 nm.^{58,59} The product distribution from Λ-Cr(en)₃³⁺ also is wavelength independent and the isomers of (en)₂Cr(enH)(OH₂)⁴⁺ produced are 65% trans, 27% Λ-cis and 8% Δ-cis. The theory of Vanquickenborne and Cuelemans,⁶⁰ which is often used to explain product distribution in this area, is not consistent with the dominant trans product and unspecified steric effects have been invoked as a rationalization of this failure. More recently, Irwin and Kirk have reported a flash photolysis study with conductivity monitoring.⁶¹ The rate constants for doublet decay and chemical change at pH <3 are very similar. For pH <3.9, the conductivity shows an exponential decrease due to the following reaction:



However, at higher pH the system shows an initial rise in conductivity that the authors ascribe to the following reaction:



Analogous observations were made earlier⁶² with *cis*-Cr(cyclam)(NH₃)₂³⁺ and more recently for the N₆-macrocycle Cr(sen)³⁺.⁶³ Kirk⁶⁴ has argued that all these reactions occur from the quartet state after BISC from the doublet.

Both Cr(phen)₃³⁺ and Cr(bpy)₃³⁺ differ from Cr(en)₃³⁺ in that the quantum yields are low, <0.04, and the doublet-state lifetimes are ~10² longer. It also is thought that the doublet state is photoactive. The low quantum yields are suggestive of a mechanism different from that of Cr(en)₃³⁺. Doublet-state quenching studies^{65,66} show that this state is definitely

involved, but do not eliminate the possibility of BISC. The main argument against the BISC pathway and for doublet activity comes from the temperature studies of Hoffman and co-workers.⁶⁷ They concluded that BISC from doublet to quartet would need to be nearly barrierless to be consistent with their observations, but it seems very unlikely that the quartet is as low in energy as the doublet.

The $\text{Cr}(\text{phen})_3^{3+}$ and $\text{Cr}(\text{bpy})_3^{3+}$ systems are unusual in showing an increase in quantum yield for solvolysis in alkaline solution. This may result because the doublet state persists on the millisecond time scale and therefore is able to undergo bimolecular reactions with OH^- with rate constants of the order of $10^3 \text{ M}^{-1} \text{ s}^{-1}$. Lille et al.⁶⁸ proposed opening of the chelate ring and coordination of an ionizable water, while Neshvad et al.⁶⁹ suggested an ionizable, intraligand bound water without ring opening.

The tris-acetylacetonate complex, $\text{Cr}(\text{acac})_3$, may be taken as an example of an O-donor system. In 50% ethanol/water, this complex undergoes solvolysis with a quantum yield of 0.011.⁷⁰ The latter is independent of wavelength between 366 and 730 nm and of pH between 0 and 13. The ΔH^\ddagger is $3.7 \text{ kcal mol}^{-1}$, compared to $24.9 \text{ kcal mol}^{-1}$ for the thermal reaction. The fac-isomer of the trifluoromethyl derivative of $\text{Cr}(\text{acac})_3$ isomerizes to the mer-isomer with quantum yields of $\sim 1 \times 10^{-3}$, which are independent of wavelength between 366 and 546 nm.⁷¹ Since the process is unaffected by H_2SO_4 and the quantum yield is only slightly different in benzene and ethanol, the process appears to be an intramolecular rhombic-bend rearrangement. A femtosecond photophysics study⁷² of $\text{Cr}(\text{acac})_3$ in acetonitrile has given rate constants for quartet to doublet intersystem crossing, doublet vibrational relaxation and doublet to ground state decay of $>10^{13}$, 10^{12} and $\sim 10^9 \text{ s}^{-1}$, respectively. It is notable that vibrational relaxation is slower than intersystem crossing.

7.5.3 Cr(III) Amine Complexes

There has been a great deal of work on the photoaquation of complexes of the general type $\text{Cr}(\text{A})_5\text{X}$, $\text{Cr}(\text{A})_4(\text{X})_2$, $\text{Cr}(\text{A})_3(\text{X})_3$ and their isomers, where A is an amine ligand. The reactions are often, but not always, antithermal, showing loss of the amine ligand. Information on these systems is summarized in the review by Kirk.⁶⁴ The first attempt to explain the variation in products and quantum yields was made by Adamson.⁷³ This led to what are termed *Adamson's rules*, which are summarized as follows:

1. The axis with the lowest average $10 Dq$ will be the most labilized.
2. If two different ligands are on that axis, the one with the larger Dq will photoaquate.
3. The quantum yield will be about the same as that for the CrL_6 complex, where L are the lower Dq axis ligands.

Some complexes that obey Adamson's rules are given by the first four examples in Table 7.6.

Table 7.6. Quantum Yields for Photoaquation of NH_3 (Φ_{N}) and X (Φ_{X}) from Some Cr(III) Amine Complexes^a

Complex	Φ_{N}	Φ_{X}
$\text{Cr}(\text{NH}_3)_5\text{Cl}^{2+}$	0.36	0.005
<i>trans</i> - $\text{Cr}(\text{en})_2(\text{Cl})_2^+$	<0.001	0.32
<i>trans</i> - $\text{Cr}(\text{NH}_3)_4(\text{Cl})_2^+$	0.003	0.44
<i>trans</i> - $\text{Cr}(\text{en})_2(\text{NH}_3)\text{Cl}^{2+}$	0.34	<0.01
<i>trans</i> - $\text{Cr}(\text{en})_2(\text{F})_2^{+b}$	0.20	0.02
<i>trans</i> - $\text{Cr}(\text{en})_2(\text{NH}_3)\text{F}^{2+}$	0.27	0.14

^a Unless otherwise indicated, original references are given by Kirk, A. D. *Coord. Chem. Rev.* **1981**, *39*, 225.

^b Manfrin, M. F.; Sandrini, A.; Juris, A.; Gandolfi, M. T. *Inorg. Chem.* **1978**, *17*, 90.

The fluoride complexes do not obey the "rules" because the Dq of F^- is smaller than that of the amine nitrogen. This led to considerable soul searching and the rationalization that what is really required is a measure of the Cr—X bond strength. With F^- , it was suggested that the Dq was anomalously low because of π -bonding effects, so that Dq does not reflect the σ -bond strength. This resulted in ligand field theory rationalizations, such as those proposed by Zinck⁷⁴ and Vanquickenborne and Cuelemans.⁶⁰ The observation⁷⁵ that *trans*- $\text{Cr}(\text{H}_2\text{N}(\text{CH}_2)_3\text{NH}_2)_2(\text{F})_2^+$ gives mainly F^- loss ($\Phi_{\text{F}} = 0.34$, $\Phi_{\text{N}} = 0.18$) and is much different from the ethylenediamine analogue shows that subtle effects (steric or ring strain) can influence the course of the photochemical process.

The quantum yields for competitive water exchange and NH_3 aquation⁷⁶ also are not consistent with the theoretical approaches. Some of these results are given in Table 7.7. The first entry is consistent with Adamson's and other predictions, but the second should predominantly give NH_3 loss and the third and fourth should mainly give water exchange; the last entry conforms to the "rules".

Table 7.7. Quantum Yields for the Water Exchange (Φ_{exch}) and NH_3 Loss (Φ_{NH_3}) from Some Cr(III) Complexes

Complex	Φ_{exch}	Φ_{NH_3}
$\text{Cr}(\text{NH}_3)_5(\text{OH}_2)^{3+}$	0.078	0.195
<i>cis</i> - $\text{Cr}(\text{NH}_3)_4(\text{OH}_2)_2^{3+}$	0.057	0.058
<i>trans</i> - $\text{Cr}(\text{NH}_3)_4(\text{OH}_2)_2^{3+}$	0.001	0.025
<i>fac</i> - $\text{Cr}(\text{NH}_3)_3(\text{OH}_2)_3^{3+}$	0.040	0.053
<i>trans</i> - $\text{Cr}(\text{NH}_3)_2(\text{OH}_2)_4^{3+}$	0.072	0.004

The antithermal nature of the photochemical reactions has been reassessed.⁷⁷ The thermal reaction of $\text{Cr}(\text{NH}_3)_5(\text{OH}_2)^{3+}$ at 50°C is mainly water exchange ($k = 1.37 \times 10^{-3} \text{ s}^{-1}$, $\Delta H^\ddagger = 99.1 \text{ kJ mol}^{-1}$) but a minor route produces *cis*- $\text{Cr}(\text{NH}_3)_4(\text{OH}_2)_2^{3+}$ ($k = 4.03 \times 10^{-6} \text{ s}^{-1}$, $\Delta H^\ddagger = 110.5 \text{ kJ mol}^{-1}$). If one happened to work at a high enough temperature, then the ammonia loss could be the dominant thermal reaction. It was suggested that the photochemical process provides access, in the electronic ground state, to a pentagonal bipyramidal transition state that is about 10 kJ mol⁻¹ higher in energy than the transition state for thermal water exchange.

Evidence for stereomobility of the photochemical transition state has been obtained⁷⁸ with *trans*- $\text{Cr}(\text{cyclam})(\text{Cl})_2^+$, a rigid macrocyclic system, that has a very low quantum yield for Cl^- aquation of 3×10^{-4} . This has been attributed to the macrocycle preventing rearrangements that normally lead to less energetic configurations in the photoactive states which lead to aquation. The *trans*- $\text{Cr}(\text{cyclam})(\text{NH}_3)_2^{3+}$ is similar to its dichloro analogue, but *cis*- $\text{Cr}(\text{cyclam})(\text{NH}_3)_2^{3+}$ has $\Phi_{\text{NH}_3} = 0.2$,⁷⁹ although the *trans* isomer has a much longer lived doublet state ($\tau = 55 \times 10^{-6} \text{ s}$, versus $2 \times 10^{-6} \text{ s}$ at 293 K). The authors propose that the photoactive state is the quartet state, which may be reached by back intersystem crossing. The latter process is less effective with the *trans* isomer because the energy separation is 22.2 kcal mol⁻¹ compared to 19.0 kcal mol⁻¹ for the *cis* isomer.

Volumes of activation have been measured by Angermann et al.⁸⁰ for some of the reactions and the results are given in Table 7.8. The authors suggest that the negative values of ΔV^\ddagger are consistent with associative activation for the photochemical process and the thermal reaction. Solvent electrostriction effects should make a larger negative contribution when X^- is the leaving group compared to NH_3 . Since this difference is not reflected in the ΔV^\ddagger values, Angermann et al. proposed that the ammonia release process is "more associative" than the X^- release.

It has been noted by Kirk⁶⁴ that there is a mechanistic anomaly for many of these Cr(III) systems. The theory of Vanquickenborne and Cuelemans⁶⁰ assumes a dissociative mechanism from the quartet state, but the negative ΔV^\ddagger values seem more consistent with associative activation.

Table 7.8. Volumes of Activation for Photochemical and Thermal Aquation of Some Cr(III) Complexes

Complex	ΔV^\ddagger (cm ³ mol ⁻¹)		
	Φ_{NH_3}	Φ_{X^-}	Thermal
$\text{Cr}(\text{NH}_3)_5\text{Cl}^{2+}$	-9.4	-13.0	-10.8
$\text{Cr}(\text{NH}_3)_5\text{Br}^{2+}$	-10.2	-12.2	-10.2
$\text{Cr}(\text{NH}_3)_5(\text{NCS})^{2+}$	-11.4	-9.8	-8.6
$\text{Cr}(\text{NH}_3)_6^{3+}$	-12.6		

7.6 PHOTOCHEMISTRY OF RUTHENIUM(II) COMPLEXES

Ruthenium(II) forms a wide range of d^6 , low-spin, octahedral complexes. The crystal field electronic states are analogous to those of Co(III) shown in Figure 7.1, however the larger Dq of Ru(II) causes the ligand field bands to occur at higher energies in the wavelength region of 300 to 400 nm. It is generally found that Ru(II) acts as a π -electron donor to ligands which have π^* -acceptor orbitals and such complexes have metal-to-ligand charge-transfer, MLCT, bands that often overlap with the ligand field bands. The latter transitions generate what can be viewed as an $\text{Ru}^{\text{III}}\text{---L}^-$ excited state, which can yield photoredox chemistry. The area of Ru(II) photochemistry has been reviewed by Tfouni.⁸¹

7.6.1 Ru(II) Complexes of Saturated Amines

Since saturated amine ligands lack π^* orbitals, their photochemistry tends to be more straightforward to interpret because the ligand field bands are not obscured by more intense charge transfer bands. Some systems with heteroligands that have π^* orbitals will be considered here, but the important class of polypyridine complexes is deferred to the next section.

The photolysis of $\text{Ru}(\text{NH}_3)_6^{2+}$ and $\text{Ru}(\text{en})_3^{2+}$ was studied initially by Matsubara and Ford at pH 3 in 0.2 M NaCl.⁸² They found that aquation was the dominant process and the quantum yield of 0.25 for $\text{Ru}(\text{NH}_3)_6^{2+}$ was constant between 313 and 405 nm. However, the quantum yield for $\text{Ru}(\text{en})_3^{2+}$ decreased from 0.18 to 0.06 between 313 and 366 nm; as yet there is no definitive explanation for this effect. More recently, Neumann and co-workers⁸³ have used sensitizers and quenchers to study the $\text{Ru}(\text{NH}_3)_6^{2+}$ system. They concluded that the photoactive state is $17.3 \pm 0.4 \times 10^3 \text{ cm}^{-1}$ above the ground state and that it is the ${}^3T_{1g}$ state. Although the spin-forbidden transition to this state has not been observed, it is predicted by theory⁸⁴ to occur at $17.7 \times 10^3 \text{ cm}^{-1}$, i.e. 565 nm.

Below 280 nm, the quantum yield for aquation decreases to ~ 0.05 and redox chemistry becomes the dominant process with quantum yields increasing with decreasing wavelength to values in the range of 0.5 to 1 at 214 nm. Matsubara and Ford assigned the absorbance in this region to a charge transfer to solvent, CTTS, transition. The decrease in quantum yield for aquation indicates that there is not efficient intersystem crossing between the CTTS excited state(s) and the ligand field states. The photochemical reaction for $\text{Ru}(\text{NH}_3)_6^{2+}$ was shown to produce H_2 and Ru(III) and was proposed to proceed by reduction of H^+ by the photoactive species to yield H^\bullet and Ru(III). The H^\bullet further reacts with H^+ and Ru(II) to yield H_2 and another Ru(III).

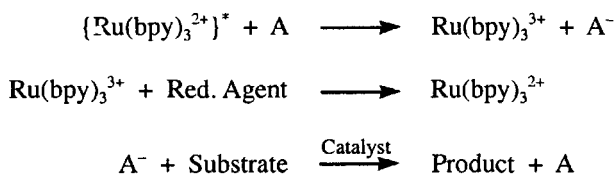
For $\text{Ru}^{\text{II}}(\text{NH}_3)_5\text{X}$ systems, the same pattern of photoactivity was observed for $\text{X} = \text{NCCH}_3$,⁸⁵ with quantum yields at 366 nm for loss of X and NH_3 of 0.16 and 0.01, respectively. Loss of NH_3 can yield cis and/or trans isomers, but the isomer distribution was not determined. More generally the redox

7.6.2 Ru(II)polypyridine Complexes

Much of the work in the Ru(II) polypyridine area has concentrated on Ru(bpy)₃²⁺ and its derivatives. The electronic spectra are dominated by an intense charge-transfer band at ~450 nm with $\epsilon \approx 10^4 \text{ M}^{-1} \text{ cm}^{-1}$; Ru(bpy)₃²⁺ shows modest photosubstitution activity with quantum yields <0.1.⁹⁰ Photochemical methods have proven useful in the preparation of several derivatives,⁹¹ including the unusual isomer *trans*-Ru(bpy)₂(OH)₂²⁺ and Ru(bpy)₂(dmbpy)(NCCH₃)₂²⁺,⁹² where dmbpy is the monodentate ligand 3,3'-dimethyl-2,2'-bipyridine.⁹³

There is interest in Ru(bpy)₃²⁺ because of its use in photochemical energy transfer, and its photophysics and applications have been the subject of several reviews.⁹⁴⁻¹⁰⁰ Parris and Brandt¹⁰¹ first observed that this complex has a relatively long-lived emission ($\tau \approx 600 \text{ ns}$ in water). This, together with its electronic spectral properties, allows the system to trap visible light energy long enough for the photoexcited state to undergo further chemical reactions. The long-lived excited state is a metal-to-ligand charge-transfer triplet, which can act as a reducing agent to give Ru(bpy)₃³⁺ or as an oxidizing agent to give Ru(bpy)₃⁺. Therefore, the energy-transfer process may be coupled to either an oxidizing or a reducing agent. An oxidative coupling is shown in Scheme 7.7.

Scheme 7.7



Much of the interest in these systems has been concerned with the cleavage of water. For example, an oxidative system has been used¹⁰² and studied in detail¹⁰³ in which A = Rh(bpy)₃³⁺, triethanolamine is the reducing agent, H₂O is the substrate, Pt⁰ is the catalyst and the product is H₂.

A reductive scheme¹⁰⁴ uses A = ascorbate and the oxidizing agent Co(bpy)_n²⁺ which is reduced to Co(bpy)_n⁺. It is proposed that the latter reacts with H⁺ to form a hydride that decomposes to H₂. A major problem in these applications is the loss of Ru(bpy)₃²⁺ due to photoaquation. Balzani and co-workers¹⁰⁵ have prepared several caged Ru(II) polypyridine complexes that are much more stable and have electronic properties similar to Ru(bpy)₃²⁺.

Sun and Hoffman¹⁰⁶ reported that the triplet state of Ru(bpy)₃²⁺ gives emission at ~625 nm and that it decays with a rate constant of $3.5 \times 10^5 \text{ s}^{-1}$ at 25°C in water. The decay has an E_a of ~45 kJ mol⁻¹, and the authors suggested that this occurs mainly by rate-controlling intersystem crossing to a photoactive ligand field state.

7.7 ORGANOMETALLIC PHOTOCHEMISTRY

Photochemical conditions are widely used in synthetic organometallic studies, and there is a steadily increasing number of quantitative studies concerned with quantum yields and elucidation of the photochemical mechanism. Most of the systematic work has been done on metal carbonyls and their derivatives, and the following discussion will be limited to this class of compounds.

A substantial barrier to mechanistic studies is the uncertainty about the assignment of the bands in the electronic spectrum of even the binary carbonyls. A typical spectrum for an $M(\text{CO})_6$ complex is shown in Figure 7.4. The spectra are dominated by intense MLCT bands, but there are weaker bands in the 320 and 270 nm regions. Beach and Gray¹⁰⁷ assigned the latter bands as vibrational components of ligand field transitions and this was supported by later theoretical studies.¹⁰⁸ This assignment and the feeling that MLCT excited states would not promote ligand dissociation, because they make the metal more electropositive, led to many qualitative and more advanced^{109,110} ligand field models to explain the photoactivity and product distribution in many metal carbonyl systems. Theoretical studies by Baerends and co-workers¹¹¹ on $\text{Mn}_2(\text{CO})_{10}$ suggest that the ligand field transitions are at much higher energy than previously assumed. Shortly thereafter, Pierloot et al.¹¹² found that this was definitely true for the more representative $\text{Cr}(\text{CO})_6$. Further calculations by Baerends¹¹³ and by Gray¹¹⁴ and their co-workers confirmed that the weak features in the spectrum are orbitally forbidden MLCT bands.

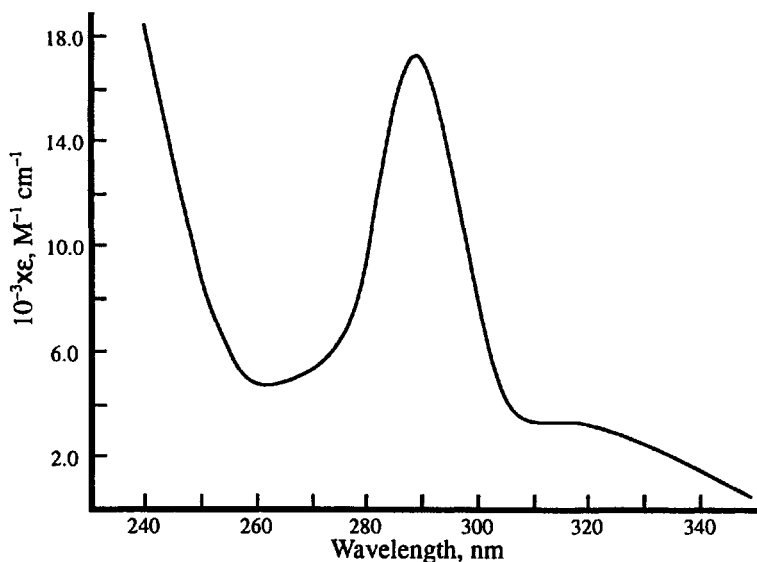


Figure 7.4. A typical electronic spectrum of an $M(\text{CO})_6$ complex.

This spectrum reassignment has significant consequences for models of photochemical mechanisms. Models which rely on excitation of the MLCT states followed by intersystem crossing to the ligand field states appear much less viable because the latter are at higher energy. A proposal which seems applicable to several systems is described in a review by Baerends and Rosa.¹¹⁵ The theory abandons the common assumption that orbital energies are always those of some equilibrium configuration. It then allows these energies to vary as a ligand dissociates and this results in calculated potential energy curves for the orbitals. The general observation is that, as the ligand moves away from the metal, at least one of the empty antibonding ligand field orbitals drops in energy and mixing with the original photoexcited state produces a highly dissociative state. The earlier perception that ligand field states are dissociative is retained but, with the more recent picture, it is not necessary to directly populate such states for them to participate in the photochemistry.

7.7.1 Metal Hexacarbonyls

Nasielski and Colas¹¹⁶ studied the following reaction in benzene and cyclohexane with $M = W$:



They found that the quantum yield ($\Phi \approx 0.7$) is independent of wavelength between 254 and 366 nm and is independent of $[L]$ (py or CH_3CN). The reaction is sensitized by $Ph_2C=O$ ($\Delta E^* = 289 \text{ kJ mol}^{-1} = 414 \text{ nm}$) but not by triphenylene ($\Delta E^* = 280 \text{ kJ mol}^{-1} = 427 \text{ nm}$). The reaction is not quenched by bibenzene ($\Delta E^* = 272 \text{ kJ mol}^{-1}$) or naphthalene ($\Delta E^* = 255 \text{ kJ mol}^{-1}$) and no phosphorescence was observed. The lack of quenching and phosphorescence indicates that the photoactive state is quite short-lived. The lack of concentration dependence is consistent with a dissociative mode of activation. The original suggestion was that the photoactive state was a ligand field triplet state, but this no longer seems tenable in view of the spectrum reassignment discussed above. A flash photolysis study by Joly and Nelson¹¹⁷ revealed that CO is fully dissociated in $\sim 350 \text{ fs}$. They suggest that this is remarkably fast for any intersystem crossing to a triplet but rather indicates that the reaction occurs from the initial excited state. Theoretical details for $M = Cr$ have been described by Baerends and co-workers.¹¹⁸

Flash photolysis of $Cr(CO)_6$ in cyclohexane¹¹⁹ produces the transient solvent complex $Cr(CO)_5(C_6H_{12})$ which was identified by IR. The $Cr-(C_6H_{12})$ bond strength has been estimated as $\sim 53 \text{ kJ mol}^{-1}$ by photoacoustic calorimetry.¹²⁰ This species reacts with CO and H_2O with rate constants of 3.6×10^6 and $4.5 \times 10^7 \text{ M}^{-1} \text{ s}^{-1}$ at 25°C , respectively, both with $\Delta H^* = 22 \text{ kJ mol}^{-1}$. The reaction of $Cr(CO)_5(OH_2)$ with C_6H_{12} has

$k = 670 \text{ s}^{-1}$ and $\Delta H^* \approx 75 \text{ kJ mol}^{-1}$. The identification of the H_2O complex is of general interest because water is a potential contaminant in many studies. Similar studies^{117,121} in aliphatic alcohols indicate initial formation of a CH-coordinated species that rearranges to the OH-coordinated isomer with $k \approx 2 \times 10^{10} \text{ s}^{-1}$.

Other work^{122,123} using picosecond laser spectroscopy has shown that these reactions proceed via a solvent intermediate, $\text{M}(\text{CO})_5(\text{solvent})$, which forms in a few picoseconds after the laser pulse and then decays to products. Lee and Harris¹²⁴ have observed formation of the solvated species $\text{Cr}(\text{CO})_5(\text{C}_6\text{H}_{12})$ with $\tau = 17 \text{ ps}$ and the decay of the vibrationally excited $\text{Cr}(\text{CO})_5$ with $\tau \approx 21 \text{ ps}$ (apparently at ambient temperature). These observations are at variance with those of Spears and co-workers,¹²⁵ who claim that the bare $\text{Cr}(\text{CO})_5$ persists on the 100-ps time scale at 22°C . Hopkins and co-workers¹²⁶ have used resonance Raman detection to show that the 100-ps process is due to thermal relaxation of the excited vibrational state, probably of $\text{Cr}(\text{CO})_5(\text{C}_6\text{H}_{12})$.

The kinetics of ligand substitution on $\text{Cr}(\text{CO})_5(\text{heptane})$ was studied by Yang et al.¹²⁷ and the rate constants vary by ~ 20 for different entering groups. As noted above, the ΔH^* for CO and H_2O substitution on $\text{Cr}(\text{CO})_5(\text{C}_6\text{H}_{12})$ is smaller than the $\text{Cr}-(\text{C}_6\text{H}_{12})$ bond strength. These observations seem most consistent with associative activation. On the other hand, van Eldik and co-workers¹²⁸ have done several studies in mixed alkane/amine solvents and interpret the observed values of ΔV^* in terms of dissociative activation.

Burkey and co-workers have reported high pressure photoacoustic results for alkane complex formation and further reaction with other nucleophiles with $\text{M} = \text{Cr}^{129}$ and W^{130} . They obtain overall ΔH° and ΔV° values and derive the M -alkane bond strengths that are $\sim 50 \text{ kJ mol}^{-1}$ for both metals.

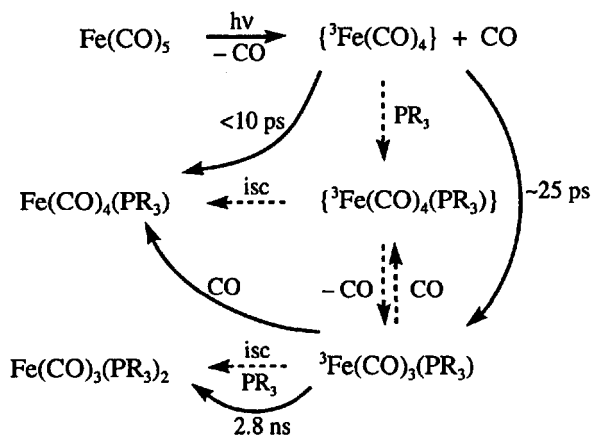
The photoinitiated reaction of 1-hexyne with $\text{M}(\text{CO})_6$ complexes has been studied on the femto- to picosecond time scale by Harris and co-workers.¹³¹ With infrared detection, they observed different lifetimes at two wavelengths. They assigned the shorter one, $\tau \approx 35 \text{ ps}$, to a mixture of vibrational relaxation and complexation of the alkyl part of the alkyne; the longer lifetime, $\tau \approx 68 \text{ ps}$, was assigned to rearrangement to the π -complex. The most rapid rearrangement was observed for the W system, which is expected to have the strongest π -alkyne bond, and the authors suggested some associative assistance to explain the faster rearrangement. In an extension of the study to the millisecond time scale, no tautomerism to the vinylidene species was observed.

Photolysis of $\text{Fe}(\text{CO})_5$ initially gives $\text{Fe}(\text{CO})_4$, but this species is unusual because it has a triplet ground state.¹³² General aspects of this area have been reviewed by Leadbetter.¹³³ Photolysis in the gas phase at 351 nm in the presence of CO or H_2 has shown that these gases combine with triplet $\text{Fe}(\text{CO})_4$ about 10^3 times more slowly than singlet state analogues.¹³⁴ This was attributed to the spin-forbidden nature of a reaction between triplet and

singlet state partners. It is often assumed that a similar reactivity pattern extends to triplet $\text{Fe}(\text{CO})_4$ in solution. A more recent study¹³⁵ of $\text{Fe}(\text{CO})_5$ in the gas phase suggests that it relaxes to singlet $\text{Fe}(\text{CO})_4$ in ~ 50 fs and then eliminates a second CO with $\tau = 3.3$ ps. Intersystem crossing of singlet $\text{Fe}(\text{CO})_4$ to the triplet state takes more than 500 ps. It should be noted that gas and solution phase observations can be different because vibrational excited states are relaxed more efficiently in solution.

The products of photolysis of $\text{Fe}(\text{CO})_5$ at 337 nm in cyclohexane with various added phosphines and CO have been reported by Burkey and co-workers.¹³⁶ The products are $\text{Fe}(\text{CO})_4(\text{PR}_3)$ and $\text{Fe}(\text{CO})_3(\text{PR}_3)_2$ with quantum yields independent of $[\text{PR}_3] \geq 1$ mM and $[\text{Fe}(\text{CO})_5] \approx 10$ mM. Addition of CO decreases the relative amount of $\text{Fe}(\text{CO})_3(\text{PR}_3)_2$. It also was found that $\text{Fe}_2(\text{CO})_9$, formed by reaction of $\text{Fe}(\text{CO})_4$ with $\text{Fe}(\text{CO})_5$, reacts thermally with PR_3 to give a different product ratio. Later, Harris and co-workers¹³⁷ studied the flash photolysis of $\text{Fe}(\text{CO})_5$ at 295 nm in neat PEt_3 . They were unable to detect either of the triplet state intermediates ${}^3\text{Fe}(\text{CO})_4$ or ${}^3\text{Fe}(\text{CO})_4(\text{PR}_3)$, and only saw the singlet state of the latter product and an intermediate after ~ 200 ps. The intermediate decays with $\tau = 2.8$ ns to yield $\text{Fe}(\text{CO})_3(\text{PR}_3)_2$. They identified the intermediate as ${}^3\text{Fe}(\text{CO})_3(\text{PR}_3)$ by making it independently by photolysis of $\text{Fe}(\text{CO})_4(\text{PR}_3)$ in heptane. To make the flash photolysis results consistent with the CO competition observations of Burkey and co-workers, it might be assumed that the high concentration of PEt_3 in the former work makes the lifetimes of ${}^3\text{Fe}(\text{CO})_4$ and ${}^3\text{Fe}(\text{CO})_4(\text{PR}_3)$ too short to be detected. On the other hand, one might assume that the persistent intermediate ${}^3\text{Fe}(\text{CO})_4(\text{PR}_3)$ can react competitively with PEt_3 and CO to explain how CO lowers the yield of the $\text{Fe}(\text{CO})_3(\text{PR}_3)_2$. Scheme 7.8 summarizes the flash photolysis results with curved arrows and the mechanism of Burkey and co-workers with dashed arrows; isc means intersystem crossing from triplet to singlet.

Scheme 7.8



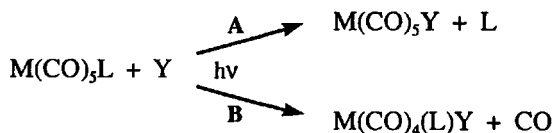
Harris and co-workers¹³⁷ also studied reactions of ${}^3\text{Fe}(\text{CO})_4$ with alcohols. They concluded that the triplet state reacts more rapidly than singlet state species and gives the O-bonded alcohol directly. This pattern of reactivity is consistent with earlier experimental¹³⁸ and theoretical¹³⁹ suggestions that triplet species would interact less strongly with alkyl groups than singlet species. Thus, in the singlet systems, the rate of O-bonded alcohol formation is limited by rearrangement from the alkyl-bonded isomer. A similar reason has been given¹⁴⁰ for the fact that Et_3SiH reacts much more rapidly with ${}^3\text{Fe}(\text{CO})_4$ than with singlet $(\text{Cp})\text{Rh}(\text{CO})$.

The nature of the photoactive state(s) in $\text{Fe}(\text{CO})_5$ remains uncertain. Theory^{141,142} suggests that a ligand field excited state is close in energy to the MLCT states and could be populated by intersystem crossing. Daniel and co-workers¹⁴¹ argued that dissociation of CO in the gas phase, which occurs with $\tau \approx 0.3$ ps, is too fast for intersystem crossing and the initially excited state must be the photoactive one. This implies that it is a MLCT state since the photons are mostly absorbed by the intense MLCT bands.

7.7.2 Substituted Metal Carbonyls: $\text{M}(\text{CO})_5\text{L}$

Photoactivated substitution on $\text{M}(\text{CO})_5\text{L}$ systems has been reported by Wrighton¹⁴³ and by Dahlgren and Zinck.¹⁴⁴ The photochemical reaction proceeds by two paths that yield different products: L elimination (path A) and CO elimination (path B), as shown in Scheme 7.9.

Scheme 7.9



Wrighton found that for $\text{M} = \text{Mo}$ and $\text{L} = \text{Y} = n\text{-PrNH}_2$, chosen so that only path B is observed, the quantum yield decreases with increasing irradiation wavelength ($\Phi_{366} = 0.24$, $\Phi_{405} = 0.20$, $\Phi_{436} = 0.057$). When $\text{M} = \text{W}$, the values of Φ are about five times less. With $\text{M} = \text{W}$, $\text{L} = n\text{-PrNH}_2$ and $\text{Y} = 1\text{-pentene}$, path A is dominant and the quantum yield is less sensitive to wavelength, even increasing slightly at longer wavelength ($\Phi_{366} = 0.60$, $\Phi_{405} = 0.65$, $\Phi_{436} = 0.73$). The results were interpreted by a ligand field model with photoactive triplet states, as shown in Figure 7.5. Longer wavelength radiation was proposed to populate the $d_{x^2-y^2}$ orbital and labilize the cis-CO ligands. This model is included here for historical background. As discussed above, current levels of theory now indicate that the ligand field transitions are at much higher energy and photolysis is activated by population of the MLCT bands. The theory described by Lammertsma and co-workers¹⁴² for $\text{Cr}(\text{CO})_5\text{L}$ systems is likely to be applicable to other $\text{M}(\text{CO})_5\text{L}$ species.

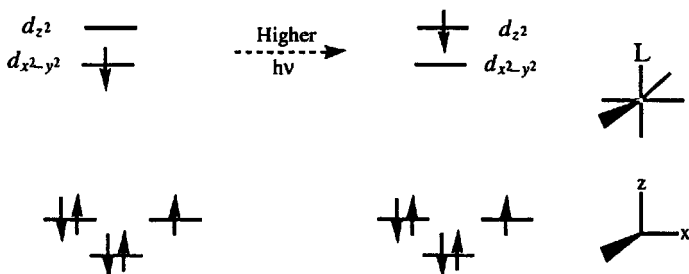
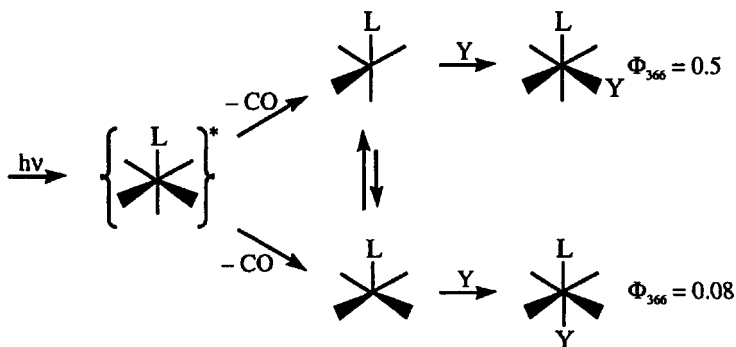


Figure 7.5. Ligand field excited states for $\text{Mo}(\text{CO})_4(\text{L})\text{Y}$ complexes.

Dahlgren and Zinck¹⁴⁴ studied $\text{W}(\text{CO})_5\text{L}$ systems at 436 nm and found that the importance of the two pathways depends on the nature of L. When L is a nitrogen-donor ligand (pyridine, piperidine, ammonia, acetonitrile), pathway A is dominant ($\Phi_{\text{A}} \approx 0.5$, $\Phi_{\text{B}} < 0.01$). When L is a phosphine, the two pathways have about equal quantum yields ($\Phi_{\text{A}} \approx \Phi_{\text{B}} \approx 0.3$). The observations were rationalized in terms of the M—C bond strengths as reflected by the CO stretching frequencies. Since the N-donors do not give back π bonding, the M—C bond is stronger and CO loss is not as favored as with the phosphines, which can compete with CO for π electrons on the metal, thereby weakening the M—C bond.

Darensbourg and Murphy¹⁴⁵ studied the photosubstitution reactions of $\text{Mo}(\text{CO})_5(\text{PPh}_3)$ with $\text{Y} = \text{PPh}_3$ or ^{13}CO (in THF at 313 and 366 nm). They observed loss of CO and the products were a mixture of cis and trans isomers. The results can be understood in terms of two five-coordinate intermediates, as shown in Scheme 7.10, where $\text{L} = \text{PPh}_3$. The interequilibration of the intermediates is indicated by the fact that *trans*- $\text{Mo}(\text{CO})_4(\text{PPh}_3)_2$ photoisomerizes with $\Phi_{366} = 0.3$.

Scheme 7.10



Wrighton et al.¹⁴⁶ examined the photolysis of $\text{W}(\text{CO})_5(\text{pyX})$ systems at 436 and 515 nm in 1:2 by volume 1-pentene/isooctane. The X substituent

was varied in such a way that the MLCT to π^* on pyX band was shifted between 347 and 470 nm. Loss of pyX is the major photoreaction. The experimental concept was based on the earlier work of Malouf and Ford⁸⁷ on $(\text{H}_3\text{N})_5\text{Ru}(\text{pyX})^{2+}$, as described in Section 7.6.1. It was observed by Wrighton et al. that Φ_{436} decreased from 0.82 to 0.12 when the MLCT band shifted from ~ 420 to 435 nm. They interpreted this to mean that the MLCT to π^* on py state is not photoactive and this seems correct. However, they attributed the activity to what they believed was a $d-d$ band in the 400-nm region. With the benefit of recent theoretical developments, one can see that this band is actually a MLCT to π^* on CO band and may produce the photoactive state.

Further work has been done by Lees and co-workers¹⁴⁷ on the Cr and Mo systems to try and elucidate the photoactive state. Their observations for $\text{Mo}(\text{CO})_5\text{L}$, where L are various substituted pyridines, were analogous to those of Wrighton et al. and they offered a similar explanation. These systems also have a band at ~ 400 nm which now would be assigned to a MLCT to π^* on CO band, and as the irradiation wavelength moves from 405 to 458 nm the quantum yield decreases. The observations suggest that absorbance at ~ 400 nm yields the photoactive state and that the MLCT to π^* on py state is not highly photoactive. Lees and co-workers reported weak luminescence from the latter state with emission maxima at ~ 650 nm.

Pulsed-laser studies¹⁴⁸ with $\text{W}(\text{CO})_5\text{L}$ (L = pyridine or piperidine) have essentially confirmed the earlier observations. This work also showed that a solvent complex is formed within 10 ps of the laser flash and this "intermediate" is the ultimate source of the substitution products. These authors also reported that if 1-hexene is the entering ligand, then the first product has $\text{W}(\text{CO})_5$ complexed to the "alkyl portion" of the hexene and this species rearranges in about 10 ns to the η^2 -hexene product. These observations may be relevant to those of Stoutland and Bergman on the addition of ethylene to $\text{Ir}(\text{Cp}^*)(\text{PMe}_3)$ discussed in Section 5.5.

The volumes of activation for the photosubstitution of $\text{W}(\text{CO})_5(\text{py})$ and 4-substituted pyridines have been determined¹⁴⁹ using $\text{P}(\text{OEt})_3$ as the entering group. This work also involved a study of the effect of pressure on the emission lifetimes, and the effect was found to be small compared to the effect of pressure on the quantum yield. The ΔV^\ddagger values are positive and somewhat dependent on the nature of the pyridine (py, $5.7 \text{ cm}^3 \text{ mol}^{-1}$; 4-cyanopy, $6.3 \text{ cm}^3 \text{ mol}^{-1}$; 4-acetylpy, $9.9 \text{ cm}^3 \text{ mol}^{-1}$). The results are consistent with a dissociative mode for photosubstitution.

The photolysis of $\text{cis-W}(\text{CO})_4(\text{pyX})_2$ complexes in benzene have been studied using a chelating phosphine¹⁵⁰ and phen¹⁵¹ as entering groups. The studies have good agreement on the Φ values, and the later study by Lees and co-workers¹⁵¹ determined that the Φ values are essentially independent of temperature for irradiation between 360 and 465 nm. But at 514 nm, the activation energy was $6.8 \text{ kcal mol}^{-1}$. This was ascribed to intersystem crossing from the MLCT to π^* on py state to the reactive state.

The $W(CO)_4(en)$ system is analogous to those in the above paragraph in that it has two N-donor atoms, but en has no π^* orbitals and photoactivation results in loss of CO. The path to the understanding of this system parallels that of other systems described in this section. The electronic spectrum has a shape similar to that in Figure 7.4. The intense band at 397 nm has been traditionally assigned to a ligand field transition and the weaker band at ~ 450 nm to a spin-forbidden transition that gives a ligand field triplet state. Lees and co-workers¹⁵² found that the Φ values decrease from 0.23 to 0.007 between 313 and 476 nm and concluded that the triplet state is not photoactive. More recently, theoretical and experimental work by Vlcek and co-workers¹⁵³ has shown that the ligand field bands are at much higher energy and the bands in the visible region are assigned to a CT transition from the $W(CO_{eq})_2$ moiety to CO_{ax} , where CO_{eq} and CO_{ax} are the equatorial and axial CO ligands, respectively. The absorbance at 398 nm yields the singlet state, while the weaker one gives the triplet state. A transient infrared spectrum of the latter was obtained on the picosecond time scale. To be consistent with the observed Φ values, the authors suggest that the singlet state is much more photoactive than the triplet.

There have been many studies of $M(CO)_4(\alpha\text{-diimine})$ systems, where the α -diimine is bpy or phen or their derivatives.¹⁵⁴ There is a π^* system on the diimine as well as the π^* orbitals on the CO. The theory, electronic spectrum assignments and photochemistry have been reviewed recently by Vlcek.¹⁵⁵ The spectra typically show a strong band in the visible region, a weaker band at ~ 400 nm and a much stronger band in the UV region. If one takes some liberties with the orbital complexity of the excited states, these transitions can be regarded respectively as MLCT to $\pi^*(\alpha\text{-diimine})$, to $\pi^*(CO)$ and to higher π^* orbitals on both ligands. In earlier work, the 400-nm band was assigned to a ligand field transition.

Vlcek and co-workers^{156,157} have shown that photolysis of $Cr(CO)_4(bpy)$ gives prompt CO dissociation in <400 fs in dichloromethane or toluene and yields only *fac*- $Cr(CO)_3(bpy)(\text{solvent})$. This result shows that an axial CO is lost. The authors suggested that the photoactive state is formed by the MLCT to $\pi^*(CO)$ transition and that it decays to two nearly degenerate, photoinactive triplet states, which involve the $\pi^*(\alpha\text{-diimine})$ orbital that can be viewed as $Cr^1(bpy^{\bullet-})$. The latter decay to the ground state with τ values of 8 and 87 ps, respectively. The quantum yield is controlled by branching of the photoactive state between capture of the entering group or solvent and decay to the triplet states.

Several studies¹⁵⁸ using PPh_3 as the entering group have found that Φ is independent of $[PPh_3]$ for $M = Cr$, but increases linearly with $[PPh_3]$ for $M = Mo$ and W . This has been taken to indicate an associative component to the mechanism for the latter systems. The tendency of the $M(CO)_6$ species of this group to show a duality of substitution mechanisms was noted in Section 5.1.1, but thermal substitution on $W(CO)_4(bpy)$ also involves monodentate bpy, as described in Section 5.1.2.2.

7.7.3 Manganese Pentacarbonyls

Faltynek and Wrighton¹⁵⁹ studied the photosubstitution of $\text{Mn}(\text{CO})_5^-$ and $\text{Mn}(\text{CO})_4(\text{PPh}_3)^-$ in the presence of PPh_3 or $\text{P}(\text{OMe})_3$ and found quantum yields of ~ 0.3 . In $\text{Mn}(\text{CO})_4(\text{PPh}_3)^-$, only substitution of the PPh_3 is observed.

Oxidative addition to $\text{Mn}(\text{CO})_5^-$ is also photoactivated. A competition study of substitution versus oxidative addition gave the results shown in Scheme 7.11. The constancy of the oxidative addition yield suggests that this path may involve an ion pair. Unfortunately, the concentration of PPh_4^+ was not varied to test this hypothesis.

Scheme 7.11

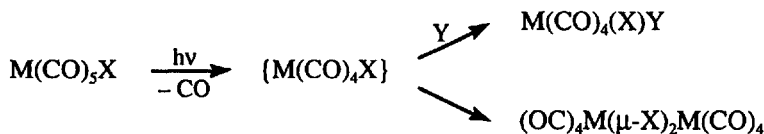


M	M	M	Percent	Percent
0.01	0.01	0.01	35	38
0.01	0.01	0.06	31	32
0.01	0.01	0.22	28	82

Ford and co-workers¹⁶⁰ studied the flash photolysis of $\text{Mn}(\text{CO})_5(\text{CH}_3)$ at 308 nm in hydrocarbons and THF. They found that the solvent reacts with the transient $\{\text{Mn}(\text{CO})_4(\text{CH}_3)\}$ to give *cis*- $\text{Mn}(\text{CO})_4(\text{CH}_3)(\text{Solvent})$ about 5×10^3 faster than it reacts with CO to give reactant. The solvent complexes with C_6H_{12} and THF have rate constants for their reactions with CO of 2×10^6 and $1.4 \times 10^2 \text{ M}^{-1} \text{ s}^{-1}$, respectively. More recent work¹⁶¹ has focused on the insertion product $\text{Mn}(\text{CO})_5(\text{C}(\text{O})\text{CH}_3)$ with the finding that it photodissociates CO to give an η^2 -acyl intermediate or a *cis*-THF complex of the parent.

The photochemical information on $\text{M}(\text{CO})_5\text{X}$ systems ($\text{M} = \text{Mn, Re}$; $\text{X} = \text{Cl, Br, I}$) is largely based on qualitative observations which suggest that CO loss is the major process and that the reactions proceed as in the following Scheme:

Scheme 7.12



For $\text{M} = \text{Mn}$, Bamford et al.¹⁶² identified the dimeric product and suggested that it can further photolyse to $\text{Mn}_2(\text{CO})_{10}$. Berry and Brown¹⁶³ observed that CO exchanges into both the axial and equatorial positions on irradiation at 400 nm. Rest and co-workers¹⁶⁴ obtained the infrared

spectrum of the intermediate at 12 K and identified it as a trigonal bipyramid with an equatorial Cl ligand. Quantum yields for reactant loss were reported by Wrighton et al.¹⁶⁵ for $\text{Re}(\text{CO})_5\text{X}$ in CCl_4 ($\text{X} = \text{Cl}, \text{Br}, \text{I}$) at 313 and 366 nm. With no Y present, the dimeric product was formed, while with $\text{Y} = \text{py}$ or PPh_3 , at unspecified concentrations, the same Φ values were obtained for a particular X. This, plus the observation of only *cis*- $\text{Re}(\text{CO})_4(\text{X})\text{Y}$ product, led the authors to suggest a common square pyramidal intermediate with a CO ligand at the apex. The stereospecificity and structure of the intermediate seem to be different from the Mn system.

Wrighton et al. interpreted their observations in terms of the ligand field model on the assumption that ligand field transitions occur in the 350-nm region. However, recent theoretical treatments¹⁶⁶ of $\text{Mn}(\text{CO})_5\text{Cl}$ suggest that it is excitation from $\pi^*(\text{Mn } d_{xz} \text{ or } d_{yz}, \text{Cl } 3p)$ to the σ^* orbital of the Mn—Cl bond. Calculated potential energy curves indicate that this excited state will lead to dissociation of either equatorial or axial CO.

7.7.4 $\text{Mn}_2(\text{CO})_{10}$ and Related Systems

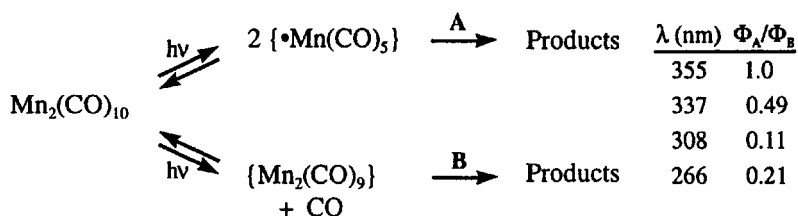
The $\text{Mn}_2(\text{CO})_{10}$ system has been of interest because it is a prototype for metal–metal bonded systems and because of the suggestion that $\bullet\text{Mn}(\text{CO})_5$ radicals may be involved in the thermal substitution reactions. The photochemistry of metal–metal bonded systems has been reviewed by Meyer and Caspar.¹⁶⁷ Bonding theory for $\text{Mn}_2(\text{CO})_{10}$ suggests that irradiation can populate the σ^* orbital of the Mn—Mn bond and therefore might be expected to cleave that bond and produce the $\bullet\text{Mn}(\text{CO})_5$ radical. Recent theoretical studies¹⁶⁸ are generally consistent with the earlier work. The $\sigma \rightarrow \sigma^*$ transition is observed at ~ 340 nm, and several studies^{169,170} using 366-nm irradiation have found evidence for radical pathways for decomposition and substitution that are consistent with initial formation of $\bullet\text{Mn}(\text{CO})_5$. The final products in the presence of N-donor ligands are $\text{Mn}(\text{CO})_5^-$ and $\text{Mn}(\text{N})_6^{2+}$. A radical chain process has been proposed for the decomposition. The radical $\bullet\text{Mn}(\text{CO})_5$ can be detected by its halogen atom abstraction reaction with CCl_4 ($k \approx 10^6 \text{ M}^{-1} \text{ s}^{-1}$). This type of reaction with chloroalkanes is a test for the presence of radicals.

Studies by Church et al.¹⁷¹ found that the recombination of $\bullet\text{Mn}(\text{CO})_5$ occurs at a near diffusion-controlled rate ($k = 1 \times 10^9 \text{ M}^{-1} \text{ s}^{-1}$ in heptane). The IR spectra indicate that the radical has a square pyramidal structure. A species with a bridging CO has been identified from a peak at 1760 cm^{-1} and was suggested to have a $\mu(\eta^1:\eta^2\text{-CO})$. This species reacts with CO in C_7H_{16} to form $\text{Mn}_2(\text{CO})_{10}$ with a rate constant of $2.7 \times 10^6 \text{ M}^{-1} \text{ s}^{-1}$. Similar observations were made by Seder et al.¹⁷² in the gas phase, where the rate constant is a surprisingly similar $2.4 \times 10^6 \text{ M}^{-1} \text{ s}^{-1}$ and the radical recombination rate constant is $4.5 \times 10^{10} \text{ M}^{-1} \text{ s}^{-1}$, both at 323 K. These observations may be relevant to the thermolysis of the Mn—Mn bond.

Hepp and Wrighton¹⁷³ reported that photolysis at 355 nm in the presence of PPh_3 gives $\sim 30\%$ CO dissociation and subsequent substitution. Later

work¹⁷⁴ on the wavelength dependence of the quantum yields indicates that CO dissociation is more important as the irradiation wavelength decreases. This trend was confirmed down to 193 nm in the gas phase by Seder et al.,¹⁷² and more recently in cyclohexane at further wavelengths by Sarakha and Ferraudi.¹⁷⁵ The situation is summarized in Scheme 7.13. The increase in CO dissociation at shorter wavelengths is consistent with irradiation into π^* orbitals of the M—CO bond.

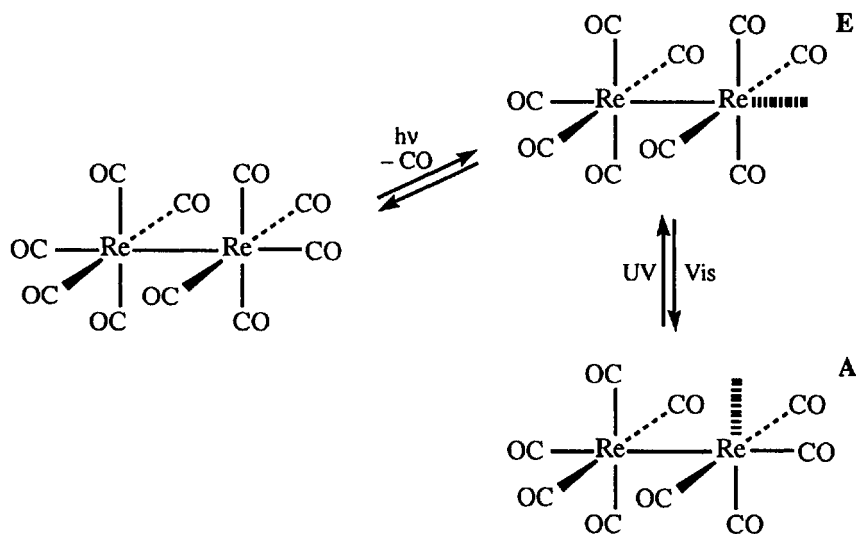
Scheme 7.13



Analogous behavior has been observed for $\text{Re}_2(\text{CO})_{10}$.^{174,175} The trapping of $\{\bullet\text{Mn}(\text{CO})_5\}$ by PPh_3 has been observed to depend on $[\text{PPh}_3]$ and was taken to indicate an associative mechanism for substitution on the 17-electron radical.

Turner and co-workers¹⁷⁶ have compared the photochemistry of $\text{Mn}_2(\text{CO})_{10}$, $\text{MnRe}(\text{CO})_{10}$ and $\text{Re}_2(\text{CO})_{10}$ in liquid argon and xenon. The former two are quite similar, but $\text{Re}_2(\text{CO})_{10}$ does not appear to form a bridged species. The low-temperature studies in inert gases with IR spectroscopy also revealed the intermediates shown in Scheme 7.14.

Scheme 7.14



The first intermediate, **E**, with an equatorial vacancy, is quite persistent in liquid xenon and returns to reactant over a period of several hours. The second intermediate, **A**, with an axial vacancy, is formed by irradiation of **E** by visible light and returns to **E** when UV light is used. Both intermediates react with N_2 to give the corresponding dinitrogen complex. More recently, Brown and Zhang¹⁷⁷ found that flash photolysis of $MnRe(CO)_{10}$ in 3-methylpentane glass gives the solvento complex $MnRe(CO)_9(\text{solvent})$ which, on warming, recombines with CO to give the reactant. Continuous irradiation of the solvento complex with visible light (>450 nm) produces a new species that was assigned to the semibridging form $MnRe(CO)_8(\mu-\eta^1, \eta^2-CO)$. Under the similar conditions, $Re_2(CO)_{10}$ gave no semibridging species.

Harris and co-workers¹⁷⁸ found that laser flash photolysis of $Mn_2(CO)_{10}$ in C_6H_{12} at 295 nm with visible detection initially formed $Mn_2(CO)_9$ which isomerizes to a bridged species in <3 ps. The latter vibrationally relaxes by two paths with τ values of 15 and 170 ps and persists for many nanoseconds. The $\bullet Mn(CO)_5$ radical relaxes in <10 ps and also persists for many nanoseconds. A later study¹⁷⁹ on $Re_2(CO)_{10}$ in halocarbon solvents with infrared detection revealed that the $\bullet Re(CO)_5$ radicals interact weakly with the solvent and recombine within the solvent cage with $\tau \approx 50$ ps and ~ 500 ps as they diffuse out of the cage. Once the radicals have diffused apart, they abstract $Cl\bullet$ from the solvent on the nanosecond time scale. Still later,¹⁸⁰ it was reported that $Re_2(CO)_9$ in CCl_4 gives an equatorial solvate, analogous to **E** in Scheme 7.14, which persists for >2.5 μs . In hexane, a similar but weaker solvate is observed which undergoes reaction after a time >50 ns to form what the authors believe is the unsolvated species with the $Re(CO)_5$ part of the molecule forming a trigonal bipyramid.

Owruksy and co-workers studied $Mn_2(CO)_{10}$ with infrared detection and photolysis at 310¹⁸¹ and 400¹⁸² nm. In the first study, they note that the extraction of lifetimes is complicated by vibrational relaxation processes which occur on the 50-ps time scale, and that no bridged species is observed in isopropanol. This may be due to complexation of $Mn_2(CO)_9$ by the solvent. For the longer wavelength irradiation, $\bullet Mn(CO)_5$ is the only product and its vibrational relaxation times were estimated to be the same, within experimental uncertainty, in cyclohexane and isopropanol. None of these studies suggest any solvento complexes for the $\bullet Mn(CO)_5$ species.

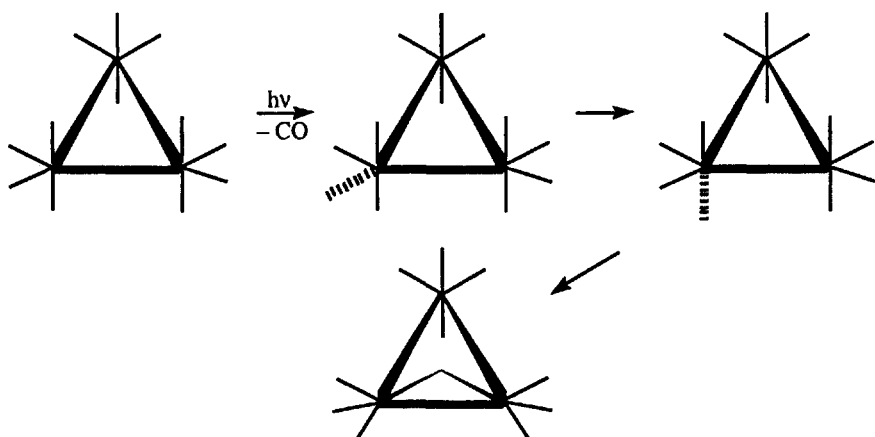
7.7.5 $M_3(CO)_{12}$ Systems: M = Fe, Ru, Os

Photochemical studies of these cluster compounds by Bentsen and Wrighton¹⁸³ and by Ford and co-workers¹⁸⁴ revealed some general patterns of reactivity. For wavelengths below ~ 350 nm, the dominant photoactivated process is CO loss and substitution by solvent or added nucleophiles. For wavelengths above 400 nm, the dominant process is photofragmentation in which the trinuclear species breaks into $M(CO)_5$, $M(CO)_4L$, $M_2(CO)_3L$ and so on. The reactions are unaffected by

chlorinated organic solvents, and this is evidence against radical reaction pathways. The area was reviewed by Ford,¹⁸⁵ and theoretical aspects of the bonding and spectra are described by Calhorda et al.¹⁸⁶ The theory is generally consistent with the traditional interpretation that the longer wavelength irradiation should activate the M—M bonds.

Bentsen and Wrighton proposed that short-wavelength irradiation of the Fe and Ru systems liberates an equatorial CO to give an intermediate that either captures solvent or added nucleophiles or rapidly rearranges to a more stable form with an axial vacancy. The latter rearranges to a bridged species with IR bands in the region of 1830 cm^{-1} . The Os system is similar, except that the bridged form has not been detected. The proposed structures of the intermediates are shown in Scheme 7.15.

Scheme 7.15



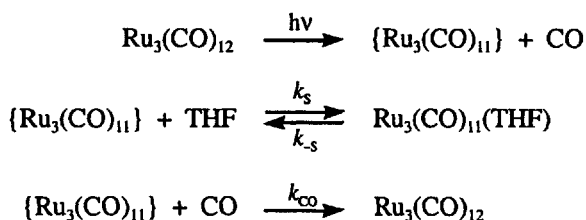
Harris and co-workers¹⁸⁷ studied the flash photolysis of $\text{Fe}_3(\text{CO})_{12}$ in cyclohexane and concluded that the major product is the bridged species that forms in ≤ 1.5 ps. It returns to the ground state with a τ value of 150 ps. However, about 20% of the $\text{Fe}_3(\text{CO})_{12}$ does not return, but fragments to form mono- and dinuclear species. The fragmentation process has shorter τ values, in the 6- to 14-ps range, as the observation wavelength is changed from 720 to 800 nm. Harris et al. have attributed these observations to fragmentation of vibrationally excited forms of $\text{Fe}_3(\text{CO})_{12}$, whose absorbance in the electronic spectrum shifts to longer wavelength with the increasing extent of vibrational excitation.

Grevels and co-workers studied $\text{Ru}_3(\text{CO})_{12}$ by flash photolysis at 308 nm in cyclohexane.¹⁸⁸ Their observations suggest that initial loss of CO produces $\text{Ru}_3(\text{CO})_{10}(\mu\text{-CO})$ which can add CO to give $\text{Ru}_3(\text{CO})_{11}(\mu\text{-CO})$. The latter can return to reactant, but it also can add a second CO to give $\text{Ru}_3(\text{CO})_{12}(\mu\text{-CO})$ in the presence of excess CO. Then, fragmentation and addition of another CO yields the products $\text{Ru}_2(\text{CO})_9$ and $\text{Ru}(\text{CO})_5$. More recently, Hartl and co-workers¹⁸⁹ studied the photolysis at 400 nm in

heptane and found $\text{Ru}_3(\text{CO})_{11}(\mu\text{-CO})$ as the primary photoproduct. The τ values for formation of this species and its return to reactant were estimated to be ~ 4 and 57 ps, respectively.

The study of Ford and co-workers¹⁸⁴ on $\text{Ru}_3(\text{CO})_{12}$ indicates that the intermediate $\text{Ru}_3(\text{CO})_{11}$, produced by 308-nm irradiation in isooctane, reacts with CO with $k_{\text{CO}} = 2 \times 10^9 \text{ M}^{-1} \text{ s}^{-1}$ at ambient temperature. With THF added, a THF adduct is formed and the kinetics of the reformation of $\text{Ru}_3(\text{CO})_{12}$ are consistent with Scheme 7.16.

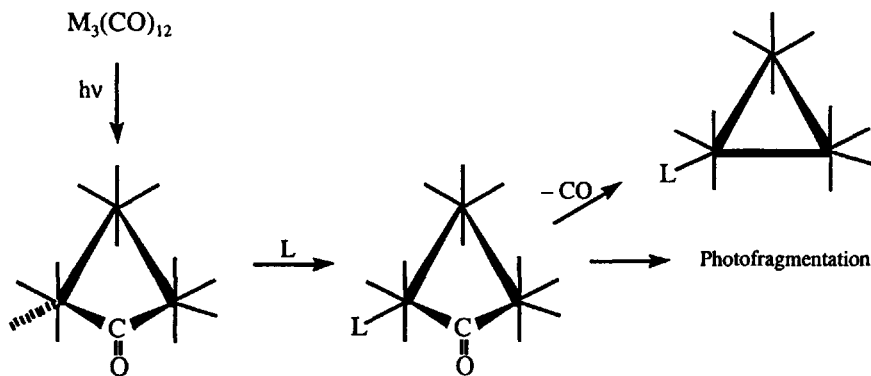
Scheme 7.16



From the dependence of the rate on $[\text{CO}]$ and $[\text{THF}]$ and the known value of k_{CO} , the authors obtain $k_{-S} = 2.1 \times 10^6 \text{ s}^{-1}$ and $k_S = 6 \times 10^9 \text{ M}^{-1} \text{ s}^{-1}$. The values of k_{CO} and k_S are near the diffusion-controlled limit and imply that isooctane is weakly solvating the intermediate $\text{Ru}_3(\text{CO})_{11}$. The value of k_{CO} is much larger than that with $\text{Mn}_2(\text{CO})_9$ in which a bridging CO is proposed to inhibit the reaction.

The long-wavelength process has been investigated by Bentsen and Wrighton,¹⁸³ and by Ford and co-workers.¹⁹⁰ The quantum yields are low, < 0.02 , and dependent on the nature of the added nucleophiles and the solvent. Product studies reveal that PPh_3 and $\text{P}(\text{OEt})_3$ favor associative substitution to give $\text{M}_3(\text{CO})_{11}(\text{PR}_3)$. The results have been interpreted as indicating a common intermediate that is an unstable isomer of $\text{M}_3(\text{CO})_{12}$, suggested to be the bridged isomer shown in Scheme 7.17.

Scheme 7.17



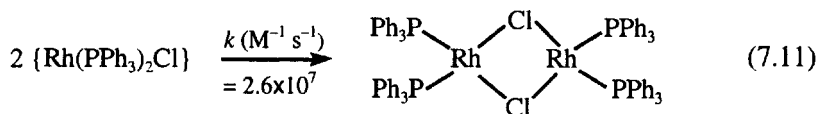
Ford has given a detailed analysis of the kinetics of this type of scheme in terms of the concentration dependence of the quantum yields for the Ru system. In cyclohexane, these results indicate that the ratio of the rate constants for substitution by L versus return to the ground state are 112, 79 and 71 for L = CO, P(OCH₃)₃ and PPh₃, respectively. The insensitivity of these ratios to the nature of L could mean that the unsaturated bridged species is unselectively scavenging any available ligand. Lower-limit values of *k* for substitution by L and return to the ground state were estimated as 5 × 10⁶ M⁻¹ s⁻¹ and 5 × 10⁴ s⁻¹, respectively.

Photolysis of Os₃(CO)₁₂ at ~436 nm in benzene was studied by Pož and Sekhar.¹⁹¹ The product is Os₃(CO)₁₁(P(OEt)₃) when P(OEt)₃ is added, but Os(CO)₄(η²-octene) and Os₂(CO)₄(μ-η¹,η¹-octene) are formed in the presence of 1-octene. The quantum yield increases with increasing concentration of the nucleophile to a limiting value of ~0.04 for both nucleophiles. The observations were interpreted in terms of formation of a reactive intermediate, Os₃(CO)₁₁(μ-CO). This may undergo substitution or revert to the nonbridged reactant. The mechanism is analogous to that discussed above for the longer-wavelength photolysis of Ru₃(CO)₁₂.

7.8 PHOTOCHEMICAL GENERATION OF REACTION INTERMEDIATES

An increasingly important application of photochemistry is in the production of proposed intermediates in thermal reactions. Flash photolysis and pulsed-laser techniques at low temperatures can produce these species and allow for their spectroscopic characterization and studies of their reactivity. Examples of this have been seen in the areas of C—H activation and the addition of alkenes to metal centers. Some aspects of this area were reviewed by Harris and co-workers.¹⁹² In order to be relevant to the thermal mechanism, the species must be in its electronic and thermal ground state.

An example of this type of application is the photochemistry of the derivative of Wilkinson's catalyst, Rh(PPh₃)₂(CO)Cl, studied by Wink and Ford.¹⁹³ The flash photolysis was studied in benzene for wavelengths longer than 315 nm, and a transient species was observed with a much higher absorbance than the reactant in the 390- to 550-nm region. The transient species, which reacts with CO to produce the reactant, has been assigned as Rh(PPh₃)₂Cl. It was also possible to determine the rate constant for the following dimerization reaction:

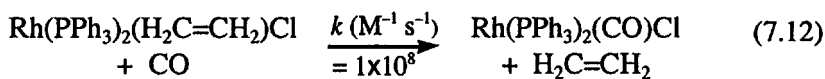


The reactivity of this transient with several species was studied and the results are summarized in Scheme 7.18.

Scheme 7.18

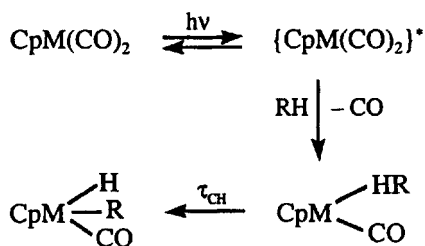
Rh(PPh ₃) ₂ (CO)Cl	L	<i>k_L</i> (M ⁻¹ s ⁻¹)
- CO ↓ <i>hν</i>	CO	6.9 × 10 ⁷
{Rh(PPh ₃) ₂ Cl}	C ₂ H ₄	>4 × 10 ⁷
L ↓ <i>k_L</i>	PPh ₃	3.0 × 10 ⁶
Rh(PPh ₃) ₂ (L)Cl	H ₂	1.0 × 10 ⁵
	D ₂	6.8 × 10 ⁴

These results are in general agreement with the values or limits determined from conventional kinetic studies by Halpern and Wong¹⁹⁴ and Tolman et al.¹⁹⁵ It was found that the dimer and the dihydrogen adduct react with CO rather slowly ($k \approx 2 \text{ s}^{-1}$) and by a unimolecular process. A remarkable feature of these results is the large rate constant for displacement of ethylene by CO, as shown in the following reaction:



Now, one has a quite complete picture of the reactivity of the species thought to be important in the operation of this catalytic system.

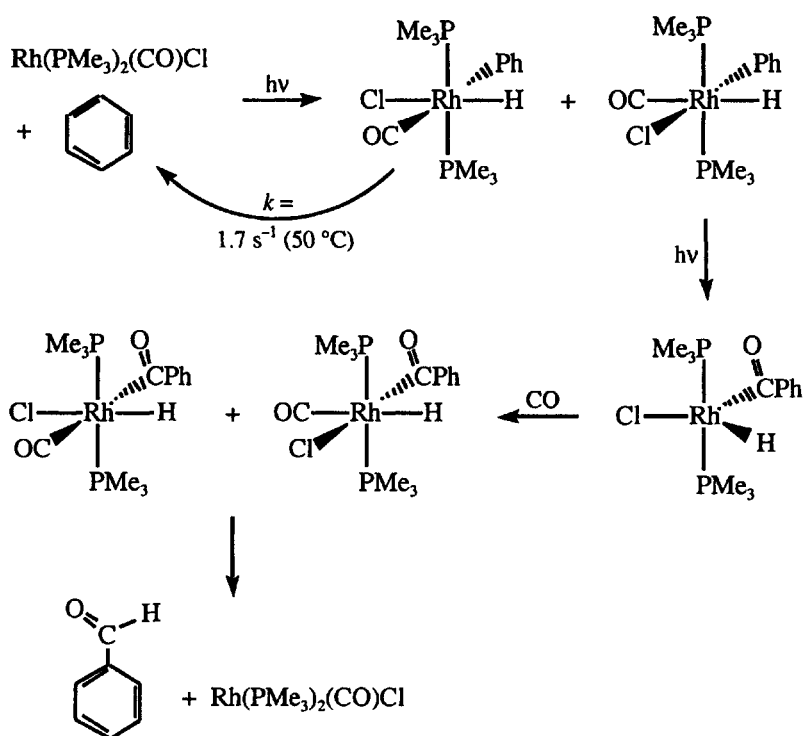
The process of C—H bond activation, discussed in Section 5.6.4, has been examined in some detail. The observations on CpM(CO)₂ systems by Bergman and co-workers¹⁹⁶ are summarized in the following Scheme:

Scheme 7.19

For both M = Rh and Ir in hydrocarbon solvents, about 80% of the initial photoexcited state decays to the ground state with $\tau \approx 40$ ps. The remaining 20% dissociates CO and forms the solvent complex on the 10-ps time scale. However the τ_{CH} value is ~ 2 ps for Ir but >500 ps for Rh in cyclohexane. This great difference in reactivity is consistent with earlier theoretical predictions.¹⁹⁷

A more complex system which involves the photoactivated oxidative addition of benzene to $\text{Rh}(\text{PMe}_3)_2(\text{CO})\text{Cl}$ is outlined in Scheme 7.20. The system is unusual in having two photoactivated steps and the general reactions shown are based on the observations of Field¹⁹⁸ and Goldman¹⁹⁹ and their co-workers. The oxidative addition yields two isomers; the one with the CO and Ph cis to each other is photoactivated to give CO insertion in competition with return to reactants. In the presence of CO, the acyl intermediate reacts by CO addition and reductive elimination to give benzaldehyde and the catalyst.

Scheme 7.20



The evidence for this scheme comes from several observations. The reaction is promoted rather than inhibited by CO, so that the initial photochemical event is not CO elimination. The photochemical behavior is unusual because the quantum yield changes if the light source is pulsed on and off. Tanaka and co-workers²⁰⁰ reported that the rate decreases by a factor of 10 when the pulse rate is changed from 10 s^{-1} to 1 s^{-1} , and the phenomenon was confirmed by Goldman et al. In Scheme 7.20, this is accounted for by competition between return to reactants and the photoactivated insertion step. Goldman and co-workers have identified the various octahedral species by low temperature NMR.

References

1. Balzani, V.; Carassiti, V. *Photochemistry of Coordination Compounds*; Academic Press: New York, 1970.
2. *Concepts of Inorganic Photochemistry*; Adamson, A. W.; Fleischauer, P., Eds.; Wiley: New York, 1975.
3. Geoffrey, G. L.; Wrighton, M. S. *Organometallic Photochemistry*; Academic Press: New York, 1979.
4. *Homogeneous and Heterogeneous Photocatalysis*; Pelizzetti, E.; Serpone, N., Eds.; Reidel: Dordrecht, The Netherlands, 1986.
5. *Photochemistry and Photophysics of Coordination Compounds*; Yersin, H.; Vogler, A., Eds.; Springer-Verlag: Berlin, 1987.
6. Adamson, A. W.; Waltz, W. L.; Zinato, E.; Watts, D. W.; Fleischauer, P. D.; Lindholm, R. D. *Chem. Rev.* **1968**, *68*, 541.
7. Crosby, G. A. *Acc. Chem. Res.* **1975**, *8*, 231.
8. Wrighton, M. S. *Top. Curr. Chem.* **1976**, *65*, 37.
9. Koerner von Gustof, E. A.; Linders, L. H. G.; Fischler, I.; Perutz, R. N. *Adv. Inorg. Chem. Radiochem.* **1976**, *19*, 65.
10. Hollebhone, B. R.; Langford, C. H.; Serpone, N. *Coord. Chem. Rev.* **1981**, *39*, 181.
11. Kirk, A. D. *Coord. Chem. Rev.* **1981**, *39*, 225.
12. Ford, P. C.; Wink, D.; DiBenedetto, J. *Prog. Inorg. Chem.* **1983**, *30*, 213.
13. Verhoeven, J. W. *Pure Appl. Chem.* **1996**, *68*, 2223.
14. Wegner, E. E.; Adamson, A. W. *J. Am. Chem. Soc.* **1966**, *88*, 394.
15. Wilson, R. B.; Solomon, E. I. *J. Am. Chem. Soc.* **1980**, *102*, 4085.
16. Scandola, F.; Scandola, M. A.; Bartocci, C. *J. Am. Chem. Soc.* **1975**, *97*, 4757.
17. Nishazawa, M.; Ford, P. C. *Inorg. Chem.* **1981**, *20*, 294.
18. Wong, C. F. C.; Kirk, A. D. *Can. J. Chem.* **1976**, *54*, 3794.
19. Braden, D. A.; Parrack, E. E.; Tyler, D. R. *Coord. Chem. Rev.* **2001**, *211*, 279.
20. Kirk, A. D.; Kneeland, D. M. *Inorg. Chem.* **1989**, *28*, 4274.
21. Kirk, A. D.; Kneeland, D. M. *Inorg. Chem.* **1995**, *34*, 1536.
22. Endicott, J. F.; Ferraudi, G. J.; Barber, J. R. *J. Phys. Chem.* **1975**, *79*, 630; *Ibid. J. Am. Chem. Soc.* **1975**, *97*, 219; *Ibid.* 6406.
23. Weit, S. K.; Kutal, C. *Inorg. Chem.* **1990**, *29*, 1455.
24. Hennig, H.; Walther, D.; Thomas, P. *Z. Chem.* **1983**, *23*, 446.
25. Wang, Z.; Kutal, C. *Inorg. Chim. Acta* **1994**, *226*, 285.
26. Kutal, C. *Coord. Chem. Rev.* **2001**, *211*, 353.
27. Cope, V. W.; Hoffman, M. Z. *J. Phys. Chem.* **1978**, *82*, 2665.
28. Ferraudi, G.; Perkovic, M. *Inorg. Chem.* **1993**, *32*, 2587.
29. Poznyak, A. L.; Pavlovski, V. I. *Angew. Chem. Int. Ed. Engl.* **1988**, *27*, 789; Poznyak, A. L. *Koord. Chim.* **1991**, *17*, 1261.
30. Kawaguchi, H.; Yoshida, M.; Yonemura, T.; Ama, T.; Okamoto, K.; Yasui, T. *Bull. Chem. Soc. Jpn.* **1995**, *68*, 874.
31. Poznyak, A. L.; Pavloski, V. I.; Chuklannova, E. B.; Polynova, T. N.; Porai-Koshits, M. A. *Monatsh. Chem.* **1982**, *113*, 561.

32. Natarajan, E.; Natarajan, P. *Inorg. Chem.* **1992**, *31*, 1215.
33. Hartshorn, R. M.; Telfer, S. G. *J. Chem. Soc., Dalton Trans.* **1999**, 3565.
34. Horner, J. H.; Tanaka, N.; Newcomb, M. *J. Am. Chem. Soc.* **1998**, *120*, 10379, and references therein.
35. Pincock, J. A. *Acc. Chem. Res.* **1997**, *30*, 43, and references therein.
36. Hartshorn, R. M.; Telfer, S. G. *J. Chem. Soc., Dalton Trans.* **2000**, 2801.
37. Mønsted, L.; Mønsted, O. *Coord. Chem. Rev.* **1989**, *94*, 109.
38. Skibsted, L. H. *Coord. Chem. Rev.* **1989**, *94*, 151.
39. Ford, P. C. *Inorg. Chem.* **1975**, *14*, 1440.
40. Forster, L. S. *Coord. Chem. Rev.* **2002**, *227*, 59.
41. Bergkamp, M. A.; Watts, R. J.; Ford, P. C. *J. Am. Chem. Soc.* **1980**, *102*, 2627.
42. Weber, W.; van Eldik, R.; Kelm, H.; DiBenedetto, J.; Ducommun, Y.; Offen, H.; Ford, P. C. *Inorg. Chem.* **1983**, *22*, 623.
43. Wieland, S.; DiBenedetto, J.; van Eldik, R.; Ford, P. C. *Inorg. Chem.* **1986**, *25*, 4893.
44. DiBenedetto, J.; Ford, P. C. *Coord. Chem. Rev.* **1985**, *64*, 361.
45. Skibsted, L. H. *Coord. Chem. Rev.* **1985**, *64*, 343.
46. Billadeau, M. A.; Wood, K. V.; Morrison, H. *Inorg. Chem.* **1994**, *33*, 5780.
47. Menon, E. L.; Perera, R.; Navarro, M.; Kuhn, R. J.; Morrison, H. *Inorg. Chem.* **2004**, *43*, 5373.
48. Kelly, T. L.; Endicott, J. F. *J. Am. Chem. Soc.* **1972**, *94*, 1797; *Ibid. J. Phys. Chem.* **1972**, *76*, 1937.
49. Carlos, R. M.; Frink, M. E.; Tfouni, E.; Ford, P. C. *Inorg. Chim. Acta* **1992**, *193*, 159.
50. Zinato, E.; Lindholm, R. D.; Adamson, A. W. *J. Am. Chem. Soc.* **1969**, *91*, 1076.
51. Waltz, W. L.; Lillie, J.; Lee, S. H. *Inorg. Chem.* **1983**, *23*, 1768.
52. Friesen, D. A.; Lee, S. H.; Nashiem, R. E.; Mezyk, S.; Waltz, W. L. *Inorg. Chem.* **1995**, *34*, 4026.
53. Kane-Maguire, N. A. P.; Langford, C. H. *J. Chem. Soc., Chem. Commun.* **1971**, 895.
54. Wasgestian, H. F. *Z. Phys. Chem. N. F.* **1969**, *67*, 39.
55. Angermann, K.; van Eldik, R.; Kelm, H.; Wasgestian, F. *Inorg. Chim. Acta* **1981**, *49*, 247.
56. Ricciari, P.; Zinato, E. *Inorg. Chem.* **1990**, *29*, 5035.
57. Cimolino, M. C.; Shipley, N. J.; Linck, R. G. *Inorg. Chem.* **1980**, *19*, 3291.
58. Cimolino, M. C.; Linck, R. G. *Inorg. Chem.* **1981**, *20*, 3499.
59. Kirk, A. D.; Scandola, M. A. R. *J. Phys. Chem.* **1982**, *86*, 4141.
60. Vanquickenborne, L. G.; Cuelemans, A. *Coord. Chem. Rev.* **1983**, *48*, 157.
61. Irwin, G.; Kirk, A. D. *Coord. Chem. Rev.* **2001**, *211*, 25.
62. Friesen, D. A.; Lee, S. H.; Lillie, W. L.; Vincze, L. *Inorg. Chem.* **1991**, *30*, 1975.
63. Irwin, G.; Kirk, A. D.; Nera, J. *Inorg. Chem.* **2002**, *41*, 874.
64. Kirk, A. D. *Chem. Rev.* **1999**, *99*, 1607.

65. Kane-Maguire, N. A.; Langford, C. H. *J. Am. Chem. Soc.* **1972**, *94*, 2125.
66. Boletta, F.; Maestri, M.; Mogi, L.; Jamieson, M. A.; Serpone, N.; Henry, M. S.; Hoffman, M. Z. *Inorg. Chem.* **1983**, *22*, 2502.
67. Jamieson, M. A.; Serpone, N.; Hoffman, M. Z. *J. Am. Chem. Soc.* **1983**, *105*, 2933.
68. Lillie, J.; Waltz, W. L.; Lee, S. H.; Gregor, L. L. *Inorg. Chem.* **1986**, *25*, 4487.
69. Neshvad, G.; Hoffman, M. Z.; Bolte, M.; Sriram, R.; Serpone, N. *Inorg. Chem.* **1987**, *26*, 2984.
70. Zinato, E.; Riccieri, P.; Sheridan, P. S. *Inorg. Chem.* **1979**, *18*, 720.
71. Kutal, C.; Yang, D. B.; Ferraudi, G. *Inorg. Chem.* **1980**, *19*, 2907.
72. Juban, E. A.; McCusker, J. K. *J. Am. Chem. Soc.* **2005**, *127*, 6857.
73. Adamson, A. W. *J. Phys. Chem.* **1967**, *71*, 798.
74. Zinck, J. I. *J. Am. Chem. Soc.* **1972**, *94*, 8039; *Ibid.* **1974**, *96*, 4464.
75. Kirk, A. D.; Namasivayam, C.; Ward, T. *Inorg. Chem.* **1986**, *25*, 2225.
76. Mønsted, L.; Mønsted, O. *Coord. Chem. Rev.* **1989**, *94*, 109.
77. Mønsted, L.; Mønsted, O. *Acta Chem. Scand. A* **1986**, *40*, 637.
78. Kutal, C.; Adamson, A. W. *Inorg. Chem.* **1973**, *12*, 1990.
79. Kane-Maguire, N. A. P.; Wallace, K. C.; Miller, D. B. *Inorg. Chem.* **1985**, *24*, 597.
80. Angermann, K.; van Eldik, R.; Kelm, H.; Wasgestian, F. *Inorg. Chem.* **1981**, *20*, 955.
81. Tfouni, E. *Coord. Chem. Rev.* **2000**, *196*, 281.
82. Matsubara, T.; Ford, P. C. *Inorg. Chem.* **1978**, *17*, 1747.
83. Carlos, R. M.; Tfouni, E.; Neumann, M. G. *J. Photochem. Photobiol. A* **1997**, *103*, 121.
84. Carlos, R. M.; Neumann, M. G.; Tfouni, E. *Inorg. Chem.* **1996**, *35*, 2229.
85. Hintze, R. E.; Ford, P. C. *J. Am. Chem. Soc.* **1975**, *97*, 2664.
86. Mazzetto, S. E.; Tfouni, E.; Franco, D. W. *Inorg. Chem.* **1996**, *35*, 3509.
87. Malouf, G.; Ford, P. C. *J. Am. Chem. Soc.* **1974**, *96*, 601; *Ibid.* **1977**, *99*, 7213.
88. Chaisson, D. A.; Hintze, R. E.; Stuermer, D. H.; Petersen, J. D.; McDonald, D. P.; Ford, P. C. *J. Am. Chem. Soc.* **1972**, *94*, 6665; Durante, V. A.; Ford, P. C. *Inorg. Chem.* **1979**, *18*, 588.
89. Winkler, J. R.; Netzel, T. L.; Creutz, C.; Sutin, N. *J. Am. Chem. Soc.* **1987**, *109*, 2381.
90. Durham, B.; Caspar, J. V.; Nagle, J. K.; Meyer, T. J. *J. Am. Chem. Soc.* **1982**, *104*, 4803.
91. Durham, B.; Walsh, J. L.; Carter, C. L.; Meyer, T. J. *Inorg. Chem.* **1980**, *19*, 860.
92. Durham, B.; Wilson, S. R.; Hodgson, D. J.; Meyer, T. J. *J. Am. Chem. Soc.* **1980**, *102*, 600.
93. Tachiyashiki, S.; Ikezawa, H.; Mizumachi, K. *Inorg. Chem.* **1994**, *33*, 623.
94. Kalyanasundaram, K. *Coord. Chem. Rev.* **1982**, *46*, 159.
95. Meyer, T. J. *Pure Appl. Chem.* **1986**, *58*, 1193.

96. Juris, A.; Balzani, V.; Barigelletti, F.; Campagna, S.; Belser, P.; von Zelewsky, A. *Coord. Chem. Rev.* **1988**, *84*, 85.
97. Krausz, E.; Ferguson, J. *Prog. Inorg. Chem.* **1989**, *37*, 293.
98. Meyer, T. J. *Acc. Chem. Res.* **1989**, *22*, 163.
99. DeArmond, M. K.; Myrick, M. L. *Acc. Chem. Res.* **1989**, *22*, 364.
100. Balzani, V.; Juris, A. *Coord. Chem. Rev.* **2001**, *211*, 97.
101. Parris, T. P.; Brandt, W. W. *J. Am. Chem. Soc.* **1959**, *81*, 5001.
102. Kirch, M.; Lehn, J.-M.; Sauvage, J.-P. *Helv. Chim. Acta* **1979**, *62*, 1345; Lehn, J.-M.; Sauvage, J.-P. *Nouv. J. Chim.* **1981**, *5*, 291.
103. Chan, S.-F.; Chou, M.; Creutz, C.; Matsubara, T.; Sutin, N. *J. Am. Chem. Soc.* **1981**, *103*, 369.
104. Krishnan, C. K.; Sutin, N. *J. Am. Chem. Soc.* **1981**, *103*, 2140.
105. Barigelletti, F.; De Cola, L.; Balzani, V.; Belser, P.; von Zelewsky, A.; Vögtle, F.; Ebmeyer, F.; Grammenudi, S. *J. Am. Chem. Soc.* **1989**, *111*, 4662.
106. Sun, H.; Hoffman, M. Z. *J. Phys. Chem.* **1993**, *97*, 11956.
107. Beach, N. A.; Gray, H. B. *J. Am. Chem. Soc.* **1968**, *90*, 5713.
108. Pierloot, K.; Verhulst, J.; Verbeke, P.; Vanquickenborne, L. G. *Inorg. Chem.* **1989**, *28*, 3059; Kotzian, M.; Rösch, N.; Schröder, H.; Zerner, M. C. *J. Am. Chem. Soc.* **1989**, *111*, 7687.
109. Pierloot, K.; Hoet, P.; Vanquickenborne, L. G. *J. Chem. Soc., Dalton Trans.* **1991**, 2363.
110. Daniel, C.; Veillard, A. *Nouv. J. Chimie* **1986**, *10*, 83; Veillard, A. *Chem. Rev.* **1991**, *91*, 743; Matsubara, T.; Daniel, C.; Veillard, A. *Organometallics* **1994**, *13*, 4905.
111. Rosa, A.; Ricciardi, G.; Baerends, E. J.; Stufkens, D. J. *Inorg. Chem.* **1995**, *34*, 3425; *Ibid.* **1996**, *35*, 2886.
112. Pierloot, K.; Tsokos, E.; Vanquickenborne, L. G. *J. Phys. Chem.* **1996**, *100*, 16545.
113. Rosa, A.; Baerends, E. J.; van Gisbergen, S. J. A.; van Lenthe, E.; Groeneveld, J. A.; Snijders, J. G. *J. Am. Chem. Soc.* **1999**, *121*, 10356.
114. Hummel, P.; Oxgaard, J.; Goddard, W. A. III; Gray, H. B. *J. Coord. Chem.* **2005**, *58*, 41; *Ibid. Inorg. Chem.* **2005**, *44*, 2454.
115. Baerends, E. J.; Rosa, A. *Coord. Chem. Rev.* **1998**, *177*, 97.
116. Nasielski, J.; Colas, A. *Inorg. Chem.* **1978**, *17*, 237.
117. Joly, A. G.; Nelson, K. A. *Chem. Phys.* **1990**, *152*, 69.
118. Pollak, C.; Rosa, A.; Baerends, E. J. *J. Am. Chem. Soc.* **1997**, *119*, 7324.
119. Church, S. P.; Grevels, F.-H.; Hermann, H.; Schaffner, K. *Inorg. Chem.* **1984**, *23*, 3830; *Ibid.* **1985**, *24*, 418.
120. Morse, J. M.; Parker, G. H.; Burkey, T. J. *Organometallics* **1989**, *8*, 2471.
121. Xie, X.; Simon, J. D. *J. Am. Chem. Soc.* **1990**, *112*, 1130.
122. Langford, C. H.; Moralejo, C.; Sharma, D. K. *Inorg. Chim. Acta* **1987**, *126*, L11.
123. Simon, J. D.; Xie, X. *J. Phys. Chem.* **1987**, *91*, 5538; *Ibid.* **1989**, *93*, 291.
124. Lee, M.; Harris, C. B. *J. Am. Chem. Soc.* **1989**, *111*, 8963.

125. Wang, L.; Zhu, X.; Spears, K. G. *J. Am. Chem. Soc.* **1988**, *110*, 8695; *Ibid. J. Phys. Chem.* **1989**, *93*, 2.
126. Yu, S.-C.; Xu, X.; Lingle, R., Jr.; Hopkins, J. B. *J. Am. Chem. Soc.* **1990**, *112*, 3668.
127. Yang, G. K.; Peters, K. S.; Vaida, V. *Chem. Phys. Lett.* **1986**, *125*, 566.
128. Zhang, S.; Bajal, H. C.; Zang, V.; Dobson, G. R.; van Eldik, R. *Organometallics* **1992**, *11*, 3901, and references therein.
129. Farrell, G. J.; Burkey, T. J. *J. Photochem. Photobiol.* **2000**, *137*, 135.
130. Jiao, T.; Leu, G.-L.; Farrell, G. J.; Burkey, T. J. *J. Am. Chem. Soc.* **2001**, *123*, 4960; Gittermann, S.; Jiao, T.; Burkey, T. J. *Photochem. Photobiol.* **2003**, *2*, 817.
131. Shanoski, J. E.; Payne, C. K.; Kling, M. F.; Glascoe, E. A.; Harris, C. B. *Organometallics*, **2005**, *24*, 1852.
132. Poliakoff, M.; Weitz, E. *Acc. Chem. Res.* **1987**, *20*, 408.
133. Leadbetter, N. *Coord. Chem. Rev.* **1999**, *188*, 35.
134. Ryther, R. J.; Weitz, E. *J. Phys. Chem.* **1991**, *95*, 9841.
135. Trushin, S. A.; Fuss, W.; Kompa, K. L.; Schmid, W. E. *J. Phys. Chem A* **2000**, *104*, 1997.
136. Nyak, S. K.; Farrell, G. J.; Burkey, T. J. *Inorg. Chem.* **1994**, *33*, 2236.
137. Snee, P. T.; Payne, C. K.; Mebane, S. D.; Kotz, K. T.; Harris, C. B. *J. Am. Chem. Soc.* **2001**, *123*, 6909.
138. Bengali, A. A.; Bergman, R. G.; Moore, C. B. *J. Am. Chem. Soc.* **1995**, *117*, 3879.
139. Siegbahn, P. E. M.; Svenson, M. *J. Am. Chem. Soc.* **1994**, *116*, 10124.
140. Snee, P. T.; Payne, C. K.; Kotz, K. T.; Yang, H.; Harris, C. B. *J. Am. Chem. Soc.* **2001**, *123*, 2255.
141. Rubner, O.; Engel, V.; Hachey, M. R.; Daniel, C. *Chem. Phys. Lett.* **1999**, *302*, 489.
142. Goumans, T. P. M.; Ehlers, A. W.; van Hemert, M. C.; Rosa, A.; Baerends, E. J.; Lammertsma, K. *J. Am. Chem. Soc.* **2003**, *125*, 3558.
143. Wrighton, M. S. *Inorg. Chem.* **1974**, *13*, 905.
144. Dahlgren, R. M.; Zinck, J. I. *Inorg. Chem.* **1977**, *16*, 3154.
145. Darensbourg, D. J.; Murphy, M. A. *J. Am. Chem. Soc.* **1978**, *100*, 463.
146. Wrighton, M. S.; Abrahamson, H. B.; Morse, D. L. *J. Am. Chem. Soc.* **1976**, *98*, 4105.
147. Lees, A. J. *J. Am. Chem. Soc.* **1982**, *104*, 2038; Kolodziej, R. M.; Lees, A. J. *Organometallics* **1986**, *5*, 450.
148. Moralejo, C.; Langford, C. H.; Sharma, D. K. *Inorg. Chem.* **1989**, *28*, 2205.
149. Wieland, S.; van Eldik, R.; Crane, D. R.; Ford, P. C. *Inorg. Chem.* **1989**, *28*, 3663.
150. Abrahamson, H. B.; Wrighton, M. S. *Inorg. Chem.* **1978**, *12*, 3385.
151. Chun, S.; Getty, E.; Lees, A. J. *Inorg. Chem.* **1984**, *23*, 2155.
152. Panesar, R. S.; Dunwoody, N.; Lees, A. J. *Inorg. Chem.* **1998**, *37*, 1648.
153. Zális, S.; Farrell, I. R.; Vlcek, A., Jr. *J. Am. Chem. Soc.* **2003**, *125*, 4580.
154. Stufkens, D. J. *Coord. Chem. Rev.* **1990**, *104*, 39; Vlcek, A., Jr.; Vichova, J.; Hartl, F. *Coord. Chem. Rev.* **1994**, *132*, 167.

155. Vlcek, A., Jr. *Coord. Chem. Rev.* **2002**, *230*, 225.
156. Virrels, I. G.; George, M. W.; Turner, J. J.; Peters, J.; Vlcek, A., Jr. *Organometallics* **1996**, *15*, 4089; Farrell, I. R.; Matousek, P.; Vlcek, A., Jr. *J. Am. Chem. Soc.* **1999**, *121*, 5296.
157. Farrell, I. R.; Matousek, P.; Towrie, M.; Parker, A. W.; Grills, D. C.; George, M. W.; Vlcek, A., Jr. *Inorg. Chem.* **2002**, *41*, 4318.
158. Fu, W.-F.; van Eldik, R. *Inorg. Chem.* **1998**, *37*, 1044, and references therein.
159. Faltynek, R. A.; Wrighton, M. S. *J. Am. Chem. Soc.* **1978**, *100*, 2701.
160. Belt, S. T.; Ryba, D. W.; Ford, P. C. *Inorg. Chem.* **1990**, *29*, 3633.
161. Boese, W. T.; Ford, P. C. *J. Am. Chem. Soc.* **1995**, *117*, 8381; Massick, S. M.; Mertens, V.; Marhenke, J., Ford, P. C. *Inorg. Chem.* **2002**, *41*, 3553.
162. Bamford, C. H.; Burley, J. W.; Coldbeck, M. *J. Chem. Soc., Dalton Trans.* **1972**, 1846.
163. Berry, A.; Brown, T. L. *Inorg. Chem.* **1972**, *11*, 1165.
164. McHugh, T. M.; Rest, A. J.; Taylor, D. J. *J. Chem. Soc., Dalton Trans.* **1980**, 1803.
165. Wrighton, M. S.; Morse, D. L.; Gray, H. B.; Ottesen, D. K. *J. Am. Chem. Soc.* **1976**, *98*, 1111.
166. Wilms, M. P.; Baerends, E. J.; Rosa, A.; Stufkens, D. J. *Inorg. Chem.* **1997**, *36*, 1541.
167. Meyer, T. J.; Caspar, J. V. *Chem. Rev.* **1985**, *85*, 187.
168. Rosa, A.; Ricciardi, G.; Baerends, E. J.; Stufkens, D. J. *Inorg. Chem.* **1995**, *34*, 3425; *Ibid.* **1996**, *35*, 2886.
169. McCullen, S. B.; Brown, T. L. *Inorg. Chem.* **1981**, *20*, 3528.
170. Stiegman, A. E.; Tyler, D. R. *Inorg. Chem.* **1984**, *23*, 527.
171. Church, S. P.; Poliakoff, M.; Timmey, J. A.; Turner, J. J. *J. Am. Chem. Soc.* **1981**, *103*, 7515; Church, S. P.; Hermann, H.; Grevels, F.-W.; Schaffner, K. *J. J. Chem. Soc., Chem. Commun.* **1984**, 785.
172. Seder, T. A.; Church, S. P.; Weitz, E. *J. Am. Chem. Soc.* **1986**, *108*, 7518.
173. Hepp, A. F.; Wrighton, M. S. *J. Am. Chem. Soc.* **1983**, *105*, 5934.
174. Kobayashi, T.; Yasufuku, K.; Iwai, J.; Yesaka, H.; Noda, H.; Ohtani, H. *Coord. Chem. Rev.* **1985**, *64*, 1.
175. Sarakha, M.; Ferraudi, G. *Inorg. Chem.* **1999**, *38*, 4605.
176. Firth, S.; Klotzbücher, W. E.; Poliakoff, M.; Turner, J. J. *Inorg. Chem.* **1987**, *26*, 3370.
177. Brown, T. L.; Zhang, S. *Inorg. Chem.* **1995**, *34*, 1164.
178. Zhang, J. Z.; Harris, C. B. *J. Chem. Phys.* **1991**, *95*, 4024.
179. Yang, H.; Snee, P. T.; Kotz, K. T.; Payne, C. K.; Frei, H.; Harris, C. B. *J. Am. Chem. Soc.* **1999**, *121*, 9227.
180. Yang, H.; Snee, P. T.; Kotz, K. T.; Payne, C. K.; Harris, C. B. *J. Am. Chem. Soc.* **2001**, *123*, 4204.
181. Owrutsky, J. C.; Baronavski, A. P. *J. Chem. Phys.* **1996**, *105*, 9864.
182. Steinhurst, D. A.; Baronavski, A. P.; Owrutsky, J. V. *Chem. Phys. Lett.* **2002**, *361*, 513.
183. Bentsen, J. G.; Wrighton, M. S. *J. Am. Chem. Soc.* **1987**, *109*, 4518; *Ibid.* 4530.

184. DiBenedetto, J. A.; Ryba, D. W.; Ford, P. C. *Inorg. Chem.* **1989**, *28*, 3503.
185. Ford, P. C. *J. Organomet. Chem.* **1990**, *383*, 339.
186. Calhorda, M. J.; Costa, P. J.; Hartl, F.; Vergeer, F. W. C. *R. Chimie* **2005**, *8*, 1477.
187. Tro, N. J.; King, J. C.; Harris, C. B. *Inorg. Chim. Acta* **1995**, *229*, 469.
188. Grevels, F.-W.; Klotzbücher, W. E.; Schickel, J.; Schaffner, K. *J. Am. Chem. Soc.* **1994**, *116*, 6229.
189. Vergeer, F. W.; Hartl, F.; Matousek, P.; Stufkens, D. J.; Towrie, M. *Chem. Commun.* **2002**, 1220.
190. Desrosiers, M. F.; Wink, D. A.; Trautman, R.; Friedman, A. E.; Ford, P. C. *J. Am. Chem. Soc.* **1986**, *108*, 1917.
191. Poë, A. J.; Sekhar, C. V. *J. Am. Chem. Soc.* **1986**, *108*, 3673.
192. Yang, H.; Kotz, K. T.; Asplund, M. C.; Wilkens, M. J.; Harris, C. B. *Acc. Chem. Res.* **1999**, *32*, 551.
193. Wink, D. A.; Ford, P. C. *J. Am. Chem. Soc.* **1987**, *109*, 436.
194. Halpern, J.; Wong, S. W. *J. Chem. Soc., Chem. Commun.* **1973**, 629.
195. Tolman, C. A.; Meakin, P. Z.; Lindner, D. L.; Jesson, J. P. *J. Am. Chem. Soc.* **1974**, *96*, 2762.
196. Asbury, J. B.; Ghosh, H. N.; Yeston, J. S.; Bergman, R. G.; Lian, T. *Organometallics* **1998**, *17*, 3417; Asbury, J. B.; Hang, K.; Yeston, J. S.; Cordaro, J. G.; Bergman, R. G.; Lian, T. *J. Am. Chem. Soc.* **2000**, *122*, 12870; Asplund, M. C.; Snee, P. T.; Yeston, J. S.; Wilkens, M. J.; Payne, C. K.; Yang, H.; Kotz, K. T.; Frei, H.; Bergman, R. G.; Harris, C. B. *J. Am. Chem. Soc.* **2002**, *124*, 10605.
197. Zeigler, T.; Tschinke, V.; Fan, L.; Becke, A. D. *J. Am. Chem. Soc.* **1989**, *111*, 9177; Su, M. D.; Chu, S. Y. *J. Phys. Chem. A* **1997**, *101*, 6798.
198. Boyd, S. E.; Field, L. D.; Partridge, M. G. *J. Am. Chem. Soc.* **1994**, *116*, 9492.
199. Rosini, G. P.; Boese, W. T.; Goldman, A. S. *J. Am. Chem. Soc.* **1994**, *116*, 9498.
200. Moriyama, H.; Sakakura, T.; Yabe, A.; Tanaka, M. *Mol. Catal.* **1990**, *60*, L9.

8

Bioinorganic Systems

The field of bioinorganic chemistry has grown tremendously in the past 25 years. Much of the work is concerned with establishing the coordination site, ligand geometry and metal oxidation state in biologically active systems. The field also extends to the preparation and characterization of simpler model complexes that mimic the spectroscopic properties and perhaps some of the reactivity of the biological system. Much of this characterization work must precede meaningful mechanistic studies. Williams¹ has provided an interesting overview of metal ions in biology from an inorganic perspective. There are several early review series² and specialized journals³ devoted to the subject, and a recent issue of *Chemical Reviews*⁴ is devoted to the area. There also are several books covering general aspects of the subject.⁵

The field is so large and the systems are so individualistic that it is necessary, for the purposes of a text such as this, to choose a few sample systems as illustrative of the mechanistic achievements and problems.

8.1 BASIC TERMINOLOGY

Studies of bioinorganic systems inevitably use some terminology from biochemistry which may be unfamiliar to an inorganic chemist. The examples in this Chapter are all metalloenzymes which catalyze some process. Clearly they contain a metal, but there are other components of an enzyme, and terms used to describe these are summarized as follows:

Apoenzyme

An apoenzyme is a polypeptide whose composition, peptide sequence and structure depend on the biological source of the metalloenzyme. Typically, the molar mass of the polypeptide is in the range of $1.5\text{--}5 \times 10^5$ daltons. The polypeptide is folded into coils and sheets whose shape is determined by electrostatics and hydrogen bonding.

Coenzyme or Cofactor

These terms designate the same type of component, but one or the other is used more commonly for a particular system. This is a nonprotein component which binds to the apoenzyme to produce the active

catalyst. It is not covalently bonded to the apoenzyme and can be removed by relatively mild denaturation of the polypeptide. Common bioinorganic examples are coenzyme B₁₂, discussed in Section 8.3, and Zn(II) in carbonic anhydrase, discussed in Section 8.4.

Prosthetic Group

A prosthetic group is analogous to a coenzyme except that a prosthetic group is believed to be covalently bonded to the apoenzyme. Compared to a coenzyme, a prosthetic group is more difficult to either separate from or rejoin to the apoenzyme. The iron-porphyrin component of myoglobin, discussed in Section 8.5, is an example.

Holoenzyme

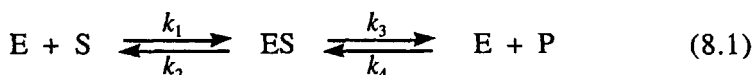
A holoenzyme is most often used to refer to a coenzyme-apoenzyme complex, while a system with a prosthetic group is simply referred to as an enzyme.

Isozyme

Isozymes are members of a family of enzymes which have differences in the amino-acid sequence and structure of the apoenzyme but carry out the same process, albeit with somewhat different activities.

8.2 TERMS AND METHODS OF ENZYME KINETICS

The simplest picture of an enzymic reaction is given by



where E is the enzyme, S is the substrate, ES is the enzyme-substrate complex and P is the product. These systems are often studied under steady-state conditions in which the enzyme (usually $<10^{-6}$ M) and substrate (usually $>10^{-4}$ M) are mixed in a buffered solution and the initial rate of loss of S or formation of P is determined. The formation of ES is assumed to be a rapid pre-equilibrium and only the initial rate is studied, so that P does not accumulate and the k_4 step is ignored. This system was analyzed in Section 2.3 and the rate, in biochemical terms, is given by the Michaelis-Menten equation:

$$\frac{d[P]}{dt} = v_i = \frac{k_3[E]_T[S]}{[S] + \frac{k_2}{k_1}} = \frac{k_3[E]_T[S]}{[S] + K_m} \quad (8.2)$$

where v_i is the initial rate, $[E]_T = [E] + [ES]$ is the total concentration of enzyme and K_m is the *Michaelis constant*. Since $K_m = [E][S]/[ES]$, it

would be called a dissociation constant by inorganic chemists, and smaller values of K_m indicate stronger enzyme to substrate binding. This rate law gives what inorganic kineticists call saturation behavior and the rate reaches a maximum when $[S] \gg K_m$, so that $V_{\max} = k_3[E]_T$. The ratio $V_{\max}/[E]_T = k_3$ is called the *turnover number*. Since the total enzyme concentration may not be precisely known, it is useful to substitute V_{\max} into Eq. (8.2) to obtain the more conventional form of the Michaelis–Menten equation. This equation can be rearranged by taking the reciprocal of both sides to obtain

$$\frac{1}{v_i} = \frac{K_m}{V_{\max} [S]} + \frac{1}{V_{\max}} \quad (8.3)$$

which predicts that a plot of v_i^{-1} versus $[S]^{-1}$, called a Lineweaver–Burke plot, will be linear with an intercept of $-K_m^{-1}$ when $v_i^{-1} = 0$.

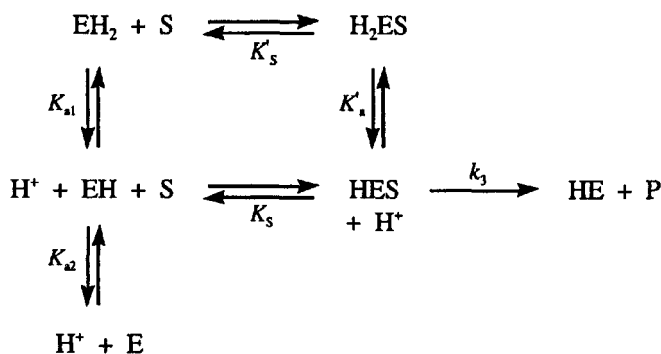
If a steady-state approximation for $[ES]$ is used (see Section 2.2) instead of the rapid-equilibrium assumption, then one obtains Eq. (8.4), known as the Briggs–Haldane equation:

$$\frac{d[P]}{dt} = v_i = \frac{k_3[E]_T[S]}{[S] + \frac{k_2 + k_3}{k_1}} \quad (8.4)$$

This equation has the same mathematical form as Eq. (8.2), except that $K_m = (k_2 + k_3)/k_1$. The K_m will be the same as defined previously only if $k_2 \gg k_3$; otherwise, K_m is always larger than k_2/k_1 .

The variation of the rate of the enzyme-catalyzed reaction with pH can provide information about the ionization of functional groups on the enzyme and substrate that are important for the reaction. Such a system might be described by Scheme 8.1, which has been simplified by omitting ionizations of the substrate in order to give a more tractable result.

Scheme 8.1



If it is assumed that the substrate binding and proton equilibria are rapidly maintained, then the initial rate can be put in the standard Michaelis–Menten form:

$$\frac{v_i}{[E]_T} = \frac{k_{\text{cat}}[S]}{[S] + K_m} \quad (8.5)$$

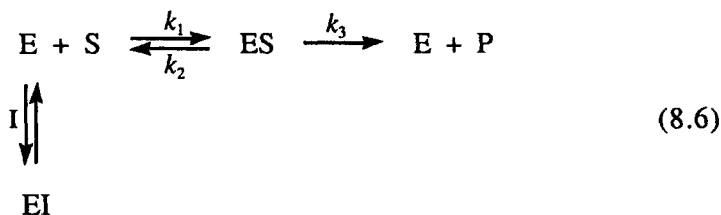
where

$$k_{\text{cat}} = \frac{k_3}{\left(1 + \frac{[H^+]}{K'_a}\right)} \quad \text{and} \quad K_m = K_s \frac{\left(1 + \frac{[H^+]}{K_{a1}} + \frac{K_{a2}}{[H^+]}\right)}{\left(1 + \frac{[H^+]}{K'_a}\right)}$$

If the conditions are such that $[S] \gg K_m$ (called swamping conditions), then the variation of k_{cat} with pH can be used to determine K'_a . On the other hand, if $K_m \gg [S]$, then k_{cat}/K_m is independent of K'_a and the values of K_{a1} and K_{a2} can be determined.

Many enzyme systems are affected by inhibitors. The structure of the inhibitors may be helpful in defining the size and binding requirements of the active site, but they may bind elsewhere and cause distortions of the peptide that affect the active site. The kinetic effect of inhibitors can be described by three possibilities, and mixtures of these possibilities may be observed.

A system with a *competitive inhibitor*, I, is described by the sequence



The inhibitor competes with the substrate for the enzyme. If a steady state is assumed for $[\text{ES}]$ and the inhibitor reaction with E is a rapidly maintained equilibrium with $K_1 = [\text{E}][\text{I}]/[\text{EI}]$, then

$$v_i = \frac{k_3[\text{E}]_T[\text{S}]}{[\text{S}] + \frac{(k_2 + k_3)}{k_1} \left(\frac{K_1 + [\text{I}]}{K_1}\right)} = \frac{k_3[\text{E}]_T[\text{S}]}{[\text{S}] + K_m \left(\frac{K_1 + [\text{I}]}{K_1}\right)} \quad (8.7)$$

An *uncompetitive inhibitor* is one that prevents the enzyme–substrate complex from following the main reaction pathway, as described by the sequence

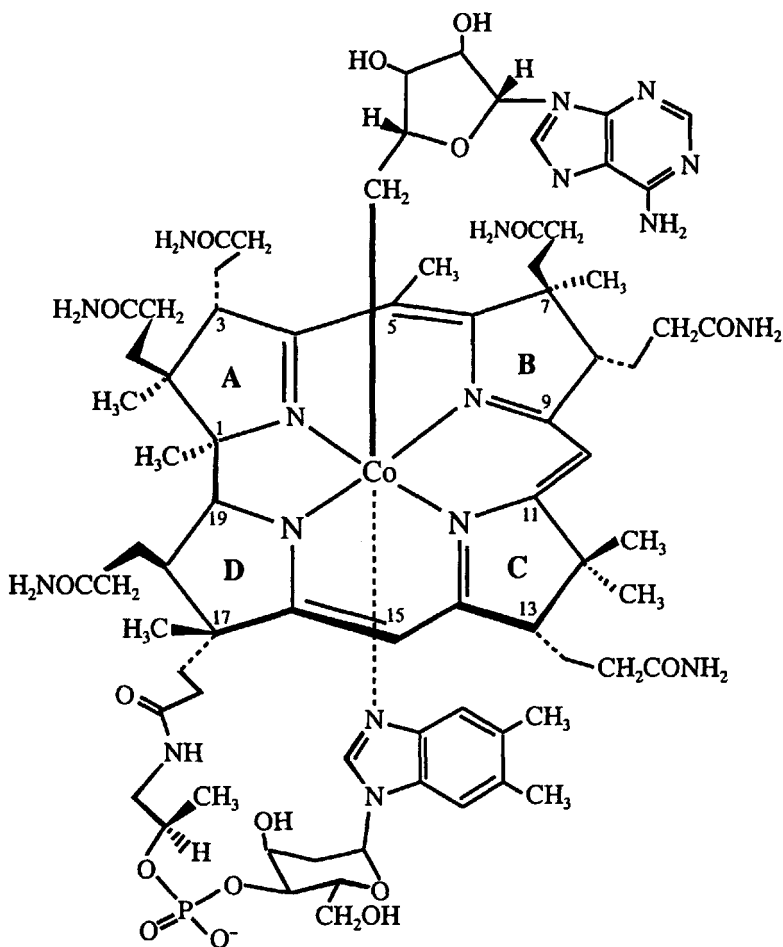


Figure 8.1. Coenzyme B₁₂.

B_{12r}, and further reduction gives the super-reduced Co(I) species, B_{12s}. These are all in a low-spin state and can be distinguished by their electronic spectra, and B_{12r} is EPR active. The benzimidazole function can be removed by hydrolysis at the phosphate-CH(CH₃) linkage to give a series of complexes known as cobinamides. These are often designated as Cbi⁺, so that one has AdoCbi⁺ and MeCbi⁺ when the organic group is 5'-deoxyadenosyl or methyl, respectively.

The structure⁸ and coordination of coenzyme B₁₂ are unusual in several aspects. It is an organometallic Co(III) complex with a cobalt-carbon bond to the 5'-carbon of 5'-deoxyadenosine. The four coordination positions in the plane are occupied by nitrogens from a corrin ring. The pyrrole rings are designated A through D, as shown in

Figure 8.1, where part of the conventional numbering system also is shown. The corrin ring differs from the more common porphyrin in that two of the pyrrole rings, A and D, are directly bonded, rather than having an intervening methylene group. The stereochemistry of the side chains makes the two faces of the corrin ring inequivalent. These faces are referred to as α and β , and the 5'-deoxyadenosyl is on the β face in Figure 8.1.

The corrin ring is somewhat flexible and puckered to varying degrees, as discussed in detail by Pett et al.⁹ Randaccio et al.¹⁰ have discussed the structures of a number of XCbl systems. If the 5'-deoxyadenosyl ligand is replaced by a methyl group, the Co—C bond length shortens from 2.02 to 1.98 Å and the Co—N(benzimidazole) also shortens from 2.21 to 2.16 Å. There have been reports of much longer Co—N bonds in holoenzymes, but it now seems that these have resulted from reduction of Co(III) to Co(II) in the crystal caused by the X-rays.¹¹ In a recent structure determination,¹² a bond length of 2.48 Å was attributed to this effect. The crystal structure of cob(II)alamin¹³ indicates that the Co(II) is five-coordinate, with the Co(II) 0.12 Å below the plane of the corrin nitrogens toward the benzimidazole. Because of this movement, the bond to the nitrogen of benzimidazole is shorter in the Co(II) derivative (2.13 Å) than in coenzyme B₁₂ (2.21 Å). An EXAFS study¹⁴ has suggested that the benzimidazole-N—Co(II) bond is even shorter (1.99 Å).

In coenzyme B₁₂, the benzimidazole may be displaced by solvent and protonated (pK_a 5–6) to give the base-off form. Until a few years ago, it was believed that the apoenzyme kept the benzimidazole coordinated to Co(III) in the holoenzyme in what is called the base-on form. Then in 1994, Ludwig and co-workers¹⁵ reported the structure of a holoenzyme in which the benzimidazole was replaced by the imidazole part of a histidine from the apoenzyme. The first indication of histidine binding came from the EPR hyperfine splitting observed in a Co(II) holoenzyme in which the apoenzyme contained ¹⁵N-enriched histidine. Since the first structure report, several analogous structures have been reported with other holoenzymes,^{16,17} and this has come to be known as the "base-off/hist-on" form. More recently, several holoenzymes have been found to be in the base-on form.^{12,18,19} It should be noted that many of these structures seem to be in the Co(II) form, due to X-ray damage, so that mechanistic arguments based on the structures should be viewed with caution. The history of X-ray crystallography of vitamin B₁₂ and its derivatives has been reviewed by Perry and Marques.²⁰

There are a number of simple model complexes of cobalt that mimic various aspects of the chemistry of coenzyme B₁₂. Examples, such as Co(DMGH)₂,²¹ Co(C₂(DO)(DOH))_{pn},²² and Co(salen),²³ are shown in Figure 8.2. These complexes have derivatives with cobalt in the (III), (II) and (I) oxidation states, analogous to coenzyme B₁₂. They form a

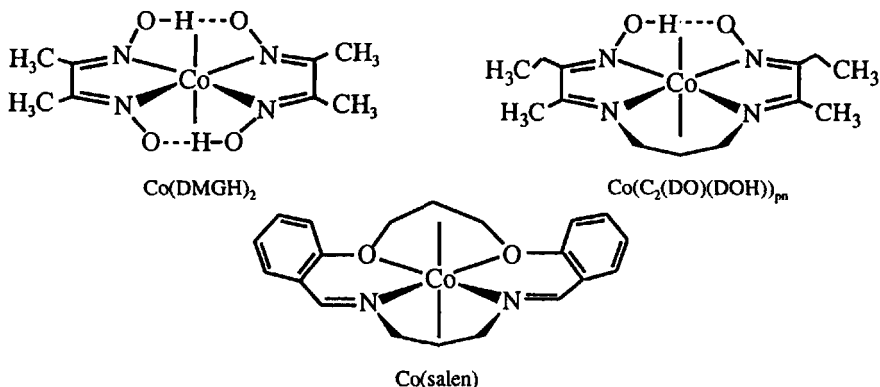


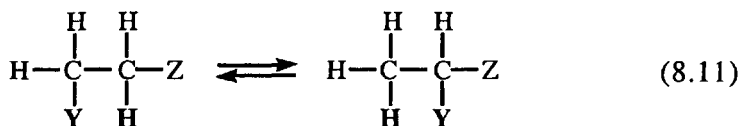
Figure 8.2. Some coenzyme B_{12} model systems.

wide range of organometallic Co(III) species in which both the organic group and the sixth ligand can be varied. The models have been particularly useful for the characterization of the electronic and EPR spectral features of coenzyme B_{12} and its derivatives.

There have been a number of studies of ligand substitution kinetics on several model systems, as well as AdoCbl and its derivatives, RCbl , where R is various alkyl and halo-substituted alkyl groups. Although these contain inert low-spin Co(III) , the reactions typically are on the stopped-flow time scale due to the trans-labilizing effect of the R group. The reaction of AdoCbl and RCbl derivatives with CN^- has been extensively studied by van Eldik and co-workers and the results have been reviewed recently.²⁴ The available evidence indicates that the reaction proceeds through a relatively labile equilibrium in which water replaces the benzimidazole to give a base-off form. Then CN^- displaces the aqua ligand by an I_d mechanism to give RCblCN . With AdoCbl , this process was too fast to measure and only the slower replacement of Ado by CN^- could be observed. The unusual substitution lability of these low-spin Co(III) systems and the dissociative character of the reactions can be attributed to the strong trans effect of the R group.

8.3.2 Functions of Adenosylcobalamin Dependent Systems

The most common transformation carried out by these systems is the interchange of H and some group $\text{Y} = \text{OH}, \text{NH}_2$ or CO_2H , as shown in the following reaction, where the transferring groups are in bold type.



In biochemical parlance, these systems are called mutases, or sometimes isomerases. When $Z = \text{OH}$ and $Y = \text{OH}$ or NH_2 , the product eliminates an aldehyde and either H_2O or NH_3 so that the process is irreversible. Such systems sometimes are referred to as eliminases, dehydrases or ammonia-lyases. Examples of these various types of systems are shown by the first five examples in Figure 8.3, where $(\text{CoA})-\text{S}$ represents coenzyme A. It should be noted that the amino mutases, such as ornithine amino mutase, also require pyridoxal phosphate as a cofactor.

The last example in Figure 8.3 shows the quite different function of ribonucleotide triphosphate reductase. A $\text{C}-\text{OH}$ group is reduced to $\text{C}-\text{H}$ while two thiols from the peptide are oxidized to a disulfide.

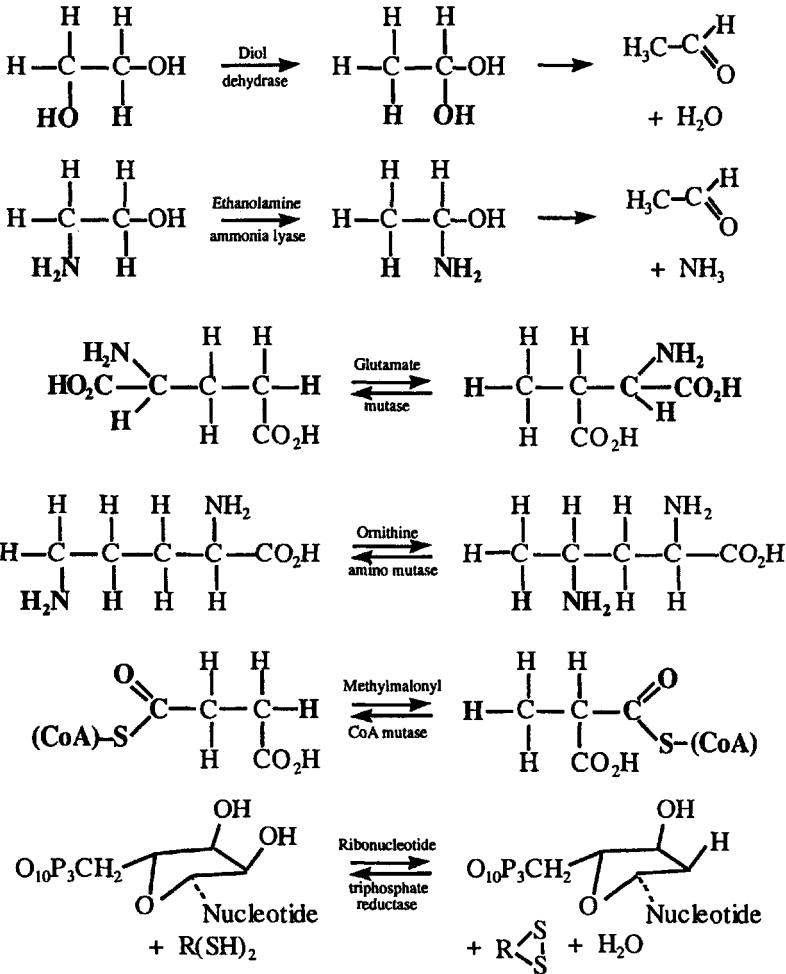
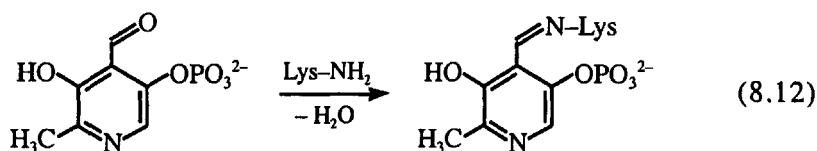


Figure 8.3. Some coenzyme B_{12} reactions.

To emphasize some of the common features, these systems have been separated into three classes: Class I are the mutases, such as glutamate mutase, in which a C—C bond is broken, and all exist in the base-off/hist-on form; Class II are the eliminases which involve C—O or C—N bond cleavage and ribonucleotide triphosphate reductase, and are in the base-on form; Class III are the amino mutases which interchange H and NH₂ and require pyridoxal phosphate as a cofactor. The structure of one member of this class has been determined and found to be in the base-off/hist-on form.²⁵ The pyridoxal phosphate is covalently bonded to a lysine, Lys—NH₂, of the peptide, as shown in the following reaction:



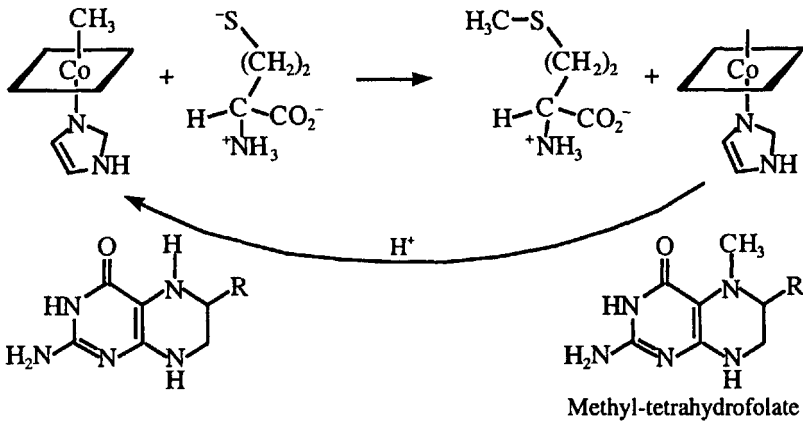
The pyridoxal phosphate is near the active site of the enzyme, and it is suspected that the amine substrate displaces the lysine, thereby releasing the pyridoxal phosphate from the protein. The substrate–pyridoxal phosphate species then undergoes the actual rearrangement induced by the coenzyme B₁₂.

8.3.3 Functions of Methylcobalamin as a Methyltransferase

Methylcobalamin is a cofactor for transfer of a methyl group in several processes, such as amino acid synthesis and CO₂ fixation. Methionine synthase is a well studied system which converts homocysteine to methionine. The structure of the holoenzyme was reported by Ludwig et al.¹⁵ with the surprising result that the 5,6-dimethylbenzimidazole loop serves to anchor the cofactor to the protein and the axial position on cobalt is occupied by an imidazole nitrogen from a histidine in the protein. This was the first report of the base-off/hist-on bonding motif, but, as noted above, it also has been observed for AdoCbl systems. A different motif is shown by a corrinoid/iron–sulfur protein involved in acetate biosynthesis. The benzimidazole has a 5-methoxy substituent, but has no ligand coordinated to the methylcobalamin in any of the oxidation states of the Co.²⁶ This totally base-off form is sometimes invoked as a precedent for analogous reactive intermediates in these methyl transfer systems. Further background on the methyltransferases is given in recent general reviews⁷ and more specifically by Mathews.²⁷ Banerjee and Ragsdale²⁸ describe more biochemical aspects.

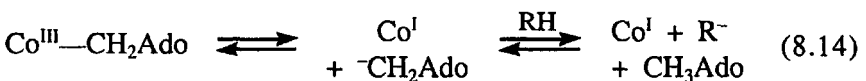
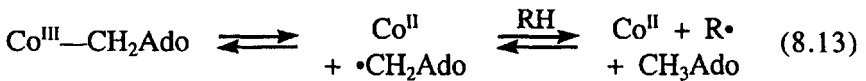
In methyltransferases, methylcobalamin transfers a methyl group to the substrate, and the methyl group must be replaced. In methionine synthase, methyl-tetrahydrofolate serves this purpose, as shown in the following Scheme:

Scheme 8.2



8.3.4 Reaction Pathways for Adenosylcobalamin Systems

A key step in the enzymic reactions of AdoCbl is the cleavage of the Co—C bond, followed by reaction of the organic fragment with the substrate RH. It is generally accepted that this may occur by a radical mechanism, as in reaction (8.13), or by an ionic mechanism, as in reaction (8.14).



The radical mechanism involves homolysis of the Co—C bond and the ionic mechanism involves heterolysis of this bond. Since coenzyme B₁₂ has both Co(II) and Co(I) derivatives, either of these mechanisms is chemically reasonable. The radical pathway provides low-spin Co(II) which is EPR active and therefore easily detectable. However, detection alone does not prove that this is the catalytic pathway. It should be noted that an important function of the protein in these systems is to constrain and protect reactive intermediates and inhibit unwanted side reactions. For example, the substrate radical or anion might combine with the cobalt to give an organocobalt complex as the product of the second step in both reactions (8.13) and (8.14).

Tritium and deuterium labeling experiments have established that a hydrogen of the substrate is transferred to the 5'-carbon of the deoxyadenosine during the reactions of diol dehydrase.²⁹ This supports

Co—C bond cleavage, but is consistent with either homolysis or heterolysis. Diol dehydrase gives inversion at the C-2 carbon when 1,2-propanediol is the substrate, and glutamate mutase also gives inversion. The reactions of methylmalonyl-CoA mutase and ribonucleotide triphosphate reductase proceed with retention. This stereospecificity indicates that the reacting carbon center of the substrate does not pass through a planar intermediate.

Several lines of evidence favor the radical mechanism and it is now widely accepted for AdoCbl. The presence of substrate radicals and Co(II) as B_{12r} has been established by EPR when substrate is added to the ethanolamine ammonia lyase,³⁰⁻³² diol dehydrase,³³ ribonucleotide reductase,^{34,35} glutamate mutase³⁶ and methylmalonyl-CoA mutase.^{37,38} Banerjee and co-workers³⁸ suggested a base-off/hist-on structure for methylmalonyl-CoA by using ^{15}N labeled protein and observing the superhyperfine coupling in the EPR of the Co(II) derivative. The crystal structure³⁹ of the Co(III) form also has shown a histidine nitrogen coordination. Stubbe and co-workers⁴⁰ have given a detailed analysis of the EPR spectra for ribonucleotide reductase and described the effect that can result from long-range coupling of Co(II) and the organic thyl radical derived from a peptide cysteine. In no case has the $\bullet CH_2Ado$ radical been detected, suggesting that it is very reactive and short-lived.

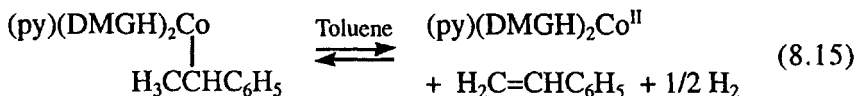
In stopped-flow studies with spectrophotometric observation, one can observe the disappearance of AdoCbl in the holoenzyme. When a solution of apoenzyme and AdoCbl is mixed with substrate, the rate is typically at the stopped-flow limit, with $k > 3 \times 10^2 \text{ s}^{-1}$ for ethanolamine ammonia lyase,⁴¹ ribonucleotide reductase,³⁵ glutamate mutase⁴² and methylmalonyl-CoA mutase.⁴³ In the latter two systems, it was found that the deuterated form of the substrate reacted about 30 times more slowly. These observations were taken to suggest that Co—C bond homolysis is not the rate-controlling step but is coupled to hydrogen atom abstraction from the substrate. This is consistent with the failure to observe the $\bullet CH_2Ado$ radical.

It should be noted that ethanolamine ammonia lyase does not show any change in the rate of disappearance of AdoCbl when perdeuterated ethanolamine is the substrate.⁴⁴ Taoka et al.⁴⁵ confirmed these results and found that methylmalonyl-CoA mutase does not show a magnetic field effect on the rate. The magnetic field is believed to affect the transition from the initially produced singlet state, in which the unpaired electrons on Co(II) and $\bullet CH_2Ado$ have opposite spins, and the triplet state, in which the electrons have the same spin. The latter state is believed to undergo much slower recombination to form reactants, but will react similar in subsequent hydrogen atom abstraction from the substrate. Possible explanations offered for the differences were that the mechanisms might be different or that stronger spin-spin coupling in the mutase may make the transition to the triplet more difficult.⁴⁵

For diol dehydrase, a radical mechanism has been implicated from the observation that glycolaldehyde deactivates the enzyme.⁴⁶ Theory⁴⁷ suggests that this results because the radical $\text{H}(\text{HO})\text{C}^{\bullet}\text{CH}(\text{=O})$ formed by H atom abstraction is so stable that it will not abstract an H atom from H_3CAdo to allow reformation of $\text{Co}-\text{CH}_2\text{Ado}$.

Considerable effort has been devoted to the radical pathway because it seems to have solid support for some systems, as noted above. There are two chemical problems with the radical mechanism: the first is the thermal stability of the $\text{Co}-\text{C}$ bond compared to the high reactivity of the enzymic reactions; the second is the very limited precedent for the type of radical rearrangements that are required. Various aspects and approaches to these problems are summarized in several reviews.⁴⁸⁻⁵⁰

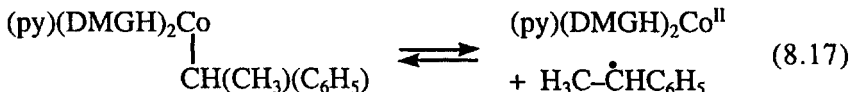
There have been a number of studies of the $\text{Co}-\text{C}$ homolysis rate and the bond energy in model compounds and, more recently, in coenzyme B_{12} itself. Halpern et al.⁵¹ studied the temperature dependence of the equilibrium constant for reaction (8.15) and determined that ΔH° is $22.1 \text{ kcal mol}^{-1}$.



They combined this value with the ΔH° of $-2.2 \text{ kcal mol}^{-1}$ for the reaction



to obtain a ΔH° of $19.9 \text{ kcal mol}^{-1}$ for the reaction



that defines the $\text{Co}-\text{C}$ bond energy of the reactant in reaction (8.15).

A kinetic method also was devised to determine the bond energy. The rate of reaction (8.15) in the absence of H_2 is first-order in the reactant, and it was assumed that the rate-controlling step is the forward reaction of (8.17), with $k_f = 7.8 \times 10^{-4} \text{ s}^{-1}$ (25°C), $\Delta H_f^\ddagger = 21.2 \text{ kcal mol}^{-1}$ and $\Delta S_f^\ddagger = -1.4 \text{ cal mol}^{-1} \text{ K}^{-1}$. Other work⁵² indicates that the reverse of reaction (8.17) will be near the diffusion-controlled limit and therefore should have a low value of $\Delta H_r^\ddagger \sim 2 \text{ kcal mol}^{-1}$. These results predict the ΔH° for reaction (8.17) as $21.2 - 2 = 19.2 \text{ kcal mol}^{-1}$, in agreement with the value from the equilibrium measurements. This provides the basis for the determinations of a number of $\text{Co}-\text{C}$ bond energies by measurement of the homolysis kinetics, especially if a radical scavenger

can be added to drag the reaction to completion.

Variations in the values of ΔH° for reactions such as (8.17) with different axial bases and alkyl groups may be due to other bond energy differences in reactants and products and not just to the Co—C bond energy changes. Measurements⁵³ of the Co—C stretching frequency ($\sim 500\text{ cm}^{-1}$) in $L(\text{DMGH})_2\text{Co—CH}_3$ systems have been interpreted to indicate that apparent bond energy variations with L are more reflective of changes in the stability of the Co(II) product than of the Co(III) reactant. Spiro and co-workers⁵⁴ came to a similar conclusion for AdoCbl , based on resonance Raman studies of the base-on and base-off forms. The applications and complications of the kinetic method for these bond energy determinations are the subject of several discussions.^{55,56} In the absence of trapping agents, the radical from thermolysis or photolysis may react with the planar N_4 ligand system to give a stable product, as observed⁵⁷ with the benzyl derivative of the $\text{Co}(\text{C}_2(\text{DO})(\text{DOH}))_{\text{pn}}$ model (see Figure 8.2), for example. Various equilibrium, competition and kinetic methods for determining Co—C bond energies have been described by Wayland and co-workers.⁵⁸

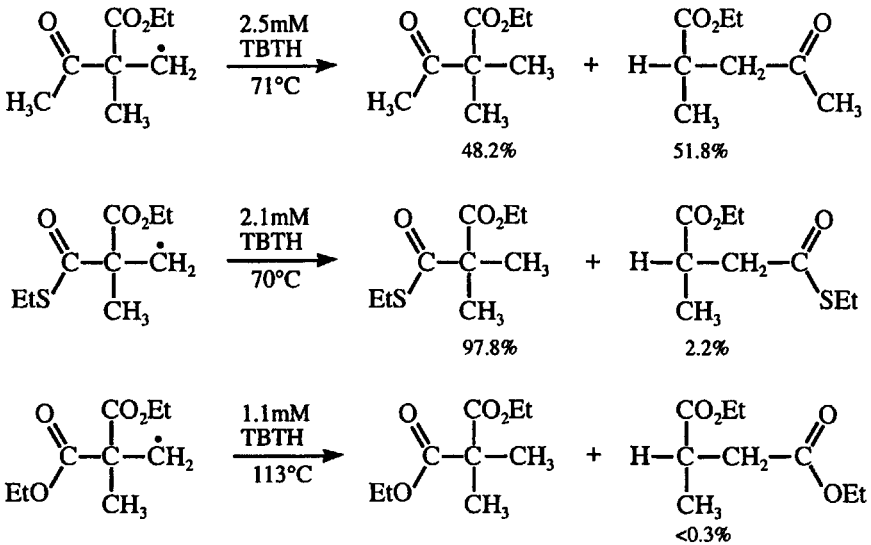
The temperature dependence of the thermal decomposition of coenzyme B_{12} was studied first in ethylene glycol by Finke and Hay,⁵⁹ then in water by Halpern et al.⁶⁰ and, most recently, again in water by Hay and Finke.⁶¹ The latter authors criticized the earlier aqueous study for its failure to separate all the reaction pathways and in particular the heterolysis reaction, which is significant for the base-off form of the coenzyme. Heterolysis is found to contribute between 77% (85°C) and 45% (110°C) of the product at the pH of 4.3 of the earlier study. From results between 85°C and 110°C at pH 7, after correction for heterolysis and the base-off form, Finke and Hay found the kinetic parameters for homolysis to be $\Delta H_h^\ddagger = 33 \pm 2\text{ kcal mol}^{-1}$ and $\Delta S_h^\ddagger = 11 \pm 3\text{ cal mol}^{-1}\text{ K}^{-1}$, which give $k_h = 1 \times 10^{-9}\text{ s}^{-1}$ (25°C). The Co—C bond dissociation energy is then estimated to be $\sim 30\text{ kcal mol}^{-1}$ after correction for the activation energy for the reverse reaction. Martin and Finke⁶² used a similar method to estimate a Co—C bond dissociation energy of 37 kcal mol^{-1} for methylcobalamin. The results of these studies have been discussed by Waddington and Finke.⁶³

The small value of $k_h \sim 10^{-9}\text{ s}^{-1}$ for the coenzyme is noteworthy in comparison to values of $\sim 2 \times 10^2\text{ s}^{-1}$ estimated for the rate-determining step in the diol dehydrase and ethanolamine ammonia lyase systems. This shows one of the problems in using the radical mechanism. This difficulty usually is explained by assuming that the enzyme somehow distorts the coenzyme so that the homolysis is about 15 kcal mol^{-1} more favorable in the holoenzyme. This distortion may destabilize the reactant and/or stabilize the transition state in order to hasten homolysis in the holoenzyme. For some time, it was thought that the axial base might promote these distortions, but Hay and Finke⁶⁴ found that

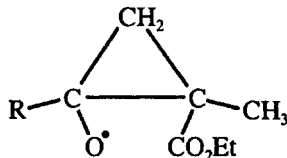
replacement of the 5,6-dimethylbenzimidazole in AdoCbl by water only decreased the homolysis rate by a factor of 10^2 . Brown et al.⁶⁵ found that an axial imidazole slightly decreases the rate of homolysis. Garr et al.⁶⁶ have given further examples of the effect of the axial base on the thermal homolysis rate and products of AdoCbl⁺. It is now generally accepted that the axial base has a minor effect on heterolysis of the Co—C bond.

The problem of precedents for the organic rearrangements required by the radical mechanism has been addressed and discussed by Wollowitz and Halpern.⁶⁷ They reacted $(n\text{-Bu})_3\text{SnH}$, TBTH, in C_6H_6 with various bromide derivatives to generate the radicals and obtained some rearranged product, as shown for typical conditions in Scheme 8.3.

Scheme 8.3

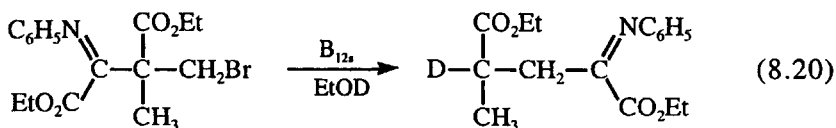
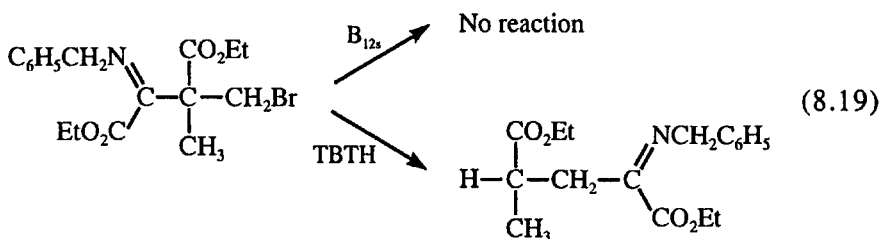
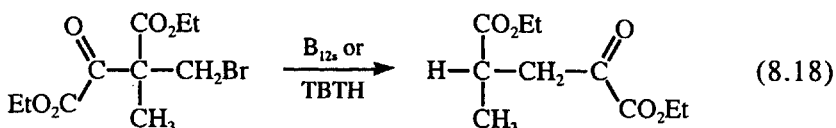


The product ratios were determined as a function of $(n\text{-Bu})_3\text{SnH}$ concentration, in order to determine the relative rates of rearrangement and $\text{H}\cdot$ abstraction from $(n\text{-Bu})_3\text{SnH}$ by the parent radical. It is clear from the product amounts in Scheme 8.3 that the migratory aptitudes of the groups are $\text{O}=\text{CCH}_3 > \text{O}=\text{CSEt} > \text{O}=\text{COEt}$. The rearrangement is envisaged as proceeding through the a cyclopropyloxy intermediate or transition state, such as the following:



Rearrangement with the O=CSEt group seems relevant to the methylmalonyl-CoA reductase system, but there are still no precedents for the OH and NH₂ migration. In addition, Wollowitz and Halpern observed rearrangements in the corresponding anions that would result from heterolysis such as that shown in reaction (8.14).

Choi and Dowd⁶⁸ have reported substantial amounts of rearranged products for the following reactions:



These reactions are expected to proceed by nucleophilic attack of B_{12s} on the halide to give the organo-B₁₂ derivative that would undergo homolysis to products. However, the reactivity patterns with B_{12s} and the formation of the deuterated product in EtOD are more easily rationalized if the reactions are proceeding through an anionic organic intermediate, which might be produced by reduction of the organic radical by excess B_{12s} or other reducing agents used to prepare the B_{12s}. Murakami et al.⁶⁹ have noted that anionic rearrangements are more facile than those involving radicals. They observed that addition of cyanide to organo-B₁₂ derivatives yields the organic anion under photolysis conditions because the NC—Co^{II} homolysis product reduces the radical to the anion, which then is rearranged.

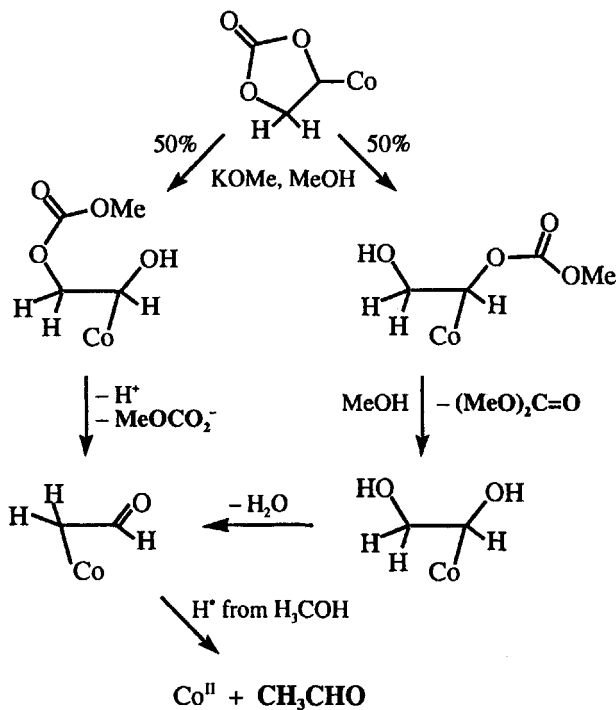
Dowd et al.⁷⁰ found that no rearranged product was obtained for the B₁₂ derivative Co—CH₂CH(CO₂H)CH(CO₂⁻)(NH₃⁺) under thermal or photochemical decomposition. However, Murakami et al.⁷¹ observed substantial rearrangement in the organic products with the same and several related species when photolysis is done while the complex is bound to an anionic surfactant (octopus azaparacyclophane). They proposed that the surfactant is acting in a way analogous to the enzyme

in the biological system. *These results indicate that studies on the coenzyme alone may not be appropriate models for the enzyme.*

To test for radical intermediates, Dowd and co-workers have used a pendant 4-pentenyl side chain trap⁷² and a cyclopropyl substituent on the substrate.⁷³ If radicals are formed, the trap should give cyclization through the 5-hexenyl radical and the cyclopropyl ring should open. Substantial amounts of unrearranged product were found in both cases and it was concluded that any radicals that might form must have very short lifetimes, in the microsecond range.

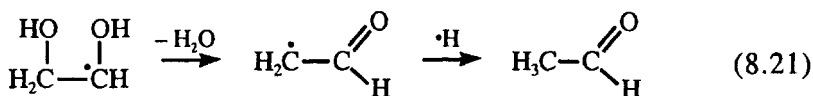
Finke et al.⁷⁴ found that, with the model $\text{Co}(\text{C}_2(\text{DO})(\text{DOH}))_{\text{pn}}$ in Figure 8.2, the $\text{Co}-\text{CH}_2\text{CH}(\text{=O})$ complex was too stable to be an intermediate in the diol to acetaldehyde reaction in their system. The stability of the aldehyde complex is consistent with earlier work of Silverman and Dolphin,⁷⁵ who found that the analogous B_{12} complex decomposed by an acid-catalyzed path with $k_{\text{obsd}} = 2.1 \times 10^3 [\text{H}^+] \text{ s}^{-1}$ at 25°C. Finke and co-workers appear to have found a synthetic scheme that proceeds at least in part through the organometallic diol complex, as shown in Scheme 8.4, where identified products are in bold.

Scheme 8.4



The intermediates in Scheme 8.4 apparently are too unstable to be isolated and have been identified through the nature and stoichiometry

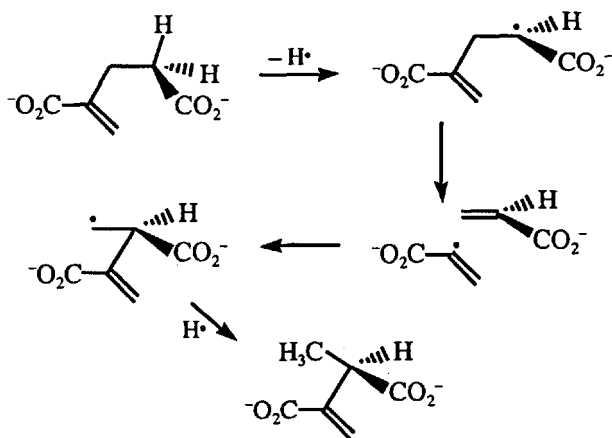
of their decomposition products ($\text{Co}^{\text{II}}:\text{CH}_3\text{CHO}:\text{CH}_3\text{OCO}_2^- = 2:2:1$) and radical trapping experiments. The decomposition is too fast to be consistent with the formation of the relatively stable aldehyde complex as an intermediate. The observations have been interpreted by assuming that the radical formed after homolysis escapes from the solvent cage and undergoes a normal radical decomposition, as shown in reaction (8.21), without the intervention of a cobalt complex.



However, this mode of decomposition does not involve the 1,1-diol intermediate shown to be required by the elegant stereochemical and labeling studies of Arigoni and co-workers⁷⁶ on diol dehydrase. Finke et al.⁴⁸ proposed a bound radical mechanism for the enzyme in which formation of the 1,1-diol assists in binding the radical to the enzyme by hydrogen bonding. The bound radical mechanism involves rehydration of the radical intermediate in reaction (8.21) to give the 1,1-diol.

For systems such as glutamate mutase, 2-methyleneglutarate mutase and methylmalonyl-CoA, Golding and co-workers⁷⁷ have proposed the rather different radical rearrangement mechanism illustrated in Scheme 8.5 for 2-methyleneglutarate mutase.

Scheme 8.5



A theoretical study⁷⁸ of the fully protonated species in the gas phase indicates that this fragmentation pathway has a higher activation energy than the more conventional radical cyclization and ring-opening mechanism. However, Chih and Marsh⁷⁹ identified acrylate as a product with glutamate mutase, and proposed that the glutamate radical fragments to acrylate and a glycinate radical.

The kinetics of radical interactions with coenzyme B₁₂ have been the subject of several flash photolysis studies.⁸⁰ The general picture is that photolysis yields a geminate radical pair, which may undergo recombination or escape the solvent cage and then recombine or undergo other reactions. Grissom and co-workers⁸¹ found that the geminate pair of Co(II) and the adenosyl radical recombine with a rate constant of $1 \times 10^9 \text{ s}^{-1}$ in water, but the value for the methyl radical is much smaller, with an upper limit of $\sim 2 \times 10^8 \text{ s}^{-1}$. The difference was attributed to the planar geometry of the methyl radical. Sension and co-workers have studied the photochemistry of a number of coenzyme B₁₂ derivatives.⁸² They recently reported⁸³ a recombination rate constant of $1 \times 10^9 \text{ s}^{-1}$ for AdoCbl bound to glutamate mutase. This value is just 30% smaller than that for AdoCbl in ethylene glycol⁸⁴ and suggests that the protein does not greatly lengthen the lifetime of the $\cdot\text{CH}_2\text{Ado}$ radical.

8.3.5 Reaction Pathways for Methylcobalamin Systems

The most intensively studied of these systems is methionine synthase and the available evidence indicates its reaction pathways have much in common with other enzymes in this group. Therefore the discussion here will concentrate on methionine synthase, whose essential chemistry is shown in Scheme 8.2. However, this Scheme does not show the mechanistic possibilities and complexities of the system.

These systems are complicated by the fact that they catalyze two methyl-transfer reactions, one from MeCbl to the substrate and the other from some reagent to cobalt to regenerate MeCbl. For methionine synthase, it is known that the reactions go with overall retention of the stereochemistry of the methyl group. This shows that both transfers occur either with retention or inversion. This observation, plus the absence of EPR signals indicative of Co(II) or organic radicals, suggest that these reactions do not proceed by homolysis of the Co—C bond.

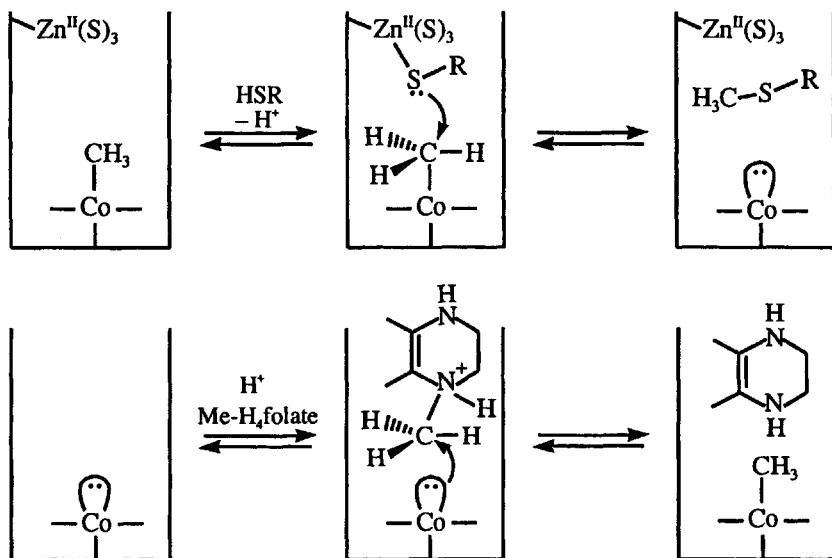
It is known from model systems that the Co(I) in B_{12s} is likely to be an excellent nucleophile since the models react readily with X—CH₃ to form X⁻ and Co^{III}—CH₃ complexes. These reactions proceed by nucleophilic attack of Co(I) to give inversion at the carbon center. This would seem to be a probable mode for transfer of the methyl group from methyl tetrahydrofolate, Me-H₄folate. An alternative is oxidative addition to give a *cis*-Co^{III}(X)(CH₃) complex, but this is not observed in the model systems and seems sterically improbable with the corrin ring system in B_{12s}. Transfer of the methyl group from MeCbl to homocysteine could then proceed by nucleophilic attack of the thiolate group on the coordinated CH₃ to yield methionine and B_{12s}.

There are two mechanistic problems with the above scenario. One is that primary amines, such as that in Me-H₄folate, are too electron rich to undergo nucleophilic attack by Co(I). The amine needs to be activated by protonation. Smith and Matthews⁸⁵ found that Me-H₄folate is

protonated with $pK_a \approx 5.1$, but the protonated form does not complex with the apoenzyme. However, a later study⁸⁶ found that the protonated form is present in the apoenzyme- B_{12s} -Me- H_4 folate tertiary complex. The second problem is that the thiol group of homocysteine has $pK_a \approx 10$ and will not be present in significant amounts as the thiolate at pH 7. However, it is known that methionine synthase requires Zn(II) for activity and that binding of homocysteine releases one proton from the enzyme. An EXAFS study⁸⁷ indicates that the Zn(II) in the holoenzyme has three thiolate ligands and gains a fourth thiolate when homocysteine is added.

The overall picture which emerges for the mechanism of methionine synthase is summarized in Scheme 8.6, where HSR is homocysteine and only the reacting part of Me- H_4 folate is shown.

Scheme 8.6



In the above Scheme, the axial base coordinated to Co is not specified, although it is known to be an imidazole from histidine in the Co(III) state. A study by Matthews and co-workers⁸⁸ indicates that switching from the base-on to base-off form does not have a major influence on the reaction with Me- H_4 folate.

8.4 A ZINC(II) ENZYME: CARBONIC ANHYDRASE

Zinc is the second most abundant metal, after iron, in humans. There are a number of enzyme systems in which Zn(II) is bound to a peptide (apoenzyme) and is at the active site in the enzyme. Examples of these

enzymes are carbonic anhydrase, carboxypeptidase A and B, alkaline phosphatase, alcohol dehydrogenase and RNA polymerase. In most cases, these systems bring about the making or breaking of covalent bonds in an organic substrate, but they also may use an oxidizing or reducing coenzyme to produce a redox change of the substrate. The area has been the subject of several reviews⁸⁹ and compilations.⁹⁰ The next section describes studies on carbonic anhydrases which are representative of the methods used to elucidate a considerable range of enzyme mechanisms. Since Zn(II) complexes are colorless, standard electronic spectroscopy is of little use in this area.

8.4.1 Mechanism of Carbonic Anhydrase Action

The carbonic anhydrase enzymes catalyze the hydration of CO₂, shown by the following reaction:

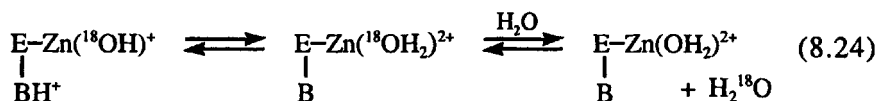
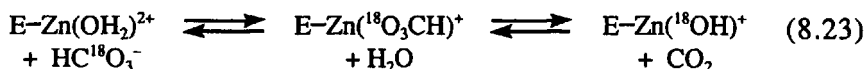


They also catalyze the hydrolysis of organic esters and the hydration of aldehydes, but with such low efficiency that this does not seem to be a significant biological function. Various aspects are discussed in the general references on Zn enzymes noted above and in several more specific reviews⁹¹ and compilations.⁹²

In mammals, there are three distinct isozymes of carbonic anhydrase, designated as CA I, CA II and CA III. Their maximum turnover numbers at 25°C are 2×10^5 , 1×10^6 and $3 \times 10^3 \text{ s}^{-1}$, respectively, and CA II is one of the most efficient of all known enzymes. Although they have different reactivities and amino acid sequences, the structures of CA I and II are known to be homologous. The active site is typically a conical cleft, about 15 Å wide at the base and 12 Å deep, with a Zn(II) atom at the apex coordinated to three imidazole nitrogens from histidines and probably a water molecule, giving a distorted tetrahedral coordination about the zinc. The zinc can be removed by chelating agents, and the resulting apoenzyme reacts with various metals, such as Co(II), Cu(II), Cd(II) and Ni(II). The Co(II) derivative has about 50% of the catalytic activity of the zinc enzyme, and various spectroscopic measurements on the cobalt analogue have been helpful in elucidating the coordination chemistry.

The lack of simple spectroscopic handles for the CA systems has made kinetic studies somewhat difficult. In one study, the ¹³C line-broadening method has been used.⁹³ The most common technique is the stopped-flow indicator method in which a solution of CO₂/HCO₃⁻ is mixed with a solution of buffer, enzyme and indicator.⁹⁴ The small pH change caused by formation or loss of H⁺ due to reaction (8.22) can be monitored spectrophotometrically. More recently, the method of choice has been to use ¹⁸O-enriched CO₂/HCO₃⁻ in combination with a mass

spectrometer, and to measure both the loss of ^{18}O in CO_2 and the gain of ^{18}O in the solvent H_2O . The relevant reactions for these two processes are given by reactions (8.23) and (8.24), respectively:



where E is the apoenzyme and BH^+ is an acidic group attached to E. Studies with various mutants have shown that this is a protonated imidazole from a histidine which is $\sim 7.5 \text{ \AA}$ from the $\text{Zn}(\text{II})$ in CA II. For the CO_2 exchange reaction, the kinetics are typically interpreted in terms of a standard Michaelis–Menten rate law

$$v_c = \frac{k_{\text{cat}}[\text{S}][\text{E}]}{K_m + [\text{S}]} \quad (8.25)$$

where [S] is the concentration of the substrate, variously defined as $[\text{CO}_2]$ or $[\text{CO}_2 + \text{HCO}_3^-]$. For typical conditions, $K_m \gg [\text{S}]$ so that the kinetics give values of k_{cat}/K_m . For the water exchange, the rate law is

$$v_w = \frac{k_B[\text{E}]}{\left(1 + \frac{K_B}{[\text{H}^+]}\right)\left(1 + \frac{[\text{H}^+]}{K_E}\right)} \quad (8.26)$$

where K_B and K_E are the acid dissociation constants of the BH^+ and ZnOH_2 components, respectively.

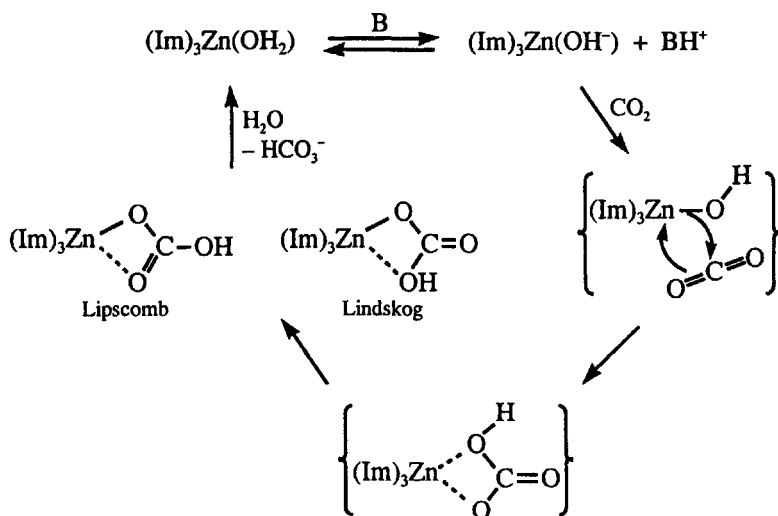
As an example of the kinetic parameters, the variation of v_w with pH for CA II has given $k_B = 0.8 \times 10^6 \text{ s}^{-1}$, $\text{p}K_B = 7.2$ and $\text{p}K_E = 6.8$ at 25°C .⁹⁵ The assignment of these ionizations to particular subunits has been an area of controversy. Simpler model systems would predict that $\text{p}K_E$ is due to an imidazole nitrogen of histidine and that $\text{p}K_B$ is due to ionization of $(\text{Im})_3\text{Zn}-\text{OH}_2^{2+}$. It was observed that replacement of the $\text{Zn}(\text{II})$ in CA I by $\text{Co}(\text{II})$ ⁹⁶ or $\text{Cd}(\text{II})$ ⁹⁷ gave $\text{p}K$ values of 6.5 and ~ 9.5 , respectively, and this metal ion sensitivity is consistent with the kinetic assignment. The latter also is consistent with results from other CA isozymes and mutants⁹⁸ and now is generally accepted. It also should be noted that HCO_3^- and 4-methylimidazole have been shown to be active proton donors in mutants lacking the histidine that is normally present.^{95,99}

The problem with the model $\text{Zn}(\text{II})$ complexes^{100,101} which led to the prediction that $\text{p}K_E > 8$ has now been resolved and attributed to the fact

that these models were five- or six-coordinate species, rather than four-coordinate as in CA. Kimura et al.¹⁰² reported the first model which seems to mimic some properties of CA. This trinitrogen chelate, [12]aneN₃, of Zn(II), has a pK_a of 7.3 and mimics the aldehyde hydration and ester hydrolysis activity of CA. The biomimetic chemistry of this system has been reviewed,¹⁰³ and the more recent review by Parkin lists more examples of (N)₃Zn(OH₂) systems with pK_a values between 6.2 and 7.5.

The catalytic cycle is shown in Scheme 8.7, with the first step being the formation of (Im)₃Zn(OH⁻) by proton transfer to some base B.

Scheme 8.7



The next step is the hydration of the CO₂, which is taken to be attack of the zinc-bound OH⁻ on CO₂, for which there are ample precedents¹⁰⁴ in the chemistry of carbonate complexes of inert metal ions. This may proceed through the intermediate at the bottom of Scheme 8.7 since Zn(II) can be five-coordinate. The latter rearranges to give zinc-bound bicarbonate, for which two possibilities have been suggested,^{105,106} as shown in Scheme 8.7. Both proposals suggest stabilization through hydrogen bonding to threonine-199, but there is little consensus on which one is correct.

The final step for CO₂ hydration is replacement of bicarbonate by water in the coordination sphere of the zinc. This will be a facile process because of the substitution lability of Zn(II). The (Im)₃Zn(OH₂) then is converted to (Im)₃Zn(OH⁻) by proton transfer to some base. The base most often suggested is the imidazole from histidine(64), which is connected by a water-bridged hydrogen-bonding network to the OH₂ of the Zn(OH₂).

Theoretical work by Merz and co-workers¹⁰⁷ essentially follows the pathway in Scheme 8.7 and finds that the bicarbonate is bound in the Lipscomb model, with the Lindskog structure being an intermediate or transition state on the pathway to the more stable form. More recent theory¹⁰⁸ has emphasized the importance of H₂O and other groups at the active site in facilitating the proton transfer reactions. It should be noted that the theoretical conclusions have changed and evolved with time¹⁰⁹ and must be viewed accordingly. Two X-ray structures with bicarbonate bound to CA I¹¹⁰ and a CA II¹¹¹ mutant have been used to support the Lindskog structure. In simple models, both bidentate and monodentate HCO₃⁻ has been observed in Cu(II) complexes,¹¹² while examples of bidentate Co(III)¹¹³ and monodentate Ni(II)¹¹⁴ coordination are known. These and other models have been reviewed recently.¹¹⁵

Model systems may provide some indication of the coordination state of Zn(II) in the bicarbonate complex. Kinetic studies by van Eldik and co-workers of the Zn(II) complexes of three-coordinate [12]aneN₃ and four-coordinate [12]aneN₄ indicate that the k_{cat} of the latter is ~5 times larger than that of the former.¹¹⁶ The four-coordinate macrocycle would be expected to disfavor chelation by bicarbonate, so that these results imply that chelation is not important. Other model studies indicate that bicarbonate chelation is detrimental to reactivity.¹¹⁷

Carbonic anhydrase is inhibited by a wide range of anions. It was found by Pocker and Diets¹¹⁸ that the inhibition is of the competitive type at pH 6.6 but is uncompetitive at pH 9.9. The uncompetitive inhibition implies that Zn(OH⁻) is not complexed by inhibitor, but Zn(II) in the enzyme-substrate complex can expand its coordination number to five with the ligands being three imidazoles, substrate and either water or inhibitor. Alkyl or aryl sulfonamides are strong inhibitors for CA and bind as the anion, RSO₂NH⁻ or ArSO₂NH⁻, respectively. Dugad et al.¹¹⁹ found that *p*-fluorobenzenesulfonamide forms a bis complex, indicating that the zinc is quite capable of becoming five-coordinate. Liang and Lipscomb¹²⁰ have modeled the formation and bonding of acetamide and sulfonamide inhibitors. Phenol is a competitive inhibitor of CA II for the hydration reaction. The structure of the phenol-CA II complex¹²¹ reveals that two phenols are bound: one in the active-site pocket but not coordinated to the zinc, and the other in a hydrophobic patch, about 15 Å from the zinc. The complex was prepared at pH 10 and the phenol may be present in the neutral or anionic form.

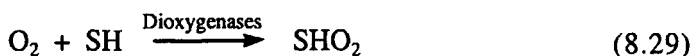
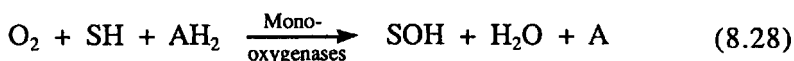
Bertini et al.¹²² showed that nitrate binds to the EH₂ and EH forms of the Co(II)-substituted enzyme. They attribute this to the EH form having tautomers E(histidine-H)Zn(OH⁻) and E(histidine)Zn(OH₂), with water replacement in the latter being the source of nitrate binding to EH. This maintains consistency with the standard interpretation that anions cannot compete with OH⁻ in the Zn(OH⁻) species.

8.5 ENZYMIC REACTIONS OF DIOXYGEN

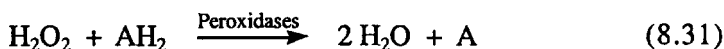
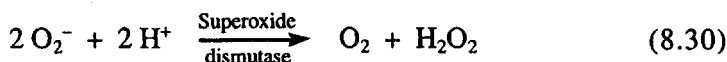
There are a number of metalloenzymes, EM, that bring about reactions of dioxygen and its derivatives, hydrogen peroxide and the superoxide ion. They may act as reversible oxygen carriers, such as hemoglobin and myoglobin in the following reaction:



The enzyme may introduce either one or two oxygens into the substrate, as shown in the following reactions:



Other enzymes protect the system¹²³ from reactions with superoxide or hydroxy radicals by catalyzing the disproportionation of O_2^- and the decomposition of hydrogen peroxide, as in reactions (8.30) and (8.31), respectively.



The oxidases and peroxidases have been succinctly reviewed.¹²⁴ The following sections discuss two examples of these metalloenzymes.

8.5.1 Oxygen Carriers: Myoglobin

Myoglobin, Mb, consists of one iron–protoporphyrin complex (heme prosthetic group) with an imidazole nitrogen of a histidine also coordinated to the iron and a single peptide chain. Since this system is simpler than hemoglobin, which has four heme units, much of the mechanistic work has been done on myoglobin. There are several sources of myoglobin that differ in the peptide composition, but the work discussed in this section is on the most common source, sperm whale myoglobin, unless otherwise indicated. The thermodynamic and structural effects of dioxygen binding to myoglobin and hemoglobin have been reviewed recently.¹²⁵

The structural features of the iron coordination in the Fe(II) deoxy form and the dioxygen complex have been determined by Takano¹²⁶ and Phillips,¹²⁷ respectively, and are shown in Figure 8.4. The Fe(II) in deoxymyoglobin is displaced by 0.42 Å out of the plane of the four porphyrin nitrogens toward the imidazole nitrogen. In the dioxygen

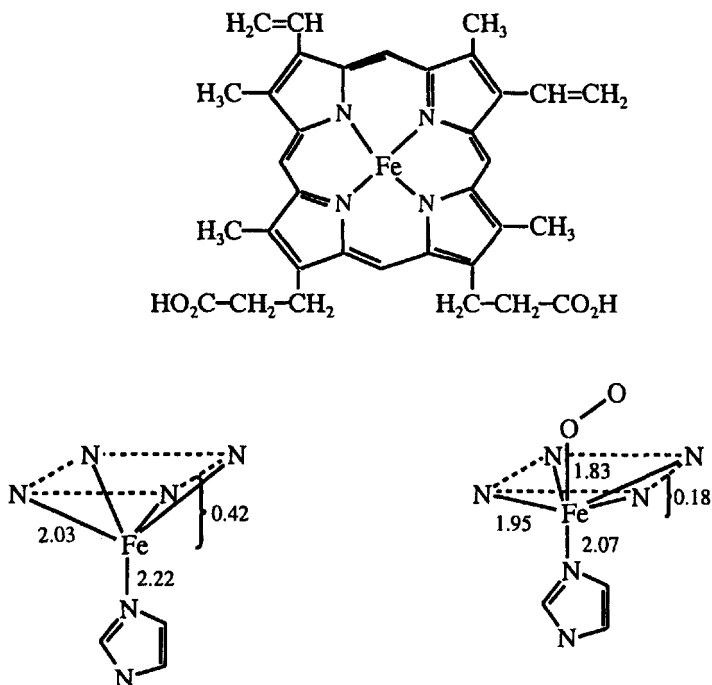
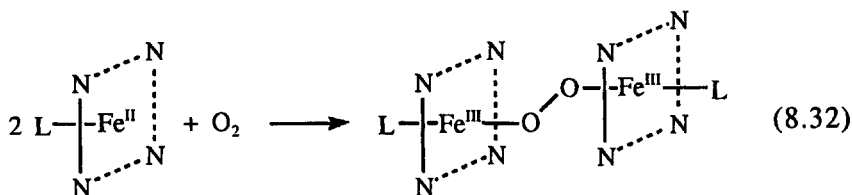


Figure 8.4. Iron protoporphyrin IX, the prosthetic group in myoglobin, and the coordination geometry of iron in myoglobin and oxymyoglobin.

complex, this displacement is reduced to 0.18 Å. The dioxygen is bonded in an end-on fashion with an Fe—O—O angle of 115°. The complexation of myoglobin by dioxygen appears to be a simple process accompanied by some structural changes. However, the Fe(II) is initially in the high-spin state and reacts with paramagnetic dioxygen to yield a diamagnetic product and a lot is happening electronically. The dioxygen complex can be pictured as Fe^{II}(O₂), Fe^{III}(O₂⁻) or Fe^{IV}(O₂²⁻). The Fe^{III}(O₂⁻) formalism is now favored as best describing the spectroscopic properties of the system. In oxymyoglobin, MbO₂, the terminal oxygen is hydrogen bonded to an imidazole of a distal histidine(64). Mutants in which this histidine is replaced by other amino acids show a lower discrimination between O₂ and CO.¹²⁸

Takano¹²⁹ reported the structure of metmyoglobin, which is the Fe(III) complex with axial water and imidazole ligands. The same structural features also are found in the model system described by Collman and co-workers,¹³⁰ where the displacement of iron depends on the steric requirements of the axial ligand, 0.086 Å with 2-methylimidazole and 0.03 Å with 1-methylimidazole.

In the development of model systems, a major problem has been that the simple Fe(II) porphyrins form diiron μ -peroxo complexes:



This can be overcome by introducing appropriate steric hindrance to dimer formation. This was achieved by Collman et al.¹³¹ by using the bulky *o*-pivalamidophenyl substituent on *meso*-tetraphenylporphyrin to prepare a model oxygen carrier. In the biological system, the peptide may serve a similar purpose.

The kinetic parameters for the binding and dissociation of some small molecules to myoglobin are given in Table 8.1. The relatively small rate constants for the isocyanides have been attributed to steric effects imposed by the peptide as these larger molecules move through the peptide cleft toward the iron. However, the kinetic difference between O₂ and CO is more remarkable. The ΔV^\ddagger for the binding of CO is quite negative, whereas that for O₂ is positive, and the CO rate constant is smaller, largely because of the less favorable ΔS^\ddagger . The binding of CO gives a low-spin Fe(II) complex with the iron 0.1 Å below the porphyrin

Table 8.1. Kinetic Parameters for Complexation of Myoglobin, Mb

Reaction	k (M ⁻¹ s ⁻¹)	ΔH^\ddagger (kJ mol ⁻¹)	ΔS^\ddagger (J mol ⁻¹ K ⁻¹)	ΔV^\ddagger (cm ³ mol ⁻¹)
Mb + O ₂ ^a	2.5 × 10 ⁷	26 ^b	-15	5.2
Mb + O ₂ ^c	1.3 × 10 ⁷	23.0	-30	7.8
Mb + O ₂ ^d	2.4 × 10 ⁷			4.6
Mb + CO ^e	3.8 × 10 ⁵	17.1	-81.1	-8.9
Mb + CO ^d	6.7 × 10 ⁵			-9.2
Mb + CO ^e	5.2 × 10 ⁵			-10.0
Mb + MeNC	1.2 × 10 ⁵ ^f			8.8
Mb + <i>n</i> -BuNC ^f	3.0 × 10 ⁴			

^a Projahn, H.-D.; Dreher, C.; van Eldik, R. *J. Am. Chem. Soc.* **1990**, *112*, 17; in 5 × 10⁻³ M Tris buffer, 0.1 M NaCl, pH 8.5, 25°C.

^b Calculated from the dissociation rate and the equilibrium constant parameters.

^c Hasinoff, B. B. *Biochemistry* **1974**, *13*, 3111; in 0.1 M phosphate buffer, pH 7.0, 25°C.

^d Adachi, S.; Morishima, I. *J. Biol. Chem.* **1989**, *264*, 18896; in 0.1 M Tris buffer, pH 7.8, 20°C.

^e Taube, D. J.; Projahn, H.-D.; van Eldik, R.; Magde, D.; Traylor, T. G. *J. Am. Chem. Soc.* **1990**, *112*, 6880; in 0.05 M bis-Tris buffer, 0.1 M NaCl, pH 7.0, 25°C.

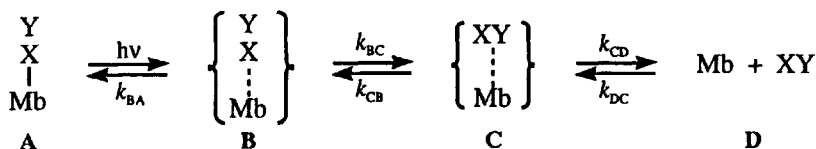
^f Rohlfs, R. J.; Olson, J. S.; Gibson, Q. H. *J. Biol. Chem.* **1988**, *263*, 1803; in 0.1 M phosphate buffer, pH 7, 20°C.

plane,¹³² compared to 0.18 Å in the O₂ complex. The O₂ is bent and hydrogen bonded to a distal histidine, whereas the CO is linear but still rather immobile according to ¹⁷O NMR studies.¹³³ The binding of O₂ is independent of pH, and CO binding is faster at lower pH.¹³⁴

For mutants in which histidine(64) is replaced, the dissociation rates of O₂ are increased by 50 to 1500 times, while the association rates for O₂ and CO increase 5 to 15 times. Resonance Raman studies¹³⁵ of Mb(CO) indicate that histidine(64) also affects the Fe—C stretching frequency, and the pH effect indicates that protonation of the histidine occurs with a pK_a of ~4.5. These studies also revealed that removal of histidine(64) increases the autooxidation rate of Mb(O₂), so that the histidine is serving some protective role as well.

It has been possible to obtain a detailed picture of the complexation process by using laser flash photolysis to dissociate the bound ligand and then watch its recombination or movement out of the active site pocket. The area was reviewed by Springer et al.¹³⁶ Martin et al.¹³⁷ studied CO dissociation from several hemes using a 250-fs laser pulse at 307 nm and concluded that the high-spin Fe(II) state is formed within 0.35 ps. Finsden et al.¹³⁸ used Raman spectrum spectroscopy to follow the Fe—N(imidazole) stretch after the dissociation of CO and O₂ from hemoglobin, and found that the deoxy form was produced within the 10-ns pulse length. This is rather surprising since low-spin to high-spin changes for octahedral Fe(II) complexes^{139,140} have rate constants of ~10⁷ s⁻¹. Traylor and co-workers¹⁴¹ observed the time evolution of difference spectra in the 400- to 500-nm range after flash photolysis and found one process on the nanosecond and another on the picosecond time scale. Olson et al.¹⁴² have done similar experiments but using essentially nanosecond time scale detection. Both groups interpret the results in terms of a four-state model, described in Scheme 8.8, where **B** is called a geminate pair and the leaving group has moved further away and probably rotated somewhat in **C**.

Scheme 8.8



The kinetic observations combined with quantum yields have been used to determine rate constants for the various steps. Some data from both studies are given in Table 8.2. The results show some variation, especially with regard to k_{BA} and k_{BC} . A transient time-dependent signal was not observed for CO dissociation, although CO dissociation has a high quantum yield.¹⁴³ This could be explained by a larger k_{BC} for CO,

Table 8.2. Rate Constants Following Flash Photolysis of Myoglobin–XY Complexes Analyzed According to Scheme 8.6

XY	k_{BA} (s ⁻¹)	k_{BC} (s ⁻¹)	k_{CB} (s ⁻¹)	k_{CD} (s ⁻¹)
O ₂ ^a	1.4×10 ¹⁰	1.5×10 ¹⁰	4.6×10 ⁶	8.8×10 ⁶
O ₂ ^b	4.9×10 ⁸	1.2×10 ⁸	8.5×10 ⁶	1.4×10 ⁷
MeNC ^a	1.3×10 ¹⁰	4.0×10 ¹⁰	7.8×10 ⁷	5.9×10 ⁶
MeNC ^b	2.4×10 ⁷	4.9×10 ⁶		
<i>n</i> -BuNC ^b	1.6×10 ⁷	1.4×10 ⁷	8.0×10 ⁵	1.2×10 ⁶
<i>t</i> -BuNC ^a	2.6×10 ¹⁰	8.0×10 ⁹	5.2×10 ⁶	3.6×10 ⁶

^a Jongeward, K. A.; Magde, D.; Taube, D. J.; Marsters, J. C.; Traylor, T. G.; Sharma, V. S. *J. Am. Chem. Soc.* **1988**, *110*, 380; in 0.1 M Tris buffer, 0.1 M NaCl, pH 7, unspecified temperature.

^b Rohlfs, R. J.; Olson, J. S.; Gibson, Q. H. *J. Biol. Chem.* **1988**, *263*, 1803; in 0.1 M phosphate buffer, pH 7, 20°C.

but the value for O₂ is at the diffusion limit according to the data of Traylor et al., so that k_{BA} must be smaller to explain the observations. Since k_{BA} and k_{CB} do not show any correlation with the steric bulk of XY, Traylor and co-workers suggested that the slower overall complexation of isocyanides is due to changes in k_{DC} caused by steric effects as the ligand enters the protein pocket. This is consistent with a crystal structure of the ethyl isocyanide complex.¹⁴⁴

Magde and co-workers¹⁴⁵ have measured k_{CD} and its Arrhenius activation energy for several complexes of horse heart myoglobin and for the O₂ sperm whale myoglobin system. For the latter, they report $k_{CD} = 7.7 \times 10^6$ s⁻¹ (25°C, 0.1 M Tris buffer, 0.1 M NaCl, pH 7.0) and $E_a = 7.4$ kcal mol⁻¹. The range of the E_a values for all the systems is 6 to 9 kcal mol⁻¹. The authors also suggested that a five-state model may be required, involving either two escape routes from the peptide pocket or a second bound site within the pocket.

The observed steady-state rate constant for Scheme 8.8 is given by

$$k_{\text{obsd}} = \frac{k_{BA}k_{CB}k_{DC}}{k_{BA}k_{CB} + k_{BA}k_{CD} + k_{BC}k_{CD}} \quad (8.33)$$

If k_{BA} is unusually small for CO, then the first two terms in the denominator of Eq. (8.33) are small relative to the third term, and the equation simplifies to $k_{\text{obsd}} = k_{BA}(k_{CB}/k_{BC})(k_{DC}/k_{CD}) = k_{BA}K_{CB}K_{DC}$. This corresponds to step B to A being rate-controlling and preceded by fast equilibria of D to C and C to B. For O₂, the first two terms in the denominator are somewhat larger than the third, so that the k_{BA} term approximately cancels in the numerator and denominator. Then, $k_{\text{obsd}} = k_{CB}(k_{DC}/k_{CD}) = k_{CB}K_{DC}$ because k_{CD} is larger than k_{CB} , and step C

to B is rate-controlling. This would explain the kinetic differences between O₂ and CO binding.

Adachi and Morishima¹⁴⁶ have determined the pressure dependence for some of the steps in Scheme 8.8 for several myoglobins. Their results, given in Table 8.3, show that changes in the peptide cause small changes in the rate constants but substantial differences in ΔV^* . The systems in Table 8.3 all have the histidine(64) residue that is involved in hydrogen bonding to the bound O₂, but they vary in the residues that may be affecting the size and structure of the pocket leading to the active site. Adachi and Morishima have given a more detailed rationalization of the effects of varying amino acid residues. Traylor and co-workers¹⁴⁷ subsequently reported activation volumes for k_{CD} with sperm whale myoglobin of 11.7, 12.6 and 9.1 cm⁻³ M⁻¹ for CO, O₂ and MeNC, respectively. For the overall formation reaction, the more negative values of $\Delta V_{obsd}^*(CO)$ can be attributed to contractions occurring at the B to A stage, which follows the rate-limiting step for O₂ binding and therefore does not influence $\Delta V_{obsd}^*(O_2)$. Projahn and van Eldik¹⁴⁸ have summarized the overall kinetic and equilibrium parameters for the CO and O₂ systems.

An interesting recent development is the use of X-ray methods to identify reaction intermediates. Schlichting et al.¹⁴⁹ flash-cooled crystals of an Mb(CO) mutant and determined the structure during continuous photolysis at 20K or 85K. They found that the intermediate for CO dissociation has the CO almost parallel to the heme plane, while the iron has moved out of the heme plane and histidine(64) has twisted away from the CO. An analogous study¹⁵⁰ of sperm whale Mb(CO) revealed

Table 8.3. Rate Constants (20°C) and Activation Volumes for the Reactions of O₂ and CO with Different Myoglobins^a

	Sperm Whale	Horse	Dog
k_{CA} (s ⁻¹) ^b	3.9×10 ⁶	3.5×10 ⁶	3.6×10 ⁶
ΔV_{CA}^* (cm ³ mol ⁻¹)	3.5	-8.4	-17.8
k_{CD} (s ⁻¹)	5.6×10 ⁶	6.2×10 ⁶	7.4×10 ⁶
ΔV_{CD}^* (cm ³ mol ⁻¹)	16.7	11.2	-2.1
k_{DC} (M ⁻¹ s ⁻¹)	5.7×10 ⁷	7.9×10 ⁷	9.1×10 ⁷
ΔV_{DC}^* (cm ³ mol ⁻¹)	10.4	12.3	8.6
k_{obsd} (M ⁻¹ s ⁻¹) ^c	2.4×10 ⁷	2.9×10 ⁷	3.0×10 ⁷
ΔV_{obsd}^* (cm ³ mol ⁻¹) ^c	4.6	3.8	0
$k_{obsd}(CO)$ (M ⁻¹ s ⁻¹) ^c	6.7×10 ⁶	6.8×10 ⁶	8.5×10 ⁶
$\Delta V_{obsd}^*(CO)$ (cm ³ mol ⁻¹) ^c	-9.2	-12.7	-18.8

^a In 0.1 M Tris buffer, pH 7.8; values are for O₂ unless otherwise indicated.

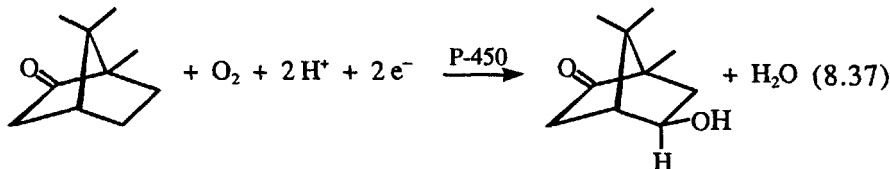
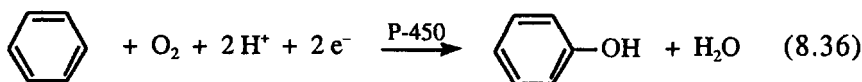
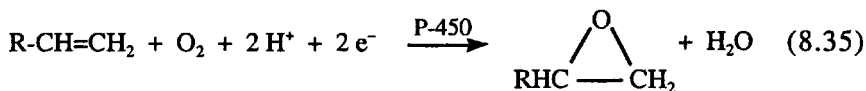
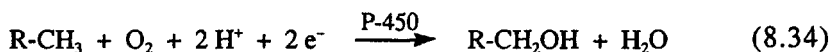
^b $k_{CA} = k_{BA}k_{CB}/(k_{BA} + k_{BC})$ from Scheme 8.8.

^c Values from steady-state conditions.

analogous features, except that no movement of the histidine was detected. More recently, time-resolved X-ray structures have revealed more details of the sites occupied by CO as it photodissociates from Mb(CO).¹⁵¹

8.5.2 Cytochrome P-450

There is a large and wide-ranging family of monooxygenase enzymes, called cytochrome P-450s, whose chemistry and biochemistry are the subjects of a recent book¹⁵² and reviews.^{153,154} Their name derives from their characteristic absorbance at 450 nm. They all contain a heme prosthetic group and catalyze the reactions of O₂ and a reducing agent to bring about transformations, such as those in reactions (8.34) to (8.37). These are only a few examples of the many reactions catalyzed by P-450 enzymes.



Reaction (8.37) represents the transformation of camphor to the exo-alcohol by P-450-CAM, one of the best characterized of these enzymes. The crystal structure of P-450-CAM and its camphor adduct have been determined by Poulos and co-workers.^{155,156} The coordination of the iron in the heme group in solution has been characterized by Dawson and co-workers^{157,158} using extended X-ray absorption fine structure, EXAFS. The resting-state prosthetic group is a six-coordinate low-spin Fe(III) heme with axial S and O ligands. The S is derived from cysteine, and Poulos has argued from bond lengths (Fe—S = 2.2 Å) that it is a thiolate cys-S⁻—Fe linkage. The O ligand is OH₂, based on electron spin-echo envelope modulation, ESEEM, results.¹⁵⁹ The Fe(III) is displaced 0.29 Å from the plane of the porphyrin nitrogens toward the S⁻. The active-site pocket contains five hydrogen-bonded waters and is lined with hydrophobic amino acids with no acid or base residues.

Since the operation of P-450 requires the enzyme plus three reagents (substrate, O_2 and reducing agent), it is possible to control the reaction conditions in order to identify intermediates and to establish the reaction pathway. If camphor is added to P-450-CAM under anaerobic conditions, then camphor displaces water and moves into the active site pocket. This complex contains five-coordinate high-spin Fe(III), with the iron atom 0.43 \AA out of the porphyrin plane and an essentially unchanged Fe—S bond length. The camphor is poised over the heme, with the C to be hydroxylated closest to the iron and the C=O of camphor hydrogen bonded to an -OH of a tyrosine. An EXAFS study by Dawson and co-workers of the low-spin Fe(II)-camphor- O_2 adduct, prepared at -40°C in water-ethylene glycol, indicated bond lengths very similar to those of a model thiolate-Fe^{II}(porphyrin)- O_2 complex.¹⁶⁰ More recently, Schlichting et al.¹⁶¹ determined tentative structures of several intermediates by low-temperature X-ray crystallography, and Davydov et al.¹⁶² showed by electron-nuclear double resonance, ENDOR, that the product is weakly bonded to the iron after the oxygen transfer. Current evidence is consistent with the sequence in Figure 8.5.

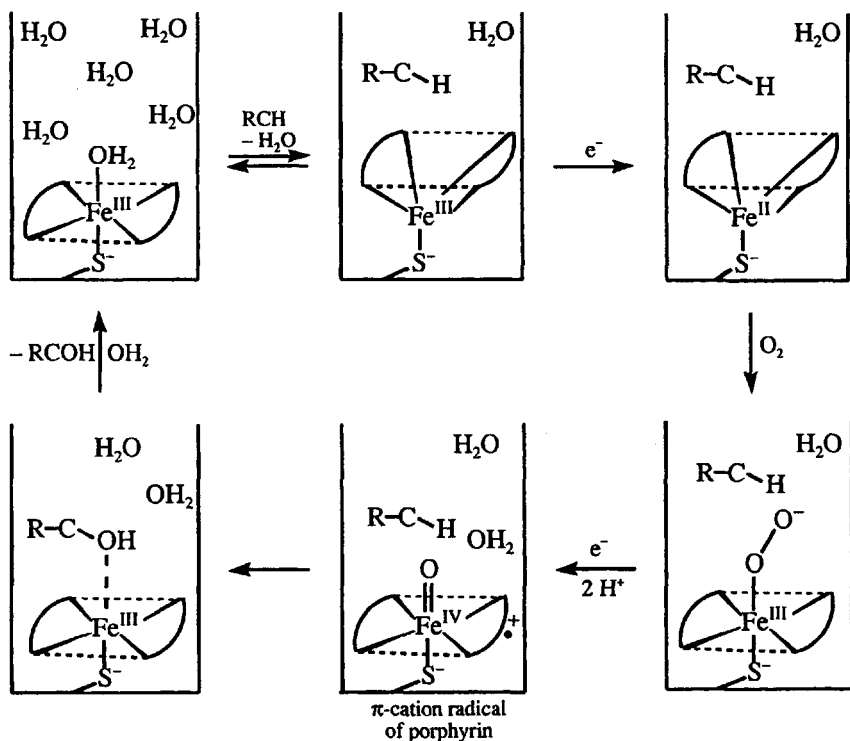
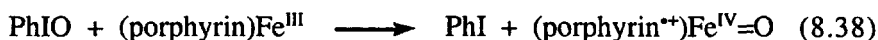


Figure 8.5. A catalytic cycle for hydroxylation by cytochrome P-450-CAM. The first four intermediates have been identified; the π -cation radical is speculative.

When the substrate (R-C-H) enters the active site pocket, a high-spin Fe(III) complex forms due to small changes in the conformation of the peptide or loss of the water ligand. This form is 0.12 V¹⁶⁵ more easily reducible than the resting enzyme and therefore favors the reduction to high-spin Fe(II), which then forms the O₂ complex similar to myoglobin. Precedent for the π -cation radical Fe=O species comes from the more stable and well-characterized intermediate, HRPI,^{164,165} of horseradish peroxidase, and it is sometimes called compound I in P-450 studies. The X-ray and ENDOR results, noted above, provide strong support for this species in P-450-CAM.

It has been shown that the Fe(III) resting state of P-450 reacts with iodobenzene, PhIO, to produce a species that hydroxylates alkanes. This can be understood if oxygen transfer from PhIO proceeds to give the π -cation radical Fe=O species, as shown in reaction (8.38).



This synthetic version causes the same hydroxylations as the natural system. However, the PhIO product gives ¹⁸O exchange with ¹⁸OH₂, while the natural system shows no exchange.¹⁶⁶ Groves et al.¹⁶⁷ found that the reaction of P-450-LM2 with its reductase gives exchange of the trans 1-H of propylene with solvent D₂O, but the enzyme with PhIO gave no exchange. Bhakta et al.¹⁶⁸ have reported substantial differences in products with PhIO and O₂ as oxidants in several P-450 systems. The PhIO reactions may be different because it complexes with the iron to form the active oxidant, rather than forming the Fe=O radical cation.

The use of *m*-chloroperbenzoic acid, mCPBA, as an oxidant has had a long and checkered history. Studies in the 1980s¹⁶⁹ indicated that the reaction of P-450-CAM with mCPBA gives two unidentified transient species. In 1994, Egawa et al.¹⁷⁰ reported that four successive species are formed when the reaction is done at pH 7.4 and 4°C. They found that the first species has absorption maxima at 367 and 694 nm and proposed that it is the Fe=O radical cation because of its spectral similarity to the known species in chloroperoxidase. In 2002, Sligar and co-workers¹⁷¹ reported that a thermostable variant of P-450 gives an initial transient with maxima at 370, 610 and 690 nm and made the same assignment as Egawa et al. However, in 2004, the Sligar group¹⁷² used freeze-quench EPR with P-450-CAM and found only tyrosine based radicals. They concluded that the Fe=O radical cation oxidizes the peptide-bound tyrosine within 8 ms. During the same period, work by Prasad and Mitra¹⁷³ on both substrate-bound and -free P-450-CAM was interpreted to show formation of the Fe=O radical cation on a time scale of ~0.5 s. Rate constants for its formation from mCPBA and H₂O₂ were reported. Most recently, Dawson and co-workers¹⁷⁴ studied the substrate-free system by stopped-flow spectrophotometry and suggest

that three intermediates are formed: an acylperoxy complex, followed by the Fe=O radical cation and then tyrosyl radical species. In summary, it appears that oxidation of the Fe(III) state of P-450-CAM by mCPBA does produce a transient Fe=O radical cation, but the species is short-lived and transforms to other products.

Further mechanistic details of the steps outlined in Figure 8.5 can be inferred from the numerous theoretical studies that have been reviewed recently.¹⁷⁵ The thiolate ligand appears to have two functions: it stabilizes the Fe^{III}—O₂H species against reduction to Fe(II) and it increases the basicity of the distal O-atom to favor formation of Fe^{III}—OOH₂ which then undergoes heterolysis to form Fe^{IV}=O and H₂O.¹⁷⁶ There are some disagreements about the theoretical details of the oxygen insertion step. However, the general consensus favors the mechanism outlined in Figure 8.6, commonly referred to as the rebound mechanism. The substrate approaches and transfers an H atom to the Fe=O unit. Then, the substrate radical moves away, reorients and finally rebounds to make the C—O bond. Then, the reaction with the alkyl radical may proceed as shown. The orbital energies depicted below each structure are a qualitative representation of the HOMOs in the systems. The three orbitals on iron are roughly equivalent to the *t*_{2g} set in a tetragonally distorted ligand field, with the two higher energy orbitals being the π* orbitals of the Fe=O bond. The H atom transfer moves an electron into one of these orbitals to make the O—H bond. One area of theoretical disagreement is whether the product of this transfer is that shown or (Por)Fe^{IV}(OH), in which an electron effectively has moved from the Fe to Por⁺. Another area of disagreement is the spin state of the first two species. The state shown is a quartet, but flipping the spin of the electron on the porphyrin produces a doublet state, and the two states may be similar in energy.

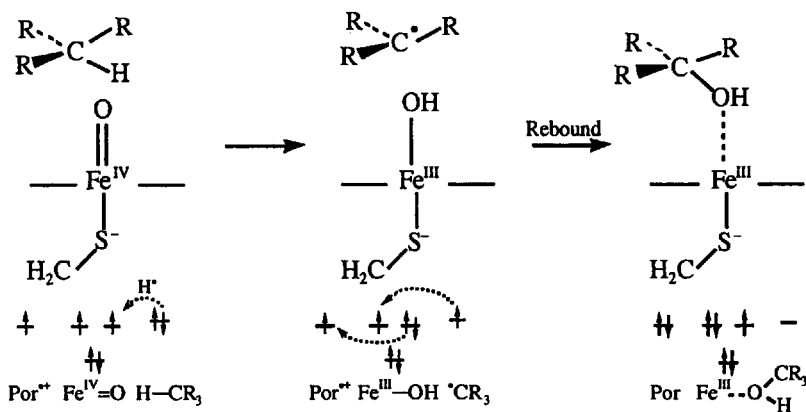
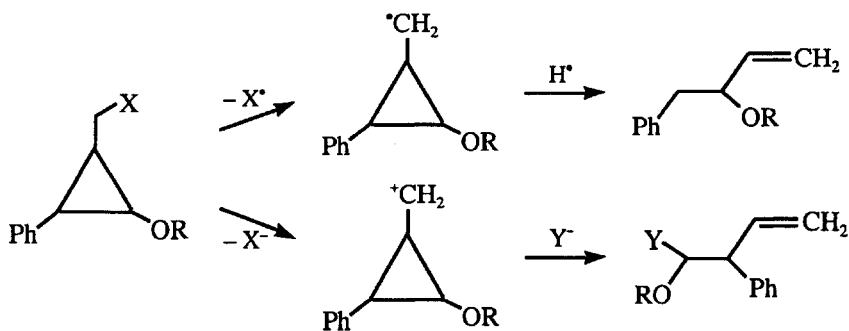


Figure 8.6. Possible steps for hydroxylation of an alkane by P-450.

The rebound step can be pictured as addition of the carbon-based radical to the half-occupied π^* orbital to make the O—C bond while an electron is transferred from iron to the porphyrin to return it to its singlet ground state. As described in the following paragraph, a critical feature of the rebound step is its timing, referred to as the rebound rate. If this rate is slow enough, then the radical may have time to undergo various types of rearrangements that will be reflected in the structure(s) of the product(s). One theoretical treatment¹⁷⁷ of the P-450-CAM system indicates that the doublet state can undergo an almost barrierless rebound, while the barrier for the quartet state is quite significant.

The intermediacy of an organic free radical in these reactions was cast into doubt through observations on radical clock reactions. Evidence for a radical came from the observation of Ortiz de Montellano and Stearns¹⁷⁸ who found that hydroxylation of bicyclo[2.1.0]pentane gave bicyclo[2.1.0]pentan-2-ol and rearranged 3-cyclopentenol, the latter being indicative of a radical intermediate. Atkinson and Ingold¹⁷⁹ used a series of five calibrated radical clocks to estimate the radical lifetime, and thereby the value of the rate constant of the oxygen transfer or rebound step. They found rather variable rate constants in the range of 1.4×10^{10} to 7×10^{12} s⁻¹. A similar study by Newcomb and co-workers¹⁸⁰ indicated a seemingly impossibly high value of 1.4×10^{13} s⁻¹. These results are all with different substrates and could indicate substrate specificity, but it has been argued that this is unlikely because the P-450 systems are so unselective with regard to substrate. Newcomb also developed the clock substrate in Scheme 8.9 that gives different rearrangement products shown from radical and cationic routes.

Scheme 8.9



With P-450 from rat liver,¹⁸¹ this substrate (X = H) gave predominantly unrearranged product with hydroxylation at the methyl group and similar amounts of Ph-hydroxylation products. The remaining product (5–15%) is derived from the cationic pathway. It was suggested that the latter may be the source of rearranged product in previous radical clock studies. More recently, using different probes and enzyme sources,

Newcomb et al.¹⁸² suggested that reaction of the Fe—OOH species as an OH⁺ donor might be the source of the cationic rearrangement products. Most recently, Ortiz de Montellano¹⁸³ and co-workers, with still different probes and enzymes, concluded that carbon hydroxylation proceeds exclusively by the radical pathway shown in Figures 8.5 and 8.6, and that the minor cationic pathway may be due to electron transfer from a radical intermediate to some reducible component of the peptide. It also was concluded, based on the similar products in D₂O and H₂O, that Fe^{III}O₂H is not the hydroxylating agent.

The epoxidation of olefins, given in reaction (8.35), presents some new mechanistic problems. Ortiz de Montellano and co-workers¹⁸⁴ have shown that the enzyme gives both epoxidation and alkylation of a pyrrole nitrogen, the latter occurring with alkenes that have a terminal =CH₂. Alkenes and alkynes alkylate a different pyrrole nitrogen. The epoxidation seems to be stereospecific, since retention is found for the reaction of *trans*-1-[1-²H]octene. The simplest explanation for these results would seem to be that the peptide controls the orientation of the substrate over the iron and the reactions proceed as shown in Figure 8.7. It should be noted that aldehydes also may be produced,¹⁸⁵ presumably through H-atom migration to give the more stable radical centered on the carbon bonded to the oxygen.

A concerted mechanism, such as that in Figure 8.7, would not predict the deuterium exchange results of Groves et al.,¹⁶⁷ and models involving organo-iron species have been invoked^{186,187} based on known model chemistry. The deuterium exchange originally was explained by a set of reversible H⁺-transfer reactions proceeding from a metallocycle, such as that shown in Scheme 8.10.

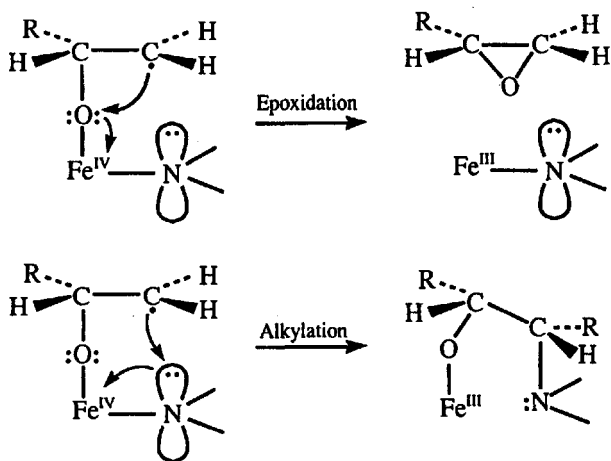
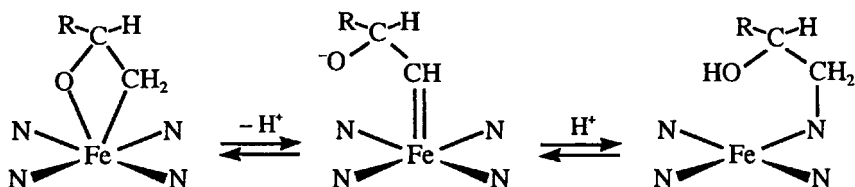


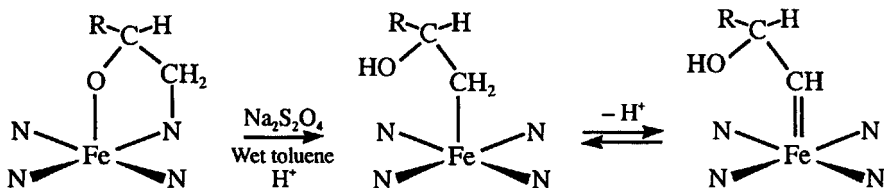
Figure 8.7. Possible routes to epoxide and N-alkylation products in the reaction of alkenes with P-450 systems.

Scheme 8.10



Dolphin et al.¹⁸⁸ have suggested, based on model studies with tetra-(2,6-dichlorophenyl)porphyrin, that a β -hydroxyalkyl species can be formed from the N-alkyl derivative under reducing conditions, as shown in Scheme 8.11. This provides an alkyl derivative that gives proton exchange through deprotonation to the carbenoid. Mansuy and co-workers¹⁸⁹ have reported efficient preparations for some carbenoids of iron *meso*-(tetraphenyl)porphyrin such as $(N)_4Fe^{IV}(=C(CH_3)COPh)$. The sterically crowded alkenes are reactive with both P-450 and model systems, yet they do not show N-alkylation and are unlikely to form carbenoids. Therefore, the latter processes appear to be side reactions of the main epoxidation process.

Scheme 8.11



Collman et al.¹⁹⁰ summarized and discussed the competition between epoxide formation and N-alkylation and the numerous mechanistic possibilities. They concluded in part that "Mechanisms ranging from a fully concerted reaction to a stepwise reaction involving an initial electron transfer may all be possible depending on the nature of the system." The theoretical results, summarized in a recent review,¹⁷⁵ reflect this mechanistic multiplicity by suggesting a concerted mechanism for the low-spin doublet state and a stepwise process for the quartet state, just as was proposed for the hydroxylation of alkanes.

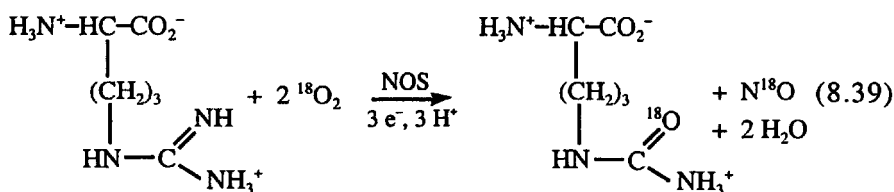
8.6 ENZYMIC REACTIONS OF NITRIC OXIDE

In 1987 it was announced by two groups^{191,192} that the endothelium-derived relaxing factor, EDRF, is nitric oxide. Previous work¹⁹³ had shown that this factor is produced in the endothelium and diffuses into the underlying muscle, where it causes smooth muscle relaxation by

triggering the conversion of guanosine triphosphate to cyclic guanosine monophosphate. Smooth muscle surrounds blood vessels and controls the resistance to blood flow in the arterial system; the relaxation of this muscle tissue can give relief from hypertension and angina pain and can assist the recovery from heart attack. Since this discovery, there has been a greatly renewed interest in the chemistry and biological functions of NO; several early reviews¹⁹⁴ and books¹⁹⁵ give further background.

With the benefit of hindsight, it is not surprising that NO is involved in smooth muscle relaxation. Angina pain has been treated for many years by vasodilators,¹⁹⁶ such as glyceryl trinitrate, amyl nitrite and isosorbide dinitrate, all of which are potential sources of NO. There is still some question as to whether NO itself or some derivative is the actual EDRF, and nitrosothiols, RS—NO, are most often invoked as possibilities.¹⁹⁷

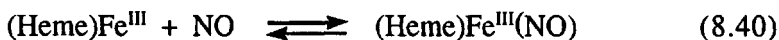
In the biological system, NO is produced by nitric oxide synthase, NOS, which occurs in at least three forms: the endothelial form, eNOS, found in endothelial cells; the neuronal form, nNOS, found in neural tissues; the inducible form, iNOS, found in macrophages. Formation of the latter is triggered by the calcium-binding protein, calmodulin. The NOS enzymes contain iron in a coordination environment like that in cytochrome P-450-CAM. The substrate is L-arginine, and the products are NO and citrulline:



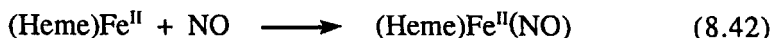
As indicated, it has been shown¹⁹⁸ that both NO and citrulline derive their oxygen from O₂. The actual system is more complicated in that two reducing coenzymes also are required: nicotinamide adenine dinucleotide phosphate hydrogen, NADPH, and tetrahydrobiopterin, H₄B. The mechanism of action may be analogous to that shown in Figure 8.7. The NADPH appears to reduce Fe(III) to Fe(II) which then reacts with O₂. The H₄B provides one electron to reduce the Fe^{III}(O₂⁻) to Fe^{III}(O₂²⁻) which undergoes protonation and cleavage to yield the Fe^{IV}=O radical cation, as in Figure 8.7.

The mechanistic details are described in several specific reviews¹⁹⁹ as well as in more general reviews on P-450 enzymes.²⁰⁰ The first step is thought to be insertion of O from Fe^{IV}=O into an NH bond of the C=NH group to yield C=NOH. Then, Fe(III) is reduced and reacts with another O₂ to form the superoxo Fe^{III}(O₂⁻) species and possibly the Fe^{III}(O₂H⁻) hydroperoxo species. There is some debate^{201,202} about which of these species is responsible for the transfer of the second O that ultimately leads to formation of NO.

The NOS enzymes are known to be inhibited by NO.²⁰³ This effect is at least in part due to binding of NO to Fe(III) and Fe(II) centers in the enzymes. There have been many studies of the binding of NO to various Fe-heme proteins and the work has been reviewed.²⁰⁴ Ford and co-workers²⁰⁵ studied the following equilibrium reaction



and determined equilibrium constants for myoglobin, Mb, horse heart cytochrome c and methemoglobin in the narrow range of 1.6×10^4 to $1.3 \times 10^4 \text{ M}^{-1}$. However, the system is complicated by the following reductive hydroxylation and complexation reactions:



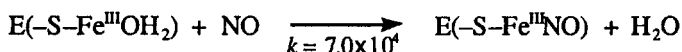
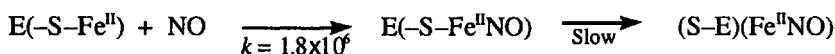
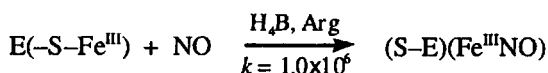
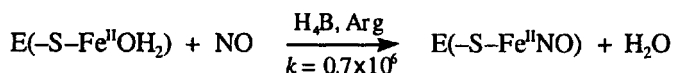
Reaction (8.41) has rate constants in the 10^2 to $10^3 \text{ M}^{-1} \text{ s}^{-1}$ range and becomes a serious complication for $\text{pH} > 7.5$. At $\text{pH} 6.4$, the rate constants for $(\text{Heme})\text{Fe}^{\text{III}} + \text{NO}$ recombination after flash photolysis were determined as 1.9×10^5 and $7.2 \times 10^2 \text{ M}^{-1} \text{ s}^{-1}$ for myoglobin and cytochrome c, respectively.²⁰⁶ The differences in rate constants were attributed to the different ligands coordinated to Fe(III). More detailed studies of the rate law and activation parameters for the NO complexes of a water soluble Fe(III) porphyrin²⁰⁷ and metmyoglobin²⁰⁸ suggest that the addition of NO to the $\text{Fe}^{\text{III}}(\text{OH}_2)$ center is controlled by dissociation of the H_2O ligand. The reactions have positive ΔS^\ddagger and ΔV^\ddagger values, and the rate of NO complexation is close to the water exchange rate²⁰⁹ for the porphyrin complex.

The $(\text{Heme})\text{Fe}^{\text{II}}$ systems in reaction (8.42) are strongly complexed by NO. Flash photolysis of such complexes²¹⁰ has indicated recombination rate constants close to the diffusion-controlled limit and analogous to those for recombination with O_2 . Champion and co-workers²¹¹ have reported observations on the picosecond time scale for the Mb(NO) system which reveals details about the relaxation of the protein and the binding sites for the initially dissociated NO. A similar study²¹² of the horseradish peroxidase system revealed a much simpler process for the rebinding of NO.

These models provide some useful guidelines, but the NOS systems are more complex because of changes in spin-state and coordination number due to dissociation of the thiolate ligand. For example,²¹³ electronic spectra indicate that iNOS, in the presence of arginine and H_4B , forms a 6-coordinate $\text{Fe}^{\text{II}}(\text{NO})$ species and a 5-coordinate high-spin $\text{Fe}^{\text{III}}(\text{NO})$ species. In the absence of arginine and H_4B , the 6-coordinate $\text{Fe}^{\text{II}}(\text{NO})$ species slowly converts to a 5-coordinate form,

while $\text{Fe}^{\text{III}}(\text{NO})$ is 6-coordinate and low-spin. With the assumption that the coordination of $\text{Fe}(\text{II/III})$ is only dependent on the presence or absence of substrate and H_4B , the kinetics²¹³ of the reaction of iNOS with NO can be summarized by Scheme 8.12, where E is the apoenzyme, Arg is L-arginine and the rate constants are in $\text{M}^{-1} \text{s}^{-1}$ at 10°C .

Scheme 8.12

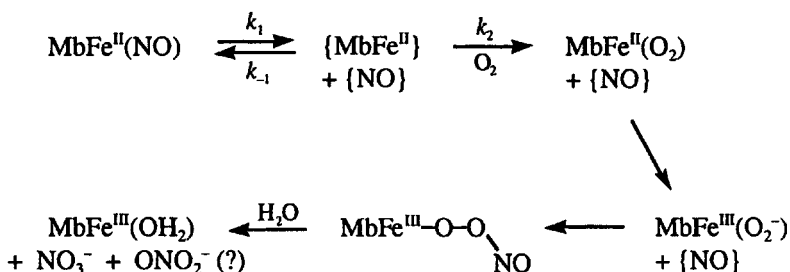


The unusual feature of these results is that the rate constant for addition of NO to $\text{Fe}(\text{III})$ in the presence of H_4B and Arg is large and of the same magnitude as for addition to $\text{Fe}(\text{II})$. This is consistent with the $\text{Fe}(\text{III})$ being 5-coordinate, so that it is not necessary to dissociate an H_2O ligand before adding the NO if the mechanism is dissociative. The smaller rate constant for addition to the 6-coordinate $\text{Fe}(\text{III})$ in the absence of H_4B and Arg is expected because now an H_2O ligand must be dissociated.

At the end of a catalytic cycle, there is evidence²¹⁴ for the presence of an $\text{Fe}^{\text{III}}(\text{NO})$ complex that is presumably in equilibrium with NO free in solution. Since the $\text{Fe}^{\text{III}}(\text{NO})$ complex is not a catalyst, this equilibrium serves as a self-regulating mechanism to prevent overproduction of NO. It also has been proposed²¹⁵ that, in the presence of the reducing cofactors, some of the $\text{Fe}^{\text{III}}(\text{NO})$ is reduced to the more stable $\text{Fe}^{\text{II}}(\text{NO})$ complex. Because of its stability, this complex probably is not a source of available NO. However, it is known that $\text{Fe}^{\text{II}}(\text{NO})$ complexes can be oxidized by O_2 , and the kinetics have been studied for $\text{MbFe}^{\text{II}}(\text{NO})$ ²¹⁶ and the analogous complex with hemoglobin.²¹⁷ These systems are of intrinsic interest because their $\text{Fe}(\text{II})$ complexes are effective scavengers for NO; they also may be models for the NOS system, although they lack the thiolate ligand. The reactions occur over several hours and produce the $\text{Fe}(\text{III})$ complex and nitrate ion. Both systems were found to be biphasic. With $\text{MbFe}^{\text{II}}(\text{NO})$, one step is independent of $[\text{O}_2]$ while the other shows saturation behavior in $[\text{O}_2]$. Both steps were found to be independent of $[\text{O}_2]$ in the hemoglobin system, although it may always

have been in the saturation region. A mechanism consistent with the kinetics for the Mb(NO) system is shown in the following Scheme, where {NO} represents NO held at some site in the protein:

Scheme 8.13



The mechanism proposes that the step showing saturation behavior is due to complexation of O_2 with the rate limited by NO dissociation, so that k_1 is the observed rate constant in the large $[\text{O}_2]$ limit. The experimental value of $k_1 = 1.3 \times 10^{-4} \text{ s}^{-1}$ at 20°C agrees reasonably with the independently determined value of $1.1 \times 10^{-4} \text{ s}^{-1}$.²¹⁸ The remaining steps, which involve coupling of NO with coordinated superoxide ion and dissociation to give peroxyntirite ion and/or rearrangement to give nitrate ion, are speculative. There is spectral evidence for a peroxyntirite intermediate in the reaction of $\text{MbFe}^{\text{III}}(\text{O}_2^-)$ with NO, but peroxyntirite was not detected as a product.²¹⁹ The large second-order rate constant of $4.4 \times 10^7 \text{ M}^{-1} \text{ s}^{-1}$ at 20°C for this reaction poses a problem for the mechanism in Scheme 8.13 because the $[\text{O}_2]$ independent step has a rate constant of $2.6 \times 10^{-4} \text{ s}^{-1}$ at 20°C . Møller and Skibsted²¹⁶ suggested that this may be due to the low effective concentration of NO and the possibility that the NO is bound in the protein.

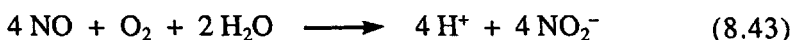
It has been argued^{220,221} that the large values of k for the reactions of NO with oxymyoglobin and oxyhemoglobin would severely limit the amount of free NO in blood. However, further work indicates that this reaction is limited by the rate of NO diffusion through the membrane of red blood cells and that there is a region near the vessel wall in flowing blood that is free of red blood cells.²²²

It should be noted that S-nitroso species, SNO or RSNO, have been proposed²²³ as biological NO carriers. These form by reaction of NO with a thiol group from cysteine in the peptide and require a further one-electron oxidation. A crystal structure supporting this mode of binding has been revised²²⁴ to suggest that the bound species is the radical RSNOH^\cdot , and a theoretical analysis²²⁵ suggests $\text{RSNH}^\cdot\text{O}$ is more consistent with the geometry of the unit. The radical may be oxidized to RSNO by O_2 in vivo. A kinetic study by Cuelemans and co-workers²²⁶ has shown that the reaction of a peptide thiol with NO is generally faster

than the reaction of NO with O₂ in vivo, and that the thiolate, RS⁻, is the reactive form with NO. Herold and Röck²²⁷ have explored the conditions that favor RSNO formation with Mb in vitro.

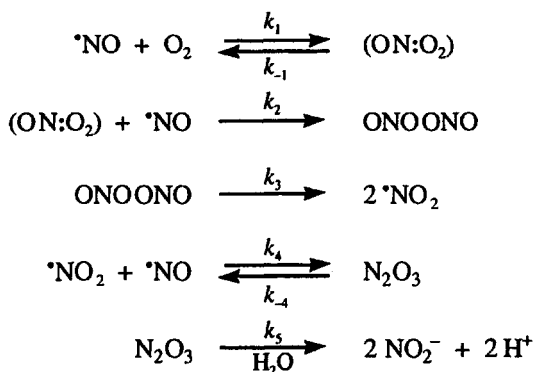
The aqueous chemistry of NO has been extensively studied. Nitric oxide has a modest solubility of 1.9 mM in water under 1 atm of NO. Descriptions of its reactivity have tended to be highly variable. Recent work indicates that NO is not highly reactive, despite having an unpaired electron, but reacts with O₂ to form reactive species. Traces of O₂ are the probable source of different conclusions about the reactivity of NO. It should be noted that there have been some recent studies of the general properties of species involved in these systems, such as the pulse radiolysis of NO,²²⁸ the pK_a values of HNO₂²²⁹ and HNO,²³⁰ the reduction potential of NO,²³¹ and the ΔG_f^o of ONO₂H.²³²

A series of papers by Goldstein and Czapski²³³ have served to clarify the pathways for the reaction of NO with O₂ and the reactivity of the intermediates. The overall reaction can be described by



There is general agreement that the rate of disappearance of O₂ is given by $-d[\text{O}_2]/dt = k[\text{O}_2][\text{NO}]^2$. The reaction pathways are described in the following Scheme:

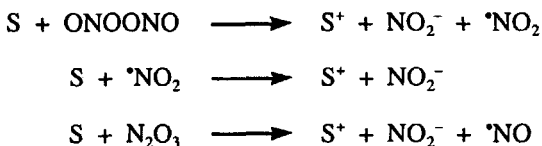
Scheme 8.14



The product of the k_1 step is uncertain and the suggested weak ON:O₂ complex is based on theoretical work by McKee.²³⁴ The known values of k_4 , k_{-4} and k_5 are $1.1 \times 10^9 \text{ M}^{-1} \text{ s}^{-1}$, $8.1 \times 10^4 \text{ s}^{-1}$ and $5.3 \times 10^2 \text{ s}^{-1}$, respectively.²¹⁰ A steady-state treatment of this mechanism gives $k = k_1 k_2 / k_{-1} = 2.5 \times 10^6 \text{ M}^{-2} \text{ s}^{-1}$.

It is expected that the intermediates in Scheme 8.14 will react with other substrates, S, and possible reactions are shown in Scheme 8.15. It was found that the rate is independent of the substrate concentration.²³⁵

Scheme 8.15



In general, the amount of reaction proceeding by these pathways will depend on the substrate and lead to variable stoichiometry for the overall substrate-oxidation reaction. For the important case of thiols, the observations suggest that $\cdot\text{NO}_2$ and/or N_2O_3 are the reactive oxidants. Goldstein and Czapski have estimated that, under physiological conditions, the nitrosation of a thiol would have a half-life of >7 min and would be too slow to produce the nitrosothiols that have been suggested as alternatives to NO as the EDRF.

Since the discovery of the involvement of NO in smooth muscle relaxation, intensive investigations have revealed additional functions of NO. The brain contains more NOS than any other organ, and NO has been suggested as the chemical messenger at the synapses. The antibacterial action of macrophages appears to involve NO production. Since superoxide ion also is produced in these systems, it has been suggested²³⁶ that the active agent is peroxynitrite, ONOO^- . Lymar and Hurst²³⁷ found that ONOO^- reacts rapidly with CO_2 to give $\text{ONO}_2\text{CO}_2^-$ and this will be the dominant pathway for removal of ONOO^- under physiological conditions. However, the product $\text{ONO}_2\text{CO}_2^-$ or its decomposition products might be active oxidants.

The mechanism of decomposition of ONOO^- has been the subject of some controversy and is discussed in two recent reviews.²³⁸ The proposed mechanisms involve either atom transfer between ONOOH and ONOO^- ²³⁹ or homolytic cleavage of the $\text{N}-\text{O}_2$ bond.²⁴⁰

Lest one think that, if a little is good then a lot of NO is better, it must be noted that NO can be a serious air pollutant and a carcinogen, although it is toxic to early tumor cells. It may be involved in mutagenesis through the conversion of 5-methylcytosine to thymine.

References

1. Williams, R. J. P. *Coord. Chem. Rev.* **1987**, *79*, 175.
2. *Metal Ions in Biological Systems*; Sigel, H., Ed.; Marcel Dekker: New York; *Advances in Inorganic Biochemistry*; Eichorn, G. L.; Marzilli, L. G., Eds.; Elsevier: New York; *Advances in Inorganic and Bioinorganic Mechanisms*; Sykes, A. G., Ed.; Academic Press: New York; *Metal Ions in Biology*; Spiro, T. G., Ed.; Wiley-Interscience: New York.
3. *J. Inorg. Biochem.*; *J. Bio. Inorg. Chem.*; *Dalton Trans.* collects bioinorganic articles on a separate WEB page.

4. *Chem. Rev.* **2004**, *104*, No. 2.
5. *Bioinorganic Chemistry: An Introduction*; Ochai, E.; Allyn and Bacon Inc.: Boston, 1977; *General Principles of Biochemistry of the Elements*; Ochai, E.; Plenum Press: New York, 1987; *Principles of Bioinorganic Chemistry*; Lippard, S. J.; Berg, J. M.; University Science Books: Mill Valley, 1994; *The Biological Chemistry of the Elements*; Faústo da Silva, J. J. R.; Williams, R. J. P.; Oxford: New York, 2001.
6. *B₁₂*; Dolphin, D., Ed.; Wiley: New York, 1982; Vols. I and II.; *Chemistry and Biochemistry of B₁₂*; Banerjee, R., Ed.; Wiley: New York, 1999.
7. Halpern, J. *Science* **1985**, *227*, 869; Pratt, J. M. *Chem. Soc. Rev.* **1985**, 161; Finke, R. G. In *Molecular Mechanisms in Bioorganic Processes*; Royal Society of Chemistry: Thomas Graham House, Science Park, Cambridge, U.K., 1990; pp 244-279; Banerjee, R. *Chem. Rev.* **2003**, *103*, 2083; Toraya, T. *Chem. Rev.* **2003**, *103*, 2095; Brown, K. L. *Chem. Rev.* **2005**, *105*, 2075; Brown, K. L. *Dalton Trans.* **2006**, 1123.
8. Lenhert, P. G.; Hodgkin, D. C. *Nature (London)* **1961**, *192*, 937; Lenhert, P. G. *Proc. R. Soc. London* **1968**, *A303*, 45; Savage, H. F.; Lindley, P. F.; Finney, J. L.; Timmins, P. A. *Acta Crystallogr.* **1987**, *B43*, 296; Bouquiere, J. P.; Finney, J. L.; Lehmann, M. S.; Lindley, P. F.; Savage, H. F. *Acta Crystallogr.* **1993**, *B49*, 79; Kräutler, B.; Konrat, R.; Stupperich, E.; Gerald, F.; Gruber, K.; Kratky, C. *Inorg. Chem.* **1994**, *33*, 4128.
9. Pett, V. B.; Liebman, M. N.; Murray-Rust, P.; Prasad, K.; Glusker, J. P. *J. Am. Chem. Soc.* **1987**, *109*, 3207.
10. Randaccio, L.; Furlan, M.; Geremia, S.; Slouf, M.; Srnova, I.; Toffoli, D. *Inorg. Chem.* **2000**, *39*, 3403.
11. Champloy, F.; Gruber, K.; Jogl, G.; Kratky, C. *J. Synchrotron Rad.* **2000**, *7*, 267; Gruber, K.; Kratky, C. *Curr. Opin. Chem. Biol.* **2002**, *6*, 598.
12. Yamanishi, M.; Yunoki, M.; Tobimatsu, T.; Sato, H.; Matsui, J.; Dokiya, A.; Iuchi, Y.; Oe, K.; Suto, K.; Shibata, N.; Morimoto, Y.; Yasuoka, N.; Toraya, T. *Eur. J. Biochem.* **2002**, *269*, 4484.
13. Kräutler, B.; Keller, W.; Kratky, C. *J. Am. Chem. Soc.* **1989**, *111*, 8936.
14. Sagi, I.; Wirt, M. D.; Chen, E.; Frisbie, S.; Chance, M. R. *J. Am. Chem. Soc.* **1990**, *112*, 8639.
15. Drennan, C. L.; Huang, S.; Drummond, J. T.; Mathews, R. G.; Ludwig, M. L. *Science*, **1994**, *266*, 1699; Ludwig, M. L.; Drennan, C. L.; Mathews, R. G. *Structure*, **1996**, *4*, 505.
16. Mancia, F.; Keep, N. H.; Nakagawa, A.; Leadlay, P. F.; McSweeney, S.; Rasmussen, B.; Boscke, P.; Diat, O.; Evans, P. R. *Structure* **1996**, *4*, 339; Mancia, F.; Evans, P. R. *Structure* **1998**, *6*, 711; McCarthy, A. A.; Baker, H. M.; Shewry, C.; Patchett, M. L.; Baker, E. N. *Structure*, **2001**, *9*, 637.
17. Ludwig, M. L.; Drennan, C. L.; Mathews, R. G. *Structure* **1996**, *4*, 505; Reitzer, R.; Gruber, K.; Jogl, G.; Wagner, U. G.; Bothe, H.; Buckel, W.; Kratky, C. *Structure* **1999**, *7*, 891.

18. Shibata, N.; Masuda, J.; Tobimatsu, T.; Toraya, T.; Suto, K.; Morimoto, Y.; Yasuoka, N. *Structure* **1999**, *7*, 997; Shibata, N.; Masuda, J.; Morimoto, Y.; Yasuoka, N.; Toraya, T. *Biochemistry* **2002**, *41*, 12607.
19. Liao, D.-I.; Dotson, G.; Turner, I., Jr.; Reiss, L.; Emptage, M. *J. Inorg. Biochem.* **2003**, *93*, 84.
20. Perry, C. B.; Marques, H. M. *South African J. Sci.* **2004**, *100*, 368.
21. Shrauzer, G. N. *Acc. Chem. Res.* **1968**, *1*, 97.
22. Finke, R. G.; Smith, B. L.; McKenna, W.; Christian, P. A. *Inorg. Chem.* **1981**, *20*, 687.
23. Costa, G. *Coord. Chem. Rev.* **1972**, *8*, 63.
24. Hamza, M. S. A.; van Eldik, R. *Dalton Trans.* **2004**, *1*.
25. Berkovitch, F.; Behshad, E.; Tang, K.-H.; Enns, E. A.; Frey, P. A.; Drennan, C. L. *Proc. Nat. Acad. Sci. U.S.A.* **2004**, *101*, 15870.
26. Ragsdale, S. W.; Lindahl, P. A.; Munck, E. *J. Biol. Chem.* **1987**, *262*, 14289; Wirt, M. D.; Kumar, M.; Ragsdale, S. W.; Chance, M. R. *J. Am. Chem. Soc.* **1993**, *115*, 2146; Wirt, M. D.; Wu, J.-J.; Scheuring, E. M.; Kumar, M.; Ragsdale, S. W.; Chance, M. R. *Biochemistry* **1995**, *34*, 5269.
27. Mathews, R. G. *Acc. Chem. Res.* **2001**, *34*, 681.
28. Banerjee, R.; Ragsdale, S. W. *Ann. Rev. Biochem.* **2003**, *72*, 209.
29. Rétey, J.; Umani-Ronchi, A.; Seibl, J.; Arigoni, D. *Experientia* **1966**, *22*, 502.
30. Babior, B. M.; Moss, T. A.; Orme-Johnson, W. H.; Beinert, H. *J. Biol. Chem.* **1974**, *249*, 4537.
31. Warncke, K.; Schmidt, J. C.; Ke, S.-C. *J. Am. Chem. Soc.* **1999**, *121*, 10522; Canfield, J. M.; Warncke, K. *J. Phys. Chem.* **2002**, *106*, 8831; Warncke, K. *Biochemistry* **2005**, *44*, 3184.
32. Bandarian, V.; Reed, G. H. *Biochemistry* **2002**, *41*, 8580.
33. Valinsky, J. E.; Abeles, J. E.; Fee, J. A. *J. Am. Chem. Soc.* **1974**, *96*, 4709.
34. Orme-Johnson, W. H.; Beinert, H.; Blakley, R. L. *J. Biol. Chem.* **1974**, *249*, 2338.
35. Licht, S.; Gerfen, G. J.; Stubbe, J. *Science* **1996**, *271*, 477.
36. Zelder, O.; Beatrix, B.; Leytbecher, U.; Buckel, W. *Eur. J. Biochem.* **1994**, *226*, 577.
37. Keep, N. H.; Smith, G. A.; Evans, M. C. W.; Diakun, G. P.; Leadlay, P. F. *Biochem. J.* **1993**, *295*, 387; Zhao, Y.; Abend, A.; Kunz, M.; Such, P.; Rétey, J. *Eur. J. Biochem.* **1994**, *225*, 891; Padmakumar, R.; Banerjee, R. *J. Biol. Chem.* **1995**, *270*, 9295.
38. Padmakumar, R.; Taoka, S.; Padmakumar, R.; Banerjee, R. *J. Am. Chem. Soc.* **1995**, *117*, 7033.
39. Mancia, F.; Keep, N. H.; Nakagawa, A.; Leadlay, P. F.; McSweeney, S.; Rasmussen, B.; Boescke, P.; Diat, O.; Evans, P. R. *Structure* **1996**, *4*, 339.
40. Gerfen, G. J.; Licht, S.; Willems, J.-P.; Hoffman, B. M.; Stubbe, J. *J. Am. Chem. Soc.* **1996**, *118*, 8192.

41. Hollaway, B. P.; White, H. A.; Joblin, K. N.; Johnson, A. W.; Lappert, M. F.; Wallis, O. C. *Eur. J. Biochem.* **1978**, *82*, 143.
42. Marsh, E. N. G.; Ballou, D. P. *Biochemistry* **1998**, *37*, 11864; Chih, H.-W.; Marsh, E. N. G. *Biochemistry* **1999**, *38*, 13684.
43. Padmakumar, R.; Padmakumar, R.; Banerjee, R. *Biochemistry* **1997**, *36*, 3713.
44. Harkins, T. T.; Grissom, C. B. *J. Am. Chem. Soc.* **1995**, *117*, 566.
45. Taoka, S.; Padmakumar, R.; Grissom, C. B.; Banerjee, R. *Bioelectromagnetics* **1997**, *18*, 506.
46. Wagner, O. W.; Lee, H. A.; Frey, P. A.; Abeles, R. H. *J. Biol. Chem.* **1966**, *249*, 1751.
47. Sandala, G. M.; Smith, D. M.; Coote, M. L.; Radom, L. *J. Am. Chem. Soc.* **2004**, *126*, 12206.
48. Finke, R. G.; Schiraldi, D. A.; Mayer, B. J. *Coord. Chem. Rev.* **1984**, *54*, 1.
49. Halpern, J. *Science* **1985**, *227*, 869.
50. Reed, G. H. *Curr. Opin. Chem. Biol.* **2004**, *8*, 477.
51. Halpern, J.; Ng, F. T. T.; Rempel, G. L. *J. Am. Chem. Soc.* **1979**, *101*, 7124.
52. Endicott, J. F.; Ferraudi, G. J. *J. Am. Chem. Soc.* **1977**, *99*, 243.
53. Nie, S.; Marzilli, P. A.; Marzilli, L. G.; Yu, N.-T. *J. Am. Chem. Soc.* **1990**, *112*, 6084.
54. Dong, S.; Padmakumar, R.; Banerjee, R.; Spiro, T. *J. Am. Chem. Soc.* **1996**, *118*, 9182.
55. Halpern, J. *Polyhedron* **1988**, *7*, 1483.
56. Koenig, T. W.; Hay, B. P.; Finke, R. G. *Polyhedron* **1988**, *7*, 1499; Koenig, T. W.; Finke, R. G. *J. Am. Chem. Soc.* **1988**, *110*, 2657.
57. Daikh, B. E.; Huthchison, J. E.; Gray, N. E.; Smith, B. L.; Weakley, J. R.; Finke, R. G. *J. Am. Chem. Soc.* **1990**, *112*, 7830.
58. Woska, D. C.; Xie, Z. D.; Gridnev, A. A.; Ittel, S. D.; Fryd, M.; Wayland, B. B. *J. Am. Chem. Soc.* **1996**, *118*, 9102.
59. Finke, R. G.; Hay, B. P. *Inorg. Chem.* **1984**, *23*, 3043; *Ibid.* **1985**, *24*, 1278.
60. Halpern, J.; Kim, S. H.; Leung, T. W. *J. Am. Chem. Soc.* **1984**, *106*, 8317; *Ibid.* **1985**, *107*, 2199.
61. Hay, B. P.; Finke, R. G. *J. Am. Chem. Soc.* **1986**, *108*, 4820.
62. Martin, B. D.; Finke, R. G. *J. Am. Chem. Soc.* **1990**, *112*, 2419.
63. Waddington, M. D.; Finke, R. G. *J. Am. Chem. Soc.* **1993**, *115*, 4629.
64. Hay, B. P.; Finke, R. G. *J. Am. Chem. Soc.* **1987**, *109*, 8012.
65. Brown, K. L.; Zou, X.; Banka, R. R.; Perry, C. B.; Marques, H. M. *Inorg. Chem.* **2004**, *43*, 8130.
66. Garr, C. D.; Sirovatka, J. M.; Finke, R. G. *J. Am. Chem. Soc.* **1996**, *118*, 11142.
67. Wollowitz, S.; Halpern, J. *J. Am. Chem. Soc.* **1988**, *110*, 3112.
68. Choi, S.-C.; Dowd, P. *J. Am. Chem. Soc.* **1989**, *111*, 2313, and references therein.

69. Murakami, Y.; Hisaeda, Y.; Ozaki, T.; Ohno, T.; Fan, S.-D.; Matsuda, Y. *Chem. Lett.* **1988**, 839.
70. Dowd, P.; Choi, S.-C.; Duak, F.; Kaufman, C. *Tetrahedron* **1988**, *44*, 2137.
71. Murakami, Y.; Hisaeda, Y.; Kikuchi, J.; Ohno, T.; Suzuki, M.; Matsuda, Y.; Matsura, T. *J. Chem. Soc., Perkin Trans. 2* **1988**, 1237.
72. Choi, G.; Choi, S.-C.; Galan, A.; Wilk, B.; Dowd, P. *Proc. Natl. Acad. Sci. U.S.A.* **1990**, *87*, 3174.
73. He, M.; Dowd, P. *J. Am. Chem. Soc.* **1996**, *118*, 711; *Ibid.* **1998**, *120*, 1133.
74. Finke, R. G.; McKenna, W. P.; Schiraldi, D. A.; Smith, B. L.; Pierpont, C. *J. Am. Chem. Soc.* **1983**, *105*, 7592; Finke, R. G.; Schiraldi, D. A. *J. Am. Chem. Soc.* **1983**, *105*, 7605.
75. Silverman, R. B.; Dolphin, D. *J. Am. Chem. Soc.* **1976**, *98*, 4633.
76. Arigoni, D. In *Vitamin B₁₂ Proceedings of the Third European Symposium on Vitamin B₁₂ and Intrinsic Cofactor*; Zagalak, B.; Friedrich, W., Eds.; Walter de Gruyter: Berlin, 1979; p 389.
77. Beartix, B.; Zelder, O.; Kroll, F. K.; Örlýgsson, G.; Golding, B. T.; Buckel, W. *Angew. Chem. Int. Ed. Engl.* **1995**, *34*, 2398.
78. Smith, D. M.; Golding, B. T.; Radom, L. *J. Am. Chem. Soc.* **1999**, *121*, 1037.
79. Chih, H.-W.; Marsh, E. N. G. *J. Am. Chem. Soc.* **2000**, *122*, 10732.
80. Endicott, J. F.; Ferraudi, G. J. *J. Am. Chem. Soc.* **1977**, *99*, 243; Chen, E.; Chance, M. R. *J. Biol. Chem.* **1990**, *265*, 12987.
81. Lott, W. B.; Chagovetz, A. M.; Grissom, C. B. *J. Am. Chem. Soc.* **1995**, *117*, 12194.
82. Sension, R. J.; Harris, D. A.; Cole, A. G. *J. Phys. Chem. B* **2005**, *109*, 21954, and references therein.
83. Sension, R. J.; Harris, D. A.; Stickrath, A.; Cole, A. G. *J. Phys. Chem. B* **2005**, *109*, 18146.
84. Yoder, L. M.; Cole, A. G.; Walker, L. A., II; Sension, R. J. *J. Phys. Chem. B* **2001**, *105*, 12180.
85. Smith, A. E.; Matthews, R. G. *Biochemistry* **2000**, *39*, 13880.
86. Matthews, R. G.; Smith, A. E.; Zhou, Z. S.; Taurog, R. E.; Bandarian, V.; Evans, J. C.; Ludwig, M. *Helv. Chim. Acta* **2003**, *86*, 3939.
87. Peariso, K.; Goulding, C. W.; Huang, S.; Matthews, R. G.; Penner-Hahn, J. E. *J. Am. Chem. Soc.* **1998**, *120*, 8410.
88. Dorweiler, J. S.; Finke, R. G.; Matthews, R. G. *Biochemistry* **2003**, *42*, 14653.
89. Vallee, B. L.; Auld, D. S. *Acc. Chem. Res.* **1993**, *26*, 543; Lipscomb, W. N.; Sträter, N. *Chem. Rev.* **1996**, *96*, 2375; Coleman, J. E. *Curr. Opin. Chem. Biol.* **1998**, *2*, 222; Parkin, G.; *Chem. Rev.* **2004**, *104*, 699.
90. *Zinc Enzymes, Prog. Inorg. Biochem. Biophys.*; Bertini, I.; Luchinat, C.; Maret, W.; Zeppezauer, M., Eds.; Birkhäuser: Boston, 1986, Vol. 1.
91. Silverman, D. N.; Lindskog, S. *Acc. Chem. Res.* **1988**, *21*, 30; Lindskog, S.; Liljas, A. *Curr. Opin. Struct. Biol.* **1993**, *3*, 915; Silverman, D. N.

- Methods Enzymol.* **1995**, *249*, 479; Christianson, D. W.; Fierke, C. A. *Acc. Chem. Res.* **1996**, *29*, 331.
92. *The Carbonic Anhydrases: New Horizons*; Chegwidde, W.R.; Carter, N. D.; Edwards, Y. H., Eds.; Birkhäuser Verlag; Basel, 2000; *Carbonic Anhydrase. Its Inhibitors and Activators. CRC Enzyme Inhibitors Series*; Supuran, C. T.; Scozzafava, A.; Conway, J., Eds.; CRC Press; Boca Raton, 2004.
93. Simonsson, I.; Jonsson, B.-H.; Lindskog, S. *Eur. J. Biochem.* **1979**, *93*, 409.
94. Khalifah, R. G. *J. Biol. Chem.* **1971**, *246*, 2561.
95. Duda, D.; Tu, C.; Qian, M.; Lapis, P.; Agbandje-McKenna, M.; Silverman, D. N.; McKenna, R. *Biochemistry* **2001**, *40*, 1741.
96. Bertini, I.; Dei, A.; Luchinat, C.; Monnanni, R. *Inorg. Chem.* **1985**, *24*, 301.
97. Bauer, R.; Limkilde, P.; Johansen, J. T. *Biochemistry* **1976**, *15*, 334; Tibell, L.; Lindskog, S. *Biochim. Biophys. Acta* **1984**, *778*, 110.
98. Bhatt, D.; Tu, C.; Fisher, S. Z.; Prada, J. A. H.; McKenna, R. *Proteins* **2005**, *61*, 239; Duda, D. M.; Tu, C.; Fisher, S. Z.; An, H.; Yoshioka, C.; Govindasamy, L.; Laipis, P. J.; Agbandje-McKenna, M.; Silverman, D. N.; McKenna, R. *Biochemistry* **2005**, *44*, 10046.
99. Tu, C.; Tripp, B. C.; Ferry, J. G.; Silverman, D. N. *J. Am. Chem. Soc.* **2001**, *123*, 5861.
100. Chaberek, S.; Courtney, R. C.; Martell, A. E. *J. Am. Chem. Soc.* **1952**, *74*, 5057.
101. Woolley, P. *Nature (London)* **1975**, *258*, 677.
102. Kimura, E.; Shiota, T.; Koike, T.; Shiro, M.; Kodama, M. *J. Am. Chem. Soc.* **1990**, *112*, 5805.
103. Kimura, E. *Prog. Inorg. Chem.* **1994**, *41*, 443.
104. Palmer, D. A.; van Eldik, R. *Chem. Rev.* **1983**, *83*, 651.
105. Lindskog, S. In *Zinc Enzymes*; Spiro, T. G. Ed.; Wiley: New York, 1983; pp 77–121.
106. Lipscomb, W. N. *Ann. Rev. Biochem.* **1983**, *52*, 17; Liang, J.-Y.; Lipscomb, W. N. *Int. J. Quantum Chem.* **1989**, *36*, 299.
107. Merz, K. M., Jr.; Banci, L. *J. Am. Chem. Soc.* **1997**, *119*, 863; Hartmann, M.; Merz, K. M., Jr.; van Eldik, R.; Clark, T. *J. Mol. Model.* **1998**, *4*, 355.
108. Loferer, M. J.; Tautermann, C. S.; Loeffler, H. H.; Liedl, K. R. *J. Am. Chem. Soc.* **2003**, *125*, 8921; Tautermann, C. S.; Loferer, M. J.; Voegelé, A. F.; Liedl, K. R. *J. Phys. Chem. B* **2003**, *107*, 12013.
109. Merz, K. M., Jr.; Hoffmann, R.; Dewar, M. J. S. *J. Am. Chem. Soc.* **1989**, *111*, 5636; Merz, K. M., Jr. *J. Am. Chem. Soc.* **1991**, *113*, 406; Aqvist, J.; Zheng, Y.-J.; Merz, K. M., Jr. *J. Am. Chem. Soc.* **1992**, *114*, 10498; Fothergill, M.; Warshel, A. *J. Am. Chem. Soc.* **1993**, *115*, 631.
110. Kumar, V.; Kannan, K. K. *J. Mol. Biol.* **1994**, *241*, 226.
111. Xue, Y.; Vidgren, J.; Svensson, L. A.; Liljas, A.; Jonsson, B.-H.; Lindskog, S. *Proteins* **1993**, *15*, 80.

112. Mao, Z.-W.; Liehr, G.; van Eldik, R. *J. Am. Chem. Soc.* **2000**, *122*, 4839; Choudhury, C. R.; Dey, S. K.; Mitra, S.; Gamlich, V. *Dalton Trans.* **2003**, 1059.
113. Baxter, K. E.; Hanton, L. R.; Simpson, J.; Vincent, B. R.; Blackman, A. G. *Inorg. Chem.* **1995**, *34*, 2795.
114. Kim, J. C.; Cho, J.; Kim, H.; Lough, A. J. *Chem. Commun.* **2004**, 1796.
115. Acharya, A. N.; Das, A.; Dash, A. C. *Adv. Inorg. Chem.* **2004**, *55*, 127.
116. Zhang, X.; van Eldik, R.; Koike, T.; Kimura, E. *Inorg. Chem.* **1993**, *32*, 5749; Zhang, X.; van Eldik, R. *Inorg. Chem.* **1995**, *34*, 5606.
117. Looney, A.; Han, R.; McNeil, K.; Parkin, G. *J. Am. Chem. Soc.* **1993**, *115*, 703.
118. Pocker, Y.; Diets, T. L. *J. Am. Chem. Soc.* **1982**, *104*, 2424.
119. Dugad, L. B.; Cooley, C. R.; Gerig, J. J. *Biochemistry* **1989**, *28*, 3955.
120. Liang, J.-Y.; Lipscomb, W. N. *Biochemistry* **1989**, *28*, 9724.
121. Nair, S. K.; Ludwig, P. A.; Christianson, D. W. *J. Am. Chem. Soc.* **1994**, *116*, 3679.
122. Bertini, I.; Dei, A.; Luchinat, C.; Monnanni, R. *Prog. Inorg. Biochem. Biophys.* **1986**, *1*, 371.
123. Imlay, J. A.; Linn, S. *Science* **1988**, *240*, 1302.
124. Dawson, J. H. *Science*, **1988**, *240*, 433.
125. Perutz, M. F.; Fermi, G.; Luisi, B.; Shaanan, B.; Liddington, R. C. *Acc. Chem. Res.* **1987**, *20*, 309.
126. Takano, T. *J. Mol. Biol.* **1977**, *110*, 569.
127. Phillips, S. E. V. *J. Mol. Biol.* **1980**, *142*, 531.
128. Springer, B. A.; Egeberg, K. D.; Sligar, S. G.; Rohlf, R. J.; Mathews, A. J.; Olson, J. S. *J. Biol. Chem.* **1989**, *264*, 3057.
129. Takano, T. *J. Mol. Biol.* **1977**, *110*, 537.
130. Jameson, G. B.; Molinaro, F. S.; Ibers, J. A.; Collman, J. P.; Brauman, J. I.; Rose, E.; Suslick, K. S. *J. Am. Chem. Soc.* **1980**, *102*, 3224.
131. Collman, J. P.; Gagne, R. R.; Halbert, T. R.; Marchon, J.-C.; Reed, C. A. *J. Am. Chem. Soc.* **1973**, *95*, 7868.
132. Norvell, J. C.; Nunes, A. C.; Schoenborn, B. P. *Science* **1975**, *190*, 569.
133. Lee, C. L.; Oldfield, E. *J. Am. Chem. Soc.* **1989**, *111*, 1584.
134. Coletta, M.; Ascenzi, P.; Traylor, T. G.; Brunori, M. *J. Biol. Chem.* **1985**, *260*, 4151.
135. Ramsden, J.; Spiro, T. G. *Biochemistry* **1989**, *28*, 3125; Morikis, D.; Champion, P. M.; Springer, B. A.; Sligar, S. G. *Biochemistry* **1989**, *28*, 4791.
136. Springer, B. A.; Sligar, S. G.; Olson, J. S.; Phillips, G. N., Jr. *Chem. Rev.* **1994**, *94*, 699.
137. Martin, J. L.; Migus, A.; Poyart, C.; Lecarpentier, Y.; Astier, R.; Antonetti, A. *Proc. Natl. Acad. Sci. U.S.A.* **1983**, *80*, 173.
138. Finsden, E. W.; Friedman, J. M.; Ondrias, M. R.; Simon, S. R. *Science*, **1985**, *229*, 661.
139. Beattie, J. K. *Adv. Inorg. Chem.* **1988**, *32*, 2.

140. Beatie, J. K.; Binstead, R. A.; West, R. J. *J. Am. Chem. Soc.* **1978**, *100*, 3046; McGarvey, J. J.; Lawthers, I.; Heremans, K.; Toftlund, H. *Inorg. Chem.* **1990**, *29*, 252.
141. Jongeward, K. A.; Magde, D.; Taube, D. J.; Marsters, J. C.; Traylor, T. G.; Sharma, V. S. *J. Am. Chem. Soc.* **1988**, *110*, 380.
142. Olson, J. S.; Rohlfs, R. J.; Gibson, Q. H. *J. Biol. Chem.* **1987**, *262*, 12930.
143. Gibson, Q. H.; Olson, J. S.; McKinnie, R. E.; Rohlfs, R. J. *J. Biol. Chem.* **1986**, *261*, 10228.
144. Johnson, K. A.; Olson, J. S.; Phillips, G. N., Jr. *J. Mol. Biol.* **1989**, *207*, 459.
145. Chatfield, M. D.; Walda, K. N.; Magde, D. *J. Am. Chem. Soc.* **1990**, *112*, 4680.
146. Adachi, S.; Morishima, I. *J. Biol. Chem.* **1989**, *264*, 18896.
147. Taube, D. J.; Projahn, H.-D.; van Eldik, R.; Magde, D.; Traylor, T. G. *J. Am. Chem. Soc.* **1990**, *112*, 6880.
148. Projahn, H.-D.; van Eldik, R. *Inorg. Chem.* **1991**, *30*, 3283.
149. Schlichting, I.; Berendzen, J.; Phillips, G. N., Jr.; Sweet, R. M. *Nature* **1994**, *371*, 808.
150. Hartmann, H.; Zinser, S.; Kominos, P.; Schneider, R. T.; Nienhaus, G. U.; Parak, F. *Proc. Natl. Acad. Sci. U.S.A.* **1996**, *93*, 7013.
151. Brunori, M.; Vallone, B.; Cutruzzola, F.; Travaglini-Allocatelli, C.; Berendzen, J.; Chu, K.; Sweet, R. M.; Schlichting, I. *Proc. Natl. Acad. Sci. U.S.A.* **2000**, *97*, 2058; Srajer, V.; Ren, Z.; Teng, T.-Y.; Schmidt, M.; Ursby, T.; Bourgeois, D.; Pradervand, C.; Schildkamp, W.; Wulff, M.; Moffat, K. *Biochemistry* **2001**, *40*, 13802; Schotte, F.; Lim, M.; Jackson, T. A.; Smirnov, A. V.; Soman, J.; Olson, J. S.; Phillips, G. N., Jr.; Wulff, M.; Anfinrud, P. A. *Science* **2003**, *300*, 1944; Bourgeois, D.; Vallone, B.; Schotte, F.; Arcovito, A.; Miele, A. E.; Sciara, G.; Wulff, M.; Anfinrud, P.; Brunori, M. *Proc. Natl. Acad. Sci. U.S.A.* **2003**, *100*, 8704; Hummer, G.; Schotte, F.; Anfinrud, P. A. *Proc. Natl. Acad. Sci. U.S.A.* **2004**, *101*, 15330.
152. *Cytochrome P-450: Structure, Mechanism and Biochemistry*, 3rd ed.; Ortiz de Montellano, P. R., Ed.; Plenum Klewer: New York, 2005.
153. Sligar, S. G.; Makris, T. M.; Denisov, I. G. *Biochem. Biophys. Res. Commun.* **2005**, *338*, 346.
154. Denisov, I. G.; Makris, T. M.; Sligar, S. G.; Schlichting, I. *Chem. Rev.* **2005**, *105*, 2253.
155. Poulos, T. L.; Howard, A. J. *Biochemistry* **1987**, *26*, 8165; Poulos, T. L.; Finzel, B. C.; Howard, A. J. *J. Mol. Biol.* **1987**, *195*, 687.
156. Poulos, T. L. *Adv. Inorg. Biochem.* **1987**, *7*, 1.
157. Dawson, J. H.; Kau, L.-S.; Penner-Hahn, J. E.; Sono, M.; Eble, K. S.; Bruce, G. S.; Hager, L. P.; Hodgson, K. O. *J. Am. Chem. Soc.* **1986**, *108*, 8114.
158. Dawson, J. H.; Sono, M. *Chem. Rev.* **1987**, *87*, 1255.

159. Thomann, H.; Bernardo, M.; Goldfarb, D.; Kroneck, P. M. H.; Ullrich, V. *J. Am. Chem. Soc.* **1995**, *117*, 8243.
160. Ricard, L.; Schappacher, M.; Weiss, R.; Montiel-Montoya, R.; Bill, E.; Gonser, U.; Trautwein, A. *Nouv. J. Chim.* **1983**, *7*, 405.
161. Schlichting, I.; Berendzen, J.; Chu, K.; Stock, A. M.; Maves, S. A.; Benson, D. E.; Sweet, R. M.; Ringe, D.; Petsko, G. A.; Sligar, S. G. *Science* **2000**, *287*, 1615.
162. Davydov, R.; Makris, T. M.; Kofman, V.; Werst, D. W.; Sligar, S. G.; Hoffman, B. M. *J. Am. Chem. Soc.* **2001**, *123*, 1403.
163. Sligar, S. G.; Gunsalus, I. C. *Proc. Nat. Acad. Sci. U.S.A.* **1976**, *73*, 1078.
164. Dunford, H. B. *Adv. Inorg. Biochem.* **1982**, *4*, 41.
165. Penner-Hahn, J. E.; Eble, K. S.; McMurry, T. J.; Renner, M.; Balch, A. L.; Groves, J. T.; Dawson, J. H.; Hodgson, K. O. *J. Am. Chem. Soc.* **1986**, *108*, 7819.
166. McDonald, T. L.; Burka, L. T.; Wright, S. T.; Guengerich, F. P. *Biochem. Biophys. Res. Commun.* **1982**, *104*, 620.
167. Groves, J. T.; Avaria-Neisser, G. E.; Fish, K. M.; Imachi, M.; Kuczkowski, R. L. *J. Am. Chem. Soc.* **1986**, *108*, 3837.
168. Bhakta, M. N.; Hollenberg, P. F.; Wimalasena, K. *J. Am. Chem. Soc.* **2005**, *127*, 1376.
169. Blake, R. C.; II; Coon, M. J. *J. Biol. Chem.* **1981**, *256*, 5755, and references therein; Wagner, G. C.; Palcic, M. M.; Dunford, H. B. *FEBS Lett.* **1983**, *156*, 244.
170. Egawa, T.; Shimada, H.; Ishimura, Y. *Biochem. Biophys. Res. Commun.* **1994**, *201*, 1464.
171. Kellner, D. G.; Hung, S.-C.; Weiss, K. E.; Sligar, S. G. *J. Biol. Chem.* **2002**, *277*, 9641.
172. Schünemann, V.; Lenzian, F.; Jung, C.; Contzen, J.; Barras, A.-L.; Sligar, S. G.; Trautwein, A. X. *J. Biol. Chem.* **2004**, *279*, 10919.
173. Prasad, S.; Mitra, S. *Biochem. Biophys. Res. Commun.* **2004**, *314*, 610.
174. Spolitak, T.; Dawson, J. H.; Ballou, D. P. *J. Biol. Chem.* **2005**, *280*, 20300.
175. Shaik, S.; Kumar, D.; de Visser, S. P.; Altun, A.; Thiel, W. *Chem. Rev.* **2005**, *105*, 2279.
176. Ogliaro, F.; de Visser, S. P.; Shaik, S. *J. Inorg. Biochem.* **2002**, *91*, 554.
177. Schöneboom, J. C.; Cohen, S.; Lin, H.; Shaik, S.; Thiel, W. *J. Am. Chem. Soc.* **2004**, *126*, 4017.
178. Ortiz de Montellano, P. R.; Stearns, R. A. *J. Am. Chem. Soc.* **1987**, *109*, 3415.
179. Atkinson, J. K.; Ingold, K. U. *Biochemistry* **1993**, *32*, 9209.
180. Newcomb, M.; Le Tadic, M.-H.; Putt, D. A.; Hollenberg, P. F. *J. Am. Chem. Soc.* **1995**, *117*, 3312.
181. Newcomb, M.; Le Tadic-Biadatti, M.-H.; Chestney, D. L.; Roberts, E. S.; Hollenberg, P. F. *J. Am. Chem. Soc.* **1995**, *117*, 12085.

182. Newcomb, M.; Shen, R.; Choi, S.-Y.; Toy, P. H.; Hollenberg, P. F.; Vaz, A. D. N.; Coon, M. J. *J. Am. Chem. Soc.* **2000**, *122*, 2677.
183. Jiang, Y.; He, X.; Ortiz de Montellano, P. R. *Biochemistry* **2006**, *45*, 533.
184. Kunze, K. L.; Mangold, B. L. K.; Wheeler, C.; Beilan, H. S.; Ortiz de Montellano, P. R. *J. Biol. Chem.* **1983**, *258*, 4202; Ortiz de Montellano, P. R.; Mangold, B. L. K.; Wheeler, C.; Kunze, K. L.; Reich, N. O. *J. Biol. Chem.* **1983**, *258*, 4208.
185. Groves, J. T.; Gross, Z.; Stern, M. K. *Inorg. Chem.* **1994**, *33*, 5065; Gross, Z.; Nimri, S.; Barzilay, C. M.; Simkovich, L. *J. Biol. Chem.* **1997**, *2*, 492.
186. Brothers, P. J.; Collman, J. P. *Acc. Chem. Res.* **1986**, *19*, 209.
187. Mansuy, D. *Pure Appl. Chem.* **1987**, *59*, 759.
188. Dolphin, D.; Matsumoto, A.; Shortman, C. *J. Am. Chem. Soc.* **1989**, *111*, 411.
189. Artaud, I.; Gregoire, N.; Battioni, J.-P.; Dupre, D.; Mansuy, D. *J. Am. Chem. Soc.* **1988**, *110*, 8714.
190. Collman, J. P.; Hampton, P. D.; Brauman, J. I. *J. Am. Chem. Soc.* **1990**, *112*, 2986.
191. Palmer, R. M. J.; Ferrige, A. G.; Moncada, S. *Nature* **1987**, *327*, 524.
192. Ignarro, L. J.; Buga, G. M.; Wood, K. S.; Byrns, R. E.; Chaudhuri, G. *Proc. Natl. Acad. Sci. U.S.A.* **1987**, *84*, 9265.
193. Furchgott, R. F.; Zawadzki, J. V. *Nature* **1980**, *288*, 373.
194. Moncada, S.; Palmer, R. M. J.; Higgs, E. A. *Pharmacol. Rev.* **1991**, *43*, 109; Snyder, S. H.; Brecht, D. S. *Scientific American* **1992**, *226* (May), 28; Butler, A. R.; Williams, D. L. H. *Chem. Soc. Rev.* **1993**, 233; Clarke, M. J.; Gaul, J. B. *Structure and Bonding*, Vol. 81; Springer-Verlag: Berlin, 1993; pp 47–181; Feldman, P. L.; Griffith, O. W.; Stuehr, D. J. *Chem. Eng. News* **1993** (December 20), 26; Williams, R. J. P. *Chem. Soc. Rev.* **1996**, 78; Cooper, C. E. *Biochim. Biophys. Acta* **1999**, *1411*, 290.
195. *The Biology of Nitric Oxide*; Moncada, S.; Marletta, M. A.; Hibbs, J. B.; Higgs, E. A., Eds.; Portland Press: London, 1992; Vols. 1 and 2; *Nitric Oxide in the Nervous System*; Vincent, S. R.; Academic Press: New York, 1995; *Nitric Oxide: Principles and Actions*; Lancaster, J., Jr., Ed.; Academic Press: San Diego, 1996.
196. Wang, P. G.; Xian, M.; Tang, X.; Wu, X.; Wen, Z.; Cai, T.; Janczuk, A. J. *Chem. Rev.* **2002**, *102*, 1091.
197. Myers, P. R.; Minor, R. L.; Guerra, R.; Bates, J. N.; Harrison, G. D. *Nature* **1990**, *345*, 161; Stamler, J. S.; Simon, D. I.; Osborne, J. A.; Mullins, M. E.; Jaraki, O.; Michel, T.; Singel, D. J.; Loscalzo, J. *Proc. Natl. Acad. Sci. U.S.A.* **1992**, *89*, 444.
198. Leone, A. M.; Palmer, R. M. J.; Knowles, R. G.; Francis, P. L.; Ashton, D. S.; Moncada, S. *J. Biol. Chem.* **1991**, *226*, 23790.
199. Alderton, W. K.; Cooper, C. E.; Knowles, R. G. *Biochem. J.* **2001**, *357*, 593; Wei, C.-C.; Crane, B. R.; Stuehr, D. J. *Chem. Rev.* **2003**, *103*, 2365; Li, H.; Poulos, T. L. *J. Inorg. Biochem.* **2005**, *99*, 293; Rousseau, D. L.; Li, D.; Couture, M.; Yeh, S.-R. *J. Inorg. Biochem.* **2005**, *99*, 306.

200. Meunier, B.; de Visser, S. P.; Shaik, S. *Chem. Rev.* **2004**, *104*, 3947.
201. Jia, Q.; Cai, T.; Huang, M.; Li, H.; Xian, M.; Poulos, T. L.; Wang, P. G. *J. Med. Chem.* **2003**, *46*, 2271.
202. Hurshman, A. R.; Marletta, M. A.; *Biochemistry* **2002**, *41*, 3439; Davydov, R.; Ledbetter-Rogers, A.; Martasek, P.; Larukin, M.; Sono, M.; Daeson, J. H.; Masters, B. S.; Hoffman, B. M. *Biochemistry* **2002**, *41*, 10375.
203. Wang, J. L.; Rousseau, D. L.; Abu-Soud, H. M.; Stuehr, D. J. *Proc. Natl. Acad. Sci. U.S.A.* **1994**, *91*, 10512; Abu-Soud, H. M.; Wang, J. L.; Rousseau, D. L.; Fukuto, J. M.; Ignarro, L. J.; Steuhr, D. J. *J. Biol. Chem.* **1995**, *270*, 22997.
204. Ford, P. C.; Lorkovic, I. M. *Chem. Rev.* **2002**, *102*, 993; Møller, J. K. S.; Skibsted, L. H. *Chem. Rev.* **2002**, *102*, 1167.
205. Hoshino, M.; Maeda, M.; Konishi, R.; Seki, H.; Ford, P. C. *J. Am. Chem. Soc.* **1996**, *118*, 5702.
206. Hoshino, M.; Ozawa, K.; Seki, H.; Ford, P. C. *J. Am. Chem. Soc.* **1993**, *115*, 9568.
207. Laverman, L. E.; Hoshino, M.; Ford, P. C. *J. Am. Chem. Soc.* **1997**, *119*, 12663.
208. Laverman, L. E.; Wanat, A.; Oszejca, J.; Stochel, G.; Ford, P. C.; van Eldik, R. *J. Am. Chem. Soc.* **2001**, *123*, 285.
209. Ostrich, I. J.; Gordon, L.; Dodgen, H. W.; Hunt, J. P. *Inorg. Chem.* **1980**, *19*, 619.
210. Traylor, T. G.; Magde, D.; Marsters, J.; Jongeward, K.; Wu, G.-Z.; Walda, K. *J. Am. Chem. Soc.* **1993**, *115*, 4808.
211. Ionascu, D.; Gruia, F.; Ye, X.; Yu, A.; Rosca, F.; Beck, C.; Demidov, A.; Olson, J. S.; Champion, P. M. *J. Am. Chem. Soc.* **2005**, *127*, 16921.
212. Ye, X.; Yu, A.; Champion, P. M. *J. Am. Chem. Soc.* **2006**, *128*, 1444.
213. Abu-Soud, H. M.; Wu, C.; Ghosh, D. K.; Stuehr, D. J. *Biochemistry* **1998**, *37*, 3777.
214. Boggs, S.; Huang, L.; Stuehr, D. J. *Biochemistry* **2000**, *39*, 2332.
215. Santolini, J.; Adak, S.; Curran, C. M.; Stuehr, D. J. *J. Biol. Chem.* **2001**, *276*, 1233; Santolini, J.; Meade, A. L.; Stuehr, D. J. *J. Biol. Chem.* **2001**, *276*, 48887.
216. Møller, J. K. S.; Skibsted, L. H. *Chem. Eur. J.* **2004**, *10*, 2291.
217. Herold, S.; Röck, G. *Biochemistry* **2005**, *44*, 6223.
218. Khaitnov, V. G.; Sharma, V. S.; Magde, D.; Koesling, D. *Biochemistry* **1997**, *36*, 6814.
219. Herold, S.; Exner, M.; Nauser, T. *Biochemistry* **2001**, *40*, 3385.
220. Butler, A. R.; Megson, I. L.; Wright, P. G. *Biochim. Biophys. Acta* **1998**, *1425*, 168.
221. Liu, X.; Miller, M. J. S.; Joshi, M. S.; Sadowska-Krowicka, H.; Clark, D. A.; Lancaster, J. R., Jr. *J. Biol. Chem.* **1998**, *273*, 18709.
222. Liao, J. C.; Hein, T. W.; Vaughn, M. W.; Huang, K.-T.; Kuo, L. *Proc. Natl. Acad. Sci. U.S.A.* **1999**, *96*, 9027.

223. Gow, A. J.; Lushinger, B. P.; Pawloski, J. R.; Singel, D. J.; Stamler, J. S. *Proc. Natl. Acad. Sci. U.S.A.* **1999**, *96*, 9027.
224. Chan, N.-L.; Kavanaugh, J. S.; Rogers, P. H.; Arnone, A. *Biochemistry* **2004**, *43*, 118.
225. Zhao, Y.-L.; Houk, K. N. *J. Am. Chem. Soc.* **2006**, *128*, 1422.
226. Aravindakumar, C. A.; De Ley, M.; Ceulemans, J. *J. Chem. Soc., Perkin Trans. 2* **2002**, 663.
227. Herold, S.; Röck, G. *J. Biol. Chem.* **2003**, *278*, 6623.
228. Lymar, S. V.; Shafirovich, V.; Poskrebyshev, G. A. *Inorg. Chem.* **2005**, *44*, 5212.
229. Riordan, E.; Minogue, N.; Healy, D.; O'Driscoll, P.; Sodeau, J. R. *J. Phys. Chem. A* **2005**, *109*, 779.
230. Shafirovich, V.; Lymar, S. V.; *Proc. Natl. Acad. Sci. U.S.A.* **2002**, *99*, 7340.
231. Bartberger, M. D.; Liu, W.; Ford, E.; Miranda, K. M.; Switzer, C.; Fukuto, J. M.; Farmer, P. J.; Wink, D. A.; Houk, K. N. *Proc. Natl. Acad. Sci. U.S.A.* **2002**, *99*, 10958.
232. Merényi, G.; Lind, J.; Czapski, G.; Goldstein, S. *Inorg. Chem.* **2003**, *42*, 3796.
233. Goldstein, S.; Czapski, G. *J. Am. Chem. Soc.* **1995**, *117*, 12078.
234. McKee, M. L. *J. Am. Chem. Soc.* **1995**, *117*, 1629.
235. Goldstein, S.; Czapski, G. *J. Am. Chem. Soc.* **1996**, *118*, 3419, 6806.
236. Beckman, J. S.; Beckman, T. W.; Chen, J.; Marshall, P. A.; Freeman, B. A. *Proc. Natl. Acad. Sci. U.S.A.* **1990**, *87*, 1620.
237. Lymar, S. V.; Hurst, J. K. *J. Am. Chem. Soc.* **1995**, *117*, 8867.
238. Kissner, R.; Nauser, T.; Kurz, C.; Koppenol, W. H. *HUBMB Life* **2003**, *55*, 567; Goldstein, S.; Lind, J.; Merényi, G. *Chem. Rev.* **2005**, *105*, 2457.
239. Kissner, R.; Koppenol, W. H.; *J. Am. Chem. Soc.* **2002**, *124*, 234, and references therein.
240. Lymar, S. V.; Khairutdinov, R. F.; Hurst, J. K. *Inorg. Chem.* **2003**, *42*, 5259, and references therein.

9

Kinetics in Heterogeneous Systems

In this Chapter, a heterogeneous system is one in which the reactants are present in at least two phases. The discussion will concentrate on two such conditions, two-phase gas/liquid systems and three-phase gas/liquid/solid systems. Chemists tend to favor homogeneous conditions, with the reactants all in one phase, because they provide more controlled and reproducible conditions. However, heterogeneous conditions are often preferred in industrial processes because of the ease of separating the catalyst from the products. In many mechanistic studies, heterogeneity adds a complicating feature to be avoided, but there are times when this cannot be done, or when it happens unexpectedly.

In gas/liquid systems, the gas often has limited solubility in the liquid which contains the other reagents. As a consequence, there can be problems of mass transport of the gaseous reactant from the gas to the liquid phase. Mass transport can limit the concentration of the gas in the liquid and/or become a rate-limiting feature of the system. These features can confuse interpretations of product distributions and rate laws.

The gas/liquid/solid systems generally involve reactants in the gas and liquid phases and a catalyst as the solid phase. In some cases, the solid may be produced from initially homogeneous conditions, and a question arises as to whether the real catalyst is the original species added or the solid product formed under the reaction conditions. There are further questions about the factors that may control the rate of the catalytic process.

9.1 GAS/LIQUID HETEROGENEOUS SYSTEMS

In the chemistry laboratory, these systems are most often encountered with the gases H_2 or CO reacting with substrate and possibly a catalyst in the liquid phase. For the mechanistic interpretation of kinetic observations, an important factor is the rate of mass transfer of the gas to the liquid phase. The rate of gas absorption into the liquid is typically represented as a first-order process, driven by the difference between the saturated gas concentration $[G(t)]_s$ and the concentration at any time $[G(t)]$, as given by

$$\frac{d[G(t)]}{dt} = k_L A ([G(t)]_f - [G(t)]) \quad (9.1)$$

where $k_L A$ is an effective first-order rate constant. This constant is taken as a product of an inherent absorption rate constant, k_L , and something related to the surface area of the liquid phase, A . In principle, k_L depends on the gas and the solvent, while A depends on the configuration of the reactor and the nature and rate of mixing.

Application of mass balance conditions to the total moles of G in the gas and liquid phases at any time and at the end of the process, along with the ideal gas law gives

$$\frac{PV_{(g)}}{RT} + [G(t)]V_{(l)} = \frac{P_f V_{(g)}}{RT} + [G(t)]_f V_{(l)} \quad (9.2)$$

where $V_{(g)}$ and $V_{(l)}$ represent the volumes of the gas and liquid phases, respectively. Rearrangement gives

$$[G(t)]_f - [G(t)] = \frac{(P - P_f)V_{(g)}}{RTV_{(l)}} \quad (9.3)$$

and differentiation of Eq. (9.3) gives

$$\frac{d[G(t)]}{dt} = - \left(\frac{V_{(g)}}{RTV_{(l)}} \right) \frac{dP}{dt} \quad (9.4)$$

Substitution from Eq. (9.3) and (9.4) into Eq. (9.1) gives a differential equation in P which can be integrated over the limits $P = P_0$ to P_f and $t = 0$ to t to obtain the standard first-order equation

$$\ln(P - P_f) - \ln(P_0 - P_f) = -k_L A t \quad (9.5)$$

A plot of the first term on the left versus time should be linear with a slope of $-k_L A$. It should be noted that the pressures in these equations refer to the partial pressures of the gas being absorbed and will be less than the total pressure if the solvent has a significant vapor pressure.

In studies concerned with the rate of this process, $k_L A$ is determined by degassing the solvent, introducing the reactant gas at some known pressure, P_0 , and then turning on the stirrer and measuring the pressure, P , as a function of time. Since gas absorption is slow in the absence of mixing, the fastest rates measured generally are limited only by the time response of the pressure sensor.

Although values of $k_L A$ obviously depend on a number of parameters that are particular to the system, it is possible to provide some typical magnitudes. These measurements are rarely found in standard chemistry

sources, and some representative references are given.¹ The recent study of Bellefon and co-workers,² comparing turbine and magnetic stirring in small reactors, may be particularly relevant to chemists. For a standard benchtop reactor, $k_L A$ typically is in the range of ~ 0.005 to 2 s^{-1} as the mixing rate increases from ~ 100 to 1500 rpm . Two examples from a study by Morisi and co-workers³ are shown in Figure 9.1.

With an appropriate mixing propeller or baffles to minimize vortex formation, $k_L A$ often becomes independent of the rate of mixing at values $\geq 1500\text{--}2000 \text{ rpm}$. Standard mixers found in chemistry laboratories have upper limit rates of 1000 rpm , often producing vortexing and therefore poorer mixing towards the upper rate limit. Although these are rather sweeping generalizations, it is clear that gas absorption into a liquid can occur with half-times of several tens of seconds for a typical reactor at moderate mixing rates.

Another factor of interest for studies in this area is the solubility of the gas in the liquid phase. This is needed to calculate the mass transfer rate and the molar concentration at saturation of the gas at a particular partial pressure of the gas. However, gas solubilities are rarely given in molar units. Most commonly, one finds the Ostwald coefficient, L , which is the concentration in the liquid phase divided by the concentration in the gas phase (i.e. the equilibrium constant for $G_{(g)}$ to $G_{(l)}$), or the Henry's law constant, H , which usually is defined as the partial pressure of the gas, $P_{(g)}$,

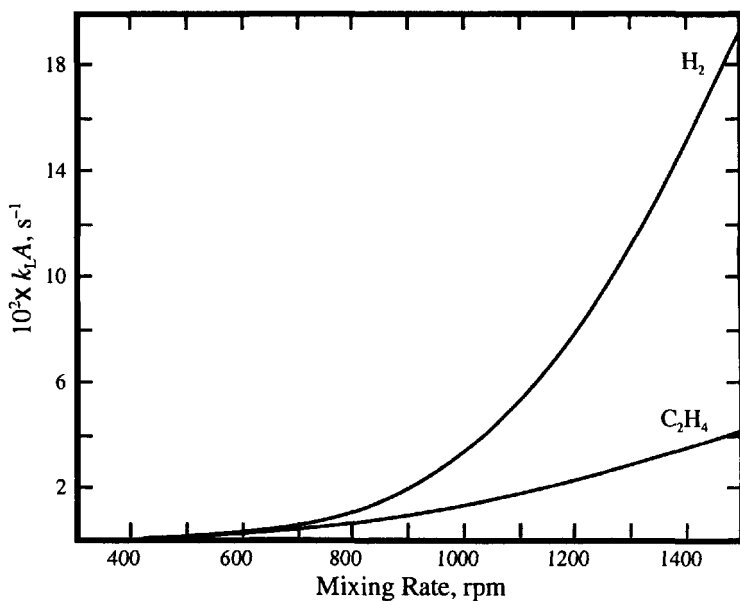


Figure 9.1. Variation of $k_L A$ with mixing rate for absorption of H_2 and C_2H_4 into n -hexane in a reactor with a 12.5 cm internal diameter.

divided by the mole fraction of gas in the liquid phase, $\chi_{(l)}$, or simply $\chi_{(l)}$ at a specified $P_{(g)}$. The relationships between these quantities and other less frequently used terms are given in the review by Battino and Clever.⁴

The solubilities of some gases are given in Tables 9.1 and 9.2. These values, at 1.00 atm partial pressure of the gas, can be extended to other pressures since Henry's law is reasonably obeyed by these gases for pressures ≤ 10 atm. The solubilities in Table 9.1 are calculated from the L values of Katayama and Nitta⁵ and the temperature dependencies of their L values have been fitted to $L_T = L_0 \exp(E_L/RT)$ to obtain the values of L_0 and E_L in Table 9.1. It may be noted that the E_L values seem to be a property of the gas rather than the solvent.

It is apparent from these examples that these gases have modest solubilities in the 2–10 mM range at 1 atm partial pressure in various solvents, and that CO is about three times more soluble than H₂. Table 9.1 shows that the molar solubility may decrease or increase with decreasing temperature. Many more data are available from the series edited by Cargill,⁶ the review of Battino and Clever⁴ and the book by Fogg and Gerrard.⁷

In studies with kinetic and mechanistic goals, it obviously is an advantage to work under conditions for which the gas/liquid mass transfer is not rate limiting. Otherwise, the experimental rate law may give an incorrect picture of the molecular mechanism. One way to avoid such problems is to work under conditions in which the rate of the chemical reaction is much slower than mass transfer. This typically would require reaction half-times on the tens of minutes time scale. Standard tests for mass transfer control are to increase the mixing rate and/or decrease the reaction rate by reducing the concentrations of reactants in the liquid phase. If mass transfer is not a limitation, then mixing rate should not affect the rate, and concentration changes should not affect the rate law.

For many systems of interest to chemists, the simplest test is to change the concentration of the catalyst and observe the effect on the rate constant, with the assumption that the rate is first-order in the catalyst. Simulated

Table 9.1. Solubilities (mM) of H₂ and N₂ at 1.00 atm.

Solvent	Gas	Temp (°C)					L_0	E_L (cal mol ⁻¹)
		25	0	-20	-40	-60		
Methanol	H ₂	3.94	3.59	3.27	2.91	2.51	0.6896	-1165.8
<i>n</i> -Propanol	H ₂	3.07	2.78	2.52	2.23	1.91	0.5750	-1205.6
<i>n</i> -Hexane	H ₂	5.26	4.72	4.23	3.70	3.13	1.0963	-1269.0
Methanol	N ₂	6.57	6.86	7.09	7.32	7.55	0.2636	-293.0
<i>n</i> -Propanol	N ₂	5.23	5.46	5.65	5.84	6.02	0.2092	-290.8
<i>i</i> -Propanol	N ₂	5.86	6.09	6.26	6.43	6.59	0.2485	-325.4
<i>n</i> -Hexane	N ₂	10.3	10.5	10.7	10.9	11.0	0.4964	-290.8

Table 9.2. Solubilities (mM) of H₂ and CO in Various Solvents at 25°C and 1.00 atm.

Solvent	[H ₂]	[CO]
Methanol	3.94 ^a	9.5 ^b , 8.3 ^c
Ethanol	3.34 ^a	8.35 ^c
<i>n</i> -Propanol	3.07 ^a	
2-Propanol		7.90 ^c
<i>n</i> -Hexane	5.26 ^a	13.5 ^c
Toluene	2.99 ^d	7.32 ^c
Acetone	3.65 ^d	14.8 ^c
Acetonitrile	3.38 ^d	
Carbon tetrachloride	3.34 ^e	8.89 ^e , 9.02 ^e
1,1,2-Trichloroethane	2.1 ^f	5.2 ^f

^a Katayama, T.; Nitta, T. *J. Chem. Eng. Data* **1976**, *21*, 194.

^b Liu, Q.; Takemura, F.; Yabe, A. *J. Chem. Eng. Data* **1996**, *41*, 589.

^c Cargill, R. W., Ed. *Carbon Monoxide. Solubility Data Series*; Pergamon Press, Oxford, **1990**; Vol. 43.

^d Brunner, E. *J. Chem. Eng. Data* **1985**, *30*, 269.

^e Tominga, T.; Battino, R.; Gorowara, H. K.; Dixon, R. D.; Wilhelm, E. *J. Chem. Eng. Data* **1986**, *31*, 175.

^f Lyke, S. E.; Lilge, M. A.; Ozanich, R. M.; Nelson, D. A.; James, B. R.; Lee, C.-L. *Ind. Eng. Chem. Prod. Res. Dev.* **1986**, *25*, 517.

results for such a system are shown in Figure 9.2, where the dynamic processes are absorption of H₂ into the solvent and hydrogenation of a substrate with a rate that is first-order in the concentrations of both H₂ and catalyst. The overall rate of loss of substrate is approximately zero-order because the concentrations of H₂ and catalyst do not change for a particular run. By changing the catalyst concentration, the half-time is changed from ~220 min to ~10 min, and $k_1A = 0.03 \text{ s}^{-1}$. From the dashed line in Figure 9.2, it can be seen that k_0 is close to first-order in catalyst concentration as long as the value of $k_0 \leq 2.5 \times 10^{-5} \text{ M s}^{-1}$, but then starts to level off and approach the condition where H₂ absorption becomes rate-limiting at the higher catalyst concentrations. In applying this test, one should observe that $k_0/[\text{Catalyst}]$ is constant as long as mass transfer is not a limitation, but will become progressively smaller as the catalyst concentration increases and mass transfer becomes important.

This background information on mass transport and gas solubility can be made more relevant by discussion of some examples. A question about mass transfer already has been raised by Blackmond and co-workers⁸ with regard to the study of Landis and Halpern⁹ on the hydrogenation of methyl-Z- α -acetamidocinnamate by Rh(dipamp)⁺ in methanol with a magnetically stirred reactor. This issue has been mentioned in Chapter 5. A preliminary analysis would suggest that mass transport should not have been a problem

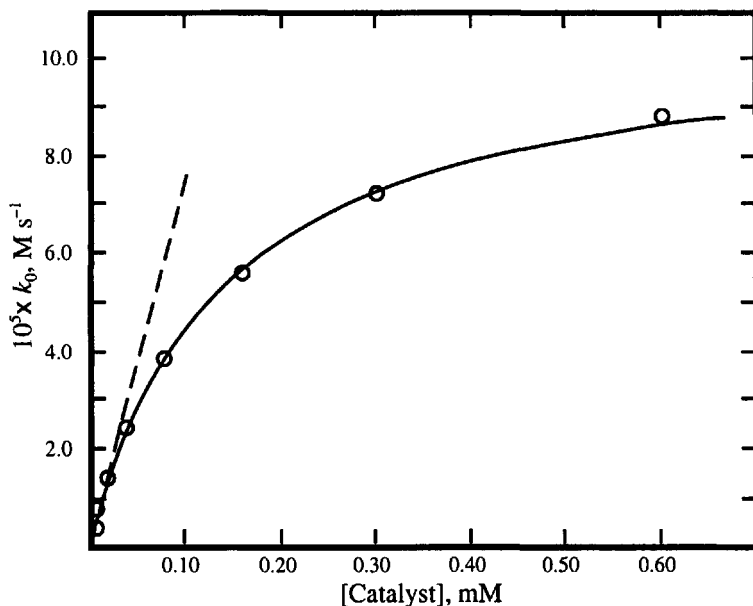


Figure 9.2. Variation of the rate constant, k_0 , with catalyst concentration. The dashed line represents the behavior if k_0 is first-order in [Catalyst].

for Landis and Halpern because the reactions occur on the tens of minutes time scale under their conditions. In this system, the rate of production of the dominant *S*-product shows saturation kinetics with increasing H_2 pressure, while the rate for the minor *R*-product is simply first-order in H_2 pressure. As a result, the percentage of *S*-product decreases significantly for pressures >1 atm. Blackmond and co-workers discussed the possibility that this change in product ratio might be due to changing H_2 concentrations due to mass transfer effects. They are somewhat ambiguous in their conclusions since they initially claim "that it is possible to reproduce their (Landis and Halpern's) observed variation of enantioselectivity with pressure, while holding hydrogen pressure constant and instead systematically changing $[\text{H}_2]$ by varying the gas-liquid mass transfer rate". But later they note "that the implicit assumption that the solution was near $[\text{H}_2]_{\text{sat}}$ made (by Landis and Halpern) is valid at 1000 kPa provided that the $k_L A$ value in the experimental system was 0.05 s^{-1} or greater". The latter seems reasonable on the basis of the above discussion of the magnitude of $k_L A$, but Blackmond and co-workers never show the time relationship of mass transfer and product formation for the actual conditions used by Landis and Halpern. This is shown in Figure 9.3 for their fastest run at 25°C . It should be noted that Landis and Halpern never actually give the H_2 concentration in methanol, but one can deduce from the parameters derived from the saturation kinetics that they are using a

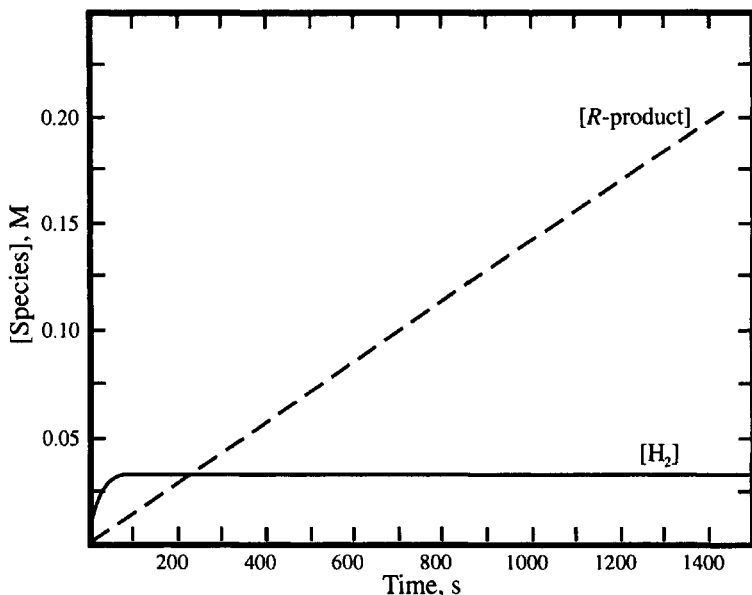


Figure 9.3. Time dependence of the concentrations of H₂ and major product during the reaction of methyl-Z- α -acetamidocinnamate (0.4 M) and H₂ (9.07 atm) catalysed by Rh(dipamp)⁺ (0.45 mM) in methanol at 25°C.

solubility of ~4.0 mM at 1 atm of H₂ (close to values in Table 9.1) and this value has been used in Figure 9.3. The Figure shows the time dependence of the concentration of H₂ and R-product for about 50% of reaction. It is apparent that mass transfer effects are complete in ~80 s and the [H₂] is at its saturation value for the remainder of the reaction, as assumed by Landis and Halpern.

The above example provides some hints as to when mass transfer could be a complicating factor in stereoselective hydrogenations. If the reaction half-time is of the order of minutes, and the product distribution depends on H₂ pressure, then mass transfer might affect the observations. In either case, the effects of mixing rate and catalyst concentration (i.e. variation of the overall rate) should be investigated.

It is rather rare to find published studies in this area in which some evaluation of mass transfer characteristics are reported. An exception is the study of Noyori and co-workers¹⁰ on the hydrogenation in methanol of α -(acylamino)acrylic esters by Ru(CH₃CO₂)₂(*S*-BINAP), where BINAP is 2,2'-bis(diphenylphosphino)-1,1'-binaphthyl. However, the observations are sometimes more confusing than enlightening. The reactor was a Teflon-coated stainless steel autoclave with an overhead stirrer, normally driven at 600 rpm, and containing 15 mL of solvent at 30°C. The kinetics seem to be moderately well behaved over somewhat limited ranges of

concentrations of catalyst (0.1–1 mM), H₂ (0.7–1.2 atm), substrate (100–400 mM), product (0–250 mM) and acetic acid (0–10 mM). The pseudo-first-order rate constants are in the range of (1–10)×10⁻⁵ s⁻¹ and show a first-order dependence on the concentration of catalyst and H₂ pressure, and inhibition by increasing substrate concentration. The authors note that first-order plots are nonlinear for pressures <0.7 atm, and suggest that this is due to a mass transfer problem. This seems unexpected on the basis of the previous discussion because the time scale for the reactions is typically from ~10 to 200 min and the rate should be slower at the lower H₂ pressure, and therefore mass transfer effects should be less important. However, detailed inspection reveals a more serious problem with these results. The rate was found to have an inverse dependence on the concentration of the reactant olefin, (as shown in the Supporting Information¹⁰) yet the rate constants are determined from normal first-order plots of ln [olefin] versus time. In fact, all of the runs with varying [olefin] give reasonably linear plots of the appropriate integrated inverse-order rate law, as shown in Section 5.6.3.1.

Reactions between gases and liquid phase reactants in NMR sample tubes can be expected to be especially prone to mass transfer problems. The liquid has a relatively small area exposed to the gas and there is essentially no mixing while the sample is in the NMR spectrometer. Oldham and Heinekey¹¹ have reported one such study on the reaction of H₂ with the hydridotris(1-pyrazolyl)borate complex, (Tp)Ir(PPh₃)(C₂H₄), in CD₂Cl₂. They observed a linear plot of -ln [(Tp)Ir(PPh₃)(C₂H₄)] versus time for an H₂ pressure of 750 Torr, but noted that the plots showed significant curvature at lower pressures (550 and 359 Torr). They ascribed this to a mass transfer effect, but again it seems strange that the slower reactions would be more affected by mass transfer. An explanation of these observations can be based on the fact that the saturated H₂ concentration (2.3–1.1 mM) is somewhat less than the initial (Tp)Ir(PPh₃)(C₂H₄) concentration (3.51 mM) and that the samples were shaken for 60 s before insertion into the NMR probe. During the latter period, one might expect that the [H₂] would reach close to its saturation value, but would be depleted by the reaction once in the probe because of slow mass transfer and the relatively high concentration of (Tp)Ir(PPh₃)(C₂H₄). This depletion would be more significant at the lower initial concentrations, i.e. pressures of H₂, and could be the source of the nonlinear plots at lower pressures. Simulations based on this model and the published pseudo-first-order rate constants are shown in Figure 9.4. The simulations assume that [H₂] reaches 90% of its saturation value during the initial mixing period in the NMR probe, with $k_L A = 5 \times 10^{-4} \text{ s}^{-1}$. The latter is required to produce a close to linear plot at 750 Torr, but clearly gives increasing nonlinearity as the pressure is reduced. The $k_L A$ value suggests that mass transfer is ~100 times slower in an NMR tube compared to a batch reactor with normal stirring rates.

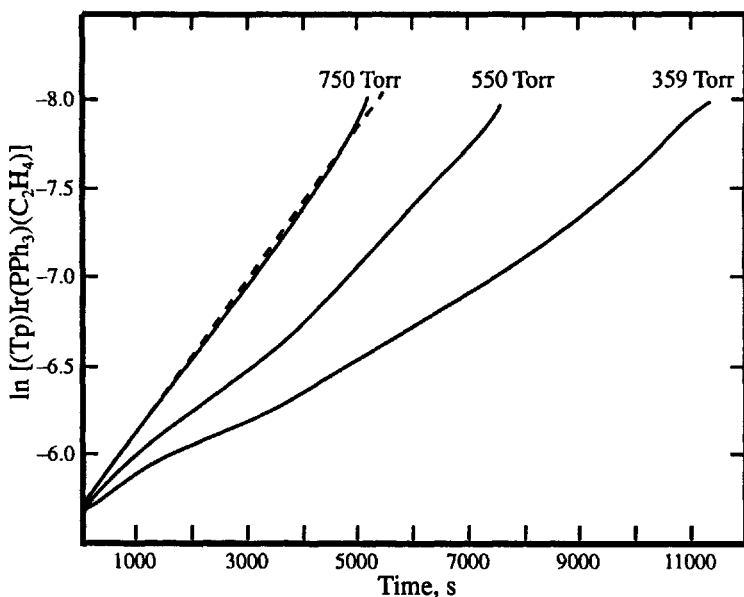


Figure 9.4. Simulation of the variation of $\ln [(Tp)Ir(PPh_3)(C_2H_4)]$ with time for the reaction of $(Tp)Ir(PPh_3)(C_2H_4)$ with H_2 in an NMR tube, based on parameters described in the text. The dashed line shows a possible linear fit at 750 Torr of H_2 .

An example where the reaction times would indicate a potential problem with mass transfer occurs in the study of Garrou and Heck¹² on the reaction of CO with a wide range of *trans*- $M(PR_3)_2(R')X$ complexes ($M = Ni, Pd, Pt$). The observed rate constants are often $>10^{-3} s^{-1}$, especially for Ni and Pd systems, so that the half-times are <10 min. It should be noted that this study was done by first saturating the solvent with CO before adding the metal complex, whose concentration (~ 0.01 – 0.03 M) was substantially higher than the saturated CO concentration. Mass transfer might explain the very similar reactivities of the $Ni(P(C_6H_5)_3)_2(C_6H_5)X$ complexes, where $X = Cl^-, Br^-,$ and I^- , and failure of the iodo complex to give good first-order kinetics. The observation that some systems show initial rapid partial CO uptake followed by slower uptake of the complete 1 equivalent of CO also could be a mass transfer effect of a somewhat different sort. The metal complex may initially consume all of the dissolved CO and this will start to be replaced from the gaseous layer of solvent vapor and CO immediately above the liquid. The CO from the bulk gas phase will move into this layer by a slower gas diffusion process, unless the gas phase also is mixed. The liquid layer is protected to a certain extent by a layer of its own vapor which has a lower partial pressure of CO than the bulk gas phase. Mixing of the gas phase is not a typical feature of gas reactors in the chemistry laboratory.

9.2 GAS/LIQUID/SOLID HETEROGENEOUS SYSTEMS

In many systems, a solid catalyst is present along with reactants in the gas and liquid phases. The new feature in these systems is the solid, and there are several aspects of this phase that must be defined. The solid generally is considered to contain one or more types of active sites where reactants are adsorbed and the catalytic chemistry occurs. These sites may be categorized as surface sites and internal sites, and are shown in an idealized fashion in Figure 9.5. The surface sites are types A and B, and may be on different faces of the solid, as shown in Figure 9.5, or all on one face. Sometimes, special attributes are assigned to edge or corner sites (not shown). The C sites in Figure 9.5 are internal, and those shown are pores in the solid. Internal sites also may be along the sides of channels through the solid.

The main mechanistic difference between surface and internal sites is that the latter have an additional mass transfer problem of getting the reactant(s) through the pore or channel to the active internal site, and then moving the product away from the site. This disadvantage for internal sites may be overcome by their greater reactivity and selectivity. For a bimolecular reaction of species adsorbed at surface sites, there is a mass transfer problem of bringing the two species together from the sites to which they are attached. This is often pictured as migration or slippage across the surface. Tests for these mass transfer limitations are discussed later in this Chapter. The gas/liquid mass transfer situation is analogous to that described in the previous Section. It generally is observed that the presence of solid in the stirred liquid has minor effects on $k_L A$ for the gas/liquid transfer, but it is always best to actually determine $k_L A$ under the actual conditions with the solid present.

There are two generally recognized modes for adsorption of the reactant(s) at the active sites. Physical adsorption or physisorption involves moderately weak interactions such as hydrogen bonding, electrostatic dipole-dipole forces and/or van der Waals forces. Physisorption causes

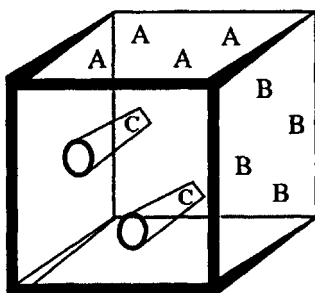


Figure 9.5. Schematic diagram of the active sites on the surface (A, B) and in a pore (C) of a solid.

only modest changes in the structure and bonding, and the adsorbed species are often considered to be in moderately labile equilibrium with the species in solution. Chemical adsorption or chemisorption involves some form of chemical bonding between the reactant and the atoms, molecules or ions at the active sites in the solid. This process can be highly variable in nature, such as formation of π -complexes or actual dissociation of the reactant, as occurs when H_2 reacts with Pt metal to give Pt-H species at the active sites. The latter type of process is referred to as dissociative adsorption. In kinetic models, chemisorption sometimes is treated as an irreversible process because the forces involved generally are much stronger than those for physisorption, but there is clearly a gray area between weak chemisorption and physisorption.

9.2.1 Kinetic Aspects of Gas/Liquid/Solid Systems

The following discussion is concerned with systems in which the catalyst is known or assumed to be a solid. The general reaction pathways are described for the adsorption of the reactants at the active site(s) on the catalyst. Rate laws for several commonly assumed reaction sequences are developed and are discussed for the widely studied hydrogenation of nitrobenzene. The situation in which the state of the catalyst may be uncertain is the subject of Section 9.3.

To clarify the analysis that follows, it is necessary to describe the way that the amounts of species in the different phases are designated. For a solid, S , the number of active sites will be indicated by (S_0) , usually taken to be moles per unit mass of the solid. A species, X , adsorbed on the solid will be indicated by $(X \cdot S)$, in the same units as (S_0) . If X is in solution, its molar concentration will be given as usual by $[X]$. In short, round brackets are used for species in the solid, and square brackets for species in solution. The concentration of X in the gas phase will be represented by the partial pressure of X , P_X . In the literature, one encounters a wide range of ways to designate these quantities, such as C for some generic concentration, n for the number of moles and χ for the mole fraction.

9.2.1.1 Kinetic Models and Examples

Reactions on solid surfaces can pose complicated kinetic possibilities and it often is necessary to make some assumptions before deriving a rate law and then to test the initial assumptions by comparing the result to the observations. Scheme 9.1 outlines the main possibilities for a system in which a gaseous species $D_{(g)}$ dissolves in the liquid phase to give $D_{(l)}$ and some species $E_{(l)}$ which is initially in the liquid phase. Both D and E may be adsorbed on the solid catalyst S to give $D \cdot S$ and $E \cdot S$, respectively. Since the solid is a catalyst, it is assumed that at least one, or possibly both, of the adsorbed species are reacting to form an adsorbed product, $P_i \cdot S$, which dissociates to give various products P_i in the liquid phase and a vacant site.

Scheme 9.1

The process in (i) is gas/liquid mass transfer that already has been discussed in detail. Steps (ii) and (iii) suggest a solid, S, with only one type of active site which is competitively adsorbing species D and E, but there could be two types of sites which selectively adsorb D and E. It also is possible that one or both of the adsorption steps (ii) and (iii) are not reversible, possibly because of chemisorption. To simplify the system, it is often assumed that the product is weakly adsorbed so that the second step in each of steps (iv)–(vi) is not rate controlling.

The rate controlling step typically is taken to be the first step in reactions (iv)–(vi) because adsorption must be the source of the catalysis. This inevitably leads to the amount or concentration of the adsorbed species, $D \cdot S$ and/or $E \cdot S$, appearing in the rate law, and one needs some means of expressing this quantity. This is most commonly done by the Langmuir isotherm which assumes that the adsorption process is a rapidly maintained equilibrium. If only species D is adsorbed and there is only one type of active site with a total number of active sites (S_0), then $(S_0) = (S) + (D \cdot S)$, where (S) represents the number of unoccupied sites. The equilibrium constant for the adsorption process is defined by

$$K_D = \frac{(D \cdot S)}{[D](S)} \quad (9.6)$$

After taking the reciprocal of both sides of Eq. (9.6), and adding 1 to both sides, one obtains, after rearrangement, the Langmuir isotherm equation

$$\sigma_D = \frac{(D \cdot S)}{(S_0)} = \frac{K_D[D]}{1 + K_D[D]} \quad (9.7)$$

where σ_D is the fraction of sites that are occupied. This allows one to

express the number of occupied sites ($D \cdot S$) in terms of $[D]$, K_D and (S_0) . The Langmuir isotherm equation is most often developed for gas/solid systems, in which case $[D]$ is replaced by the partial pressure of the gas. If D and E are adsorbed at independent sites, S_D and S_E , respectively, then a completely analogous development gives

$$(D \cdot S) = (S_{D0}) \frac{K_D [D]}{1 + K_D [D]} \quad \text{and} \quad (E \cdot S) = (S_{E0}) \frac{K_E [E]}{1 + K_E [E]} \quad (9.8)$$

where (S_{D0}) and (S_{E0}) are the total numbers of each type of site, and K_D and K_E are the equilibrium constants for adsorption at the respective sites. If D and E are adsorbed competitively at one type of site, then

$$(D \cdot S) = (S_0) \frac{K_D [D]}{1 + K_D [D] + K_E [E]} \quad (9.9)$$

$$(E \cdot S) = (S_0) \frac{K_E [E]}{1 + K_D [D] + K_E [E]}$$

These expressions have direct analogues for equilibria in solution which may in part explain their common usage in the analysis of solid state catalysis.

It is often noted that the Langmuir isotherm does not provide an adequate description when a large fraction of the sites are occupied. This problem is ascribed to the fact that the sites are not independent at high coverage, so that K actually decreases as the coverage increases, or the sites may be similar but not identical and therefore have a range of K values. On the other hand, it may be possible to independently determine effective K values under the experimental conditions and compare them to values from the kinetic analysis. For competitive adsorption, this might be done by using a derivative of E which has the functions thought to be involved in adsorption but not the function that reacts with $D \cdot S$. An obvious limitation of the Langmuir isotherm is that it requires adsorption to be a rapidly reversible process on the time scale of the overall reaction. Therefore, it may not be applicable to some cases of chemisorption.

Recently, Ostrovskii¹³ has suggested that molar heats of chemisorption are constant "over wide ranges of coverage", consistent with the Langmuir isotherm, and that earlier calorimetric measurements suggesting variations with coverage suffer from experimental difficulties. This is supported by the earlier study of Weller and co-workers¹⁴ who found that the Langmuir isotherm was as good or better than the Temkin or Freundlich isotherms for 16 of the 19 systems they examined. Ostrovskii has proposed that this may resolve the long-standing paradox^{15,16} that kinetic studies seemed to be adequately described by the Langmuir isotherm, even under conditions where it might be expected that this isotherm would not apply. On the other

hand, heats of adsorption on single crystals of metals¹⁷ sometimes show substantial differences between crystal faces and changes with coverage. Even the state of NO adsorbed on Ni{100} changes from dissociated N and O atoms at low coverage to molecular NO at modest coverage.¹⁸ The seeming disparity between the single crystal and more macroscopic observations could just reflect that the latter are giving an overall average of the various processes, or are dominated by the thermodynamically most favorable process. In any case, the message for the moment seems to be that the Langmuir isotherm is adequate for most kinetic studies, but this does not guarantee that the adsorption is a simple process.

Mechanistic formulations in this area usually begin from one of two simplified mechanisms, both of which assume the conditions of the Langmuir isotherm. The Langmuir–Hinshelwood mechanism¹⁹ assumes that the rate controlling step is between the two adsorbed species D•S and E•S, so that the overall mechanism includes steps (ii), (iii) and (vi) in Scheme 9.1. The Eley–Rideal or Rideal mechanism²⁰ assumes that the rate controlling step is between a species in solution and an adsorbed species. Thus, if D is the adsorbed species, the mechanism would include steps (ii) and (v) in Scheme 9.1.

For the case of independent or noncompetitive adsorption, the expressions in Eq. (9.8) can be used to obtain the rate of production of product. The Langmuir–Hinshelwood mechanism gives

$$\frac{d(P_3)}{dt} = k_6(D\bullet S)(E\bullet S) = k_6(S_{D0})(S_{E0}) \left(\frac{K_D[D]}{1 + K_D[D]} \right) \left(\frac{K_E[E]}{1 + K_E[E]} \right) \quad (9.10)$$

while the Eley–Rideal mechanism gives

$$\frac{d(P_2)}{dt} = k_5[E](D\bullet S) = k_5(S_{D0})[E] \left(\frac{K_D[D]}{1 + K_D[D]} \right) \quad (9.11)$$

For competitive adsorption, substitutions for (D•S) and (E•S) from Eq. (9.9) into Eq. (9.10) gives for the Langmuir–Hinshelwood mechanism

$$\frac{d(P_3)}{dt} = k_6(S_0)^2 \frac{K_D K_E [D][E]}{(1 + K_D[D] + K_E[E])^2} \quad (9.12)$$

and substitution for (D•S) from Eq. (9.9) into Eq. (9.11) gives for the Eley–Rideal mechanism

$$\frac{d(P_2)}{dt} = k_5(S_0)[E] \left(\frac{K_D[D]}{1 + K_D[D] + K_E[E]} \right) \quad (9.13)$$

The magnitudes of $K_D[D]$ and $K_E[E]$ relative to each other and to 1 can transform the rates from being first-order in [D] and/or [E] to being

independent of reactant concentrations. For noncompetitive adsorption, the Eley-Rideal mechanism, Eq. (9.11), is always first-order in [E]. For competitive adsorption, the Langmuir-Hinshelwood mechanism, Eq. (9.12), can be inverse-first-order in [D] or [E].

For the special case where D is H_2 undergoing dissociative adsorption into two $H\cdot S$ fragments, the equilibrium constant for adsorption is given by $K_H = (H\cdot S)/(S)[H_2]^{1/2}$ and the fraction of occupied sites is

$$\theta_H = \frac{(H\cdot S)}{(S_0)} = \frac{K_H[H_2]^{1/2}}{1 + K_H[H_2]^{1/2}} \quad (9.14)$$

In this case, the first-order dependencies in Eq. (9.10)–(9.13) become half-order. Clearly, there is an analogous difference for any species adsorbed as two equivalent halves, such as C_2H_6 forming two $H_3C\cdot S$, or C_2H_4 giving two $H_2C\cdot S$. Similar modifications must be made when chemisorption gives two different species, such as propane giving $H_3C\cdot S$ and $H_5C_2\cdot S$.

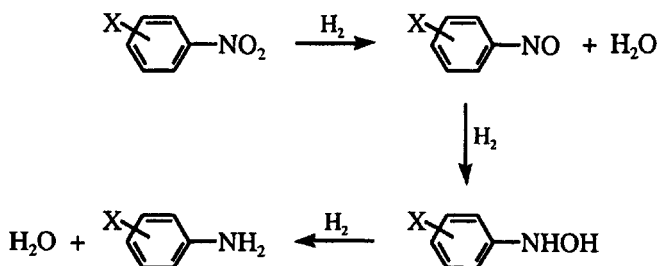
As usual for kinetic studies designed to determine rate laws, it is important to ensure that mass transfer limitations are not affecting the observations. This issue has already been discussed for the gas/liquid mass transfer step. For solid catalysts, there is the additional step of transfer of reactants to active sites on the catalyst. Criteria for this effect are discussed in the review of Singh and Vannice.²¹ The best test seems to be that of Madon and Boudart²² which relies on changing the number of active sites per unit mass of solid catalyst, (S_0) . As can be seen from Eq. (9.10)–(9.13), the rate increases with an increase in (S_{D0}) or (S_0) for all mechanisms. For surface sites on a homogeneous solid, (S_0) can be increased by increasing the surface area of the catalyst, although changing the particle size can affect other mass transfer issues.²³ For catalysts bound to a solid support, (S_0) can be changed simply by changing the loading of the catalyst on the support. For catalysts with the active sites in pores or channels, the situation is more complex and requires an estimate of the diffusivity within the pore or channel. The standard method seems to be the Weisz-Prater criterion²⁴ which requires that the ratio of the measured rate to the estimated diffusion controlled rate should be $\ll 1$ if mass transfer in the pores is not a factor.

There are many studies on gas/liquid/solid systems and it is difficult and inevitably somewhat arbitrary to select examples that illustrate general kinetic or mechanistic features. In addition, these studies on a particular reaction are often difficult to discuss as a group because of differences in the type and preparation of the catalyst and the solvent. As a result, differences in kinetic observations or mechanistic interpretations between studies simply may be a consequence of differences in the solid catalyst.

A system that illustrates these features is the oft-studied hydrogenation of nitrobenzene, NB, and its derivatives to give the corresponding aniline, catalyzed by Pt or Pd dispersed on some solid support. The kinetics are

most often determined from the rate of H_2 consumption, or periodic sampling and analysis of the reactant solution by gas chromatography. The reaction is generally thought to proceed through the nitrosobenzene and phenylhydroxylamine intermediates, as shown in Scheme 9.2.

Scheme 9.2



The results of representative studies from the groups of Rempel,²⁵ Chaudhari,²⁶⁻²⁸ Renken,²⁹ Chandalia^{30,31} and Blackmond³² are summarized in Table 9.3. Renken and co-workers found that up to 30% of the nitrosobenzene intermediate was present during the hydrogenation of NB over Pt on a glass fiber support, but the intermediate species constituted $\leq 7\%$ of the total at any time for hydrogenation over Pd. In most studies and kinetic interpretations, the possibility of intermediate species has been ignored and a single rate-determining step has been assumed.

The studies in Table 9.3 show the use of a number of different conditions, especially with regard to the substrate, solvent and the support for Pd and Pt. The conditions often result from a limited survey by the authors to find the solvent and catalyst that give optimum rate and selectivity for their chosen substrate. For example, Khilnani and Chandalia³¹ found that hydrogenation of *m*-dinitrobenzene was much faster in acetone than in ethanol, and studied the kinetics in acetone. Despite these differences, one might hope to find some common kinetic features in these studies, at least for those using the same metal and similar solvents.

Four of the five systems using Pd show saturation kinetics in the NB substrate concentration and have K_{NB} values of similar magnitude. They also show a first-order dependence on H_2 pressure, at least up to ~ 12 atm, and saturation kinetics were only observed for the study extended to 28 atm of H_2 . When no H_2 saturation kinetics were observed, a simple non-competitive Eley-Rideal mechanism was adopted by the authors. For these systems, Eq. (9.11) can be modified by letting $k_5(S_{\text{D}_0}) = k_{\text{cat}}$ and by using Henry's law to replace the H_2 concentration by its partial pressure, P_{H_2} . Then, the rate of formation of aniline, AN, is given by

$$\frac{d[\text{AN}]}{dt} = k_{\text{cat}} P_{\text{H}_2} \left(\frac{K_{\text{NB}}[\text{NB}]}{1 + K_{\text{NB}}[\text{NB}]} \right) \quad (9.15)$$

Table 9.3. Summary of the Hydrogenation of Nitrobenzene Derivatives, NBX, by Metal Supported Catalysts.

X	Catalyst/ Substrate	Solvent	Temp (°C)	NB (M) order ^b	H ₂ (atm) order ^b	K _H ^a (atm ⁻¹)	K _{NB} ^a (M ⁻¹)	Ref.
H	1.4% Pd/ acrylate gel	HOAc/ MeOH	31	0.005-0.9 1(s)	0.13-0.7 1(s)	≤1.3 ^c	≤7.3 ^c	25
2-NO ₂ 4-CH ₃	5% Pd/ Al ₂ O ₃	EtOAc	50-90	0.05-0.9 1(s)	3-28 1(s)	-0.06	-1.5	27
H	0.2% Pd/ glass fibre	91% iPrOH	50	0.12-0.68 1(s)	4-12.5 1		7.2	29
2-NO ₂	5% Pd/C	Acetone	20-40	0.3-0.89 <0	10-34 0			31
4-OC ₂ H ₃	10% Pd/C	EtOH	20-80	0.6 {1(s)} ^d	1 {1} ^d		5	32
3-Cl	1% Pt/C	MeOH	40-90	0.2-1.2 1(s)	6-68 1		~5	26
4-Cl	5% Pt/C	MeOH	28-60	0.32 1 ^e	10-34 1			30
4-OH	1% Pt/C	EtOH	35-80	0.12-0.96 1(s)	13.5-67 1(s)	-0.03	-1.1	28

^a Adsorption coefficients estimated from the published data by letting $K_H P_{H_2} + K_{NB}[NB] = 1$ for the conditions at which the rate reaches half of its maximum value. If saturation kinetics were not observed for one component, then it was ignored in making the estimate.

^b (s) indicates saturation kinetics, i.e. the rate was initially first-order in the reactant and became independent of it at higher concentrations.

^c The adsorption coefficients are upper limits because the authors suggest that the higher rates may be affected by mass transfer.

^d The order in [H₂] is assumed, and it is not clear how K_{NB} was determined since only one substrate concentration is mentioned.

^e The order was judged from the linearity of the usual semilogarithmic first-order plot at one concentration.

If H₂ saturation kinetics really are a general feature of these systems, then an Eley-Rideal mechanism with competitive adsorption, Eq. (9.13), could be consistent with the observations. With the substitution that $k_5(S_0) = k_{cat}$ in Eq. (9.13), this mechanism gives the rate of product formation as

$$\frac{d[AN]}{dt} = k_{cat} P_{H_2} \left(\frac{K_{NB}[NB]}{1 + K_{NB}[NB] + K_H P_{H_2}} \right) \quad (9.16)$$

The K_H and K_{NB} values in Table 9.3 are based on this model. In all of these experimental studies, a single value of [NB] or P_{H₂} was kept constant while

the other was varied, and the initial rate will reach half of its saturation value when $1 + K_{\text{NB}}[\text{NB}] + K_{\text{H}}P_{\text{H}_2} = 2$. This simple relationship was used to estimate the K values given in Table 9.3. Saturation kinetics in both reactants can be explained by a noncompetitive Langmuir–Hinshelwood mechanism, with $k_6(S_{\text{D}_0})(S_{\text{E}_0}) = k_{\text{cat}}$ in Eq. (9.10), to give

$$\frac{d[\text{AN}]}{dt} = k_{\text{cat}} \left(\frac{K_{\text{H}}P_{\text{H}_2}}{1 + K_{\text{H}}P_{\text{H}_2}} \right) \left(\frac{K_{\text{NB}}[\text{NB}]}{1 + K_{\text{NB}}[\text{NB}]} \right) \quad (9.17)$$

Figure 9.6 shows examples of the saturation kinetic curves that might be obtained from these three possible alternative explanations. The curves are calculated with K_{H} and K_{NB} values that are representative of those with Pd in Table 9.3. Different k_{cat} values have been used for the Eley–Rideal and Langmuir–Hinshelwood models in order to scale the curves for clearer presentation. Figure 9.6 shows that any of these models might explain the kinetic observations, but P_{H_2} must be >10 atm to clearly show saturation kinetics for the P_{H_2} dependence of the initial rate. If K_{H} is smaller than the assumed value of 0.1 atm^{-1} , then this pressure limit would be larger.

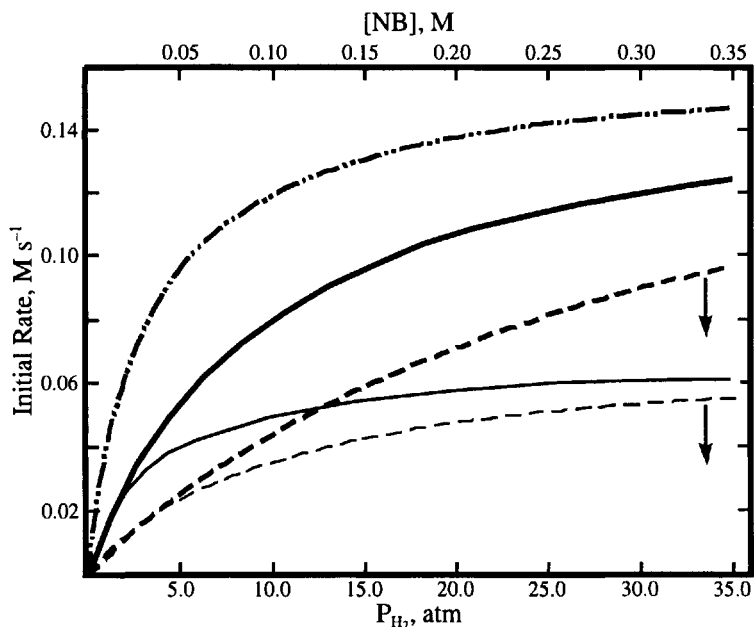


Figure 9.6. Calculated variation of the initial rate of hydrogenation of nitrobenzene, NB, for various models. (— · — · —) simple Eley–Rideal varying [NB]; (—) full Eley–Rideal varying [NB]; (— — —) full Eley–Rideal varying P_{H_2} ; (—) Langmuir–Hinshelwood varying [NB]; (— — —) Langmuir–Hinshelwood varying P_{H_2} . Curves are calculated with $K_{\text{H}} = 0.1 \text{ atm}^{-1}$, $K_{\text{NB}} = 6 \text{ M}^{-1}$, nonvarying concentrations of $[\text{NB}] = 0.4 \text{ M}$ and $P_{\text{H}_2} = 20 \text{ atm}$.

The exceptional system is the hydrogenation of *m*-dinitrobenzene in acetone,³¹ where the rate was found to increase with decreasing concentration of the substrate and to be almost independent of the pressure of H₂. An inverse dependence on [NB] would only be consistent with the competitive adsorption Langmuir–Hinshelwood mechanism, Eq. (9.12). If the denominator of this equation is expanded, one obtains a term $(K_{\text{NB}}[\text{NB}])^2$ and cancellation of [NB] in the numerator and denominator leaves a term $K_{\text{NB}}^2[\text{NB}]$ in the denominator as the source of the inverse dependence on [NB]. The authors did not attempt to analyze the [NB] versus time dependence, and acknowledged that more detailed studies would be necessary to establish the rate equation.

Another unusual effect was noted by Hawkins and Makowski³³ in the hydrogenation of 4-nitroacetophenone and studied further by Blackmond and co-workers.³² Hawkins and Makowski reported for one set of conditions (0.6 M substrate in ethanol with 0.9 M methanesulfonic acid under 1.7 atm of H₂ over 10% Pd/C at 25°C), that the rate of consumption of the first equivalent of H₂ was slower than that for the next two equivalents. They attributed this to inhibition of reduction of the nitroso-intermediate by the 4-nitroacetophenone, but the kinetic details were not explored because the focus was on catalyst optimization. Blackmond and co-workers studied the reaction by heat-flow calorimetry under similar conditions, but without methanesulfonic acid. They observed zero-order kinetics for most of the reaction, but the rate increased rather abruptly at about 90% conversion to the aniline derivative. This behavior was ascribed to the low substrate concentration at the end of the reaction causing a change from an Eley–Rideal mechanism to a Langmuir–Hinshelwood mechanism. It should be noted that this phenomenon was observed for only one particular Pd/C catalyst formulation and was not observed for unsubstituted nitrobenzene. It is not certain that these observations from the two studies are even concerned with the same phenomenon, since the rate increase noted by Hawkins and Makowski covers a longer time and a much greater extent of reaction. Nevertheless, these studies do point to complications that may arise from the interactions of adsorbed species. This feature is often ignored in mechanistic studies in this area because the kinetic data is too sparse to reveal such complexities. Zaera has reviewed advances in this area;³⁴ although many of the examples are from the cleaner gas/solid systems, the principles still apply when a liquid is present.

9.3 WHERE IS THE CATALYST?

There is increasing awareness that catalysts introduced into a system as a solid may partially dissolve or react to give the real catalyst in the liquid phase. Conversely, species introduced in solution may react to produce some solid that is actually the catalyst. This Section will discuss the methods that may be used to identify the phase of the active catalyst.

The problem of an initially homogeneous catalyst reacting to form a potential solid catalyst seems to occur most frequently, but not exclusively, for hydrogenation reactions. The strongly reducing conditions, i.e. the presence of H_2 , and the common usage of complexes of easily reducible late transition metals as catalysts, make reduction to the elemental metal, $M(0)$, thermodynamically favorable. Although H_2 normally is not a kinetically reactive reducing agent, reduction to $M(0)$ can occur because of the somewhat forcing conditions of high H_2 pressures and temperatures $>50^\circ C$. Of course, other reducing agents, such as phosphines or even the substrate, may be implicated. The question at this stage is not so much how the metal was formed, but rather, has it formed and if so, is it the active catalyst? The methods for answering these questions have been discussed in detail in the recent reviews by Widegren and Finke,³⁵ and by Dyson.³⁶ The methods described below are only some of the more widely used, potentially useful or essential techniques.

An initial warning sign of formation of metal is a darkening of the color of the reacting solution and possibly the formation of a metallic film on the container. The latter may not be observed because, under dilute conditions, many elemental metals form colloids or suspensions, and these may be stabilized by other components in the system. One test for such conditions is that the electronic spectrum characteristically has a strong but rather featureless appearance in the visible and near ultra-violet regions. In principle, the solids can be removed by filtration or centrifugation, but special procedures are required to separate the nanoclusters of $M(0)$ sometimes encountered. If separation is successful, then the filtrate can be tested for the catalytic activity of any homogeneous species.

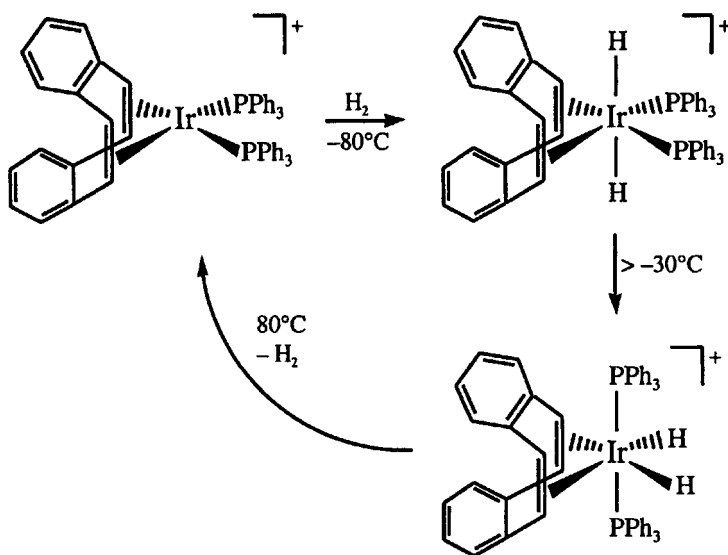
A standard chemical test for catalytic activity of the $M(0)$ species, which seems to have been applied first in this general area by Whitesides and co-workers,³⁷ is to add $Hg(0)$ to the system. The principle is that $Hg(0)$ will amalgamate or coat the surface of the $M(0)$ species and greatly reduce or eliminate the catalytic activity. It is necessary to add a substantial excess of $Hg(0)$, with vigorous stirring to ensure mixing with the $M(0)$ species, and to test that $Hg(0)$ does not react with any of the reactants or products.

A second but less widely used test is to poison the $M(0)$ surface with additives such as CS_2 , thiophene or PPh_3 . The principle is that the poison will adsorb at the active sites on the metal and inhibit or stop other catalytic reactions. The assumption is that the poison is essentially irreversibly adsorbed, but this becomes doubtful if modest to high temperatures ($>50^\circ C$) are required. Finke and co-workers have pointed out that less than 1 equivalent of poison per metal should be effective because a substantial amount of the metal will be in the bulk rather than at active sites. Of course, it must again be shown that the poison does not react with the reactants or products.

A method that is complementary to the above two was proposed and tested by Anton and Crabtree.³⁸ They found that several homogeneous Rh,

Ru and Ir catalysts are poisoned by dibenzo[*a,e*]cyclooctatetraene, DCT, but DCT has little effect on heterogeneous Rh, Pd and Pd systems. This test is based on the idea that the homogeneous catalyst must have some substitution lability and will react with DCT to form a stable diene complex. The reactions of the Ir complex under hydrogenation conditions are shown in Scheme 9.3.³⁹

Scheme 9.3



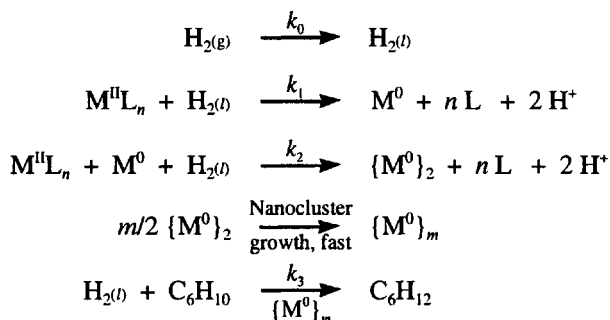
Hydrogenation of DCT was never observed; this was rationalized by noting that one C=C group cannot insert into an M-H bond without the other C=C bond becoming detached. The Ru(DCT)(PPh₃)₂⁺ complex did not react with H₂. The suggested protocol for the test is to generate the proposed catalyst under H₂ in the normal way, remove the H₂ and add 1 equivalent of DCT per metal, stir for 2 h and start the normal hydrogenation of the substrate. Despite the rather unique information provided, this test does not seem to have been used since the original study, possibly because DCT is not commercially available, but an efficient synthesis has been published recently.⁴⁰ The other drawback is that the 2 h reaction time might give any nascent heterogeneous catalyst time to deactivate through agglomeration or poisoning by the ligands displaced by the DCT.

Another characteristic of systems that form heterogeneous catalysts adventitiously in situ is that they tend to give irreproducible rates. This might not be the case if all the conditions, such as concentrations, temperature and mixing, were carefully controlled during the formation of the catalytic solid, but this is not usually the case if the initial assumption is that no significant solid is forming. The importance of the synthetic conditions is shown in the series of studies by Finke and co-workers on the

formation of catalytic nanoclusters.⁴¹⁻⁴⁴ It should be noted that irreproducible rates are only apparent from published data when the minimum time for substantial conversion of substrate to product is reported. It is not uncommon in synthetic studies to choose an arbitrary reaction time which always gives substantial conversion but which may be much longer than the time actually required for some runs.

Finke and co-workers have argued that a critical test for the formation of a heterogeneous catalyst during hydrogenation is the observation of an initial induction period followed by a more rapid stage for consumption of substrate or formation of product. Of course, this requires a detailed monitoring of the time dependence for substrate disappearance or product formation. The kinetic model initially suggested by Lin and Finke has been expanded somewhat in more recent reports by Watzky and Finke⁴⁵ and by Hornstein and Finke.⁴⁶ To illustrate this test, a somewhat modified version of the reaction sequence proposed by Finke and co-workers is shown in Scheme 9.4.

Scheme 9.4



The modifications are: addition of the $\text{H}_{2(\text{g})}$ mass transfer step, k_0 ; designation of the precatalyst as some species $\text{M}^{\text{II}}\text{L}_n$; inclusion of the products of the reduction step, k_1 . The third step, k_2 , is crucial for the kinetic analysis and is a somewhat unspecified nucleation of M^0 species which grow in non-rate-limiting steps to form $\{\text{M}^0\}_m$ nanoclusters that are proposed to be the actual hydrogenation catalysts. The last step, k_3 , is the actual hydrogenation of the substrate, which is cyclohexene in Scheme 9.4. This step was included by Watzky and Finke, but they concluded it was not rate-limiting for their standard conditions. In the more recent work of Hornstein and Finke, this step has been ignored and replaced by an agglomeration of the nanoclusters to produce an inactive form of M^0 . Finke and co-workers have discussed in detail the aspects of nanocluster formation and growth and these issues will not be considered here. The discussion which follows will concentrate on the kinetic behavior predicted for such a system and how it provides a test for formation of such heterogeneous catalysts from dissolved precatalysts.

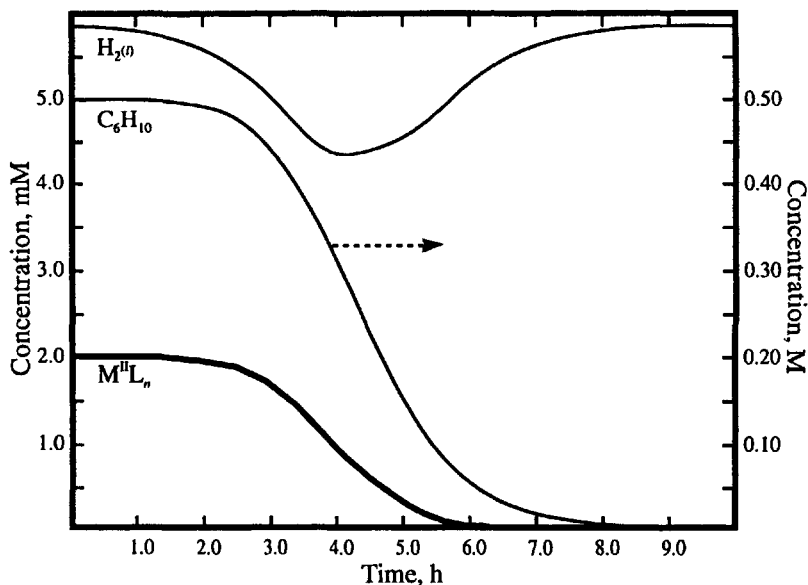


Figure 9.7. Time dependence of reactant concentrations predicted by Scheme 9.4 for initial conditions of $P_{\text{H}_2} = 1.5$ atm, $[\text{C}_6\text{H}_{10}] = 0.5$ M, $[\text{M}^{\text{II}}\text{L}_n] = 2.0$ mM, and rate constants of $k_{\text{L}}A = 0.03$ s $^{-1}$, $k_1 = 5 \times 10^{-5}$ M $^{-1}$ s $^{-1}$, $k_2 = 50$ M $^{-2}$ s $^{-1}$, $k_3 = 30$ M $^{-2}$ s $^{-1}$.

The typical kinetic profile for a system following Scheme 9.4 is shown in Figure 9.7. The magnitudes of the concentrations and rate constants are based on the observations of Watzky and Finke, who studied the hydrogenation of cyclohexene with a (1,5-COD)Ir(I) precatalyst. Similar profiles have been reported by Finke and co-workers for other systems. The sigmoidal shape of the time dependence of the concentration of the precatalyst or substrate is taken to be diagnostic of formation of a heterogeneous metal catalyst from the precursor. The initial induction is controlled by the slow formation of $\text{M}(0)$ by the k_1 step, but as more of this is formed, the k_2 step becomes faster, generating more of the active catalyst $\{\text{M}^0\}_m$ and this causes the rate of substrate consumption to increase. During this more rapid phase, the mass transfer of $\text{H}_2(\text{g})$ to the liquid phase may not be fast enough to maintain the saturation concentration of $\text{H}_2(\text{l})$. This is shown by the dip in the concentration of the latter in Figure 9.7.

It was observed in the study by Watzky and Finke that the duration of the induction period was independent of the C_6H_{10} concentration, but the rate of H_2 consumption showed saturation kinetics in the C_6H_{10} concentration during the faster phase. The authors noted that most of their study with $[\text{C}_6\text{H}_{10}] = 1.65$ M was under conditions where the rate was independent of $[\text{C}_6\text{H}_{10}]$, but did not explain the saturation kinetics because they did not include the k_3 step in their model. The curves in Figure 9.8 show that the model does predict that the rate increases with increasing $[\text{C}_6\text{H}_{10}]$, but then

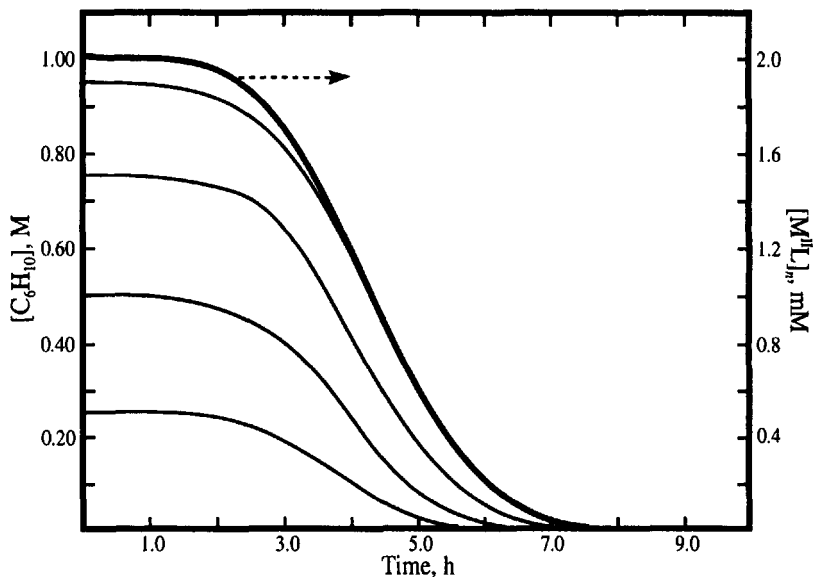


Figure 9.8. Time dependence of $[C_6H_{10}]$ (—) and $[M^{II}]_n$ (---) with varying initial concentrations of C_6H_{10} as predicted by Scheme 9.4. Other initial conditions and rate constants as in Figure 9.7, except $k_3 = 60 \text{ M}^{-2} \text{ s}^{-1}$.

reaches an upper limit of the rate of $\{M^0\}_m$ production as the initial $[C_6H_{10}]$ approaches 1 M, i.e. the model predicts the saturation behavior.

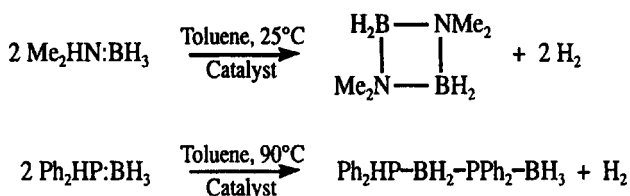
In their review, Widegren and Finke have tabulated 31 reports between 1973 and 2002 in which metal particle formation may be an issue for the catalytic process. More recently, Finke and co-workers⁴⁷ have examined $(\eta^6-C_6Me_6)(OAc)_2Ru(II)$ which was originally reported⁴⁸ to catalyse the hydrogenation of benzene. Simple observation, as well as transmission electron and X-ray photoelectron spectroscopies, established that a Ru(0) film is deposited in this system. Mercury poisoning showed that the Ru(0) is the hydrogenation catalyst. It also was found that the kinetics for the system follow the sigmoidal pattern predicted by Scheme 9.4 and illustrated in Figure 9.7. Previously, this kinetic behavior had been established for nanocluster formation, but it appears to work equally for formation of the Ru(0) film. It also was noted that the length of the induction period was quite variable and this was attributed to Ru(0) impurities in the precatalyst which serve as nucleation sites for metal formation. It was suggested that the Ru(0) deposits in the reactor in the original study may have served a similar purpose in promoting formation of the catalytic Ru(0) film.

A study⁴⁹ of the catalyst $(Rh(\eta^5-C_5Me_5)(Cl)_2)_2$, developed by Maitlis and co-workers,⁵⁰ has shown how the nature of the catalyst can depend on the reaction conditions. The hydrogenation of cyclohexene was observed at

22°C and found to be homogeneous. However, the hydrogenation of benzene requires temperatures >50°C and was concluded to involve a heterogeneous nanoparticle catalyst. Another study⁵¹ of a triruthenium cluster cation has concluded that hydrogenation of benzene at 110°C uses primarily $\text{Ru}(0)_n$ metal as the catalyst.

A curious case that illustrates some of the perversities that can be observed has been reported by Jaska and Manners.⁵² They studied the dehydrocoupling reactions shown in Scheme 9.5 using various rhodium catalysts.

Scheme 9.5



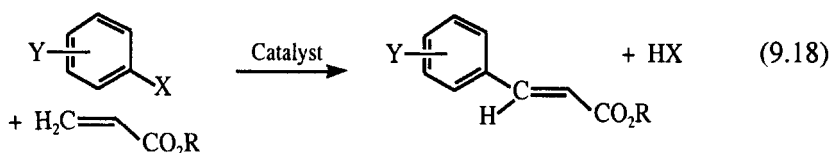
The reaction of $\text{Me}_2\text{HN:BH}_3$ with $\{\text{Rh}(1,5\text{-COD})(\mu\text{-Cl})\}_2$ as the catalyst showed all the signs of being heterogeneously catalyzed. The solutions changed from orange to black over 2 h, and the electronic spectrum was similar to that of colloidal $\text{Rh}(0)$. Eventually, a black precipitate and a metallic mirror were observed in the reactor. Addition of $\text{Hg}(0)$ stopped the reaction, PPh_3 caused the rate to decrease and filtration through a 0.5 μm filter gave a solution with very little catalytic activity. Standard transmission electron microscopy was found to degrade the catalyst to some metal particles, but lowering the energy of the electron beam showed that $\text{Rh}(0)$ particles were present in the reaction solution. The kinetics gave a sigmoidal plot of product concentration versus time, with an induction period of ~200 min. All of these observations are consistent with catalysis by colloidal and/or larger particles of $\text{Rh}(0)$. It was also noted that $\text{Rh}(0)$ supported on Al_2O_3 catalysed the reaction but was not poisoned by $\text{Hg}(0)$, while colloidal $\text{Rh}(0)$ catalysed the reaction but was not poisoned by $\text{Hg}(0)$. This has interesting implications for the generality of the $\text{Hg}(0)$ poisoning test.

On the other hand, the reaction of $\text{Ph}_2\text{HP:BH}_3$ with the same catalyst at 90°C showed none of the features expected for heterogeneous catalysis. The solutions changed from orange to dark red, but never to black, and never gave a precipitate. Neither addition of $\text{Hg}(0)$ nor filtration had any effect on the catalytic activity, and no induction period was observed. All these observations suggest that the catalyst is some dissolved Rh species. With $\text{Rh}/\text{Al}_2\text{O}_3$, a greatly reduced catalytic activity was observed which was attributed to leaching of some Rh from the solid support to yield a dissolved Rh species. Neither colloidal $\text{Rh}(0)$ nor the catalytic solution

prepared from $\text{Me}_2\text{HN}:\text{BH}_3$ and $\{\text{Rh}(1,5\text{-COD})(\mu\text{-Cl})\}_2$ showed any reaction with $\text{Ph}_2\text{HP}:\text{BH}_3$. Similarly, the catalytic solution from $\text{Ph}_2\text{HP}:\text{BH}_3$ showed no reaction with $\text{Me}_2\text{HN}:\text{BH}_3$.

Jaska and Manners⁵² tentatively suggest several reasons for the different behavior of the two systems, such as the greater reducing power of the BH_3 fragment in the $\text{Me}_2\text{HN}:\text{BH}_3$ adduct and the thermal liberation of PPh_2H in $\text{Ph}_2\text{HP}:\text{BH}_3$. The PPh_2H may stabilize the soluble Rh species and may react by oxidative addition to dissolve any $\text{Rh}(0)$ formed. Such factors can explain why $\text{Ph}_2\text{HP}:\text{BH}_3$ does not yield insoluble $\text{Rh}(0)$ species, but there also must be mechanistic differences in the dehydrocoupling reactions to explain why a catalyst, in whatever form, for one system does not work for the other.

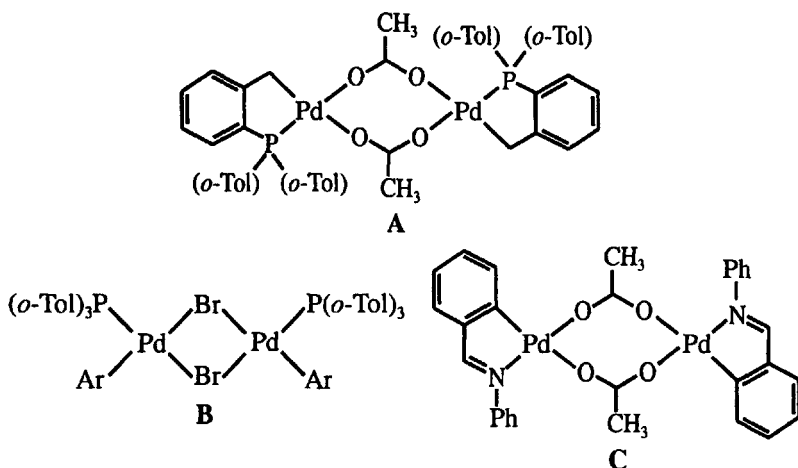
The nature and form of the catalyst in the Heck reaction⁵³ has generated a substantial amount of research activity. The example of this reaction that has most often been studied with regard to this question is shown in Eq. (9.18), where the reactants are an aryl halide and an ester of acrylic acid. For the halides, X, the reactivity order is $\text{I} > \text{Br} \gg \text{Cl}$.



Various palladium species catalyze the reaction, and a common procedure is to start with $\text{Pd}(\text{OAc})_2$, PPh_3 , NaOAc and sometimes NEt_3 . The reaction generally is done at elevated temperatures (100–150°C) in a polar solvent, such as dimethylacetamide or dimethylformamide. The reaction usually proceeds with formation of at least some Pd metal. The standard reaction sequence involves first reduction of $\text{Pd}(\text{II})$, possibly by phosphine or amine, to a ligated $\text{Pd}(0)$ species, often represented as PdL_2 . The latter is proposed to undergo oxidative addition with the aryl halide, and the resulting $\text{Pd}^{\text{II}}(\text{Ar})(\text{X})(\text{L})_2$ species loses an L and coordinates the olefin. Then, the aryl group inserts into the Pd—olefin bond. This is followed by β -hydride elimination, possibly assisted by base, liberation of the product and re-coordination of L to regenerate the catalyst. Further details can be found in recent reviews by Crisp,⁵⁴ Beletskaya and Cheprakov⁵⁵ and Amatore and Jutland.⁵⁶ It should be noted that the electrochemical studies of the latter workers indicate that the $\text{Pd}(0)$ is present as an anionic complex, such as $\text{Pd}(\text{L})_2(\text{OAc})^-$, and that the oxidative addition gives a 5-coordinate $\text{Pd}(\text{II})$ species, such as $\text{Pd}(\text{Ar})(\text{X})(\text{L})_2(\text{OAc})^-$.

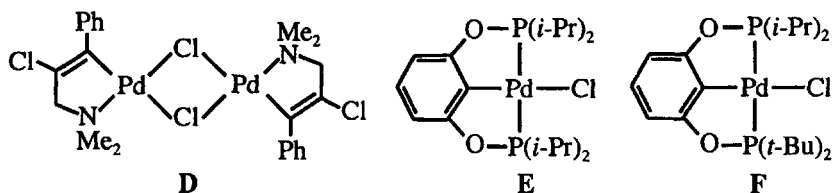
The above mechanism received two blows from different directions in the mid-1990s. Herrmann and co-workers⁵⁷ observed that a $\text{Pd}(\text{II})$ metallacycle, A, in the presence of $n\text{-Bu}_4\text{NBr}$ is an excellent catalyst for the Heck reaction, but the reaction only starts after addition of the olefin. This led Shaw⁵⁸ to propose a different mechanism, at least for these

systems, which involved a Pd(II)/Pd(IV) cycle, rather than the more usual Pd(II)/Pd(0) cycle. Subsequently, Böhm and Herrmann⁵⁹ studied the products of the coupling of styrene with a number of different aryl bromides and the catalysts Pd(P(*o*-Tol)₃)₂, the palladacycle **A** and the Pd(II) dimer **B**. They concluded that all the catalysts were proceeding via analogous mechanisms and that **A** was not using the Pd(II)/Pd(IV) cycle.



Blackmond and co-workers⁶⁰ studied the kinetics of the reaction of *p*-bromobenzaldehyde and butyl acrylate with the palladacycle **C** as the catalyst. They observed an induction period whose duration depended on the water concentration and which they ascribed to dissociation of the dimer and reduction by the olefin to a Pd(0) species. The latter undergoes oxidative addition by the aryl bromide in a process that shows saturation kinetics as the oxidative addition becomes faster than the dissociation and reduction steps.

More recent studies by Dupont and co-workers,⁶¹ using the palladacycle **D**, and Eberhard,⁶² using several monomeric chelates, such as **E** and **F**, indicate that these systems decompose to Pd(0) species under normal reaction conditions. In both cases, Hg(0) stops the reaction, and Eberhard showed that CS₂, thiophene and PPh₃ are effective poisons, even at 180°C.



The general conclusion from these observations seems to be that Pd metal particles are essential for catalysis. This is consistent with the earlier report of Blackmond and co-workers⁶³ that stabilized Pd(0) colloids are

effective catalysts for the Heck coupling. The way in which Pd metal particles may participate is suggested by the results of Davies et al.⁶⁴ They found that Pd on solid supports is solubilized by oxidative addition with aryl iodides and bromides to produce Pd(II) species in solution.

The second blow for the traditional mechanism was the discovery by Jeffery that a phosphine was not needed to carry out the Heck reaction. Jeffery⁶⁵ found that an effective catalyst operating at -60°C could be made from $\text{Pd}(\text{OAc})_2$ in aqueous media containing $n\text{-Bu}_4\text{NBr}$ or $n\text{-BuN}_4\text{Cl}$ as necessary components, and with Na_2CO_3 or K_2CO_3 as the base. These are now called ligand-free conditions. De Vries et al.⁶⁶ found respectable activity for reaction of iodobenzene with n -butylacrylate at 80°C , starting with $\text{Pd}(\text{OAc})_2$ and NEt_3 in 1-methyl-2-pyrrolidone, but with no BuN_4^+ salt. However, the Pd(0) recovered after reaction on silica showed greatly reduced activity which could only be restored by treatment with I_2 or Br_2 . In a later publication, de Vries et al.⁶⁷ found that aryl bromides could be activated at 135°C by a similar catalyst preparation, as long as the amount of catalyst was kept below 0.1 mol%. They suggested that the slower oxidative addition of aryl bromides compared to iodides allowed more Pd(0) to accumulate and agglomerate into inactive forms at higher Pd concentrations. As an interesting sidelight, they also found that their catalyst had almost the same activity as that originating from the palladacycle A. Köhler and co-workers⁶⁸ took a slightly different approach to the agglomeration problem by dispersing low levels of Pd(0) on TiO_2 or Al_2O_3 or a commercially available zeolite, NaY. The zeolite support gave the best activity, which the authors suggest might be due to diffusion limitations in the pores of the zeolite which inhibit agglomeration. They also reported that the reaction of bromobenzene with styrene has an induction period of ~ 25 min at 140°C , and the product formation correlates with the amount of Pd in solution. The observations differ somewhat from those in an earlier paper by Djakovitch and Köhler,⁶⁹ but the solvent has been changed from dimethylacetamide to 1-methyl-2-pyrrolidone.

But what and where is the catalyst in this system? The simplest explanation of the various observations seems to be that the resting state of the catalyst is Pd(0) particles in solution or adsorbed on some support. However, the actual catalyst may be a dissolved Pd(II) species which is formed by oxidative addition of the aryl halide to the Pd(0) particles.⁷⁰ The poisons would inhibit the latter process by coating or occupying the reactive sites on the Pd metal. It also seems that the complexes of Pd(II) which were tested as catalysts are much more susceptible to reduction to Pd(0) than was originally suspected. Thus, the common products found from three precatalyst sources by Böhm and Herrmann⁵⁹ could be explained by the precatalysts all ultimately forming Pd(0). Differences in reactivity could be due to different forms or particle sizes of the Pd metal, which would depend on how rapidly the precatalyst decomposed and the particles grew. The $n\text{-Bu}_4\text{N}^+$ ion found to be important by Jeffery⁶⁵ might

be stabilizing nanoclusters or colloidal Pd metal. In a recent review,⁷¹ de Vries proposes that soluble Pd(0) clusters undergo oxidative addition by the aryl halide in competition with agglomeration to inactive Pd black, and summarizes the background information that supports this view.

References

1. Beenackers, A. A. C. M.; van Swaani, W. P. M. *Chem. Eng. Sci.* **1993**, *48*, 3109; Sun, Y.; Wang, J.; LeBlond, C.; Landau, R. N.; Blackmond, D. G. *J. Catal.* **1996**, *161*, 759; Setinc, M.; Levec, J. *Chem. Eng. Sci.* **2001**, *56*, 6081; Hoffer, B. W.; Schoenmakers, P. H. J.; Mooijman, P. R. M.; Hamminga, G. M.; Berger, R. J.; van Langeveld, A. D.; Moulijn, J. A. *Chem. Eng. Sci.* **2004**, *59*, 259.
2. Meille, V.; Pestre, N.; Fongarland, P.; de Bellefon, C. *Ind. Eng. Chem. Res.* **2004**, *43*, 924.
3. Li, J.; Tekie, Z.; Mizan, T. I.; Morisi, B. I.; Maier, E. E.; Singh, C. P. P. *Chem. Eng. Sci.* **1996**, *51*, 549.
4. Battino, R.; Clever, H. L. *Chem. Rev.* **1966**, *66*, 395.
5. Katayama, T.; Nitta, T. *J. Chem. Eng. Data* **1976**, *21*, 194.
6. Cargill, R. W., Ed. *Carbon Monoxide. Solubility Data Series*; Pergamon Press, Oxford, 1990.
7. Fogg, P. G. T.; Gerrard, W. *Solubility of Gases in Liquids*; J. Wiley & Sons, New York, 1991.
8. Sun, Y.; Landau, R. N.; Wang, J.; LeBlond, C.; Blackmond, D. G. *J. Am. Chem. Soc.* **1996**, *118*, 1348.
9. Landis, C. R.; Halpern, J. *J. Am. Chem. Soc.* **1987**, *109*, 1746.
10. Kitamura, M.; Tsukamoto, M.; Bessho, Y.; Yoshimura, M.; Kobs, U.; Wildhalm, M.; Noyori, R. *J. Am. Chem. Soc.* **2002**, *124*, 6649.
11. Oldham, W. J., Jr.; Heinekey, D. M. *Organometallics* **1997**, *16*, 467.
12. Garrou, P. E.; Heck, R. F. *J. Am. Chem. Soc.* **1976**, *98*, 4115.
13. Ostrovskii, V. E. *Ind. Eng. Chem. Res.* **2004**, *43*, 3113.
14. Corma, A.; Llois, F.; Monton, J. B.; Weller, S. *Chem. Eng. Sci.* **1988**, *43*, 785.
15. Boudart, M. *Ind. Eng. Chem. Res.* **1989**, *28*, 379.
16. Weller, S. W. *Catal. Rev.* **1992**, *34*, 227.
17. Brown, W. A.; Kose, R.; King, D. A. *Chem. Rev.* **1998**, *98*, 797.
18. Vattuone, L.; Yeo, Y. Y.; King, D. A. *J. Chem. Phys.* **1996**, *104*, 8096.
19. Langmuir, I. *Trans. Farad. Soc.* **1921**, *17*, 621; Hinshelwood, C. N. *Kinetics of Chemical Change in Gaseous Systems*; Clarendon, Oxford, 1926, p 145.
20. Eley, D. D.; Rideal, E. K. *Proc. R. Soc. London, Ser A* **1941**, *178*, 452.
21. Singh, U. K.; Vannice, M. A. *Applied Catalysis A* **2001**, *213*, 1.
22. Madon, R. J.; Boudart, M. *Ind. Eng. Chem. Fundam.* **1982**, *21*, 438.
23. Chambers, R.; Boudart, M. *J. Catal.* **1995**, *154*, 364.
24. Fogler, H. S. *Elements of Chemical Reaction Engineering*, 3rd Ed., Prentice Hall, Englewood, N. J., 1999, Chapter 12.

25. Tong, S. B.; O'Driscoll, F. K.; Rempel, G. L. *Can. J. Chem. Eng.* **1978**, *56*, 340.
26. Rode, C. V.; Chaudhari, R. V. *Ind. Eng. Chem. Res.* **1994**, *33*, 1645.
27. Rajashekharam, M. V.; Nikalje, D.; Jaganathan, R.; Chaudhari, R. V. *Ind. Eng. Chem.* **1997**, *36*, 592.
28. Vaidya, M. J.; Kulkarni, S. M.; Chaudhari, R. V. *Org. Process Res. Dev.* **2003**, *7*, 202.
29. Höller, V.; Wegricht, D.; Yuranov, I.; Kiwi-Minsker, L.; Renken, A. *Chem. Eng. Tech.* **2000**, *23*, 251.
30. Khilnani, V. L.; Chandalia, S. B. *Org. Process Res. Dev.* **2001**, *5*, 257.
31. Khilnani, V. L.; Chandalia, S. B. *Org. Process Res. Dev.* **2001**, *5*, 263.
32. LeBars, J.; Dini, S.; Hawkins, J. M.; Blackmond, D. G. *Adv. Synth. Catal.* **2004**, *346*, 943.
33. Hawkins, J. M.; Makowski, T. W. *Org. Process Res. Dev.* **2001**, *5*, 328.
34. Zaera, F. *Acc. Chem. Res.* **2002**, *35*, 129; *Ibid. J. Phys. Chem. B* **2002**, *106*, 4043.
35. Widegren, J. A.; Finke, R. G. *J. Mol. Cat.* **2003**, *198*, 317.
36. Dyson, P. J. *Dalton Trans.* **2003**, 2964.
37. Foley, P.; DiCosimo, R.; Whitesides, G. M. *J. Am. Chem. Soc.* **1980**, *102*, 6713; Whitesides, G. M.; Hackett, M.; Brainard, R. L.; Lavalleye, J.-P. P.M.; Sowinski, A. F.; Izumi, A. N.; Moore, S. S.; Brown, D. W.; Staudt, E. M. *Organometallics* **1985**, *4*, 1819.
38. Anton, D. R.; Crabtree, R. H. *Organometallics*, **1983**, *2*, 85.
39. Anton, D. R.; Crabtree, R. H. *Organometallics*, **1983**, *2*, 621.
40. Chaffins, S.; Brettreich, M.; Wudl, F. *Synthesis* **2002**, 1191.
41. Lyon, D. K.; Finke, R. G. *Inorg. Chem.* **1990**, *29*, 1787.
42. Lin, Y.; Finke, R. G. *Inorg. Chem.* **1994**, *33*, 4891.
43. Aiken, J. D., III; Finke, R. G. *J. Am. Chem. Soc.* **1998**, *120*, 9545.
44. Besson, C.; Finney, E. E.; Finke, R. G. *Chem. Mater.* **2005**, *17*, 4925; *Ibid. J. Am. Chem. Soc.* **2005**, *127*, 8179.
45. Watzky, M. A.; Finke, R. G. *J. Am. Chem. Soc.* **1997**, *119*, 10382.
46. Hornstein, B. J.; Finke, R. G. *Chem. Mater.* **2004**, *16*, 139.
47. Widegren, J. A.; Bennett, M. A.; Finke, R. G. *J. Am. Chem. Soc.* **2003**, *125*, 10301.
48. Bennett, M. A.; Ennett, J. P. *Inorg. Chim. Acta* **1992**, *198–200*, 583.
49. Hagen, C. M.; Widegren, J. A.; Maitlis, P. M.; Finke, R. G. *J. Am. Chem. Soc.* **2005**, *127*, 4423.
50. Maitlis, P. M. *Acc. Chem. Res.* **1978**, *11*, 301.
51. Hagen, C. M.; Vielle-Petit, L.; Laurenczy, G.; Süß-Fink, G.; Finke, R. G. *Organometallics* **2005**, *24*, 1819.
52. Jaska, C. A.; Manners, I. *J. Am. Chem. Soc.* **2004**, *126*, 9776.
53. Heck, R. F. *J. Am. Chem. Soc.* **1968**, *90*, 5518; Heck, R. F.; Nolley, J. P. *J. Org. Chem.* **1972**, *14*, 2320.
54. Crisp, G. T. *Chem. Soc. Rev.* **1998**, *27*, 427.
55. Beletskaya, I. P.; Cheprakov, A. V. *Chem. Rev.* **2000**, *100*, 3009.

56. Amatore, C.; Jutland, A. *Acc. Chem. Res.* **2000**, *33*, 314.
57. Herrmann, W. A.; Brossmer, C.; Öfele, K.; Reisinger, C.-P.; Riermeier, T. H.; Beller, M.; Fischer, H. *Angew. Chem. Int. Ed. Engl.* **1995**, *34*, 1844; Herrmann, W. A.; Brossmer, C.; Reisinger, C.-P.; Riermeier, T. H.; Öfele, K.; Beller, M. *Chem. Eur. J.* **1997**, *3*, 1357.
58. Shaw, B. L. *New J. Chem.* **1998**, *22*, 77.
59. Böhm, V. P. W.; Herrmann, W. A. *Chem. Eur. J.* **2001**, *7*, 4191.
60. Rosner, T.; Le Bars, J.; Pfaltz, A.; Blackmond, D. G. *J. Am. Chem. Soc.* **2001**, *123*, 1848; Rosner, T.; Pfaltz, A.; Blackmond, D. G. *J. Am. Chem. Soc.* **2001**, *123*, 4621.
61. Consorti, C. S.; Zanini, M. L.; Leal, S.; Ebeling, G.; Dupont, J. *Org. Lett.* **2003**, *5*, 983.
62. Eberhard, M. R. *Org. Lett.* **2004**, *6*, 2125.
63. Le Bars, J.; Specht, U.; Bradley, J. S.; Blackmond, D. G. *Langmuir*, **1999**, *15*, 7621.
64. Davies, I. W.; Matty, L.; Hughes, D. L.; Reider, P. J. *J. Am. Chem. Soc.* **2001**, *123*, 10139.
65. Jeffery, T. *Tetrahedron* **1996**, *52*, 10113.
66. De Vries, A. H. M.; Parlevliet, F. J.; Schmieder-van de Vondervoort, L.; Mommers, J. H. M.; Henderickx, H. J. W.; Walet, M. A. M.; de Vries, J. G. *Adv. Synth. Catal.* **2002**, *344*, 996.
67. De Vries, A. H. M.; Mulders, J. M. C. A.; Mommers, J. H. M.; Henderickx, H. J. W.; de Vries, J. G. *Org. Lett.* **2003**, *5*, 3285.
68. Pröckl, S. S.; Kleist, W.; Gruber, M. A.; Köhler, K. *Angew. Chem. Int. Ed. Eng.* **2004**, *43*, 1881.
69. Djakovitch, L.; Köhler, K. *J. Am. Chem. Soc.* **2001**, *123*, 5990.
70. Biffis, A.; Zecca, M.; Basato, M. *Eur. J. Inorg. Chem.* **2001**, 1131.
71. De Vries, J. G. *Dalton Trans.* **2006**, 421.

Experimental Methods

A kinetic study generally proceeds after the reactants, products and stoichiometry of the reaction have been satisfactorily characterized. The more one knows about the chemistry of the reaction, the better the conclusions that one can draw from a kinetic study. The discussion here describes techniques often used in inorganic studies, emphasizes their time range and general area of applicability and gives some examples of their use. Further details can be found in other sources.^{1,2}

Any experimental kinetic method must somehow monitor change of concentration with time. Many studies are done under pseudo-first-order conditions, and then one must monitor the deficient reactant or product(s) because the other species undergo small changes in concentration. The kinetic method(s) of choice often will be dictated by the time scale of the reaction. The detection method(s) will be determined by the spectroscopic properties of the species to be monitored. The efficient use of materials can be a significant factor in the choice of method because a kinetic study generally involves a number of runs at different concentrations and temperatures, and conservation of difficult to prepare or expensive reagents may be a critical factor.

The detection method should be as species specific as possible, and ideally one would like to measure both reactant disappearance and product formation. The method must not be subject to interference from other reactants and should be applicable under a wide range of concentration conditions so that the rate law can be fully explored. Often there is a practical trade-off between specificity, sensitivity and reaction time. For example, NMR is quite specific but rather slow and has relatively low sensitivity, unless the system allows time for signal accumulation. Spectrophotometry in the UV and visible range often has good sensitivity and speed, but the specificity may be poor because absorbance bands are broad and intermediates may have chromophoric properties similar to those of the reactant and/or product. Vibrational spectrophotometry can be better if the IR bands are sharp, as in the case of metal carbonyls, but the solvent must be chosen to provide an appropriate spectral window. Conductivity change can be very fast but is rather unspecific, except for reactions that involve the production or consumption of the H^+ or OH^- ions, because of their unusually large specific conductivities.

10.1 FLOW METHODS

In these methods, the reagent solutions are brought together by flowing them through a mixer from which the reaction solution emerges to be analyzed. The flow may simply be driven by gravity or by mechanical pressure applied to syringes containing the reagents. The minimum time scale depends on various factors, such as the reagent flow rate, the efficiency of the mixer and the response time of the analyzer. This general process has been adapted in various ways to minimize the amount of reagents used, optimize the detection sensitivity and shorten the accessible reaction time. Some of these adaptations are described in the following sections.

10.1.1 Quenched Flow

This method involves driving the reagent solutions through a mixer and then having some means of stopping (quenching) the reaction as the solution emerges from the mixer. The reaction time can be controlled by changing the length of tubing between the mixer and quencher. Calibration with a reaction of known rate is necessary. The main trick is to find an effective quenching method, and this will depend on the chemical reaction; adding acid, base or precipitating agents, and rapid cooling are common methods. The short time limit is ~20 ms, but this depends on the effectiveness of the quenching method.

The advantages of this method are that the apparatus is simple and that analysis of the quenched solution can be done without time constraints. The disadvantages are the sometimes tedious analysis of many samples and the consumption of substantial amounts of reagents for each kinetic run. The method has been used especially for isotope exchange reactions where the subsequent analysis of isotopic content is a slow process.

10.1.2 Stopped Flow

For reactions with half-times in the 10-ms to ~60-s range, stopped flow is the most popular technique, and several commercial instruments are available.³

In a typical instrument, the reagent solutions are contained in two drive syringes whose plungers can be advanced by activating an air pressure or electrical drive system. This moves the solutions through a mixer into an observation cell and then to a stopping syringe. A mechanical stop on the stopping syringe or drive mechanism stops the flow and triggers the observation and data recording system. The standard system mixes equal volumes (~0.2–0.5 mL) of each reagent solution and uses single-wavelength, single-beam, UV–visible spectrophotometry as the detection method. A number of variations have been described using other detection methods (conductivity, fluorimetry, NMR,⁴ ESR,⁵ EXAFS⁶) and multiwavelength detection.⁷ Instruments have been described for

measurements at high pressure⁸ and at subzero temperatures.⁹ Systems are available¹⁰ for first mixing two reagents and then a third after some time interval. In general, the method is quite adaptable and widely applicable.

The time range limitations are determined on the short end by the deadtime of the system (the time for mixing of reagents and transfer to the observation cell) and on the long end by the diffusion of reagents into the observation cell. The experimental first-order rate constant, k_{exp} , can be corrected for the mixing time effect, k_{mix} , to obtain the true pseudo-first-order rate constant, k_{true} , from the relationship suggested by Dickson and Margerum¹¹ that $(k_{\text{true}})^{-1} = (k_{\text{exp}})^{-1} - (k_{\text{mix}})^{-1}$. The rearranged version of this expression, given by

$$k_{\text{true}} = k_{\text{exp}} \left(1 - \frac{k_{\text{exp}}}{k_{\text{mix}}} \right)^{-1} \quad (10.1)$$

shows that the true rate constant is always larger than the experimental value, but the correction will be insignificant if $k_{\text{exp}}/k_{\text{mix}} \ll 1$. To determine k_{mix} , measurements can be done on a well-characterized system under pseudo-first-order conditions with $k_{\text{true}} = k_1[\text{R}]$, where k_1 is known and R is the excess reagent whose concentration can be varied to change k_{true} . Then, the variation of k_{exp} with [R] is used to determine k_{mix} . Margerum and co-workers¹² have reported values of k_{mix} for Durrum and Hi-Tech instruments of 1.7×10^3 and $2.9 \times 10^3 \text{ s}^{-1}$, respectively.

The deadtime is due primarily to the physical separation of the mixer and observation cell and also depends on the flow velocity. Typical deadtimes are in the 1- to 5-ms range and can be determined by extrapolation of the observable back to the known value at true time zero, as shown by the dashed lines in Figure 10.1.

The experimentally recorded time, t_{exp} , equals zero when the stopping syringe triggers the observation, and the actual time, t , is related to t_{exp} and the deadtime, t_d , by

$$t = t_{\text{exp}} + t_d \quad (10.2)$$

For spectrophotometric detection, Figure 10.1 illustrates the relationship between these times and A_0^{pred} , the predicted absorbance at true zero time, and A_0^{obsd} , the initial absorbance at the start of the detection system. The reaction has a pseudo-first-order rate constant $k_{\text{exp}} = k_1[\text{R}]$, so that the time dependence of the absorbance change is given by

$$(A_{\infty} - A) = (A_{\infty} - A_0^{\text{pred}}) e^{-k_{\text{exp}} t} \quad (10.3)$$

where A_{∞} is the final absorbance and A is the absorbance at any time t . Both sides of Eq. (10.3) can be multiplied by $e^{k_{\text{exp}} t_d}$, and noting that $t_{\text{exp}} = t - t_d$, one obtains

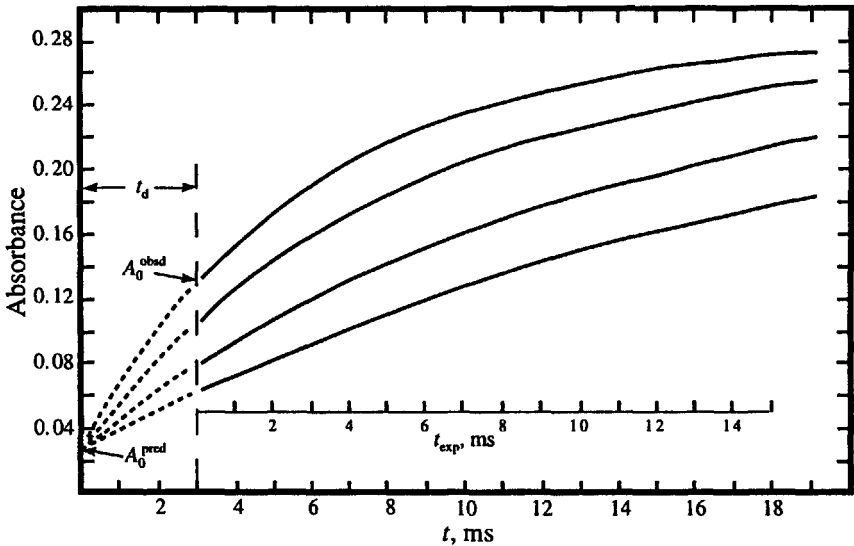


Figure 10.1. Schematic stopped-flow recordings with varying first-order rate constants, showing the variation of the observed initial absorbance, A_0^{obsd} , with the rate constant.

$$\begin{aligned} (A_\infty - A)e^{k_{\text{exp}}t_d} &= (A_\infty - A_0^{\text{pred}})e^{-k_{\text{exp}}(t - t_d)} \\ &= (A_\infty - A_0^{\text{pred}})e^{-k_{\text{exp}}t_{\text{exp}}} \end{aligned} \quad (10.4)$$

Substitution of the limiting condition that $A = A_0^{\text{obsd}}$ when $t_{\text{exp}} = 0$ into Eq. (10.4) and rearrangement yields the expression

$$(A_\infty - A_0^{\text{obsd}}) = (A_\infty - A_0^{\text{pred}})e^{-k_{\text{exp}}t_d} \quad (10.5)$$

which can be used to determine t_d from the measurable quantities k_{exp} , A_0^{obsd} and A_0^{pred} . Since $k_{\text{exp}} = k_1[\text{R}]$, then R can be varied in a series of experiments and A_0^{obsd} should change, as shown in Figure 10.1, so that an average t_d , which should be independent of [R], can be calculated.

Substitution from Eqs. (10.2) and (10.5) into Eq. (10.3) gives

$$(A_\infty - A) = (A_\infty - A_0^{\text{obsd}})e^{-k_{\text{exp}}t_{\text{exp}}} \quad (10.6)$$

which shows that k_{exp} is independent of t_d and is determined from the dependence of $(A_\infty - A)$ on t_{exp} .

The situation is more complex for studies under second-order conditions because the reagent concentrations at the true zero time must be known. Meagher and Rorabacher¹³ have analyzed the second-order system of reactants A + B coming to equilibrium with products C + D and have given

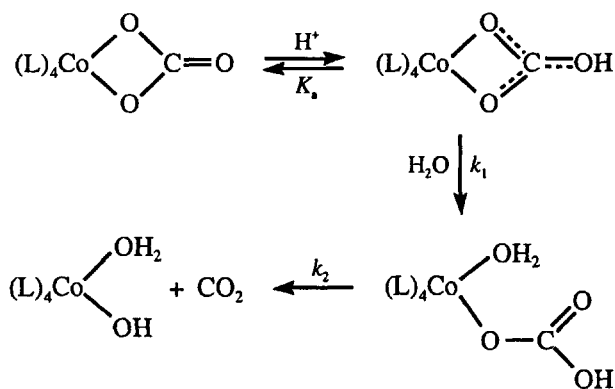
the integrated expression for the time dependence of the concentration change. The deadtime could be adjusted to give the A_0^{pred} , if this value is known, and Meagher and Rorabacher have suggested an empirical way of dealing with the mixing problem.

Another limitation of stopped-flow mixing is that the reagent solutions should be of similar composition in order to avoid spurious effects due to inhomogeneous mixing. It is always advisable to do blank observations to ensure that no apparent reaction is observed in the absence of each reactant.

There are numerous applications of this method in which the collection and analysis of the experimental rate constants are entirely straightforward. Modern instruments also allow for the collection and global analysis of data at several wavelengths. The few examples described below illustrate some special aspects or address problems of long-standing interest.

The hydrolysis of Co(III) carbonate chelates in acidic solution has been the subject of numerous studies and may be a model for the carbonic anhydrase catalyzed dehydration of CO_2 . The results have been reviewed and reanalyzed.¹⁴ Buckingham and Clark¹⁵ have provided new insight into this reaction by taking advantage of the multiwavelength observation capabilities of modern instruments. As a result, it has been possible to show that the reactions are often biphasic and to identify the optimum wavelength to observe the biphasic character. The elements of the mechanism are shown in the Scheme 10.1.

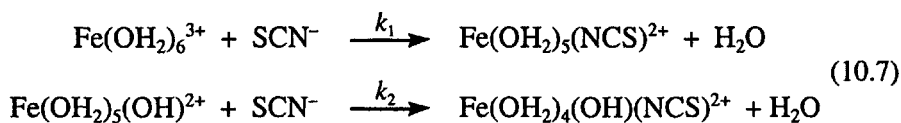
Scheme 10.1



For some systems, the protonated species has been detected and the K_a determined. The two steps in the reaction are assigned to chelate ring opening, k_1 , and decarboxylation, k_2 , of the monodentate bicarbonate complex. This work provides an example of the ambiguity in assigning each rate constant to the correct reaction in biphasic systems. The $[\text{H}^+]$ dependence was used to assign the larger rate constant to the chelate ring opening step for $\text{Co}(\text{NTA})(\text{O}_2\text{CO})^{2-}$ and $\text{Co}(\text{tren})(\text{O}_2\text{CO})^+$, but to the

decarboxylation for $\text{Co}(\text{gly})_2(\text{O}_2\text{CO})^-$ and $\text{Co}(\text{NH}_3)_4(\text{O}_2\text{CO})^+$. It was found that $K_a \sim 1 \text{ M}$ and $k_2 \sim 1 \text{ s}^{-1}$ (25°C , 1.0 M NaClO_4) for all the systems studied. This insensitivity to the ancillary ligands is consistent with protonation at a site remote from the $\text{Co}(\text{III})$, and for the $\text{O}-\text{C}$ rather than the $\text{Co}-\text{O}$ bond breaking for the decarboxylation. However, k_1 changes by $\sim 10^4 \text{ s}^{-1}$ for different $(\text{L})_4$ systems because the $\text{Co}-\text{O}$ bond is broken. Buckingham and Clark¹⁵ suggest a detailed mechanism that involves an intermediate or minor equilibrium species with a proton transferred to a carbonate oxygen bound to $\text{Co}(\text{III})$.

Reactions of aqueous $\text{Fe}(\text{III})$ with various ligands often yield highly colored products. The classic example of this is the deep red thiocyanate complex, $\text{Fe}(\text{OH}_2)_5(\text{NCS})^{2+}$. This system is ideal for study because of the large absorbance change and the ready availability of reagents. There is some mechanistic interest because reactivity arguments have suggested that the substitution mechanism is associative for $\text{Fe}(\text{OH}_2)_6^{3+}$ and dissociative for $\text{Fe}(\text{OH}_2)_5(\text{OH})^{2+}$. A number of pressure-dependent studies have been done in the expectation that ΔV^\ddagger values would help to validate the reactivity arguments. There is general agreement that the reaction proceeds by the following two pathways:



Earlier studies,¹⁶⁻¹⁸ mainly using pressure- and temperature-jump relaxation methods, obtained values of $(1.2-1.5) \times 10^2 \text{ M}^{-1} \text{ s}^{-1}$ for k_1 and $(1-4) \times 10^4 \text{ M}^{-1} \text{ s}^{-1}$ for k_2 , at 25°C . But stopped-flow methods^{19,20} have given values of $70-90 \text{ M}^{-1} \text{ s}^{-1}$ for k_1 and $(4-7) \times 10^3 \text{ M}^{-1} \text{ s}^{-1}$ for k_2 . Furthermore, the activation volumes from six studies range from -6.1 to $+6.7 \text{ cm}^3 \text{ M}^{-1}$ for k_1 , and from 0 to $+16.5 \text{ cm}^3 \text{ M}^{-1}$ for k_2 . The most recent study by Grace and Swaddle²¹ used high-pressure stopped flow, low concentrations and second-order conditions for $\text{Fe}(\text{III})$ and SCN^- , in order to avoid higher-order thiocyanate complexes. They obtained ΔV^\ddagger values of $-5.7 \text{ cm}^3 \text{ M}^{-1}$ and $+9.0 \text{ cm}^3 \text{ M}^{-1}$ for k_1 and k_2 , respectively. These results agree with the earlier stopped-flow study of Funahashi et al.²⁰ with a large excess of SCN^- , but not with results from temperature-jump and pressure-jump relaxation methods. Funahashi et al. suggested that some of the earlier work was affected by nitrate ion complexation from the $\text{NaNO}_3/\text{HNO}_3$ medium used, but the results of Capitan et al.¹⁹ show rather small differences in rate constants at 25°C between nitrate and perchlorate media. Grace and Swaddle²¹ noted that some relaxation studies might be affected by incorrect speciation, but reanalysis did not remove the disparity. They proposed that electric discharge effects in the temperature-jump measurements may affect the observations. It may be relevant that Betts and Dainton²² have observed the oxidation of SCN^- by aqueous $\text{Fe}(\text{III})$.

10.1.3 Continuous Flow

Historically, continuous flow preceded stopped flow as a method for studying moderately fast reactions. The reactant solutions continuously flow through the mixer and observation chamber, and the time is varied by changing the flow rate or by changing the distance between observation point and mixer. The apparatus is simple, but large amounts of reagents are consumed. Pulsed continuous flow,²³ a method in which continuous flow is established for a short time, can reduce reagent consumption to ~5 mL, and fast jet mixers have lowered the accessible reaction half-time to the 10- μ s range. The concentration of the reagent being monitored can be lowered if integrating observation is used, in which the flowing solution is viewed down the length of the observation cell. A combined continuous flow with integrating observation and stopped-flow system has been described.²⁴

10.1.4 Pulsed Accelerated Flow

This method may be viewed as an adaptation of pulsed continuous flow, in which the flow rate through the mixer and observation chamber is varied during the course of one run. Most applications of this method have been from Margerum and co-workers.²⁵ The method can be used for half-times down to ~10 μ s, compared to ~10 ms for stopped flow. The complexity of the analysis limits the method to first-order reaction conditions.

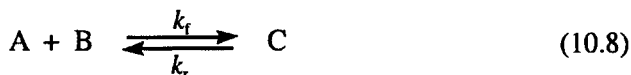
10.2 RELAXATION METHODS

In these methods, a system at equilibrium is subjected to a perturbation and the kinetics of the system relaxing to the new equilibrium condition is followed. The perturbation normally is a change in temperature, pressure or concentration of one of the reagents, and the methods are known as temperature-jump, pressure-jump and concentration-jump, respectively. The advantage of these methods is that the perturbation, especially of temperature and pressure, can be applied very quickly and reactions with half-times in the microsecond range can be observed. The pioneering work on these methods by Eigen and co-workers²⁶ greatly extended the time scale for solution kinetic studies. The major limitation is that the equilibrium position of the reaction must involve significant concentrations of both reactants and products; therefore, relaxation methods are not applicable to essentially irreversible reactions. These methods are especially useful for Lowry-Brønsted acid-base reactions, in which the equilibrium position can be adjusted simply by changing the pH of the solution, and for ligand substitution reactions that involve proton production or consumption.

It is a noteworthy feature of relaxation methods that the changes in concentration caused by the perturbation should not be too large, so that the mathematical analysis can be simplified. This poses some limitations

for the detection method, in that it must be fast but also sensitive enough to detect these small concentration changes. However, it is possible to repeat the perturbation and improve the signal to noise ratio through signal averaging.

The mathematical analysis may be illustrated for the following system:



After the perturbation, the system comes to a new equilibrium with final concentrations $[A_e]$, $[B_e]$ and $[C_e]$, and these may be related to the concentration at any time through the concentration change variable Δ , so that $[A] = [A_e] + \Delta$, $[B] = [B_e] + \Delta$ and $[C] = [C_e] - \Delta$. For more complex stoichiometries, Δ must be multiplied by the appropriate factors. Then, simple differentiation shows that $d\Delta/dt = d[A]/dt = d[B]/dt = -d[C]/dt$, and one can write the usual differential equation for the system as follows:

$$\begin{aligned} \frac{d\Delta}{dt} &= \frac{d[A]}{dt} = -k_f[A][B] + k_r[C] \\ &= -k_f([A_e] + \Delta)([B_e] + \Delta) + k_r([C_e] - \Delta) \end{aligned} \quad (10.9)$$

Expansion and collection of terms gives

$$\frac{d\Delta}{dt} = -k_f([A_e] + [B_e])\Delta - k_r\Delta - k_f[A_e][B_e] + k_r[C_e] - k_f\Delta^2 \quad (10.10)$$

At equilibrium, $k_f[A_e][B_e] = k_r[C_e]$, and these terms cancel. Next, the assumption is made that Δ is very small, so that the term in Δ^2 can be neglected and Eq. (10.10) simplifies to

$$\frac{d\Delta}{dt} = -(k_f([A_e] + [B_e]) + k_r)\Delta = \frac{1}{\tau}\Delta \quad (10.11)$$

where τ is defined as the relaxation time.

If experiments are done with varying positions of the equilibrium, then a plot of τ^{-1} versus $[A_e] + [B_e]$ should have a slope of k_f and an intercept of k_r . This is different from the normal pseudo-first-order system coming to equilibrium where the experimental rate constant is equal to $k_f + k_r$.

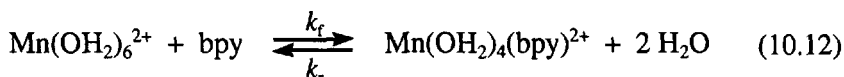
10.2.1 Temperature Jump

For a system at equilibrium, if the temperature is changed by ΔT , then the equilibrium concentrations will change because of the thermodynamic relationship $(\delta \ln K/\delta T)_p = -\Delta H_{rxn}^\circ/RT^2$ between the equilibrium constant and the enthalpy change for the reaction, ΔH_{rxn}° . In most applications and commercial instruments, the sample is contained between two electrodes

and is subjected to a voltage of ~10–100 kV across the electrodes to produce a discharge and a temperature increase of ~5°C. This requires that the solution be electrically conducting, and clearly is somewhat invasive on the sample. It has been noted²⁷ that ion polarization at the charged electrodes can cause spurious but reproducible signals.

For nonconducting solutions, applications of pulsed microwave heating have been described.^{28,29} Heating by an iodine laser has been used,³⁰ photons at 1315 nm are absorbed by overtone vibrations of OH bonds in the solvent to cause the heating.

Hague and Martin³¹ used T-jump to study the complexation of aqueous Mn(II) by 2,2'-bipyridine, shown by reaction (10.12). The work was extended by Doss and van Eldik³² to determine the pressure dependence (21°C, 0.3 M NaClO₄, pH ~6.8).



From both studies, $k_f \approx 2 \times 10^5 \text{ M}^{-1} \text{ s}^{-1}$, and the pressure dependence gave $\Delta V_f^* = -3 \text{ cm}^3 \text{ M}^{-1}$. This negative value was taken as evidence for an I_a mechanism for substitution on $\text{Mn}(\text{OH}_2)_6^{2+}$.

It has been suggested³³ that, with proper calibration, the magnitude of the T-jump change can be used to determine K and $\Delta H_{\text{rxn}}^\circ$. Secco and co-workers³⁴ have done such a study on the reaction of Fe(III) with the thiocyanate ion. They obtained $K = 1.2 \times 10^2 \text{ M}^{-1}$, $\Delta H_{\text{rxn}}^\circ = -1.6 \text{ kcal mol}^{-1}$ and $k_1 = 6 \times 10^2 \text{ M}^{-1} \text{ s}^{-1}$ (25°C, 0.5 M HClO₄). Unfortunately, these values are not in agreement with current stopped-flow values of $K \approx 2 \times 10^2 \text{ M}^{-1}$ and $k_1 \approx 1 \times 10^2 \text{ M}^{-1} \text{ s}^{-1}$. Secco and co-workers overlooked the earlier studies of Brower¹⁶ and Funahashi et al.,²⁰ and the contribution of the k_2 pathway.

10.2.2 Pressure Jump

This method requires a finite volume change for the reaction, $\Delta V_{\text{rxn}}^\circ$, so that the equilibrium constant will change with pressure due to the relationship $(\delta \ln K / \delta P)_T = -\Delta V_{\text{rxn}}^\circ / RT$. The experiment is done by putting the sample under high pressure and then suddenly reducing the pressure by piercing a diaphragm. High-pressure equipment and observation cells are required, but the perturbation seems less invasive on the sample than T-jump by electrical discharge. A P-jump system with conductivity detection has been described recently.³⁵

10.2.3 Concentration Jump

The system is perturbed by adding a small amount of one of the species in the equilibrium reaction. Generally, the apparatus is much simpler compared to the T-jump or P-jump methods, but the perturbation cannot be done as quickly so that the short-time limit is in the millisecond range.

10.3 ELECTROCHEMICAL METHODS

There are several electrochemical methods, such as cyclic voltammetry, polarography, chronoamperometry and chronopotentiometry, which can be used to measure homogeneous reaction rates. It is beyond the scope of this text to explore all the variations and intricacies of electrochemical methods, but they are described in several sources.³⁶ The purpose here is to give some basic background and some examples of the technique.

In general, electrochemical observations can give information about homogeneous reaction rates when an electrode reaction is coupled to a homogeneous chemical reaction and the rate of the latter becomes rate limiting for the process at the electrode. Sometimes, the chemical rate constant can be extracted fairly directly from the observations, or it may require curve matching of experimental and simulated curves computed with various rate constants. Since the size and composition of the electrode and the diffusion coefficients of reagents affect the kinetics of the electrode reaction, these factors will influence the observations and the effective time range for these methods.

The field has a well-developed nomenclature and symbolism. The one-electron electrode reaction is designated by **E** and a chemical reaction by **C**. There are extensions of this system, such as **E+E** for a two-electron electrode reaction, $\bar{\text{E}}$ and $\bar{\text{E}}$ for reduction and oxidation, **C1** and **C2** for first- and second-order reactions and **C1'** for a pseudo-first-order reaction. Cyclic voltammetry is the most widely used technique because of the availability of appropriate instrumentation, and the number of applications is likely to increase with the recent availability of software^{37,38} to simulate cyclic voltammograms. Such simulations generally are essential for the determination of meaningful kinetic parameters.

An idealized cyclic voltammogram, CV, and some terminology of this technique are shown in Figure 10.2. The experiment is carried out by changing the voltage, E , of the working electrode at some constant sweep rate, ν , and measuring the current, i . Then, the sweep rate and reagent concentrations are changed and the changes in cathodic and anodic peak potentials, E_{pc} and E_{pa} , respectively, and peak current, i_p , are analyzed.

The quantitative analysis requires knowledge of the rate(s) of the heterogeneous electrode reaction(s), reagent diffusion coefficients and the transfer coefficient. If the electrode reaction is reversible, most of these parameters can be determined from the CV experiments. The formal reduction potential, $E^{\circ'}$, differs from the standard potential, E° , because the latter is obtained by extrapolation to infinite dilution, while the former refers to the actual experimental conditions of ionic strength and temperature. For a fast, reversible process, $E^{\circ'} \approx E_{1/2} \pm 10$ mV if the diffusion coefficients of the oxidized and reduced forms are within a factor of two. Potentials are reported relative to some standard electrode, such as ferrocene/ferrocinium ion, saturated calomel, SCE, or Ag/AgCl, and this must be taken into account in comparing results from different sources.

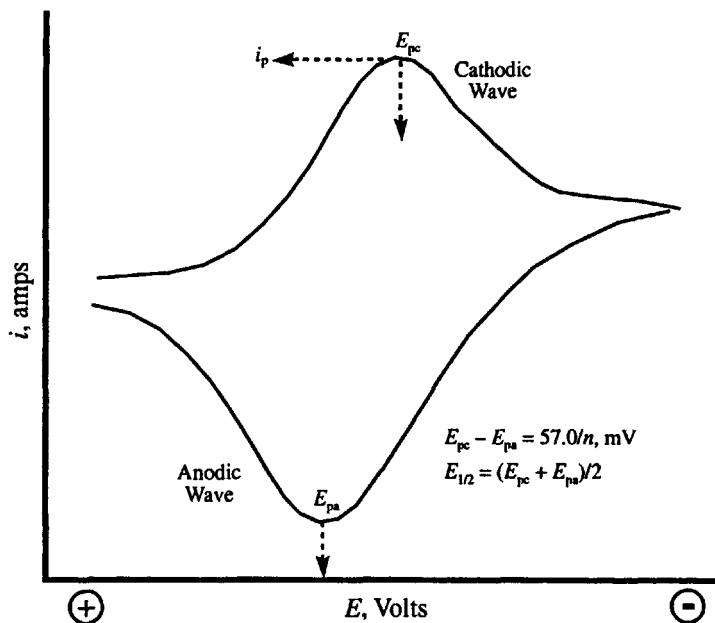


Figure 10.2. Sketch of a cyclic voltammogram for a reversible electrode reaction.

One restriction on these methods is that the medium must contain an "inert" electrolyte to maintain electrical conductivity. Typically, 0.1 M tetraalkylammonium salts of PF_6^- , CF_3SO_3^- or ClO_4^- are used. Problems can arise due to adsorption of reagents on the electrodes and uncertainties in the chemical characterization of the product of the electrode reaction. The experiment can give the number of electrons, n , involved and the reduction potential. Then, the nature of the electrochemically generated reagent often is inferred by chemical reasoning and analogy. It is possible to couple the system to some spectroscopic technique, such as EPR³⁹ or IR spectroscopy with transparent electrodes,⁴⁰ to give further characterization.

The electrochemical behavior of aqueous Cu(II) and Cu(I) complexed by 2,9-dimethyl-1,10-phenanthroline, DMP, has been studied by Lei and Anson.⁴¹ The measurements involved cyclic and rotating-disk voltammetry with glassy carbon electrodes at pH 5.2 in a buffer containing 0.04 M aqueous acetic, phosphoric and boric acids, at ambient temperature. Glassy carbon electrodes were used to minimize adsorption of electroactive species on the electrode. If the initial ratio of DMP to Cu(II) is ≥ 2 , then a normal CV is observed and assigned to the following reaction:



With equal concentrations of DMP and Cu(II), the electrochemical response is more complicated. Cathodic and anodic peaks appear at the

same positions as in the $\text{Cu}(\text{DMP})_2^{2+}/\text{Cu}(\text{DMP})_2^+$ system, and a new cathodic peak is observed at ~ 0.1 V and assigned to the reaction



There is no anodic peak, however, and the sum of the cathodic peak currents is smaller than expected for reduction of all the Cu(II) present. This may be accounted for by the ligand redistribution reaction



which removes $\text{Cu}(\text{DMP})_2^+$ and forms Cu^{2+} . Uncomplexed Cu^{2+} was not detected because it would appear below the experimental scan range, at -0.1 V. When the scan rate is increased from 50 to 250 mV s^{-1} , the anodic part of the $\text{Cu}(\text{DMP})_2^{2+}/\text{Cu}(\text{DMP})_2^+$ reaction appears, indicating that the scanning is faster than the ligand redistribution reaction (10.15) that removes $\text{Cu}(\text{DMP})_2^+$ at low scan rates. This reaction must be faster than the redistribution of the Cu(II) species, shown by the following reaction:



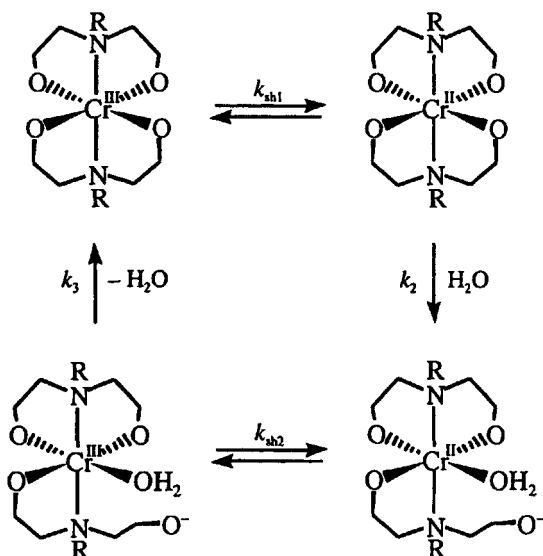
Otherwise, no $\text{Cu}(\text{DMP})_2^{2+}/\text{Cu}(\text{DMP})_2^+$ wave would be observed.

Quantitative analysis, based on a comparison of the experimental and simulated voltamograms, indicates values of $k_1 = 1.1 \times 10^4 \text{ M}^{-1} \text{ s}^{-1}$ and $k_2 = 5 \times 10^2 \text{ M}^{-1} \text{ s}^{-1}$, with equilibrium constants for the same reactions of 3×10^3 and 7.9×10^{-2} , respectively. Further analysis gave complex formation constants for $\text{Cu}(\text{DMP})_2^+$ and $\text{Cu}(\text{DMP})_2^{2+}$ of 6.7×10^8 and $1.5 \times 10^{10} \text{ M}^{-1}$, respectively. It is the large value of the latter that leads to much of the complexity of the system.

The substitution inertness of Cr(III) and the lability of Cr(II) have allowed Hecht et al.⁴² to observe some ring-opening and ring-closing reactions of amino-carboxylate ligands. The experiments used a stationary Hg drop electrode in 1.0 M Na_2SO_4 at pH 8.5, apparently at ambient temperature. Their observations can be explained by Scheme 10.2, where the aliphatic substituent R gives the *trans*-N,N geometry shown.

For such systems, initial CV reduction of the Cr(III) complex shows a broad cathodic wave whose position shifts from about -1.4 to -1.6 V as the sweep rate is increased. This is typical of an irreversible reduction with sluggish electrode kinetics and is assigned to the k_{sh1} process. If the voltage sweep is reversed after the irreversible reduction and the CV continued, then anodic (-1.18 V) and cathodic (-1.25 V) peaks appear, typical of a reversible process. These were assigned to k_{sh2} , the oxidation/reduction of the ring-opened species. Values of k_{sh1} and k_2 were determined by comparison of voltamograms at various sweep rates to the digital

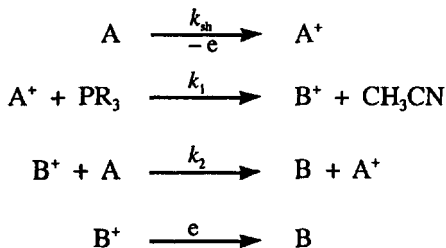
Scheme 10.2



simulations, and values of k_{sh2} and k_3 were obtained similarly from pre-electrolyzed solutions containing the Cr(II) complex. The results gave k_2 and k_3 values of 35 ± 6 and $1.3 \pm 0.2 \text{ s}^{-1}$, respectively, for $R = \text{Me}$, and $(7.3 \pm 3.4) \times 10^2$ and $(2.2 \pm 0.2) \times 10^2 \text{ s}^{-1}$ for $R = \text{Et}$.

Kochi and co-workers⁴³ used cyclic voltammetry to study the oxidation of $\text{Mn}(\eta^5\text{-H}_3\text{CC}_5\text{H}_4)(\text{CO})_2(\text{NCCH}_3)$ with 0.1 M Et_4NClO_4 in acetonitrile at a platinum electrode. The acetonitrile complex has a reversible CV wave ($E^\circ = 0.19 \text{ V}$ vs $\text{Fe}(\text{Cp})_2^+/\text{Fe}(\text{Cp})_2$), but when another ligand, PR_3 , is added to the system, the observations can be understood in terms of Scheme 10.3.

Scheme 10.3



$k_1, \text{M}^{-1} \text{s}^{-1}$	$\text{P}(\text{OPh})_3$	$\text{P}(\text{Ph-4-Cl})_3$	PPh_3	$\text{P}(\text{Me})\text{Ph}_2$
	12	9.5×10^2	1.3×10^2	$> 1 \times 10^5$

The reduction wave for the A^+ species is decreased to an extent dependent on the PR_3 concentration and the scan rate, and a new wave appears due to B/B^+ . This is attributed to relatively rapid substitution of $NCCH_3$ by PR_3 in the 17-electron A^+ species, with a second-order rate constant k_1 . By digital simulation of the voltamograms, the values of k_1 shown on Scheme 10.3 were determined for various PR_3 at 25°C. The span of these values provides an indication of the dynamic range of the method. This system is somewhat unusual because the k_2 reaction is thermodynamically favorable and provides the propagation step for a catalytic pathway for substitution of CH_3CN by PR_3 . This work was extended⁴⁴ to substituted pyridines as leaving groups, and leaving and entering group effects were analyzed.

Later, Sweigart and co-workers⁴⁵ used electrochemical oxidation to make the analogous anions $Mn(\eta^5-R_nC_5H_{5-n})(CO)_3^+$ ($R = Me, Ph, ^nBu; n = 2, 3$) and studied their reactions with $P(OEt)_3$ in CH_2Cl_2 at 25°C. The rate constants found for the formation of $Mn(\eta^5-MeC_5H_4)(CO)_2(P(OEt)_3)^+$ and then $Mn(\eta^5-MeC_5H_4)(CO)(P(OEt)_3)_2^+$ were 1×10^8 and $3.1 \times 10^3 \text{ M}^{-1} \text{ s}^{-1}$, respectively. The larger value was determined by the pre-wave method of Parker and Tilset⁴⁶ under conditions of a deficiency of $P(OEt)_3$, such as $[P(OEt)_3]/[Mn] = 0.55$. The rapid reaction depletes the concentration of $P(OEt)_3$ at the electrode surface so that the later part of the wave appears as a normal wave of the unreacted cation.

10.4 NUCLEAR MAGNETIC RESONANCE METHODS

There is a wide variety of applications of NMR to problems in inorganic kinetics. The time scale depends on the type of system and can vary from hours for simply monitoring concentration changes of reactants and products, to microseconds for studying exchange and fluxional processes on paramagnetic systems. One great advantage of NMR is that the temperature can be changed over a wide range, from about -200°C to +150°C, without significant instrument modification. Another advantage is the molecular specificity of the NMR signal, which often permits an assignment of the composition and structure of stable intermediates and products. The specificity is augmented by the ability to detect a wide range of NMR active nuclei; 1H , ^{13}C , ^{19}F and ^{31}P are standard for most modern NMR instruments, and many metals have NMR active isotopes that can be observed with appropriate modifications. A feature that is almost unique to NMR is the ability to measure rates of reactions in which there is no net chemical change, such as solvent exchange and ligand fluxionality. The major limitation of NMR is sensitivity, and concentrations must be typically about 0.01 M, unless signal averaging is possible. However, the small sample size of 0.5–2 mL allows for modest materials consumption.

Discussions of the theory and quantitative analysis in this area often use the lifetime, τ , of a nucleus in a particular site as the kinetic feature of interest. This lifetime has the conventional definition (see Section 1.1) of

the concentration of nuclei in the site divided by their rate of disappearance from the site. To establish the relationship between the rate constant and the lifetime, it is necessary to define τ clearly because of ambiguities due to the number and populations of sites.

For example, the exchange of nuclei between a hydrated metal ion $M(\text{OH}_2)_n^{z+}$ and bulk solvent water can be represented by reaction (10.17) with whole water molecule exchange, or by reaction (10.18) with just proton exchange.



In either case, there are two lifetimes, τ_m for the water ligands and τ_s for the bulk solvent. There is an ambiguity as to whether one is considering whole water molecule exchange with n coordinated sites, as in reaction (10.17), or proton exchange with $2n$ such sites, as in reaction (10.18). If ^{17}O NMR is used, then only whole molecule exchange will be observed and the definitions are straightforward and given by

$$\tau_m = \frac{n[M^{z+}]}{\text{Rate}} \quad \tau_s = \frac{[\text{H}_2\text{O}]}{\text{Rate}} \quad \text{Rate} = k[M^{z+}]^x[\text{H}_2\text{O}]^y \quad (10.19)$$

If ^1H NMR is used, then the populations in each site are multiplied by 2 because there are two hydrogens per water molecule and the lifetimes are defined by

$$\tau'_m = \frac{2n[M^{z+}]}{\text{Rate}} \quad \tau'_s = \frac{2[\text{H}_2\text{O}]}{\text{Rate}} \quad \text{Rate} = k'[M^{z+}]^x[\text{H}_2\text{O}]^y \quad (10.20)$$

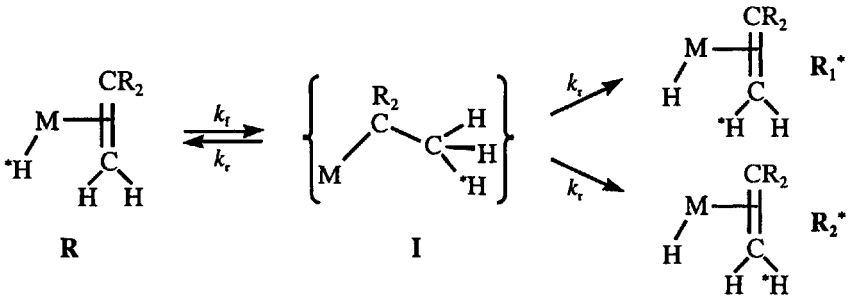
If one believes that the exchange involves a water molecule, then k in Eq. (10.19) is the rate constant for exchange of one water ligand. But k' in Eq. (10.20) is for exchange of one H and, since there are two H atoms per ^{17}O , then $k = k'/2$. However, if H exchange occurs only by reaction (10.18), then k' is the rate constant as defined by Eq. (10.20). Therefore, ^{17}O NMR will give k for water molecule exchange, but the k' from ^1H NMR has an ambiguous assignment. For other solvents, such as acetonitrile, DMF and DMSO, where independent exchange of the methyl protons is very unlikely, the site population factor in Eq. (10.20) is often implicitly omitted and the τ definitions refer to whole solvent molecule exchange.

Fluxional processes present another example where it is important to define the rate and to understand the relationship between the rate constant from the NMR measurement and that for the chemical event. The latter aspect has been discussed in detail by Johnson and Moreland⁴⁷ and more recently by Green et al.⁴⁸

A simple example is the H exchange in an η^2 -alkene metal hydride. The NMR experiment may be done by labeling either the hydride or alkene hydrogens, and this leads to different relationships between the NMR rate constant and the rate constant for the H shift. The labeling might be done by isotope substitution or by selective spin saturation or inversion in a pulsed NMR experiment.

The hydride labeling experiment is proposed to proceed through an η^1 -alkyl intermediate, **I**, as shown in Scheme 10.4.

Scheme 10.4



The general principle can be illustrated with the simplifying assumption that the H atoms in the η^2 -alkene (**R**) are magnetically equivalent and then the products (**R₁*** and **R₂***) are identical in the NMR spectrum. The NMR experiment monitors the conversion of **R** to **R₁*** + **R₂***, and the problem is to determine how the rate of this process is related to k_f . First, one can make a steady-state assumption for the intermediate **I**

$$\frac{d[\mathbf{I}]}{dt} = k_f[\mathbf{R}] - 3k_r[\mathbf{I}] = 0 \quad (10.21)$$

and obtain the steady-state concentration, given by

$$[\mathbf{I}] = \frac{k_f[\mathbf{R}]}{3k_r} \quad (10.22)$$

Then, the rate of loss of **R** that is measured by NMR is given by

$$-\frac{d[\mathbf{R}]}{dt} = k_f[\mathbf{R}] - k_r[\mathbf{I}] \quad (10.23)$$

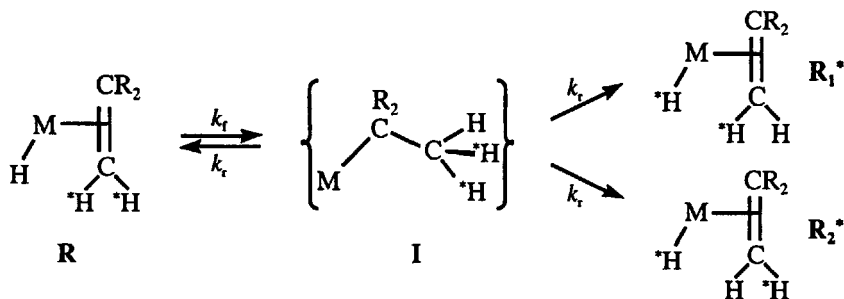
Substitution for **I** from Eq. (10.22) and rearrangement gives

$$-\frac{d[\mathbf{R}]}{dt} = \frac{2}{3}k_f[\mathbf{R}] \quad (10.24)$$

This is the rate measured by NMR and the observed rate constant is $k_{\text{obsd}} = (2/3)k_f$.

If the experiment is done by labeling the CH₂ protons, then the system is represented by Scheme 10.5.

Scheme 10.5



The steady-state concentration of **I** is given by Eq. (10.22), but the two reactions at the right return half of the magnetization or label to the original site **R** so that the rate of disappearance from **R** is given by

$$-\frac{d[\mathbf{R}]}{dt} = k_f[\mathbf{R}] - k_r[\mathbf{I}] - 0.5k_r[\mathbf{I}] - 0.5k_r[\mathbf{I}] \quad (10.25)$$

Substitution from Eq. (10.22) and rearrangement gives

$$-\frac{d[\mathbf{R}]}{dt} = \frac{1}{3}k_f[\mathbf{R}] \quad (10.26)$$

The measured rate constant is $k_{\text{obsd}} = (1/3)k_f$ in this case. The difference between Eqs. (10.24) and (10.26) results from the different populations of the sites and requires that the H atoms of the alkene are magnetically equivalent. Further examples are given by Green and co-workers.⁴⁸

In the following discussion, the NMR methods are separated into four categories, roughly in the order of decreasing time scale of their applicability. However, the latter is quite dependent on the system and different methods might be used in different temperature ranges. The important variables of the chemical system are the correct assignment of the spectrum, the chemical shift differences of the species or sites involved in the reaction and the nuclear relaxation times of the nuclei being observed. There have been several recent reviews of dynamic NMR applications and the field is referred to as DNMR.^{49,50}

10.4.1 Signal Monitoring

This method refers to the simple monitoring of the changes with time of the concentration of reactants and products, as determined from the integrated intensities of the appropriate peaks in the NMR spectrum. The short time scale is the few minutes required for temperature equilibration

and instrument setup and the long time is limited only by sample stability. For pulsed Fourier transform instruments, it is important to remember that the repetition rate or relaxation delay must be 8–10 times longer than the nuclear longitudinal relaxation time(s), T_1 , in order to obtain correct relative intensities. The T_1 values for ^1H and ^{13}C nuclei can be in the 1- to 10-s range, and this puts a limitation on the repetition rate.

A special example of this type of application is the measurement of exchange reactions using appropriate isotopes. For example, the exchange between free CO and CO ligands in metal carbonyls can be measured using ^{13}C -enriched CO, and the exchange between H_2O and oxo anions⁵¹ or water ligands can be measured in suitably inert systems using ^{17}O enrichment.⁵² Deuterium replacement of ^1H can be used to measure proton exchange between water and weakly acidic ligands, such as amines.⁵³ Isotopically labeled ligands can be used to measure electron-exchange rates when one of the partners is diamagnetic.⁵⁴

10.4.2 Magnetization Transfer

This method is simple to qualitatively envisage and interpret.⁵⁵ A selective pulse (or DANTE series of pulses⁵⁶) is used to produce spin inversion or saturation at one site. After a variable waiting period, t_m , a 90° pulse is used to generate the normal spectrum of the system. As exchange proceeds, the inverted nuclei appear in other sites and the intensities of the sites involved in the exchange will decrease. The pattern of the intensity changes is indicative of the exchange pathways in multisite systems. As t_m is increased to the stage where $t_m > T_1$, the natural nuclear relaxation processes tend to restore the intensity and the intensity of the sites involved in the exchange will increase due to T_1 processes.

The accessible range of exchange lifetimes, τ , for this method is determined on the short end by t_m and on the long end by T_1 . For typical spectrometers, t_m can be as short as ~ 0.01 s and T_1 for protons is often ~ 1 s, so that first-order rate constants of ~ 1 – 100 s^{-1} can be determined. Because T_1 usually has a lower activation energy (~ 5 – 10 kJ mol^{-1}) than τ , it is often possible to adjust the temperature to meet the requirement of this method that $T_1 \geq \tau$. The apparent necessity to selectively invert only one signal could be a problem if resonances are close, but this limitation can be overcome by the suggestion of Muhandiram and McClung⁵⁷ to treat both the initial and final intensities as variables in the analysis. Inversion of a multiplet due to spin–spin coupling can be achieved with a single pulse, broad enough to cover the multiplet for small coupling constants, or by pulses of different frequencies in the DANTE sequence for large coupling constants. It has been found⁵⁸ that spin–spin coupling does not adversely affect rate constant determinations by this method. Because of the competition between exchange and the T_1 processes, it is advantageous for quantitative analysis to measure the T_1 values independently under slow exchange conditions.

10.4.3 Two-Dimensional Exchange Spectroscopy

This method is discussed in detail in the review by Perrin and Dwyer⁵⁰ and is called 2D EXSY. In the experiment, a 90° pulse is applied to rotate the magnetization from the +z to the -x axis. After a time t_1 , called the evolution or labeling time, a second 90° pulse rotates the magnetization from the xy plane into the xz plane and a field gradient or homospoil pulse is applied to dephase the magnetization along the x axis. After a further time t_m , called the mixing time, a third 90° pulse rotates the magnetization to the y axis and the free induction decay, FID, is collected during a time t_2 . The magnetization evolves in the xy plane during the two time periods, t_1 and t_2 . For a single site, the angular rate of precession is ω , and maxima will occur when $\cos(\omega t_1)$ and $\cos(\omega t_2)$ equal 1. Then, a three-dimensional plot of intensity versus t_1 and t_2 will show a maximum when this condition is satisfied for t_1 and t_2 . The peak is often represented by intensity contours and is really a cone. For a multisite system, nuclei in different environments have different precessional rates, ω_i , but will give maxima when $\cos(\omega_i t_1)$ and $\cos(\omega_i t_2)$ equal 1 and will give peaks along the diagonal of the t_1 - t_2 plane when $t_1 = t_2$.

When the system is undergoing chemical exchange, magnetization can transfer between the sites during the mixing time, and this produces off-diagonal cross peaks in the final three-dimensional plot of the spectra. These cross peaks give a map of the sites that are undergoing exchange. The evaluation of rate constants from the information is based on the intensities or, more properly, the volumes of the cross peaks. This analysis is not trivial, especially for multisite systems, and requires special care in the collection and processing of the data to ensure that the volumes of the peaks are properly evaluated.

There are several other sources of cross peaks in the 2D EXSY experiment. Dipolar coupling with nearby nuclei (nuclear Overhauser effects) produces cross peaks, as observed in standard Nuclear Overhauser Enhancement Spectroscopy, NOESY. These can be identified because exchange usually has a larger temperature dependence than dipolar coupling. Scalar coupling interferes with 2D EXSY by producing so-called J cross peaks that can be eliminated by phase cycling.⁵⁹

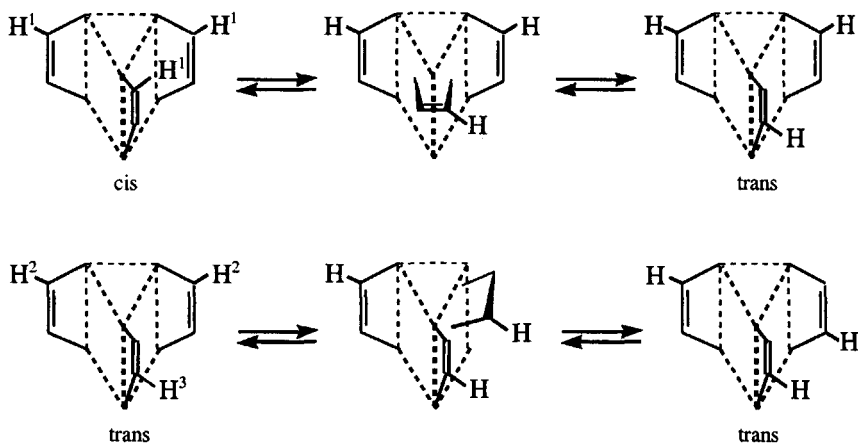
The choice of the mixing time is crucial for this method because it is quite time consuming to do studies by varying t_m as well as t_1 and t_2 . If t_m is too short, then little mixing will occur and the intensities of the cross peaks will be small and difficult to analyse; if t_m it is too long, the intensities approach those of the diagonal peaks and become insensitive to the exchange rate. For a two-site system, AB, with known or estimated values for T_1 and the rate constants, k_{AB} and k_{BA} , Perrin and Dwyer⁵⁰ suggested that the optimum mixing time is given by

$$t_{m(\text{opt})} = \frac{1}{T_1^{-1} + k_{AB} + k_{BA}} \quad (10.27)$$

Clearly, for a multisite system with different exchange rates, there will not be a single optimum value. In any case, the accessible range of rate constants is limited by the nuclear relaxation rate T_1^{-1} , and therefore is similar to the range for magnetization transfer.

The 2D EXSY method has been applied⁶⁰ to the rearrangements of tris(dithiolene) complexes of the general type $M(S_2C_2R_1R_2)_3$, where M is W or Mo, R_1 is phenyl or substituted phenyl and R_2 is H or phenyl. The structures in solution are believed to be trigonal prismatic, based on the crystal structures of analogous complexes,⁶¹ and the asymmetric substitution gives the possibility of cis and trans isomers. However, there is the possibility that these are fac and mer isomers. The authors' structural assignments are shown by the left-hand structures in Scheme 10.6, where the R_1 substituents have been omitted for clarity and $R_2 = H$.

Scheme 10.6



For $R_2 = H$, the low-temperature 1H NMR spectrum has three peaks in the expected region that were assigned to H^1 , H^2 and H^3 , as shown at the left in Scheme 10.6. The peaks have approximately a 1:2:1 intensity ratio, respectively, due to the ~3:1 equilibrium mixture of trans:cis isomers. The results of a 2D EXSY experiment on $W(S_2C_2H(p-CH_3OPh))_3$ are shown schematically in Figure 10.3. In addition to the diagonal peaks, cross peaks are observed for all the protons, indicating that all the sites are undergoing exchange with each other. The cross peaks for the H^1-H^3 protons are weakest and give less certain rate constants for this interchange.

Kataakis and co-workers⁶⁰ suggested that the fluxionality is due to the rearrangement reactions shown in Scheme 10.6. The rotation of any ring in either isomer appears to have $\Delta H^\ddagger \approx 60 \text{ kJ mol}^{-1}$. The relative rate constants for the interchange of the different proton types are reasonably consistent with the proposal. For the Mo analogue, bandshape analysis was found to be consistent with the same fluxionality mechanism.

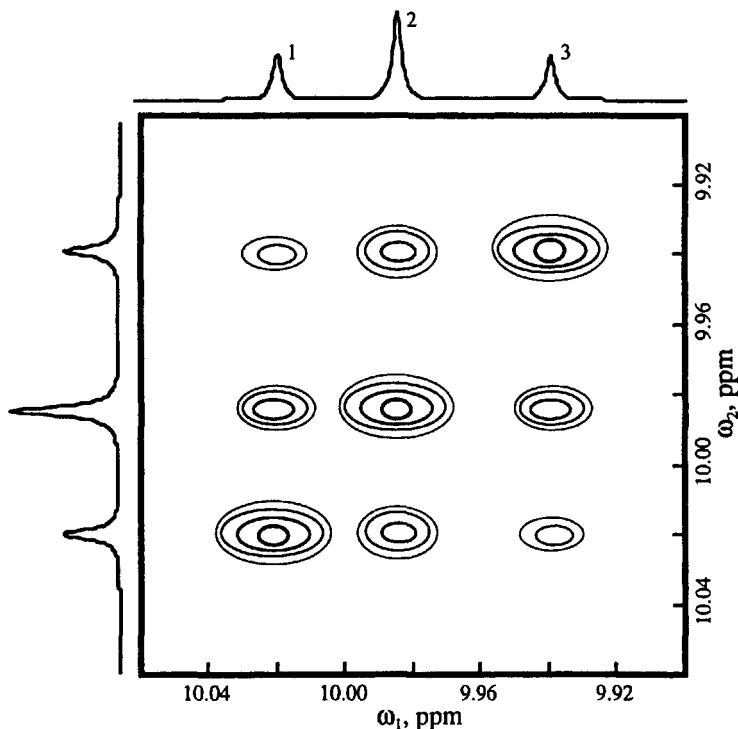


Figure 10.3. The 2D EXSY spectrum of $W(S_2C_2H(p-CH_3OPh))_3$ at $-40^\circ C$ in the dithiolenic proton region with $t_m = 2$ s.

10.4.4 Bandshape Analysis

This method was the first one used to show the applicability of NMR to dynamic processes, and was the only method available during the era of continuous wave NMR. For a system with two sites, in the slow-exchange or low-temperature limit, one observes the normal spectrum with two peaks. If the temperature is raised and exchange starts to occur, then the two peaks begin to broaden and come together. The peaks will coalesce at some temperature, the coalescence temperature, which depends on the exchange rate and the chemical shift separation between the peaks in the absence of exchange. As the temperature is increased further, the signal changes to a single sharp resonance in the fast-exchange limit. For systems with several sites and therefore several peaks in the slow-exchange limit, it is possible to observe the broadening and coalescence of the exchanging sites. The quantitative analysis normally takes the form of calculating the spectrum for various exchange models and rate constants and then choosing the model that best fits the observed spectra and gives rate constants that have the normal temperature dependence. Computer programs are available to generate the calculated spectra.⁶²

The time scale for this method depends on the chemical shift difference, $\Delta\nu_0$, between the exchanging sites. At the coalescence temperature, the rate constant is given by

$$k = \frac{\pi\Delta\nu_0}{\sqrt{2}} = 2.22\Delta\nu_0 \quad (10.28)$$

Below the coalescence temperature, in the slow-exchange region, two peaks are observed that are broadened over their natural full linewidth at half-height by $\delta\nu$, and $k \approx 2\pi\delta\nu$ in this region. Above the coalescence temperature, in the fast-exchange region, only one peak is observed with a linewidth of $\delta\nu$, and $k \approx 4\pi\Delta\nu_0^2/\delta\nu$. For typical parameters in ^1H NMR of $\delta\nu \approx 5$ Hz and $\Delta\nu_0 = 100$ Hz, k can range from ~ 30 to $\sim 3 \times 10^4$ s $^{-1}$. Since $\Delta\nu_0$ depends directly on the magnetic field strength, the range can be extended to larger k by working at higher fields. For other nuclei, such as ^{13}C , ^{19}F and ^{31}P , and for paramagnetic systems, the $\Delta\nu_0$ can be much larger and the upper limit is greatly extended. The lower end of the range for bandshape analysis overlaps the upper range for the two methods discussed above, but the upper limit is extended by $\sim 10^2$ by bandshape analysis.

A limitation of bandshape analysis is that one needs the chemical shifts and linewidths for the nonexchanging system. When possible, this is done by cooling the sample to well below the slow-exchange limit, but the temperature dependence of the shifts and line widths is rarely determined, and they are treated as constants in the analysis. Another problem is that the exchange pathways are not always clearly delineated by bandshape analysis, especially in multisite systems. A model is chosen and fitted to the data, but the initial choice is somewhat subjective, and some pathways may be missed. A problem can arise in the data collection on pulsed Fourier transform instruments. The pulse repetition rate must be substantially longer than the T_1 of any nuclei of interest to ensure that there are no intensity distortions, but there is always the temptation to shorten the repetition time in order to shorten the data collection time. A fairly typical application of bandshape analysis to an inorganic mechanism problem is the recent study of Raymond and co-workers⁶³ on the fluxionality of tris-catecholate complexes of Ga(III), where the ligands are 2,3-dihydroxy-*N,N'*-substituted-terephthalamides. Under slow-exchange conditions, the ^1H NMR at 300 MHz of the isopropyl derivative shows two methyl resonances due to the chirality, as discussed in Section 4.2.3. In D_2O , as the temperature is raised these two peaks merge and coalesce at $\sim 57^\circ\text{C}$. Further increase in temperature produces the expected sharpening to one methyl signal. The spectra over the temperature range of 20°C to 95°C were fitted by bandshape simulations to obtain $\Delta H^* = 55.2$ kJ mol $^{-1}$ and $\Delta S^* = -39$ J mol $^{-1}$ K $^{-1}$ (pD 9.8). The fluxional process was assigned to an intra- rather than an intermolecular ligand rearrangement because the rate was independent of the concentration of free ligand added. From parallel observations in DMSO, the authors suggested that the solvent

effect is minor and therefore also consistent with an intramolecular process. However, the solvent effect analysis was based on calculations of ΔG^\ddagger at the respective coalescence temperatures⁶⁴ of 57°C in D₂O and 87°C in DMSO. The resulting 7 kJ mol⁻¹ difference was considered minor. This analysis represents an example of the all too common practice in this area of comparing two kinetic parameters at different coalescence temperatures. At 57°C, the calculated rate constants are 15.6 s⁻¹ in DMSO and 126 s⁻¹ in D₂O, and the eightfold difference in rate constants might not seem so minor.

Similar studies were reported⁶³ on the unsymmetrical amide ligand with a benzyl group on one nitrogen and a tertiary butyl on the other. This system has cis and trans isomers and the types of interconversion have been discussed in Section 4.2.4. The trans isomer undergoes inversion without isomerization with a coalescence temperature of 22°C, but a full analysis was not possible because the low-temperature limiting spectrum was not reached at 0°C. The cis–trans isomerization was observed at higher temperatures with coalescence at ~67°C. The inversion without isomerization of the trans isomer indicates a trigonal twist mechanism for the rearrangement.

10.4.5 Relaxation Rate Measurements

This type of application is a specialized extension of bandshape analysis in which the temperature dependence of the transverse nuclear relaxation time, T_2 , is used to measure rates of exchange. The T_2 can be determined from the line width of the NMR peak, or more accurately by special pulse sequences. The method is generally applied to simple systems with well-separated peaks in the NMR spectrum. It has been especially useful for measurements of solvent exchange rates from paramagnetic metal ions, such as the example in reaction (10.17). This special application assumes a two-site system with the NMR spectrum dominated by one peak, that of the bulk solvent. Swift and Connick⁶⁵ first published the basic equations that are a solution of the Bloch equations modified for chemical exchange by McConnell.⁶⁶ Analogous equations have been given for T_1 , for the three-site problem⁶⁷ and for the rotating-frame relaxation time⁶⁸ in such systems. The method and results are the subject of several reviews.⁶⁹

An idealized temperature dependence of the relaxation rates is shown in Figure 10.4. The parameter plotted, T_{ip}^{-1} , is the difference between the relaxation rate in the presence of the exchanging species and the rate for the pure solvent, divided by the metal ion concentration. In the high-temperature limit at the left of Figure 10.4, exchange is fast and relaxation is controlled by the nuclear relaxation rate in the inner coordination sphere of the metal ion, T_{2m}^{-1} . As the temperature is lowered, exchange becomes slower and relaxation is controlled by dephasing of the nuclear precession frequency due to the difference in chemical shift between the bulk and coordinated nucleus, $\Delta\omega_m$. The slower the exchange, the more effective is

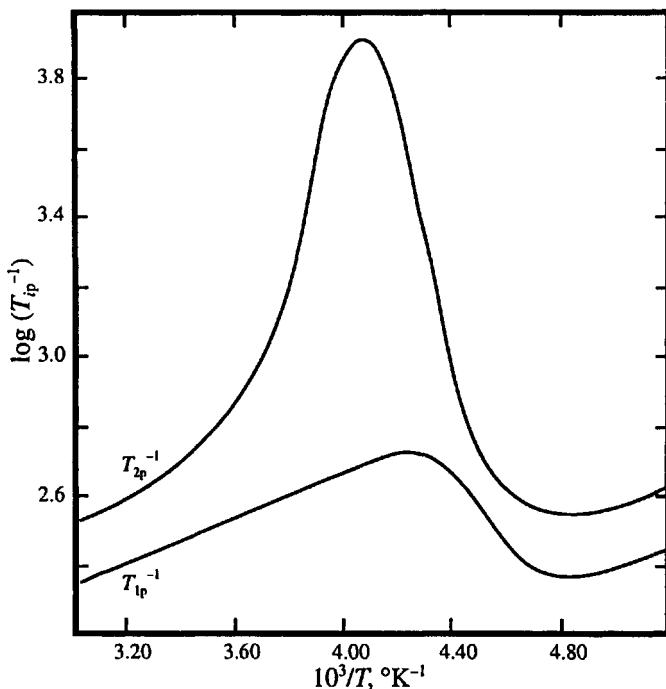


Figure 10.4. Representation of the temperature dependence of T_{2p}^{-1} and T_{1p}^{-1} for an idealized system in which all the regions are observable.

the dephasing, so that the measured relaxation rate increases with decreasing temperature in what is called the non-Arrhenius region. At still lower temperature, the exchange becomes slow enough so that the dephasing is controlled by the exchange lifetime, τ_m , and the relaxation rate decreases with decreasing temperature in the Arrhenius region. Finally, at low temperature, inner-sphere solvent exchange is so slow that only relaxation due to outer-sphere interactions, T_{2o}^{-1} , is observed. The latter effect actually occurs at all temperatures but is generally obscured by the more effective relaxation processes. At the maximum between the Arrhenius and non-Arrhenius regions, $\tau_m^{-1} = \Delta\omega_m$. Since $\Delta\omega_m$ can be in the range of 10^3 to 10^5 s^{-1} for paramagnetic systems, this gives some indication of the range of applicability of this method.

In practice, a particular system often will show only two or three of these specific regions. The problem is to fit this temperature dependence to the known functions, primarily to determine ΔH^* and ΔS^* for the exchange process. This also requires some knowledge or estimates of the activation energies, E_m and E_o , for T_{2m} and T_{2o} , respectively. Measurements of T_1^{-1} can be helpful in this regard because T_1 is not affected by dephasing and exchange is apparent only in the Arrhenius region, as shown in Figure 10.4. The main difficulty is separating the various factors that affect the

temperature dependence of T_2^{-1} when the limiting regions are not well defined. Least-squares analysis is far more satisfactory than the early graphical methods.

This methodology is especially useful for labile paramagnetic systems, and many of the solvent-exchange kinetic parameters given in Tables 3.13 and 3.18 have been determined by this method. A further application is discussed in Section 4.1.2 and described in Figure 4.2.

10.5 ELECTRON PARAMAGNETIC RESONANCE METHODS

This is a powerful technique for the detection and monitoring of species with unpaired electrons. This type of spectroscopy is designated by several acronyms: EPR, electron paramagnetic resonance; ESR, electron spin resonance; EMR, electron magnetic resonance. EPR is quite sensitive, with detection limits in the range of 10^{-6} M in favorable cases. It also can be quite informative as to structure because of electron–nuclear hyperfine coupling to metal and ligand nuclei. The main disadvantage is that many species with unpaired electrons do not give a useful EPR signal in solution because efficient electron spin relaxation leads to broad or undetectable signals. Signals are more generally detectable in the crystalline or frozen glassy state. For the first-row transition metals in their common oxidation states, solution EPR is useful for complexes of V(IV), Mn(II) and Cu(II), while Cr(III) and Fe(III) often give broad spectra in solution. Most organic radicals give EPR signals that are quite useful for detection and identification of such species as reaction intermediates.

Most EPR spectra are measured at X-band frequency of 9.4 GHz in the microwave region of the electromagnetic spectrum, and the magnetic field of ~ 0.3 T is changed to give the resonance condition for signal detection. The sample tube should be quartz, in order to avoid impurity signals found in Pyrex, and the tube should be flattened for solvents with high dielectric constants, such as water, to minimize dielectric loss in the microwave cavity. The concentrations of paramagnetic species should be $<10^{-3}$ M, in order to minimize signal broadening due to intermolecular relaxation interactions. EPR spectra are usually displayed as plots of the derivative of signal intensity versus magnetic field. Double integration of such data is necessary to get proper integrated signal intensities. With proper calibration, the signal intensity can give a direct measure of the concentration of the EPR-active species.

Pulsed EPR is becoming more widely available. A 90° pulse is typically in the range of 10 to 30 ns. The free induction decay, FID, after such a pulse can be used to measure the electron spin relaxation time or to monitor the decay of radicals⁷⁰ that have been produced by some fast method, such as flash photolysis or pulse radiolysis. Electron spin-echo envelope modulation, ESEEM, spectroscopy⁷¹ is a pulse method used primarily for detecting weak hyperfine coupling.

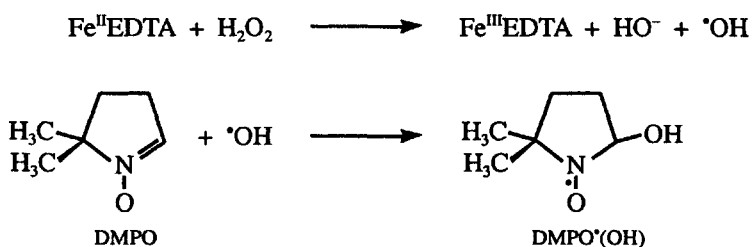
Most applications use EPR as a detection method for reactants or products. Various flow methods can be coupled with EPR to monitor the time dependence of EPR-active species. It is also possible to use EPR line broadening to measure exchange rates, and in this area the time scale is in the range of 10^{-7} to 10^{-9} s.

Margerum and co-workers⁷² used EPR coupled with stopped flow to measure the electron exchange rate between complexes of Ni(II) and Ni(III) with half-times of ~ 1 s. The Ni(III) species is EPR active and was enriched with ^{61}Ni , which broadens the EPR signal due to hyperfine coupling. As electron exchange proceeds, the $^{61}\text{Ni(III)}$ is exchanged for the more abundant $^{58}\text{Ni(III)}$ and $^{60}\text{Ni(III)}$, which have no nuclear spin. As a result, the EPR signal sharpens and provides a measure of the extent of exchange. It was suggested that this method might be applied to other metals using isotopes such as ^{57}Fe , ^{99}Ru and ^{53}Cr .

Spin trapping can be used to convert radical intermediates into more stable species that can be detected by EPR. For example, fumarate ion was used⁷³ to trap the aryl radicals, $\cdot\text{Ar}$, formed in the oxidation of Fe(II) by benzenediazonium ions, ArN_2^+ , in a stopped-flow EPR study. The $\text{}^{-}\text{O}_2\text{C}(\text{C}_6\text{H}_5)\text{CH}\cdot\text{CHCO}_2\text{}^{-}$ radical is sufficiently stable relative to dimerization so that its concentration after the 35-ms mixing time could be used to determine the rate of the initial oxidation reaction.

The much studied reaction of $\text{Fe}^{\text{II}}\text{EDTA}$ with H_2O_2 has been investigated⁷⁴ in a stopped-flow system with a deadtime of 18 ms using 5,5-dimethyl-1-pyrroline N-oxide, DMPO, to trap the $\cdot\text{OH}$ radicals. The general reactions are shown in Scheme 10.7.

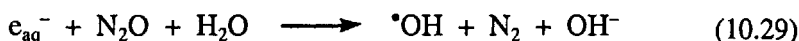
Scheme 10.7



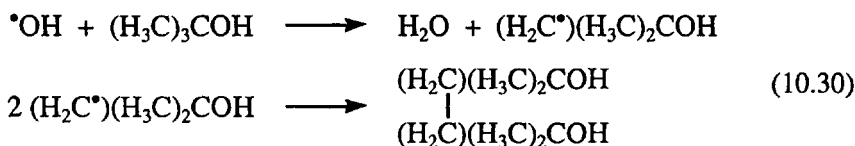
The $\text{DMPO}\cdot(\text{OH})$ radical could be detected at the $5\text{-}\mu\text{M}$ level, and the time dependence of its formation was studied as a function of reagent concentrations. It was concluded from initial rates that the reaction is first-order in $[\text{Fe}^{\text{II}}\text{EDTA}]$ and $[\text{H}_2\text{O}_2]$, but that only $\sim 20\%$ of the expected amount of $\text{DMPO}\cdot(\text{OH})$ is formed with initial concentrations of $100\ \mu\text{M}$ Fe(II), $200\ \mu\text{M}$ EDTA, $600\ \mu\text{M}$ H_2O_2 and $20\ \text{mM}$ DMPO at pH 7.4. The amount of $\text{DMPO}\cdot(\text{OH})$ decreased as the $[\text{Fe(II)}]/[\text{H}_2\text{O}_2]$ ratio increased. This indicates that $\cdot\text{OH}$ is reacting by other pathways, in addition to being trapped by DMPO. One known reaction is that of $\text{Fe}^{\text{II}}\text{EDTA}$ with $\cdot\text{OH}$.⁷⁵

10.6 PULSE RADIOLYSIS METHODS

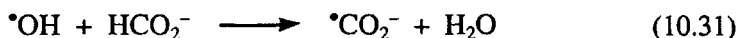
It is possible to quickly generate reactive species and solvated electrons by passing a high-energy pulse of electrons through a solution. Results have been summarized and discussed in several reviews.⁷⁶ The pulse is typically 5–100 ns long with energies in the range of 2 to 20 MeV, depending on the source apparatus. The high-energy electrons initially are present in hot spots or spurs and the thermalized species are present after $\sim 10^{-7}$ s. In water, the species and number produced per 100 eV of energy absorbed, in brackets, are: e_{aq}^- (2.65), $\cdot\text{OH}$ (2.65), $\cdot\text{H}$ (0.65), H_2O_2 (0.72), H_2 (0.45). In most applications, the initial radiolysis products are scavenged by additives that remove undesired species or produce a new reactive species. For example, water saturated with N_2O (~ 0.022 M under 1 atm of N_2O) converts e_{aq}^- to $\cdot\text{OH}$ in ~ 50 ns by the following reaction:



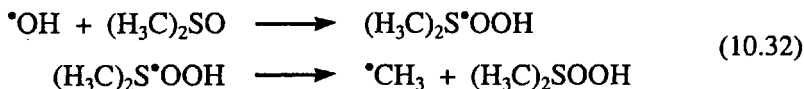
The $\cdot\text{OH}$ radicals can be scavenged by *t*-butanol through reactions (10.30), but the *t*-butanol radical can be intercepted by sufficiently reactive substrates. Other alcohols react similarly, but their radicals are generally 5 to 10 times more reactive with substrates than the *t*-butanol radical.



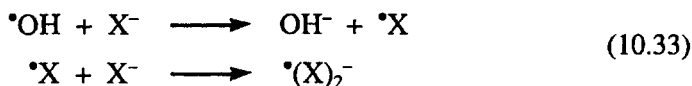
Sodium formate can be used to form the $\cdot\text{CO}_2^-$ radical by the following reaction:



If O_2 is present, $\cdot\text{CO}_2^-$ will react to give CO_2 and the superoxide radical $\cdot\text{O}_2^-$. Methyl radicals can be produced from DMSO by the following sequence⁷⁷:



Bromide and thiocyanate ions can produce the corresponding $\cdot(\text{X})_2^-$ radical anion by the following reactions:



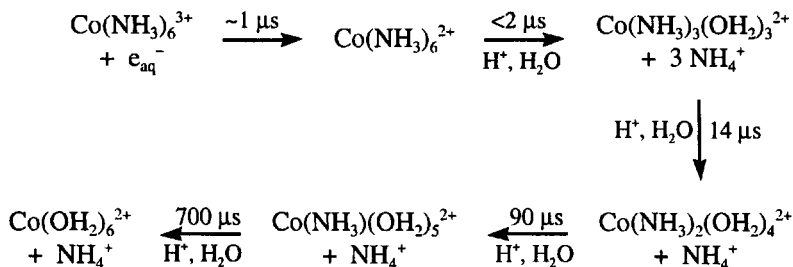
The $^{\bullet}(\text{SCN})_2^-$ radical is moderately stable, with an absorbance maximum at 478 nm. The amount of $^{\bullet}(\text{SCN})_2^-$ produced during radiolysis of a 0.01 M SCN^- solution is commonly used as a dosimeter⁷⁸ to determine the number of radicals produced per electron pulse. With azide ion, the reaction stops at the first stage in reaction (10.33) to give predominantly $^{\bullet}\text{N}_3$, but $^{\bullet}(\text{N}_3)_2$ may be produced at high N_3^- concentrations.⁷⁹

Combinations of reagents are used to produce the dominant radiolysis product of interest. For example, to study reactions of $^{\bullet}\text{OH}$, the sample solution would be saturated with N_2O , but to study $^{\bullet}\text{CO}_2^-$, the solution would also contain ~ 0.1 M HCO_2^- . The radicals produced in the above reactions are generally quite reactive: e_{aq}^- and $^{\bullet}\text{CO}_2^-$ are strong reducing agents; $^{\bullet}\text{OH}$, $^{\bullet}\text{N}_3$ and $^{\bullet}\text{Br}_2^-$ are strong oxidizing agents. These species also tend to decay by dimerization or disproportionation, but their concentrations are sufficiently low (1–10 μM) so that these second-order reactions are often slow compared to reactions with other substrates that are added at the mM level.

Most studies in this area use spectrophotometric detection and the time scale can be from microseconds to seconds. Because the products are produced at low concentrations, it is often possible to do multiple radiation pulses on the same sample. The main problem is the lack of molecular specificity of the spectrophotometric method, so that the nature of the reaction and the products are often inferred by analogy and by the concentration dependence of the reaction rate.

Pulse radiolysis was used⁸⁰ to rapidly generate $\text{Co}(\text{NH}_3)_6^{2+}$ and then follow the aquation of the NH_3 ligands. The radiolysis was done on solutions of $\text{Co}(\text{NH}_3)_6^{3+}$ at $\text{pH} < 4.5$ in the presence of *t*-butanol to scavenge $^{\bullet}\text{OH}$ so that e_{aq}^- is the reducing agent. Detection was by conductivity change due to the loss of H_3O^+ by formation of NH_4^+ . The overall observations are summarized in Scheme 10.8, where the times are half-times for the various steps. Similar rates were observed when several pentaammine and tetraammine Co(III) complexes were studied.

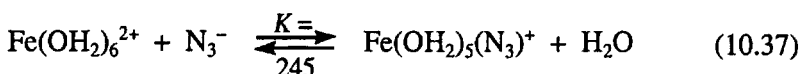
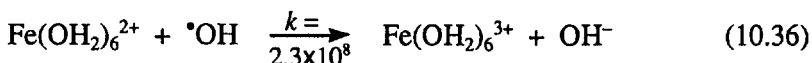
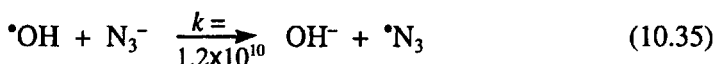
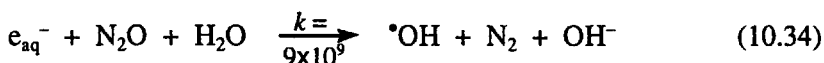
Scheme 10.8



The rate of aquation of $\text{Co}(\text{en})_3^{2+}$, produced from $\text{Co}(\text{en})_3^{3+} + e_{\text{aq}}^-$, is slower than in the ammine systems in Scheme 10.8. The half-time for loss

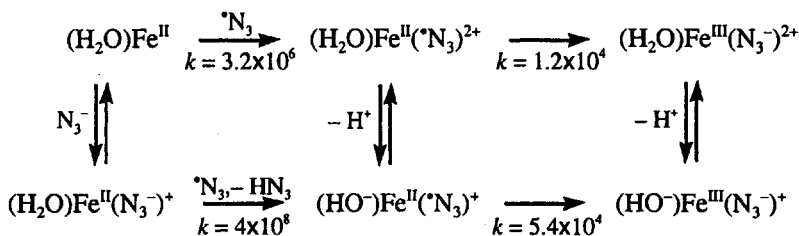
of the first ethylenediamine is pH-dependent and varies from 320 to 910 μs between pH 2.5 and 4.6. This effect was attributed to a protonated monodendate intermediate.

There have been several pulse radiolysis studies of the oxidation of aquo and other complexes of the M(II) ions of the first transition series. In several cases, the pulse radiolysis observations indicate that the reactions can be more complex than simple oxidation to the M(III) ion. For example, pulse radiolysis of N_2O saturated solutions of $\text{Fe}(\text{OH}_2)_6^{2+}$ and N_3^- involves the following initial reactions and equilibria⁸¹ (rate constants at 25°C in $\text{M}^{-1} \text{s}^{-1}$):



The pH was 5.4–6.2, so that HN_3 is fully dissociated to N_3^- . When the Fe(II) concentration ($\sim 0.01 \text{ M}$) is 10 to 15 times larger than that of N_3^- , the major products after 0.26 μs are Fe(III) and $\cdot\text{N}_3$ from the reactions (10.35) and (10.36), respectively. However, when the N_3^- concentration is the same or larger than that of Fe(II), then $\cdot\text{OH}$ reacts mainly by reaction (10.35) and the product after 28 μs has absorbance maxima at 300 and 419 nm. This spectrum does not correspond either to $\cdot\text{N}_3$ or to the oxidized complex $\text{Fe}^{\text{III}}(\text{OH}_2)_5(\text{N}_3)^+$, and was assigned to aqueous $\text{Fe}^{\text{II}}(\cdot\text{N}_3)^{2+}$. This intermediate decays to the final Fe(III) products, and the conclusions and rate constants ($\text{M}^{-1} \text{s}^{-1}$ or s^{-1}) of Parsons et al.⁸¹ are summarized in Scheme 10.9, where only one H_2O ligand is shown for clarity.

Scheme 10.9



Reactions of $\text{Fe}(\text{OH}_2)_6^{2+}$ with $\cdot\text{N}_3$, $\cdot\text{Br}_2$ and $\cdot\text{O}_2\text{H}$ have rate constants in the narrow range of $(1.2\text{--}3.6) \times 10^6 \text{ M}^{-1} \text{ s}^{-1}$, and it appears that the reaction

is limited by water ligand dissociation from $\text{Fe}(\text{OH}_2)_6^{2+}$. Similar observations have been reported for analogous reactions at other metal centers by van Eldik et al.⁸² The larger rate constant for $\text{Fe}(\text{OH}_2)_6^{2+} + \cdot\text{OH}$ in reaction (10.36) indicates that this reaction proceeds by H atom abstraction.

With regard to the intermediate assigned as $\text{Fe}^{\text{II}}(\cdot\text{N}_3)^{2+}$, it was noted by Parsons et al.⁸¹ that the spectrum of this species is similar to that observed in the reaction of $\text{Mn}^{\text{II}}(\text{NTA})$ with $\cdot\text{OH}$ ⁷⁵ and $\text{Fe}^{\text{II}}(\text{NTA})$ with $\cdot\text{CO}_2^-$.⁸³ The former was assigned to a product of H abstraction from the ligand in $\text{Mn}^{\text{II}}(\text{NTA})$, and the latter to $\text{Fe}^{\text{III}}(\text{NTA})(\text{OH}_2)(\text{CO}_2)^{2-}$ with an Fe—C bond. Presumably the correspondence in these spectra is accidental, but it shows the difficulty in assigning species from their electronic spectra alone.

A recent study⁸⁴ has revised the reaction pathways for decomposition of NO under pulse radiolysis conditions. It has been concluded that NO reacts with $\cdot\text{H}$ to form $\cdot\text{HNO}$ in the singlet state, but with e_{aq}^- to give NO^- in a triplet state. These two species do not rapidly interconvert by H^+ transfer because of their different spin states. They both react with NO to ultimately yield N_3O_3^- , which dissociates with $k \approx 3 \times 10^2 \text{ s}^{-1}$ to give N_2O and NO_2^- .

10.7 FLASH PHOTOLYSIS METHODS

This technique is somewhat analogous to pulse radiolysis in that the system is subjected to a short high-energy pulse and then subsequent events are monitored. In flash photolysis the pulse usually is provided by a laser beam of photons and the immediate product is some photoexcited state of the absorbing reactant(s). Subsequent events are monitored on the nanosecond or longer time scale, most commonly by Fourier transform IR or UV–visible spectrophotometry. Flash photolysis is much cleaner than pulse radiolysis in that there is not the multiplicity of initial reactants or the need to add reagents to remove undesired reactants. In both methods, there is the problem of identifying the reactive intermediates from the often limited spectroscopic signatures that they provide.

There have been many studies of the activation of C—H bonds by the coordinatively unsaturated species that can be generated by flash photolysis.⁸⁵ In a recent study, Harris and co-workers⁸⁶ have observed the flash photolysis of $\text{Rh}(\text{Tp}^*)(\text{CO})_2$ in pentane with a 295-nm laser pulse ($\text{Tp}^* = \text{hydridotris}(3,5\text{-dimethylpyrazolyl})\text{borate}$). They observed reformation of $\text{Rh}(\text{Tp}^*)(\text{CO})_2$ at 2054 cm^{-1} , with $\tau \approx 70 \text{ ps}$, and cooling of a vibrationally excited intermediate, with $\tau \approx 23 \text{ ps}$, to give a vibrational ground state absorbing at 1972 cm^{-1} . This intermediate decays with $\tau \approx 200 \text{ ps}$ and seems to convert with the same rate to another intermediate absorbing at 1992 cm^{-1} . The final product, $\text{Rh}(\text{Tp}^*)(\text{CO})(\text{R})\text{H}$, appears on a longer time scale of $\sim 500 \text{ ns}$. The intermediates were suggested to be weakly and more strongly solvated species, but their 20 cm^{-1} difference in CO stretching frequencies was acknowledged to be unexpected for such a model. It

should be noted that the Tp^* ligand in this system is known to undergo a rapid fluxional η^3 to η^2 change, but the η^3 form is dominant.⁸⁷ The wavelength dependence of the quantum yields and other chemistry of this system have been reported by Purwoko and Lees⁸⁸, and some synthetic and structural aspects are given by Chauby et al.⁸⁹

Flash photolysis also provides access to electronic excited states, whose photochemistry, energy transfer and electron transfer properties can be observed after the flash. One of the most widely studied such systems is $\text{Ru}(\text{bpy})_3^{2+}$, in which the photochemically generated excited state is both a good oxidizing and reducing agent.⁹⁰ Binding of analogues of this complex to proteins and then photoactivating the system has been exploited to study electron transfer in proteins.⁹¹ Barton and co-workers⁹² have used Ru and Os analogues to study electron and energy transfer for such complexes intercalated in DNA.

The flash photolysis of vitamin B_{12} and its derivatives has been studied by Sension and co-workers⁹³ to reveal details of the radical recombination after homolysis of the Co—C bond.

References

1. Caldin, E. F. *Fast Reactions in Solution*; Blackwell: Oxford, 1964; Hague, D. N. *Fast Reactions*; Wiley-Interscience: London, 1971; Bradley, J. N. *Fast Reactions*; Oxford University Press: Oxford, 1975; Bernasconi, C. F. *Relaxation Kinetics*; Academic Press: New York, 1976; Wilkins, R. G. *Kinetics and Mechanism of Reactions of Transition Metal Complexes*, 2nd ed.; VCH: Weinheim, 1991; Pilling, M. J.; Seakins, P. W. *Reaction Kinetics*; Oxford University Press: Oxford, 1995.
2. Wilkins, R. G. *Adv. Inorg. Bioinorg. Mech.* **1983**, 2, 139.
3. Applied Photophysics (<http://www.photophysics.com/>); Hi-Tech Scientific (<http://www.hi-techsci.co.uk/>); OLIS, On-Line Instrument Systems Inc. (<http://www.olisweb.com>).
4. Funahashi, S.; Ishihara, K.; Aizawa, S.; Sugata, T.; Ishi, M.; Inada, Y.; Tanaka, M. *Rev. Sci. Instr.* **1993**, 64, 130.
5. Sienkiewicz, A.; Qu, K. B.; Scholes, C. P. *Rev. Sci. Instr.* **1994**, 65, 68.
6. Inada, Y.; Funahashi, S. *Rev. Sci. Instr.* **1994**, 65, 18.
7. Gerhard, A.; Gaede, W.; Neubrand, A.; Zang, W.; van Eldik, R.; Stanitzek, P. *Instrum. Sci. Technol.* **1994**, 22, 1.
8. van Eldik, R.; Palmer, D. A.; Schmidt, R.; Kelm, H. *Inorg. Chim. Acta* **1981**, 50, 131; Nichols, P. J.; Ducommun, Y.; Merbach, A. E. *Inorg. Chem.* **1983**, 22, 3993. Ishihara, K.; Miura, H.; Funahashi, S.; Tanaka, M. *Inorg. Chem.* **1988**, 27, 1706.
9. Balny, C.; Saldana, T.-L.; Dahan, N. *Anal. Biochem.* **1987**, 163, 309.
10. Bourke, G. C. M.; Thompson, R. C. *Inorg. Chem.* **1987**, 26, 903.
11. Dickson, P. N.; Margerum, D. W. *Anal. Chem.* **1986**, 58, 3153.
12. Beckwith, R. C.; Cooper, J. N.; Margerum, D. W. *Inorg. Chem.* **1994**, 33, 5144.
13. Meagher, N. E.; Rorabacher, D. B. *J. Phys. Chem.* **1994**, 98, 12590.

14. Palmer, D. A.; van Eldik, R. *Chem. Rev.* **1983**, *83*, 651; Massoud, S.; Jordan, R. *B. Inorg. Chim. Acta* **1994**, *221*, 9.
15. Buckingham, D. A.; Clark, C. R. *Inorg. Chem.* **1994**, *33*, 6171.
16. Brower, K. R. *J. Am. Chem. Soc.* **1968**, *90*, 5401.
17. Jost, A. *Ber. Bunsenges. Phys. Chem.* **1976**, *80*, 316.
18. Doss, R.; van Eldik, R.; Kelm, H. *Ber. Bunsenges. Phys. Chem.* **1982**, *86*, 825; Martinez, P.; Mohr, R.; van Eldik, R. *Ber. Bunsenges. Phys. Chem.* **1986**, *90*, 609.
19. Capitan, M. J.; Munoz, E.; Graciani, M. M.; Jiminez, R.; Tejera, I.; Sanchez, F. *J. Chem. Soc., Faraday Trans. I* **1989**, *85*, 4193.
20. Funahashi, S.; Ishihara, K.; Tanaka, M. *Inorg. Chem.* **1983**, *22*, 2070.
21. Grace, M. R.; Swaddle, T. W. *Inorg. Chem.* **1992**, *31*, 4674.
22. Betts, R. H.; Dainton, F. S. *J. Am. Chem. Soc.* **1953**, *75*, 5721.
23. Gerischer, H.; Heim, W. *Ber. Bunsenges. Phys. Chem.* **1967**, *71*, 1040.
24. Gerischer, H.; Holzwarth, J. F.; Seifert, D.; Strohmaier, L. *Ber. Bunsenges. Phys. Chem.* **1969**, *73*, 952; Eck, V.; Marcus, M.; Stange, G.; Westerhausen, J.; Holzwarth, J. F. *Ber. Bunsenges. Phys. Chem.* **1981**, *85*, 869; Bruhn, H.; Nigam, S.; Holzwarth, J. F. *Disc. Faraday Soc.* **1982**, *74*, 129.
25. Fogelman, K. D.; Walker, D. M.; Margerum, D. W. *Inorg. Chem.* **1989**, *28*, 986; Beckwith, R. C.; Wang, T. X.; Margerum, D. W. *Inorg. Chem.* **1996**, *35*, 995.
26. Eigen, M. *Pure Appl. Chem.* **1963**, *6*, 97.
27. Marcandalli, B.; Winzek, C.; Holzwarth, J. F. *Ber. Bunsenges. Phys. Chem.* **1984**, *88*, 368.
28. Ertl, G.; Gerischer, H. *Z. Electrochem.* **1962**, *66*, 560.
29. Aubard, J.; Nozeran, J. M.; Levoir, P.; Meyer, J. J.; Dubois, J. E. *Rev. Sci. Instrum.* **1979**, *50*, 52.
30. Dawson, A.; Gormally, J.; Wyn-Jones, E.; Holzwarth, J. F. *J. Chem. Soc., Chem. Commun.* **1981**, 386; Bannister, J. J.; Gormally, J.; Holzwarth, J. F.; King, T. A. *Chem. Br.* **1984**, *20*, 227; *Ibid.* 232; Fletcher, P. D. I.; Holzwarth, J. F. *J. Phys. Chem.* **1991**, *95*, 2550; Alexandridis, P.; Holzwarth, J. F.; Hatton, A. T. *Langmuir* **1993**, *9*, 2045.
31. Hague, D. N.; Martin, S. R. *J. Chem. Soc., Dalton Trans.* **1974**, 254.
32. Doss, R.; van Eldik, R. *Inorg. Chem.* **1982**, *21*, 4108.
33. Winkler-Oswatitsch, R.; Eigen, M. *Angew. Chem. Int. Ed. Engl.* **1979**, *18*, 20.
34. Citi, M.; Secco, F.; Venturi, M. *J. Phys. Chem.* **1988**, *92*, 6399.
35. Stanley, B. J.; Marshall, D. B.; *Rev. Sci. Instr.* **1994**, *65*, 199.
36. Faulkner, L. R.; Bard, A. J. *Electrochemical Methods*; Wiley: New York, 1980; Osteryoung, J. *Acc. Chem. Res.* **1993**, *26*, 77; Rieger, P. H. *Electrochemistry*, 2nd ed.; Chapman & Hall: New York, 1994.
37. O'Dea, J. J.; Osteryoung, J. G.; Lane, T. *J. Phys. Chem.* **1986**, *90*, 2761; Rudolph, M. *J. Electrochem. Interfacial Electrochem.* **1991**, *314*, 13.
38. Rudolph, M.; Reddy, D. P.; Feldberg, S. W. *Anal. Chem.* **1994**, *66*, 589A. DigiSim 1.0 program; Bioanalytical Systems Inc., West Lafayette, Indiana (<http://www.bioanalytical.com:80/>).

39. Connelly, N. G.; Orpen, A. G.; Rieger, A. L.; Rieger, P. H. *J. Chem. Soc., Chem. Commun.* **1992**, 1293.
40. Pike, R. D.; Alavosus, T. J.; Camaioni-Neto, C. A.; Williams, J. C.; Sweigart, D. A. *Organometallics* **1989**, *8*, 2631; Zhang, Y.; Gosser, D. K.; Rieger, P. H.; Sweigart, D. A. *J. Am. Chem. Soc.* **1991**, *113*, 4062; Shaw, M. J.; Geiger, W. E. *Organometallics*, **1996**, *15*, 13.
41. Lei, Y.; Anson, F. C. *Inorg. Chem.* **1995**, *34*, 1083.
42. Hecht, M.; Schultz, F. A.; Speiser, B. *Inorg. Chem.* **1996**, *35*, 5555.
43. Hershberger, J. W.; Klingler, R. J.; Kochi, J. K. *J. Am. Chem. Soc.* **1983**, *105*, 61.
44. Zizelman, P. M.; Amatore, C.; Kochi, J. K. *J. Am. Chem. Soc.* **1984**, *106*, 3771.
45. Huang, Y.; Carpenter, G. B.; Sweigart, D. A.; Chung, Y. K.; Lee, B. Y. *Organometallics* **1995**, *14*, 1423.
46. Parker, V. D.; Tilset, M. J. *J. Am. Chem. Soc.* **1987**, *109*, 2521.
47. Johnson, C. S., Jr.; Moreland, C. G. *J. Chem. Educ.* **1973**, *50*, 477.
48. Green, M. L. H.; Wong, L.-L.; Sella, A. *Organometallics* **1992**, *11*, 2660.
49. Orrell, K. G.; Sik, V. *Ann. Rep. NMR Spectrosc.* **1987**, *19*, 79; *Ibid.* **1993**, *27*, 103.
50. Perrin, C. L.; Dwyer, T. J. *Chem. Rev.* **1990**, *90*, 935;
51. Brasch, N. E.; Buckingham, D. A.; Evans, A. B.; Clark, C. R. *J. Am. Chem. Soc.* **1996**, *118*, 7969.
52. Aygen, S.; Hanssum, H.; van Eldik, R. *Inorg. Chem.* **1985**, *24*, 2853; Gonzalez, G.; Moullet, B.; Martinez, M.; Merbach, A. E. *Inorg. Chem.* **1994**, *33*, 2330; Galsbol, F.; Mønsted, L.; Mønsted, O. *Acta Chem. Scand.* **1992**, *47*, 43; Cusanelli, A.; Frey, U.; Richens, D. T.; Merbach, A. E. *J. Am. Chem. Soc.* **1996**, *118*, 5265.
53. Buckingham, D. A.; Marzilli, L. G.; Sargeson, A. M. *J. Am. Chem. Soc.* **1968**, *90*, 6028; Jackson, W. G. *Inorg. Chim. Acta* **1987**, *131*, 105.
54. Bernhard, P.; Helm, L.; Ludi, A.; Merbach, A. *J. Am. Chem. Soc.* **1985**, *107*, 312.
55. Gesmar, H.; Led, J. J. *J. Magn. Reson.* **1986**, *68*, 95; Grassi, M.; Mann, B. E.; Pickup, B. T.; Spencer, C. M. *J. Magn. Reson.* **1986**, *69*, 92.
56. Freeman, R. *Chem. Rev.* **1991**, *91*, 1397.
57. Muhandiram, D. R.; McClung, R. E. D. *J. Magn. Reson.* **1987**, *71*, 187; *Ibid.* **1988**, *76*, 121.
58. McClung, R. E. D.; Aarts, G. H. M. *J. Magn. Reson.* **1995**, *115A*, 145.
59. Johnson, E. R.; Dellwo, M. J.; Hendrix, J. *J. Magn. Reson.* **1986**, *66*, 399.
60. Argyropoulos, D.; Mitsopoulou, C.-A.; Katakis, D. *Inorg. Chem.* **1996**, *35*, 5549.
61. Smith, A. E.; Schrauzer, G. N.; Mayweg, V. P.; Heinrich, W. *J. Am. Chem. Soc.* **1965**, *87*, 5798.
62. Binsch, G. *J. Am. Chem. Soc.* **1969**, *91*, 1304; Binsch, G.; Kleier, D. A. *DNMR3, Program 165, Quantum Chem. Prog. Exchange*, Indiana University, **1970**; Binsch, G.; Stephenson, D. *J. Magn. Reson.* **1978**, *32*, 145; Szymanski, S. *J. Magn. Reson.* **1988**, *77*, 320; Bain, A. D.; Duns, G. J. *J. Magn. Reson.* **1995**, *112A*, 258.
63. Kersting, B.; Telford, J. R.; Meyer, M.; Raymond, K. N. *J. Am. Chem. Soc.* **1996**, *118*, 5712.

64. The relationship between ΔG^\ddagger and the rate constant k_c at the coalescence temperature T_c given in reference 63 contains minor errors and should be $\Delta G^\ddagger(\text{kJ mol}^{-1}) = 19.145 \times 10^{-3}(10.319 + \log(T_c/k_c))$.
65. Swift, T. J.; Connick, R. E. *J. Chem. Phys.* **1962**, *37*, 307.
66. McConnell, H. *J. Chem. Phys.* **1958**, *28*, 430.
67. Angerman, N. S.; Jordan, R. B. *Inorg. Chem.* **1969**, *8*, 1824; Led, J. S.; Grant, D. M. *J. Am. Chem. Soc.* **1977**, *99*, 5845; Jen, J. *J. Magn. Reson.* **1978**, *30*, 111.
68. Chopra, S.; McClung, R. E. D.; Jordan, R. B. *J. Magn. Reson.* **1984**, *59*, 361.
69. Merbach, A. E. *Pure Appl. Chem.* **1987**, *59*, 161; Merbach, A. E.; Akitt, J. W. *NMR Basic Princ. Prog.* **1990**, *24*, 189; van Eldik, R.; Merbach, A. E. *Comments Inorg. Chem.* **1992**, *12*, 341.
70. Mezyk, S.; Bartels, D. A. *J. Chem. Soc., Faraday Trans.* **1995**, *91*, 3127.
71. Kang, P. C.; Eaton, G. R.; Eaton, S. S. *Inorg. Chem.* **1994**, *33*, 3660; Wirt, M. D.; Bender, C. J.; Peisach, J. *Inorg. Chem.* **1995**, *34*, 1663.
72. Wang, J.-F.; Kumar, K.; Margerum, D. W. *Inorg. Chem.* **1989**, *28*, 3481.
73. Gilbert, B. C.; Hanson, P.; Jones, J. R.; Whitwood, A. C.; Timms, A. W. *J. Chem. Soc., Perkin Trans. 2* **1992**, 629.
74. Jiang, J.; Bank, J. F.; Scholes, C. P. *J. Am. Chem. Soc.* **1993**, *115*, 4742.
75. Lati, J.; Meyerstein, D. *J. Chem. Soc., Dalton Trans.* **1978**, 1105.
76. van Eldik, R. *Pure and Appl. Chem.* **1993**, *65*, 2603; Buxton, G. V.; Mulazzani, Q. G.; Ross, A. B. *J. Phys. Chem. Ref. Data* **1995**, *24*, 1055.
77. Veitwisch, D.; Janata, E.; Asmus, K. D. *J. Chem. Soc., Perkin Trans.* **1980**, 146.
78. Buxton, G. V.; Stuart, C. R. *J. Chem. Soc., Faraday Trans.* **1995**, *91*, 279.
79. Butler, J.; Land, E. J.; Swallow, A. J.; Prutz, W. A. *Radiat. Phys. Chem.* **1984**, *23*, 265.
80. Lillie, J.; Shinohara, N.; Simic, M. G. *J. Am. Chem. Soc.* **1976**, *98*, 6516.
81. Parsons, B. J.; Zhao, Z.; Navaratnam, S. *J. Chem. Soc., Faraday Trans.* **1995**, *91*, 3133.
82. van Eldik, R.; Cohen, H.; Meyerstein, D. *Inorg. Chem.* **1994**, *33*, 1566.
83. Goldstein, S.; Czapski, G.; Cohen, H.; Meyerstein, D. *J. Am. Chem. Soc.* **1988**, *110*, 3903.
84. Lyman, S. V.; Shafirovich, V.; Poskrebyshev, G. A. *Inorg. Chem.* **2005**, *44*, 5212.
85. Perutz, R. N. *Chem. Soc. Rev.* **1993**, 361; Arndtsen, B. A.; Bergman, R. G.; Mobley, T. A.; Peterson, T. H. *Acc. Chem. Res.* **1995**, *28*, 154.
86. Lian, T.; Bromberg, S. E.; Yang, H.; Proulx, G.; Bergman, R. G.; Harris, C. B. *J. Am. Chem. Soc.* **1996**, *118*, 3769.
87. Ghosh, C. K.; Graham, W. A. G. *J. Am. Chem. Soc.* **1987**, *109*, 4726; Ghosh, C. K. Ph.D. Dissertation, University of Alberta, Edmonton, Canada, 1988.
88. Purwoko, A. A.; Lees, A. J. *Inorg. Chem.* **1996**, *35*, 675.
89. Chauby, V.; Serra Le Berre, C.; Kalck, Ph.; Daran, J.-C.; Commenges, G. *Inorg. Chem.* **1996**, *35*, 6354.
90. Juris, A.; Balzani, V.; Barigelletti, F.; Campagna, S.; Belser, P.; von Zelewsky, A. *Coord. Chem. Rev.* **1988**, *84*, 85; Sykora, J.; Sima, J. *Coord. Chem. Rev.* **1990**, *107*, 1.
91. Gray, H. B. *Chem. Soc. Rev.* **1986**, *15*, 17.

92. Murphy, C. J.; Arkin, M. R.; Ghatalia, N. D.; Bossmann, S.; Turro, N. J.; Barton, J. K. *Proc. Natl. Acad. Sci. U.S.A.* **1994**, *91*, 5315; Holmlin, R. E.; Stemp, E. D. A.; Barton, J. K. *J. Am. Chem. Soc.* **1996**, *118*, 5236.
93. Yoder, L. M.; Cole, A. G.; Walker, L. A., II; Sension, R. J. *J. Phys. Chem. B* **2001**, *105*, 12180; Sension, R. J.; Harris, D. A.; Cole, A. G. *J. Phys. Chem. B* **2005**, *109*, 21954; Shiang, J. J.; Cole, A. G.; Sension, R. J.; Huang, K.; Weng, Y.; Trommel, J. S.; Marzilli, L. G.; Lian, T. *J. Am. Chem. Soc.* **2006**, *128*, 801.

Problems

CHAPTER 1

1. The following reaction is studied in *t*-butanol at 35°C by measuring the integrated peak intensity, I , of the ^1H NMR of the product:

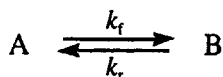


The experimental conditions for several kinetic runs and the values of I at various times are given in the table below.

- (a) Determine the experimental rate constant for each of the runs.
(b) Plot the experimental rate constants versus the bromide ion concentration and calculate the specific rate constant for the reaction, if possible.

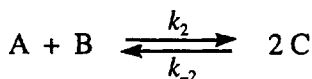
$\text{M}(\text{NH}_3)_2(\text{Cl})_2$ (M)	3.0×10^{-3}	5.0×10^{-3}	8.0×10^{-3}		
Br^- (M)	0.060	0.085	0.110		
Time (s)	I	Time (s)	I	Time (s)	I
50	0.30	50	0.68	50	1.4
100	0.58	100	1.30	100	2.56
150	0.80	150	1.80	150	3.50
200	1.02	200	2.24	200	4.30
300	1.40	300	2.94	250	4.94
400	1.70	400	3.48	300	5.48
600	2.16	500	3.88	350	5.92
800	2.44	600	4.16	400	6.28
1000	2.64	800	4.54	450	6.60
1300	2.80	1000	4.74	500	6.82
1600	2.90	1300	4.90	600	7.21
2000	2.96	1600	4.96	800	7.64
3500	3.00	2500	5.00	2000	8.00

- 2.(a) Develop an equation that can be used to determine the experimental rate constant from measurements of absorbance versus time for the following system:

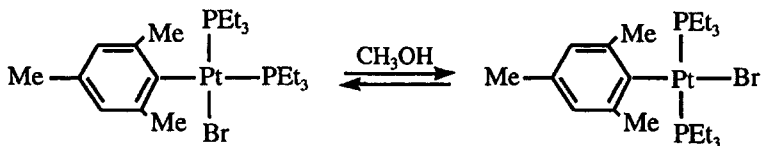


Assume that both A and B are absorbing at the observation wavelength and that both species obey Beer's law and have molar absorptivities ϵ_A and ϵ_B , respectively.

- (b) Show how the final absorbance can be used to determine the equilibrium constant for the reaction if ϵ_A and ϵ_B are known.
3. Develop an expression that could be used to determine the second-order rate constant for the following system. (See Section 1.2.4.)



4. There have been two studies of the following isomerization reaction:



The results of the studies of the variation of the rate constant with temperature are given in the table below.

- (a) Use each set of data to calculate the activation enthalpy and entropy for the reaction.

t (°C)	$10^4 \times k_{\text{exp}}$ (s ⁻¹) ^a	t (°C)	$10^4 \times k_{\text{exp}}$ (s ⁻¹) ^b
25	1.0	17.0	0.45
30	1.7	23.5	0.95
35	2.7	30.0	1.9
40	4.0	36.2	3.9
45	6.0	44.6	9.4

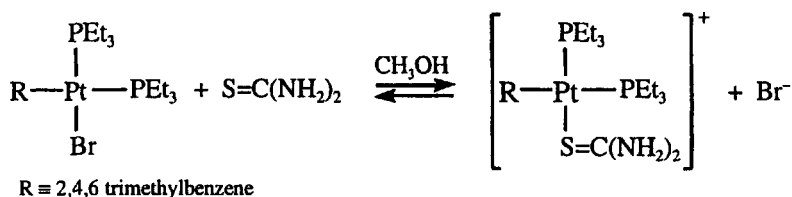
^a Romeo, R.; Minniti, D.; Trozzi, M. *Inorg. Chem.* **1976**, *15*, 1134, using 5×10^{-5} M Pt(II) in 0.01 M LiClO₄.

^b van Eldik, R.; Palmer, D. A.; Kelm, H. *Inorg. Chem.* **1979**, *18*, 572, using 5×10^{-4} M Pt(II) without added inert salt.

- (b) Romeo et al.¹ found that the rate of the reaction is affected by the bromide ion concentration. This is unlikely to be an ionic strength effect because both reactants are uncharged. The results at 30°C are given in the following table. Devise an empirical expression that will describe the dependence of k_{exp} on $[\text{Br}^-]$.

$10^4 \times [\text{Br}^-] \text{ (M)}$	0.0	2.0	4.0	6.0	8.0
$10^4 \times k_{\text{exp}} \text{ (s}^{-1}\text{)}$	2.13	1.05	0.69	0.53	0.43

- (c) Van Eldik et al.² also studied the pressure dependence of the following substitution reaction:



Under pseudo-first-order conditions (1.0×10^{-4} M Pt(II), 0.01–0.1 M $\text{S}=\text{C}(\text{NH}_2)_2$) they found that the rate constant is given by the following two-term expression:

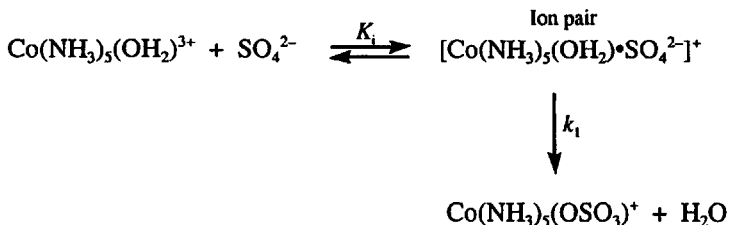
$$k_{\text{exp}} = k_1 + k_2[\text{S}=\text{C}(\text{NH}_2)_2]$$

Use the pressure dependencies of k_1 and k_2 in the following table to calculate the volume of activation for each rate constant.

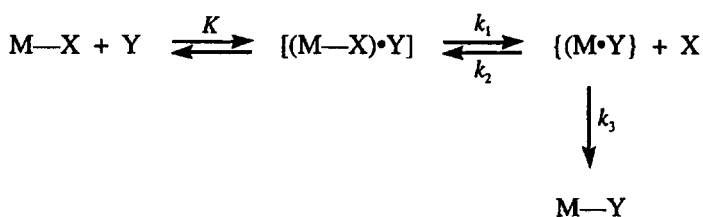
P (bar)	$10^4 \times k_1 \text{ (s}^{-1}\text{)}$	$10^3 \times k_2 \text{ (s}^{-1}\text{)}$
1	2.25	3.25
250	2.53	4.27
500	3.08	4.82
750	3.72	5.54
1000	4.36	5.56

CHAPTER 2

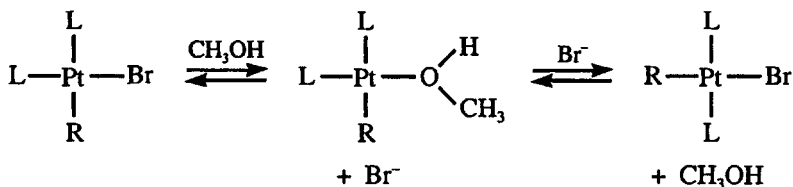
- Develop the expression for the pseudo-first-order rate constant for the following ion-pair substitution mechanism. Assume that the solvent is water and that K_i represents a rapidly maintained equilibrium and that $[\text{SO}_4^{2-}] \gg [\text{Co(III)}]_{\text{total}}$.



2. Develop the expression for the pseudo-first-order rate constant for the following mechanism. Assume that $[\text{Y}]$ and $[\text{X}] \gg [\text{M}]_{\text{total}}$, that the first step is a rapidly maintained equilibrium and that there is a steady state for the intermediate $\{(\text{M}) \cdot \text{Y}\}$.



3. The mechanism shown below might be suggested as an explanation for the effect of bromide ion on the isomerization reaction in Problem 4(b) of Chapter 1:



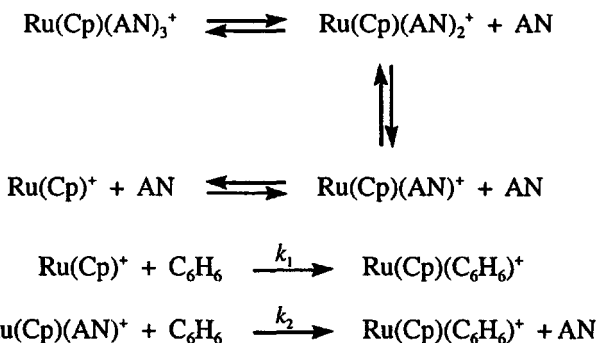
- (a) Develop the rate law for this mechanism by assuming a steady state for the intermediate methanol complex.
- (b) Does the predicted pseudo-first-order rate constant have a dependence on $[\text{Br}^-]$ consistent with the data in Problem 4(b) of Chapter 1?
- (c) Is the mechanism shown consistent with the principle of microscopic reversibility?
4. The rate law for the reaction given below has been determined in aqueous 0.10 M HClO_4 with Fe^{3+} in excess. The rate is first-order in the Cr-benzyl complex concentration and independent of the Fe^{3+} concentration. Suggest a mechanism consistent with this rate law. (*Hint*: see Zhang and Jordan.³)



5. The substitution reaction of benzene with $\text{Ru}(\text{Cp})(\text{AN})_3$ ($\text{Cp} = \eta^5\text{-C}_5\text{H}_5$, $\text{AN} = \text{CH}_3\text{CN}$) has been studied in acetone by Koefod and Mann.⁴ They find that the rate is given by

$$\text{Rate} = \left(\frac{a}{[\text{AN}]^3} + \frac{b}{[\text{AN}]^2} \right) [\text{C}_6\text{H}_6][\text{Ru}(\text{Cp})(\text{AN})_3]$$

under conditions where $[\text{AN}]$ and $[\text{C}_6\text{H}_6] \gg [\text{Ru}]$. The authors interpret these observations on the basis of the following rapidly maintained equilibria and the rate-limiting reactions given by k_1 and k_2 :



- (a) Develop the rate law for this system. Assume that the reactant species are related by the relationships

$$\beta_1 = \frac{[\text{Ru}(\text{Cp})(\text{AN})^+]}{[\text{Ru}(\text{Cp})^+][\text{AN}]}, \quad \beta_2 = \frac{[\text{Ru}(\text{Cp})(\text{AN})_2^+]}{[\text{Ru}(\text{Cp})^+][\text{AN}]^2}, \quad \beta_3 = \frac{[\text{Ru}(\text{Cp})(\text{AN})_3^+]}{[\text{Ru}(\text{Cp})^+][\text{AN}]^3}$$

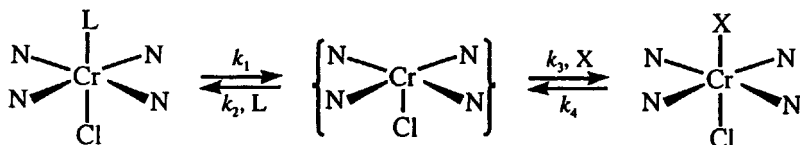
and the total reactant concentration is given by

$$[\text{R}]_{\text{tot}} = [\text{Ru}(\text{Cp})^+] + [\text{Ru}(\text{Cp})(\text{AN})^+] + [\text{Ru}(\text{Cp})(\text{AN})_2^+] + [\text{Ru}(\text{Cp})(\text{AN})_3^+]$$

- (b) Compare your result in (a) to the experimental rate law and describe under what conditions the observations correspond to your rate law.

CHAPTER 3

1. The substitution reactions of (tetraphenylporphinato)chromium(III) chloride have been studied with several different leaving and entering groups.⁵ The kinetic results have been interpreted in terms of a limiting D mechanism, as described by the following sequence:



Some of the kinetic results (25°C in toluene) are summarized in the following table:

L	X	k_1 (s ⁻¹) ^a	k_3/k_2 ^a	log K^a
PPh ₃	MeIm ^b	4.6	1.03×10 ³	4.8
P(OPr) ₃	MeIm ^b	95	24	4.1
P(C ₂ H ₄ CN) ₃	MeIm ^b	80	~2×10 ²	(5.3) ^c
py	MeIm ^b	5.0	1.7	2.5
PPh ₃	py	3.6		2.6

^aO'Brien, P.; Sweigart, D. A. *Inorg. Chem.* **1982**, *21*, 2094.

^bMeIm is N-methylimidazole.

^cCalculated from data in the table.

- Use other data in the table to predict k_3/k_2 for the last system listed.
 - Determine the order of nucleophilicity of the L and X ligands based on the k_3/k_2 values. Analyze this ordering on the basis of the Hard-Soft theory of acids and bases and other factors thought to affect nucleophilicity.
 - Calculate k_4 from the overall equilibrium constant and the kinetic data for the three systems with X = MeIm and L = PPh₃, P(OPr)₃ and py. Are these values of k_4 consistent with the mechanistic proposal? Suggest how the value of log K for P(C₂H₄CN)₃ was calculated.
 - Calculate k_4 for the system with L = PPh₃ and X = py. Is the result consistent with other results in the table?
2. Substitution reactions on Pt(II) are thought to proceed with associative activation. The following reaction has been studied by Romeo et al.⁶ using various amine, Am, entering groups:



The pseudo-first-order rate constant is given by $k_{\text{obsd}} = k_1 + k_2[\text{Am}]$. The table below gives some representative results at 25°C in CH₂Cl₂ and some extrakinetic parameters.

- Suggest a mechanism for the k_1 pathway consistent with the data.

Am ^a	pK _a	Cone Angle (deg)	E _r (kcal M ⁻¹)	10 ⁴ κk ₁ (s ⁻¹)	10 ² κk ₂ (M ⁻¹ s ⁻¹)
NH ₂ ⁿ Pr	10.56	106	31	1.83	8.39
NH ₂ Cy	10.62	115	41	1.64	6.82
NH ₂ ⁿ Bu	10.64	113	43	1.97	4.66
NH ₂ ^t Bu	10.65	123	53	1.72	2.18
Pip	11.12	121	61	1.91	3.26
NHEt ₂	10.92	125	73	1.74	0.669
NH ⁱ Pr ₂	11.09	137	105	1.72	0.039
NEt ₃	10.76	150	109	1.69	
NHCy ₂		133	113	1.71	

^a Abbreviations: ⁿPr = *n*-propyl; ⁿBu = *n*-butyl; ^tBu = *t*-butyl; Pip = piperidine; ⁱPr = *iso*-propyl.

- (b) Discuss the variation of k_2 with cone angle. Does this pathway exhibit a steric threshold? Estimate values of k_2 for NEt₃ and NHCy₂. Do these estimates seem consistent with the apparent inability to evaluate k_2 relative to k_1 for [am] = 1.0 M?
- (c) Discuss the variation of k_2 with E_r by considering the same factors described in (b).
3. Will the following complexes be labile or inert as defined by Taube? Cr^{II}(L)₆, octahedral low spin; V^{III}(L)₆, octahedral; Rh^{II}(L)₆, octahedral.
4. Various types of evidence indicate that the substitution reactions on Co(OH₂)₆²⁺ in water have a **D** mechanism. If this is correct, explain why the reaction rates are observed to be first-order in the entering ligand.
- 5.(a) Use the *d* orbital energies in Table 3.14 to calculate the crystal field activation energies for an octahedral *d*³ system undergoing substitution by a trigonal pyramidal and by a pentagonal bipyramidal transition state. Use these results and the data in Table 3.15 to predict the most favorable transition state of regular geometry and the mechanism for such a system.
- (b) Calculate the crystal field activation energy for a square-planar *d*⁸ system undergoing associative substitution by square-pyramidal and trigonal-bipyramidal transition states.
6. Several studies have shown that the replacement of L in Fe^{II}(CN)₅L complexes has kinetic properties typical of a **D** mechanism. The rate shows a saturation effect at high entering group concentrations, which is

consistent with Eq. (3.3). Reddy and van Eldik⁷ have determined the ΔV^\ddagger for k_1 for such reactions with L = various amines as the entering group. The partial molar volume, \bar{V}° , of the amines was varied to determine the effect on ΔV^\ddagger . The results are tabulated below:

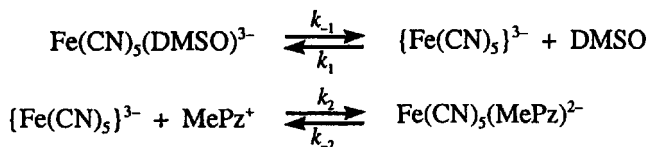
	NH ₃	NH ₂ CH ₃	NH ₂ C ₂ H ₅	NH ₂ C ₃ H ₇	NH ₂ CH ₂ Ph
ΔV^\ddagger (cm ³ M ⁻¹)	16.6	24.0	16.3	18.5	17.4
\bar{V}° (cm ³ M ⁻¹)	24.8	41.7	58.4	85.6	109

- (a) What is unusual about these results, since, for a D mechanism

$$\Delta V^\ddagger = \bar{V}^\circ(\text{Fe}(\text{CN})_5) + \bar{V}^\circ(\text{L}) - \bar{V}^\circ(\text{Fe}(\text{CN})_5\text{L})$$

- (b) Suggest an explanation for these observations. (*Hint*: See Jordan.⁸)

7. The kinetics of the reaction of the N-methylpyrazinium ion, MePz⁺, with $\text{Fe}(\text{CN})_5(\text{DMSO})^{3-}$ were studied by Malin and co-workers.⁹ The results were interpreted in terms of the following D mechanism:



- (a) Develop the expression for the pseudo-first-order rate constant for the system, under the conditions that $[\text{DMSO}], [\text{MePz}^+] \gg [\text{Fe}^{\text{II}}]_{\text{tot}}$, and with a steady-state assumption for $[\{\text{Fe}(\text{CN})_5\}^{3-}]$.
- (b) The rate constant, k_{obsd} , shows an unusual dependence on $[\text{MePz}^+]$, as indicated by the following data for $[\text{DMSO}] = 5 \times 10^{-3}$ M.

[MePz ⁺] (M)	0.006	0.012	0.025	0.050	0.100	0.200
$10^4 \times k_{\text{obsd}}$ (s ⁻¹)	1.35	1.06	0.926	0.820	0.772	0.750

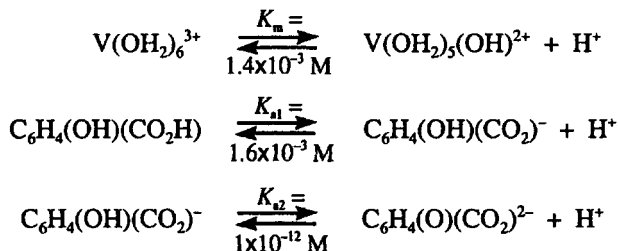
Determine the limiting conditions required for the answer in (a) to reduce to a form consistent with the fact that k_{obsd} decreases with increasing $[\text{MePz}^+]$. Make a plot of the data based on this reduced form to extract values of rate constant(s) and/or their quotients.

- (c) It might be expected that $k_1 \approx k_2$ because $\{\text{Fe}(\text{CN})_5\}^{3-}$ would be rather indiscriminant in its reaction with nucleophiles. In an earlier study, Toma and Malin¹⁰ determined that $k_{-2} = 2.8 \times 10^{-4}$ s⁻¹. Use this information and the results in (b) to calculate k_1/k_2 . Is the value of the ratio consistent with expectations?

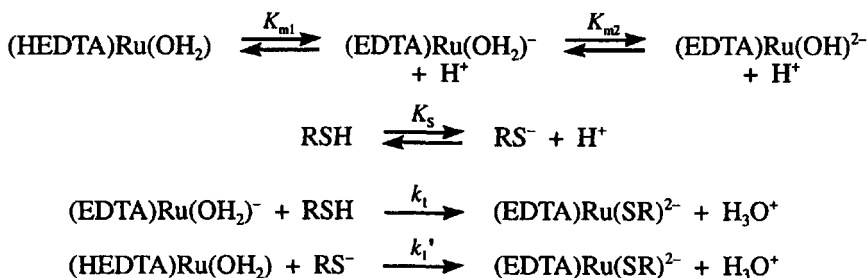
8. The reaction of aqueous V(III) with salicylic acid has the following rate law:

$$\text{Rate} = \left(6.0 + \frac{2.6}{[\text{H}^+]}\right)[\text{V(III)}]_{\text{total}}[\text{salicylic acid}]_{\text{total}}$$

The relevant ionization reactions in this system are the following:



- (a) Propose two reaction schemes that are consistent with the rate law.
- (b) Calculate the specific rate constants for each scheme in (a) and determine which, if any, is more probable on the basis of other data in Table 3.22.
9. The complex of Ru(III) with EDTA in water has an η^5 -EDTA with an uncoordinated acetate group on the N cis to the OH_2 ligand. The fully protonated complex is often abbreviated as $(\text{HEDTA})\text{Ru}(\text{OH}_2)$, and it undergoes successive ionizations to form $(\text{EDTA})\text{Ru}(\text{OH}_2)^-$ and $(\text{EDTA})\text{Ru}(\text{OH})^{2-}$. In early work¹¹ it was found that $(\text{EDTA})\text{Ru}(\text{OH}_2)^-$ is unusually substitution labile for a low-spin d^5 system. The rates of ligand substitution have a strong dependence on the nature of the entering group, and an associative mechanism was proposed. This is consistent with the negative values of ΔS^\ddagger and ΔV^\ddagger found in later work.¹² The area has been reviewed recently.¹³ Several thiol entering groups, RSH, have been studied and observed to have substitution rates that are nearly independent of pH in the 5–6 region.¹⁴ It also appears that the rates are not very dependent on the basicity of the thiols, as judged by their $\text{p}K_a$ values. These studies may be interpreted in terms of the following equilibria and reactions:



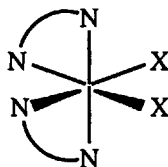
- (a) For the conditions that $[\text{RSH}]_{\text{tot}} \gg [\text{Ru}]_{\text{tot}}$, develop an expression for the pseudo-first-order rate constant, k_{obsd} , for this system.
- (b) Show that for pH 5–6, the expression for k_{obsd} is independent of $[\text{H}^+]$, given that $K_{\text{m1}} = 5 \times 10^{-3} \text{ M}$, $K_{\text{m2}} = 3.9 \times 10^{-8} \text{ M}$, and $K_{\text{s}} > 10^{-8} \text{ M}$.
- (c) The answer to (a) should reveal that there is a proton ambiguity between the assignment to the k_1 or k_1' paths. The published data has been assigned to k_1 , and some results are tabulated below. Make the opposite assignment and calculate values for k_1' . Do these values show some correlation with the basicity of RS^- , and are they consistent with diffusion-control limits?

RSH	cysteine	glutathione	N-acetylcysteine	2-mercaptoethanol
$K_{\text{s}} (\text{M})$	5.5×10^{-9}	3.3×10^{-9}	3.3×10^{-10}	2.5×10^{-10}
$k_1 (\text{M}^{-1} \text{ s}^{-1})$	152	288	276	530

CHAPTER 4

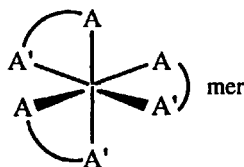
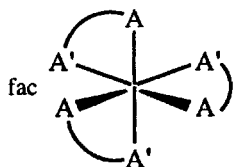
1. For the following complex, draw diagrams describing a process that:

- (a) Causes racemization but no isomerization.
 (b) Causes cis–trans isomerization.

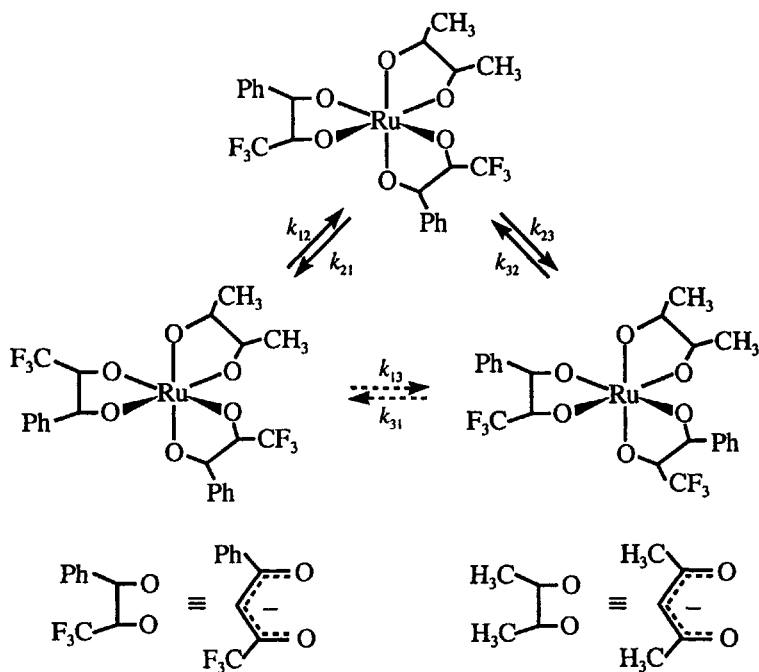


2. For each of the isomers of the following asymmetric chelate:

- (a) Predict the products if the reaction proceeds by one-ended dissociation of A' to give a trigonal-bipyramidal intermediate with the monodentate ligand in the trigonal plane. Assume that ring closing occurs with equal probability along the trigonal edges.
- (b) Indicate if a new structural isomer or stereoisomer of the reactant has formed in each case.



3. Stereochemical mobility in a square-based pyramidal molecule may be due to an "anti-Berry" pseudorotation in which the intermediate in the normal pseudorotation is actually the reactant. Sketch an anti-Berry process for a square-based pyramidal molecule.
4. The fluxional behavior of the Ru(III) acetylacetonate derivatives in the following scheme have been studied by Hoshino et al.¹⁵ The authors isolated the isomer in the lower left of the scheme and deduced that, as it isomerizes in DMF, it does not convert directly to the isomer on the lower right, i.e., k_{13} and k_{31} are much smaller than the other rate constants. However, the isomer at the top of the scheme can interconvert to both of the other isomers. This behavior places restrictions on the types of rearrangement that occur.



- (a) Show two intramolecular twist mechanisms that will bring about the k_{13} reaction. These are presumably eliminated as mechanistic possibilities because this change is not observed.
- (b) Show two mechanisms that proceed by trigonal-bipyramidal intermediates and give the k_{21} and k_{23} process. Assume that the bond broken is always that of an O next to CF_3 .
- (a) Determine if the process described in (b) gives the k_{13} process.
5. Show with clear diagrams why an $\eta^2\text{-C}_6\text{H}_6$ system should be more readily fluxional than an $\eta^4\text{-C}_6\text{H}_6$ system.

6. For $\text{Rh}(\eta^5\text{-C}_5\text{H}_5)(\text{C}_2\text{F}_4)(\text{C}_2\text{H}_4)$, the pressure dependence of the rotation of ethylene has been measured by Peng and Jonas¹⁶ using ^1H NMR line shape analysis. Some results in pentane at 0°C are given below. Note that the solvent viscosity, η , increases with increasing pressure.

P (MPa)	0.10	105	202	308	401	495
k (s^{-1})	235	295	340	359	346	313
η (cP)	0.448	0.762	1.21	1.87	2.60	3.47

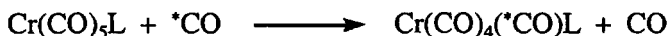
The observations are unusual because the rate constant goes through a maximum. The results were fitted to a polynomial to obtain

$$\ln k = 5.461 + 2.508 \times 10^{-3}P - 3.585 \times 10^{-6}P^2$$

- (a) Since $(\delta(\ln k)/\delta P)_T = -\Delta V^\ddagger/RT$, the derivative of this polynomial can be used to calculate the value of ΔV^\ddagger at any pressure. Calculate ΔV^\ddagger at pressures of 0, 100, 200, 300, 400 and 500 MPa.
- (b) The authors have ascribed the pressure-dependent component of ΔV^\ddagger to a frictional effect of the solvent. Intuitively, one might expect such an effect to correlate with the solvent viscosity. Plot the ΔV^\ddagger values in (a) versus η to determine if this supposition is reasonable.

CHAPTER 5

1. Explain the trends in the rate constants given in the table below for the following reaction:



Compound	k (s^{-1} , 30°C) ^a
$\text{Cr}(\text{CO})_6$	1.0×10^{-12}
$\text{Cr}(\text{CO})_5(\text{PMe}_2\text{Ph})$	1.5×10^{-10}
$\text{Cr}(\text{CO})_5(\text{PPh}_3)$	3.0×10^{-10}
$\text{Cr}(\text{CO})_5\text{Br}^-$	2.0×10^{-5}
$\text{Cr}(\text{CO})_5\text{Cl}^-$	1.5×10^{-4}

^a Atwood, J. D.; Brown, T. L. *J. Am. Chem. Soc.* **1976**, *98*, 3160, and references therein.

2. Substitution reactions on some metal carbonyls proceed by parallel dissociative and associative pathways and the reaction may have significant reversibility. The situation has been considered recently by Schneider and van Eldik.¹⁷ If the entering group is Y and the leaving

group is CO, then Eq. (3.17) can be readily adapted to give the dissociative contribution to k_{exp} , and k_5 and k_{-5} can be defined as the forward and reverse rate constants for the parallel associative pathway. Then, the pseudo-first-order rate constant is given by

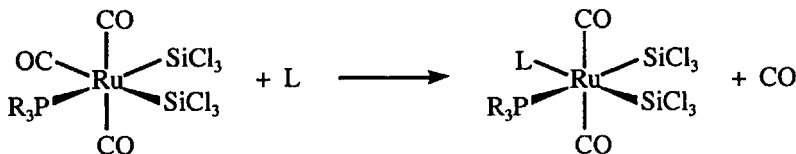
$$k_{\text{exp}} = \frac{k_1 k_3 [\text{Y}] + k_2 [\text{CO}] k_4}{k_2 [\text{CO}] + k_3 [\text{Y}]} + k_5 [\text{Y}] + k_{-5} [\text{CO}]$$

- (a) Apply the principle of detailed balancing to this cyclic system by noting that the equilibrium constant $K = k_1 k_3 / k_2 k_4 = k_5 / k_{-5}$. Use these relationships to eliminate the reverse rate constants, k_4 and k_{-5} , and express k_{exp} in terms of the other rate constants and K .
- (b) If the limiting conditions are such that $k_1 k_3 [\text{Y}] \gg k_2 k_4 [\text{CO}]$ and $k_3 [\text{Y}] \gg k_2 [\text{CO}]$, then the expression for k_{exp} appears to reduce to

$$k_{\text{exp}} = k_1 + k_5 [\text{Y}] + k_{-5} [\text{CO}]$$

Show that this equation must be simplified further to be consistent with the assumptions and the principle of detailed balancing.

3. For the following reaction, the rate constant in toluene has been found to be independent of the nature and concentration of L.

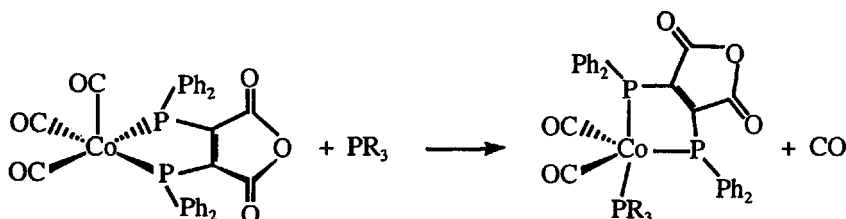


Results for various PR_3 ligands are given in the following table:

Phosphine	$\text{p}K_a$	Cone Angle	$-\log k^a$
$\text{P}(\text{OCH}_2)_3\text{CEt}$	1.74	101	5.96
$\text{P}(\text{OMe})_3$	2.6	107	5.14
$\text{PPh}(\text{OMe})_2$	2.64	120	4.95
PPhMe_2	6.50	122	4.72
$\text{P}(\text{OPh})_3$	-2.0	128	4.70
$\text{PPh}_2(\text{OMe})$	2.69	132	4.64
PPh_2Me	4.57	136	4.15
$\text{P}(p\text{-FC}_6\text{H}_4)_3$	1.97	145	3.12
PPh_3	2.73	145	3.05
$\text{P}(p\text{-MeC}_6\text{H}_4)_3$	3.84	145	3.08
$\text{P}(m\text{-MeC}_6\text{H}_4)_3$	3.3	165	2.89
$\text{P}(m\text{-ClC}_6\text{H}_4)_3$	1.03	165	3.02

^aChalk, K. L.; Pomeroy, R. K. *Inorg. Chem.* **1984**, *23*, 444; at 40°C in toluene, k in s^{-1} .

- (a) Suggest a mechanism, based on the observations with varying L.
- (b) The relative constancy of the rate constants for PR_3 ligands with cone angles of 145° but different pK_a indicates that the reaction is insensitive to σ -donor effects. However, k seems to vary with the cone angle. Make a plot of $\log k$ versus cone angle and analyze the steric effects in terms of their influence on the ground state and transition state for the reaction. (*Hint*: see Giering and co-workers¹⁸)
4. Nineteen-electron organometallic complexes are rare and generally quite reactive. Recently, the ligand substitution kinetics have been studied for the following system:



This may be viewed as a 19-electron system, or as Co(I) with a reduced ligand radical, P_2^- . In any case, the mechanism of substitution is of interest, and the data below have been obtained with $[\text{PR}_3]_{\text{tot}} \gg [\text{Co}]_{\text{tot}}$:

Table A. Rate Constants (25°C) for $\text{Co}(\text{CO})_3(\text{P-P}) + \text{PPh}_3$ in CH_2Cl_2

$[\text{PPh}_3]$ (M)	0.148	0.296	0.371	0.445	0.556	0.704
$10^3 k$ (s^{-1})	5.48	5.45	5.47	5.52	5.42	5.50

Table B. Rate Constants for $\text{Co}(\text{CO})_3(\text{P-P}) + \text{PPh}_3$ in CH_2Cl_2

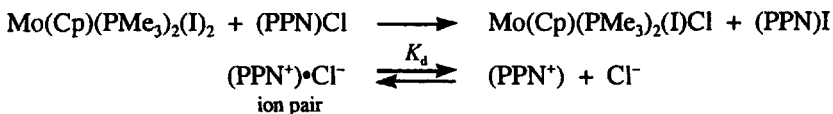
t ($^\circ\text{C}$)	10.0	15.0	20.0	25.0	30.0
$10^3 k$ (s^{-1})	0.598	1.26	2.67	5.47	10.2

Table C. Rate Constants (25°C) for $\text{Co}(\text{CO})_3(\text{P-P}) + \text{PR}_3$ in CH_2Cl_2

PR_3	PPh_3	$\text{P}(\text{OPh})_3$	PMePh_2	PBu_3	$\text{P}(\text{OMe})_3$
$10^3 k$ (s^{-1})	5.47	5.18	5.20	5.58	5.03

- (a) Are the kinetic results consistent with an I_a mechanism?
- (b) Are the kinetic results consistent with an A mechanism?
- (c) Are the kinetic results consistent with rate-controlling chelate ring opening followed by substitution? (See Scheme 5.4.)
- (d) Are the kinetic results and activation parameters for PPh_3 consistent with an I_d mechanism?

5. Substitution on 17-electron systems usually proceeds with associative activation. $\text{Mo}(\text{Cp})(\text{PMe}_3)_2(\text{I})_2$ is unusual for a 17-electron complex because it is more readily reduced than oxidized. This suggests that it is not a willing electron acceptor and therefore might undergo substitution by an associative pathway. Linck and co-workers¹⁹ have studied the following system in dichloromethane:



$(\text{PPN})\text{Cl}$ = (triphenylphosphonium)iminium chloride

The study is complicated by the ion pairing, and the general problem is to determine if the active nucleophile is free Cl^- or the ion pair, $(\text{PPN}^+)\cdot\text{Cl}^-$, and if there is a dissociative component to the rate. The ion pair formation constants were determined from conductivity studies by Algra and Balt.²⁰ Therefore, one can calculate the amount of free Cl^- and ion pair, $(\text{PPN}^+)\cdot\text{Cl}^-$, for a particular total $(\text{PPN})\text{Cl}$ concentration. Typical results at 30°C and $K_d = 4 \times 10^{-4} \text{ M}$ are tabulated below:

$10^2 \times [(\text{PPN})\text{Cl}] \text{ (M)}$	0.546	1.224	2.372	3.400	6.490
$10^2 \times [\text{Cl}^-] \text{ (M)}$	0.139	0.219	0.313	0.379	0.532
$10^2 \times [(\text{PPN}^+)\cdot\text{Cl}^-] \text{ (M)}$	0.407	1.005	2.059	3.021	5.958
$10^5 \times k_{\text{obsd}} \text{ (s}^{-1}\text{)}$	0.60	0.92	1.48	1.83	3.00

- (a) If $[\text{Cl}^-]$ is assumed to be the only nucleophile, then least-squares analysis gives

$$k_{\text{obsd}} = -(1.86 \pm 0.95) \times 10^{-6} + (5.43 \pm 0.40) \times 10^{-3} [\text{Cl}^-]$$

Why does this assumption appear unreasonable?

- (b) If the ion pair, $(\text{PPN}^+)\cdot\text{Cl}^-$, is assumed to be the only nucleophile, then least-squares analysis gives

$$k_{\text{obsd}} = (4.35 \pm 0.36) \times 10^{-6} + (4.58 \pm 0.24) \times 10^{-4} [(\text{PPN}^+)\cdot\text{Cl}^-]$$

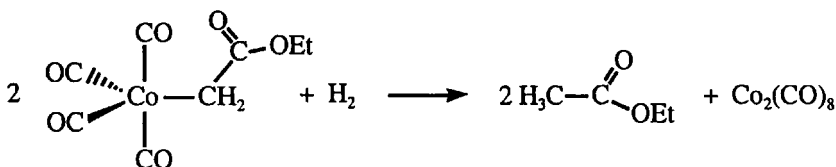
What could be the significance of the term that is independent of $[(\text{PPN}^+)\cdot\text{Cl}^-]$ in this equation?

- (c) If one assumes that both Cl^- and the ion pair are reactive, then

$$k_{\text{obsd}} = (3.64 \pm 0.22) \times 10^{-3} [\text{Cl}^-] + (1.64 \pm 0.34) \times 10^{-4} [(\text{PPN}^+)\cdot\text{Cl}^-]$$

Do the relative values of the rate constants for these two nucleophiles seem reasonable?

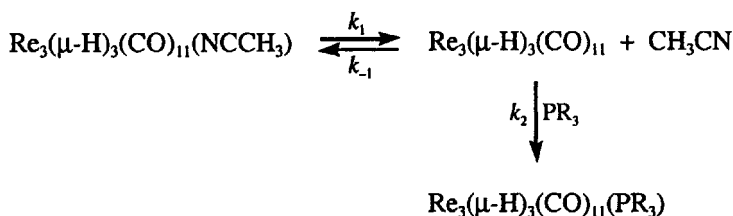
6. It has been observed that $cis\text{-Pt}(\text{PEt}_3)_2(\text{H})(\text{Solv})^+$ (Solv = methanol or acetone) reacts with 1-hexene but only brings about the isomerization of the 1-hexene to 2-hexene and 3-hexene. Suggest a mechanism for this process.
7. Assume that the reaction of $\text{Rh}(\text{Cp}^*)(\text{CO})\text{Kr}$ with cyclohexane involves rate-controlling dissociation of Kr. Verify that the k_{exp} has the form of Eq. (5.53) and the conclusion of Bergman and co-workers²¹ that α should be independent of the nature of the alkane.
8. The following reaction is of possible relevance to the mechanism of the hydroformylation reaction:



The dependence of the reaction rate on H_2 and CO concentrations has been determined at 35°C in *n*-heptane, and the results are given in the following table:

$10^3 \times [\text{H}_2]$ (M)	3.68	3.68	9.94	3.30	2.59	2.13
$10^3 \times [\text{CO}]$ (M)	1.31	1.31	3.56	2.30	4.16	5.35
$10^5 \times k_{\text{exp}}$ (s^{-1})	1.89	1.93	1.60	1.03	0.43	0.25

- (a) Deduce the rate law that seems to describe the results best.
- (b) Suggest a mechanism that is consistent with the rate law in (a).
- (c) Suggest a further type of experiment or kinetic study that would help to confirm your suggestion in (b).
9. In a study of the substitution reactions of $\text{Re}_3(\mu\text{-H})_3(\text{CO})_{11}(\text{NCCH}_3)$, Beringhelli et al.²² have proposed the dissociative mechanism in the following scheme:



- (a) Determine if this mechanism is consistent with the dependence of k_{obsd} on the reagent concentrations given in the following table for the reaction at 300 K in CDCl_3 :

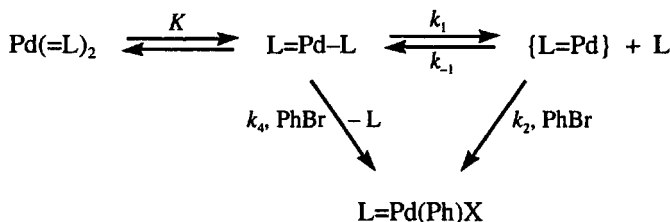
$[\text{Re}_3]_{\text{tot}}$ (M)	0.019	0.014	0.0141	0.0121
$[\text{PPh}_3]$ (M)	0.219	0.143	0.290	0.143
$[\text{CH}_3\text{CN}]$ (M)	0.262	0.367	0.152	0.265
$10^5 k_{\text{obsd}}$ (s^{-1})	1.71	0.89	3.68	1.22

- (b) For several phosphines, the analysis gave values of k_2/k_{-1} , as tabulated below along with some extrakinetic factors. Discuss the trends in this ratio with respect to the basicity of the phosphine and steric factors, as measured by the cone angle or the repulsion parameter, E_R . Would the effect of the size of the phosphine on its diffusion coefficient be relevant? (*Hint*: see Section 1.9)

Phosphine	$\text{p}K_a$	Cone Angle	E_R	$\log k_2/k_{-1}$
PMe_3	8.65	118	39	-0.04
PPhMe_2	6.50	122	44	-0.21
P(OMe)_3	2.6	107	52	-0.45
PPh_2Me	4.59	136	57	-0.42
P^nBu_3^a	8.43	132	64	-0.68
PPh_3	2.73	145	75	-0.92

^a n Bu is *n*-butyl.

- (c) Are the data in (a) consistent with a mechanism involving pre-equilibrium hydride-bridge opening, followed by phosphine substitution on the unsaturated metal center and then rapid bridge closing and CH_3CN elimination?
- (d) If the reaction were done as before in CDCl_3 but with some CD_3CN added, would the observations in (a) predict that CD_3CN would appear in the reactant?
10. The kinetics of the oxidative addition of PhBr to $\text{Pd}(\text{BINAP})_2$ in toluene at 45°C has been studied by Hartwig and co-workers.²³ This reaction is thought to be the rate-controlling process in the $\text{Pd}(0)$ catalyzed coupling of amines with aryl halides. The catalytic reaction has been the subject of several studies which recently have been revised and discussed by Shekhar et al.²⁴ On the basis of their kinetic results, Hartwig and co-workers proposed that the oxidative addition proceeds by the following pathways, where $\text{Pd}(=\text{L})_2$ is $\text{Pd}(\text{BINAP})_2$ and $\text{L}=\text{Pd}-\text{L}$ has one monodentate BINAP:

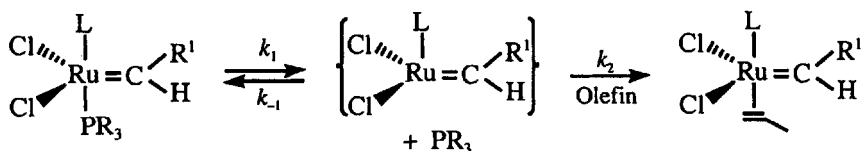


- (a) Develop an expression for the pseudo-first-order rate constant, k_{obs} , for this system for the conditions that $[\text{PhBr}] \gg [\text{Pd}(=\text{L})_2]$ and $[\text{L}]$ is constant, and with the assumptions that K represents a rapidly established equilibrium with $K \ll 1$ and a steady-state for $\{\{\text{L}=\text{Pd}\}\}$.
- (b) The data tabulated below gives the dependence of k_{obs} on $[\text{PhBr}]$ with added free $[\text{L}] = 4.1 \times 10^{-4} \text{ M}$.

$[\text{PhBr}], \text{ M}$	0.0029	0.0090	0.024	0.095	0.18	0.36	0.72	1.44	2.88
$10^5 k_{\text{obs}}, \text{ s}^{-1}$	3.0	6.8	7.6	10	12	15	20	30	45

Make a plot of $[\text{PhBr}]$ versus k_{obs} , and determine if the data are qualitatively consistent with expression for k_{obs} derived in (a).

- (c) From the data for $[\text{PhBr}] > 0.2 \text{ M}$, assume a linear dependence of k_{obs} on $[\text{PhBr}]$ and estimate values for $k_1 K$ and $k_4 K$.
- (d) It generally is found that PhI is more reactive for oxidative additions. How might a kinetic study with PhI help to substantiate the proposed mechanism.
- (e) In the paper, it is stated that, if $K k_{-1} [\text{L}] \gg k_2 [\text{PhBr}]$, the rate law is simplified. This seems difficult to justify because K is unknown. Do you agree with the statement of the authors?
11. Grubbs and co-workers²⁵ have studied the kinetic properties of several catalysts for olefin metathesis and ROMP (see Section 5.7.6). The general type of catalyst, and the authors' proposed mechanism are shown by the following reactions:



If a steady-state is assumed for the concentration of the intermediate, then the pseudo-first-order rate constant is given by

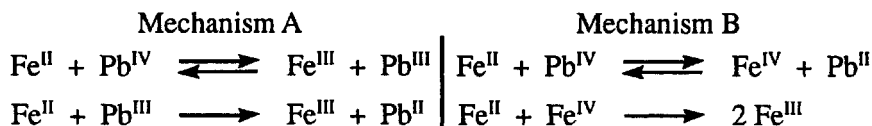
$$k_{\text{obs}} = \frac{k_1}{\frac{k_{-1}[\text{PR}_3]}{k_2[\text{Of}]} + 1}$$

where [Of] is the concentration of the olefin. The rate constants for PR_3 exchange, k_B , also were determined by magnetization transfer. The values of k_B are expected to equal k_1 .

- Since the reactant is a 16-electron system, another possible pathway could involve initial association of the olefin, and then dissociation of the phosphine. Develop the analogous rate constant expression for this mechanism.
- In the absence of added PR_3 , the rate was found to be independent of [Of] for some systems and approximately linear in [Of] for others. Do these observations differentiate between the two mechanisms?
- In experiments with ethyl vinyl ether as the olefin and 0.017 M total Ru, the k_{obs} was determined by NMR as a function of the ratio $[\text{PR}_3]/[\text{Of}]$. A linear variation of $1/k_{\text{obs}}$ with $[\text{PR}_3]/[\text{Of}]$ was found. Do these observations differentiate between the two mechanisms?
- For the system with $\text{PR}_3 = \text{L} = \text{PCy}_3$ and $\text{X} = \text{Cl}$, the slope of the plot in (c) was found to be $2.3 \times 10^4 \text{ s}^{-1}$ at 50°C in toluene. Use this information and the measured value of $k_B = 2.6 \text{ s}^{-1}$ to calculate k_{-1}/k_2 .
- The system described in (d) also was studied by spectrophotometry at 20°C with 0.77 mM total Ru. The [Of] was varied and no PCy_3 was added. The k_{obs} shows saturation kinetics in [Of] which suggest from the authors' rate expression that $[\text{Of}] \approx 0.05 \text{ M}$ when k_{obs} reaches half of its maximum value, i.e. when $[\text{Of}] = k_{-1}/k_2[\text{PCy}_3]$. Use these observations to estimate k_{-1}/k_2 and compare the result to the answer in (d).

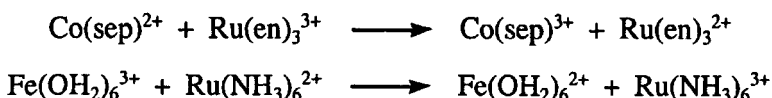
CHAPTER 6

- The oxidation of $\text{Fe}(\text{II})$ by $\text{Pb}(\text{IV})$ might proceed by either of the following mechanisms:

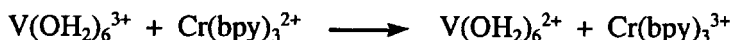


- Assume a steady state for Pb^{III} and Fe^{IV} and develop the rate law for each mechanism.
- Could these alternatives be distinguished experimentally?

2. Use the data in Table 6.2 and the Marcus relationship, Eq. (6.32), to predict the rate constants for the following reactions:



3. For the following reaction, $k = 4.2 \times 10^2 \text{ M}^{-1} \text{ s}^{-1}$ and $K = 1.3$ at 25°C :

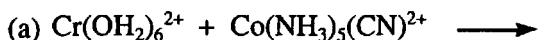


Use additional data in Table 6.2 to estimate the self-exchange rate constant for $\text{Cr}(\text{bpy})_3^{2/3+}$.

4. The Ru(IV) and Ru(III) complexes of sarcophagine, sar, undergo deprotonation to give $\text{Ru}^{\text{IV}}(\text{sar}(-\text{H}))^{3+}$ and $\text{Ru}^{\text{III}}(\text{sar}(-\text{H}))^{2+}$, and this couple has a reduction potential of 0.05 V. Bernhard and Sargeson²⁶ reported the rate constant of $7 \times 10^7 \text{ M}^{-1} \text{ s}^{-1}$ for the following reaction:



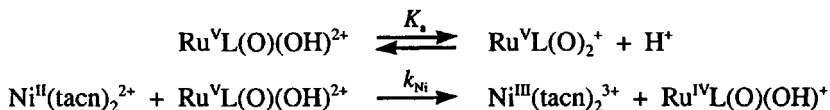
- (a) Use the simple Marcus relationship to estimate the self-exchange rate constant for $\text{Ru}^{\text{IV/III}}(\text{sar}(-\text{H}))$, given that the $\text{Ru}^{\text{III/II}}(\text{sar})$ couple has a reduction potential of 0.29 V and a self-exchange rate constant of $1.2 \times 10^5 \text{ M}^{-1} \text{ s}^{-1}$.
- (b) For the reaction of $\text{Ru}^{\text{II}}(\text{sar})^{2+}$ with O_2 , $k = 1.4 \text{ M}^{-1} \text{ s}^{-1}$ and the O_2/O_2^- couple has a reduction potential of -0.15 V . Use this and other information in (a) to estimate the self-exchange rate constant for the O_2/O_2^- couple. Compare your answer to other results in Table 6.5.
5. Predict the products of the following reactions:



6. Based on the reduction potentials and self-exchange rate constants given below, estimate whether either Ce^{IV} or MnO_4^- would be suitable analytical reagents for $\text{Fe}(\text{CN})_6^{4-}$.

Reaction	E° (V)	k ($\text{M}^{-1} \text{ s}^{-1}$)
$\text{Ce}^{\text{IV}} + \text{Ce}^{\text{III}}$	+1.44	4.6
$\text{Fe}(\text{CN})_6^{3-} + \text{Fe}(\text{CN})_6^{4-}$	+0.36	3×10^2
$\text{MnO}_4^- + \text{MnO}_4^{2-}$	+0.56	3.6×10^3

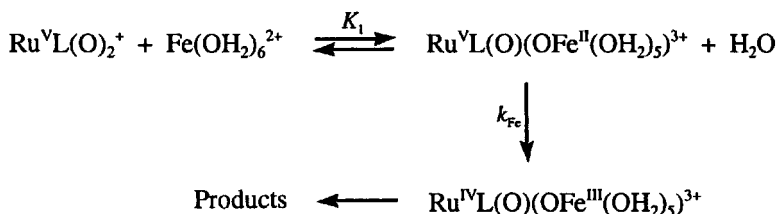
7. Yau et al.²⁷ have studied the reaction of several reducing agents with a *cis*-dioxo-Ru(V) species, $\text{RuL}(\text{O})_2^+$, where L is an N_4 donor chelate. The kinetics of the reaction with $\text{Ni}(\text{tacn})_2^{2+}$ were found to be consistent with the following reactions:



The following table gives the $[\text{H}^+]$ dependence of the second-order rate constants at 298 K and ionic strength 0.10 M.

$[\text{H}^+]$ (M)	0.005	0.010	0.020	0.050	0.080	0.100
$10 \times k_{\text{Ni}}$ ($\text{M}^{-1} \text{s}^{-1}$)	2.86	4.39	6.36	9.20	9.89	10.0

- (a) Derive the rate law for the proposed reaction pathway and determine if the data are consistent with the proposal. If possible, determine k_{Ni} and K_a from an appropriate plot of the data.
- (b) The rate of the analogous reaction with $\text{Fe}(\text{OH}_2)_6^{2+}$ was found to be independent of $[\text{H}^+]$, and the authors proposed a pathway via an inner-sphere adduct, as shown by the following reactions:



However, the authors failed to include the acid dissociation reaction, K_a , in the proposal. With the latter included, develop the rate law for the system, for the conditions of $[\text{Fe}]_{\text{tot}} \gg [\text{Ru}]_{\text{tot}}$, and show that the rate is not predicted to be independent of $[\text{H}^+]$ for the same range of $[\text{H}^+]$ as used with $\text{Ni}(\text{tacn})_2^{2+}$.

- (c) Assume that $\text{Fe}(\text{OH}_2)_6^{2+}$ reacts with both $\text{RuL}(\text{O})(\text{OH})^{2+}$ and $\text{RuL}(\text{O})_2^+$ by a simple outer-sphere mechanism and determine under what special condition this system would give a rate that is independent of $[\text{H}^+]$.
8. The self-exchange rate constant for $\text{Cr}(\text{NN})_3^{3/2+}$ systems, where NN = bpy or phen, has been the subject of some disagreement. Zahir²⁸ has recently measured several rate constants for the reaction of some $\text{Cr}(\text{NN})_3^{2+}$ systems with several oxidants. Representative results from

this and earlier work are given in the following table, where k_{BB} is the self-exchange rate constant for the oxidant.

NN	Oxidant	$\log k_{\text{AB}}$	$\log k_{\text{BB}}$	$\log K_{\text{AB}}$
5-Clphen	$\text{Ru}(\text{NH}_3)_6^{3+}$	6.85	3.48	3.74
bpy	$\text{Ru}(\text{NH}_3)_6^{3+}$	7.63	3.48	5.26
phen	$\text{Ru}(\text{NH}_3)_6^{3+}$	7.69	3.48	5.60
5-Mephen	$\text{Ru}(\text{NH}_3)_6^{3+}$	7.76	3.48	5.93
4,7-Me ₂ phen	$\text{Ru}(\text{NH}_3)_6^{3+}$	8.41	3.48	8.47
bpy	$\text{Co}(\text{bpy})_3^{3+}$	8.04	1.26	9.64
bpy	$\text{Co}(\text{phen})_3^{3+}$	8.14	1.65	10.5
bpy	$\text{Fe}(\text{OH}_2)_6^{3+}$	8.86	0.62	16.9

- Based on a logarithmic form of Eq. (6.32), devise a function that, when plotted versus $\log K_{\text{AB}}$, should give a straight line. Plot the data and determine if the result is reasonably consistent with the simplest form of Marcus theory. Use the plot to estimate $\log k_{\text{BB}}$.
- It has often been observed that $\text{Fe}(\text{OH}_2)_6^{3+}$ deviates from the predictions of Marcus theory. Is this true for this data? Would the situation be improved if its k_{BB} were $\sim 5 \times 10^3 \text{ M}^{-1} \text{ s}^{-1}$?

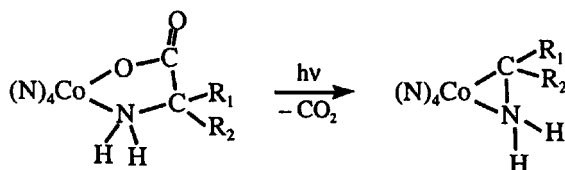
CHAPTER 7

- In Figure 7.1, assume that the photoactive state A can react by two pathways to give products P_1 and P_2 with rate constants k_1 and k_2 , respectively. Develop the expression for the quantum yields of the two products.
- The energy levels for the $d-d$ transitions in an octahedral Cr(III) complex are given in Figure 7.3. Suggest two explanations for the observation that the quantum yield for photosubstitution on such complexes is independent of the irradiation wavelength between 350 and 700 nm.
- Use Adamson's rules to:
 - Predict the product of the photolysis of $\text{cis-Cr}(\text{NH}_3)_4(\text{Cl})_2^+$.
 - Explain the very low quantum yield for the photoaquation of $\text{trans-Cr}(\text{en})_2(\text{OH}_2)_2^{3+}$.
- For Scheme 7.16, develop the kinetic expression that can be used to determine the various rate constants from the dependence of the rate on $[\text{CO}]$ and $[\text{THF}]$.

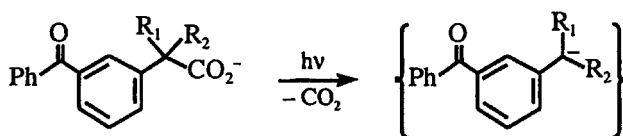
5. The activation volumes ($\text{cm}^3 \text{M}^{-1}$) for the photolysis of two chloro complexes of Cr(III) and Rh(III) are given in the table below. Suggest rationalizations for the similarities and differences.

	$\Delta V^\ddagger(\Phi_{\text{Cl}})$	$\Delta V^\ddagger(\Phi_{\text{NH}_3})$
$\text{Cr}(\text{NH}_3)_2\text{Cl}^{2+}$	-13	-9.4
$\text{Rh}(\text{NH}_3)_3\text{Cl}^{2+}$	-8.6	+9.3

6. The photodecarboxylation of amino acid complexes of Co(III) in water proceeds as follows:

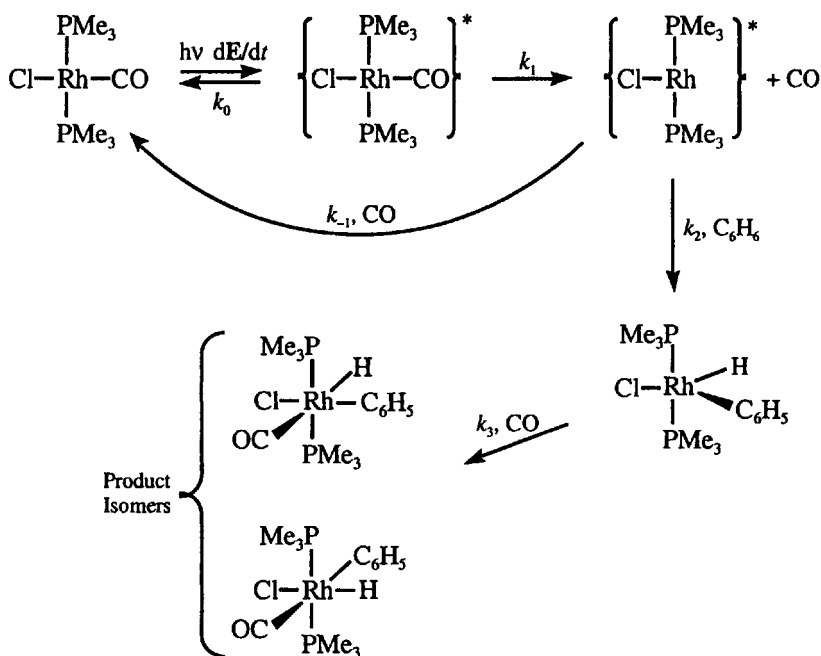


Radical clock studies by Hartshorn and Telfer,²⁹ as shown in Scheme 7.4, suggest that the mechanism may not involve radicals. Sciano and co-workers³⁰ have shown that the photodecarboxylation of ketoprofen derivatives in water proceeds via a carbanion intermediate, as shown in the following reaction:



Depending on the substituents, R_1 and R_2 , this intermediate can undergo rearrangements and cyclizations in competition with the protonation by H_2O .

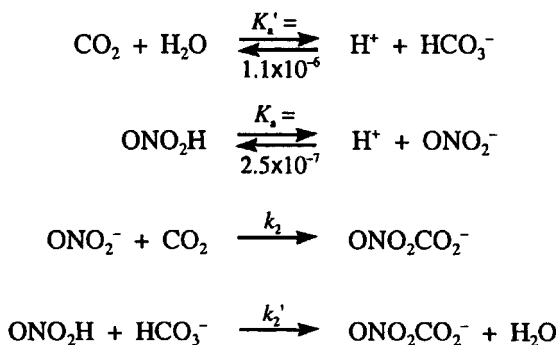
- On the basis of the ketoprofen systems, suggest a mechanism for the Co(III) complexes that does not involve a radical as the species undergoing ring closure to make the Co—C bond.
 - What might be the effect on the products in your answer to (a) if the photolysis were done in acidic solution? (*Hint*: carbanions are normally rapidly protonated by H^+ .)
7. The photolysis of *trans*- $\text{Rh}(\text{PMe}_3)_2(\text{CO})\text{Cl}$ in benzene/THF solution has been studied and the products and proposed reaction pathways are shown in the following scheme:



- (a) Develop the expression for the quantum yield of the products, assuming a steady state for all intermediate species and that excess CO and benzene are present.
- (b) Would a study of the variation of product quantum yield with the concentration of benzene and CO help to establish the validity of the proposed scheme?
- (c) The interconversion of the product isomers has been proposed to proceed through an η^2 -benzene intermediate. Show, with clear diagrams, how this might occur.
8. The photolysis of $\text{Re}_2(\text{CO})_{10}$ in acetonitrile produces a mixture of $\text{Re}_2(\text{CO})_9(\text{NCCH}_3)$ and $\text{Re}(\text{CO})_5$. In the absence of other reagents, two $\text{Re}(\text{CO})_5$ radicals recombine with $k = 1 \times 10^{10} \text{ M}^{-1} \text{ s}^{-1}$. Sarakha and Ferraudi³¹ observed that the addition of various macrocyclic complexes of Cu(II) of the general form $\text{Cu}(\text{N})_4^{2+}$ had no effect on the decay of the $\text{Re}(\text{CO})_5$ radical unless halide ions (Cl^- , Br^- or I^-) were added to the acetonitrile solution. It also was observed that NaCl or NaBr alone did not affect the spectrum or decay of the $\text{Re}(\text{CO})_5$ radical.
- (a) Suggest a mechanism for the reaction. (*Hint*: see Section 6.4.)
- (b) On the basis of your mechanism, suggest other species that might be added to promote the reaction of $\text{Re}(\text{CO})_5$ and $\text{Cu}(\text{N})_4^{2+}$.
- (c) Suggest a single species that might act like $\text{Cu}(\text{N})_4^{2+}$ plus halide.

CHAPTER 8

- Describe in detail the complete mechanistic sequence proposed by Finke et al.³² for the reaction of diol dehydrase with ethylene glycol.
- For a system with competitive inhibition, develop expressions for the slope, intercept when $[S]^{-1} = 0$ and intercept when $v_i^{-1} = 0$ for Lineweaver–Burke plots, by rearrangement of Eq. (8.7).
 - For a system showing uncompetitive inhibition, develop expressions for the slope, intercept when $[S]^{-1} = 0$ and intercept when $v_i^{-1} = 0$ for Lineweaver–Burke plots, by rearrangement of Eq. (8.9).
 - Draw sketches to show how the Lineweaver–Burke plots would vary with $[I]$ for competitive and uncompetitive inhibition.
- Assume that the hydrolysis of phenyl acetate by carbonic anhydrase proceeds by a mechanism analogous to that for CO_2 hydration. Describe the sequence of reactions that would be involved in the ester hydrolysis.
- Show that the steady-state solution for Scheme 8.8 yields Eq. (8.33).
- Consider the electronic structure of the reactants and suggest why the rate-controlling step for CO binding to myoglobin may be formation of the Fe—CO bond, while this step is not rate-controlling for O_2 binding.
- Show that the mechanism in Scheme 8.14 gives the experimental rate law for NO oxidation. Make any steady-state approximations that are necessary.
- If reactants are involved in protolytic equilibria, there is often a proton ambiguity as to the state of protonation of the actual reacting species. In the case of the reaction of peroxyxynitrite ion with carbon dioxide, Lyman and Hurst³³ were able to show that the reactants are CO_2 and ONO_2^- . The overall system can be described by the following scheme:

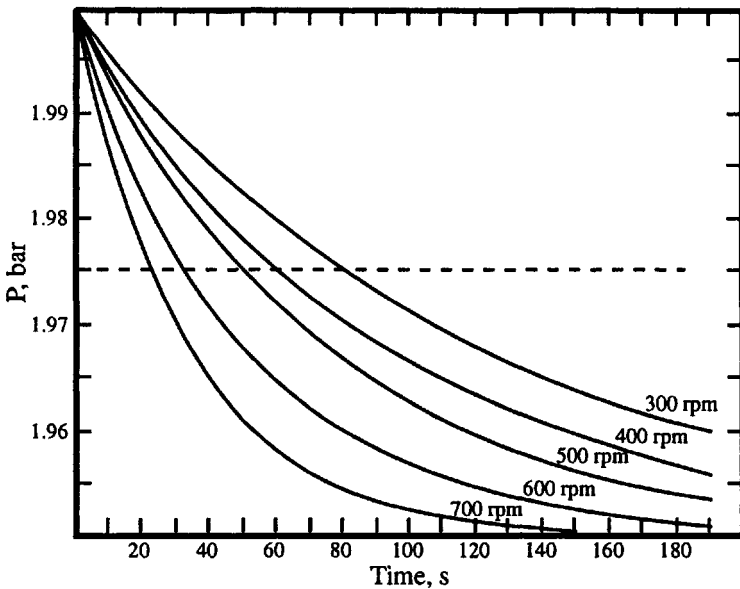


- (a) Develop two rate expressions in terms of total carbonate species and total peroxyxynitrite species for the above scheme, assuming that the reaction proceeds exclusively either by the k_2 path or by the k_2' path. Assume that the equilibria are rapidly maintained.
- (b) In the above development, the assumption that the CO_2 hydration is rapid is not really true. It has a half-time of ~ 25 s at pH 7. Explain how this would allow the actual nature of the reacting species to be determined.

CHAPTER 9

1. Garland and co-workers³⁴ have reported results for the mass transfer of H_2 into toluene with magnetic stirring. The reactor has a total volume of 25 mL and 11 mL of toluene were used in the experiments. The pressure decrease as a function of time was measured for several mixing rates. Simulated results of the observations are shown in the graph below.

- (a) From the graph, estimate the half-time, $t_{1/2}$, for each mixing rate. The dashed line shows the point at which the pressure has undergone half of its total change. Calculate $k_t A$ for each mixing rate.
- (b) From the graph, estimate the time it will take for 90% of the H_2 to be absorbed at a mixing rate of 500 rpm.



2. Although adsorption coefficients often are extracted from the kinetic models for heterogeneous systems, it is rather rare for the values to be

confirmed by independent measurements of adsorption isotherms. The determination of an adsorption coefficient illustrated here is based on the experiments of Fonseca and co-workers³⁵ for the adsorption of benzaldehyde, A, onto a Pd on carbon catalyst, S, although the data are not those from the paper. The experiment involved the addition of various masses of catalyst, m_s , to a constant amount of A, 2.40×10^{-5} mol, in 20.0 mL of THF. Then, spectrophotometry can be used to determine the concentration of A in solution after complete adsorption, $[A_{\text{sol}}]$ M. The amount of A adsorbed, A_{ad} mol, can be determined by difference. The following data might be obtained.

m_s (g)	0.100	0.150	0.200	0.300	0.400	0.600	0.900
$10^4 \times [A_{\text{sol}}]$ (M)	9.89	8.91	8.00	6.40	5.08	3.23	2.03
$10^5 \times A_{\text{ad}}$ (mol)	0.422	0.617	0.800	1.12	1.38	1.74	1.99

The equilibrium constant for the adsorption process can be defined as $K = (A_{\text{ad}})(S)^{-1}[A_{\text{sol}}]^{-1}$, where (S) mol g^{-1} is the number of free sites remaining at equilibrium after A has been adsorbed and (A_{ad}) is the mol of A adsorbed per g. One also can define the maximum number of sites for adsorption as $(S)_{\text{max}} = n_s$, where n_s , mol g^{-1} , is the total number of sites per unit mass. Then, the value of (S) is obtained by difference as $(S) = (S)_{\text{max}} - (A_{\text{ad}}) = n_s - (A_{\text{ad}})$, and the equilibrium constant is given by

$$K = \frac{(A_{\text{ad}})}{(n_s - (A_{\text{ad}}))[A_{\text{sol}}]}$$

- Rearrange this expression to show that a plot of (A_{ad}) versus $(A_{\text{ad}})/[A_{\text{sol}}]$ should be linear. (*Hint*: equate the reciprocal of both sides of the expression and rearrange terms.)
 - Make the plot indicated in (a) and determine K and n_s .
 - It should be noted that this model might not work in real life when a large fraction of the sites are occupied, because of interactions between the adsorbed species. Use the value of n_s from (b), and calculate the fraction of sites that are occupied for values of m_s of 0.100, 0.400 and 0.900 g.
3. There is evidence that adsorption of H_2 on Pd occurs by dissociation, so that the isotherm given by Eq. (9.14) should apply. This in turn suggests that catalytic hydrogenation by H_2 on Pd should have an $[\text{H}_2]^{1/2}$ dependence and might show saturation behavior when $K_{\text{H}}[\text{H}_2]^{1/2} > 1$. It is therefore surprising that the hydrogenation of various nitrobenzenes, summarized in Table 9.3 seem to show a first-order dependence on $[\text{H}_2]$. The noncompetitive Langmuir–Hinshelwood and both Eley–Rideal

mechanisms, Eqs. (9.10), (9.11) and (9.13), predict that, if initial rates, v_i are measured as a function of $[D]$ while $[E]$ is held constant, then

$$v_i = a[D]/(1 + b[D])$$

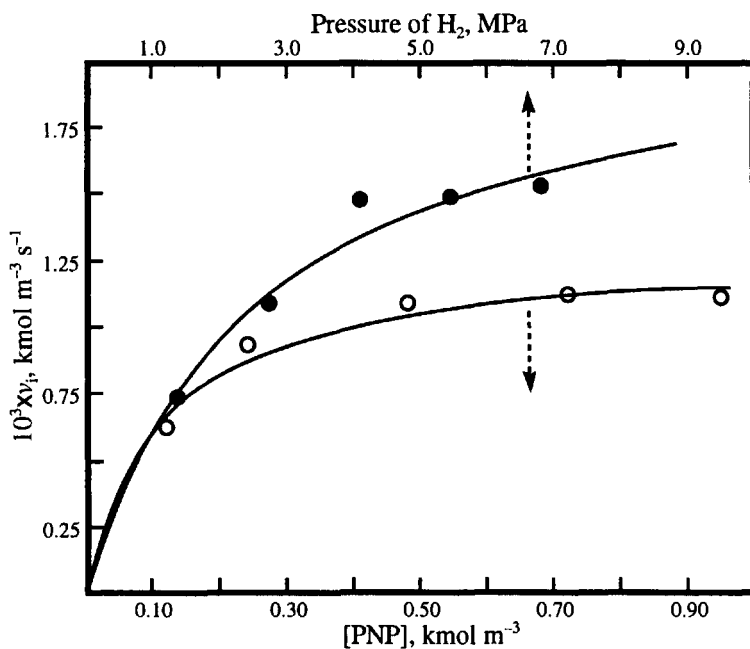
where a and b are constants. When D is H_2 , then $[D]$ may be given by P_{H_2} for physisorption or $(P_{H_2})^{1/2}$ for dissociative chemisorption.

- (a) The hydrogenation of 2,4-dinitrotoluene on 5% Pd/Al₂O₃ was found³⁶ to give the initial rates as a function of P_{H_2} tabulated below. On the basis of appropriate double-reciprocal plots, determine if the data can distinguish between the modes of attachment of H_2 to Pd.

P_{H_2} (MPa)	0.325	0.725	1.43	2.78
$10^3 v_i$ (kmol m ⁻³ s ⁻¹), 343 K	0.34	0.61	0.92	1.15
$10^3 v_i$ (kmol m ⁻³ s ⁻¹), 363 K	0.80	1.16	1.25	1.65

- (b) Based on the results at 363 K, could the two possibilities be better distinguished by a measurement of v_i at lower pressure, i.e. 0.1 MPa, or higher pressure, i.e. 4.0 MPa? Assume that the v_i values have an uncertainty of $\pm 10\%$.

5. The figure below shows the initial rate, v_i , for hydrogenation of *p*-nitrophenol, PNP, over 1% Pt on carbon in ethanol.³⁷



The initial rates are at 353 K as a function of [PNP] with P_{H_2} constant at 2.72 MPa, and as a function of P_{H_2} with [PNP] constant at 0.479 kmol m^{-3} . The amounts of catalyst and solvent were the same in all of the runs. Clearly, a saturation effect is observed in both cases.

- (a) Which of the four models described by Eqs. (9.10)–(9.13) is not consistent with the observations?
- (b) For the noncompetitive Langmuir–Hinshelwood mechanism, Eq. (9.10) can be rewritten for the condition that [D] is constant and [E] is varied, to obtain

$$v = \left(\frac{k_6(S_{D0})(S_{E0})K_D[D]}{1 + K_D[D]} \right) \left(\frac{K_E[E]}{1 + K_E[E]} \right) = v_{\max} \left(\frac{K_E[E]}{1 + K_E[E]} \right)$$

where v_{\max} is the rate when $K_E[E] \gg 1$ and will be a constant, as defined in the equation, for runs in which [D] and the amount of catalyst are held constant. An analogous equation is easily obtained for the condition that [E] is constant and [D] is varied. For the system under consideration, species E and D are PNP and H_2 , respectively, and [D] can be replaced by P_{H_2} . From these equations, a least-squares analysis of the data with [D] constant yields values of $K_E = 9.2 \text{ kmol}^{-1} \text{ m}^3$ and $v_{\max} = 1.3 \times 10^{-3} \text{ kmol m}^{-3} \text{ s}^{-1}$, while with [E] constant, the analysis yields values of $K_D = 0.395 \text{ MPa}^{-1}$ and $v_{\max} = 2.2 \times 10^{-3} \text{ kmol m}^{-3} \text{ s}^{-1}$. Calculate the ratio of the values of v_{\max} under the two conditions. Compare the calculated and observed ratios to determine if the model is internally consistent.

- (c) An analogous grouping of constant and variable terms can be done for the competitive Eley–Rideal mechanism, Eq. (9.13), to obtain for constant [E]

$$v = \frac{k_5(S_0)[E]}{1 + K_E[E]} \left(\frac{K_D[D]}{1 + \frac{K_D}{1 + K_E[E]}[D]} \right) = v_{\max} \left(\frac{K_D[D]}{1 + \frac{K_D}{1 + K_E[E]}[D]} \right)$$

This equation and its analogue for constant [D] have the same mathematical form as those in (b), but the meaning of the parameters is different. Use the numerical values of $K_D(1 + K_E[E])^{-1}$ and $K_E(1 + K_D[D])^{-1}$ to produce two equations that can be solved for K_D and K_E . Is this model consistent with the observations?

6. In two studies, the hydrogenation of cyclohexene was studied with the catalysts 2.3% Pt on SiO_2 ³⁸ and 4.88% Pd on Al_2O_3 .³⁹ Otherwise, the solvent, cyclohexane and temperature, 308 K, were the same. Both studies found that the rate was directly proportional to the mass of

catalyst and was independent of the concentration of cyclohexene. The rates were reported as turnover frequencies, TOF, defined as moles of cyclohexene consumed per moles of surface Pt or Pd atoms per second.

- (a) For the Pt/SiO₂ system, the variation of TOF with P_{H₂} gave the following data:

P _{H₂} , kPa	20	40	60	80	110
TOF, s ⁻¹	1.8	3.7	5.5	7.5	9.6

Determine the order of the rate with respect to P_{H₂}.

- (b) Choose a Langmuir–Hinshelwood or Eley–Rideal mechanism that is consistent with the observed dependencies on P_{H₂} and cyclohexene concentration.
- (c) For the Pd/Al₂O₃ system, the following data was obtained:

P _{H₂} , kPa	27.4	38.3	54.0	80.9
TOF, s ⁻¹	3.8	4.6	5.6	6.9

The authors concluded that the dependence of the TOF on P_{H₂} was different from that found for the Pt/SiO₂ system. From an analysis of the data, give any reasons that lead you to agree or disagree with this conclusion.

- (d) Propose a kinetic model that is consistent with the rate law for the Pd/Al₂O₃ system.

References

- Romeo, R.; Minniti, D.; Trozzi, M. *Inorg. Chem.* **1976**, *15*, 1134.
- van Eldik, R.; Palmer, D. A.; Kelm, H. *Inorg. Chem.* **1979**, *18*, 572.
- Zhang, Z.; Jordan, R. B. *Inorg. Chem.* **1994**, *33*, 680.
- Koefod, R. S.; Mann, K. R. *J. Am. Chem. Soc.* **1990**, *112*, 7287.
- O'Brien, P.; Sweigart, D. A. *Inorg. Chem.* **1982**, *21*, 2094.
- Romeo, R.; Arena, G.; Scolaro, L. M.; Plutino, M. R. *Inorg. Chem.* **1994**, *33*, 4029.
- Reddy, K. B.; van Eldik, R. *Inorg. Chem.* **1991**, *30*, 596.
- Jordan, R. B. *Inorg. Chem.* **1996**, *35*, 3725.
- Toma, H. E.; Malin, J. M.; Giesbrecht, E. *Inorg. Chem.* **1973**, *12*, 2084.
- Toma, H. E.; Malin, J. M. *Inorg. Chem.* **1973**, *12*, 1039.
- Matsubara, T.; Creutz, C. *Inorg. Chem.* **1979**, *18*, 1956.
- Baja, H. C.; van Eldik, R. *Inorg. Chem.* **1988**, *27*, 4052.
- Chatterjee, D. *Coord. Chem. Rev.* **1998**, *168*, 273.

14. Povse, V. G.; Olabe, J. A, *Transition Met. Chem.* **1998**, *23*, 657; Shoukry, M. M.; Shehata, M. R.; Hamza, M. S. A.; van Eldik, R. *Dalton Trans.* **2005**, 3921.
15. Hoshino, Y.; Takahashi, R.; Shimizu, K.; Sato, G. P.; Aoki, K. *Inorg. Chem.* **1990**, *29*, 4816.
16. Peng, X.; Jonas, J. *J. Chem. Phys.* **1990**, *93*, 2192.
17. Schneider, K. J.; van Eldik, R. *Organometallics* **1990**, *9*, 92; *Ibid.* 1235.
18. Rahman, M. M.; Liu, H.-Y.; Prock, A.; Giering, W. P. *Organometallics* **1987**, *6*, 650; Lorsbach, B. A.; Bennett, D. M.; Prock, A.; Giering, W. P. *Organometallics* **1995**, *14*, 869.
19. Poli, R.; Owens, B. E.; Linck, R. G. *Inorg. Chem.* **1992**, *31*, 662.
20. Algra, G. P.; Balt, S. *Inorg. Chem.* **1981**, *20*, 1102.
21. Schultz, R. H.; Bengali, A. A.; Tauber, M. J.; Weiller, B. H.; Wasserman, E. P.; Kyle, K. R.; Moore, C. B.; Bergman, R. G. *J. Am. Chem. Soc.* **1994**, *116*, 7369.
22. Beringhelli, T.; D'Alfonso, G.; Minoja, A. P.; Freni, M. *Inorg. Chem.* **1991**, *30*, 2757.
23. Shekhar, S.; Ryberg, P.; Hartwig, J. F. *Org. Lett.* **2006**, *8*, 851.
24. Shekhar, S.; Ryberg, P.; Hartwig, J. F.; Mathew, J. S.; Blackmond, D. G.; Strieter, E. R.; Buchwald, S. L. *J. Am. Chem. Soc.* **2006**, *128*, 3584.
25. Sanford, M. S.; Love, J. A.; Grubbs, R. H. *J. Am. Chem. Soc.* **2001**, *123*, 6543.
26. Bernhard, P.; Sargeson, A. M. *Inorg. Chem.* **1988**, *27*, 2754; *Ibid. J. Am. Chem. Soc.* **1989**, *111*, 597.
27. Yau, S. K. W.; Che, C.-M.; Lau, T.-C. *J. Chem. Soc., Dalton Trans.* **2002**, 2697
28. Zahir, K. O. *Can. J. Chem.* **2001**, *79*, 1124.
29. Hartshorn, R. M.; Telfer, S. G. *J. Chem. Soc., Dalton Trans.* **1999**, 3565; *Ibid.*, **2000**, 2801.
30. Cosa, G.; Llauger, L.; Sciano, J. C.; Miranda, M. A. *Org. Lett.* **2002**, *18*, 3083; Llauger, L.; Miranda, M. A.; Cosa, G.; Sciano, J. C. *J. Org. Chem.* **2004**, *69*, 7066; Lukeman, M.; Sciano, J. C. *J. Am. Chem. Soc.* **2005**, *127*, 7698.
31. Sarakha, M.; Ferraudi, G. *Inorg. Chem.* **1996**, *35*, 313.
32. Finke, R. G.; Schiraldi, D. A.; Mayer, B. J. *Coord. Chem. Rev.* **1984**, *54*, 1.
33. Lymar, S. V.; Hurst, J. K. *J. Am. Chem. Soc.* **1995**, *117*, 8867.
34. Gao, F.; Ng, P.; Li, C.; Krummel, K. I.; Allian, A. D.; Garland, M. *J. Catal.* **2006**, *237*, 49.
35. Brigas, A. F.; Fonseca, C. S. C.; Johnstone, R. A. W. *J. Mol. Catal. A* **2006**, *246*, 100.
36. Rajashekharan, M. V.; Nikalje, D. D.; Jaganathan, R.; Chaudhari, R. V. *Ind. Eng. Chem. Res.* **1997**, *36*, 592.
37. Vaidya, M. J.; Kulkarni, S. M.; Chaudhari, R. V. *Org. Process Res. Dev.* **2003**, *7*, 202.
38. Madon, R. J.; O'Connell, J. P.; Boudart, M. *AIChE J.* **1978**, *24*, 904.
39. Gonzo, E. E.; Boudart, M. *J. Catal.* **1978**, *52*, 462.

Chemical Abbreviations

acac	acetylacetonate, 2,4-pentanedionate
Ar	aryl
azacapten	1-methyl-3,13,16-trithia-6,8,10,19-tetraazabicyclo[6.6.6]eicosane
bpy	2,2'-bipyridyl
Bu	butyl
COD	1,5-cyclooctadiene
Cp	cyclopentadienide
Cp*	pentamethylcyclopentadienide
Cy	cyclohexyl
cyclam	1,4,8,11-tetraazacyclotetradecane
dien	diethylenetriamine
DMA	<i>N,N</i> -dimethylacetamide
DMF	<i>N,N</i> -dimethylformamide
DMSO	dimethylsulfoxide
EDTA	ethylenediaminetetraacetate
en	ethylenediamine; 1,2-diaminoethane
Et	ethyl
Et ₄ dien	tetraethyldiethylenetriamine
gly	glycine
hfac	hexafluoroacetylacetonate
HOAc	acetic acid
Im	imidazole
isn	isonicotinamide
Me	methyl
nic	nicotinamide
NTA	nitrilotriacetic acid
OAc	acetate ion
<i>o</i> -Tol	<i>ortho</i> -tolyl
ox	oxalate
Ph	phenyl
phen	1,10-phenanthroline
Pr	propyl

Prop carb	propylene carbonate; 1,2-propanediol cyclic carbonate
py	pyridine
sar	sarcophagine; 3,6,10,13,16,19-hexaazabicyclo[6.6.6]eicosane
sep	sepulchrate; 1,3,6,8,10,13,16,19-octaazabicyclo[6.6.6]eicosane
sen	4,4',4''-ethylidynetris(3-azabutan-1-amine)
tacn	1,4,7-triazacyclononane
THF	tetrahydrofuran
tn	trimethylenediamine; 1,3-diaminopropane
TPP	tetraphenylporphine; 5,10,15,20-tetraphenyl-21H,23H-porphine
tren	triethylenetetramine
Trf	triflate ion; trifluoromethane sulfonate
ttacn	1,4,7-trithiacyclononane
[9]aneS ₃	1,4,7-trithiacyclononane

This page intentionally left blank

Index

- Absorption, gas into liquid
rate, 391
rate constant, 392
rate law, 392
- Acetonitrile complexes, reaction with nucleophiles, 81
- Actinometer, 292
- Activated complex, 18, 20
- Activation
Associative, 44
Dissociative, 44
- Activation energy
crystal field theory, 86, 87(T)
- Activation enthalpy (see enthalpy of activation), 19
- Activation entropy (see entropy of activation), 19
- Activation parameters, Marcus theory, for cross reactions, 272
- Activation volume (see volume of activation), 21
- Active sites, solid catalysts, 400
- Adamson's rules for Cr(III) amine photoaquation, 307
- Adenosylcobalamin, AdoB₁₂, AdoCbl, 341
functions, 344
heterolysis, 347
homolysis, 347
substitution kinetics, 344
- Adiabatic process, transmission coefficient, 256
- Adiabaticity, Ehrenfest, 256
- Adsorption on solid
dissociative isotherm for H₂, 405
Langmuir isotherm, 402
competitive, 403
limitations, 403
noncompetitive, 403
- Agostic interaction
alkene insertion, 191
 β -hydride elimination, 191
methyl migration, 171
olefin metathesis, 234
W(CO)₃(PCy₃)₂ stabilization, 160, 182
- Al(III) complexes, trigonal twist, 128
- Al(DMSO)₆³⁺, chelate formation with
2,2'-bipyridine, 104
2,2',6',2''-terpyridine, 104
- Aliphatic halides, oxidative addition, 182
side-on pathway, theory, 184
solvent effects on, 184
stereochemistry of, 183
to Ir(CO)(PR₃)₂Cl, kinetic parameters, 183(T)
to Ir(CO)₂(I₂)⁻, pathways, 184
to Pt(PPh₃)₂, by halogen abstraction, 184
to Zr(η^5 -Cp)₂(PMePh₂), radical pathway, 184
- Alkene (also see olefin)
addition to
Co(η^5 -Cp)(NO)₂, 192
rate constants, 193(T)
Fe(P₂(CH₂)₂(R)₄)₂(H)₂, 191
Ir(η^2 -HBPF₃)(CO)(C₂H₄), σ and π complex, 191
epoxidation by cytochrome P-450, 372
concerted mechanism, 372
exchange on Co(η^5 -Cp)(NO)₂, 193
rate law, 194
fluxionality, π -bonded, 137
in Rh(η^5 -Cp)(C₂F₄)(C₂H₄), 23
hydrogenation, catalytic, 195
hydride route, 196
olefin route, 196
symmetry restrictions, 195
lifetime, NMR, η^2 -complex, 437
migratory insertion, 191
in Co(PMe₃)₃(H)(C₂H₄), 191
theory, 191
 π -complex formation, 189
 σ -complex formation, 189
substitution reactions, 188
- Alkoxide-metal bonds, CO₂ insertion, 175
- Alkyne, reaction with
Ir(OC(Me)CHCPh)(PPh₃)₂(OCMe₂)⁺, 192
metal hydride, 191
- Allyl complexes
bonding, 139
endo-exo isomers, η^3 -complex, 140

- flip mechanisms, 140
fluxionality, 139
 mechanisms in η^3 -allyls, 140
 olefin rotation mechanisms, 140
 π - σ - π mechanisms, 140
- Allyl rotation in
 Fe(Cp)(CO)(η^3 -C₃H₅), 141
 Mo(Cp)(CO)₂(η^3 -C₃H₄R), 141
 Ru(Cp)(CO)(η^3 -C₃H₅), 141
- Amino acid amide chelates of Co(III), ring closing, 80
- Amino acid ester chelates of Co(III), ring closing, 79
- Angular overlap model for solvent exchange, 88
- Anionic mechanism for rearrangements by coenzyme B₁₂, 352
- Antarafacial sigmatropic shift, 133
- Anti-lock-and-key mechanism, 202
- Antithermal pathway
 photoaquation of Co^{III}(NH₃)₅X, 301
 photolysis of Cr(III) complexes, 304
- Apoenzyme, 337
- Aquocobalamin, B_{12a}, 341
- Aromatic halides, oxidative addition, 184
 and coupling, 187
 anion effects, 186
 catalytic pathways, 185
 to Pd(P)₂, theory, 186
 trans product, 186
- Arrhenius activation energy, 17
- Arrhenius equation, 17
- Arrhenius pre-exponential factor, 17
- As(III) ligands
 cone angles, 71(T)
 electronic parameters, 71(T)
 steric repulsion parameters, 71(T)
- Ascorbic acid species, self-exchange rate constants, 269
- Associative activation, 44
- Associative interchange mechanism, I_a, 44
- Associative mechanism, A, 44
 for 17-electron systems, 168
 for 19-electron intermediate, 151
 intermediate in Pt(II) bis hydrazones, 56
 operational test for, 54
 rate constant, 54
 rate law, 54
 examples, 55
 for Pd(dien)(py)²⁺ + Cl⁻, 56
 for Rh(cyclooctadiene)(SbPh₃)Cl + amines, 55
 for Ru(NH₃)₅(OH)₂²⁺ + methylpyrazinium ion, 56
- Asymmetric hydrogenation, 201
 of C=C bonds, 202
 by chiral monodentate ligands, 204
 by diphosphine Ru(II) catalysts, 205
 by Rh(chiraphos)⁺, 202
 by Rh(dipamp)⁺, 202
 olefin route, 203
 by Rh(DuPHOS)⁺, theory, 202
 by Ru(BINAP)²⁺ speciation with methyl (Z)- α -(acetamido)-cinnamate, 207
 by Ru(BINAP)(O₂CCH₃)₂
 mechanism, 210
 rate law, 209
 with neutral substrates, 207
 by Ru(R-BINAP)(O₂CCH₃)₂, 205
 mechanism, 206
 stoichiometric, hydride formation, 204
- of C=O bonds, 211
 by H₂ addition, 211
 by transfer hydrogenation, 211
 mechanisms, 212
 with Ru(II)(η^6 -arene)((S,S)-TsDPEN), 214
 with Ru(BINAP)(DPEN), 215
 with Ru(tolBINAP)(DPEN), bifunctional catalytic pathway, 216
- Atom transfer, oxidative addition, 179
- Back intersystem crossing in Cr^{III}(L)₆, 305
- Bailar twist (see trigonal twist), 120
- Bandshape analysis for NMR kinetics, 442
- Basicity scales, need for 2 parameters, 63
- Berry pseudorotation mechanism, 129
- Beta-hydride elimination, 191
 agostic interactions, 191
- Bifunctional catalyst, 80
- Bifunctional metal-ligand catalyst
 intermediate, transfer hydrogenation, 215
 pathway for hydrogenation of C=O bonds by Ru(tolBINAP)(DPEN), 216
- BINAP(-S), structure, 205
- Bioinorganic systems, 337
- Bond energy, Co—C in
 Co(DMGH)₂(py)(CH(CH₃)(C₆H₅)), 349
 coenzyme B₁₂, 349
 methylcobalamin, 350
- Bridged electron transfer, 255
 outer-sphere mechanism, 277
 remote attack, 277
 for Co(NH₃)₅(p-formylbenzoate)²⁺ + Cr(II), 278

- Bridge-terminal CO exchange, 141
 in Co_2CO_8 , 141
 in $\text{Cr}_2(\eta^5\text{-Cp})_2(\text{NO})_4$, 143
 in $\text{Fe}_2(\eta^5\text{-Cp})_2(\text{CO})_4$, 141
 pathways, 142
 in $\text{Fe}_2(\eta^5\text{-Cp})_2(\text{P(OPh)}_3)(\text{CO})_3$, 143
 in $\text{Mn}_2(\eta^5\text{-Cp})_2(\text{NO})_2(\text{CO})_2$, 143
 in $\text{Pt}_2(\eta^5\text{-Cp})_2(\text{CO})_2$, 143
 in $\text{Ru}_2(\eta^5\text{-Cp})_2(\text{CO})_4$, 141
- Bridging ligand, 254
 adjacent atom attack, 277
 effect
 in $\text{Co}(\text{NH}_3)_5(\text{OCOH})^{2+}$, 275
 in $\text{Co}(\text{NH}_3)_5(\text{thiocarbamate})^{2+}$, linkage isomers, 276
 on electron transfer, 274
 on intervalence electron transfer, 284
 remote attack, 277
 by Cr(II), 278
 properties
 in $\text{Co}^{\text{III}}(\text{NH}_3)_5\text{X}$, 275
 π conjugation, 276
- Briggs-Haldane equation, 339
- Carbene formation in cytochrome P-450 models, 372
- Carbon acids, deprotonation, 27
- Carbon dioxide
 hydrogenation, 229
 by $\text{Ru}(\text{hfacac})(\text{Ph}_2\text{P}(\text{CH}_2)_3\text{PPh}_2)_2$, 229
 insertion, 174
 in $\text{W}(\text{CO})_5(\text{CHDCHDPh})^-$, 175
 mechanism, 175
 stereochemistry, 175
 in $\text{W}(\text{CO})_5(\text{CH}_3)^-$, kinetics, 175
 into metal-alkoxide bonds, 175
 reaction with peroxyxynitrite, 379
- Carbonato complexes
 aquation and formation, 77
 of Co(III)
 chelate ring opening, 77
 and aquation, 78
- Carbon-hydrogen bond activation, 217
 by $\text{Co}(\text{Cp})(\text{CO})$, theory, 221
 by $\text{Fe}((\text{R}_2\text{PCH}_2)_2)_2$ and $\text{Ru}((\text{R}_2\text{PCH}_2)_2)_2$, 221
 by Ir(III) and Rh(III) species, 224
 by $\text{Ir}(\text{Cp})(\text{CO})_2$, 220
 flash photolysis, 328
 by $\text{Ir}(\text{Cp}^*)\text{L}$, 217
 by Pt(II) species, 224
 theory, 225
 by $\text{Rh}(\text{Cp})(\text{CO})_2$, 220
 flash photolysis, 328
 by $\text{Rh}(\text{Cp})(\text{CO})_2(\mu\text{-CO})$, 221
 by $\text{Rh}(\text{Cp}^*)(\text{CO})_2$, 220
 of cyclohexane in inert gas solvents, 220
 by $\text{Rh}(\text{HBPz}^*)_3(\text{CO})_2$, 218
 by $\text{Rh}(\text{HPz}^*)_3(\text{CO})(\text{C}_2\text{H}_4)$, 218
 by $\text{Rh}(\text{PR}_3)_2(\text{CO})\text{Cl}$, 219
 by $\text{Rh}(\text{Tp}^*)(\text{CO})_2$, flash photolysis, 451
 energetics, 219
 theory, 221
- Carbonic anhydrase
 catalytic cycle, 359
 Co(II) derivative, NO_3^- binding, 360
 experimental methods, 357
 inhibitors, 360
 intermediate
 Lindskog model, 359
 Lipscomb model, 359
 isozymes, 357
 mechanism of action, 357
 model, $\text{Zn}[12]\text{aneN}_3$, 359
 model, $\text{Zn}[12]\text{aneN}_4$, kinetics, 360
 phenol complex, structure, 360
 pK_a assignments, 358
 rate, pH profile of CO_2 hydration, 358
 structure, 357
 with bound HCO_3^- , 360
 theory, 360
 Zn(II) enzyme, 356
- Carbonyl exchange, bridge-terminal, 141
- Catalysis, homogeneous, by organometallic compounds, 225
- Catalyst, 40
 BF_3 for CO insertion, 170
 bifunctional, 80
 for transfer hydrogenation, 215
 for epoxide polymerization, 177
 phosphine oxide for amine replacement
 in $\text{Mo}(\text{CO})_5(\text{NHR}_2)$, 159
 solid, active sites, 400
 transfer hydrogenation, mono- and dihydride routes, 214
- Catalytic
 hydrogenation of alkenes, 195
 pathways for oxidative addition of aromatic halides, 185
 reactions, coenzyme B_{12} , 345
- Cativa process for methanol carbonylation, 230
- Charge effect, interchange mechanisms, 65
- Charge symmetry in electron-transfer reactions, 259
- Chauvin mechanism for olefin metathesis, 236

- Chelate effect
 chelate ring size, 105
 in $\text{Ni}(\text{OH}_2)_6^{2+}$ + ethylenediamine, 104
 in $\text{Ni}(\text{OH}_2)_6^{2+}$ + glycine, 105
 kinetics, 104
- Chelate formation
 first bond formation step, 100
 in $\text{Al}(\text{DMSO})_6^{3+}$ + bipyridine and terpyridine, 104
 in $\text{M}(\text{OH}_2)_6$ + glycine, 100
 in $\text{Ni}(\text{OH}_2)_6^{2+}$ + ethylenediamine, 103
 K_f and rate constants, 106
 kinetics, 100
 limiting forms of the rate constant, 102
 rate constants, estimated, 102
 rate-controlling step, 100
 ring-closing step, 100
- Chelate ring closing in
 complexes of $\text{Co}(\text{III})$
 amino acid amide, 80
 amino acid ester, 79
 glycine, pathways, 81
 $\text{Cr}(\text{CO})_5(\text{N}-\text{N})$, 161
 $\text{Cr}(\text{CO})_5(\text{R}_2\text{P}-\text{PR}_2)$, 161
 $\text{Mo}(\text{CO})_5(\text{phen})$, volume of activation, 161
 $\text{Mo}(\text{CO})_5(\text{R}_2\text{P}-\text{PR}_2)$, 161
cis- $\text{Pt}(\text{Ph})_2(\text{CO})(\text{X}-\text{X})$, 161
 $\text{Ru}(\text{CO})_4(\text{R}_2\text{P}-\text{PR}_2)$, 161
- Chelate ring opening
 in complexes of $\text{Co}(\text{III})$
 carbonato, 77
 oxalato, base hydrolysis, 79
 in $\text{Cr}(\text{CO})_4(\text{S}-\text{S})$, 161
 in organometallic systems, 160
 in $\text{W}(\text{CO})_4(\text{bpy})$, 160
 rate constants of
 $\text{Ni}(\text{OH}_2)_4(\text{amino-pyridines})^{2+}$, 105
 $\text{Ni}(\text{OH}_2)_6^{2+}$ + glycine, 105
- Chemical mechanism for electron transfer, 278
- Chemical shifts, ^{13}C NMR of $\text{Ni}(\text{CO})_3\text{L}$, 71(T), 154
- Chemisorption, of gas on solid, 401
- Chiral centers
 isomerism or racemization, 126
 NMR, 126
- Cis effect, 76
 in $\text{W}(\text{CO})_5\text{L}$, 158
 ligand order, 76
 on CO exchange of $\text{Mn}(\text{CO})_5\text{X}$, 153
 on CO substitution, 158
 theory for $\text{Mn}(\text{CO})_5(\text{L}^-)$ and $\text{Cr}(\text{CO})_5\text{L}$, 77
- $\text{Co}(\text{II})$ compounds
 $\text{Co}(\text{II})$ carbonic anhydrase, NO_3^- binding, 360
 Cob(II)alamin, B_{12} , 341
 $\text{Co}(\text{NH}_2\text{R})_n^{2+}$, coordination change, NMR studies, 116
 $\text{Co}(\text{OH}_2)_6^{2+}$, substitution reactions, 96
 $\text{Co}(\text{py})_n(\text{X})_2$, coordination change, 116
- $\text{Co}(\text{II/III})$ systems
 $\text{Co}(\text{NH}_3)_6^{2/3+}$, self-exchange rates, DFT theory, 264
 $\text{Co}(\text{phen})_3^{2/3+}$, anion effects on self-exchange rates, 266
- $\text{Co}(\text{III})$ compounds
 acetonitrile complex, reaction with nucleophiles, 81
- amines
 competition studies on acid hydrolysis, 53
 Dissociative conjugate base intermediate, 53
 mechanism, 51, 73
- amino acid
 amide complex, chelate ring closing, 80
 ester complex, peptide formation, 81
 chelate ring closing, 79
- aquation, linear free energy relationship, 64
- carbonato complexes
 aquation and formation, 77
 chelate ring opening, 77
 and aquation, 78
- $\text{Co}(\text{bpy})_2(\text{glycinate})^{2+}$
 derivative, radical clock results, 300
 photochemistry, 300
- $\text{Co}(\text{C}_2(\text{DO})(\text{DOH}))_{\text{pn}}$, coenzyme B_{12}
 model, diol dehydrase
 mechanism, 353
- $\text{Co}(\text{CN})_5(\text{OH}_2)^{2-}$, substitution, D
 mechanism rate constant, 50
- $\text{Co}(\text{CN})_5\text{X}^{2-} + \text{SCN}^-$
 linkage isomers, photochemical and thermal yields, 298(T)
 photochemistry, 297
- $\text{Co}(\text{CN})_6^{3-}$, photoaquation, 297
 in water-glycerol, 297
- $\text{Co}(\text{DMG})_2(\text{L})\text{X}$, D mechanism, 50
- $\text{Co}(\text{DMGH})_2(\text{py})(\text{CH}(\text{CH}_3)(\text{C}_6\text{H}_5))$,
 Co—C bond energy, 349
- $\text{Co}(\text{en})_2(\text{A})\text{X}$, isomerism, ligand field theory, 125
- $\text{Co}(\text{en})_2(\text{L})\text{X}$, base hydrolysis
 competition studies, 52

- cis*-Co(en)₂(NH₃)X, base hydrolysis competition studies, 52(T)
- Co(en)₂(SO₃)(OH₂)⁺, substitution, D mechanism, 50
- Co(en)₂(Y)X, base hydrolysis competition studies, 52
- Co(en)₃³⁺
isomerism, ligand field theory, 125
pulse radiolysis, 449
- Co(gly)₂(CO₃)⁻, hydrolysis, 427
- Co(L)₄(aminocarboxylates),
photochemistry, 299
- Co(L)₄(CO₃), hydrolysis, 78, 426
- Co(L)₃Y, photochemistry, 297
- Co(L)₆, ligand field states, 296
photochemistry, 296
- Co(NH₃)₄(NH₂CH₃) (DMF)³⁺, aquation,
steric versus electronic effects, 68
- Co(NH₃)₄(CO₃)⁺
hydrolysis, 78, 427
photochemistry, 299
- Co(NH₂CH₃)₃X, photoredox reactions,
299
- Co(NH₂R)₃X
photochemistry, flash photolysis, 299
photoredox reactions, 298
- Co(NH₃)₅Cl²⁺ + Cr(OH₂)₆²⁺, inner-sphere
electron transfer, 255
- Co(NH₃)₅Cl²⁺ and Co(NH₂CH₃)₃Cl²⁺
aquation, kinetic parameters, 67(T)
steric effects, 67
structural parameters, 67
- Co(NH₃)₅(*p*-formylbenzoate)²⁺ + Cr(II),
bridged remote attack, 278
- Co(NH₃)₅(glycinate)²⁺ + Cr(II), bridged
outer-sphere mechanism, 277
- Co(NH₃)₅(mbpy)⁴⁺ + •CO₂⁻, electron
transfer, chemical mechanism,
279
- Co(NH₃)₅(NC)²⁺, linkage isomerism, 118
- Co(NH₃)₅(N₃)²⁺ + NO⁺, competition
studies, 53
- Co(NH₃)₅(OCOH)²⁺, bridging ligand
effect, 275
- Co(NH₃)₅(O₂CC₆H₄NO)²⁺ + •R, electron
transfer, chemical mechanism,
279
- Co(NH₃)₅(O₂CXC₆H₄•NO)⁺,
intramolecular electron transfer,
rate constants, 280(T)
- Co(NH₃)₅(ONO)²⁺
linkage isomerism, 118
pressure dependence, 22
temperature dependence, 19
- Co(NH₃)₅(OP(OCH₃)₃)³⁺, aquation,
competition studies, 53
- Co(NH₃)₅(SCN)²⁺, linkage isomerism,
117
- Co(NH₃)₅(thiocarbamate)²⁺, linkage
isomers as bridging ligands, 276
- Co(NH₃)₅X
and Cr(OH₂)₆²⁺, kinetic parameters,
275(T)
aquation, constant thermodynamic
parameters, 54
base hydrolysis, constant
thermodynamic parameters, 54
bridging ligand properties, 275
photoaquation quantum yields, 301(T)
antithermal pathway, 301
photoredox reactions, 299
- Co(NH₃)₆³⁺
photoaquation, 296
pulse radiolysis, 449
- Co(NTA)(CO₃)₂⁻, hydrolysis, 78, 426
- Co(tren)(NH₃)(OH₂)•Cl²⁺, ion pair
structure, 66
- Co(tren)(CO₃)⁺, hydrolysis, 78, 426
- electron transfer in
Co(III)–Fe(II) systems, 280, 284
Co(III)–Ru(II) systems, 280, 284
- glycine, ring-closing pathways, 81
- induced aquation, 53
- nitrito complex, formation, 79
- oxalato complex, base hydrolysis,
chelate ring opening, 79
- phosphate ester complex, hydrolysis, 82
- photochemistry, 295
- sulfite complexes, formation, 79
- trigonal twist, 128
- Co compounds, organometallic
- Co(CO)₃(NO), substitution reactions,
158
- Co(CO)₄H, hydroformylation
mechanism, 226
- Co(CO)₄(SnCl₃), substitution, radical
mechanism, 166
- Co(η⁵-Cp)(CO) and C–H bond
activation, theory, 221
- Co(η⁵-Cp)(CO)₂, slippage mechanism,
155
- Co(η⁵-Cp)(NO)₂
alkene addition, 192
rate constants, 193(T)
alkene exchange, 193
rate law, 194
- Co(PMe₃)₃(H)(C₂H₄), alkene migratory
insertion, 191

- $\text{Co}_2(\text{CO})_8$
 bridge-terminal CO exchange, 141
 hydroformylation catalysis, 226
 $\text{Co}_4(\text{CO})_8(\text{L})_p$ cluster, substitution, 166
 CO exchange in
 $\text{M}(\text{CO})_5$ systems, 151
 $\text{M}(\text{CO})_6$ systems, 152
 metal carbonyls, 150
 $\text{Mn}(\text{CO})_5\text{X}$
 cis effect, 153
 microscopic reversibility, 41
 $\text{Ni}(\text{CO})_4$, 151
 $\text{V}(\eta^5\text{-C}_5\text{R}_n)_2(\text{CO})$, 156
 CO insertion, 168
 BF_3 catalysis, 170
 in $\text{Fe}(\text{CO})_2(\text{PMe}_3)(\text{CH}_3)\text{I}$, 169
 in $\text{Fe}(\text{CO})_2(\text{PPh}_2\text{Me})(\text{CH}_3)\text{I}$, η^2 -acyl
 intermediate, 169
 in $\text{Fe}(\text{CO})_4\text{R}^-$, ion pairing, 173
 in $\text{Fe}(\eta^5\text{-Cp})(\text{CO})(\text{COCH}_3)$, photolysis,
 173
 in $\text{Fe}(\eta^5\text{-Cp})(\text{CO})(\text{PR}_3)(\text{CH}_3)$, 169
 in $\text{Fe}(\eta^5\text{-Cp})(\text{CO})_2(\text{CH}_3) + \text{PR}_3$, 173
 in $\text{Fe}(\eta^5\text{-C}_9\text{H}_7)(\text{CO})_2(\text{CH}_3) + \text{PR}_3$, 173
 in $\text{Mn}(\text{CO})_5(\text{CH}_3)$, 168
 kinetics, 171
 rate law, 171
 in $\text{Mo}(\text{Cp})(\text{CO})_3(\text{CH}_3)$, solvent effects,
 171, 172(T)
 methyl migration mechanism, 169
 phenyl migration in Pt(II) complex, 170
 CO substitution, cis effect, 158
 Cob(II)alamin, B_{12r} , 341
 Cobalamin
 adenosyl, AdoB_{12} , AdoCbl , 341
 substitution kinetics, 344
 aquo, B_{12a} , 341
 cyano, CNCbl , 341
 derivatives, substitution kinetics, 344
 methyl, H_3CCbl , 341
 structures, 343
 super-reduced, B_{12s} , 342
 Cobinamides, Cbi^+ , 342
 Co—C bond energy in
 $\text{Co}(\text{DMGH})_2(\text{py})(\text{CH}(\text{CH}_3)(\text{C}_6\text{H}_5))$, 349
 coenzyme B_{12} , 349, 350
 methylcobalamin, 350
 Coenzyme, 337
 Coenzyme B_{12} (also see
 adenosylcobalamin), 341
 anionic mechanism for organic
 rearrangements, 352
 base-off form, 343
 base-off/hist-on form, 343
 base-on form, 343
 catalyzed reactions, 345
 classes by function, 346
 Co—C bond
 energy, 349, 350
 heterolysis, 347
 homolysis, 347
 axial ligand effect, 350
 coenzyme B_{12} , rate, 349
 enzyme effect, 350
 evidence, 348
 kinetic parameters, 349, 350
 radical clock results, 353
 $\text{Co}(\text{C}_2(\text{DO})(\text{DOH}))_{pn}$, model, diol
 dehydrase mechanism, 353
 cofactor, pyridoxal phosphate, 345, 346
 corrin ring, 342
 diol dehydrase, bound radical
 mechanism, 354
 1,1-diol radical intermediate, 354
 flash photolysis, 355, 452
 functions, 344
 glutamate mutase, radical fragmentation
 mechanism, 354
 methylmalonyl-CoA, radical
 mechanism, 354
 model systems, 343
 Co—C bond energy, 349
 homolysis kinetics, 349
 organic rearrangements with surfactant,
 352
 radical mechanism for organic
 rearrangements, 351
 structure, 342
 thermal decomposition
 pathways, 350
 temperature dependence, 350
 Cofactor, 337
 Collision frequency, 259
 Competition ratios for **D** intermediates,
 51(T)
 Competition studies for
 acid hydrolysis of Co(III) amines, 53
 aquation of $\text{Co}(\text{NH}_3)_5(\text{OP}(\text{OCH}_2)_3)^{3+}$, 53
 $\text{Co}(\text{en})_2(\text{L})\text{X}$, base hydrolysis, 52
cis- $\text{Co}(\text{en})_2(\text{NH}_3)\text{X}$, base hydrolysis,
 52(T)
 $\text{Co}(\text{NH}_3)_5(\text{N}_3)^{2+} + \text{NO}^+$, 53
 the **D** intermediate, 47, 51
 Competitive inhibitor, 340
 Complementary oxidation-reduction
 reactions, 253
 Complex kinetic systems, 15
 integrated rate law, 16

- Compressibility and volume of activation, 21
- Comproportionation constant, intervalence systems, 281
- Concentration variables and rate constant, 12
in first-order irreversible system, 14
in second-order irreversible system, 14
- Concentration-jump, relaxation method, 428, 430
- Cone angles, 70
for P(III) and As(III) ligands, 71(T)
for P(III) ligands, 70
multiple, 155
steric parameters, 154
- Conformation change, ligand, 114
- Constant thermodynamic parameters for aqutation of Co(III) pentaammine complexes, 54
base hydrolysis of Co(III) pentaammine complexes, 54
the **D** mechanism intermediate, 48
- Continuous-flow method, 428
- Coordinated ligand, nucleophilic attack, 81, 82
- Coordination geometry change, 115
in $\text{Co}(\text{NH}_2\text{R})_n^{2+}$, NMR studies, 116
in $\text{Co}(\text{py})_n(\text{X})_2$, 116
octahedral to square planar, 115
tetrahedral to octahedral, 115
tetrahedral to square planar, 115
- Corrin ring, coenzyme B₁₂, 342
- Cossee mechanism, initiation of
homogeneous polymerization, 234
- Coulombic work term, Marcus theory, 260
- Cr(II) compounds
aminocarboxylate systems, electrochemistry and kinetics, 433
bridging ligand, remote attack, 278
electron transfer, bridged remote attack, rate constants, 278(T)
reactions with
 $\text{Co}(\text{NH}_3)_5(p\text{-formylbenzoate})^{2+}$, bridged remote attack, 278
 $\text{Co}(\text{NH}_3)_5(\text{glycinate})^{2+}$, bridged outer-sphere mechanism, 277
 $\text{Co}^{\text{III}}(\text{NH}_3)_5\text{X}$, kinetic parameters, 275(T)
- Cr(III) compounds
amines
aqutation, linear free energy relationship, 64
photoaqutation
Adamson's rules, 307
quantum yields, 308(T)
aminocarboxylate systems, electrochemistry and kinetics, 433
 $\text{Cr}(\text{acac})_3$, photoaqutation, 307
 $\text{Cr}(\text{C}_2\text{O}_4)_3^{3-}$, racemization, aqutation and $^{18}\text{OH}_2$ exchange, 122
 $\text{Cr}(\text{CN})_5(\text{NH}_3)^{2-}$, photoaqutation, 305
 $\text{Cr}(\text{CN})_6^{3-}$
emission lifetimes, 305
photoaqutation, volume of activation, 305
cis- $\text{Cr}(\text{cyclam})(\text{NH}_3)_2^{3+}$, photoaqutation, 306
 $\text{Cr}(\text{cyclam})(\text{X})_2$, stereomobility of photochemical transition state, 309
 $\text{Cr}(\text{en})_3^{3+}$
photoaqutation, 306
photoracemization, 306
 $\text{Cr}(\text{L})_6$
back intersystem crossing, 305
ligand field states, 304
photochemistry, 304
 $\text{Cr}(\text{LL})_3$ chelates, photochemistry, 306
 $\text{Cr}(\text{NH}_3)_5\text{Cl}^{2+}$ and $\text{Cr}(\text{NH}_2\text{CH}_2)_3\text{Cl}^{2+}$
aqutation kinetic parameters, 67(T)
steric effects, 67
structural parameters, 67
 $\text{Cr}(\text{NH}_3)_5(\text{OH}_2)^{3+}$, photochemistry, 309
 $\text{Cr}(\text{NH}_3)_5\text{X}$, photoaqutation, volumes of activation, 309(T)
 $\text{Cr}(\text{NH}_3)_6^{3+}$
emission lifetimes, solvent and pressure effects, 305
photoaqutation, 305
 $\text{Cr}(\text{NH}_3)_n(\text{OH}_2)_{6-n}^{3+}$, photosubstitution
quantum yields for H_2O and NH_3 , 308(T)
 $\text{Cr}(\text{phen})_3^{3+}$ and $\text{Cr}(\text{bpy})_3^{3+}$, photoaqutation, 306
 $\text{Cr}(\text{phen})_3^{3+}$, racemization, 122
 $\text{Cr}(\text{TPP})(\text{Cl})(\text{py})$, substitution, **D** mechanism, 51(T)
 $\text{Cr}(\text{TPP})(\text{Cl})\text{X}$, substitution, **D** mechanism, 50
fluoride complexes, photochemistry, 308
photochemistry, 304
photolysis, antithermal pathways, 304
- Cr compounds, organometallic
 $\text{Cr}(\text{CO})_4(\text{bpy})$, photochemistry, 320
 $\text{Cr}(\text{CO})_4(\text{S}-\text{S})$, chelate ring opening, 161
 $\text{Cr}(\text{CO})_5(\text{C}_2\text{H}_4)$, ethylene dissociation, 191

- $\text{Cr}(\text{CO})_5(\text{cyclohexane})$
 from flash photolysis, 314
 substitution rates, 315
 $\text{Cr}(\text{CO})_5(\text{heptane})$, substitution rates, 315
 $\text{Cr}(\text{CO})_5\text{L}$
 cis effect theory, 77
 photochemistry, 319
 $\text{Cr}(\text{CO})_5(\text{N—N})$, chelate ring closing,
 161
 $\text{Cr}(\text{CO})_5(\text{R}_2\text{P—PR}_2)$, chelate ring
 closing, 161
 $\text{Cr}(\text{CO})_5(\text{solvent})$, from flash photolysis,
 315
 $\text{Cr}(\text{CO})_5\text{X}$, substitution, theory, 154
 $\text{Cr}(\text{CO})_6$
 CO exchange and substitution, 153(T)
 flash photolysis, 314
 with 1-hexyne, 315
 photochemistry, 314
 theory, 314
 $\text{Cr}(\eta^6\text{-arene})(\text{CO})_3$, slippage mechanism,
 155
 $\text{Cr}(\eta^6\text{-C}_8\text{H}_8)(\text{CO})_3$, fluxionality, 136
 $\text{Cr}_2(\eta^2\text{-Cp})_2(\text{NO})_4$, bridge-terminal CO
 exchange, 143
 Cr, Mo, W hexacarbonyls, trends in
 reactivity, 152
 $\text{Cr}(\text{P}(\text{OR})_3)_2(\text{H})_2$, fluxionality, 181
 Cross electron-transfer reaction, 258
 Crystal field theory
 activation energy, 86
 for water exchange, 87(T)
d orbital energies, 86(T)
 enthalpy of activation, 86
 substitution reactions, 86
 $\text{Cu}^{\text{III}}(\text{DMP})_n$ systems, electrochemistry and
 kinetics, 432
 Curtin–Hammett conditions, 36
 transition-state free energy, 37
 reaction coordinate diagram, 37
 Cyanocobalamin, CNCbl, 341
 Cyclic system, 40
 Cytochrome P-450, 367
 epoxidation, 372
 concerted mechanism, 372
 epoxide and N-alkylation competition,
 372
 hydroxylation mechanism
 radical or cationic, 371
 rebound, 370
 models, carbene formation, 372
 monooxygenase enzyme, 367
 reaction with
m-chloroperbenzoic acid, 369
 iodosylbenzene, 369
 reactions, 367
 theory, 370
 Cytochrome P-450-CAM
 reaction pathway, 368
 reaction with camphor, 367
 structure, 367
 Davies equation, 25
 Deadtime determination, stopped-flow
 first-order conditions, 425
 second-order conditions, 425
 Deadtime, stopped-flow, 424
 Debye–Hückel theory
 extended law, 25
 limiting law, 25
 Decarbonylation of $\text{Mn}(\text{CO})_5(\text{OCCH}_3)$,
 product distribution, 169
 Deprotonation
 by OH^- , 27
 of carbon acids, 27
 of H_2 complexes, kinetics, 182
 of metal hydrides, 28
 Detailed balancing principle, 39
 example, 102
 Dielectric constant of solvent, effects on
 interchange mechanisms, 65
 Diffusion coefficients, 26
 Stokes–Einstein equation, 26
 Diffusion-controlled
 deprotonation, 27
 protonation, 27
 rate constants, 25
 second-order, 26
 estimated in water, 27(T)
 unimolecular, 27
 Dihydride route, transfer hydrogenation of
 C=O bonds, 212
 Diol dehydrase
 bound radical mechanism, 354
 catalyzed reactions, 345
 mechanism, 348, 349
 for $\text{Co}(\text{C}_2(\text{DO})(\text{DOH}))_{\text{pm}}$, coenzyme
 B_{12} model, 353
 rate-determining step, 350
 Dioxigen, reaction with NO, 378
 Dioxygenase, enzyme reactions, 361
 Direct transfer route for hydrogenation of
 C=O bonds, 212, 213
 Dissociation and intramolecular isomerism,
 differentiation, 121
 Dissociation isomerism mechanism, 119
 ligand field theory, 125
 Dissociative activation, 44

- Dissociative adsorption
 isotherm for H_2 , 405
 of gas on solid, 401
- Dissociative conjugate base mechanism, 73
 for Co(III) amines, 51, 73
 intermediate for Co(III) amines, 53
- Dissociative interchange mechanism, I_d , 44
- Dissociative intermediate
 16-electron, 151
 competition studies, 47
 constant thermodynamic properties, 48
 ligand site preference, theory, 158
- Dissociative ion pair mechanism, 95
- Dissociative mechanism, D, 44
 examples of tests, 49
 for $Co(CN)_5(OH_2)^{2-}$, 50
 rate constant, 50
 for $Co^{III}(DMG)_2(L)X$, 50
 for $Co(en)_2(SO_3)(OH_2)^+$, 50
 for $Cr(TPP)(Cl)(py)$, results, 51(T)
 for $Cr(TPP)(Cl)X$, 50
 for $Fe(\eta^5\text{-indenyl})(CO)_2I$, 156
 for $Rh(Cl)_5(OH_2)^{2-}$ substitution, 50
 results, 51(T)
 for $RuCl(\eta^5\text{-indenyl})(PPh_3)_2$, 156
 intermediate
 competition ratios, 51(T)
 competition studies, 51
 ion pair formation of reactants, 46
 preassociation of reactants, 46
 rate constant, 45
 rate law, 45
 reaction coordinate diagram, 49
 rearrangement of unsymmetrical
 chelates, 126
- Dissociative rate law, examples, 49
- Distance dependence, electron transfer rate
 in metalloproteins, 286
- Dithiocarbamates of Fe(IV), Fe(III) and
 Ru(III), isomerism, 128
- Dixon plot, 341
- Drago *E* and *C* scale, 60
 values for representative acids and bases,
 60(T)
- Drago solvent polarity scale, 61
 parameters, 62(T)
- Edwards nucleophilicity scale, 58
- Ehrenfest adiabaticity, 256
- Eigen–Wilkins mechanism, 95
- Einstein, 292
- Electrochemical methods, 431
 cyclic voltammetry, 431
 symbols, 431
- Electrochemistry and kinetics of
 $Cr^{IV/III}$ -aminocarboxylate systems, 433
 $Cu^{II/I}(DMP)_n$ systems, 432
 $Mn(\eta^5\text{-H}_3CC_2H_4)(CO)_2(NCCCH_3)$, 434
 $Mn(\eta^5\text{-H}_3CC_2H_4)(CO)_2(PR_3)$, 434
- Electron paramagnetic resonance methods
 (see EPR), 446
- Electron transfer
 bridged
 adjacent atom attack, 277
 outer-sphere mechanism, 277
 remote attack, 277
 by Cr(II), rate constants, 278(T)
 bridging ligand effects, 274
 in $Co(NH_3)_5(OCOH)^{2+}$, 275
 in $Co(NH_3)_5(\text{thiocarbamate})^{2+}$, linkage
 isomers, 276
 bridging ligand, H_2O , 276
 bridging ligand properties
 in $Co^{III}(NH_3)_5X$, 275
 π conjugation, 276
 chemical mechanism, 278
 for $Co(NH_3)_5(\text{mbpy})^{4+} + \bullet CO_2^-$, 279
 for $Co(NH_3)_5(O_2CC_6H_4NO_2)^{2+} + \bullet R$,
 279
 cross reaction, 258
 rate constants, 268(T)
 inner-sphere mechanism, 254
 for $Co(NH_3)_5Cl^{2+} + Cr(OH_2)_6^{2+}$, 255
 for $Co^{III}(NH_3)_5X + Cr(OH_2)_6^{2+}$, kinetic
 parameters, 275(T)
 precursor complex, 255
 successor complex, 255
 theory, 277
 intervalence, 281
 intramolecular rate constants, for
 $Co(NH_3)_5(O_2CXC_6H_4\bullet NO_2)^+$,
 280(T)
- Marcus theory
 cross relationship with
 free energies, 258
 rate and equilibrium constants, 259
 details, 259
 inverted region, 272
 metalloproteins, 285
 theory, 286
 mixed valence systems, 281
 outer-sphere, 255
 precursor and successor complex, 257
 theory, 256
 rate constants, calculated by the Marcus
 cross relationship, 268(T)
 rate distance dependence in
 metalloproteins, 286

- reactions
 - charge symmetry, 259
 - volumes of activation, 271
- Ru(II) in metalloproteins, 286
- self-exchange reaction, 258
 - rate constants, 265(T)
- Electron transfer, binuclear systems
 - Co(III)–Fe(II), 280, 284
 - Co(III)–Ru(II), 280, 284
 - Ru(II)–Ru(III), 284
 - Ru(III)–Os(II), 285
- Electronegativity, absolute, and hardness, 63
 - values for acids and bases, 63(T)
- Electronic effect, ^{13}C NMR of Ni(CO) $_3$ L, 71
- Electronic parameters for P(III) and As(III) ligands, 71(T)
- Electronic spectra for M(CO) $_6$, 313
 - and photochemistry, 314
- Eley–Rideal mechanism
 - competitive adsorption, 404
 - noncompetitive adsorption, 404
- Emission lifetime of
 - Cr(CN) $_6^{3-}$, 305
 - Cr(NH $_3$) $_6^{3+}$, solvent and pressure effects, 305
 - Ru(bpy) $_3^{2+}$, 312
- Enantiomeric excess, ee, 202
- Endothelium relaxing factor, NO, 373
- Entering group effects, on {•Mn(CO) $_5$ },
 - rate constants, 168(T)
- Enthalpy of activation, 19
 - crystal field theory, 86
 - for nonaqueous solvent exchange, 91(T)
 - for solvent exchange, empirical correlation, 92(T)
 - for water exchange, 84(T)
 - SCF theory, 89(T)
- Entropy of activation, 19
 - and volumes of activation for water exchange, 72(T)
 - for interchange mechanisms, 73
 - for nonaqueous solvent exchange, 91(T)
 - for water exchange, 84(T)
- Enzyme kinetics
 - Briggs–Haldane equation, 339
 - Dixon plot, 341
 - inhibitor
 - competitive, 340
 - noncompetitive, 341
 - uncompetitive, 340
 - Lineweaver–Burke plot, 339, 341
 - Michaelis constant, 338
 - Michaelis–Menten equation, 338
 - pH dependence, 339
 - saturation behavior, 339
 - steady-state conditions, 338
 - swamping conditions, 340
 - terms and methods, 338
 - turnover number, 339
- Enzyme reactions
 - of carbon dioxide, 357
 - of dioxygen, 361
 - of hydrogen peroxide, 361
 - of nitric oxide, 373
 - of superoxide ion, 361
 - with coenzyme B $_{12}$, 345
- Epoxidation by cytochrome P-450, 372
 - concerted mechanism, 372
- Epoxide polymerization, 176
 - catalysts, 177
- EPR, kinetics
 - methods, 446
 - flow, 447
 - pulsed, 446
 - of Ni II electron exchange, 447
- EPR, spin trapping for
 - Fe(II) oxidation by benzenediazonium ions, 447
 - Fe II (EDTA) + H $_2$ O $_2$, 447
- Ethanolamine ammonia lyase
 - catalyzed reactions, 345
 - mechanism, 348
 - rate-determining step, 350
- Ethylene
 - dissociation from Cr(CO) $_5$ (C $_2$ H $_4$), 191
 - reaction with Ir(η^5 -Cp*)(PMe $_3$), σ - and π -complex formation, 189, 319
 - rotation in
 - Fe(CO) $_4$ (ethylene), 138
 - Ir(η^5 -Cp)(C $_2$ H $_4$) $_2$, 138
 - Ir(PPhMe $_2$) $_3$ (CH $_3$)(C $_2$ H $_4$), 139
 - Ir(PPhMe $_2$) $_3$ (CH $_3$ CN)(C $_2$ H $_4$) $^+$, 139
 - Ir(PPhMe $_2$) $_4$ (C $_2$ H $_4$) $^+$, 139
 - Os(CO) $_4$ (ethylene), 138
 - Os(PPh $_3$) $_2$ (CO)(NO)(C $_2$ H $_4$), 138
 - Rh(η^5 -Cp)(C $_2$ F $_4$)(C $_2$ H $_4$), pressure dependence, 23
 - Rh(η^5 -Cp)(C $_2$ H $_4$) $_2$, 138
 - Ru(CO) $_4$ (ethylene), 138
- Ethylene–butadiene codimerization, 232
 - catalysis by
 - Ni(P(OEt) $_3$) $_4$ H, 232
 - RhCl $_3$, mechanism, 232
- Experimental methods, detection criteria, 422
- EXSY NMR method, 440

- Fe(II) compounds**
 electron transfer in Fe(II)–Co(III) systems, 280, 284
 Fe protoporphyrin (IX), structure, 362
 Fe(EDTA) + H₂O₂, EPR spin trapping, 447
 Fe(Heme) + NO, kinetics, 375
 Fe(Heme)(NO), flash photolysis, 375
 Fe(NTA) + •CO₂⁻, pulse radiolysis, 451
 Fe(OH₂)₆²⁺
 inner-sphere reaction with radicals, 450
 reaction with •OH, H atom transfer, 451
 substitution reactions, 96
 Fe(phen)₃²⁺, racemization, 122
 oxidation by benzenediazonium ions, EPR, 447
 spin-state equilibria, 123
- Fe(II/III) systems**
 aqueous, self-exchange rates, 268, 269
 Fe(CN)₆^{3/4-}, cation effects on self-exchange rates, 266
 Fe(Cp)₂^{0/+}, self-exchange rates, 263
- Fe(III) compounds**
 Fe(III) and Fe(IV) dithiocarbamates, isomerism, 128
 Fe(III) aqueous + SCN⁻, volume of activation, 427
 Fe heme complexes of NO, reductive hydroxylation, 375
 Fe(Heme), complexation by NO, 375
 recombination kinetics, 375
 Fe(Heme)(NO), flash photolysis, 375
 Fe(OH₂)₃(NCS)²⁺ formation, 427
 high-pressure stopped-flow, 427
 P-jump and T-jump, 427
 Fe(OH₂)₃(OH)²⁺, substitution rate constants, 99(T)
 Fe(OH₂)₆²⁺ + N₃⁻, pulse radiolysis, 450
 Fe(OH₂)₆³⁺, substitution reactions, 97
 rate constants, 99(T)
- Fe compounds, organometallic**
 Fe(CO)₂(η⁵-Cp)(η¹-Cp), fluxionality, 134
 Fe(CO)₂(PMe₃)(CH₃)I, CO insertion, 169
 Fe(CO)₂(PPh₂Me)(CH₃)I, CO insertion, η²-acyl intermediate, 169
 •Fe(CO)₃(PR₃)₂⁺ radical, reactivity, 167
 Fe(CO)₄(ethylene), fluxionality, 138
 Fe(CO)₄R⁻, ion pairing and CO insertion, 173
 Fe(CO)₅
 catalyst for Reppe synthesis, 227
 CO exchange and substitution, 151
 dissociation, theory, 152
 fluxionality, 130
 photochemistry, 315
 theory, 317
 reaction with
 PEt₃, flash photolysis, 316
 PR₃, photochemistry, 316
 ROH, flash photolysis, 317
 rearrangements, 128
 substitution, 152(T)
 water gas shift mechanism, 229
 Fe(Cp)(CO)(η³-C₃H₅), allyl rotation, 141
 Fe(Cp)(CO)₂(CH₂R), SO₂ insertion, 174
 Fe(Cp)₂^{0/+}, self-exchange rates, 263
 Fe(η⁵-Cp)(CO)(COCH₃), photolysis and CO insertion intermediate, 173
 Fe(η⁵-Cp)(CO)(PR₃)(CH₃), CO insertion, 169
 Fe(η⁵-Cp)(CO)₂(CH₃) + PR₃, CO insertion intermediate, 173
 Fe(η⁵-Cp)(η¹-Cp)(CO)₂, fluxionality, 131
 Fe(η⁵-Cp)(η¹-indenyl)(CO)₂, fluxionality, 132
 Fe(η⁴-C₈H₈)(CO)₂(i-PrNC), fluxionality, 136
 Fe(η⁵-C₉H₇)(CO)₂(CH₃) + PR₃, CO insertion intermediate, 173
 Fe(η⁵-indenyl)(CO)₂I, D mechanism, 156
 Fe(NO)₂(CO)₂, substitution reactions, 158
 Fe(P₂(CH₂)₂(R)₄)₂(H)₂, alkene addition, 191
 Fe((R₂PCH₂)₂)₂, photochemistry, C–H bond activation, 221
 Fe₂((η⁵-Cp)(CO)₂)₂
 bridge–terminal CO exchange mechanism, 142
 fluxionality, 141
 isomer structures, 142
 Fe₂(η⁵-Cp)₂(P(OPh)₃)(CO)₃, bridge–terminal CO exchange, 143
 Fe₃(CO)₁₂,
 flash photolysis, 325
 fluxionality, 143
 photochemistry, 324
 FeRu₂(CO)₁₂, fluxionality, 143
- First bond formation, chelate formation, 100**
First-order and second-order conditions, comparison, 10

- First-order system
 integratable equation, 34
 irreversible system, 4
 concentration variables, 14
 half-time, 5
 integrated rate law, 4
 rate and mechanism, 31
 reversible system, 6
 half-time, 7
 integrated rate law, 7
- Fischer–Tropsch reaction, 227
 catalysis by $M_x(\text{CO})_x$ systems, 228
- Flash photolysis methods, 451
- Flash photolysis of
 $\text{Co}(\text{bpy})_2(\text{glycinate})^{2+}$, 300
 coenzyme B_{12} , 355, 452
 $\text{Co}(\text{NH}_3)_4(\text{OCO}_2)^+$, 299
 $\text{Cr}(\text{CO})_6$, 314
 $\text{Cr}(\text{CO})_3(\text{cyclohexane})$ formation, 314
 $\text{Cr}(\text{CO})_3(\text{solvent})$ formation, 315
 $\text{Fe}(\text{CO})_5$, 315
 + PEt_3 , 316
 + ROH , 317
 $\text{Fe}^{\text{II}}(\text{Heme})(\text{NO})$, 375
 $\text{Fe}^{\text{III}}(\text{Heme})(\text{NO})$, 375
 $\text{Fe}_3(\text{CO})_{12}$, 325
 $\text{Ir}(\text{Cp})(\text{CO})_2$, C–H bond activation, 328
 $\text{M}(\text{CO})_6$ + 1-hexyne, 315
 $\text{Mb}(\text{NO})$, 375
 $\text{Mn}(\text{CO})_5(\text{CH}_3)$, 321
 $\text{Mn}_2(\text{CO})_{10}$, 324
 myoglobin complexes, 364
 4-state model, 364
 rate constants, 365(T)
 $\text{Os}(\text{bpy})_3^{2+}$, 452
 $\text{Rh}(\text{Cp})(\text{CO})_2$, C–H bond activation, 328
 $\text{Rh}(\text{NH}_3)_5\text{I}^{2+}$, 303
 $\text{Rh}(\text{PPh}_3)_2(\text{CO})\text{Cl}$, 327
 $\text{Rh}(\text{Tp}^*)(\text{CO})_2$, C–H bond activation, 451
 $\text{Ru}(\text{bpy})_3^{2+}$, 452
 $\text{Ru}_3(\text{CO})_{12}$, 325
 $\text{W}(\text{CO})_5(\text{py})$, 319
 + 1-hexene, 319
- Flow methods, 423
- Fluorescence, 293
- Fluxional organometallic compounds, 130
- Fluxional processes, NMR lifetime, 436
- Fluxional ring systems, 131
- Fluxionality of
 allyl complexes, 139
 $\text{Cr}(\eta^6\text{-C}_8\text{H}_8)(\text{CO})_3$, 136
 $\text{Cr}(\text{P}(\text{OR})_3)_3(\text{H})_2$, 181
 η^1 -allyl complexes, 139
 η^3 -allyl complexes, 140
 $\eta^2\text{-C}_6\text{H}_6$ systems, 1,5 shift, 135
 $\eta^4\text{-C}_6\text{H}_6$ systems, 1,3 shift, 135
 $\eta^1\text{-C}_7\text{H}_7$ systems, 1,5 shift, 135
 $\eta^2\text{-C}_8\text{H}_8$ systems, 136
 $\eta^4\text{-C}_8\text{H}_8$ systems, 136
 $\eta^6\text{-C}_8\text{H}_8$ systems, 136
 $\text{Fe}(\text{CO})_4(\text{ethylene})$, 138
 $\text{Fe}(\text{CO})_5$, 130
 $\text{Fe}(\eta^5\text{-Cp})(\eta^1\text{-Cp})(\text{CO})_2$, 131, 134
 $\text{Fe}(\eta^5\text{-Cp})(\eta^1\text{-indenyl})(\text{CO})_2$, 132
 $\text{Fe}(\eta^4\text{-C}_8\text{H}_8)(\text{CO})_2(i\text{-PrNC})$, 136
 $\text{Fe}_2(\eta^5\text{-Cp})(\text{CO})_2$, 141
 Ga(III) tris-catecholate complexes, 443
 $\text{Ir}(\eta^5\text{-Cp})(\text{C}_2\text{H}_4)_2$, 138
 $\text{Ir}(\text{PPhMe}_2)_3(\text{CH}_3)(\text{C}_2\text{H}_4)$, 139
 $\text{Ir}(\text{PPhMe}_2)_3(\text{CH}_3\text{CN})(\text{C}_2\text{H}_4)^+$, 139
 $\text{Ir}(\text{PPhMe}_2)_4(\text{C}_2\text{H}_4)^+$, 139
 $\text{IrRh}_3(\text{CO})_{12}$, 144
 $\text{Ir}_2\text{Rh}_2(\text{CO})_9(\mu\text{-CO})_3$, 144
 $\text{Ir}_4(\text{CO})_{11}(\mu\text{-SO}_2)$, 144
 $\text{M}(\text{Cp})(\text{CO})_n(\eta^3\text{-C}_3\text{H}_4\text{R})$ systems, 141
 $\text{M}_3(\text{CO})_{12}$ systems, 143
 $\text{M}_4(\text{CO})_{12}$ systems, 143
 $\text{Mn}(\text{CO})_5(\eta^1\text{-C}_3\text{H}_5)$, 139
 $\text{Mo}(\text{S}_2\text{C}_2\text{R}_2\text{R}_2)_3$, 441
 $\text{Os}(\text{CO})_4(\text{ethylene})$, 138
 $\text{Os}(\eta^3\text{-C}_7\text{H}_7)(\text{CO})_3(\text{SnPh}_3)$, 137
 $\text{Os}(\eta^6\text{-C}_8\text{H}_8)(\eta^4\text{-1,5-COD})$, 136
 $\text{Os}(\text{PPh}_3)_2(\text{CO})(\text{NO})(\text{C}_2\text{H}_4)$, 138
 π -bonded cyclic systems, 134
 π -bonded olefins, 137
 $\text{Pd}(\text{PPhMe}_2)(\text{NC}_5\text{H}_4\text{CO}_2)(\eta^1\text{-C}_3\text{H}_5)$, 139
 $\text{Pt}(\text{PPh}_3)_2(\eta^3\text{-C}_7\text{H}_6)$, 135
 $\text{Re}(\eta^1\text{-C}_7\text{H}_7)(\text{CO})_5$, 134
 $\text{Rh}(\eta^5\text{-Cp})(\text{C}_2\text{H}_4)_2$, 138
 $\text{Rh}_4(\text{CO})_{12}$, 144
 $\text{Ru}(\text{CO})_4(\text{ethylene})$, 138
 $\text{Ti}(\text{NMe}_2)_2(\eta^1\text{-C}_3\text{H}_5)$, 139
 $\text{W}(\eta^6\text{-C}_8\text{H}_8)(\text{CO})_3$, 136
 $\text{W}(\text{P}(\text{OR})_3)_3(\text{H})_2$, 181
 $\text{W}(\text{S}_2\text{C}_2\text{R}_2\text{R}_2)_3$, 441
- Franck–Condon principle, 256, 260
- Free energy of activation, 18
- Free-energy relationships, linear, 64
- Ga(III) complexes
 of tris-catecholate, fluxionality by NMR
 bandshape analysis, 443
 trigonal twist, 128
- Gas absorption into liquid
 mixing rate effect, 393
 rate, 391
 rate constant, 392
 rate law, 392

- Gas adsorption on solid
 chemisorption, 401
 dissociative, 401
 physisorption, 400
- Gas solubility
 Henry's law, 393
 of H_2 , CO, in various solvents, 395(T)
 of H_2 , N_2 , temperature dependence, 394(T)
 Ostwald coefficient, 393
- Gas/liquid systems, 391
- Gas/liquid/solid systems, 400
 kinetic models, 401
 rate-controlling steps, 402
- Geometrical isomerism (also see isomerism) 119
- Glutamate mutase
 catalyzed reactions, 345
 mechanism, 348
 radical fragmentation mechanism, 354
- Glycine
 chelate formation with $M(OH)_6$, 100
 chelate ring-closing pathways, 81
- Guggenheim method, 14
- Gutmann donor numbers, 59
 applications, 263, 282
 for common solvents and anions, 59(T)
- H_2
 asymmetric hydrogenation of
 C=C bonds, 202
 C=O bonds, 211
 complexes, deprotonation, kinetics, 182
 dissociative adsorption isotherm, 405
 heterolytic cleavage with Ru(II)
 catalysts, 207
 oxidative addition, 180
 reaction pathway, 182
 to $Ir(CO)(PR_3)_2X$, kinetic parameters, 180(T)
 to $Rh(PPh_3)_3Cl$, 197
- Half-order, rate and mechanism, 32
- Half-time, 3
 first-order
 irreversible system, 5
 reversible system, 7
 second-order irreversible system, 9
- Hard and soft acids and bases
 examples, 62
 qualitative ordering, 62
 theory, 62
- Hardness, absolute
 electronegativity relationship, 63
 values for acids and bases, 63(T)
- Heck reaction
 catalysis by oxidative addition to Pd
 metal nanoclusters, 418
 heterogeneous or homogeneous Pd
 catalyst, 416
 palladacycle catalysts, 417
 Pd metal formation, 417
 phosphine free catalysts, 418
- Hemilabile ligands, 161
- Hemilabile systems
 phenyl group in
 $Ti(\eta^5-C_5H_4C(CH_3)_2C_6H_5)(CH_3)_2^+$, 163
 rate constant, 162
 Rh dimer system, 163
 $Rh(CO)(SNS)^+$, 163
 $Ru(\eta^5-indenyl)(PPh_3)(PPh_2X)^+$, 162
- Heterogeneous catalysis
 hydrogenation of nitrobenzenes, 405
 kinetic results, 407(T)
 mechanism comparison, 408
 nanoclusters, 412
 kinetic model, 412
- Heterogeneous catalyst
 from a homogeneous precursor, 409
 tests for M(0), 410
 from $Ir^I(1,5-COD) + H_2$, 413
 from $Rh_2((1,5-COD)(\mu-Cl))_2$, 415
 from $Rh_2((\eta^5-Cp^*)(Cl))_2 + H_2$, 414
 from $Ru(\eta^6-C_6Me_6)(OAc)_2 + H_2$, 414
 induction period for formation, 412
- Heterogeneous or homogeneous Pd
 catalyst, Heck reaction, 416
- Heterogeneous systems
 Eley-Rideal mechanism for
 competitive adsorption, 404
 noncompetitive adsorption, 404
 gas/liquid, 391
 gas/liquid/solid, 400
 kinetic models, 401
 rate-controlling steps, 402
 hydrogenation of nitrobenzenes, 405
 kinetic results, 407(T)
 mechanism comparison, 408
 kinetics, 391
- Langmuir isotherm for
 adsorption on solid, 402
 competitive adsorption, 403
 noncompetitive adsorption, 403
- Langmuir-Hinshelwood mechanism for
 competitive adsorption, 404
 noncompetitive adsorption, 404
 mass transfer to active sites, 405
 in pores, 405
 mechanisms, 404

- Heteroligand replacement in, 159
 $M(CO)_3L$ systems, 159
cis- $Mo(CO)_4L_2$, 159
- Heterolysis of
 adenosylcobalamin, 347
 coenzyme B_{12} , 347
 H_2 by $Ru(II)$ catalysts, 207
- Holoenzyme, 338
- Homogeneous catalysis by organometallic compounds, 225
- Homogeneous polymerization,
 Ziegler–Natta type, 233
- catalysis by $Zr(Cp)_2(X)_2$, 233
 initiation by the
 Cossee mechanism, 234
 trigger mechanism, 234
 pathways, 233
 propagation, 234
- Homolysis
 of adenosylcobalamin, 347
 of coenzyme B_{12} , 347
 mechanism for metal–metal bonded
 carbonyls, 164
- Hopping mechanism, intervalence electron transfer, 285
- Hydride
 acidity, 181
 classical $M(H)_2$, 180
 elimination, β (see beta-hydride elimination), 191
 formation, stoichiometric, asymmetric hydrogenation, 204
 nonclassical $M(\eta^2-H_2)$, 180
 protonation, 181
 route for alkene hydrogenation, 196
 route for hydrogenation of C_6H_{10} by
 $Rh(PPh_3)_3(H)_2Cl$, 198
- Hydroformylation, 225
 catalysis by
 $Co_2(CO)_8$, 226
 $Rh(PPh_3)_2(CO)_2H$, 226
 mechanism for $Co(CO)_4H$, 226
 theory reviews, 227
- Hydrogen bonding
 solvent parameters, 62(T)
 solvent property scales, 61
 thermochemical scale, 61
- Hydrogenation,
 asymmetric, 201
 of $C=C$ bonds, 202
 of $C=O$ bonds, 211
 pathways, 196, 212
 stereoselective, 201
 symmetry restriction, 195
- Hydrogenation catalysis by
 $Ir(COD)^+$ derivatives, 199
 pathways, 200
 theory, 201
 $Mn(CO)_5H$, mechanisms, 167
 $Rh(dipamp)^+$
 mass transfer effect, 395
 pathways, 203
 $Rh(diphos)^+$, olefin route, 199
 $Rh(DUPHOS)^+$, theory, 202
 $Ru(BINAP)(CH_3CO_2)_2$
 kinetics, 205, 209
 mass transfer effect, 397
 $Ru(BINAP)(DPEN)(Cl)_2$, 215
 $Ru(PPh_3)_3(Cl)_2$, 213
 $Ru(TsDPEN)(Ar)Cl$, 214
 Wilkinson's catalyst, $Rh(PPh_3)_3Cl$, 197
- Hydrogenation of
 CO_2 by $Ru(hfacac)(Ph_2P(CH_2)_3PPh_2)$,
 229
 C_6H_{10} by $Rh(PPh_3)_3(H)_2Cl$, 198
 1-hexene by $Rh(diphos)^+$, 199
 nitrobenzene
 heterogeneous catalysis, 405
 kinetic results, 407(T)
 mechanism comparison, 408
- Hydroxylation by cytochrome P-450
 radical or cationic mechanism, 371
 rebound mechanism, 370
- Indenyl complex, D mechanism for
 $Fe(\eta^5-indenyl)(CO)_2I$, 156
 $RuCl(\eta^5-indenyl)(PPh_3)_2$, 156
- Indenyl effect
 slippage mechanism, 156
 substitution in
 $Re(\eta^5-indenyl)(CO)_2(MeCCMe)$, 157
 $Rh(\eta^5-indenyl)(CO)_2$, 156
 in $V(\eta^5-indenyl)_2(CO)$ and
 $V(\eta^5-C_5R_n)_2(CO)$, 156
- Indenyl ligand, σ -donicity, 156
- Induced aquation of $Co(III)$ complexes, 53
- Induction period for formation of
 heterogeneous catalyst, 412
- Inert and labile classification of Taube, 85
- Inert metal ions, 85
- Inhibitor
 competitive, 340
 noncompetitive, 341
 of carbonic anhydrase, 360
 uncompetitive, 340
- Initial rate method, 11
- Inner-sphere and outer-sphere mechanism,
 differences, 273

- Inner-sphere electron transfer, 254
 for $\text{Co}(\text{NH}_3)_3\text{Cl}^{2+} + \text{Cr}(\text{OH}_2)_6^{2+}$, 255
 for $\text{Cr}(\text{II}) + \text{Co}^{\text{III}}(\text{NH}_3)_3\text{X}$, kinetic parameters, 275(T)
 for $\text{Fe}(\text{II})$ aqueous + radicals, 450
 precursor and successor complex, 255
 theory, 277
- Inner-sphere reorganization, Marcus theory, 260
- Insertion of
 alkene into MH or MC bonds, 191
 CO into MC bonds, 168
- Insertion reactions (see CO insertion), 168
- Integrated rate law, 3
 complex kinetic systems, 16
 first-order system
 irreversible, 4
 reversible, 7
 parallel reactions, 17
 second-order system
 irreversible, 9
 reversible, 8
 successive reactions, 16
 zero-order system, 4
- Interchange mechanisms, 44
 associative, I_a , 44
 charge effects, 65
 dissociative, I_d ,
 entropy of activation, 73
 solvent dielectric constant effects, 65
 steric effects, 66
 volume of activation, 71
- Intermediate, 20
- Internal conjugate base mechanism for substitution on $\text{Ni}(\text{OH}_2)_6^{2+}$, 103
- Internal filtration, 293
- Intersystem crossing, 294, 296
- Intervalence electron transfer, 281
 bridging ligand effects, 284
 comproportionation constant, 281
 electronic absorption bands, 281
 for $\text{Ru}_2(\text{NH}_3)_{10}(\mu\text{-L})_5^+$, 283(T)
 enthalpy of activation effect, 285
 hopping mechanism, 285
 in Ru(II/III) systems, 281
 in Ru–Ru systems, 282
 metal–metal distance dependence, 284
 nuclear factors, 285
 Robin–Day classification, 281
 solvent effects, 282
 trapped-valence model, 282
 weakly coupled systems, 284
- Intimate mechanism, 44
 operational tests for, 57
- Intramolecular and dissociation isomerism, differentiation, 121
- Intramolecular rearrangement isomerism mechanisms, 120
 for symmetrical tris-chelates
 rhombic bend, 120
 trigonal twist, 120
 for unsymmetrical tris-chelates
 rhombic bend, 127
 trigonal twist, 127
- Inverse-order, rate and mechanism, 32
- Inverted region, Marcus theory prediction, 272
- Ion pair
 $[\text{Co}(\text{tren})(\text{NH}_3)(\text{OH}_2)\text{Cl}]^{2+}$ structure, 66
 formation constant, theory, 47
 calculated, 47(T)
 formation of reactants and the D mechanism, 46
- Ion pair dissociative mechanism, 95
- Ion pairing
 for CO insertion in $\text{Fe}(\text{CO})_4\text{R}^-$, 173
 solvent effect for $\text{Pt}(\text{Me}_4\text{en})(\text{DMSO})\text{Cl}^+ + \text{Cl}^-$, 66
- Ionic strength
 Davies equation, 25
 Debye–Hückel limiting law, 25
 dependence of rate constants, 24
- Ir compounds, organometallic
 $\text{Ir}(\text{CO})(\text{PR}_3)_2\text{Cl}$, oxidative addition of aliphatic halides, kinetic parameters, 183(T)
 $\text{Ir}(\text{CO})(\text{PR}_3)_2\text{X}$, oxidative addition of H_2 , kinetic parameters, 180(T)
 $\text{Ir}(\text{CO})_2(\text{I})_2^-$, oxidative addition of aliphatic halides, pathways, 184
 $\text{Ir}(\text{CO})_3\text{I}$, catalyst for methanol carbonylation, mechanism, 231
 $\text{Ir}(\text{COD}) + \text{H}_2$, heterogeneous catalyst formation, 413
 $\text{Ir}(\text{COD})^+$ derivatives, hydrogenation catalysts, 199
 pathways, 200
 $\text{Ir}(\eta^5\text{-Cp})(\text{C}_2\text{H}_4)_2$, ethylene rotation, 138
 $\text{Ir}(\eta^5\text{-Cp})(\text{CO})_2$
 C–H bond activation, 220
 flash photolysis and C–H bond activation, 328
 photochemistry, 220
 slippage mechanism, 155
 $\text{Ir}(\eta^5\text{-Cp})\text{L}$, C–H bond activation, 217
 $\text{Ir}(\eta^5\text{-Cp})(\text{PMe}_3) + \text{ethylene}$
 reaction coordinate diagram, 190
 σ - and π -complex formation, 189, 319

- $\text{Ir}(\eta^5\text{-Cp}^*)(\text{PMe}_3)(\text{C}_6\text{H}_5)_2\text{H}$, thermolysis with ethylene, 189
 $\text{Ir}(\eta^5\text{-Cp}^*)(\text{PMe}_3)(\text{Cy})\text{H}$, reductive elimination, 223
 $\text{Ir}(\eta^2\text{-HBPf}_3)(\text{CO})(\text{C}_2\text{H}_4)$, alkene addition, σ and π complex, 191
 $\text{Ir}(\text{OC}(\text{Me})\text{CHCPh})(\text{PPh}_3)_2(\text{OCMe}_2)^+$ + alkyne, 192
 $\text{Ir}(\text{PPhMe}_2)_3(\text{CH}_3)(\text{C}_2\text{H}_4)$, fluxionality, 139
 $\text{Ir}(\text{PPhMe}_2)_3(\text{CH}_3\text{CN})(\text{C}_2\text{H}_4)^+$, fluxionality, 139
 $\text{Ir}(\text{PPhMe}_2)_4(\text{C}_2\text{H}_4)^+$, fluxionality, 139
 $\text{Ir}(\text{Tp})(\text{PPh}_3)(\text{C}_2\text{H}_4) + \text{H}_2$ in NMR tube, mass transfer effect, 398
 $\text{IrRh}_3(\text{CO})_{12}$, fluxionality, 144 theory, 201
 $\text{Ir}_2\text{Rh}_2(\text{CO})_9(\mu\text{-CO})_3$, fluxionality, 144
 $\text{Ir}_4(\text{CO})_{11}(\mu\text{-SO}_2)$, fluxionality, 144
 $\text{Ir}_4(\text{CO})_n(\text{L})_p$ cluster, substitution, 166
 Iron protoporphyrin IX, myoglobin prosthetic group, structure, 362
Isomerism
 chiral centers, 126
 differentiation of dissociation and intramolecular mechanisms, 121
 geometrical, 119
 intramolecular rearrangements, 120
 linkage, 117
 mechanism
 dissociation, **D**, 119
 ligand field theory, 125
 ligand bite distance, 128
 rhombic bend, 120, 127
 structural features, 128
 trigonal twist, 120, 127
 ligand field theory, 124
 of $\text{Co}(\text{en})_2(\text{A})\text{X}$, ligand field theory, 125
 of $\text{Co}(\text{en})_3^{3+}$, ligand field theory, 125
 of $\text{Fe}(\text{IV})$ and $\text{Fe}(\text{III})$ dithiocarbamates 128
 of $\text{Pt}(\text{L-Met-S,N})_2$, 130
 of *cis*- $\text{Pt}(\text{NH}_3)_2(\text{Cl})_2$, 130
 of $\text{Pt}(\text{R})_2(\text{L})_2$ and $\text{Pt}(\text{Ar})_2(\text{L})_2$, 130
 of $\text{Ru}(\text{III})$ dithiocarbamates, 128
 one-ended dissociation of $\text{M}(\text{AA})_2(\text{X})_2$ systems, 119
 optical (see racemization), 119
 permutational analysis, 128
 square-planar systems, 130
 twist angle, 128
 unsymmetrical chelates, 126
 Isomerism and racemization, ligand field theory, 124
 Isozyme, 338
 of carbonic anhydrase, 357
 of nitric oxide synthase, 374
 Kinetic analysis, relaxation methods, 429
 Kinetic effects on quantum yields, 294
 Kinetic parameters for
 CO exchange on $\text{V}(\eta^5\text{-C}_5\text{R}_n)_2(\text{CO})$, 157(T)
 $\text{Co}(\text{NH}_3)_5\text{Cl}^{2+}$ and $\text{Co}(\text{NH}_2\text{CH}_3)_5\text{Cl}^{2+}$ aquation, 67(T)
 $\text{Co}^{\text{III}}(\text{NH}_3)_5\text{X} + \text{Cr}(\text{OH})_2^{2+}$, 275(T)
 $\text{Cr}(\text{NH}_3)_3\text{Cl}^{2+}$ and $\text{Cr}(\text{NH}_2\text{CH}_3)_3\text{Cl}^{2+}$ aquation, 67(T)
 electron-transfer, self-exchange, 265(T)
 myoglobins,
 O₂ and CO binding, 366(T)
 small molecule binding, 363(T)
 nonaqueous solvent exchange, 91(T)
 substitution and exchange on $\text{M}(\text{CO})_6$, 153(T)
 substitution on $\text{M}(\text{CO})_5$, 152(T)
 substitution on $\text{V}(\text{CO})_6$, 151(T)
 water exchange, 84(T)
 Kinetic system, complex, 15
 Kinetic trans effect, 75
 Kinetics and the chelate effect, 104
 Kinetics of chelate formation, 100
 King and Altman method, 34
 Labile and inert classification of Taube, 85
 Labile metal ions, 85
 Labile transition-metal ions, ligand substitution, 94
 Langmuir isotherm, adsorption on solid, 402
 competitive adsorption, 403
 limitations, 403
 noncompetitive adsorption, 403
 Langmuir-Hinshelwood mechanism
 competitive adsorption, 404
 noncompetitive adsorption, 404
 Lifetime, 3
 NMR, 436
 Ligand
 bite distance and isomerism, 128
 conformational change, 114
 electronic effect parameter χ , 154
 electronic effect, theory, 155
 hemilabile, 161
 order
 cis effect, 76
 heteroligand replacement, 159
 trans effect, $\text{Pt}(\text{II})$ complexes, 74

- parameters
 aryl effect E_{ar} , 154
 π -acidity π_p , 154
 σ -donicity χ_d , 154
 steric, 154
 rearrangements, 114
- Ligand field excited states of
 $\text{Mo}(\text{CO})_4(\text{L})\text{Y}$, 318
- Ligand field states of
 $\text{Co}^{\text{III}}(\text{L})_6$, 296
 $\text{Cr}^{\text{III}}(\text{L})_6$, 304
- Ligand field theory
 D isomerism mechanism, 125
 isomerism and racemization, 124
 trigonal twist mechanism, 124
- Ligand substitution in, 43
 labile transition-metal ions, 94
 organometallic systems, 150
- Lindskog intermediate, carbonic anhydrase, 359
- Linear free energy relationship, 64
 for aquation of
 $\text{Co}(\text{III})$ complexes, 64
 $\text{Cr}(\text{III})$ complexes, 64
 for proton transfer, 64
- Lineweaver–Burke plot, 339, 341
- Linkage isomerism in, 117
 $\text{Co}(\text{NH}_3)_5(\text{NC})^{2+}$, 118
 $\text{Co}(\text{NH}_3)_5(\text{ONO})^{2+}$, 118
 pressure dependence, 22
 temperature dependence, 19
 $\text{Co}(\text{NH}_3)_5(\text{SCN})^{2+}$, 117
 $\text{Os}(\text{IV/III})$ systems, 119
 $\text{Pd}(\text{Et}_4\text{dien})(\text{SCN})^+$, 118
 $\text{Ru}^{\text{II/III}}(\text{NH}_3)_5$ systems, 118
 $\text{Ru}(\text{NH}_3)_5(\text{DMSO})^{3+}$, 119
 $\text{Ru}(\text{NH}_3)_5(\text{nicotinamide})^{3+}$, 119
- Linkage isomers
 from $\text{Co}(\text{CN})_5\text{X}^{3-} + \text{SCN}^-$,
 photochemical and thermal
 yields, 298(T)
 of $\text{Co}(\text{NH}_3)_5(\text{thiocarbamate})^{2+}$, bridging
 ligand effect, 276
- Lipscomb intermediate, carbonic
 anhydrase, 359
- M general systems
 $\text{M}(\text{CO})_6$
 electronic spectra, 313
 photochemistry, 314
 $\text{M}(\text{OH}_2)_6 + \text{glycine}$, chelate formation,
 100
 $\text{M}(\text{OH}_2)_6^{2/3+}$, self-exchange rate trends,
 264
 $\text{M}(\text{phen})_3^{2/3+}$ and $\text{M}(\text{bpy})_3^{2/3+}$, self-
 exchange rates, 266
 $\text{M}(\text{P}(\text{OR})_2)_3$, complexes, rearrangements,
 128
- Magnetization-transfer, NMR kinetics, 439
- Marcus cross relationship
 applications, 267
 calculated electron transfer rate
 constants, 268(T)
 calculated self-exchange rate constants,
 269(T)
 for O_2/O_2^- , 271(T)
 from thermodynamics, 257
 simplified, 267
 with free energies, 258
 with rate and equilibrium constants, 259
- Marcus theory
 activation parameters, calculated for
 cross reactions, 272
 calculated outer-sphere rate constant,
 261
 coulombic work term, 260
 details, 259
 electronic transmission coefficient, 261
 inner-sphere reorganization, 260
 nuclear reorganization, 261
 precursor complex formation constant,
 260
 predicted inverted region, 272
 self-exchange rate constants, calculated
 for $\text{M}(\text{L})_n^{2/3+}$ systems, 262(T)
 solvent reorganization, 260
 work term corrections, 270
- Mass transfer effect for
 $\text{Ir}(\text{Tp})(\text{PPh}_3)(\text{C}_2\text{H}_4) + \text{H}_2$, in NMR tube,
 398
 $\text{Ni}(\text{PPh}_3)_2(\text{Ph})\text{X} + \text{CO}$, 399
 $\text{Rh}(\text{dipamp})^+ + \text{H}_2$, 395
 $\text{Ru}(\text{BINAP})(\text{CH}_3\text{CO}_2)_2 + \text{H}_2$, 397
- Mass transfer
 gas/liquid, 391
 in NMR sample tube, 398
 limit, tests, 394
 to active sites, 405
 in pores, 405
- Mechanism and rate law, 31
- Mechanistic classification of
 oxidation–reduction reactions, 254
 substitution reactions, 43
- Metal carbonyls
 CO exchange, 150
 derivatives, substitution and exchange,
 153
 substitution reactions, 150

- Metal hydride
 acidity, 181
 deprotonation, 28
 reaction with alkynes, 191
- Metal ion substitution reactivity
 labile and inert classification of Taube, 85
 crystal field theory, 86
- Metal–ligand bifunctional intermediate,
 transfer hydrogenation catalysis, 215
- Metalloproteins, electron transfer, 285
 distance dependence of rate, 286
 from Ru(II), 286
 theory, 286
- Metal–metal bonded carbonyls
 homolysis mechanism, 164
 homolysis or dissociative mechanism for CO substitution?, 166
 substitution, 164
- Metal–metal charge transfer process, 281
- Methanol carbonylation, 230
 Cativa process, 230
 Ir(CO)₃I catalysis, mechanism, 231
 Monsanto process, 230
- Methionine synthase
 mechanism, 356
 methylcobalamin structure, 346
 reaction pathways, 355
 Zn(II) requirement, 356
- Methyl migration (see CO insertion), 172
- Methylcobalamin, H₃CCbl, 341
 Co—C bond energy, 350
 functions, 346
 methionine synthase mechanism, 356
 reaction pathways, 355
 structure in methionine synthase, 346
- Methylmalonyl–CoA mutase
 catalyzed reactions, 345
 mechanism, 348
 radical mechanism, 354
- Methyl–mercury(II) scale, 58
- Methyltransferase (see methylcobalamin), 346
- Michaelis constant, 338
- Michaelis–Menten equation, 338
- Microscopic reversibility
 for CO exchange in Mn(CO)₅X, 41
 for Re^V(hydrotris(pyrazolyl)-borate)(NArMe)(OTf), substitution, 41
 for Re^V(oxo)(dithiolate), substitution, 42
 principle, 40
- Migratory insertion (see CO insertion), 168
- Mixed valence systems, electron transfer, 281
- Mixing rate, effect on gas absorption, 393
- Mixing time correction, stopped-flow, 424
- Mn(II) compounds
 Mn(NTA) + •OH, pulse radiolysis, 451
 Mn(OH₂)₆²⁺ + bpy, kinetics and volume of activation, 430
 Mn(OH₂)₆²⁺, substitution reactions, 96
- Mn compounds, organometallic
 •Mn(CO)₃(PR₃)₂, reactivity, 167
 •Mn(CO)₅
 entering group effects, rate constants, 168(T)
 from photolysis of Mn₂(CO)₁₀, 322
- Mn(CO)₅⁻
 photochemistry, 321
 photosubstitution quantum yields, 321
- Mn(CO)₅(CH₃)
 CO insertion, 168
 kinetics, 171
 rate law, 171
 flash photolysis, 321
- Mn(CO)₅(C(O)CH₃), photolysis, 171
- Mn(CO)₅(η¹-C₃H₅), fluxionality, 139
- Mn(CO)₅H
 hydrogenation mechanisms, 167
 substitution mechanisms, 167
- Mn(CO)₅(L⁻), cis effect theory, 77
- Mn(CO)₅(OCCH₃), decarbonylation, product distribution, 169
- Mn(CO)₅X
 CO exchange
 cis effect, 153
 microscopic reversibility, 41
 photochemistry, 321
 substitution, theory, 154
- Mn(Cp)(CO)₃, complex with *n*-heptane, 221
- Mn(η⁵-H₅CC₅H₄)(CO)₂(NCCH₃),
 electrochemistry and kinetics, 434
- Mn(η⁵-H₅CC₅H₄)(CO)₂(PR₃),
 electrochemistry and kinetics, 434
- Mn₂(CO)₉ + CO, photochemistry, 323
- Mn₂(CO)₁₀
 C isotope exchange, 165
 flash photolysis, 324
 homolysis and substitution, 164
 homolysis, rate law, 164
 photochemistry, 322
 photolysis to •Mn(CO)₅, 322

- $\text{Mn}_2(\eta^5\text{-Cp})_2(\text{NO})_2(\text{CO})_2$, bridge-terminal CO exchange, 143
 $\text{MnRe}(\text{CO})_{10}$
 photochemistry, 324
 substitution, 165
 Molybdenum compounds, organometallic
 $\text{Mo}(\text{CO})_4(\text{L})\text{Y}$
 ligand field excited states, 318
 photochemistry, 318
cis- $\text{Mo}(\text{CO})_4\text{L}_2$, heteroligand replacement, 159
 $\text{Mo}(\text{CO})_3\text{L}$, photochemistry, 317–319
 $\text{Mo}(\text{CO})_3(\text{NHR}_2)$, phosphine oxide catalyst for amine replacement, 159
 $\text{Mo}(\text{CO})_3(\text{phen})$, chelate ring closing, volume of activation, 161
 $\text{Mo}(\text{CO})_3(\text{R}_2\text{P—PR}_2)$, chelate ring closing, 161
 $\text{Mo}(\text{CO})_3\text{X}^-$, substitution, theory, 154
 $\text{Mo}(\text{CO})_6$, CO exchange and substitution, 153(T)
 $\text{Mo}(\text{Cp})(\text{CO})_2(\eta^3\text{-C}_3\text{H}_4\text{R})$, allyl rotation, 141
 $\text{Mo}(\text{Cp})(\text{CO})_3(\text{CH}_3)$, solvent effects on CO insertion, 171, 172(T)
 $\text{Mo}(\text{S}_2\text{C}_2\text{R}_1\text{R}_2)_3$, fluxionality by 2-dimensional NMR, 441
 Model systems for
 carbonic anhydrase, 359
 coenzyme B₁₂, 343
 myoglobin, 362
 Molecular modeling and theory, 28
 Monohydride route, transfer hydrogenation, 212
 Monooxygenase enzymes
 cytochrome P-450, 367
 reactions, 361
 Monsanto process for methanol
 carbonylation, 230
 MP_4H complexes, rearrangements, 129
 Multiple-term rate and mechanism, 32
 Myoglobin, Mb, 361
 CO complex, ¹⁷O NMR studies, 364
 CO dissociation intermediate, structure, 366
 complexation
 by O₂, spin-state changes, 364
 volume of activation, 366
 complexes
 flash photolysis, 364
 4-state model, 364
 rate constants, 365(T)
 deoxy, structure, 361, 362
 histidine(64) mutants, 364
 protonation, 364
 $\text{MbFe}^{\text{II}}(\text{NO}) + \text{O}_2$, reaction pathway, 377
 met, Mb(OH₂)₂, structure, 362
 models, formation of μ-peroxo complexes, 362
 NO complex, flash photolysis, 375
 recombination kinetics, 375
 O₂ and CO complexation
 kinetic parameters, 366(T)
 rate-controlling steps, 365
 oxyMb + NO, 377
 Fe oxidation state, 362
 Mb(O₂), structure, 361
 mutant reactions, 362
¹⁷O NMR studies, 364
 structure, 362
 prosthetic group, structure, 362
 small molecule binding, kinetic parameters, 363(T)
 Nanocluster heterogeneous catalysts, 412
 kinetic model, 412
 Ni(II) compounds
 $\text{Ni}(\text{en})_3^{2+}$, racemization, 122
 $\text{Ni}((\text{H}_3\text{CNHCH}_2)_2)_3^{2+}$, racemization, 122
 $\text{Ni}(\text{OH}_2)_4(\text{amino-pyridines})^{2+}$, chelate ring opening rate constants, 105
 $\text{Ni}(\text{OH}_2)_6^{2+}$
 internal conjugate base mechanism for substitution, 103
 substitution reaction rate constants, 94(T)
 reaction with
 ethylenediamine
 chelate effect, 104
 chelate formation, 103
 glycine, chelate effect, 105
 $\text{Ni}(\text{phen})_3^{2+}$, racemization, 122
 Ni(II/III) system
 $\text{Ni}^{\text{II/III}}$, electron exchange by EPR, 447
 Ni compounds, organometallic
 $\text{Ni}(\text{CO})_3\text{L}$
¹³C NMR chemical shifts, 71(T), 154
 electronic effect and ¹³C NMR, 71
 $\text{Ni}(\text{CO})_4$, CO exchange and substitution, 151
 $\text{Ni}(\text{P}(\text{OEt})_3)_4\text{H}^+$, ethylene-butadiene codimerization catalyst, 232
 $\text{Ni}(\text{PPh}_3)_2(\text{Ph})\text{X} + \text{CO}$, mass transfer effect, 399
 Nitric oxide
 aqueous chemistry, 378
 aqueous, pulse radiolysis, 451

- biological functions, 379
- carriers, S-nitroso species, 377
- complex of (myoglobin)Fe^{II} + O₂,
 reaction pathway, 377
- complexes
 - associative substitution, 158
 - of Fe^{III} hemes, reductive hydroxylation, 375
- endothelium relaxing factor, 373
- enzyme reactions, 373
- reaction with
 - Fe^{II}(Heme), kinetics, 375
 - Fe^{III}(Heme), kinetics, 375
 - myoglobin, kinetics, 375
 - nitric oxide synthase, Fe(II) and Fe(III), rate constants, 376
 - O₂, 378
 - O₂ and thiols, 379
 - oxymyoglobin, 377
 - superoxide ion, 379
- Nitric oxide synthase, NOS
 - coenzymes, NADPH and H₄B, 374
 - endothelial, eNOS, 374
 - Fe spin states, 375
 - inducible, iNOS, 374
 - mechanism, 374
 - neuronal, nNOS, 374
 - self-regulating mechanism, 376
- Nitrito complex of Co(III), formation, 79
- NMR methods, 435
 - bandshape analysis, fluxionality of Ga(III) tris-catecholate complexes, 443
 - chiral centers, isomerism or racemization, 126
 - fluxionality of
 - Mo(S₂C₂R₁R₂)₃, 441
 - W(S₂C₂R₁R₂)₃, 441
 - kinetics
 - by bandshape analysis, 442
 - limitations, 443
 - by 2-dimensional methods, 440
 - by magnetization-transfer, 439
 - by signal monitoring, 438
 - coalescence temperature and rate constant, 443
 - relaxation rate measurements, 444
 - lifetime in
 - η²-alkene metal hydride, 437
 - fluxional processes, 436
 - water ligand exchange, 436
 - relaxation rate, temperature dependence, 444
 - temperature dependence of ¹⁴N in Co(NH₂R)_n²⁺, 116
- NO (see nitric oxide), 373
- Nonaqueous solvent exchange, 90
 - kinetic parameters, 91(T)
- Nonclassical hydride, conversion of W(CO)₃(PR₃)₂(η²-H₂), to W(CO)₃(PR₃)₂(H)₂, kinetics, 181
- Noncompetitive inhibitor, enzyme kinetics, 341
- Noncomplementary oxidation–reduction reaction, 253
 - mechanisms, 254
- Nonradiative deactivation, 294
- n_p*, nucleophilicity scale, 58
- Nuclear magnetic resonance methods (see NMR), 435
- Nuclear reorganization, Marcus theory, 261
- Nucleophilic attack at coordinated ligand, 81, 82
- Nucleophilicity scale, 57
 - Drago *E* and *C* scale, 60
 - Edwards, 58
 - Gutmann donor number, 59
 - methyl–mercury(II), 58
 - n_p*, 58
- Numerical integration
 - examples, 39
 - methods, 38
- Observed rate constant, 10
- Octahedral to square planar coordination change, 115
- Olefin (also see alkene)
 - codimerization, 232
 - coupling, 235
 - catalysts
 - metal-carbenes of Mo and Ru, 235
 - N-heterocyclic carbenes of Ru, 235
 - Chauvin mechanism, 236
 - metathesis, 232, 235
 - catalysts
 - metal-carbenes of Mo and Ru, 235
 - N-heterocyclic carbenes of Ru, 235
 - Chauvin mechanism, 236
- π-bonded, rotations, 137
- π-bonding, 137
- route
 - alkene hydrogenation, 196
 - Rh(dipamp)⁺ asymmetric hydrogenation, 203
 - Rh(diphos)⁺ hydrogenation of 1-hexene, 199

- One-ended dissociation, isomerism of
 $M(AA)_2(X)_2$ systems, 119
- O_2/O_2^- , self-exchange rate constants, 269
 from Marcus cross relationship, 271(T)
- Operational classification of substitution
 mechanisms, 43
- Operational test for the
 A mechanism, 54
 D mechanism, 45
 intimate mechanism, 57
 stoichiometric mechanism, 44
- Optical isomerism (see racemization), 119
- Order of a
 rate law, 2
 reaction, 15
- Organic halides, oxidative addition (see
 aliphatic or aromatic halides),
 182
- Ornithine amino mutase, catalyzed
 reactions, 345
- Os(II) compounds
 electron transfer in Os(II)–Ru(III)
 systems, 285
 $Os(bpy)_3^{2+}$, flash photolysis, 452
- Os(II/III) systems
 electron transfer in Os–Ru systems, 282
 linkage isomerism, 119
- Os compounds, organometallic
 $Os(CO)_4$ (ethylene), fluxionality, 138
 $Os(CO)_5$
 CO exchange and substitution, 151
 dissociation, theory, 152
 substitution, 152(T)
 $Os(\eta^3-C_3H_7)(CO)_3(SnPh_3)$, fluxionality,
 137
 $Os(\eta^6-C_8H_8)(\eta^4-1,5-COD)$, fluxionality,
 136
 $Os(PPh_3)_2(CO)(NO)(C_2H_4)$, ethylene
 rotation, 138
 $Os_3(CO)_9(\mu-C_4Ph_4)$, substitution, steric
 effects, 166
 $Os_3(CO)_{10}(\mu_2-H)_2$ substitution
 associative, steric threshold, 166
 volumes of activation, 166
 $Os_3(CO)_{12}$
 fluxionality, 143
 photochemistry, 324
 $Os_3(CO)_4(L)_p$ cluster, substitution, 166
- Outer-sphere and inner-sphere mechanism,
 differences, 273
- Outer-sphere electron transfer, 255
 precursor and successor complex, 257
 reaction coordinate diagram, 257
 theory, 256
- Oxalato chelate of Co(III), base hydrolysis,
 chelate ring opening, 79
- Oxidation–reduction reactions (also see
 electron transfer), 253
 complementary, 253
 inner-sphere, 254
 mechanistic classification, 254
 noncomplementary, 253
 mechanisms, 254
 outer-sphere, 255
 stoichiometric classification, 253
- Oxidative addition, 177
 atom transfer, 179
 examples, 178
 mechanisms, 179
 of aliphatic halides, 182
 side-on pathway, theory, 184
 solvent effects, 184
 Reichardt's solvent parameter, 184
 stereochemistry, 183
 to $Ir(CO)(PR_3)_2Cl$, kinetic parameters,
 183(T)
 to $Ir(CO)_2(I)_2^-$, pathways, 184
 to $Pt(PPh_3)_2$, by halogen abstraction,
 184
 to $Zr(\eta^5-Cp)_2(PMePh_2)$, radical
 pathway, 184
- of aromatic halides, 184
 anion effects, 186
 catalytic pathways, 185
 coupling, 187
 to Pd(0) metal nanoclusters, Heck
 reaction, 418
 to $Pd(P_2)$, theory, 186
 trans product, 186
- of H_2 , 180
 to $Ir(CO)(PR_3)_2X$, kinetic parameters,
 180(T)
 reaction pathway, 182
 photoactivated, C_6H_6 to
 $Rh(PMe_3)_2(CO)Cl$, 329
 rate law, 178
- Oxo reaction, 225
- Oxygen carriers, myoglobin, 361
- Oxygen, O_2 , enzymic reactions, 361
- Oxygen/superoxide, self-exchange rate
 constants, 269
 from Marcus cross relationship, 271(T)
- P(III) ligands
 cone angles, 70, 71(T)
 electronic parameters, 71(T)
 pK_a values, 71(T)
 steric repulsion parameters, 71(T)

- Palladacycle catalysts, Heck reaction, 417
 catalyst poisoning, 417, 418
 Pd metal formation, 417
- Parallel reactions
 integrated rate law, 17
 rate constants, 17
 rate law, 16
- Partial molar volume calculation for
 $M(OH_2)_n^{z+}$ ions, 93
- Pd compounds
 Pd(0) nanoclusters, oxidative addition,
 Heck reaction, 418
 Pd(dien)(py)²⁺ + Cl⁻, A rate law, 56
 Pd(Et₄dien)(SCN)⁺, linkage isomerism,
 118
 Pd(P)₂, oxidative addition of aromatic
 halides, theory, 186
 Pd(PPhMe₂)(Cl)(η³-allyl), π-σ-π
 mechanism, 140
 Pd(PPhMe₂)(NC₅H₄CO₂)(η¹-C₃H₅),
 fluxionality, 139
- Peptide formation with Co(III) amino acid
 ester complexes, 81
- Permutational analysis of isomerism, 128
- Peroxidase, enzyme reaction, 361
- Peroxyinitrite
 decomposition, 379
 reaction with CO₂, 379
- Phenyl migration to CO in Pt(II) complex,
 170
- Phosphate ester hydrolysis
 catalyst requirements, 82
 in Co(III) complexes, 82, 83
 in labile metal complexes, 83
- Phosphine oxide, catalyst for amine
 replacement in Mo(CO)₅(NHR₂),
 159
- Phosphorescence, 293
- Photoactive state, steady-state assumption,
 295
- Photoaquation of
 Co(CN)₆³⁻, 297
 in water-glycerol, 297
 Cr^{III}(NH₃)₅X
 antithermal pathway, 301
 quantum yields, 301(T)
 Co(NH₃)₆³⁺, 296
 Cr(III) amines, 307
 quantum yields, 308(T)
 Cr(acac)₃, 307
 Cr(CN)₅(NH₃)²⁻, 305
 Cr(CN)₆³⁻, 305
 cis-Cr(cyclam)(NH₃)₂³⁺, 306
 Cr(en)₃³⁺, 306
 Cr^{III}(NH₃)₅X, volumes of activation,
 309(T)
 Cr(NH₃)₆³⁺, 305
 Cr(phen)₃³⁺ and Cr(bpy)₃³⁺, 306
 cis-Rh(bpy)₂(L)Cl²⁺, volumes of
 activation, 302
 Rh^{III}(N)₄(L)X isomers, 302
 quantum yields, 303(T)
 Rh(NH₃)₅Cl²⁺, volumes of activation,
 302
 Rh(NH₃)₅I²⁺, 303
- Photochemical
 energy transfer of Ru(bpy)₃²⁺, 312
 generation of reaction intermediates, 327
 transition state, stereomobility of
 Cr^{III}(cyclam)(X)₂, 309
- Photochemistry (also see flash photolysis)
 basic terminology, 292
 kinetic effects on quantum yield, 294
 organometallic, 313
- Photochemistry of
 C-H bond activation by
 Ir(Cp)(CO)₂, 220, 328
 Ir(Cp^{*})(CO)₂, 218
 Ir(Cp^{*})(PMe₃)(H)₂, 217
 Rh(Cp)(CO)₂, 221, 328
 (Rh(Cp)(CO))₂(μ-CO), 221
 Rh(Cp^{*})(CO)₂, 220
 Rh(HBPz^{*})₃(CO)₂, 218
 Rh(PMe₃)₂(CO)Cl, 219, 329
- Co(III) complexes, 295
 Co(bpy)₂(glycinate)²⁺, 300
 Co(CN)₅X³⁻ + SCN⁻, 297
 Co^{III}(L)₄(aminocarboxylates), 299
 Co^{III}(L)₅Y, 297
 Co^{III}(L)₆, 296
 Co(NH₃)₄(OCO₂)⁺, 299
 Cr(III) complexes, 304
 of fluoride, 308
 Cr(CO)₄(bpy), 320
 Cr(CO)₅L, 319
 Cr(CO)₆, 314
 theory, 314
 Cr^{III}(L)₆, 304
 Cr^{III}(LL)₃ chelates, 306
 Cr(NH₃)₅(OH)₂³⁺, 309
 Fe(CO)₅, 315
 theory, 317
 with PR₃, 316
 Fe₃(CO)₁₂, 324
 Ir(Cp)(CO)₂, 220
 M(CO)₅L systems, 317
 M(CO)₆, 314
 electronic spectra, 314

- $M_3(CO)_{12}$
 bridged intermediate, 326
 structures of intermediates, 325
 $Mn(CO)_5^-$, 321
 $Mn(CO)_5X$, 321
 $Mn_2(CO)_9 + CO$, 323
 $Mn_2(CO)_{10}$, 322
 $MnRe(CO)_{10}$, 324
 $Mo(CO)_4(L)Y$, 318
 $Mo(CO)_5L$, 317–319
 $Os_3(CO)_{12}$, 324
 $Re(CO)_5X$, 322
 $Re_2(CO)_{10}$, 323
 Rh(III) complexes, 301
 $Rh(Cp^*)(CO)_2$ in inert gas solvents, 220
cis- $Rh(phen)_2(Cl)_2^+$, 303
 $Rh(PPh_3)_2(CO)Cl$, 327
 Ru(II) amines, 310
 Ru(II) complexes, 310
 Ru(II) polypyridine complexes, 312
 $Ru(bpy)_3^{2+}$, 312
 $Ru(en)_3^{2+}$, 310
 $Ru(NH_3)_5(pyX)^{2+}$, 311
 $Ru^{II}(NH_3)_5X$, 310
 $Ru(NH_3)_6^{2+}$, 310
 $Ru_3(CO)_{12}$, 324
 $W(CO)_4(bpy)$, 320
 $W(CO)_4(en)$, 320
 $W(CO)_5L$, 317, 318
 $W(CO)_5(pyX)$, 318
 $W(CO)_6$, 314
 Photolysis of
 $Fe(\eta^5-Cp)(CO)(COCH_3)$, CO insertion
 intermediate, 173
 $Mn(CO)_5(C(O)CH_3)$, 171
 Photoracemization of $Cr(en)_3^{3+}$, 306
 Photoredox reactions of
 $Co^{III}(NH_2CH_2)_5X$, 299
 $Co^{III}(NH_2R)_5X$, 298
 $Co^{III}(NH_3)_5X$, 299
 $Rh(NH_3)_5I^{2+}$, 303
 Photostationary state, 294
 Photosubstitution on
 $Cr(NH_3)_n(OH_2)_{6-n}^{3+}$, quantum yields for
 H_2O and NH_3 , 308(T)
 $Mn(CO)_5^-$, quantum yields, 321
 $Rh(NH_3)_5Cl^{2+}$ in various solvents, 302
 quantum yields, 302(T)
 $W(CO)_4(pyX)_2 + (R_2P-PR_2)$, quantum
 yields, 319
 $W(CO)_5(pyX) + P(OEt)_3$, volumes of
 activation, 319
 Physisorption, of gas adsorption on solid,
 400
 Polymerization of epoxides, 176
 catalysts, 177
 pathways, 176
 Preassociation of reactants, **D** mechanism,
 46
 Precursor complex
 formation constant, Marcus theory, 260
 inner-sphere electron transfer, 255
 outer-sphere electron transfer, 257
 Pressure dependence of
 emission lifetimes of $Cr(NH_3)_6^{3+}$, 305
 ethylene rotation in
 $Rh(\eta^5-Cp)(C_2F_4)(C_2H_4)$, 23
 linkage isomerism of $Co(NH_3)_5(ONO)^{2+}$,
 22
 rate constants, 21
 viscosity effect, 22
 Pressure-jump method, 430
 Principle of detailed balancing, 39
 Principle of microscopic reversibility, 40
 Prosthetic group, 338
 Proton ambiguity, 98
 for substitution on $Fe(OH_2)_6^{3+}$, 97
 Proton transfer, linear free energy
 relationship, 64
 Protonation
 by H_3O^+ , 27
 of metal hydrides, 181
 Pseudo-first order
 rate constant, 10
 reaction conditions, 9
 example, 10
 Pseudorotation mechanism, 129
 Pt(II) compounds
 bis hydrazones, **A** intermediate, 56
 for C–H bond activation, 224
 theory, 225
 ligand trans effect order, 74
 phenyl migration to CO, 170
 $Pt(L-Met-S,N)_2$, isomerism, 130
 $Pt(Me_4en)(DMSO)Cl^+ + Cl^-$, anation,
 solvent effect on ion pairing, 66
cis- $Pt(NH_3)_2(Cl)_2$, isomerism, 130
 $Pt(PEt_3)_2(R)Cl + py$, steric effects, 68
 rate constants, 69(T)
 Pt compounds, organometallic
 $Pt(Me_2phen)(CH_3)(PPhMe_2)$,
 intramolecular twist, 123
cis- $Pt(Ph)_2(CO)(X-X)$, chelate ring
 closing, 161
 $Pt(PPh_3)_2$, oxidative addition of aliphatic
 halides by halogen abstraction,
 184
 $Pt(PPh_3)_2(\eta^3-C_7H_6)$, fluxionality, 135

- Pt(R)₂(L)₂ and Pt(Ar)₂(L)₂, isomerism, 130
- Pt₂(η⁵-Cp)₂(CO)₂, bridge-terminal CO exchange, 143
- Pulse radiolysis
 methods, 448
 products in water, 448
 radical products, 449
- Pulse radiolysis of
 aqueous NO, 451
 Co(en)₃³⁺, 449
 Co(NH₃)₆³⁺, 449
 Fe^{II}(NTA) + •CO₂⁻, 451
 Fe(OH)₂²⁺ + N₃⁻, 450
 Mn^{II}(NTA) + •OH, 451
- Pulsed accelerated flow method, 428
- Pyridoxal phosphate, coenzyme B₁₂, cofactor, 345, 346
- Qualitative Analysis of Ligand Effects, QUALE, 154
- Quantum mechanics models, solvent exchange, 89
- Quantum yield, 292
 kinetic factors, 294
- Quenched-flow method, 423
- Quencher, 294
- Racemization, aquation and ¹⁸OH₂ exchange of
 Cr(C₂O₄)₃³⁻, 122
 Rh(C₂O₄)₃³⁻, 121(T)
- Racemization of
 chiral centers, 126
 Cr(phen)₃³⁺, 122
 Fe(phen)₃²⁺, 122
 M(phen)₃ complexes, and aquation, activation parameters, 122(T)
 Ni((H₃CNHCH₂)₂)₃²⁺, 122
 Ni(en)₃²⁺, 122
 Ni(phen)₃²⁺, 122
 unsymmetrical chelates, 126
- Radiationless deactivation, 296
- Radiative deactivation, 294
- Radical clock tests on
 Co(bpy)₂(glycinate)²⁺ derivative, 300
 coenzyme B₁₂ homolysis, 353
 cytochrome P-450, 371
- Radical mechanism for
 coenzyme B₁₂ with 1,1-diol, 354
 diol dehydrase, bound, 354
 glutamate mutase, fragmentation, 354
 methylmalonyl-CoA, 354
 organic rearrangements with coenzyme B₁₂, 351
 substitution
 in organometallic systems, 166
 on Mn(CO)₅H, 167
 on Re(CO)₅H, 167
- Radical reactivity
 of •Fe(CO)₃(PR₃)₂⁺, 167
 of •Mn(CO)₃(PR₃)₂, 167
 of •Re(CO)₅, 167
 theory for 17-electron systems, 168
- Rapid equilibrium assumption, 34
 rate constant, 35
- Rapid equilibrium or steady-state approximation, 37
- Rate and mechanism
 first-order, 31
 half-order, 32
 inverse-order, 32
 multiple-term, 32
 second-order, 31
- Rate and rate constant, 2
- Rate and stoichiometry, 1
- Rate constant, 2
 diffusion controlled, 25
 experimental, 10
 for hemilabile systems, 162
 for parallel reactions, 17
 for successive reactions, 16
 for the A mechanism, 54
 for the D mechanism, 45
 from concentration variables, 12
 ionic strength dependence, 24
 observed, 10
 pressure dependence, 21
 pseudo-first-order, 10
 rapid equilibrium assumption, 35
 steady-state approximation, 34
 temperature dependence, 17
- Rate law, 2
 complex, 15
 for Mn₂(CO)₁₀ homolysis, 164
 for oxidative addition, 178
 for parallel reactions, 16
 for successive reactions, 16
 for the A mechanism, 54
 examples, 55
 for the D mechanism, 45
 examples, 49
 from mechanism, 32
 to mechanism, qualitative guidelines, 31
- Rate of disappearance, 1
- Rate of formation, 1

- Rate-controlling step, chelate formation, 100
- Ray-Dutt bend (see rhombic bend), 120
- Re(V) compounds
 Re(hydrotris(pyrazolyl)borate)-(NArMe)(OTf) substitution, microscopic reversibility, 41
 Re(oxo)(dithiolate) substitution, microscopic reversibility, 42
- Re compounds, organometallic
 •Re(CO)₅ reactivity, 167
 Re(CO)₅H, substitution mechanisms, 167
 Re(CO)₅X, photochemistry, 322
 Re(η^1 -C₇H₇)(CO)₅, fluxionality, 134
 Re(η^5 -indenyl)(CO)₂(MeCCMe), indenyl effect on substitution, 157
 Re₂(CO)₁₀, photochemistry, 323
 Re isotope exchange, 165
- Reaction coordinate diagram for, 20
 Curtin-Hammett conditions, 37
 D mechanism, 49
 Ir complex + ethylene, 190
 outer-sphere electron transfer, 257
- Reaction intermediates, photochemical generation, 327
- Reaction order, 15
 log-log plots, 15
- Reaction rate, 1
- Reactions without metal-ligand bond breaking, 77
- Rearrangement
 of Fe(CO)₅, 128
 of five-coordinate systems, 128
 of M(P(OR)₃)₃ complexes, 128
 of MP₄H complexes, 129
 pseudorotation mechanism, 129
 tetrahedral jump mechanism, 129
 turnstyle mechanism, 129
- Rebound mechanism, hydroxylation by cytochrome P-450, 370
- Reductive elimination, 177, 188
 coupling, 188
 from Ir(Cp^{*})(PMe₃)(Cy)H, 223
 from W(Cp)₂(CH₃)H, 222
 theory, 223
 nonreacting ligand effects, 188
 theory, 188
 variation with
 leaving groups, 188
 metal, 188
- Reichardt, scale of solvent properties, 61
 for oxidative addition of aliphatic halides, 184
- Relativistic effects, 153
- Relaxation methods, 428
 concentration-jump, 428, 430
 kinetic analysis, 429
 limitations, 428
 P-jump, 428, 430
 T-jump, 428, 429
- Relaxation rate measurements, NMR kinetics, 444
- Relaxation time, 429
- Repe carbonylation, 227
- Repe synthesis, 227
 catalysis by Fe(CO)₅, 227
- Rh(III) compounds
 photochemistry, 301
 triplet-state decay rate constants, 301(T)
cis-Rh(bpy)₂(L)Cl²⁺, photoaquation, volumes of activation, 302
 RhCl₃, ethylene-butadiene codimerization catalyst, 232
 Rh(Cl)₅(OH₂)²⁺, substitution, D mechanism, 50, 51(T)
 Rh(C₂O₄)₃³⁻, racemization, aquation and ¹⁸OH₂ exchange, 121, 121(T)
 Rh(N)₄(L)X isomers, photoaquation, 302
 quantum yields, 303(T)
 Rh(NH₃)₅Cl²⁺, photoaquation, volumes of activation, 302
 photosubstitution, quantum yields in various solvents, 302(T)
 Rh(NH₃)₅I²⁺, flash photolysis, 303
 photoaquation, 303
 photoredox reactions, 303
cis-Rh(phen)₂(Cl)₂⁺, photochemistry, 303
- Rh compounds, organometallic
 Rh dimer, arene slippage, 163
 Rh(chiraphos)^{*}, asymmetric hydrogenation, 202
 Rh(CO)(SNS)⁺ system, hemilability, 163
 Rh(Cp)(CO)-methane complex, energetics, 221
 Rh(Cp)(CO)₂, C-H bond activation, 220
 flash photolysis, 328
 photochemistry, 221
 Rh(Cp^{*})(CO)₂, C-H bond activation, 220
 photochemistry
 in inert gas solvents, 220
 with cyclohexane, 220
 Rh(cyclooctadiene)(SbPh₃)Cl + amines, A rate law, 55
 Rh(dipamp)⁺
 asymmetric hydrogenation, 202
 olefin route, 203
 mass transfer effect, 395

- Rh(diphos)⁺, hydrogenation of 1-hexene, olefin route, 199
 Rh(DuPHOS)⁺, asymmetric hydrogenation, theory, 202
 Rh(η^5 -C₅H₄NO₂)(CO)₂ + PPh₃, solvent dielectric constant effects, 66(T)
 Rh(η^5 -Cp)(C₂F₄)(C₂H₄), ethylene rotation, pressure dependence, 23
 Rh(η^5 -Cp)(C₂H₄)₂, ethylene rotation, 138
 Rh(η^5 -Cp)(CO)₂, slippage mechanism, 155
 Rh(η^5 -indenyl)(CO)₂, indenyl effect on substitution, 156
 Rh(HBPz^{*}₃)(CO)₂, C–H bond activation, 218
 Rh(HPz^{*}₃)(CO)(C₂H₄), C–H bond activation, 218
 Rh(PMe₃)₂(CO)Cl, photoactivated oxidative addition, 329
 photochemistry, 329
 Rh(PPh₃)₂(CO)₂H₂, hydroformylation catalysis, 226
 Rh(PPh₃)₂(CO)Cl, flash photolysis, intermediate reactivity, 328
 photochemistry, 327
 Rh(PPh₃)₃Cl
 dimerization, 197
 dissociation, 197
 hydrogenation catalyst, 197
 reaction with H₂, 197
 Rh(PPh₃)₃(H)₂Cl, hydrogenation of C₆H₁₀, 198
 Rh(PR₃)₂(CO)Cl, C–H bond activation, 219
 Rh(Tp^{*})(CO)₂, flash photolysis, C–H bond activation, 451
 Rh₂((1,5-COD)(μ -Cl))₂, heterogeneous catalyst formation, 415
 Rh₂((Cp)(CO))₂(μ -CO), photochemistry and C–H bond activation, 221
 Rh₂((η^5 -Cp^{*})(Cl)₂)₂ + H₂, heterogeneous catalyst formation, 414
 Rh₄(CO)₁₂
 fluxionality, 144
 water gas shift catalyst, 228
 Rh₄(CO)_n(L)_p cluster, substitution, 166
 Rhombic bend for
 M(AA)₃ complexes, 120
 unsymmetrical chelates, 127
 Ribonucleotide reductase
 catalyzed reactions, 345
 mechanism, 348
 Ring-closing metathesis, RCM, 236
 Ring-closing step, chelate formation, 100
 Ring-opening metathesis polymerization, ROMP, 236
 Ring whizzers, 131
 Robin–Day classification of intervalence systems, 281
 Rotations of π -bonded olefins, 137
 Ru(II) catalysts
 diphosphine, asymmetric hydrogenation, 205
 heterolytic cleavage of H₂, 207
 Ru(II) compounds
 amines, photochemistry, 310
 electron transfer
 in metalloproteins, 286
 in Ru(II)–Co(III) systems, 280, 284
 polypyridine complexes,
 photochemistry, 312
 Ru(bpy)₃²⁺
 emission lifetime, 312
 flash photolysis, 452
 photochemical energy transfer, 312
 photochemistry, 312
 Ru(en)₃²⁺, photochemistry, 310
 Ru(NH₃)₅(OH)₂²⁺ + methylpyrazinium ion, A rate law, 56
 Ru(NH₃)₅(pyX)²⁺, photochemistry, 311
 Ru(NH₃)₅X, photochemistry, 310
 Ru(NH₃)₆²⁺, photochemistry, 310
 Ru(II/III) systems
 electron transfer
 in Ru–Os systems, 282
 intervalence, 281, 282, 284
 Ru(hfacac)₃^{0/1-}, self-exchange rates, 263
 Ru^{II/III}(NH₃)₅, linkage isomerism, 118
 Ru(III) compounds
 electron transfer in Ru(III)–Os(II) systems, 285
 Ru dithiocarbamates, isomerism, 128
 Ru(NH₃)₅(DMSO)³⁺, linkage isomerism, 119
 Ru(NH₃)₅(nicotinamide)³⁺, linkage isomerism, 119
 Ru₂(NH₃)₁₀(μ -L)²⁺, intervalence absorption energy, 283(T)
 Ru compounds, organometallic
 Ru(BINAP)²⁺, asymmetric
 hydrogenation of methyl (Z)- α -(acetamido)cinnamate, 207
 Ru(BINAP)(DPEN), asymmetric
 hydrogenation of C=O bonds, 215
 Ru(BINAP)(O₂CCH₃)₂, asymmetric
 hydrogenation
 catalyst, 205

- of neutral substrates, 207
- mechanism, 206, 210
- rate law, 209
- mass transfer effect, 397
- $\text{Ru}(\text{CO})_4(\text{ethylene})$, fluxionality, 138
- $\text{Ru}(\text{CO})_4\text{L}$, substitution, kinetics, 154
- $\text{Ru}(\text{CO})_4(\text{R}_2\text{P}-\text{PR}_2)$, chelate ring closing, 161
- $\text{Ru}(\text{CO})_5$
 - CO exchange and substitution, 151
 - dissociation, theory, 152
 - substitution, 152(T)
- $\text{Ru}(\eta^6\text{-arene})((S,S)\text{-TsDPEN})^+$
 - asymmetric transfer hydrogenation of C=O bonds, 214
 - transfer hydrogenation, D exchange kinetics, 214
- $\text{Ru}(\eta^6\text{-C}_6\text{Me}_6)(\text{OAc})_2 + \text{H}_2$, heterogeneous catalyst formation, 414
- $\text{Ru}(\eta^5\text{-Cp})(\text{CO})(\eta^3\text{-C}_3\text{H}_5)$, allyl rotation, 141
- $\text{Ru}(\eta^5\text{-Cp})(\eta^4\text{-C}_5\text{H}_4\text{O})\text{L}^+$, slippage mechanism, 155
- $\text{Ru}(\eta^5\text{-indenyl})(\text{PPh}_3)(\text{PPh}_2\text{X})^+$, hemilability, 162
- $\text{Ru}(\eta^5\text{-indenyl})(\text{PPh}_3)_2\text{Cl}$, D mechanism, 156
- $\text{Ru}(\text{hfacac})(\text{Ph}_2\text{P}(\text{CH}_2)_3\text{PPh}_2)$, hydrogenation of CO_2 , 229
- $\text{Ru}(\text{PPh}_3)_2(\text{CO})\text{Cl}(\eta^3\text{-CH}_2\text{CHCMe}_2)$, endo-exo isomers, 141
- $\text{Ru}((\text{R}_2\text{PCH}_2)_2)_2$, photochemistry and C-H bond activation, 221
- $\text{Ru}(\text{tolBINAP})(\text{DPEN})$, asymmetric hydrogenation of C=O bonds, bifunctional catalytic pathway, 216
- $\text{Ru}_2((\eta^5\text{-Cp})(\text{CO}))_2$, bridge-terminal CO exchange, 141
- $\text{Ru}_3(\text{CO})_{12}$
 - flash photolysis, 325
 - fluxionality, 143
 - photochemistry, 324
 - water gas shift catalyst, 228
- $\text{Ru}_3(\text{CO})_n(\text{L})_p$ cluster, substitution, 166
- $\text{Ru}_3(\mu_3\text{-}\eta^2\text{-}(2\text{-PhNpy})(\text{CO}))_9^+$, associative substitution, 166
- $\text{Ru}_5\text{C}(\text{CO})_{15}$ cluster, substitution, 166
- $\text{Ru}_6\text{C}(\text{CO})_{17}$ cluster, substitution, 166
- Runge-Kutta method, 38
- Saturation behavior, 45
 - enzyme kinetics, 339
- Secondary photolysis, 293
- Second-order
 - irreversible system, 9
 - concentration variables, 14
 - half-time, 9
 - integrated rate law, 9
 - rate and mechanism, 31
 - reversible system, 7
 - integrated rate law, 8
- Second-order and first-order conditions, comparison, 10
- Self-exchange electron-transfer reaction, 258
 - kinetic parameters, 265(T)
 - asymmetry
 - calculated by the Marcus cross relationship, 269(T)
 - for ascorbic acid species, 269
 - for $\text{M}(\text{L})_n^{2/3+}$ systems, calculated by Marcus theory, 262(T)
 - for O_2/O_2^- , 269
 - calculated from Marcus cross relationship, 271(T)
- rates
 - counter ion effects, 266
 - for $\text{Co}(\text{NH}_3)_6^{2/3+}$, DFT theory, 264
 - for $\text{Co}(\text{phen})_3^{2/3+}$, anion effects, 266
 - for Fe(II/III) aqueous, 268, 269
 - for $\text{Fe}(\text{CN})_6^{3/4-}$, cation effects, 266
 - for $\text{Fe}(\text{Cp})_2^{0/+}$, 263
 - for $\text{M}(\text{OH}_2)_6^{2/3+}$, trends, 264
 - for $\text{M}(\text{phen})_3^{2/3+}$ and $\text{M}(\text{bpy})_3^{2/3+}$, 266
 - for $\text{Ru}(\text{hfacac})_3^{0/1-}$, 263
 - quantum theory, 263
 - spin-state changes, 266
- Sensitizer, 293
- Shilov reaction, 224
- Sigma-donicity, indenyl ligand, 156
- Sigmatropic shifts
 - symmetry rules, 132
 - allowed, suprafacial, 133
 - forbidden, antarafacial, 133
 - 1,3 antarafacial, 133
 - 1,5 suprafacial, 134
 - 1,7 antarafacial, 134
 - 1,9 suprafacial, 134
- Slip mechanism, 137
- Slippage mechanism, 155
 - in $\text{Co}(\eta^5\text{-Cp})(\text{CO})_2$, 155
 - in $\text{Cr}(\eta^6\text{-arene})(\text{CO})_3$, 155
 - in $\text{Ir}(\eta^5\text{-Cp})(\text{CO})_2$, 155
 - in $\text{Rh}(\eta^5\text{-Cp})(\text{CO})_2$, 155
 - in $\text{Ru}(\eta^5\text{-Cp})(\eta^4\text{-C}_5\text{H}_4\text{O})\text{L}^+$, 155
 - indenyl effect, 156
- Softness, absolute, 63

- Solvatochromic solvent properties scale, 61
parameters, 62(T)
- Solvent effects
dielectric constant change on interchange mechanisms, 65
for $\text{Rh}(\eta^5\text{-C}_5\text{H}_4\text{NO}_2)(\text{CO})_2 + \text{PPh}_3$, 66(T)
on emission lifetimes of $\text{Cr}(\text{NH}_3)_6^{3+}$, 305
on intervalence electron transfer, 282
on ion pairing for $\text{Pt}(\text{Me}_4\text{en})(\text{DMSO})\text{Cl}^+ + \text{Cl}^-$ anation, 66
on oxidative addition of aliphatic halides, 184
on photosubstitution, quantum yields for $\text{Rh}(\text{NH}_3)_5\text{Cl}^{2+}$, 302(T)
- Solvent exchange
angular overlap model, 88
aqueous, 83
empirical correlation, 92
enthalpy of activation, 92(T)
kinetic parameters
aqueous, 84(T)
nonaqueous, 91(T)
nonaqueous, 90
quantum mechanics models, 89
volume of activation, 93
theory, 93
- Solvent property scales, 61
Drago, 61
hydrogen bonding, 61
Reichardt, 61
representative parameters, 62(T)
solvatochromic, 61
- Solvent reorganization, Marcus theory, 260
- Spin trapping, EPR, 447
- Spin-state changes, self-exchange rates, 266
- Spin-state equilibria, Fe(II) complexes, 123
- Square-planar systems, isomerism, 130
- Steady-state, approximation, 32
rate constant, 34
- Steady-state conditions, enzyme kinetics, 338
- Steady-state, or rapid equilibrium approximation?, 37
- Stereochemical change, 114
- Stereochemistry of CO_2 insertion, 175
oxidative addition of aliphatic halides, 183
- Stereoselective hydrogenation, 201
- Steric effects
for aquation of $\text{Cr}(\text{NH}_3)_5\text{Cl}^{2+}$ and $\text{Cr}(\text{NH}_2\text{CH}_3)_5\text{Cl}^{2+}$, 67
for interchange mechanisms, 66
for $\text{Pt}(\text{PEt}_3)_2(\text{R})\text{Cl} + \text{py}$, 68
rate constants, 69(T)
for substitution on $\text{Os}_3(\text{CO})_9(\mu\text{-C}_4\text{Ph}_4)$, 166
threshold, 71
versus electronic effects for, $\text{Co}(\text{NH}_2\text{CH}_3)(\text{NH}_3)_4(\text{DMF})^{3+}$ aquation, 68
- Steric parameters
cone angle, 70, 154
for P(III) and As(III) ligands, 71(T)
steric repulsion energy, 70, 155
for P(III) and As(III) ligands, 71(T)
symmetric deformation coordinate, 155
- Stern–Volmer plots, 293
- Stoichiometric classification of oxidation-reduction reactions, 253
- Stoichiometric mechanism, 44
operational tests, 44
- Stokes–Einstein equation, 26
- Stopped-flow method, 423
deadtime, 424
determination for
first-order conditions, 425
second-order conditions, 425
high-pressure, 427
mixing time correction, 424
time range, 424
- Structural parameters for
Co(III) pentaamine complexes, 67
Cr(III) pentaamine complexes, 67
- Substitution and exchange on
 $\text{M}(\text{CO})_5$, 151
 $\text{M}(\text{CO})_6$, 152
kinetic parameters, 153(T)
theory, 153
metal carbonyl derivatives, 153
 $\text{Ni}(\text{CO})_4$, 151
- Substitution and homolysis of $\text{Mn}_2(\text{CO})_{10}$, 164
- Substitution mechanism
operational classification, 43
trends in volumes of activation, 96
- Substitution, radical mechanism
for $\text{Co}(\text{CO})_4(\text{SnCl}_3)$, 166
for organometallic systems, 166
- Substitution rate, variation with metal ion, 83
- Substitution reactions, 43
crystal field theory, 86
mechanism classification, 43

- of alkenes, 188
- of $\text{Co}(\text{OH}_2)_6^{2+}$, 96
- of $\text{Co}_4(\text{CO})_n(\text{L})_p$ cluster, 166
- of $\text{Cr}(\text{CO})_5$ (cyclohexane), 315
- of $\text{Cr}(\text{CO})_5$ (heptane), 315
- of $\text{Fe}(\text{OH}_2)_5(\text{OH})^{2+}$, rate constants, 99(T)
- of $\text{Fe}(\text{OH}_2)_6^{2+}$, 96
- of $\text{Fe}(\text{OH}_2)_6^{3+}$, 97
 - rate constants, 99(T)
- of $\text{Ir}_4(\text{CO})_n(\text{L})_p$ cluster, 166
- of $\text{M}(\text{CO})_5$, 152(T)
- of $\text{M}(\text{CO})_5\text{X}^-$ systems, theory, 154
- of metal carbonyls, 150
- of metal-metal bonded carbonyls, 164
- of $\text{Mn}(\text{CO})_5\text{H}$, mechanisms, 167
- of $\text{Mn}(\text{OH}_2)_6^{2+}$, 96
- of $\text{MnRe}(\text{CO})_{10}$, 165
- of $\text{Ni}(\text{OH}_2)_6^{2+}$, rate constants, 94(T)
- of NO complexes, 158
- of $\text{Os}_3(\text{CO})_9(\mu\text{-C}_6\text{Ph}_4)$, steric effects, 166
- of $\text{Os}_3(\text{CO})_n(\text{L})_p$ cluster, 166
- of $\text{Os}_3(\mu_2\text{-H})_2(\text{CO})_{10}$, associative, steric threshold, 166
- of $\text{Re}(\text{CO})_5\text{H}$, mechanisms, 167
- of $\text{Re}(\eta^5\text{-indenyl})(\text{CO})_2(\text{MeCCMe})$, indenyl effect, 157
- of $\text{Rh}(\eta^5\text{-indenyl})(\text{CO})_2$, indenyl effect, 156
- of $\text{Rh}_4(\text{CO})_n(\text{L})_p$ cluster, 166
- of $\text{Ru}_3(\text{CO})_n(\text{L})_p$ cluster, 166
- of $\text{Ru}_3(\mu_3\text{-}\eta^2\text{-}(2\text{-PhNpy})(\text{CO})_9)^+$, associative, 166
- of $\text{Ru}_3\text{C}(\text{CO})_{15}$ cluster, 166
- of $\text{Ru}_3\text{C}(\text{CO})_{17}$ cluster, 166
- of $\text{Ti}(\text{OH}_2)_6^{3+}$, 96(T)
- of $\text{V}(\text{CO})_6$, 150
 - kinetic parameters, 151(T)
- of $\text{V}(\eta^5\text{-C}_5\text{R}_n)_2(\text{CO})$, 156
- of $\text{V}(\text{OH}_2)_6^{3+}$, 96, 97(T)
- of $\text{W}(\text{CO})_3(\text{PCy}_3)_2$, 160
- of $\text{W}(\text{CO})_4(\text{bpy})$, 160
- Successive reactions
 - integrated rate law, 16
 - rate constants, 16
 - rate law, 16
- Successor complex
 - inner-sphere electron transfer, 255
 - outer-sphere electron transfer, 257
- Sulfito complexes of Co(III), formation, 79
- Sulfur dioxide
 - complex formation, 78
 - insertion, 174
 - in $\text{Fe}(\text{Cp})(\text{CO})_2(\text{CH}_2\text{R})$, 174
 - in $\text{W}(\text{CO})_5(\text{Y}(\text{CH}_3)_3)$, 174
- Superoxide dismutase, reaction, 361
- Superoxide/oxygen
 - self-exchange rate constants, 269
 - calculated from Marcus cross relationship, 271(T)
- Suprafacial sigmatropic shift, 133
- Swamping conditions, enzyme kinetics, 340
- Symmetry restrictions for alkene hydrogenation, 195
- Symmetry rules, sigmatropic shifts, 132
- Taube, labile and inert classification of metal ions, 85
- Taube-Creutz compound, 281
- Temperature dependence of $\text{Co}(\text{NH}_3)_5(\text{ONO})^{2+}$ linkage isomerism, 19
 - rate constants, 17
- Temperature-jump method, 429
 - determination of K and ΔH° , 430
- Tests, operational, for the
 - A mechanism, 54
 - D mechanism, examples, 49
 - intimate mechanism, 57
 - stoichiometric mechanism, 44
- Tetrahedral jump mechanism, 129
- Tetrahedral to octahedral coordination change, 115
- Tetrahedral to square planar coordination change, 115
- Thermodynamic trans effect, 74
- Thiols, reaction with $\text{NO} + \text{O}_2$, 379
- Ti compounds
 - $\text{Ti}(\eta^5\text{-C}_5\text{H}_4\text{C}(\text{CH}_3)_2\text{C}_6\text{H}_5)(\text{CH}_3)_2^+$, hemilabile phenyl group, 163
 - $\text{Ti}(\text{NMe}_2)_2(\eta^1\text{-C}_3\text{H}_5)$, fluxionality, 139
 - $\text{Ti}(\text{OH}_2)_6^{3+}$, substitution reactions, 96(T)
- Trans effect, 74
 - kinetic, 75
 - ligand order for Pt(II) complexes, 74
 - thermodynamic, 74
- Transfer hydrogenation of C=O bonds, 211
 - bifunctional metal-ligand intermediate, 215
 - by $\text{Ru}(\eta^6\text{-arene})((S,S)\text{-TsDPEN})^+$, 214
 - D exchange kinetics, 214
 - direct transfer route, 213
 - mechanisms, 212
 - mono- and dihydride routes, 214
 - differentiation, 213
 - Transition state, 18, 20
 - Transition-state free energies for Curtin-Hammett conditions, 37
 - Transition-state theory, 18

- Transmission coefficient, 18
 electronic, Marcus theory, 261
 for adiabatic processes, 256
- Trapped-valence model, intervalence
 electron transfer, 282
- Trigger mechanism, homogeneous
 polymerization initiation, 234
- Trigonal twist isomerism mechanism
 for Al(III) complexes, 128
 for Co(III) complexes, 128
 for Ga(III) complexes, 128
 for M(AA)₃ complexes, 120
 for unsymmetrical chelates, 127
 ligand field theory, 124
- Triplet-state decay rate constants of Rh(III)
 complexes, 301(T)
- Turnover frequency, TOF, 202
- Turnover number, TON, 202
 enzyme kinetics, 339
- Turnstyle mechanism, 129
- Twist angle and isomerism, 128
- Uncompetitive inhibitor, enzyme kinetics,
 340
- Unstable intermediate, 32
- Unsymmetrical chelate rearrangement by a
 D mechanism, 126
 rhombic bend, 127
 trigonal twist, 127
- V(III) compounds
 V(OH₂)₆³⁺, substitution reactions, 96
 rate constants, 97(T)
- V compounds, organometallic
 V(CO)₆, substitution reactions, 150
 kinetic parameters, 151(T)
- V(η⁵-C₅R_n)₂(CO)
 CO exchange, kinetic parameters,
 157(T)
 indenyl effect, 156
 substitution reactions, 156
- V(η³-indenyl)₂(CO), indenyl effect, 156
- van't Hoff equation, 21
- Viscosity, pressure dependence, 22
- Vitamin B₁₂ (see coenzyme B₁₂), 341
- Volume of activation, 21
 compressibility factor, 21
 for Cr(CN)₆³⁻, photoaquation, 305
 for Cr(CO)₄(S—S), chelate ring opening,
 161
 for electron-transfer reactions, 271
 for Fe(III) aqueous + SCN⁻, 427
 for interchange mechanisms, 71
 for Mn(OH₂)₆²⁺ + bpy, 430
 for Mo(CO)₅(phen), chelate ring closing,
 161
 for myoglobin, complexation, 366
 for nonaqueous solvent exchange, 91(T)
 for Os₃(μ₂-H)₂(CO)₁₀, substitution
 reactions, 166
 for photoaquation of
 Cr^{III}(NH₃)₅X, 309(T)
cis-Rh(bpy)₂(L)Cl²⁺, 302
 Rh(NH₃)₅Cl²⁺, 302
 for photosubstitution of W(CO)₅(pyX) +
 P(OEt)₃, 319
 for solvent exchange, 93
 theory, 93
 for water exchange, 72, 84(T)
 and entropies of activation, 72(T)
 trends and substitution mechanism, 96
- Volume, partial molar of M(OH₂)_n^{z+} ions,
 calculation, 93
- W compounds, organometallic
 W(CO)₃(PCy₃)₂
 agostic bond stabilization, 160
 substitution reactions, 160
- W(CO)₃(PR₂)₂(H₂), η²-H₂ isomer, 180
 structure, 180
- W(CO)₃(PR₃)₂(H₂) conversion to
 W(CO)₃(PR₃)₂(H)₂, kinetics, 181
- W(CO)₄(bpy)
 chelate ring opening, 160
 photochemistry, 320
 substitution, 160
- W(CO)₄(en), photochemistry, 320
- W(CO)₄(pyX)₂ + (R₂P—PR₂),
 photosubstitution quantum yields,
 319
- W(CO)₅(CH₃)⁻, CO₂ insertion, kinetics,
 175
- W(CO)₅(CHDCHDPh)⁻, CO₂ insertion
 mechanism, 175
 stereochemistry, 175
- W(CO)₅L
cis effect, 158
 photochemistry, 317, 318
- W(CO)₅(py), flash photolysis, 319
 in 1-hexene, 319
- W(CO)₅(pyX)
 photochemistry, 318
 photosubstitution with P(OEt)₃,
 volumes of activation, 319
- W(CO)₅X⁻, substitution, theory, 154
- W(CO)₅(Y(CH₃)₃)⁻, SO₂ insertion, 174
- W(CO)₆
 CO exchange and substitution, 153(T)

- flash photolysis in 1-hexyne, 315
- photochemistry, 314
- $W(Cp)_2(CH_3)H$
 - reductive elimination, 222
 - theory, 223
- $W(\eta^6-C_8H_8)(CO)_3$, fluxionality, 136
- $W(P(OR)_3)_5(H)_2$, fluxionality, 181
- $W(S_2C_2R_1R_2)_3$, fluxionality, 2-
dimensional NMR, 441
- Water as a bridging ligand, 276
- Water exchange
 - entropies and volumes of activation, 72(T)
 - kinetic parameters, 84(T)
 - crystal field theory, 87(T)
 - NMR lifetime, 436
 - range of rates, 85
 - rates, 83
 - SCF theory, enthalpy of activation, 89(T)
- Water gas shift reaction, 228
 - catalysis
 - by $Rh_4(CO)_{12}$ and $Ru_3(CO)_{12}$, 228
 - by $Fe(CO)_5$, mechanism, 229
 - theory, 228
- Wilkinson's catalyst, $Rh(PPh_3)_3Cl$
 - dimerization, 197
 - dissociation, 197
 - hydrogenation, 197
 - of C_6H_{10} , 198
 - reaction with H_2 , 197
- Woodward–Hoffmann rules for
sigmatropic shifts, 132
- Work term corrections, Marcus theory, 270
- Zero-order reaction, 3
 - integrated rate law, 4
- Ziegler–Natta homogeneous
polymerization, 233
 - by $Zr(Cp)_2(X)_2$, 233
 - initiation by the
 - Cossee mechanism, 234
 - trigger mechanism, 234
 - pathways, 233
 - propagation, 234
- Zinc(II) enzyme, carbonic anhydrase, 356
- Zinc(II) requirement for methionine
synthase, 356
- $Zn[12]aneN_3$, carbonic anhydrase model,
359
- $Zn[12]aneN_4$, carbonic anhydrase model,
kinetics, 360
- $Zr(\eta^5-Cp)_2(PMePh_2)$, oxidative addition of
aliphatic halides, radical
pathway, 184